

THE PETROGENESIS AND GEOCHEMISTRY OF THE BRITISH CALEDONIAN GRANITES,  
WITH SPECIAL REFERENCE TO MINERALIZED INTRUSIONS.

Thesis presented for the Degree of  
Doctor of Philosophy  
University of Leicester 1985

Catherine O'Brien (BSc Leicester).

To Julian and my two furry friends Bear and Woodstock.

## CONTENTS.

	Page.	
Chapter 1.	Introduction.	1
Chapter 2.	Tectonic setting of the British Caledonides.	3
2:1.	Introduction.	3
2:2.	The tectonic evolution of the northern margin of Iapetus.	5
2:2:i.	The early events in the Moine.	5
2:2:ii.	The development of the Dalradian basin and the Grampian orogeny.	8
2:2:iii.	The development of the Ordovician-Silurian accretionary prism in Southern Scotland and the last events of the Caledonian orogeny.	12
2:3.	The tectonic evolution of the southern margin of Iapetus.	20
2:3:i.	The age and nature of the pre-Caledonian basement.	20
2:3:ii.	Ensialic sedimentary basins and volcanism in the Cambrian and Ordovician.	22
2:3:iii.	Deformation, metamorphism, granite intrusion and the end of the Caledonian orogeny.	23
2:4.	Summary.	25
Chapter 3.	Petrology and mineral chemistry.	28
3:1.	Introduction.	28
3:2.	Mineralogy of the Caledonian intrusions.	29
3:3.	Crystallization sequences from textural information.	30

3:3:1.	Scotland.	30
3:3:1:i.	Pyroxene bearing intrusives.	30
3:3:1:ii.	Hornblende bearing intrusives.	30
3:3:1:iii.	Biotite granites.	33
3:3:1:iv.	Two mica granites.	34
3:3:2.	The English Lake District.	34
3:3:2:i.	Pyroxene bearing intrusives.	34
3:3:2:ii.	Biotite granites.	35
3:3:2:iii.	Garnet granites.	36
3:4.	Secondary alteration products and textures.	37
3:4:1	Scottish granites.	38
3:4:1:i.	Pyroxene bearing intrusions.	38
3:4:1:ii.	Hornblende bearing intrusions.	39
3:4:1:iii.	Biotite granites.	39
3:4:2.	The Lake District.	40
3:4:2:i.	Pyroxene bearing intrusions.	41
3:4:2:ii.	Biotite granites.	41
3:4:2:iii.	Garnet granites.	42
3:5.	Mineral chemistry.	43
3:5:i.	Pyroxenes.	43
3:5:ii.	Amphiboles.	44
3:5:iii.	Biotites.	48
3:5:iv.	Feldspars.	53
3:5:v.	Chlorites.	58
3:5:vi.	Muscovites.	61
3:5:vii.	Oxides.	63
3:5:viii.	Garnets.	63
3:5:ix.	Accessory rare earth bearing minerals.	63

3:6.	Summary and conclusions.	64
Chapter 4.	Criteria for the classification of the Caledonian granites.	65
Chapter 5.	Mineralization, metallogenesis and late stage processes in the Caledonian granites.	73
5:1.	Introduction.	73
5:2.	Mineralization, metallogenesis and late stage processes in the Caledonian granites of the English Lake District	74
5:2:i.	Effects of metasomatism and hydrothermal alteration on the major and trace element composition of the intrusions.	77
5:2:ii.	The effects of greisenization.	80
5:2:iii.	Geochemistry of metasomatism other than greisenization.	83
5:3.	Mineralization and metasomatism in the Caledonian granites of Scotland.	84
5:3:i.	The porphyry copper molybdenum granites.	84
5:3:ii.	The metalliferous tin tungsten granites of eastern Scotland.	88
5:3:iii.	Fracture induced uranium mineralization at Helmsdale	91
5:4.	Summary and conclusions.	92
Chapter 6.	The geochemistry of the Caledonian granitoids and geochemical modelling of selected intrusions.	94
6:1.	Introduction.	94
6:2.	Major and trace element variations.	94
6:2:i.	Internal geochemical variations of the Lake District intrusions.	103

6:2:ii.	Internal geochemical variations in the Scottish Caledonian intrusives.	105
6:3.	Geochemical modelling.	119
6:3:1.	Major element modelling.	121
6:3:2.	Trace element modelling.	124
6:3:2:i.	The Lake District.	127
6:3:2:ii.	The Scottish Caledonian granitoids.	131
6:4.	The Rare earth elements.	143
6:5.	The role of the continental crust in the generation of the Caledonian granites.	148
6:5:i.	The Lake District granites.	149
6:5:ii.	The Scottish granitoids.	150
6:6.	Summary.	153
Chapter 7.	Petrogenesis and regional variations.	156
7:1.	Introduction.	156
7:2.	Petrogenetic variation in the Lake District granitoids.	157
7:3.	Petrogenetic variation in the Scottish Caledonian granitoids.	159
7:4.	Isotopic evidence of source variation.	172
7:5.	Source variation between the intrusions of the northern and southern plates.	174
7:6.	Discussion and conclusions.	176
Chapter 8.	Summary of conclusions.	177

## LIST OF TABLES.

	Page.
Chapter 2.	
Table 2:1. Published isotopic data on the Caledonian granitoids.	16
Table 2:2. Pb isotopic data from Pidgeon & Aftalion 1978.	17
Table 2:3. Combined Rb-Sr Sm-Nd data for the Caledonian granitoids.	18
Table 2:4. Isotopic dates of the Lake District granites.	25
Chapter 3.	
Table 3:1. Summary of the mineralogy of the Scottish Caledonian intrusions.	31
Table 3:2. Summary of the mineralogy of the Lake District intrusions.	35
Table 3:3. Summary of secondary alteration products in Scottish intrusions.	37
Table 3:4. Summary of secondary alteration products in Lake District intrusions.	38
Table 3:5. Representative microprobe data for pyroxenes from Caledonian intrusions.	45
Table 3:6. Representative microprobe data for amphiboles from Caledonian intrusions.	46
Table 3:7. Representative microprobe data for biotites from Caledonian granites.	51
Table 3:8. Representative microprobe data for feldspars from Caledonian intrusions.	54
Table 3:9. Representative microprobe analyses of chlorites from Caledonian intrusions.	59
Table 3:10. Representative microprobe data for primary muscovites from Caledonian granites.	61

Table 3:11. Representative microprobe analyses of secondary muscovites in Caledonian granites.	62
Chapter 4.	
Table 4:1. Summary of Read's classification of the Caledonian granites.	67
Table 4:2. Reclassification of Read's newer and last granites according to Pankhurst & Sutherland (1982).	68
Table 4:3. Geochemical classification of the Caledonian granites.	72
Chapter 5.	
Table 5:1. Selected trace element abundances for average Glen Gairn and Skiddaw greisens.	90
Chapter 6.	
Table 6:1. Mean analyses for the British Caledonian intrusives.	96
Table 6:2. Mean cumulus mineral assemblages calculated using major element modelling.	123
Table 6:3. Mineral/melt distribution coefficients used in magmatic models.	127
Table 6:4a) Average mineral/melt distribution coefficients of the rare earth elements in basaltic and andesitic rocks.	145
Table 6:4b) Average mineral/melt distribution coefficients of rare earth elements in dacitic and rhyolitic rocks.	145
Table 6:5. Average major and trace element data for crustal units in the Caledonides of Britain.	152

## LIST OF FIGURES.

### Chapter 1.

Fig. 1:1. The location and extent of the Caledonide fold belt.

Fig. 1:2. The location of the Caledonian granites under consideration.

### Chapter 2.

Fig. 2:1.  $\epsilon$  Nd vs.  $\epsilon$  Sr variation diagram for the Caledonian granitoids, data from Halliday (1984).

### Chapter 3.

Fig. 3:1. Simplified Ab. Or. Qtz. phase diagrams for S and I type granites.

Fig. 3:2. Pyroxene compositions.

Fig. 3:3. Cationic Fe/Fe+Mg vs. Mn compositions of biotites from the Scottish granitoids.

Fig. 3:4. Cationic Fe vs. Mg compositions of biotites from Scottish granitoids.

Fig. 3:5. Biotite compositions from the Lake District granitoids.

Fig. 3:6. Feldspar compositions from the Scottish granitoids.

Fig. 3:7. Feldspar compositions from the Lake District granitoids.

Fig. 3:8.  $TiO_2$  vs.  $K_2O$  variation in biotites and chlorites.

Fig. 3:9.  $MgO$  vs.  $K_2O$  variation in biotites and chlorites.

Fig. 3:10.  $FeO$  vs.  $K_2O$  variation in biotites and chlorites.

Fig. 3:11. Fe-Mn-Ti variation in oxide phases.

#### Chapter 4.

Fig. 4:1. Mantle normalized trace element plots for S-type granites.

Fig. 4:2. Mantle normalized trace element plots for the more evolved juvenile granites.

Fig. 4:3. Mantle normalized trace element plots for the less evolved juvenile granites.

#### Chapter 5.

Fig. 5:1. Frequency distribution of tin in Caledonian granites.

Fig. 5:2. Frequency distribution of tungsten in Caledonian granites.

Fig. 5:3. Frequency distribution of molybdenum in Caledonian granites.

Fig. 5:4. Frequency distribution of copper in Caledonian granites.

Fig. 5:5. Frequency distribution of boron in caledonian granites.

Fig. 5:6. Frequency distribution of uranium in Caledonian granites.

Fig. 5:7. Frequency distribution of thorium in Caledonian granites.

Fig. 5:8. Frequency distribution of lithium in Caledonian granites.

Fig. 5:9. Frequency distribution of beryllium in Caledonian granites.

Fig. 5:10. LIL element variation diagrams for the Lake District granitoids.

Fig. 5:11. LIL element variation diagrams for the Lake District granitoids.

Fig. 5:12.  $TiO_2$  vs. V and B vs. Ga variation diagrams for the Lake District granitoids.

Fig. 5:13. Comparison of mantle normalized trace element plots for granites and greisens from the Lake District.

Fig. 5:14. Selected trace element variations for the Skiddaw granite.

Fig. 5:15. Selected trace element variations for the Eskdale intrusion.

Fig. 5:16. Selected trace element variations for the Carrock Fell and Shap intrusions.

Fig. 5:17. Selected trace element variations for the Threlkeld microgranite.

Fig. 5:18. Selected trace element variations for the Kilmelford complex.

Fig. 5:19. Selected trace element variations for the Ballachulish complex.

Fig. 5:20. Selected trace element variations for the Comrie complex.

Fig. 5:21. Comparison of mantle normalized trace element plots for the Cairngorm and Dartmoor intrusions.

Fig. 5:22. Selected trace element variations for the Glen Gairn intrusion.

Fig. 5:23. Selected trace element variations for the Helmsdale intrusion.

## Chapter 6.

Fig. 6:1. Major and trace element variations for the Skiddaw granite.

Fig. 6:2. Major and trace element variations for the Eskdale intrusion.

Fig. 6:3. Major and trace element variations for the Carrock Fell intrusion.

Fig. 6:4. Major and trace element variations for the Ennerdale, Threlkeld and Shap intrusions.

Fig. 6:5. Major and trace element variations for the Helmsdale granite.

Fig. 6:6. Major and trace element variations for the Migdale, Rogart and Grudie intrusions.

Fig. 6:7. Major and trace element variations for the Strontian and Cluanie intrusions.

Fig. 6:8. Major and trace element variations for the Ballachulish intrusion.

Fig. 6:9. Major and trace element variations for the Ben Nevis and Etive intrusions.

Fig. 6:10. Major and trace element variations for the Moor of Rannoch and Strath Ossian granodiorites.

Fig. 6:11. Major and trace element variations for the Foyers intrusion.

Fig. 6:12. Major and trace element variations for the Moy, Peterhead and Ben Rinnes granites.

Fig. 6:13. Major and trace element variations for the Ardclach, Stritchen, Aberdeen and Cove Bay granites.

Fig. 6:14. Major and trace element variations for the Blackburn, Glenlivet and Dorback granites.

Fig. 6:15. Major and trace element variations for the Hill of Fare, Mt. Battock and Cromar granites.

Fig. 6:16. Major and trace element variations for the Bennachie granite.

Fig. 6:17. Major and trace element variations for the Lochnagar granite.

Fig. 6:18. Major and trace element variations for the Glen Gairn granite.

Fig. 6:19. Major and trace element variations for the Cairngorm granite.

Fig. 6:20. Major and trace element variations for the Comrie complex.

Fig. 6:21. Major and trace element variations for the Garabal Hill complex.

Fig. 6:22. Major and trace element variations for the Kilmelford complex.

Fig. 6:23. Major and trace element variations for the Cairnsmore of Fleet granite.

Fig. 6:24. Trace element modelling for the Skiddaw granite.

Fig. 6:25. Trace element modelling for the Eskdale intrusion.

Fig. 6:26. Trace element modelling for the Carrock Fell granophyre.

Fig. 6:27. Trace element modelling for the Rogart complex.

Fig. 6:28. Trace element modelling for the Strontian complex.

Fig. 6:29. Trace element modelling for the Ballachulish complex.

Fig. 6:30. Trace element modelling for the Ben Nevis complex.

Fig. 6:31. Trace element modelling for the Lochnagar granite.

Fig. 6:32. Trace element modelling for the Cairngorm granite.

Fig. 6:33. Chondrite normalized REE patterns for the Lake District intrusions.

Fig. 6:34. REE modelling for selected Lake District granitoids.

Fig. 6:35. Chondrite normalized REE patterns for selected Scottish granitoids.

Fig. 6:36. Chondrite normalized REE patterns for selected Scottish granitoids.

Fig. 6:37. Chondrite normalized REE patterns for selected Scottish granitoids.

Fig. 6:38. Chondrite normalized REE patterns for selected Scottish granitoids.

Fig. 6:39. REE modelling for the Cairngorm granite.

#### Chapter 7.

Fig. 7:1.  $\text{SiO}_2$  vs. Zr variation diagram for the Lake District granitoids.

Fig. 7:2.  $\text{SiO}_2$  vs. Nb variation diagram for the Lake District granitoids.

Fig. 7:3.  $\text{SiO}_2$  vs. Cr variation diagram for the Lake District granitoids.

Fig. 7:4.  $\text{SiO}_2$  vs. V variation diagram for the Lake District granitoids.

Fig. 7:5.  $\text{SiO}_2$  vs. Y variation diagram for the Lake District granitoids.

Fig. 7:6.  $\text{SiO}_2$  vs. Ce variation diagram for the Lake District granitoids.

Fig. 7:7.  $\text{SiO}_2$  vs. Sr variation diagram for the Lake District granitoids.

Fig. 7:8.  $\text{SiO}_2$  vs. Ba variation diagram for the Lake District granitoids.

Fig. 7:9.  $\text{SiO}_2$  vs. Rb variation diagram for the Lake District granitoids.

Fig. 7:10.  $\text{SiO}_2$  vs. Rb/Sr variation diagram for the Lake District granitoids.

Fig. 7:11. AFM diagrams for the Lake District and Scottish granitoids.

Fig. 7:12. Statistical contour map of Sr for the Scottish granite samples with 68-73% SiO<sub>2</sub>.

Fig. 7:13. Statistical contour map of Rb for the Scottish granite samples with 68-73% SiO<sub>2</sub>.

Fig. 7:14. SiO<sub>2</sub> vs. TiO<sub>2</sub> variation diagram for the Scottish granitoids.

Fig. 7:15. SiO<sub>2</sub> vs. Al<sub>2</sub>O<sub>3</sub> variation diagram for the Scottish granitoids.

Fig. 7:16. SiO<sub>2</sub> vs. Fe<sub>2</sub>O<sub>3</sub> variation diagram for the Scottish granitoids.

Fig. 7:17. SiO<sub>2</sub> vs. MnO variation diagram for the Scottish granitoids.

Fig. 7:18. SiO<sub>2</sub> vs. MgO variation diagram for the Scottish granitoids.

Fig. 7:19. SiO<sub>2</sub> vs. CaO variation diagram for the Scottish granitoids.

Fig. 7:20. SiO<sub>2</sub> vs. Na<sub>2</sub>O variation diagram for the Scottish granitoids.

Fig. 7:21. SiO<sub>2</sub> vs. K<sub>2</sub>O variation diagram for the Scottish granitoids.

Fig. 7:22. SiO<sub>2</sub> vs. P<sub>2</sub>O<sub>5</sub> variation diagram for the Scottish granitoids.

Fig. 7:23. SiO<sub>2</sub> vs. Rb variation diagram for the Scottish granitoids.

Fig. 7:24. SiO<sub>2</sub> vs. Ba variation diagram for the Scottish granitoids.

Fig. 7:25. SiO<sub>2</sub> vs. Sr variation diagram for the Scottish granitoids.

Fig. 7:26. SiO<sub>2</sub> vs. V variation diagram for the Scottish granitoids.

Fig. 7:27. SiO<sub>2</sub> vs. Cr variation diagram for the Scottish granitoids.

Fig. 7:28. SiO<sub>2</sub> vs. Y variation diagram for the Scottish granitoids.

Fig. 7:29. SiO<sub>2</sub> vs. Rb/Sr variation diagram for the Scottish granitoids.

Fig. 7:30. SiO<sub>2</sub> vs. Nb variation diagram for the Scottish granitoids.

Fig. 7:31. SiO<sub>2</sub> vs. Zr variation diagram for the Scottish granitoids.

Fig. 7:32. SiO<sub>2</sub> vs. Ce variation diagram for the Scottish granitoids.

Fig. 7:33. SiO<sub>2</sub> vs. Th variation diagram for the Scottish granitoids.

Fig. 7:34. SiO<sub>2</sub> vs. U variation diagram for the Scottish granitoids.

Fig. 7:35. SiO<sub>2</sub> vs. U/Th variation diagram for the Scottish granitoids.

Fig. 7:36. SiO<sub>2</sub> vs. Rb/Zr variation diagram for the Scottish granitoids.

Fig. 7:37. Rb/Zr vs. Nb variation diagram for the Scottish granitoids.

Fig. 7:38. Rb/Zr vs. Y variation diagram for the Scottish granitoids.

KEY TO FIG 1:2.

1. Reay diorite.
2. Helmsdale.
3. Lairg-Rogart.
4. Grudie.
5. Migdale.
6. Cluanie.
7. Strontian.
8. Kilmelford.
9. Ballachulish.
10. Ben Nevis.
11. Foyers.
12. Moy.
13. Ardclach.
14. Ben Rinnes.
15. Stritchen.
16. Peterhead.
17. Cove Bay.
18. Aberdeen.
19. Black Burn.
20. Bennachie.
21. Hill of Fare.
22. Mt. Battock.
23. Cromar.
24. Glenlivet.
25. Dorback.
26. Glen Gairn.
27. Lochnagar.
28. Cairngorm.
29. Strath Ossian.
30. Moor of Rannoch.
31. Etive.
32. Garabal Hill.
33. Comrie.
34. Cairnsmore of Fleet.
35. Carrock Fell granophyre.
36. Skiddaw.
37. Threlkeld.
38. Shap.
39. Ennerdale.
40. Eskdale.

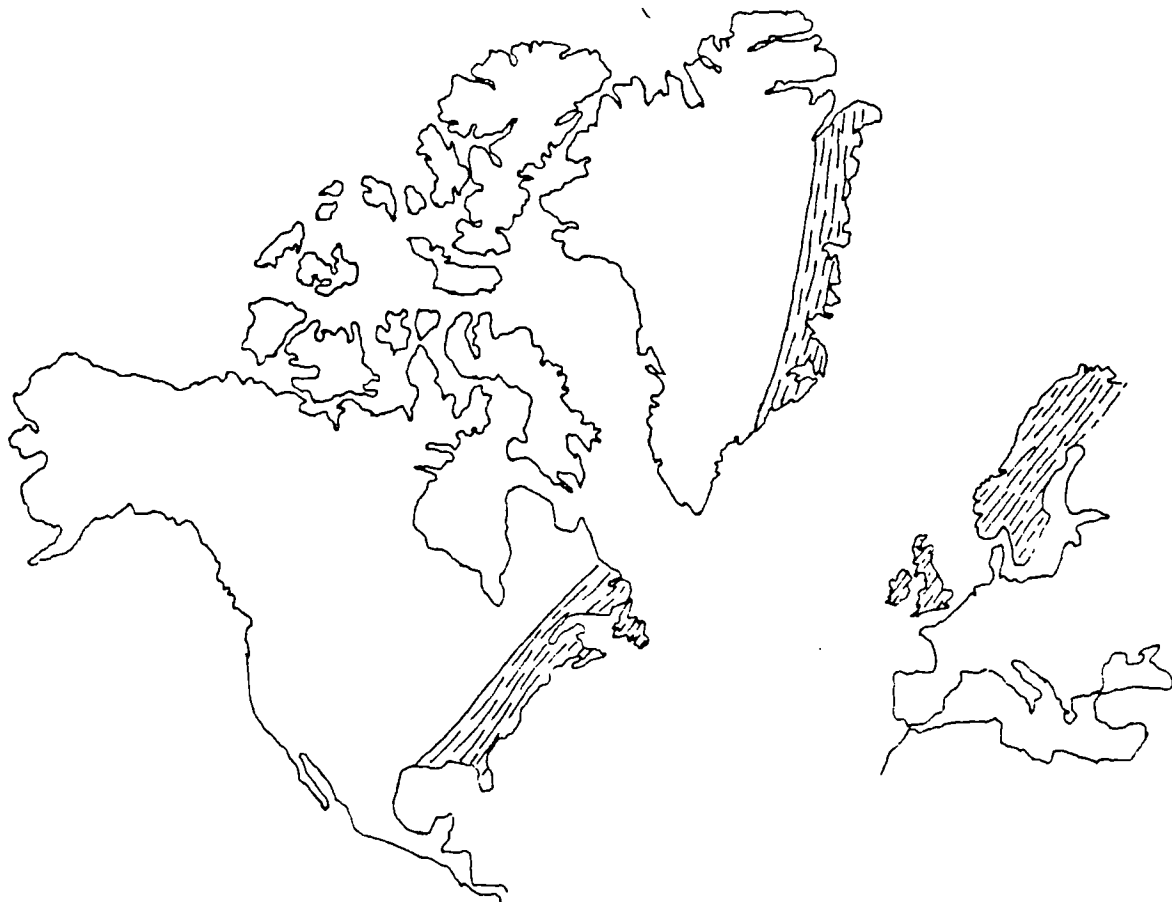
## CHAPTER 1. INTRODUCTION.

The Caledonian fold belt of Britain forms part of a major orogenic belt now to be found along the east coast of north America (Appalachians), northeast Greenland, the British Isles and western Scandinavia, (Fig 1:1). Intrusive granitic rocks of Caledonian age are found in all parts of the fold belt, on both sides of the suture, which, in the British Isles is thought to pass along a line through the Solway Firth. The British section of the Caledonian fold belt has been extensively studied and mapped, and to a wealth of detail has accumulated on the metamorphic, structural and tectonic aspects of the fold belt. However there has been no previous comprehensive geochemical study of the granitic intrusive rocks, although some individual intrusions have been examined in detail.

Fig. 1:2 shows the location of the granitic intrusions from both sides of the suture which are under consideration in this thesis. The intrusions range in composition from tonalites to biotite granites. The local names of each individual intrusion are given in Fig. 1:2 and are used throughout this thesis. The British Caledonian fold belt has been extensively mapped hence this study has focused on the petrography and geochemistry of the intrusions.

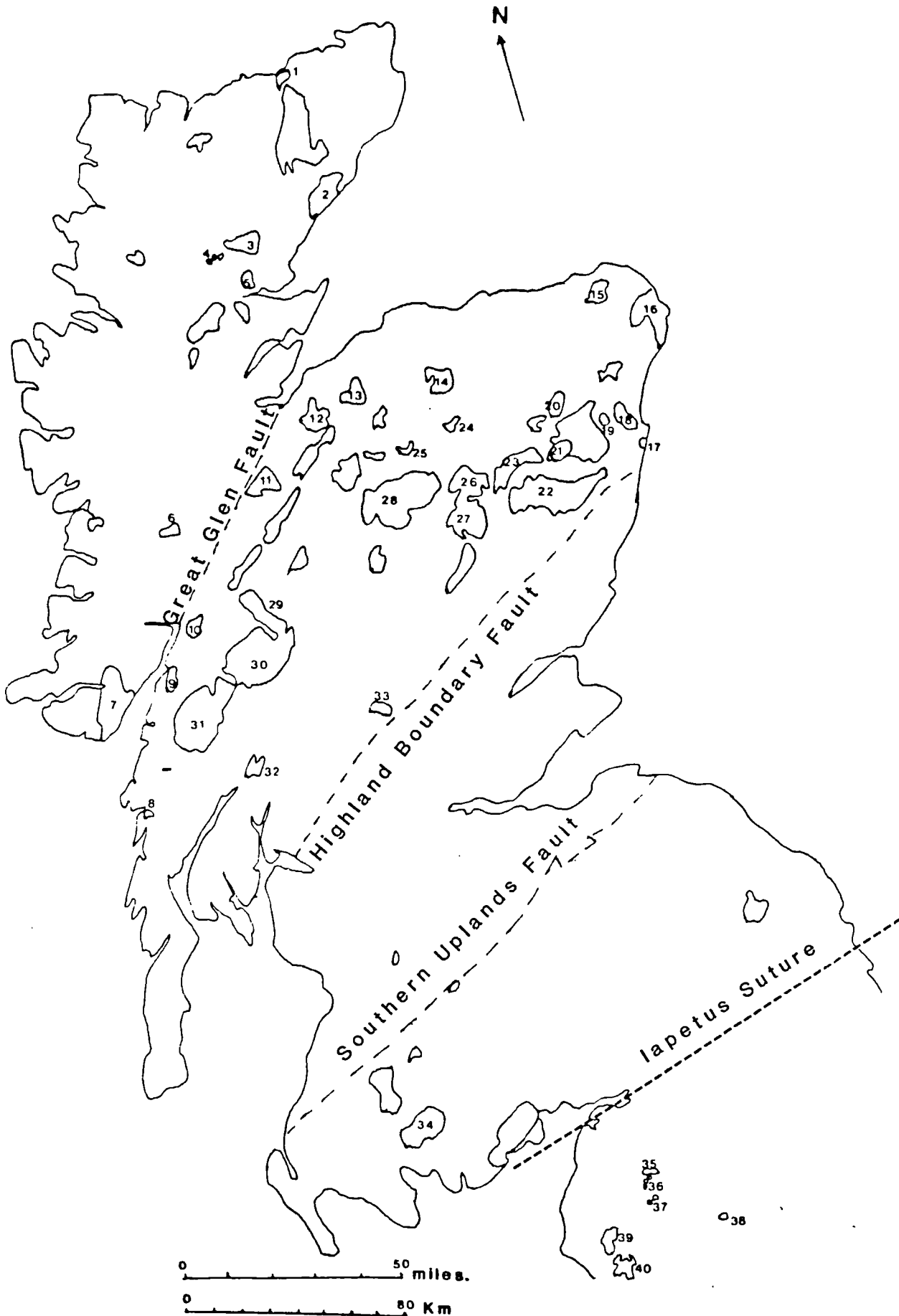
The sampling of the 40 intrusions covered in this study was initiated by the Applied Geochemistry Group of the British Geological Survey, and the majority of the material studied came from this source. Additional field sampling was undertaken of specific intrusions, and these were supplemented by collections made by Dr. A.M. Evans (University of

Fig. 1:1. Map showing the extent of the Caledonide fold belt on present day continent configurations.



Area affected by the Caledonian orogeny.

Fig. 1:2. The location of the granitic intrusions under consideration in this thesis, key on facing page.



Leicester) and Dr. G.C. Brown (Open University). The petrographic rock type, source of sample and National Grid Reference for each sample is listed in appendix A, the sample locations are also noted on the map in the back cover of this volume. The aim of this project was to produce a comprehensive body of major and trace element data on the Caledonian granitoids which would provide a regional framework within which the petrogenesis of the granites could be considered, both individually and collectively, along with the effects of element distributions during fractional crystallization, hydrothermal alteration and mineralization.

Key to Figs. in Chapter 2.

Fig. 2:1.

- \* - Eskdale granite.
- O - Shap granite.
- ☒ - Cairnsmore of Fleet granite.
- W - Ben Nevis granite.
- E - Etive Ben Starav.
- E - Etive Ben Cruachan.
- F - Foyers tonalite and granodiorite.
- Ⓢ - Foyers granite.
- S - Strontian tonalite and granodiorite.
- Ⓢ - Strontian granite.
- ✱ - Cluanie granodiorite.
- L - Lochnagar granite.
- G - Garabal Hill granodiorite.
- A - Aberdeen granite.
- T - Stritchen granite.
- - Helmsdale granite.
- - Southern uplands sediments.
- x - Moine metasediments.

## CHAPTER 2. TECTONIC SETTING OF THE BRITISH CALEDONIDES.

### 2:1. INTRODUCTION.

The Caledonides of Britain form part of a complex Palaeozoic mobile belt comprising rock units of various ages and metamorphic state, affected by or formed during the collision of at least two lithospheric plates. However, as the events leading up to continental collision took place more than 400 million years ago, precise tectonic interpretations of the Caledonian fold belt are rather difficult and subsequent events have destroyed or masked vital evidence concerning the development of the orogen. The incomplete record of the evidence which is available for the Caledonides in Britain has resulted in numerous individualistic tectonic interpretations. There is now general agreement that plate tectonic models can be applied to the Caledonides following the initial work of Wilson (1966) and Dewey (1969). However, details of the evolution of the orogen in terms of plate tectonics are still in dispute, with different models proposing various numbers of continental plates or microplates, subduction zones and spreading centres to explain the observed evidence.

The pre-Caledonian stable continental blocks were the Archaean cratons extending through N.W. Scotland, Greenland, N. America and Scandinavia, and a late Precambrian southern "continent" forming the basement to England and N. France. There is no evidence of Archaean crust in the Southern continent and this block may represent a series of island arcs (Le Bas 1981) generated in the late Proterozoic. The existence of an ocean (Iapetus) separating these older cratonic blocks during the

development of the Caledonides has been inferred from faunal evidence from the Cambrian through to the Silurian, with different distinct faunal groups in the sediments on the continental shelves of the older cratonic blocks until the Silurian when the faunal types become intermixed (Cowie 1960, Palmer 1969, Williams 1969, McKerrow & Cocks 1976). Thus we have clear evidence of a well established ocean as far back in the geological record as the Cambrian. How much further back in geological time the Iapetus extends is a matter of debate; some authors would extend it back to at least 1000 Ma (Wright 1976) others would place continental rifting in the late Precambrian corresponding to the development of the Dalradian sedimentary basin (Lambert & McKerrow 1976, Anderton 1982, Dewey & Shackleton 1984).

This chapter attempts to summarize the more important aspects of the tectonic development of the Caledonian fold belt. This is a necessary prelude to any discussion of the genesis of the Caledonian granites, as models for granite genesis may depend on the relative timing of crustal thickening and metamorphic events. Moreover the nature of the crust into which the granites were intruded has influence on the type of material which may be assimilated into a mantle derived calc-alkaline magma, and can influence the metallogenic aspects of Caledonian granites. This chapter is divided into two main sections; the tectonic evolution of the northern margin of Iapetus (i.e. Scotland north of the Solway Firth) and the tectonic evolution of the southern margin of Iapetus (i.e. England).

## 2:2 THE TECTONIC EVOLUTION OF THE NORTHERN MARGIN OF IAPETUS.

The tectonic evolution of the northern margin of Iapetus may be considered in several stages. Firstly, the Grenvillian-Morar events which are not closely connected with the later events and may represent a separate orogenic phase; secondly, the events during the Ordovician comprising the Grampian phase of the Caledonide orogeny; thirdly, the events associated with the final closure of Iapetus during or after the late Silurian.

### 2:2:i EARLY EVENTS IN THE MOINE.

The stable foreland of the Caledonian orogen in N.W. Scotland is composed of Archaean Lewisian gneisses which suffered their last major tectonothermal event in the Laxfordian 1600-1700 Ma (Giletti et al. 1961). The Moine series was deposited unconformably on top of deeply eroded Lewisian; direct evidence for this can be seen at the tectonic inlier of Lewisian within the Moine at Glenelg, where a basal conglomerate separates the Lewisian from the Moine (Ramsey 1958). The metamorphic grade of the Lewisian tectonic inliers is generally higher than the surrounding Moine (Rathbone & Harris 1979), although this distinction decreases eastwards with the increasing metamorphic grade of the Moines. The Moine series was deposited as a sequence of sandstones and muds in what is thought to have been a shallow marine to shelf environment. Subsequent to their deposition the Moine series has undergone at least 5 phases of deformation and three phases of metamorphism.

Until relatively recently, all the deformation and metamorphism displayed by the Moines was thought to be Ordovician in age, corresponding to the metamorphism and deformation observed in the younger Dalradian. For instance, the thrusts along the N.W. margin of the Moines cut through the Cambro-Ordovician rocks of the shelf sequence deposited on top of the Lewisian and Torridonian foreland (Anderton et al. 1979). However, recent isotopic studies of the metasediments, pegmatites and granite segregations have shown that the metamorphic history of the Moines is much older than Ordovician. The Ardgour gneiss has been dated at  $1050 \pm 46$  Ma (Brooke et al. 1976) and the Morar pelites at  $1024 \pm 96$  Ma (Brooke et al. 1977). These ages are thought to reflect an early metamorphic event affecting the Moines, roughly contemporaneous with the Grenvillian episode in N. America and the Gothide event in Scandinavia, which also appears to be chronologically equivalent to the  $F_2$  deformational phase in the Morar area of the Moine (Powell 1974). Pegmatites, which are pre- $F_2$  in the Carn Gorm and Glenfinnan areas, give a range of Rb-Sr muscovite ages from  $767 \pm 44$  to  $546 \pm 105$  (vanBreemen et al. 1974). Similar ages for the Moine rocks have been obtained by earlier workers (Gilletti et al. 1961, Long & Lambert 1963). The apparent disparity of the dating of the Moine  $F_2$  event could be explained in terms of incomplete resetting of the isotopic systems of the minerals by subsequent Caledonian deformation and metamorphism; this places the maximum metamorphic temperature in the Moines of Morar and Knoydart at between 300 and  $500^\circ\text{C}$  - the blocking temperatures for Sr and Rb diffusion (Purdy and Jager 1976), which would concur with the development of gneisses in this area in the Grenvillian (Brewer et al. 1979). Alternatively a younger deformation event (Morarian) of about 750 Ma has been postulated (Wright 1976).

It is thought that the metamorphic grade of the Ordovician (Grampian) events c467 Ma increases eastwards, culminating in Sutherland as sillimanite migmatites (Soper & Brown 1971). However, little isotopic work has been done in this area other than K-Ar dating of biotite and muscovite which have a blocking temperature of 300-350<sup>o</sup>C (Purdy & Jager 1976), and which yeild only Grampian - Caledonian ages (Pankhurst 1973). So it is arguable whether the Grenvillian event extended throughout the whole of the Moines into Sutherland.

To the south of the Great Glen fault the Central Highland Division and the Grampian Division had been assigned to the Moines (Johnstone 1975) on the basis of their similarity to the Loch Eil Division of the Moines. Later they were assigned to the Dalradian (Anderton et al. 1979) and ultimately reassigned to the Moine on the basis of Rb-Sr dating of muscovite in folded and sheared pegmatites, which gave ages ranging from 573<sub>-13</sub> to 718<sub>+19</sub>, the younger ages coming from the most sheared samples (Piasecki & vanBreemen 1979). These isotopic dates appear to affirm that this group belongs to the Moine Supergroup. Geochemical distinction between the Moines of the Central Highlands and the Dalradian is also possible; trace element differences between the two groups indicate different sediment sources (Lambert, Holland & Winchester 1982).

These older events preserved within the Moine must represent a separate orogenic phase of Grenville-Morar age. The Grenvillian-Morarian event has been recognised in a linear belt extending from N. America through Scotland to Scandinavia; but finding an acceptable tectonic interpretation for this event is difficult. Was it closure of an earlier

ocean before the development of Iapetus (Johnson 1975), or was the tectonic event simply caused by subduction along the northwestern margin of Iapetus (Wright 1976). There is no direct evidence to choose between the two hypotheses although the latter fits better with the later events in this area.

## 2:2:ii THE DEVELOPMENT OF THE DALRADIAN BASIN AND THE GRAMPIAN OROGENY.

Dalradian sedimentation began in the late Precambrian and lasted through to the lower Ordovician (Arenig) of the Highland Border group (Currey 1982). The lower Dalradian (Appin group) comprises shallow water sediments deposited in a stable subsiding environment (Harris et al. 1978, Hickman 1975). In the succeeding Argyll group the shallow water sediments are followed by deep water turbidites, indicating development of syndepositional faulted basins (Harris et al. 1978, Anderton 1979). This resulted in increased crustal thinning and instability, culminating in the eruption of the volcanics of the Southern Highland group, which have tholeiitic affinities (Graham 1976, Graham & Bradbury 1981, Wilson & Leake 1972).

The tectonic setting of the Dalradian sedimentation is disputed. Recent geophysical investigations into the crustal structure of the Caledonides show a thinned pre-Caledonian basement beneath the Dalradian (Bamford et al. 1978), which adds weight to the argument that the Dalradian was deposited in an ensialic basin (Phillips et al. 1976, Powell 1971, Harris et al. 1978, Watson & Dunning 1979). The same pre-Caledonian basement appears to stretch as far south as the Southern

Uplands fault (Bamford et al. 1978, Graham & Upton 1978). Moreover palaeocurrent determinations for some units in the Argyll Group of the Dalradian indicate derivation from a sediment source to the southwest (Klein 1970, Anderton 1971b, Howarth 1971, Spencer 1969, 1971) thus requiring some continental landmass to the south. The source area of sediments to the south contained granites and metamorphic rocks (Roberts 1973, Harris 1972). It appears therefore that an ensialic tensional basin model for the Dalradian has more substance than the earlier concept of Dalradian sedimentation in a continental margin environment (Lambert & McKerrow 1976, Wright 1976). It also appears that, although the Dalradian basin was largely ensialic, the presence of what appears to have been ocean floor in the Highland Border Complex can also be interpreted as representing ocean floor developed in the Dalradian basin (Henderson & Robertson 1982).

There are two possible tectonic environments for the development of an ensialic-oceanic basin in the Dalradian: (a) that of a subsidiary basin related to continental rifting and ocean development, or (b) that of a marginal basin developed as a result of extension in the back arc region related to subduction. The link between the Dalradian basin and the opening of Iapetus has been suggested recently on the basis that sediments which are derived from the south are too voluminous to be explained by derivation from the Midland Valley basement block (Anderton 1982). Yardley et al. (1982) hypothesise that the source of these sediments has been removed by strike-slip faulting since the development of the Dalradian basin. Geochemical evidence from the basaltic volcanics within the Upper Dalradian appears to relate these volcanics to a

subduction environment as opposed to a continental rifting environment (Graham & Bradbury 1981). This, together with the early date for the subduction related Portsoy granite ( $669^{+17}$  Ma; Pankhurst 1974) and the presence of granite clasts in the Dalradian groups derived from the south, suggests a subduction related environment for the Dalradian basin. This would indicate a prolonged existence of the Iapetus ocean as suggested by Wright (1976).

The whole Dalradian basin underwent deformation and metamorphism at c500-c460 Ma during what is termed the Grampian orogeny. This event also remetamorphosed the Moines as shown by dates of between 573 and 420 Ma for pegmatites within the Moine (Piasecki & Breemen 1979, Brewer et al. 1979) and the date of c 560 Ma for the Carn Chuinneag granite (Pidgeon & Johnson 1974). This tectonic event appears to be related to the closure of the Dalradian sedimentary basin. Whether active subduction took place within the Dalradian basin is uncertain. However all authors touching this subject link the compressional tectonic regime of the Grampian orogeny with the subduction of the Iapetus oceanic plate under the northern plate.

Since both the extensional and compressional phases of the development of the Dalradian basin appear to be related to subduction processes, the change from back arc extension to compression in the back arc region must be related to changes in the physical conditions in the subduction zone; i.e. change in angle of the subduction zone due to differences in buoyancy of the downgoing slab and changes in the rate of subduction. There are several modern analogues to the development of the Dalradian

basin and subsequent compression, e.g. Bransfield Strait, Antarctic Peninsula (Weaver et al. 1979), Sarmiento (Saunders et al. 1979) and Aysen, S. Chile (Bartholomew & Tarney 1984).

The timing of this collisional compressive phase can be constrained on the basis of isotopic dating of intrusions within the metamorphic complex; intrusions which show regional metamorphic fabrics may be either pre- or syn-metamorphic and give an indication of the timing of the onset of the Grampian event. The Carn Chuinneag granite which is dated structurally at pre-D<sub>2</sub> to D<sub>4</sub> and the main metamorphism (Shepherd 1973) has a radiometric age of ~560 Ma (Long 1964, Pidgeon & Johnson 1974). The Glen Dessary syenite, situated within the Moines north of the Great Glen Fault, and which can be structurally dated at pre-D<sub>3</sub> and possibly pre-D<sub>2</sub> gives a radiometric age of ~456 Ma (vanBreemen et al. 1979). The Loch Borrolan complex, which appears to have been intruded during the last stages of brittle movement along the Moine Thrust, has an isotopic age of ~429 Ma (vanBreemen et al. 1979b) and marks the end of the Grampian event in the N.W. Highlands.

South of the Great Glen fault, and within the Grampian group of the Moine, the Glen Kyllachy granite was emplaced at ~444 Ma (vanBreemen & Piasecki 1983) and intruded towards the end of D<sub>3</sub>. The Ben Vuirich granite intruded into the Dalradian is structurally constrained between D<sub>2</sub> and D<sub>3</sub> (Bailey 1925, Bradbury et al. 1976) and is dated at ~514 Ma (Pankhurst & Pidgeon 1976). The Dunfallandy Hill granite is considered to be post-D<sub>2</sub> but pre-D<sub>3</sub> (although also considered to be contemporaneous with D<sub>3</sub>; Bradbury et al. 1976) and yields an isotopic age of ~491 Ma

(Pankhurst & Pidgeon 1976). The newer gabbros of Aberdeenshire, which were intruded during the peak of  $D_3$  in a Buchan type metamorphic environment (1-3 Kb and 500-600°C) are dated at ~510 Ma (Pankhurst 1969).

It therefore appears that the metamorphic climax is diachronous between the Moines of N.W. Scotland (including the Grampian Highlands) and the Dalradian; the peak of metamorphism in the Dalradian is much earlier and less longlived than that in the Moines, which would be compatible with the Dalradian having been at a structurally higher level than the Moines. This metamorphic diachronism is also supported by the respective K-Ar mineral ages from the Moines and the Dalradian: these ages represent the passage of the rock through the blocking temperature of 300-350°C, below which the equilibration of this isotopic system is frozen. Dewey and Pankhurst (1970) showed that the K-Ar determinations for the Dalradian gave significantly older ages than those for the Moine, indicating faster uplift and cooling in the Dalradian; thermochron maps published by Pankhurst (1973) show that the areas of slow uplift correspond closely to areas of highest grade metamorphism, which did not pass through this blocking temperature until ~390 Ma.

## 2:2:iii THE DEVELOPMENT OF THE ORDOVICIAN-SILURIAN ACCRETIONARY PRISM IN SOUTHERN SCOTLAND AND THE LAST EVENTS OF THE CALEDONIAN OROGENY.

It is apparent that regional uplift was a persistent feature of the late orogenic period in the Scottish Highlands north of the Highland Boundary fault. Uplift and erosion appears to have begun some 20-30 million years before the metamorphic climax (England & Richardson 1977) and continued for about 100 million years over the Highlands as a whole.

During the peak of the Grampian orogeny the crust over the Highlands region may have had a total thickness of 60-70 Km, some 30 Km of which was removed prior to the Devonian. Much of this material cannot be accounted for in the sedimentary basins represented by the Southern Uplands (Watson 1984). From about 430 Ma most of the Scottish Highlands appears to have been buried under less than 10 Km of crust above the present level of exposure; thus most of the erosion took place before this date (Pankhurst 1973, Watson 1984).

During the later stages of the Grampian orogeny ductile deformation gave way to brittle fracturing; this style of deformation was established by about 420 Ma (Watson 1984). These faults and fractures appear to control the location of the major post tectonic granites. These large scale vertical movements of crustal units has been thought to cause the generation of granitic magma in the base of the crust, through relief of pressure (Pitcher 1982), or contact between hot mantle and cooler units at the base of the crust (Leake 1978).

During this period of uplift and erosion, subduction continued, resulting in the development of the Southern Uplands accretionary prism. The oldest units of this complex, containing basalts and chert at the base, date from the Arenig. The youngest units are Wenlock in age. The middle and upper units lack cherts or basalts at the base, and decollement at the base of the graptolitic shales, (the least competent of the sedimentary succession), appears to be the reason for the incomplete sequence (Leggett et al. 1979). It is reasonable to suppose that the missing parts of the succession have been subducted; this would

therefore imply increasing subduction of sediment from the late Ordovician onwards, and has important petrogenetic implications for magma genesis, as noted by Thirlwall (1983). The type of deformation observed in the Southern Uplands was considered by Leggett et al. (1979) to indicate a low rate of underthrusting along the northwestern margin of the Iapetus Ocean. Therefore much of the observed deformation within the Southern Uplands occurred during the active process of subduction over a long period of geological time rather than representing a collisional event.

Contemporary with the build up of the Southern Uplands accretionary prism was the intrusion of the post tectonic Caledonian granites belonging to the "newer" and "last" granites of Read (1961). Most of these granites have been isotopically dated (Table 2:1), and range from Strichen ~475 Ma to Cairnsmore of Fleet ~390 Ma. The older granites of this group are relatively close, temporally, to the peak of metamorphism and their  $^{87}\text{Sr}/^{86}\text{Sr}$  initial ratios suggest that they had a larger component of crustal material in their source than the later granites, which would be consistent with higher temperatures within the crust during their intrusion.

The post tectonic granites have been extensively studied using isotopic techniques. The relative contributions of mantle and crustal sources to this magmatism remain controversial. Studies of U-Pb systematics of these granites reveal evidence of a crustal contribution through the presence of inherited zircons, (Table 2:2), (Pidgeon & Aftalion 1978). For these granites with inherited zircons the upper intersections on the

concordia diagram are relatively close in age and tend to group at 1500-1600 Ma, similar to the intersections for the pre-tectonic granites (Pidgeon & Aftalion 1978). This must imply a common crustal component in the sources of all these granites and, although the initial  $^{87}\text{Sr}/^{86}\text{Sr}$  ratios for most of the post tectonic granites do not indicate large scale anatexis of the available crustal units (Lewisian, Moine and Dalradian), some crustal contribution is compatible with this data.

More recent work using combined Rb-Sr and Nd-Sm isotopic techniques has been carried out on a number of the post tectonic granites and potential source units, (Table 2:3 and Fig 2:1). This shows that the Southern Uplands sediments have a similar isotopic signature to many of the post tectonic granites, with the appearance of a mixing line between the Southern Uplands sediments and the mantle array. Halliday (1984) regards this as evidence of underthrusting of Southern Uplands sediments under the northern continent. However this is not a real tectonic possibility. Thirlwall (1983), observing the same mixing processes for the late Silurian-Devonian lavas, concludes that the Southern Uplands sediments were subducted and mixed with mantle melts to produce the observed andesitic volcanics. This is more plausible tectonic interpretation bearing in mind the mechanisms which generated the Southern Uplands accretionary prism.

Fig. 2:1. Sr and Nd isotope variation in the Caledonian granites (see over page).

Fig. 2:1. Sr and Nd isotope variation in the Caledonian granites, data from Hamilton et al. (1980) and Halliday (1984), key to symbols on fold out sheet.



---

**TABLE 2:1. PUBLISHED ISOTOPIC DATA ON THE CALEDONIAN GRANITOIDS.**

Granite	Age	Method	$^{87}\text{Sr}/^{86}\text{Sr}$	Reference
Stritchen	462 $\pm$ 22	Rb-Sr	0.7172	Pankhurst 1974
	475 $\pm$ 5	U-Pb monazite		Pidgeon & Aftalion 1978
Aberdeen	440	Rb-Sr	0.7162	Halliday 1984
Strontian	435 $\pm$ 10	Rb-Sr	0.7060	Harmon & Halliday 1980
	435	U-Pb zircon		Pidgeon & Aftalion 1978
Kilmelford	427	Rb-Sr	0.7040	Harmon & Halliday 1980
Helmsdale	420	Rb-Sr	0.7065	Harmon & Halliday 1980
	420	U-Pb zircon		Pidgeon & Aftalion 1978
Cluanie	417	Rb-Sr	0.7048	Halliday et al. 1979
	417	U-Pb zircon		Pidgeon & Aftalion 1978
Lochnagar	415 $\pm$ 5	Rb-Sr	0.7065	Halliday et al. 1979
Hill of Fare	413 $\pm$ 3	Rb-Sr	0.7057	Halliday et al. 1979
Etive (Cruachan) (Starav)	410	Rb-Sr	0.7048	Halliday et al. 1979
		Rb-Sr	0.7047	Hamilton et al. 1980
Ballachulish	410	Rb-Sr	0.7042	Harmon & Halliday 1980
Cairngorm	408 $\pm$ 3		0.706	Pankhurst & Sutherland 1982
Grudie	405 $\pm$ 15			Pankhurst & Sutherland 1982
Garabal Hill	406	Rb-Sr	0.7074	Harmon & Halliday 1980
Migdale	400	Rb-Sr	0.7059	Halliday et al. 1979
Strath Ossian	409 $\pm$ 9	Rb-Sr	0.7056	Halliday et al. 1979
Foyers	400	Rb-Sr	0.7061	Halliday et al. 1979
	415	Rb-Sr	0.7045	Pankhurst 1979
Ben Nevis	410	Rb-Sr	0.7043	Harmon & Halliday 1980
Moor of Rannoch	410	Rb-Sr	0.7048	Harmon & Halliday 1980
Cairnsmore of Fleet	392 $\pm$ 2	Rb-Sr	0.7071	Harmon & Halliday 1980

---

---

**TABLE 2:2 Pb ISOTOPIC DATA FROM PIDGEON & AFTALION 1978**

Granite	inherited zircons	upper intersection of concordia (Ma)	lower intersection of concordia (Ma)
Stritchen	Yes	>1000	450
Aberdeen	Yes	>1000	3-400
Strontian (tonalite)	No		425-445
Helmsdale	Yes	~2050	420
Cluanie	Yes	>1000	417
Lochnagar	trace		400-415
Hill of Fare	trace		400
Etive (Cruachan)	trace		405
Migdale	Yes	1400-1800	400
Strath Ossian	Yes	>1000	400
Foyers (granodiorite)	Yes	>1000	385
Cairnsmore of Fleet	No		390
Shap	No		390
Eskdale	Trace		460

---

---

**TABLE 2:3. COMBINED Rb-Sr Sm-Nd DATA FOR THE CALEDONIAN GRANITOIDS.**

Granite	I Sr	I Nd	$\epsilon$ Nd	$\epsilon$ Sr	Reference
Strontian (ton)	0.7055	0.512104	-0.2	+25	Hamilton et al. 1980
(ton)	0.70598	0.511996	-2.3	+35	
(gd)	0.70583	0.511968	-2.8	+32	
(gd)	0.70534	0.512101	-0.3	+23	
(gd)	0.70550	0.511999	-2.2	+26	
(g)	0.70713	0.511754	-6.8	+57	
Foyers (ton)	0.70605	0.511738	-7.5	+36	
(gd)	0.70692	0.511680	-8.7	+52	
(gd)	0.70819	0.511668	-8.9	+77	
(g)	0.70458	0.511743	-7.5	+7.6	
(g)	0.70461	0.511757	-7.3	+8.0	
(g)	0.70436	0.511806	-6.3	+3.3	
Ben Nevis	0.70455	0.511734	-8.0	+6.5	
Stritchen	0.7161	0.511484	-11	+230	
Etive (Starav)	0.70542	0.511636	-9.8	+23	Halliday 1984
	0.70503	0.511618	-10	+16	
(Cruachan)	0.70482	0.511873	-5.4	+12	
	0.70475	0.51179	-6.3	+11	
Helmsdale	0.70621	0.51179	-5.9	+31	
Cluanie	0.70602	0.51216	+1.3	+10	
Migdale	0.70847	0.51177	-6.8	+27	
Hill of Fare	0.7057	0.51201	-1.8	+24	
Strath Ossian	0.7060	0.51180	-6.3	+28	
Aberdeen	0.71792	0.51142	-12.7	+107	
Lochnagar	0.70630	0.51196	-2.7	+33	
Garabal Hill	0.70778	0.51192	-3.7	+54	
Cairnsmore of Fleet	0.70629	0.51201	-2.4	+32	
	0.7083	0.51198	-2.9	+60	
	0.7074	0.51198	-3.0	+47	
Shap	0.7075	0.512027	-2.6	+63	Hamilton et al. 1980
Eskdale	0.7076	0.51182	-5.1	+51	Halliday 1984
Southern Uplands sediments	0.70473	0.51218	+1.1	+10	
	0.71048	0.51178	-6.6	+92	
	0.70872	0.51185	-5.2	+67	

---

One category of the late granites are closely associated with calc-alkaline andesitic to rhyolitic lavas (Glen Coe, Ben Nevis, Ben Cruachan, Lochnagar). These granites have ring faults and cone sheets with evidence of cauldron subsidence (Read 1961). Many of these volcanics are associated with continental sediments of the Old Red Sandstone which are dated on palaeontological grounds as lower Devonian (Westoll 1945), although this has come under dispute more recently with some faunas being possibly as old as the Llandovery (Lamont 1952). There is some controversy over the relationship of these post-tectonic plutonics and volcanics with active subduction. Some authors consider that these late magmas are "continental" and not strictly related to subduction (Brown 1979, Stillman & Francis 1979). However the geochemistry of the Devonian volcanics shows that there is a conclusive link between this magmatism and subduction (Thirlwall 1983, 1984). It is therefore considered that subduction did continue into the Devonian and that these late volcanics and plutonics are related to this process (Groome & Hall 1974, French 1979, Mitchell & Mckerrow 1975, Phillips et al. 1976, Johnstone et al. 1979, Thirlwall 1981). The occurrence of Caledonian granites, such as Loch Doon, Criffle-Dalbeaty, Cheviot, Cairnsmore of Carspthean and Cairnsmore of Fleet, within the Southern Uplands accretionary prism implies that the subduction zone responsible for their generation must have been at least 90 Km further south, if comparison is made with modern arc-trench gaps. It is during this last stage of subduction that strike slip faulting may be responsible for the large scale removal of crustal units in the region of the subduction zone (Phillips et al. 1976) resulting in the juxtaposition of the Southern Uplands accretionary prism with the English Lake District without the

intervening forearc regions. Thus active subduction may have continued into the Devonian. The fact that there is no appreciable deformation of strata which date from the Silurian to the Devonian in Scotland would indicate that the final collision was not a major tectonic event in the British Caledonides. This contrasts with the Caledonides of Scandinavia where there is considerable deformation of rocks of Silurian to Devonian age.

## 2:3 TECTONIC EVOLUTION OF THE SOUTHERN MARGIN OF IAPETUS.

### 2:3:i THE AGE AND NATURE OF THE PRE-CALEDONIAN BASEMENT.

The pre-Caledonian basement of the southern or European plate is very poorly exposed, covered not only by sediments of Cambrian to Devonian age but also later continental shelf sediments of various ages. Isolated inliers of pre-Caledonian basement occur in North Wales, South Wales, the Welsh Borders and central England. These inliers reveal a complex picture of volcanics and sediments. The volcanics are generally calc-alkaline (Thorpe 1982). All of the pre-Caledonian units which have been isotopically dated give ages of between c700 and c500 Ma (Cribb 1975, Patchett et al. 1980, Beckinsale et al. 1981, Bath 1974, Patchett & Jocelyn 1979, Beckinsale & Thorpe 1979) and are therefore late Proterozoic to early Palaeozoic. There is no evidence from isotopic studies of intrusions within the southern plate for crust older than 1200 Ma, although the amount of crust sampled by this type of study is rather limited (Hampton & Taylor 1983, Pidgeon & Aftalion 1978). However Pb isotopic studies of post Caledonian galenas from the N. Pennines

suggests their derivation from crustal material >1700 Ma in age (Wedepohl et al. 1978).

The seismic velocities of the basement under the southern plate are lower than those characteristic of the Lewisian type basement of the northern plate (Bamford et al. 1978). Heat flow studies over the southern plate indicate that the predominant metamorphic grade is low down to about 15 Km (Richardson & Oxburgh 1978). The low metamorphic grade of the basement is evident from surface exposures, which are generally folded and at greenschist grade metamorphism, and are in places intensely sheared and tectonised (Lambert & Holland 1971, Thorpe 1972). The exception to this is the Mona complex of Anglesey where there are gneisses which show some evidence of migmatisation (Greenly 1923). The Mona complex also contains characteristic components of a subduction zone environment with ophiolites, melanges and blueschists (Wood 1974). The deformation and tectonism observed in the Mona complex, and to a lesser extent in the other inliers of late Precambrian age, together with the indications of subduction, imply that some type of collision event had taken place in this area in the late Precambrian, probably the closure of a marginal basin (Thorpe 1974, Wright 1976). This event was considered by Thorpe (1974) to explain some of the older calc-alkali volcanics in this region. It has been suggested (Le Bas 1982) that the whole of the southern continent represents a series of small continental blocks or island arcs which accreted during the late Proterozoic to early Palaeozoic. However this process of accretion must have ceased by the lower Cambrian because the shelf facies sediments which unconformably cover the basement units of the Midlands are not appreciably deformed.

2:3:ii ENSIALIC SEDIMENTARY BASINS AND VOLCANISM IN THE CAMBRIAN AND ORDOVICIAN.

During the Cambrian and Ordovician two major sedimentary basins were developed on the southern plate, the Welsh basin and the Lake District - Isle of Man basin. Both of these sedimentary basins appear to be ensialic on the basis of seismic profiles (Bamford et al. 1976) and other geological considerations (Dunning & Max 1975). The Welsh basin is not relevant to this study as only the granites of the Lake District have been investigated. However the geochemistry of the volcanics within the Welsh basin are compatible with a subduction zone to the north of the Lake District (Fitton & Hughes 1970).

The Lake District - Isle of Man basin appears to have been a continental margin environment (Moseley 1977) in which the Skiddaw slates, more than 3 Km of graptolitic mudstones with subsidiary greywacke and sandstones of Arenig to upper Llanvirn age, were deposited (Wadge 1978a). These are interpreted as turbiditic sequences deposited in relatively deep water (Jackson 1978). Associated with the Skiddaw slates are the Eycott volcanics which have some geochemical affinities with island arc tholeiites (Fitton et al. 1982, Fitton & Hughes 1970). The Carrock Fell granophyre and ferro-gabbros are thought to be related to this volcanism (Hunter 1980), although the isotopic age of the Carrock Fell granophyre may not be consistent with this. The Skiddaw slates were deformed prior to the deposition of the Borrowdale volcanic group (Wadge 1972, Jeans 1972), and are presumably present beneath the Borrowdale volcanics throughout the Lake District area and crop out to the south of

the Borrowdale volcanics group in isolated inliers. The volcanics of the Borrowdale group comprise a sequence of subaerial to subaqueous calc-alkaline lavas and tuffs which are compatible with a continental margin environment (Fitton & Hughes 1970) and are dated at about 457 Ma (Thirlwall & Fitton 1983), being stratigraphically Llandeilo to Caradoc in age. The Skiddaw slates and Borrowdale volcanic group are unconformably overlain by limestones, shales, mudstones and greywackes of upper Caradoc and Ashgill ages.

### 2:3:iii DEFORMATION, METAMORPHISM, GRANITE INTRUSION AND THE END OF THE CALEDONIAN OROGENY.

The type of deformation and metamorphism observed in the Lake District is less extensive and intense than that observed in the northern plate. There were several phases of deformation in the Lake District, the main phase being at the end of the Silurian (Soper & Roberts 1971), making interpretation of earlier structures difficult. The first phase, prior to the eruption of the Borrowdale volcanics, was probably minor. In the Black Combe inlier, for instance, the contact between the Skiddaw slates and the Borrowdale volcanics is conformable (Helm 1970). The second phase of deformation took place in the late Ordovician, prior to the deposition of the rocks of Ashgillian age (Soper & Numan 1974). The last and main phase of deformation, accompanied by the development of cleavage, took place during the end of the Silurian, at about the same time as the intrusion of the Shap and Skiddaw granites (Bouter & Soper 1973, Soper & Roberts 1971). The metamorphism which accompanied this deformation is of lower greenschist facies.

Granite magmatism in the Lake District appears to have taken place in a number of episodes according to published isotopic data, (Table 2:4). It began with Threlkeld in the lower Ordovician, followed by Eskdale and Ennerdale (although field evidence does not support this order of intrusion) and the Carrock granophyre, and the Shap and Skiddaw intrusions in the lower Devonian. This last event appears to have been associated with the emplacement of a large granite of batholithic proportions, proposed on the basis of the residual gravity anomaly (Bott 1974) and possibly connected at depth with the Weardale granite dated at  $410 \pm 10$  (Holland & Lambert 1970). Recent geophysical modelling suggests that the Eskdale granite is the surface expression of the Lake District batholith (Lee 1984). However the high regional heat flow of the Lake District (Brown et al. 1980) is not consistent with a batholith with a chemical composition similar to the Eskdale granite, which is not a high heat production granite, but would be consistent with a batholith of similar composition to the Skiddaw granite. The granites of the Lake District do not have any evidence of inherited zircons (Pidgeon & Aftalion 1978). The sequence of granite emplacement is broadly comparable with that of the northern province, particularly in the emplacement of large volumes of granite magma at the end of the Caledonian event.

---

**TABLE 2:4. ISOTOPIC DATES OF THE LAKE DISTRICT GRANITES**

Granite	age	method	$^{87}\text{Sr}/^{86}\text{Sr}$	Reference
Skiddaw	392 $\pm$ 4	K-Ar biotite		Shepperd et al. 1976
Shap	393 $\pm$ 3	Rb-Sr	0.70767	Wadge et al. 1978
Carrock Fell granophyre	416 $\pm$ 20	Rb-Sr	0.70708	Rundle 1979
Ennerdale	420 $\pm$ 4	Rb-Sr	0.70568	Rundle 1979
Eskdale	429 $\pm$ 4	Rb-Sr	0.70756	Rundle 1979
Threlkeld	438 $\pm$ 15	Rb-Sr	0.7057	Rundle 1981
Carrock Fell gabbro	468 $\pm$ 10	K-Ar biotite		Rundle 1979

---

#### 2:4 SUMMARY.

The tectonic history of the Caledonides appears sometimes to be confusing and is certainly complicated. The significance of the nature and age of the crustal units involved in the orogeny is only of importance to this thesis when discussing the contribution of crustal units to the genesis of the Caledonian granites. The sequence and nature of the tectonic events are more important since this constrains the hypotheses relating to the genesis of the granitoids in terms of tectonic acceptability.

The major tectonic events in the development of the Caledonide orogen in the British Isles are as follows.

a) The Dalradian supergroup appears (from the geochemical signature of the Dalradian basic volcanics) to have been deposited in a back arc extensional environment, which implies active subduction along the northern margin of Iapetus as far back as the Late Precambrian.

b) The major crustal thickening event in the Ordovician (Grampian Orogeny) does not mark the cessation of subduction and continent-continent collision since the development of the Southern Uplands accretionary prism continued into the Wenlock phase of the Silurian. But this event does mark the closure of the Dalradian back arc basin. It is uncertain whether active subduction took place within the Dalradian basin or whether the event was totally ensialic. The change in tectonic conditions in the Dalradian basin, by analogy with more recent examples, must result from a change in physical conditions in the subduction zone. Active subduction continued during the compressional stage from evidence from the newer gabbro suite, which has geochemical affinities with subduction related volcanics.

c) The southern plate has a shorter geological history and may have evolved as a series of island arcs during the Late Proterozoic to Early Palaeozoic, becoming stabilised during the Cambrian.

d) The final closure of the Iapetus ocean took place during or after the Wenlock phase of the Silurian and did not result in major crustal thickening or metamorphism in the Caledonides of the British Isles. However most of the Caledonian granites examined in this study are associated with this phase of the Caledonide orogeny. The major debate

on the origin of these granites centres on whether active subduction continued into the early Devonian and on the length of time after active subduction ceases that calc-alkaline magmas can be generated from the mantle wedge or downgoing slab before truly continental magmatism begins.

Key to Figs. in Chapter 3.

Fig. 3:2.

- I - Kilmelford diorite.
- Z - Comrie diorite.
- G - Garabal Hill gabbro.
- D - Garabal Hill diorite.
- F - Garabal Hill fine grained granodiorite.

Figs. 3:3, 3:4 and 3:6.

- A - Aberdeen granite.
- C - Cairngorm granite.
- D - Dorback granite.
- E - Etive complex.
- G - Garabal Hill complex.
- H - Hill of Fare granite.
- I - Kilmelford diorite.
- K - Mt. Battock granite.
- L - Lochnagar granite.
- N - Bennachie granite.
- Q - Cromar granite.
- R - Ben Rinnes granite.
- S - Strontian complex.
- U - Ballachulish complex.
- W - Ben Nevis complex.
- Z - Comrie complex.
- △ - Ardclach granite.
- ◇ - Cove Bay granite.
- ▽ - Glen Gairn granite.
- \* - Moy granite.
- ⌘ - Moor of Rannoch granodiorite.
- - Strath Ossian granodiorite.

Fig. 3:5.

- + - Eskdale granodiorite and granite.
- △ - Skiddaw granite.
- - Shap granite.

Fig. 3:7.

- ⊙ - Shap granite.
- △ - Skiddaw granite.
- \* - Eskdale granodiorite and granite.
- ⊠ - Ennerdale granophyre.
- - Carrock Fell granophyre.
- ▽ - Threlkeld microgranite.

Fig. 3:8.

- W - Ben Nevis complex.
- H - Hill of Fare granite.
- - Shap granite.
- + - Eskdale granodiorite and granite.

Fig. 3:11 a).

- E - Etive complex.
- G - Garabal Hill complex.
- H - Hill of Fare granite.
- I - Kilmelford diorite.
- K - Mt. Battock granite.
- L - Lochnagar granite.
- N - Bennachie granite.
- Q - Cromar granite.
- Z - Comrie complex.
- \* - Moy granite.

Fig. 3:11 b).

- △ - Skiddaw granite.
- + - Eskdale granodiorite and granite.
- ⊠ - Ennerdale granophyre.
- - Carrock Fell granophyre.
- - Shap granite.

## CHAPTER 3. PETROGRAPHY AND MINERAL CHEMISTRY.

## 3:1 INTRODUCTION.

The comprehensive range of Caledonian plutons covered in this study precludes detailed petrographic descriptions of individual plutons or parts of plutons, and many of the intrusions are so petrographically similar that they may be grouped together for this purpose to avoid repetition. In any case detailed petrographic descriptions of many of the intrusions covered in this study are to be found in the literature (Grant-Wilson 1882, 1886, 1890, Harker 1895, Hinxman 1896, Hinxman et al. 1902, 1915, 1923, Barrow 1912, Barrow & Cunningham-Craig 1912, Barrow et al. 1913, Crampton & Carruthers 1914, Grantham 1928, Mackie 1928, Bisset 1932, Hitchen 1934, Anderson 1935, 1937, 1939, Trotter et al. 1936, Nockolds 1941, Leedal 1952, Bailey 1960, Sabine 1963, Harry 1965, Haslam 1968, Eastwood et al. 1968, Soper 1969, Marston 1971, Munroe 1971, Oldershaw 1974, Firman 1978, Pankhurst & Sutherland 1982).

Ideally, to assist modelling of the geochemical evolution of individual Caledonian plutons, it would be helpful to identify phases which may be cumulus minerals in the broadest sense of the term i.e. those minerals which have crystallized early and may have become separated from the residual liquid to a certain extent through a variety of processes including gravitational settling and filter pressing. In the granite system crystallization rarely produces a clear division between "cumulate" and "liquid" rock types due to the viscous nature of the magmas. Coarse grained granitic rocks are best regarded as variable mixtures of cumulus crystals and interstitial liquid (McCarthy & Groves 1979). However it is apparent that processes such as filter pressing may

be capable of providing some separation of cumulus crystals from the granitic liquids, although this is probably less efficient than gravitational settling as petrological evidence indicates that this process is not always complete.

Granitic magmas are often volatile rich, and in the late stages of crystallization hydrous fluid phases become concentrated and promote secondary alteration effects such as sericitization of plagioclases. This process is exacerbated if the intrusion is hosted by low grade water rich slates or shales, as in the Lake District where connate water may enter the cooling intrusion. This process may lead to the development of mineral deposits in the form of veins (e.g. Skiddaw), or porphyry type deposits (e.g. Kilmelford) or secondary uranium enrichments (e.g. Helmsdale).

### 3:2 MINERALOGY OF THE CALEDONIAN INTRUSIONS.

The Caledonian granites studied may be divided into two major groups (1) Scotland and (2) the Lake District. These groups for the purpose of description can be subdivided according to their mineralogy as follows: pyroxene bearing intrusions, hornblende bearing intrusions, biotite granites, two mica granites and garnet granites. A summary of the primary mineralogy of these groups is given in Tables 3:1 and 3:2. Most of the intrusions studied have some secondary alteration, ranging from minor sericitization of feldspars and chloritization of biotites through to localized pervasive greisenization. Although this aspect is described in detail in chapter 3:4 and the geochemistry of metasomatized granites

in chapter 5, a summary of the secondary mineralogy of these intrusions is given in Tables 3:3 and 3:4.

### 3:3 CRYSTALLIZATION SEQUENCES FROM TEXTURAL INFORMATION.

#### 3:3:1. SCOTLAND.

##### 3:3:1:i. PYROXENE BEARING INTRUSIVES.

The pyroxene bearing intrusives can be divided into two groups in terms of textures; the Garabal Hill ultrabasics and gabbros, and the diorites from Garabal Hill, Comrie and Kilmelford. The Garabal Hill ultrabasics and gabbros are texturally pyroxene cumulates with intercumulus plagioclase (Plate 3:1a). The diorites have texturally cumulus pyroxene, oxides, biotite, hornblende and plagioclase with intercumulus quartz and alkali feldspar (Plate 3:1b).

##### 3:3:1:ii. HORNBLLENDE BEARING INTRUSIVES.

The hornblende bearing intrusives cover a range of rock compositions from diorites through to granites, and although the proportions of various minerals change over this range of compositions the sequence of crystallization remains roughly the same. The first phases to crystallize are hornblende, Fe-Ti oxides, sphene, allanite followed by biotite; these are generally euhedral in nature (Plate 3:1c, d, e and f) and in the more mafic intrusions occur as "clumps" of mixed hornblende, biotite and sphene (Plate 3:2a). The presence of apatite, zircon and other accessory phases within biotite implies early crystallization for these accessory phases (Plate 3:2b).

PLATE 3:1. (See over page).

PLATE 3:1.

- a) Cumulus pyroxenes (pale grey, fractured, with high relief) with intercumulus plagioclase (pale grey with lamella twinning) and biotite (mid grey); Garabal Hill diorite (GH10), cross polars, magnification x25.6.
- b) Cumulus pyroxenes (dark grey) and plagioclase (lamella twinned) with intercumulus quartz (white) and potassium feldspar (white); Kilmelford diorite (KM12), cross polars, magnification x63.
- c) Euhedral twinned hornblende; Strath Ossian granodiorite (S07), cross polars, magnification x32.
- d) Euhedral sphene (pale grey); Strontian tonalite (SRN10), plane polarised light, magnification x20.
- e) Euhedral allanite (dark grey); Ballachulish granite (B14), plane polarised light, magnification x63.
- f) Euhedral biotite (dark grey); Strath Ossian granodiorite (S010), plane polarised light, magnification x50.4.

PLATE 3:1

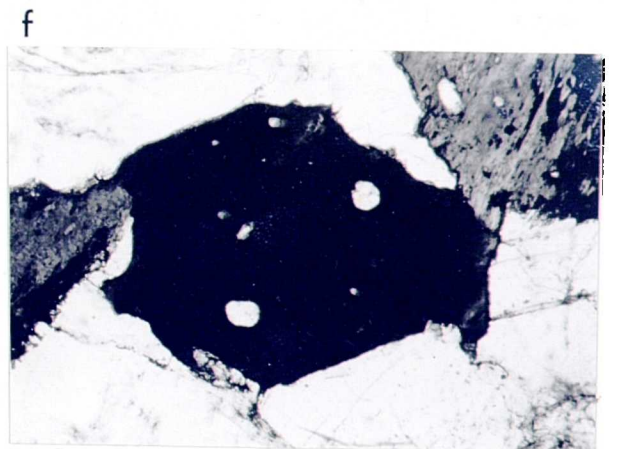
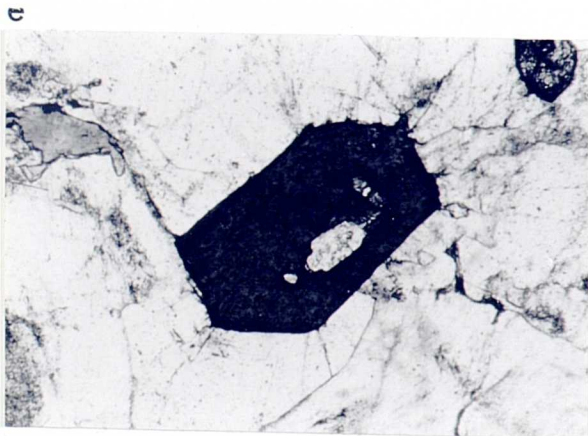
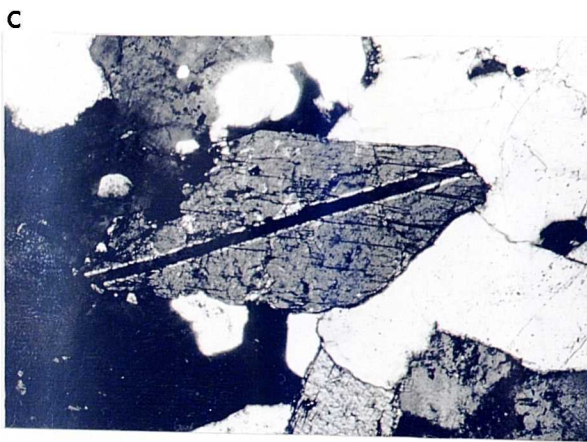
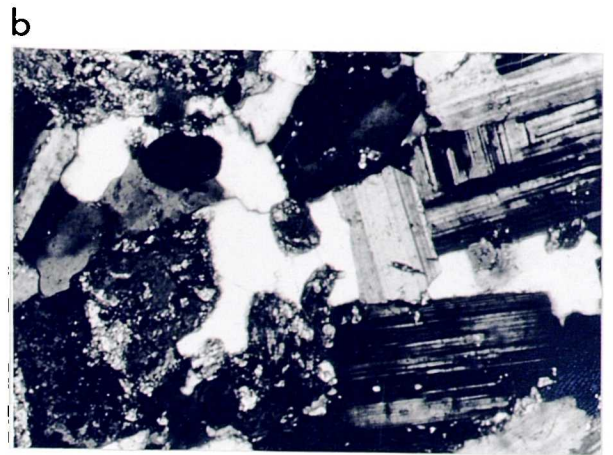
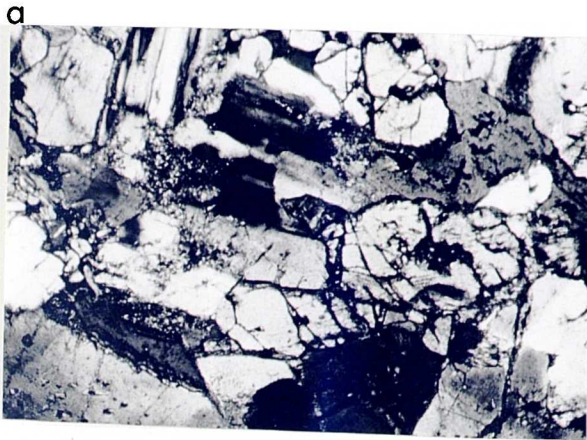
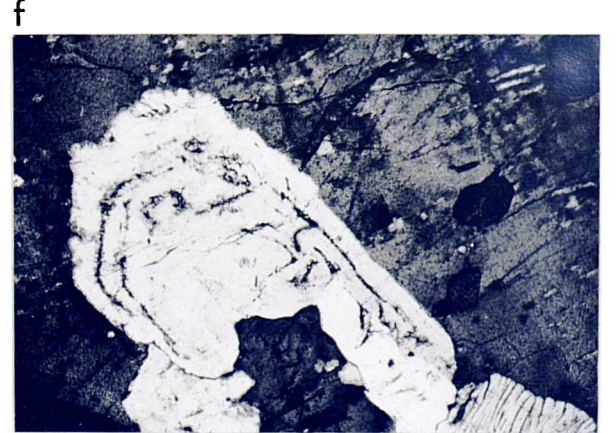
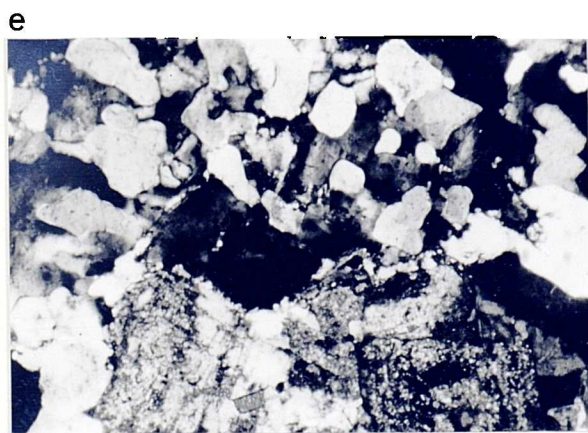
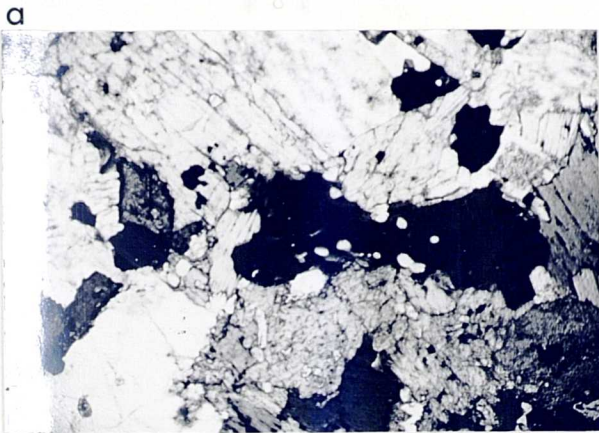


PLATE 3:2. (See over page).

PLATE 3:2.

- a) "Clump of mafics", hornblende (pale grey), biotite (mid grey), sphene (dark grey), magnetite (black) and plagioclase (white); Ben Nevis outer granite (BN13), plane polarised light, magnification x20.
- b) Accessory minerals in biotite, apatite (white) and zircon (with pleochroic halo); Dorback granite (TM18), plane polarised light, magnification x128.
- c) Biotite (mid grey) and hornblende (pale grey) within plagioclase aggregate; Moor of Rannoch granodiorite (MR4), cross polars, magnification x32.
- d) Interstitial quartz (white) and potassium feldspar (white) with cumulus plagioclase (lamella twinned) and sphene (mid grey); Foyers tonalite (F103), cross polars, magnification x32.
- e) Granophyric interstitial quartz (white) and potassium feldspar (pale-mid grey) with sericitised cumulus plagioclase; Foyers granodiorite (BPR585) cross polars, magnification x20.
- f) Perthitic potassium feldspar (mid grey) ophitically enclosing zoned plagioclase (white), sphene (dark grey) and hornblende (dark grey); Cluanie granodiorite (CL1), cross polars, magnification x20.

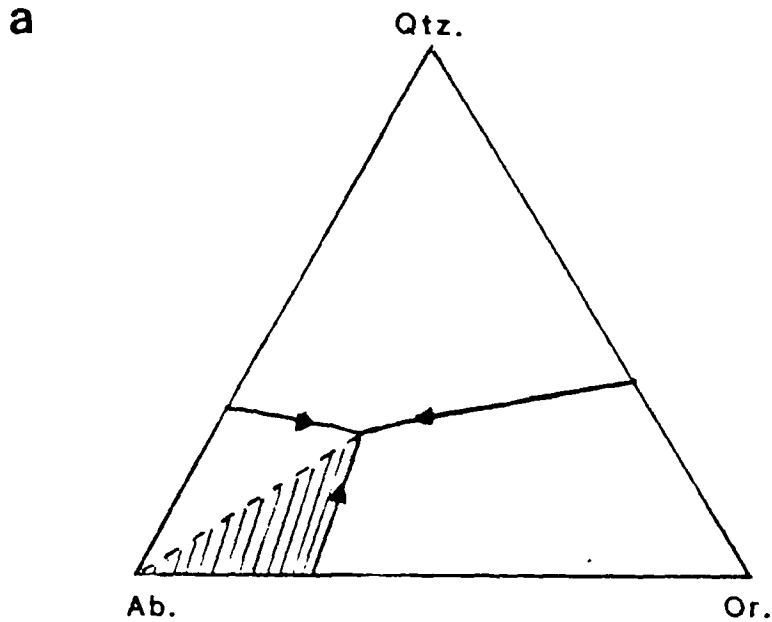
PLATE 3:2



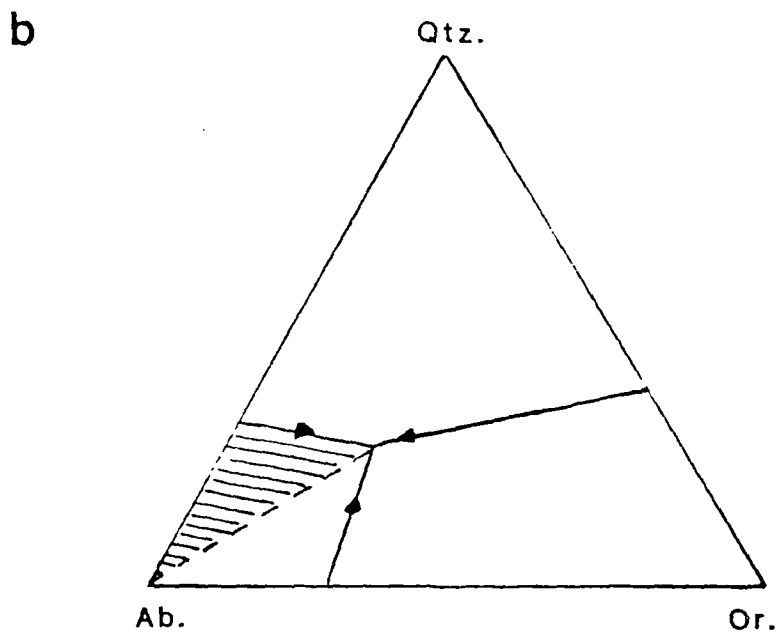
The crystallization of these mafic phases is followed by plagioclase which is generally sub-euhedral in character and often encloses mafic minerals in the core area of crystals, (Plate 3:2c). However the crystallization of plagioclase and mafic minerals probably proceeds simultaneously through a large part of the early crystallization of these plutons. Both plagioclase and the mafic minerals crystallize early and may be cumulus minerals and are present in various proportions from almost 100% in the diorites through to about 40% in the granites. The variation in the proportion of cumulus phases suggests that fractionation of these phases may have taken place.

The trapped interstitial liquid is generally represented by quartz and alkali feldspar. In the less evolved dioritic, tonalitic and granodioritic plutons, these phases are interstitial and minor in abundance, (Plate 3:2d) and may in some cases show granophyric texture (Plate 3:2e). In the more evolved plutons the interstitial nature of these minerals is more equivocal with perthitic potassium feldspar often enclosing euhedral plagioclase and mafic minerals in an "ophitic" fashion, (the term "ophitic" is used here in a general sense rather than referring to particular minerals i.e. pyroxene and plagioclase), (Plate 3:2f). In the granites the potassium feldspar may also occur as a "cumulus" phase although this cannot be shown texturally. Quartz in all cases is anhedral in character and appears to be the last phase to crystallize. This sequence of crystallization can be represented on the quartz, albite, orthoclase phase diagram (Fig 3:1a), with the liquid composition projecting into the shaded part of the albite field of the quartz, orthoclase, albite phase diagram, where precipitation of albite will push the liquid composition onto the albite, orthoclase cotectic.

Fig. 3:1. Phase diagram interpretation of crystallization sequences observed.



a) Qtz.-Ab.-Or. phase diagram at 5 Kb after Tuttle & Bowen (1958): The shaded area representing the projected liquid compositions of the mantle derived granites as inferred from their crystallization sequence.



b) Qtz.-Ab.-Or. phase diagram at 5 Kb after Tuttle & Bowen (1958): The shaded area representing the projected liquid compositions of crustally derived two mica granites as inferred from their crystallization sequence.

Cotectic crystallization of albite and orthoclase will then take the liquid composition to the quartz, albite, orthoclase ternary eutectic.

### 3:3:1:iii. BIOTITE GRANITES.

The sequence of crystallization in the biotite granites is generally similar to that of the hornblende granites. Naturally the proportion of mafic minerals, although variable, is less than observed in the hornblende granites and they appear to be cumulus in the biotite granites also. Plagioclase similarly appears to be cumulus. However the total proportion of cumulus minerals is generally lower than in the hornblende granites and varies from ca 50% to ca 30%. The perthitic potassium feldspars generally enclose plagioclase and biotite in an "ophitic" fashion. In some cases quartz is also enclosed within the potassium feldspar but generally towards the edges of the grains (Plate 3:3a). Quartz is generally anhedral but often encloses plagioclase and biotite. Thus the order of crystallization is similar to that observed in the hornblende granites, as represented in Fig. 3:1a. In the most evolved granites, namely Cairngorm, Hill of Fare, Mount Battock, Cromar, Glen Gairn and Bennachie, muscovite occurs interstitially (Plate 3:3b). If this muscovite is primary it implies that the residual liquid was undersaturated with respect to silica and alkali rich. However this very late stage crystallization may not be closely related to any residual silicate magma but rather a hydrous fluid carrying small quantities of silica and aluminium along with incompatible elements such as Rb and Li.

PLATE 3:3. (See over page).

PLATE 3:3.

a) Perthitic potassium feldspar (mid grey) ophitically enclosing euhedral plagioclase (lamella twinned) towards the center of the grain and euhedral quartz (white) in the edge of the grain, Mt. Battock granite (LU28), cross polars, magnification x20.

b) Interstitial muscovite (pale grey with prominent cleavage planes) between quartz (white to pale grey), plagioclase (lamella twinned-pale grey) and biotite (mid grey); Cairngorm granite (CN2), cross polars, magnification x20.

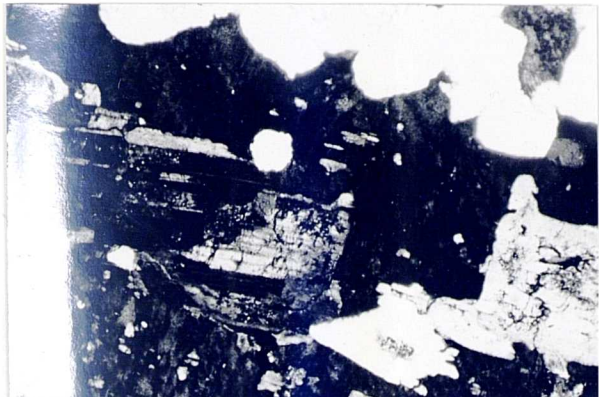
c) Primary muscovite (pale grey with prominent cleavage planes) with biotite (mid grey with prominent cleavage planes), subhedral; Ardclach granite (AD6), cross polars, magnification x20.

d) Plagioclase (lamella twinned) ophitically enclosing sub-euhedral quartz (white); Cove Bay granite (17-37), cross polars, magnification x39.4.

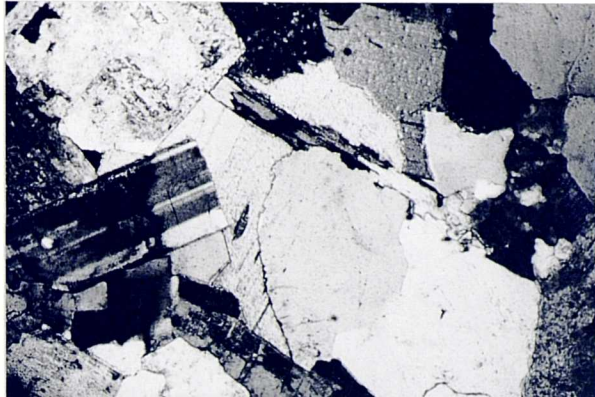
e) Microcline ophitically enclosing sub-euhedral quartz (white); Aberdeen granite (AB1), cross polars, magnification x20.

PLATE 3:3

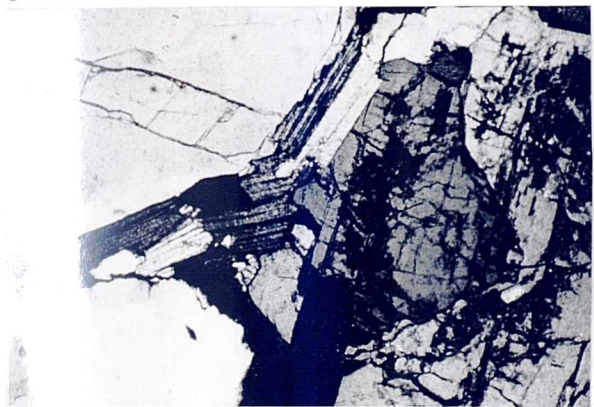
a



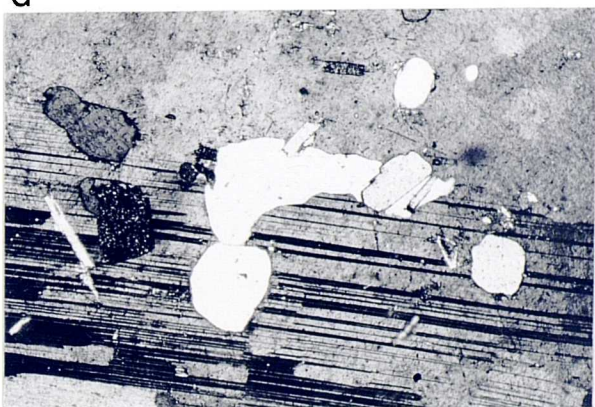
b



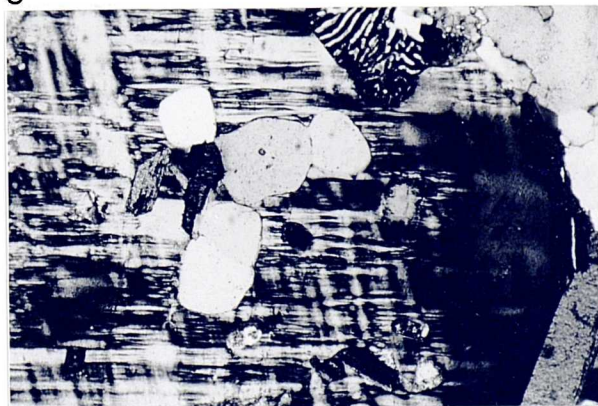
c



d



e



### 3:3:1:iv. TWO MICA GRANITES.

The two mica granites contain primary muscovite which crystallized early and occurs with biotite as well formed flakes (Plate 3:3c). Plagioclase is sub-euhedral and appears to have crystallized early. Quartz is also sub-euhedral and crystallized before plagioclase in some instances (Plate 3:3d). Perthitic potassium feldspar and microcline encloses both plagioclase and quartz in an "ophitic" fashion (Plate 3:3e), and is interstitial. Quartz also occurs interstitially. This sequence of crystallization can be explained by the phase diagram in Fig 3:1b, with the liquid composition projecting into the shaded part of the albite field in the quartz, orthoclase, albite phase diagram, where precipitation of albite will push the liquid composition onto the albite quartz cotectic. Cotectic crystallization of albite and quartz will take the liquid composition to the quartz, albite, orthoclase ternary eutectic.

### 3:3:2. THE ENGLISH LAKE DISTRICT.

#### 3:3:2:i. PYROXENE BEARING INTRUSIVES.

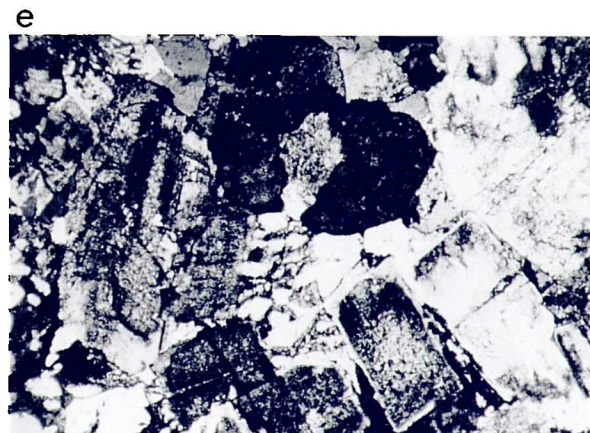
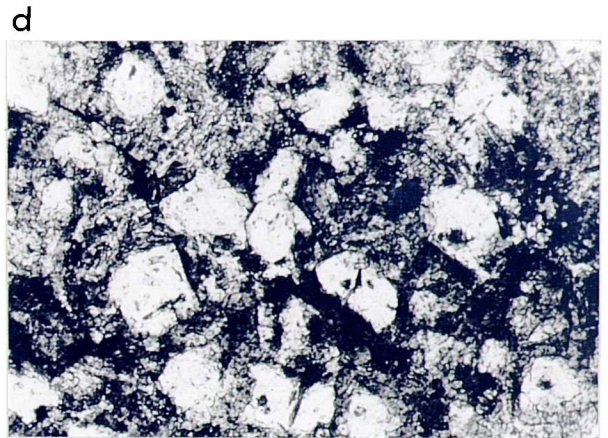
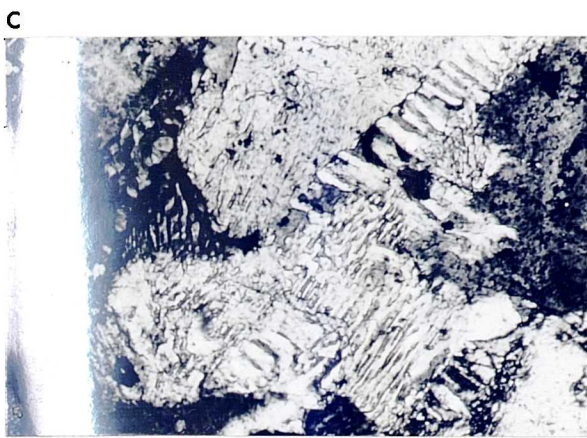
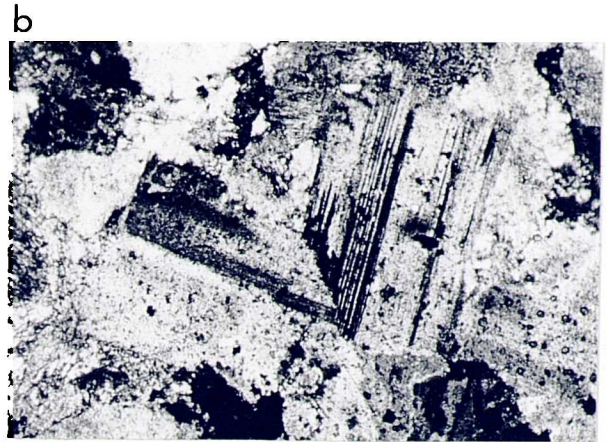
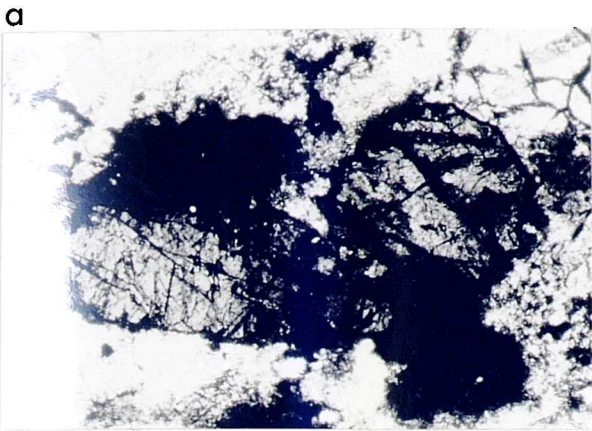
The pyroxene-bearing intrusives of the Lake District are all granophyric or fine-grained granitic bodies. The pyroxenes, which are often replaced or partially replaced by acicular hornblende, chlorite and epidote, occur as phenocrysts (Plate 3:4a) along with plagioclase (Plate 3:4b). These phenocrysts are generally surrounded by a matrix of quartz and alkali-feldspar showing granophyric or spherulitic texture, indicating rapid eutectic crystallization (Plate 3:4c). In some

PLATE 3:4. (See over page).

PLATE 3:4.

- a) Pyroxene phenocrysts (slightly altered) (mid grey); Carrock Fell granophyre (CF5), plane polarised light, magnification x50.4.
  
- b) Plagioclase phenocrysts (lamella twinned); Ennerdale granophyre (EN13), cross polars, magnification x20.
  
- c) Granophyric matrix; Carrock Fell granophyre (CF16), cross polars, magnification x63.
  
- d) Microgranitic matrix (considerably altered); Threlkeld microgranite (TH23), cross polars, magnification x63.
  
- e) Interstitial granophyric matrix between plagioclase (pale to mid grey) and altered pyroxene (dark grey); Carrock Fell hybrid suite (CF41), cross polars, magnification x20.

PLATE 3:4



instances this matrix becomes microgranitic (Plate 3:4d). The proportion of "cumulus" phenocrysts to matrix decreases from the Carrock Fell ferrogabbros and hybrid suite through to the Carrock Fell granophyres (Plate 3:4e and c). The Carrock Fell ferrogabbros may be regarded as cumulate rich relatives of the Carrock Fell granophyres.

---

TABLE 3:2. SUMMARY OF THE MINERALOGY OF THE LAKE DISTRICT INTRUSIONS.

	opx	cpx	hb	bi	sp	mag	il	all	zir	ap	monz	top	mu	gt
<u>pyroxene bearing.</u>														
Carrock Fell granophyre *	*		*		*	*		*	*					
Carrock Fell ferrogabbro*	*	*	*		*	*		*	*					
Ennerdale	*		*		*	*		*	*					
Threlkeld	*				*	*		*	*					
<u>Biotite granites.</u>														
Skiddaw				*	*	*		*	*		*			
Shap				*	*	*		*	*		*			
<u>Garnet granite.</u>														
Eskdale				*	*	*		*	*		*	*		*

---

### 3:3:2:ii. BIOTITE GRANITES.

The biotite granites of the Lake District are texturally similar to those of Scotland, having early crystallizing biotite and plagioclase (Plate 3:5a and b). Quartz and potassium feldspar appear to have crystallized later and occur either as interstitial phases in Shap (the large potassium feldspar porphyroblasts are considered to be secondary and will be discussed later), (Plate 3:5c); or in Skiddaw, where potassium feldspar encloses biotite and plagioclase, but quartz is interstitial (Plate 3:5d).

PLATE 3:5. (See over page).

PLATE 3:5.

a) Euhedral biotite (dark grey) ophitically enclosed within sericitised plagioclase (white to pale grey) implying early growth of biotite; Skiddaw granite (SD41), plane polarised light, magnification x25.6.

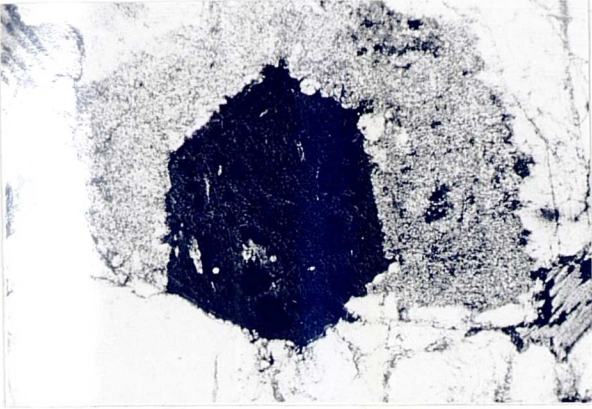
b) Euhedral plagioclase (lamella twinned, pale to mid grey) with interstitial quartz (black to dark grey), implying early growth of plagioclase; Shap granite (SH31), cross polars, magnification x20.

c) Interstitial perthitic potassium feldspar (twinned) with euhedral plagioclase (pale grey) and biotite (mid grey); Shap granite (SH30), cross polars, magnification x20.

d) Euhedral plagioclase (pale grey) ophitically enclosed in perthitic potassium feldspar (mid grey); Skiddaw granite (SD35), cross polars, magnification x20.

PLATE 3:5

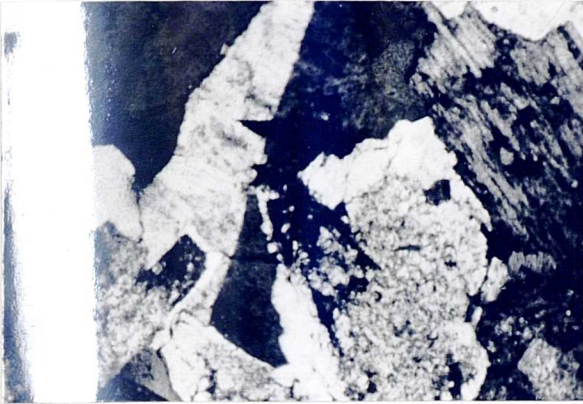
a



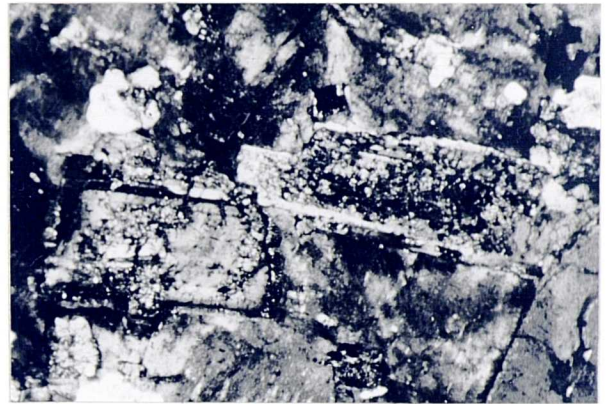
b



c



d



## 3:3:2:iii. GARNET GRANITES.

The Eskdale granite and granodiorite both contain garnet which appears to have formed early in the crystallization sequence, forming subhedral crystals which are often veined with secondary chlorite (Plate 3:6a). Garnet is also found in aplites, although it is not clear where it occurs in the order of crystallization (Plate 3:6b). Biotite and plagioclase are sub-euhedral in character as in the biotite granites (Plate 3:6c and 6d). Potassium feldspar, as in the Skiddaw granite, encloses plagioclase (Plate 3:6e), but quartz is generally anhedral and largely interstitial. Thus the crystallization sequence is similar to that in the biotite granites with no early crystallization of quartz, with the liquid composition projecting into the shaded part of the albite field in the quartz, orthoclase, albite phase diagram (Fig. 3:1a), where precipitation of albite will push the liquid composition onto the albite orthoclase cotectic. Cotectic crystallization of albite and orthoclase will then take the liquid composition to the quartz, albite, orthoclase ternary eutectic. Therefore although the presence of garnet might indicate a crustal source for the Eskdale granite the crystallization sequence is not indicative of an anatectic melt.

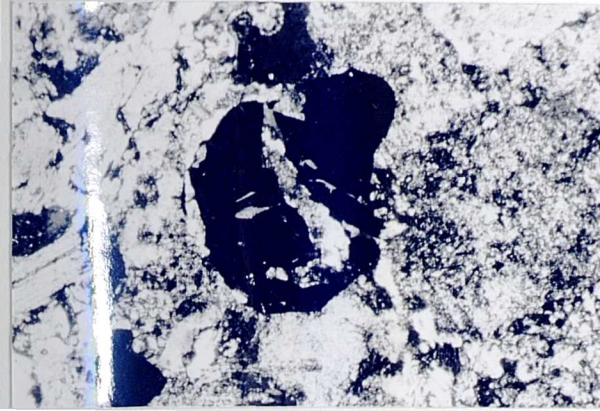
PLATE 3:6. (See over page).

PLATE 3:6.

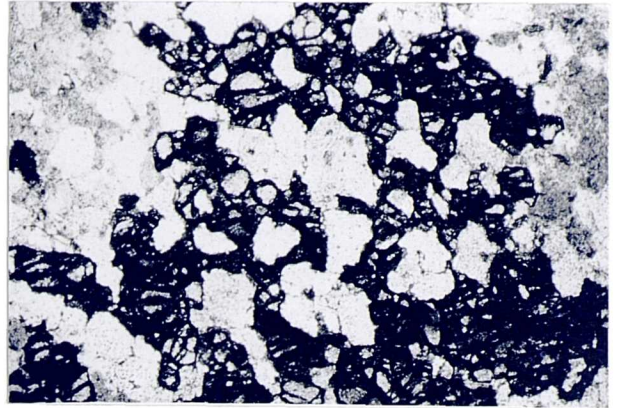
- a) Subhedral garnet (black), veined with chlorite (mid grey); Eskdale granodiorite (ED2), cross polars, magnification x32.
  
- b) Garnet (dark grey) in aplite within the Eskdale granodiorite (ED6), plane polarised light, magnification x20.
  
- c) Euhedral "early" biotite (mid grey); Eskdale granodiorite (ED8), plane polarised light, magnification x32.
  
- d) Sub-euhedral "early" plagioclase (lamella twinned); Eskdale granite (ED47), cross polars, magnification x20.
  
- e) Plagioclase (pale grey) ophitically enclosed in perthitic potassium feldspar (dark grey); Eskdale granite (ED14), cross polars, magnification x20.

PLATE 3:6

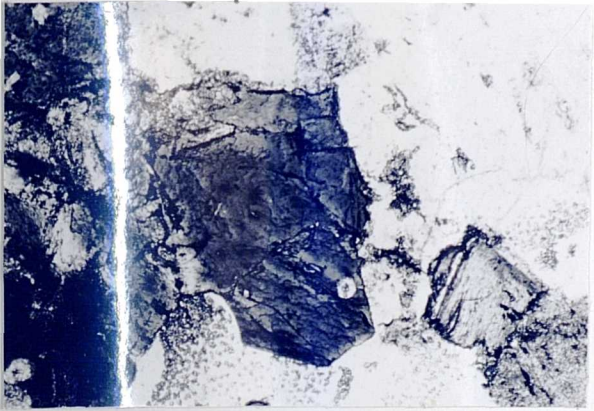
a



b



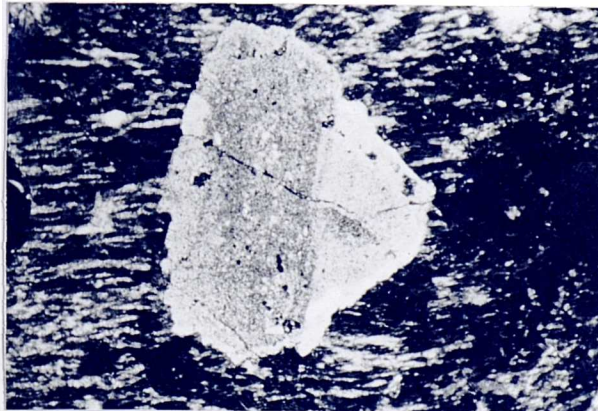
c



d



e



## 3:4 SECONDARY ALTERATION PRODUCTS AND TEXTURES.

---

**TABLE 3:3. SUMMARY OF SECONDARY ALTERATION PRODUCTS IN SCOTTISH INTRUSIONS.**

	hb	ch	ru	ep	he	mu	cc	fl	py	ccp	mo	wof
Kilmelford	*	*	*	*		*	*		*	*		
Comrie diorite		*				*						
Garabal Hill ultrabasics	*	*										
Garabal Hill pyroxene diorite												
Garabal Hill quartz diorite		*	*	*		*						
Garabal Hill fine granodiorite						*						
Garabal Hill main granodiorite						*						
Comrie quartz diorite		*	*			*	*					
Etive Ben Cruachan		*	*	*	*	*						
Strontian tonalite												
Strontian granodiorite		*	*			*	*					
Strontian granite						*						
Ben Nevis outer granite												
Foyers tonalite		*	*	*		*						
Foyers granodiorite		*	*	*		*						
Foyers granite		*	*	*		*						
Rogart		*	*			*	*					
Helmsdale		*	*		*	*	*	*				
Reay diorite												
Grudie		*	*			*	*					
Strath Ossian						*						
Moor of Rannoch		*	*									
Ballachulish granodiorite		*	*			*						
Cluanie												
Dorback		*	*			*						
Lochnagar		*	*		*	*						
Peterhead		*	*	*	*	*						
Glenlivet		*	*		*	*						
Etive Ben Starav		*	*			*						
Ben Nevis inner granite												
Comrie granite		*	*			*						*
Migdale		*	*			*						
Ballachulish granite		*	*			*				*		*
Moy						*						
Stritchen						*						
Ben Rinnes		*	*			*						
Cairngorm		*	*		*	*	*					
Bennachie		*	*			*						
Glen Gairn		*	*		*	*						
Cromar		*	*		*	*						
Hill of Fare		*	*		*	*						
Mount Battock		*	*		*	*						
Blackburn		*	*			*						
Ardclach												
Aberdeen						*						
Cove Bay						*						

---

### 3:4:1. SCOTTISH GRANITES.

#### 3:4:1:i. PYROXENE BEARING INTRUSIONS.

The Garabal Hill ultramafic and gabbroic rocks have suffered a considerable amount of secondary mineral growth. In the pyroxenites the intercumulus plagioclase is highly sericitized and the pyroxenes are partially replaced by a fibrous mixture of hornblende and chlorite leaving only kernels of unaltered pyroxene (Plate 3:7a). This type of alteration is generally limited to the ultramafic members of the Garabal Hill complex.

In the Comrie diorite the plagioclase is highly sericitized with some chlorite and calcite replacing pyroxene. The extensive nature of the alteration of the Comrie diorite is probably related to the molybdenum mineralization in the granite. The Kilmelford diorite is closely associated with porphyry copper mineralization. This has resulted in a wide range of secondary alteration, with both phyllic and propylitic alteration generally associated with porphyry type mineralization. Other than this the pyroxenes are in some instances replaced by hornblende and the biotite by chlorite. The extent of the alteration varies from only partial replacement of plagioclase by fine grained muscovite to total recrystallization with muscovite, calcite and opaques (mainly pyrite and chalcopyrite).

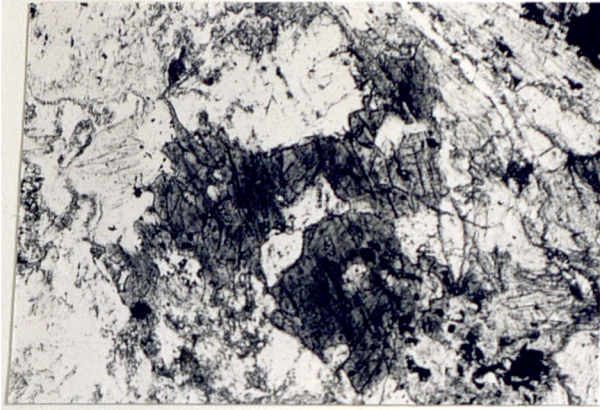
PLATE 3:7. (See over page).

PLATE 3:7.

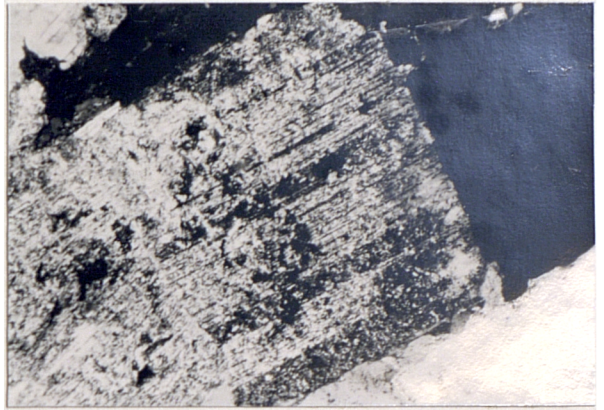
- a) Core of unaltered pyroxene (mid grey) within secondary hornblende (white), chlorite (pale grey) and magnetite (black); Garabal Hill pyroxenite (GH14), plane polarised light, magnification x20.
  
- b) Euhedral plagioclase (lamella twinned) with sericitic alteration; Foyers granodiorite (BPR505), cross polars, magnification x39.4.
  
- c) Secondary chlorite (mid grey) with accicular rutile (black) replacing biotite (dark grey); Comrie granite (CM6), plane polarised light, magnification x63.
  
- d) Secondary chlorite (mid grey) and calcite (white) after hornblende; Helmsdale granite (HD107), plane polarised light, magnification x63.

PLATE 3:7

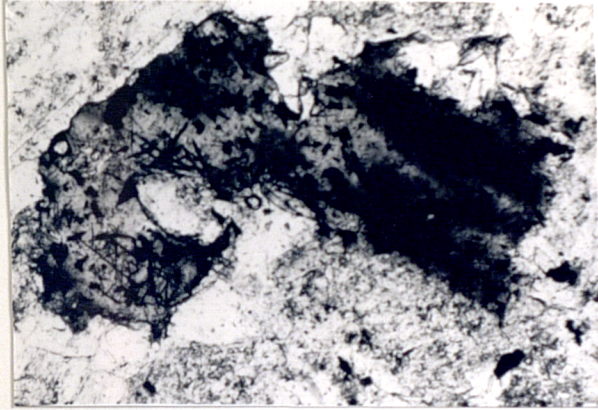
a



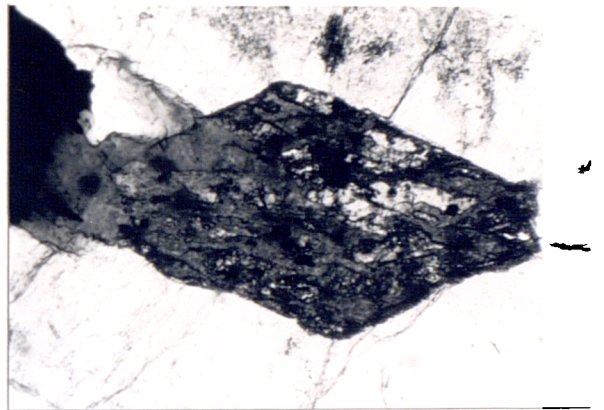
b



c



d



### 3:4:1:ii. HORNBLLENDE BEARING INTRUSIONS.

Alteration in the hornblende bearing granitoids is extremely variable. In a few intrusions there is no visible alteration (Table 3:3). The most common type of alteration is sericitization of the plagioclases (Plate 3:7b), and chlorite and rutile replacing biotite (Plate 3:7c). Less commonly epidote or a mixture of calcite and chlorite replaces hornblende (Plate 3:7d). The Ballachulish intrusion displays more intense alteration and also has associated porphyry type copper mineralization, with phyllic alteration and secondary sulphides chalcopryrite, pyrite, and malachite. The Helmsdale intrusion is also intensely altered, displaying local extensive hematization (Plate 3:8a) and also potassic alteration in shatter zones which appear to be linked to uranium mineralization (Tweedie 1979). There is also secondary fluorite and calcite, and some replacement of biotite and hornblende by chlorite and rutile.

### 3:4:1:iii. BIOTITE GRANITES.

Secondary muscovite is a common feature of the biotite granites with particularly intense potassic alteration in the Comrie and Ballachulish granites associated with porphyry type mineralization. The Comrie granite has associated molybdenite, principally on joint planes. The mineralization in the Ballachulish granite is primarily chalcopryrite and pyrite with secondary malachite. Replacement of biotite by chlorite and rutile is also a common feature of most biotite granites.

The muscovite noted as being interstitial in the Cairngorm suite of granites may also be of secondary origin, the uncertainty here being

PLATE 3:8. (See over page).

PLATE 3:8.

a) Hematised feldspars; Helmsdale granite (38a-110), plane polarised light, magnification x32.

b) Interstitial muscovite (pale grey to white) invading surrounding potassium feldspars (pale to mid grey); Cairngorm granite (CN16), cross polars, magnification x50.4.

c) Interstitial muscovite (pale grey) replacing adjacent biotite crystal (mid grey) along cleavage planes; Cairngorm granite (BL8), cross polars, magnification x25.6.

d) Two generations of secondary muscovite in the Glen Gairn greisen, both large grains with prominent cleavage planes and smaller rosettes (GG9), cross polars, magnification x25.6.

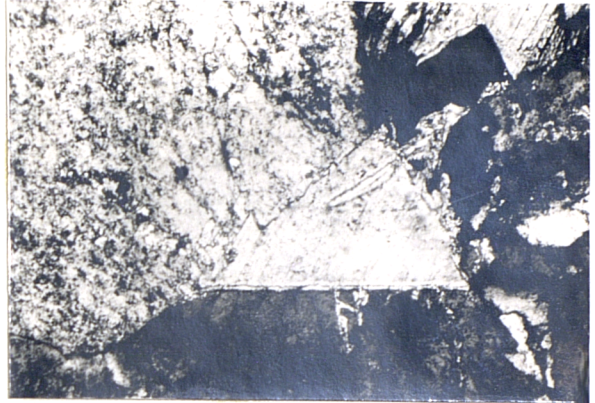
e) Pink granite and green greisen samples from the Glen Gairn intrusion, with centimeter scale.

PLATE 3:8

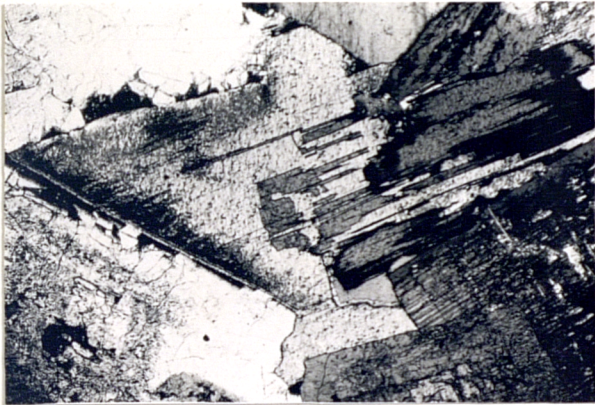
a



b



c



d



e



whether the residual liquid responsible for the growth of this mineral was a residual silicate magma or a hydrous fluid. The evidence for a secondary origin for this mineral lies in the occasional extension of this mineral across grain boundaries of enclosing feldspars where its growth is unequivocally secondary (Plate 3:8b). This also occurs where an adjacent grain is biotite with an interfingering of biotite and muscovite (Plate 3:8c). Intense alteration is rare in this group of intrusions. However the Glen Gairn granite sports patches of "greisen" which is green in colour (Plate 3:8e) and in thin section shows two generations of muscovite growth with large flakes set in a matrix of fine grained muscovite in quartz (Plate 3:8d). Granites in the Cairngorm suite also show hematitization which is variable in extent and appears to be associated with high levels of uranium, the fluids responsible for the hematitization also probably carrying uranium.

### 3:4:2. THE LAKE DISTRICT.

---

TABLE 3:4. SUMMARY OF SECONDARY ALTERATION PRODUCTS IN LAKE DISTRICT INTRUSIONS.

	hb	ch	ru	ep	he	mu	cc	fl	py	ccp	mo	wof
Carrock Fell granophyre	*	*	*	*	*	*	*					
Carrock Fell ferrogabbro	*	*	*		*	*						
Ennerdale		*	*	*	*	*						
Threlkeld		*	*			*						
Skiddaw		*	*			*	*	*	*	*	*	*
Shap		*	*	*	*	*	*	*	*	*		
Eskdale		*	*	*	*	*	*					

---

### 3:4:2:i. PYROXENE BEARING INTRUSIONS.

The state of alteration of the pyroxene bearing intrusives of the Lake District is highly variable. The Threlkeld microgranite for instance is pervasively metasomatized with extensive sericitization and chloritization and veins of secondary calcite and some pyrite. The Ennerdale and Carrock granophyres are generally less altered, although the Ennerdale granophyre has widespread epidote replacing pyroxene (Plate 3:7a), which may represent the regional greenschist metamorphic event which postdated this intrusion. There is also localized haematitization in the Ennerdale intrusion, which is probably related to the west Cumbrian haematite deposits which date from the Lower Carboniferous (Firman 1978b). In the Carrock granophyre the pyroxenes are frequently replaced by mixtures of hornblende, chlorite, epidote and hematite with some sericitization of feldspars. However adjacent to tungsten veins near Carrock Mine the granophyre is converted to a microgreisen with large scale replacement of feldspars by muscovite (Plate 3:7 b).

### 3:4:2:ii. BIOTITE GRANITES.

Both the Shap and Skiddaw granites have evidence of high temperature water-rock interaction closely associated with mineralization. In the Shap granite the large megacrysts of potassium feldspar are clearly secondary in origin, found not only in the granite but also in autoliths and xenoliths within the granite. These potassium feldspar crystals differ from the primary potash feldspars in the matrix of this granite in that they are full of anhedral inclusions of other minerals representing material which was not included in the feldspar lattice (Plate 3:9 c).

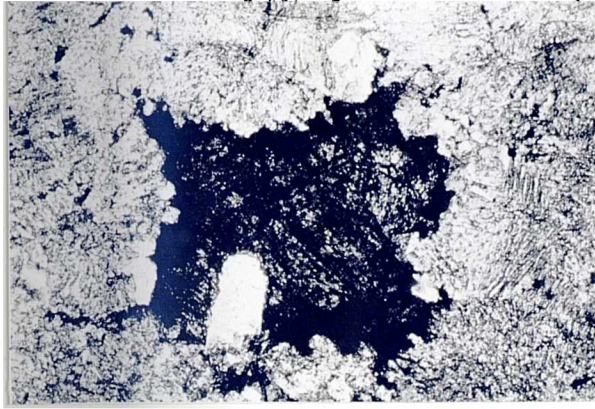
PLATE 3:9. (See over page).

PLATE 3:9.

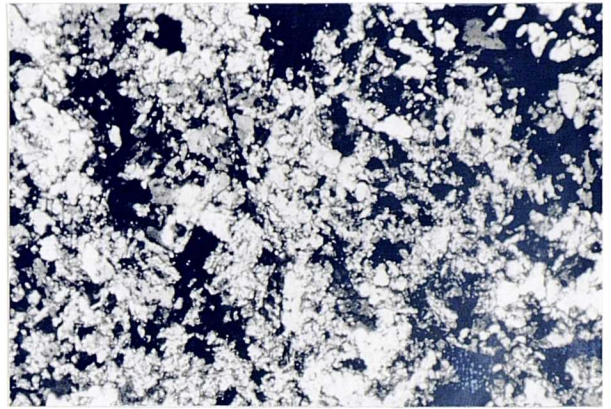
- a) Secondary epidote (dark grey) after pyroxene phenocrysts in the Ennerdale granophyre (EN18), plane polarised light, magnification x32.
  
- b) Random growth of muscovite in the microgreisen adjacent to mineral vein in the Carrock granophyre (CF6), cross polars, magnification x32.
  
- c) Anhedral inclusions (white to pale grey) within secondary potassium feldspar (mid grey); Shap granite (SH26), cross polars, magnification x20.
  
- d) Secondary hematite after sphene (black); Shap granite (SH30), plane polarised light, magnification x20.
  
- e) Secondary rutile (mid grey) in Skiddaw greisen (SD31), plane polarised light, magnification x252.

PLATE 3:9

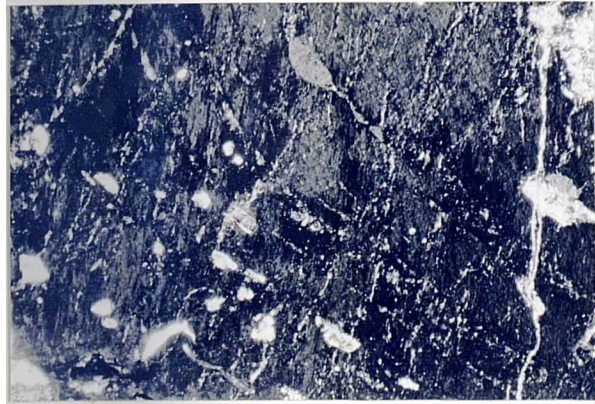
a



b



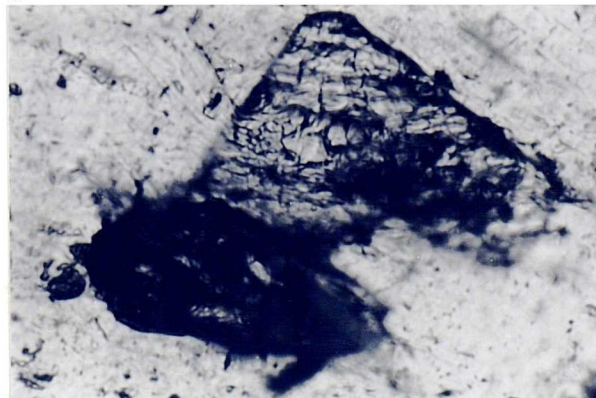
c



d



e



Accompanying the growth of potassium feldspar is some chloritization of biotites, sericitization of plagioclase, secondary hematite after sphene (Plate 3:9.d), and veinlets of calcite and baryte with fluorite, pyrite and chalcopyrite.

The Skiddaw granite shows different states of alteration in its three outcrops. Rocks of the southernmost, Siren Gill, outcrop are the least altered, showing some chlorite replacing biotite and some sericitization of the feldspars. Rocks of the central, Caldbeck, outcrop generally display more alteration with more secondary chlorite and muscovite. Rocks of the northern, Grainsgill, outcrop however are intensely altered with considerable development of greisen and all samples show total replacement of biotite with chlorite and rutile and variable replacement of feldspars with muscovite. In the greisens there is no chlorite but Ti is retained in rutile (Plate 3:9e). The greisens also contain chalcopyrite, pyrite, molybdenite, wolframite and other opaque minerals in small quantities. Fluorite and tourmaline are present in small amounts in the Caldew and Grainsgill exposures of the Skiddaw granite. An age for the hydrothermal event responsible for the greisenization was determined by K-Ar isotopic analysis of muscovites by Shepherd et al. (1976) and is close to the intrusive age of the granite.

### 3:4:2:iii. GARNET GRANITE.

The Eskdale granite and granodiorite show evidence of both high and low temperature alteration, and there are a few patches of greisen, especially around Devoke Water, where there is considerable development of secondary muscovite, representing high temperature alteration.

Secondary muscovite is also common throughout the granite and granodiorite in sericitized feldspars. Epidote is rare in the Eskdale granite, although the biotites are generally totally replaced by a mixture of chlorite, rutile, hematite and muscovite (Plate 3:10a). This type of alteration is pervasive in the granite, and with a few exceptions, in the granodiorite too. Haematitization is common in the Eskdale granite with intense hematitization occurring at North Boote iron mines where the granite is totally replaced by a mixture of haematite and carbonates (Plate 3:10b).

### 3:5 MINERAL CHEMISTRY.

A study was made of the mineral chemistry of most of the intrusions to assess the variation in mineral chemistry with major and trace element chemistry within and between intrusions. Representative mineral analyses can potentially be used for major element modelling of fractional crystallization trends. The data was collected using a Cambridge Instruments Microscan 5 with Link System 860 Energy Dispersive facility.

#### 3:5:i. PYROXENES.

Pyroxenes are only found in the more mafic intrusions. Clinopyroxene is more common than orthopyroxene. Representative analyses of pyroxenes from the Kilmelford diorite, Comrie diorite, and the Garabal Hill fine grained granodiorite, diorite and gabbro are given in Table 3:4. The compositions of these pyroxenes are variable. The clinopyroxenes from Kilmelford are diopside to subcalcic augite in composition (Fig 3:2a). In the Comrie diorite the clinopyroxenes are mainly augites with some

PLATE 3:10. (See over page).

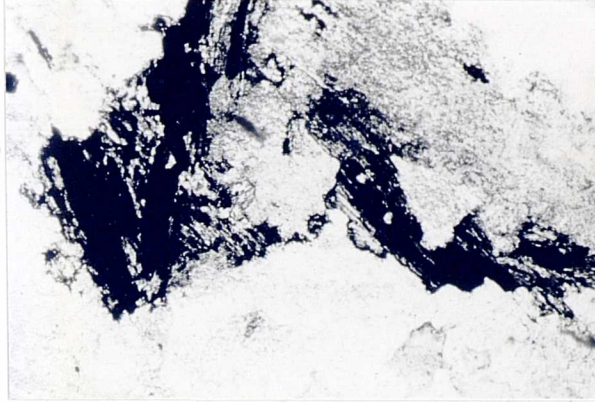
PLATE 3:10.

a) Biotite replaced by a mixture of iron oxides (black) and white mica (white); Eskdale granite (E036), plane polarised light, magnification x32.

b) Hematite (black) and calcite (pale to mid grey) totally replacing granite; Eskdale granite (E037), cross polars, magnification x32.

PLATE 3:10

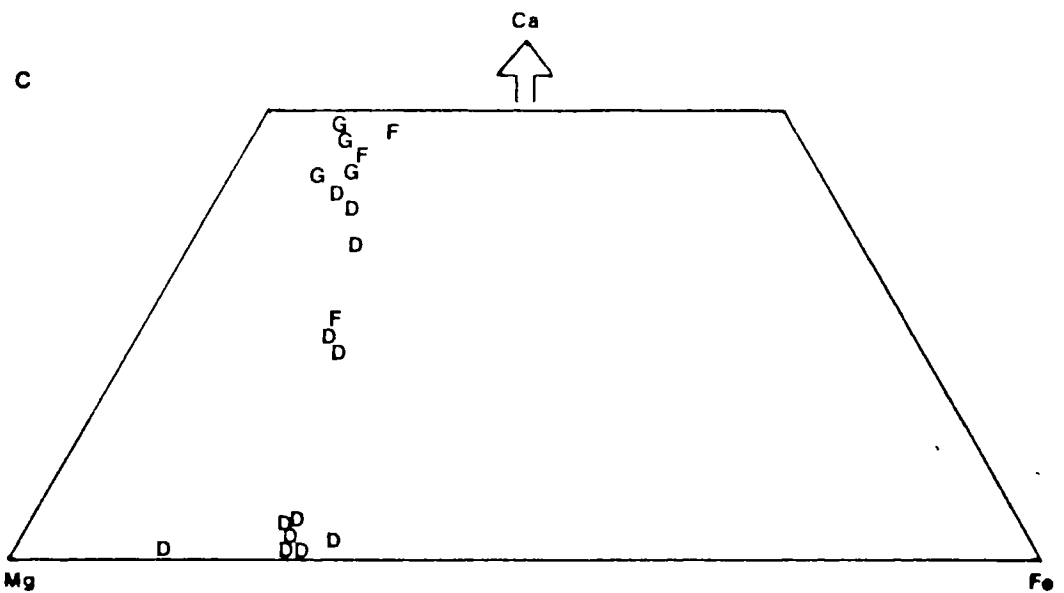
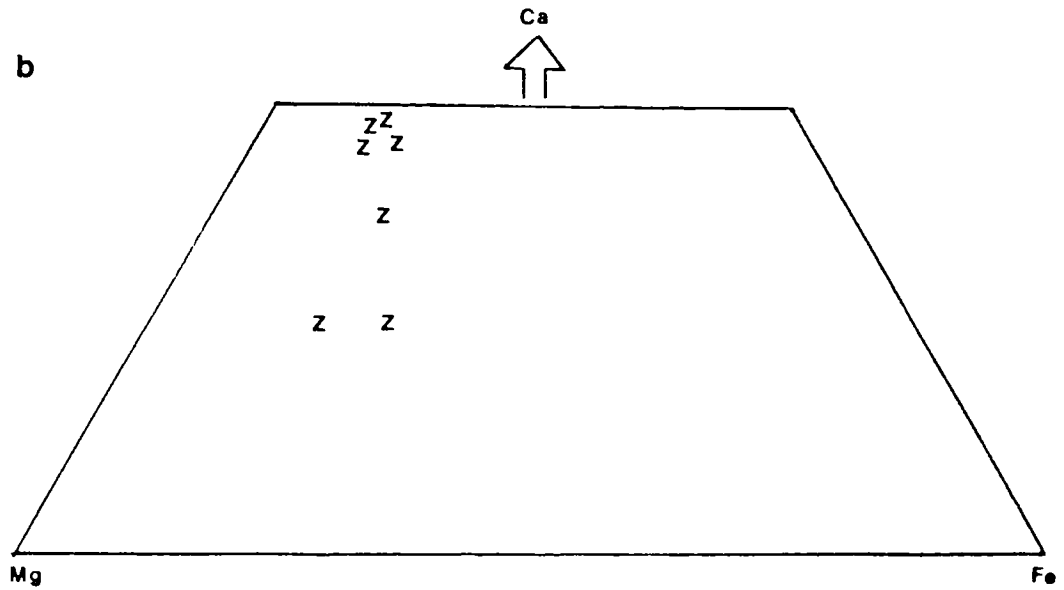
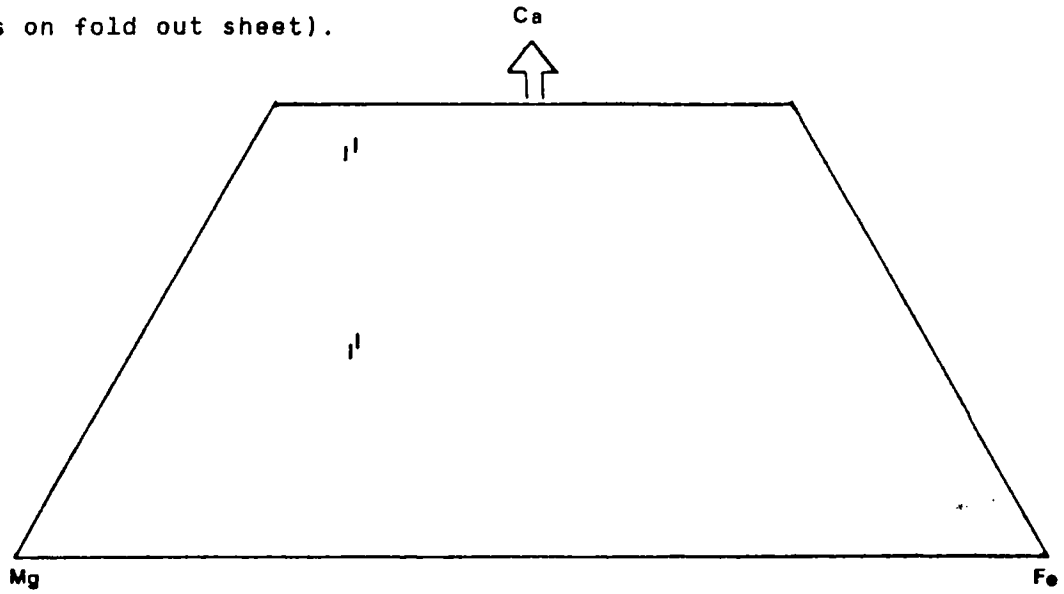
a



b



Fig. 3:2. a) compositional variation in pyroxenes in the Kilmelford diorite, b) compositional variation in pyroxenes in the Comrie diorite, c) compositional variation in pyroxenes in the Garabal Hill complex. (Key to symbols on fold out sheet).



falling in the salite field (Fig 3:2b). In the Garabal Hill complex the pyroxenes in the fine grained granodiorite are augites; in the diorites, augite and sub-calcic augite coexist with bronzite and hypersthene; in the gabbro the pyroxene is diopside (Fig 3:2c).

### 3:5:ii. AMPHIBOLES.

Amphiboles are common in granitic rocks although their distribution is confined largely to the granodioritic and tonalitic compositions. The amphiboles are generally green in colour and sub-euhedral and appear mostly to be primary and early in the sequence of crystallization. Representative analyses of hornblendes are shown in Table 3:5, where analyses are recalculated to give a minimum estimate of  $Fe_2O_3$ . However in a few cases (where the initial recalculation was unable to satisfy the charge balance equation) the mid-point from the Papike (1974) method of  $Fe_2O_3:FeO$  recalculation is used and the amphiboles are assigned names according to the method of Leake (1978). The range of composition is small, generally from edenite to actinolite. However amphiboles of actinolitic composition are generally regarded as secondary after pyroxenes, although the common presence of amphiboles of this composition in granites and granodiorites of relatively evolved chemistry, (e.g. Lochnagar) appears to cast doubt on this broad generalization. Amphiboles of this composition in the less evolved granitoids are undoubtedly secondary after pyroxenes.

TABLE 3:5 REPRESENTATIVE MICROPROBE DATA FOR PYROXENES FROM CALEDONIAN INTRUSIONS. ANALYSES ARE QUOTED AS WT% OXIDES, Fe<sup>2+</sup>/Fe<sup>3+</sup> RATIO CALCULATED BY CHARGE BALANCE.

	Kilmelford		Comrie	Garabal Hill			
	diopside	subcalcic	salite	fine grained granodiorite	diorite	opx	gabbro
		augite		augite	subcalcic	bronzite	diopside
	KM2	KM5	CM9	GH11	GH17	GH10	GH14
SiO	52.5	53.7	52.4	50.2	51.9	52.2	51.8
TiO <sup>2</sup>	0.2	0.7	0.3	0.6	0.1	0.5	0.4
Al <sup>3</sup>	0.7	4.6	0.9	2.9	4.6	0.9	1.7
Fe <sup>2</sup> O <sup>3</sup>	2.3	0.0	2.4	4.1	1.5	1.6	3.7
Fe <sup>3</sup> O <sup>3</sup>	7.2	10.9	7.0	5.4	10.7	17.8	4.8
MnO	0.4	0.3	0.2	0.4	0.2	0.4	0.2
MgO	14.5	16.1	14.3	13.8	16.6	23.4	15.5
CaO	22.1	11.2	22.0	20.9	12.1	2.7	20.6
Na <sup>0</sup>	0.6	0.7	0.6	0.7	1.3	0.4	0.7
K <sup>2</sup> O	0.0	0.7	0.0	0.1	0.1	0.0	0.1
TOT	100.4	99.0	100.1	98.9	99.0	100.0	99.4

Mineral formula units (based on 6 oxygens).

Si	1.955	1.974	1.951	1.891	1.923	1.934	1.924
Ti	0.004	0.020	0.009	0.016	0.004	0.013	0.011
Al	0.030	0.201	0.041	0.128	0.203	0.040	0.075
Fe <sup>3</sup>	0.065	0.000	0.066	0.115	0.040	0.044	0.105
Fe <sup>2</sup>	0.225	0.333	0.219	0.169	0.332	0.552	0.148
Mn	0.011	0.011	0.007	0.011	0.006	0.013	0.007
Mg	0.802	0.884	0.793	0.771	0.915	1.294	0.861
Ca	0.880	0.441	0.880	0.844	0.479	0.106	0.820
Na	0.044	0.052	0.043	0.050	0.095	0.029	0.048
K	0.000	0.031	0.000	0.006	0.002	0.001	0.048

TABLE 3:6. REPRESENTATIVE MICROPROBE DATA FOR AMPHIBOLES FROM CALEDONIAN GRANITOIDS, ANALYSES QUOTED AS WT% OXIDES.

	Garabal Hill gabbro				Garabal Hill diorite			
	actinolite	magnesio- hornblende	ferroan pargasite	edenite	magnesio- hornblende	actinolitic- hornblende	actinolite	
	GH15	GH15	GH14	GH21	GH21	GH22	GH17	
SiO <sub>2</sub>	53.7	48.2	41.7	45.1	47.7	49.2	53.6	
TiO <sub>2</sub>	0.2	0.7	3.9	1.4	1.1	0.4	0.4	
Al <sub>2</sub> O <sub>3</sub>	1.3	5.3	11.3	8.2	7.1	4.6	2.8	
Fe <sup>2+</sup> O <sub>3</sub>	0.1	1.0	0.7	1.5	1.4	1.3	0.6	
Fe <sup>3+</sup> O <sub>3</sub>	11.3	14.5	10.5	12.7	12.2	13.9	6.9	
MnO	0.5	0.5	0.4	0.4	0.4	0.8	0.0	
MgO	16.4	13.2	13.1	13.1	14.4	14.2	19.3	
CaO	12.7	11.4	11.6	11.8	12.1	10.9	12.6	
Na <sub>2</sub> O	0.5	0.9	2.1	1.5	1.4	1.2	0.6	
K <sub>2</sub> O	0.1	0.4	1.3	0.6	0.4	0.1	0.1	
TOT	96.9	96.2	96.6	96.2	98.2	96.7	97.0	
Mineral formula units based on 23 oxygens.								
Si	7.781	7.216	6.226	6.762	6.955	7.293	7.602	
Ti	0.025	0.084	0.443	0.156	0.122	0.048	0.042	
Al	0.220	0.940	1.994	1.449	1.217	0.806	0.470	
Fe <sup>3+</sup>	0.010	0.112	0.081	0.171	0.153	0.147	0.063	
Fe <sup>2+</sup>	1.375	1.810	1.315	1.596	1.488	1.719	0.825	
Mn	0.060	0.067	0.044	0.048	0.046	0.106	0.005	
Mg	3.551	2.941	2.919	2.926	3.122	3.143	4.080	
Ca	1.973	1.830	1.853	1.893	1.897	1.738	1.914	
Na	0.143	0.267	0.594	0.436	0.399	0.339	0.168	
K	0.020	0.080	0.242	0.109	0.078	0.026	0.013	
SUM	15.160	15.347	15.711	15.546	15.477	15.366	15.180	
Garabal Hill f.g granodiorite      Garabal Hill granodiorite      Ballachulish								
	magnesio- hornblende	actinolite	actinolitic hornblende	edenite	magnesio- hornblende	actinolitic hornblende	edenite	
	GH11	GH11	GH3	GH3	GGF6	GGF6	GGF6	
SiO <sub>2</sub>	47.6	52.4	50.7	46.8	47.6	48.7	48.1	
TiO <sub>2</sub>	1.0	0.1	0.4	1.4	1.2	0.8	1.2	
Al <sub>2</sub> O <sub>3</sub>	6.9	1.6	4.0	6.9	5.7	5.2	6.2	
Fe <sup>2+</sup> O <sub>3</sub>	1.1	0.7	1.9	2.4	0.7	1.9	0.3	
Fe <sup>3+</sup> O <sub>3</sub>	14.9	11.3	10.6	12.4	13.6	12.7	13.9	
MnO	0.3	0.6	0.6	0.6	0.6	0.5	0.5	
MgO	12.5	15.9	15.1	13.4	13.7	13.5	14.2	
CaO	11.9	12.2	11.6	11.2	11.8	11.5	11.7	
Na <sub>2</sub> O	0.9	0.4	1.1	2.1	1.2	1.3	1.5	
K <sub>2</sub> O	0.5	0.2	0.4	0.7	0.6	0.5	0.6	
TOT	97.6	95.3	96.2	97.8	96.7	96.7	98.3	
Mineral formula units based on 23 oxygens.								
Si	7.044	7.742	7.439	6.902	7.087	7.220	7.047	
Ti	0.122	0.010	0.041	0.153	0.135	0.094	0.127	
Al	1.202	0.271	0.698	1.207	1.008	0.914	1.075	
Fe <sup>3+</sup>	0.123	0.082	0.206	0.268	0.078	0.216	0.036	
Fe <sup>2+</sup>	1.843	1.391	1.307	1.526	1.691	1.575	1.701	
Mn	0.035	0.073	0.071	0.080	0.076	0.064	0.062	
Mg	2.752	3.506	3.297	2.939	3.048	2.978	3.107	
Ca	1.888	1.925	1.818	1.765	1.878	1.834	1.845	
Na	0.261	0.109	0.308	0.612	0.355	0.359	0.434	
K	0.100	0.034	0.079	0.122	0.116	0.095	0.106	
SUM	15.361	15.143	15.262	15.575	15.471	15.348	15.541	

TABLE 3:6 CONTINUED.

	Comrie diorite magnesian actinolite hornblende		Ben Nevis actinolite		Moor of Rannoch magnesian edenite actinolitic hornblende		
	CM9	CM1	BN16	BN16	MR1	MR5	MR5
SiO <sub>2</sub>	47.2	54.9	53.5	48.1	48.2	47.5	50.4
TiO <sub>2</sub>	0.3	0.1	0.1	0.9	1.0	1.3	0.5
Al <sub>2</sub> O <sub>3</sub>	5.6	1.5	2.1	4.9	6.1	6.2	5.0
Fe <sup>2+</sup> O <sup>3</sup>	4.0	0.8	0.4	0.2	0.5	1.4	1.0
Fe <sup>3+</sup> O <sup>3</sup>	13.2	7.3	10.4	12.4	12.9	12.5	11.0
MnO	0.2	0.4	0.6	0.4	0.3	0.6	0.4
MgO	12.4	19.5	16.8	14.5	14.2	13.8	15.5
CaO	12.3	11.9	12.7	11.8	12.2	12.1	12.0
Na <sub>2</sub> O	0.8	0.9	0.5	1.0	1.3	1.5	1.0
K <sub>2</sub> O	0.5	0.0	0.1	0.6	0.5	0.6	0.0
TOT	96.7	97.4	97.0	94.8	97.1	97.6	98
	Mineral formula units based on 23 oxygens.						
Si	7.080	7.762	7.709	7.247	7.106	7.010	7.225
Ti	0.028	0.010	0.015	0.105	0.113	0.142	0.020
Al	0.988	0.253	0.355	0.875	1.064	1.085	0.800
Fe <sup>3+</sup>	0.455	0.088	0.041	0.017	0.050	0.158	0.100
Fe <sup>2+</sup>	1.661	0.858	1.251	1.555	1.583	1.543	1.300
Mn	0.029	0.043	0.068	0.054	0.034	0.072	0.020
Mg	2.781	4.108	3.604	3.247	3.127	3.030	3.300
Ca	1.978	1.814	1.956	1.900	1.922	1.914	1.900
Na	0.241	0.236	0.145	0.286	0.557	0.438	0.200
K	0.099	0.005	0.009	0.117	0.090	0.109	0.000
SUM	15.341	15.178	15.155	15.403	15.447	15.500	15.300
	Kilmelford actinolite edenite		Strath Ossian magnesian edenite hornblende		Strontian edenite actinolitic hornblende		
	KM5	KM5	SO3	SO3	SRN8	SRN8	
SiO <sub>2</sub>	54.9	47.0	49.5	46.7	47.0	48.3	
TiO <sub>2</sub>	0.1	1.2	0.9	1.1	1.1	0.9	
Al <sub>2</sub> O <sub>3</sub>	2.5	7.6	5.6	6.1	6.0	4.9	
Fe <sup>2+</sup> O <sup>3</sup>	0.0	1.1	0.3	1.3	1.9	2.4	
Fe <sup>3+</sup> O <sup>3</sup>	11.9	8.4	13.5	13.4	13.8	11.9	
MnO	0.4	0.1	0.4	0.5	0.4	0.4	
MgO	13.3	16.0	14.2	13.4	13.7	13.7	
CaO	11.7	12.2	12.1	12.0	11.6	11.3	
Na <sub>2</sub> O	0.3	1.9	1.0	1.4	1.4	0.9	
K <sub>2</sub> O	0.2	0.2	0.4	0.7	0.7	0.6	
TOT	95.3	96.7	98.0	96.6	97.8	95.2	
	Mineral formula units based on 23 oxygens						
Si	8.018	6.914	7.224	6.993	6.970	7.252	
Ti	0.014	0.132	0.100	0.126	0.122	0.103	
Al	0.425	1.310	0.958	1.079	1.054	0.860	
Fe <sup>3+</sup>	0.000	0.126	0.031	0.151	0.215	0.266	
Fe <sup>2+</sup>	1.456	1.038	1.648	1.671	1.710	1.489	
Mn	0.051	0.015	0.054	0.061	0.055	0.047	
Mg	2.899	3.502	3.095	2.996	3.032	3.058	
Ca	1.824	1.915	1.890	1.923	1.842	1.814	
Na	0.091	0.544	0.289	0.403	0.408	0.268	
K	0.045	0.028	0.074	0.128	0.140	0.119	
SUM	14.823	15.523	15.363	15.531	15.548	15.275	

TABLE 3:6 CONTINUED.

	Dorback		Lochnagar		
	edenitic hornblende	magnesian hornblende	edenite	magnesian hornblende	actinolite
	TM21	TM21	BL48	BL48	BL48
SiO	44.4	44.5	54.9	48.4	52.2
TiO <sup>2</sup>	1.5	1.2	0.1	1.2	0.4
Al <sup>3</sup>	8.5	8.9	1.5	5.3	2.8
Fe <sup>2</sup> O <sup>3</sup>	1.4	2.9	0.8	2.2	0.0
FeO <sup>3</sup>	16.6	14.8	7.3	12.1	12.5
MnO	0.3	0.4	0.4	0.7	0.9
MgO	11.1	12.2	19.5	14.0	15.2
CaO	11.5	12.2	12.0	11.7	12.1
Na <sub>2</sub> O	1.6	1.6	0.9	1.4	0.8
K <sub>2</sub> O	0.9	0.0	0.0	0.5	0.2
TOT	97.8	97.3	97.4	97.5	97.0
	Mineral formula units based on 23 oxygens.				
Si	6.677	6.673	7.762	7.125	7.620
Ti	0.172	0.140	0.010	0.135	0.045
Al	1.509	1.578	0.253	0.916	0.480
Fe <sup>3+</sup>	0.160	0.336	0.088	0.240	0.000
Fe <sup>2+</sup>	2.090	1.856	0.858	1.494	1.527
Mn	0.040	0.047	0.043	0.081	0.111
Mg	2.494	2.414	4.108	3.080	3.296
Ca	1.858	1.956	1.814	1.843	1.887
Na	0.470	0.460	0.236	0.391	0.218
K	0.163	0.000	0.005	0.101	0.041
SUM	15.633	15.460	15.178	15.407	15.225

## 3:5:iii. BIOTITES.

Biotite is a mineral which is ubiquitous in most granite intrusions. Variations in biotite composition within some of the intrusions is large, particularly in the composite intrusions such as Comrie and Garabal Hill. Overall there is a large variation in biotite composition, reflecting the range of whole rock compositions in the Caledonian granitoids, with changes in biotite composition related to the level of geochemical evolution of the granites, (Table 3:7). Biotites are in most instances sub-euhedral and appear to form part of the fractionating mineral assemblage, therefore the composition of the biotites both reflect and cause variations in the major element compositions of the granite magmas through fractional crystallization.

The variation in biotite composition is restricted mainly to Fe, Mg, Ti, Mn, and Al through substitution; variations in these elements are directly influenced by the availability of these elements within the magma, elements present in low concentrations, such as Mg, may become rapidly depleted during fractional crystallization. The observed variation in biotites of these elements is generally 10 wt% for Al, Fe and Mg and 5 wt% for Mn. Biotites from the least evolved plutons (diorites, tonalites, granodiorites and some granites) generally have low  $Al_2O_3$  (12-15 wt%), high MgO (10-15 wt%), low MnO (0-0.5 wt%) and intermediate FeO and  $Fe_2O_3$  (15-20 wt%) with high Mg numbers. Biotites from the more geochemically evolved granites have typically higher  $Al_2O_3$  (15-23 wt%) and  $FeO + Fe_2O_3$  (20-25 wt%), lower MgO (0-10 wt%) and higher MnO (0.5-5.0 wt%) with low Mg numbers. Exceptions to this generalization are the biotites from the Glen Gairn granite which typically have low  $FeO + Fe_2O_3$  (10-17 wt%); however these biotites are also rich in Rb and Li (not systematically analysed) and are close in composition to zinwaldite (Hall & Walsh 1972).

Biotites from granites which on the basis of isotopic and textural evidence, appear to be S-type have compositions similar to those from the evolved granites, with the exception of Mn which is generally low. Thus these biotites form a separate group on a Mn vs. Fe/Fe+Mg cation diagram (Fig. 3:3). The total compositional range is shown on an Fe vs. Mg cation diagram in Fig. 3:4, and it is noted that the biotites from S-type granites also plot separately from those from the evolved and less evolved juvenile granites. The low levels of manganese observed in biotites from S-type granites is probably the result of residual spessertine rich garnet in the metasedimentary source for these granites.

Fig. 3:3. Compositional variation in biotites (see over page).

Fig. 3:3. Compositional variation in biotites (based on 22 oxygens)

a) Cationic proportions of Mn vs. Fe/Fe+Mg for biotite data from the Caledonian granitoids of eastern Scotland. (key to symbols on fold out sheet).

b) Cationic proportions of Mn vs. Fe/Fe+Mg for biotite data from the Caledonian granitoids of western Scotland. (key to symbols on fold out sheet).

c) Cationic proportions of Mn vs. Fe/Fe+Mg for biotite data from all the Caledonian granitoids of Scotland. (key to symbols on fold out sheet).

Fig. 3:3

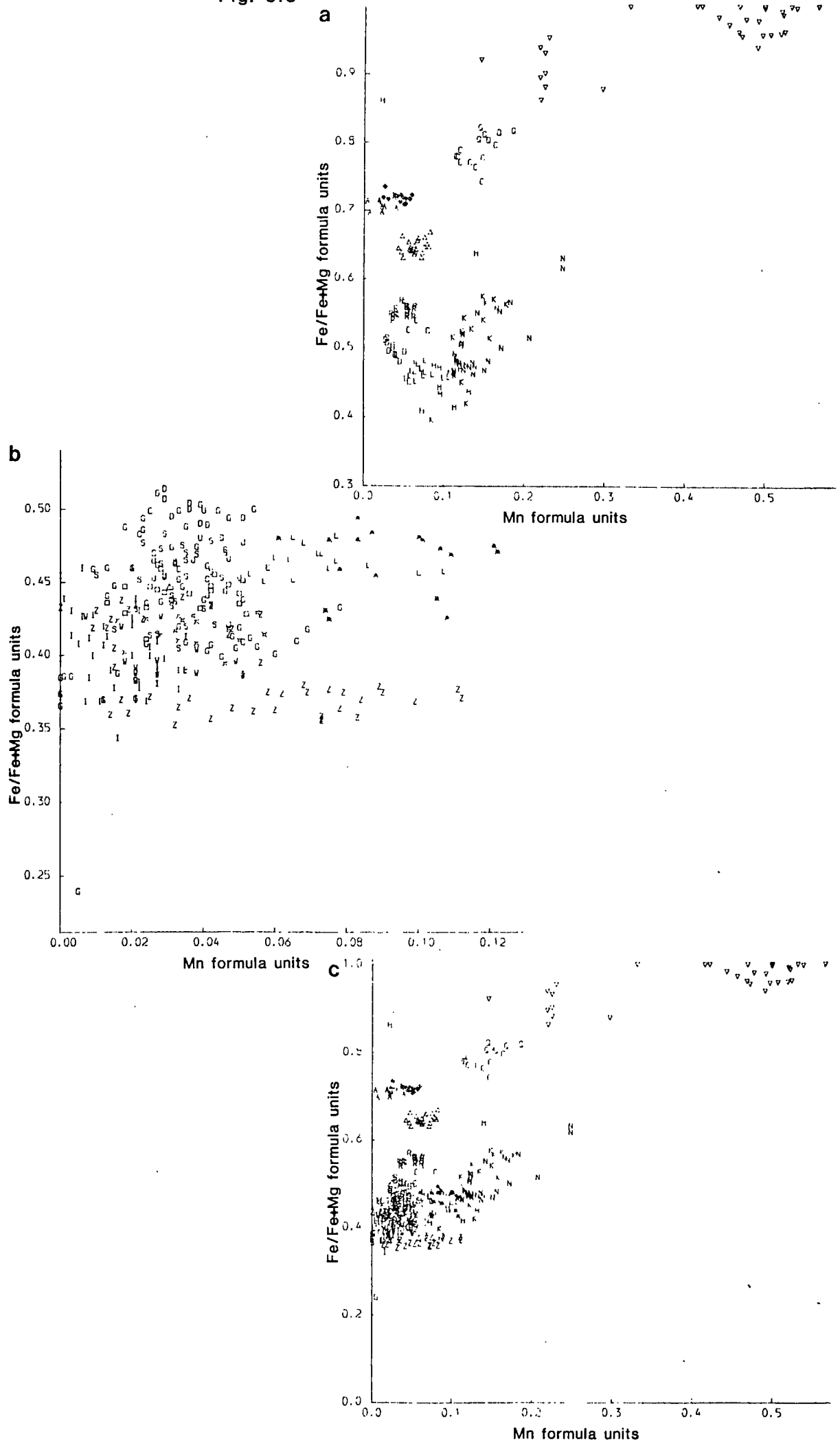


Fig. 3:4. Compositional variation in biotites (see over page).

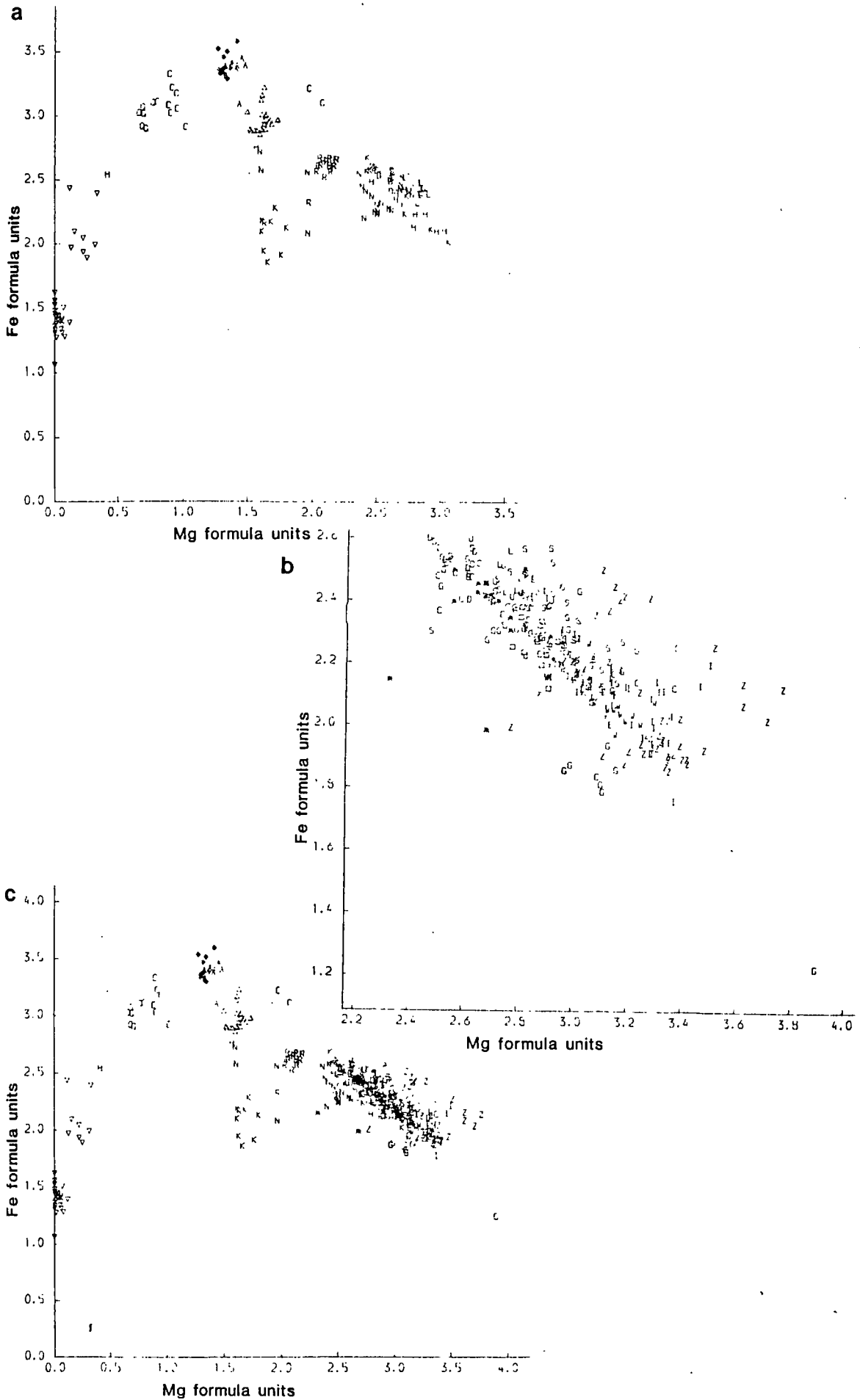
Fig. 3:4. Compositional variations in biotites (based on 22 oxygens)

a) Cationic proportions of Mg vs. Fe for biotite data from the Caledonian granitoids of eastern Scotland. (key to symbols on fold out sheet).

b) Cationic proportions of Mg vs. Fe for biotite data from the Caledonian granitoids of western Scotland. (key to symbols on fold out sheet).

c) Cationic proportions of Mg vs. Fe for biotite data from all the Caledonian granitoids from Scotland. (key to symbols on fold out sheet).

Fig. 3:4



Biotites from the Lake District granites show a much smaller compositional variation than those of the Scottish granites. Biotite compositions from the Shap and Skiddaw granites show the same trend towards manganese enrichment as biotites from the Hill of Fare, Mt Battock and Bennachie granites, whilst biotites from the Eskdale granite do not show manganese levels commensurate with the observed iron enrichment in these biotites and have compositions on Fe/Fe+Mg v. Mn cation diagram similar to those observed in the Aberdeen and Cove Bay granites (Fig. 3:5a). On the Fe v. Mg cation diagram the biotites from Eskdale are more depleted in magnesium than biotites from Aberdeen and Cove Bay (Fig. 3:5b). The low levels of manganese observed in biotites from the Eskdale granite are thought to be due to preferential partition of manganese into the garnets within the Eskdale granite.

In summary, in the more fractionated intrusions there is increasing substitution of  $\text{Al}_2\text{O}_3$  for  $\text{Fe}_2\text{O}_3$  and FeO and MnO for MgO in the biotite lattice. The substitution of FeO and MnO for MgO in the biotite lattice implies that Mg is being rapidly depleted during fractional crystallization, and the substitution of  $\text{Al}_2\text{O}_3$  for  $\text{Fe}_2\text{O}_3$  with increasing FeO has implications for changes in the oxidation state of magmas during fractional crystallization, with the most fractionated granites (Cairngorm, Cromar and Glen Gairn) probably having a higher FeO/ $\text{Fe}_2\text{O}_3$  ratio than the less evolved granites as revealed by biotite compositions.

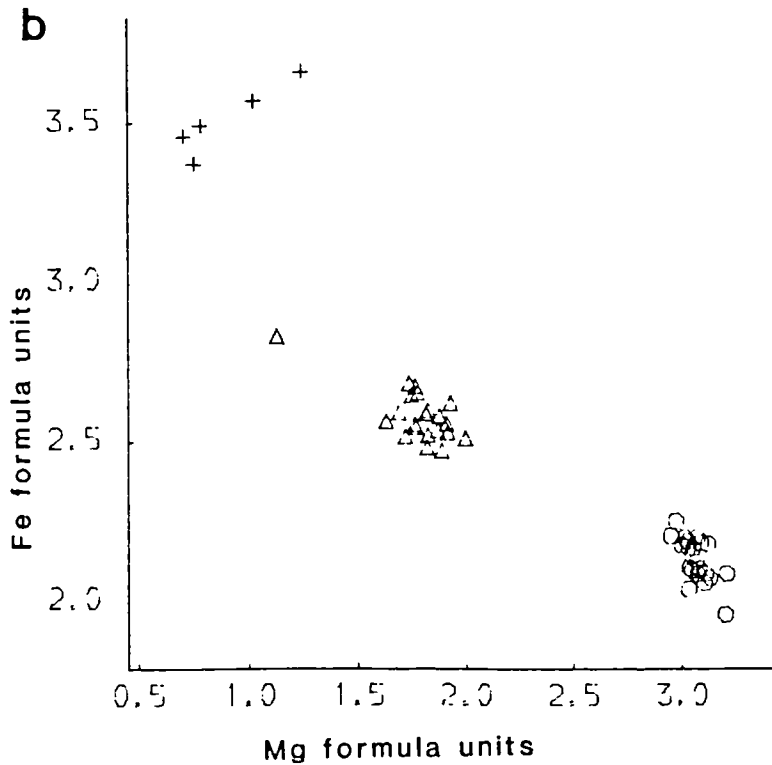
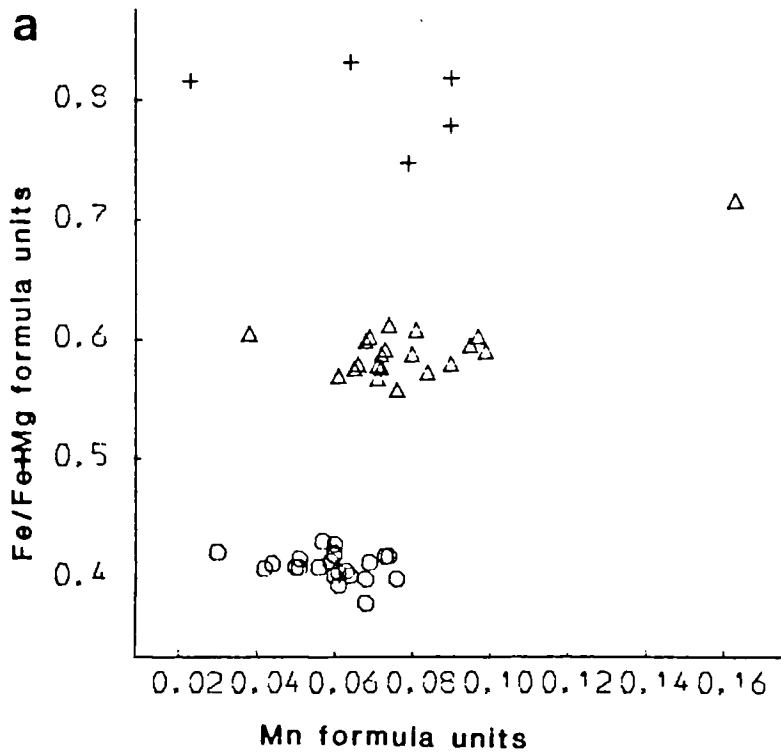


Fig. 3:5. Compositional variation in biotites (based on 22 oxygens). a) Cationic proportions of Mg vs. Fe/Fe+Mg for biotite data from the Caledonian granites of the Lake District. b) Cationic proportions of Mg vs. Fe for biotite data from the Caledonian granites of the Lake District. (key to symbols on fold out sheet).

TABLE 3:7. REPRESENTATIVE MICROPROBE DATA FOR BIOTITES FROM CALEDONIAN GRANITES (where a large compositional range was noted the end members are shown). ANALYSES ARE QUOTED IN WT% OXIDES.

	Garabal Hill Comrie				Kilmelford		Ballach- -ulish		Ben Nevis	Etive	Strontian	
	GH10	GH15	CM5	CM9	KM5	KM2	GGF6	8N13	ET7	SRN5	SRN10	
SiO <sub>2</sub>	35.7	36.1	36.9	34.3	36.7	36.6	36.3	35.7	36.7	36.0	35.7	
TiO <sub>2</sub>	6.1	3.9	4.2	5.2	5.7	5.2	3.7	4.3	5.0	2.3	4.5	
Al <sub>2</sub> O <sub>3</sub>	14.1	13.9	13.4	13.1	13.1	12.2	12.8	12.4	13.3	14.1	14.3	
Fe <sub>2</sub> O <sub>3</sub>	14.2	19.5	14.9	17.2	15.2	18.7	11.6	15.7	15.8	16.8	17.5	
MnO	0.1	0.3	0.6	0.2	0.2	0.1	0.3	0.3	0.3	0.3	0.2	
MgO	13.6	10.8	15.2	12.0	14.7	12.3	12.0	13.0	13.8	14.8	10.6	
CaO	0.1	0.0	0.0	0.0	0.0	0.0	0.0	0.1	0.0	0.2	0.0	
Na <sub>2</sub> O	0.2	0.3	0.5	0.4	0.4	0.2	0.2	0.5	0.6	0.4	0.2	
K <sub>2</sub> O	9.2	9.4	9.1	8.8	9.3	9.2	9.4	9.1	9.0	8.0	9.2	
TOT	93.3	94.2	94.8	91.0	95.4	94.4	93.3	90.9	94.5	92.9	92.3	
Mineral formula units (based on 22 oxygens).												
Si	5.46	5.61	5.57	5.47	5.52	5.65	5.67	5.66	5.57	5.56	5.61	
Ti	0.71	0.46	0.47	0.62	0.64	0.59	0.44	0.51	0.57	0.27	0.53	
Al	2.54	2.54	2.39	2.46	2.32	2.22	2.36	2.32	2.39	2.56	2.64	
Fe	1.81	2.54	1.88	2.29	1.91	2.41	2.43	2.08	2.00	2.17	2.29	
Mn	0.01	0.04	0.07	0.03	0.02	0.01	0.04	0.04	0.04	0.04	0.03	
Mg	3.10	2.51	3.42	2.84	3.29	2.83	2.80	3.08	3.13	3.41	2.48	
Ca	0.01	0.00	0.01	0.00	0.01	0.00	0.00	0.02	0.00	0.03	0.01	
Na	0.07	0.08	0.15	0.12	0.13	0.05	0.07	0.15	0.19	0.13	0.06	
K	1.80	1.86	1.76	1.79	1.79	1.80	1.87	1.84	1.75	1.57	1.85	
SUM	15.51	15.63	15.72	15.63	15.64	15.57	15.68	15.67	15.65	15.74	15.49	
Mg No.	63.1	49.8	64.5	55.4	63.2	54.0	53.6	59.7	61.0	61.1	51.9	
Moor of Strath Dorback Lochnagar Moy Ben Hill of Fare Bennachie Rannoch Ossian Rinnes												
	MR5	S010	TM21	LU20	BL48	M6	TM31	LU17	LU10	BA2	BA30	
SiO <sub>2</sub>	36.8	36.9	35.6	36.5	35.8	35.8	36.0	38.8	39.5	37.5	37.0	
TiO <sub>2</sub>	3.7	3.1	3.1	3.1	4.1	3.7	2.8	2.6	0.5	3.0	3.1	
Al <sub>2</sub> O <sub>3</sub>	14.1	13.9	14.4	14.0	12.7	13.1	15.7	11.8	24.2	13.1	14.9	
Fe <sub>2</sub> O <sub>3</sub>	16.4	17.5	19.7	17.9	19.2	17.8	20.4	15.5	20.5	18.7	20.7	
MnO	0.4	0.1	0.4	0.8	0.5	0.6	0.3	0.7	0.2	1.0	1.9	
MgO	13.0	13.0	11.4	14.8	11.7	11.8	9.5	13.3	1.9	12.4	6.8	
CaO	0.1	0.0	0.1	0.0	0.0	0.0	0.0	0.1	0.1	0.0	0.1	
Na <sub>2</sub> O	0.0	0.4	0.8	0.8	0.3	0.5	0.3	0.2	0.5	0.7	0.3	
K <sub>2</sub> O	8.7	9.5	9.4	8.1	9.5	9.6	9.6	10.1	9.2	9.9	9.2	
TOT	93.0	94.4	94.9	95.8	93.8	92.8	94.5	93.0	96.5	96.2	93.9	
Mineral formula units (based on 22 oxygens).												
Si	5.66	5.65	5.52	5.49	5.61	5.63	5.59	5.99	5.83	5.70	5.80	
Ti	0.42	0.36	0.37	0.35	0.48	0.43	0.32	0.30	0.05	0.34	0.37	
Al	2.56	2.51	2.63	2.99	2.35	2.44	2.87	2.14	4.22	2.34	2.76	
Fe	2.11	2.24	2.55	2.26	2.52	2.35	2.65	2.01	2.53	2.39	2.71	
Mn	0.06	0.02	0.05	0.09	0.07	0.08	0.04	0.09	0.02	0.12	0.25	
Mg	2.97	2.97	2.63	3.33	2.72	2.77	2.19	3.07	0.41	2.82	1.59	
Ca	0.01	0.00	0.01	0.00	0.00	0.01	0.00	0.02	0.01	0.01	0.01	
Na	0.00	0.13	0.23	0.22	0.10	0.14	0.09	0.06	0.13	0.19	0.08	
K	1.70	1.86	1.86	1.55	1.90	1.92	1.89	1.98	1.74	1.93	1.84	
SUM	15.49	15.73	15.85	15.79	15.74	15.76	15.65	15.66	14.95	15.85	15.41	
Mg No.	58.6	57.0	50.7	59.5	52.0	54.1	45.3	60.5	14.0	54.1	37.1	

TABLE 3:7 CONTINUED

	Mt Battock		Cromar		Cairngorm		Glen Gairn	Aber-	Ard-	Cove
	LU26	LU18	LU33A	TM24	CN3	TM53	GG7	-deen	-clach	Bay
								33-71	AD4	17-36
SiO <sub>2</sub>	38.1	39.0	36.6	36.6	35.3	41.0	43.0	32.9	34.9	33.8
TiO <sub>2</sub>	2.7	2.1	2.4	3.4	2.5	1.1	0.5	3.4	4.0	3.3
Al <sub>2</sub> O <sub>3</sub>	12.7	17.0	18.3	13.1	17.9	23.4	22.1	16.7	16.9	17.3
Fe <sub>2</sub> O <sub>3</sub>	17.1	16.9	23.0	23.8	25.3	16.1	11.6	25.0	22.6	25.0
MnO	0.9	1.1	1.3	0.5	0.9	1.8	3.2	0.2	0.6	0.4
MgO	11.7	7.1	3.0	9.0	3.8	1.4	0.0	5.9	6.8	5.7
CaO	0.0	0.1	0.1	0.0	0.1	0.3	0.1	0.1	0.0	0.0
Na <sub>2</sub> O	0.4	0.2	0.5	0.7	0.3	0.5	0.4	0.1	0.2	0.7
K <sub>2</sub> O	8.8	9.0	9.7	8.9	9.5	8.8	9.1	9.0	9.8	9.5
TOT	92.4	92.6	94.7	96.0	95.6	94.5	90.0	93.3	95.8	95.6

Mineral formula units (based on 22 oxygens)

Si	5.93	6.00	5.73	5.69	5.54	6.07	6.54	5.32	5.42	5.33
Ti	0.31	0.24	0.28	0.39	0.29	0.13	0.06	0.41	0.47	0.39
Al	2.34	3.08	3.38	2.39	3.31	4.08	3.97	3.18	3.09	3.21
Fe	2.23	2.17	3.01	3.09	3.32	1.99	1.48	3.38	2.93	3.29
Mn	0.12	0.15	0.17	0.06	0.12	0.22	0.42	0.02	0.08	0.05
Mg	2.73	1.62	0.69	2.08	0.89	0.32	0.00	1.42	1.57	1.35
Ca	0.00	0.02	0.02	0.00	0.02	0.05	0.01	0.01	0.00	0.00
Na	0.11	0.07	0.14	0.21	0.09	0.15	0.12	0.04	0.07	0.20
K	1.76	1.77	1.93	1.77	1.91	1.66	1.77	1.85	1.93	1.91
SUM	15.53	15.13	15.34	15.71	15.51	14.67	14.36	15.63	15.57	15.73
Mg No.	55.0	42.7	18.8	40.2	21.3	13.8	0.0	29.5	35.0	29.0

	Shap		Skiddaw		Eskdale	
	SH31	SD38	SD31	ED56	ED32	
SiO <sub>2</sub>	37.0	36.0	31.6	32.5	32.4	
TiO <sub>2</sub>	4.1	4.0	3.1	3.1	2.3	
Al <sub>2</sub> O <sub>3</sub>	13.3	16.8	17.5	15.0	19.6	
Fe <sub>2</sub> O <sub>3</sub>	16.5	19.7	19.8	26.2	25.4	
MnO	0.4	0.6	1.1	0.6	0.5	
MgO	13.3	8.8	4.4	5.0	2.9	
CaO	0.0	0.1	0.1	0.1	0.1	
Na <sub>2</sub> O	0.3	0.4	0.1	0.4	0.2	
K <sub>2</sub> O	9.0	9.6	8.3	8.4	9.1	
TOT	93.8	95.8	86.1	91.2	92.4	

Mineral formula units (based on 22 oxygens).

Si	5.67	5.48	5.41	5.42	5.29
Ti	0.47	0.46	0.39	0.38	0.28
Al	2.40	3.02	3.54	2.95	3.76
Fe	2.11	2.51	2.84	3.67	3.47
Mn	0.05	0.08	0.16	0.08	0.07
Mg	3.03	2.00	1.13	1.25	0.71
Ca	0.00	0.01	0.02	0.01	0.01
Na	0.08	0.10	0.04	0.11	0.05
K	1.76	1.86	1.82	1.79	1.88
SUM	15.58	15.53	15.36	15.67	15.52
Mg No.	59.0	44.3	28.6	25.4	16.9

## 3:5:iv. FELDSPARS.

In dealing with a large number of intrusions with varying compositions it is inevitable that the feldspar compositions will also vary considerably. The range of plagioclase compositions is larger in the intrusions of western Scotland with a range of An68 to An2 (Fig. 3:6a), with some substitution of sodium for potassium in the orthoclase. The granites of eastern Scotland have a smaller range of plagioclase compositions from An45 to An0 consistent with a smaller range in whole rock composition, with some substitution of sodium for potassium in orthoclase (Fig. 3:6b). In the two mica granites which are thought to be crustally derived, the plagioclase compositions vary from An84 to An28 consistent with the possibility of some relict plagioclase being present (Fig. 3:6c). Feldspars from the Lake District granophyres and microgranite have plagioclase compositions varying from An44 to An4 (Fig. 3:7b), and the granites from the Lake District granites have plagioclases which vary from An55 to An2 with considerable substitution of potassium and sodium (Fig. 3:7a). Representative feldspar compositions can be found in Table 3:8.

Fig. 3:6. Compositional variation of feldspars (see over page).

Fig. 3:6. Compositional variation in feldspars from the Caledonian granitoids of Scotland.

a) Or.-Ab.-An. variation diagram for feldspar compositions from Caledonian "juvenile" granitoids of western Scotland. (key to symbols on fold out sheet).

b) Or.-Ab.-An. variation diagram for feldspar compositions from Caledonian "juvenile" granitoids of eastern Scotland. (key to symbols on fold out sheet).

c) Or.-Ab.-An. variation diagram for feldspar compositions from Caledonian "S" type two mica granites of Scotland. (key to symbols on fold out sheet).

Fig. 3:6

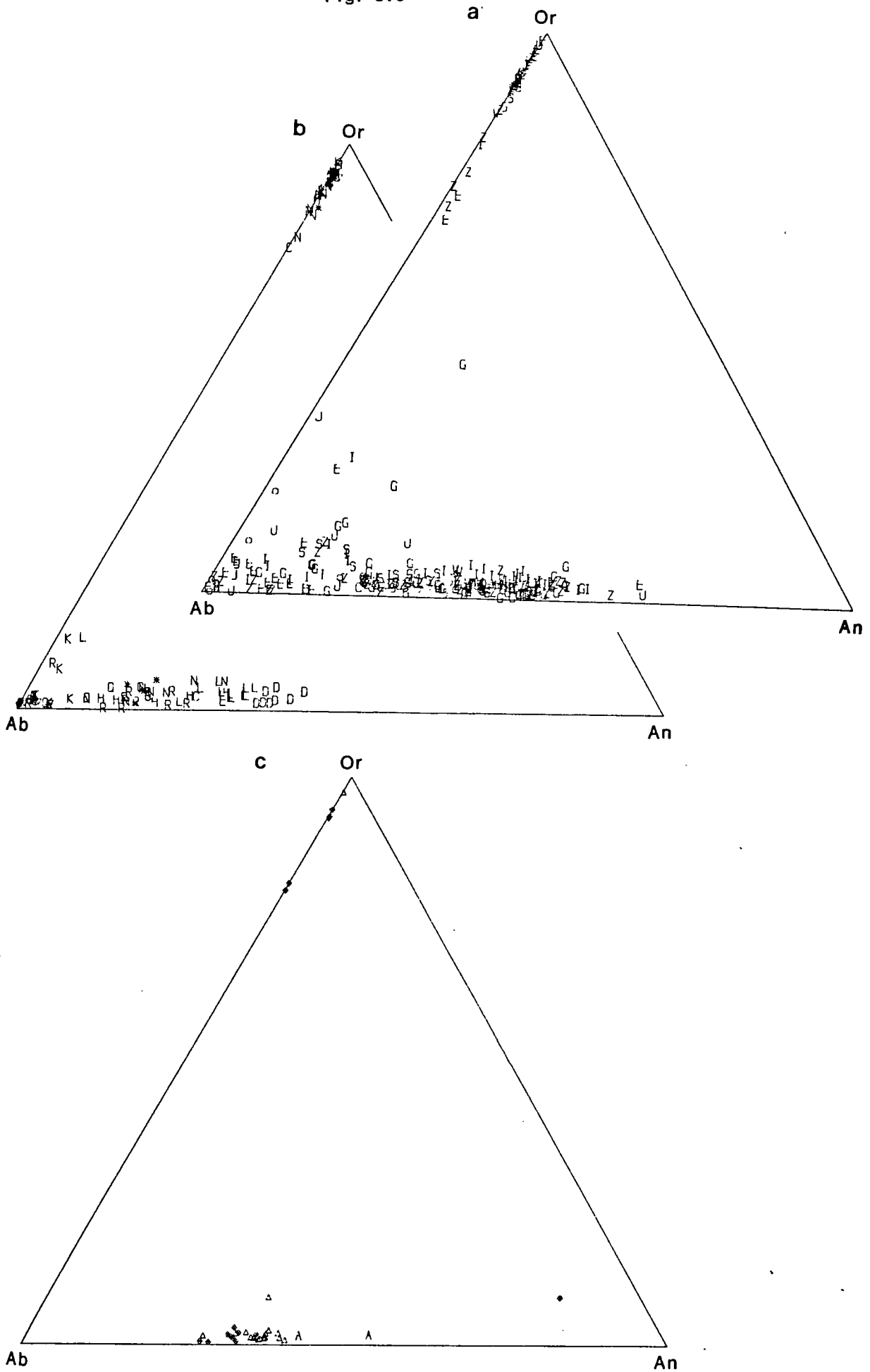


Fig. 3:7. Compositional variation in feldspars from the Caledonian granitoids from the Lake District. a) Or.-Ab.-An. variation diagram for feldspar compositions from the Caledonian granites of the Lake District. b) Or.-Ab.-An. variation diagram for feldspar compositions from the Caledonian microgranites and granophyres from the Lake District. (key to symbols on fold out sheet).

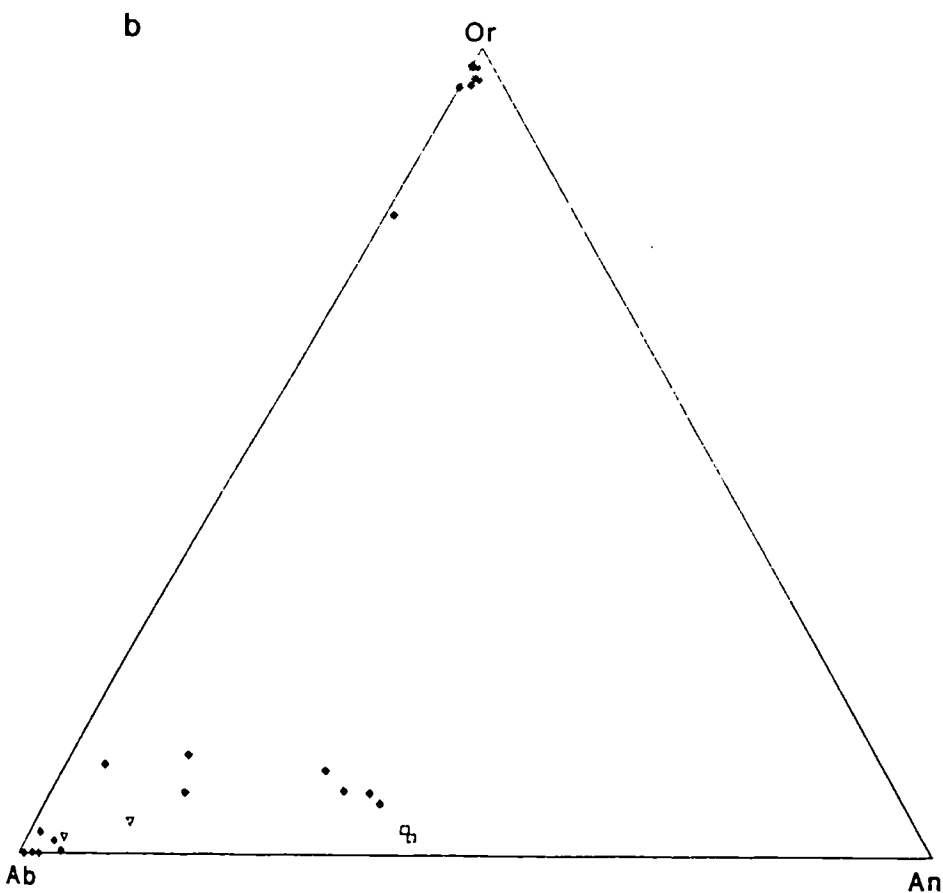
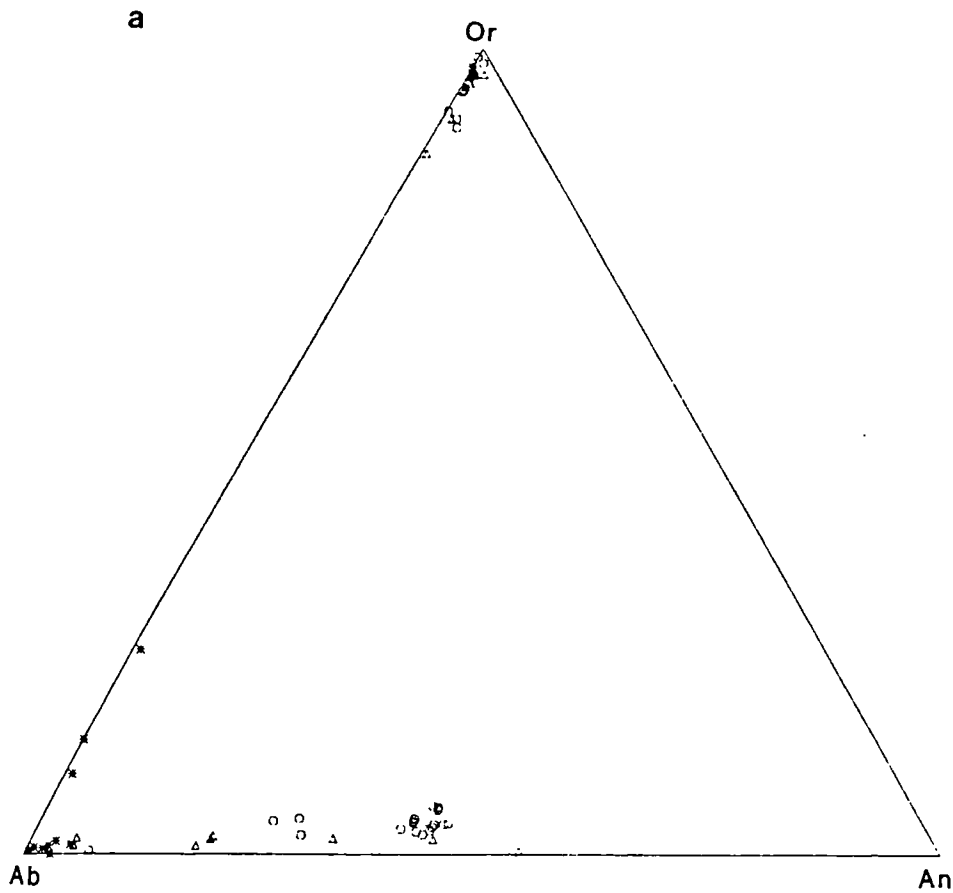


TABLE 3:8. REPRESENTATIVE MICROPROBE DATA FOR FELDSPARS FROM CALEDONIAN INTRUSIONS. ANALYSES QUOTED AS WT% OXIDES.

	Moor of Rannoch			Strath Ossian			Strontian		
	MR5	MR5	MR5	S03	S010	S03	SRN8	SRN5	SRN5
SiO <sub>2</sub>	59.3	62.9	63.9	60.0	62.0	65.3	59.3	64.4	64.5
TiO <sub>2</sub>	-	-	0.1	-	0.0	-	-	0.1	0.3
Al <sub>2</sub> O <sub>3</sub>	24.7	22.9	18.3	24.9	23.0	18.6	25.8	21.8	18.9
FeO	0.2	0.1	0.1	0.2	0.1	0.1	0.0	0.4	0.1
MnO	-	-	0.0	-	-	-	-	-	0.1
MgO	0.1	0.3	0.2	0.1	0.0	0.0	0.1	0.3	0.2
CaO	6.9	4.5	-	6.8	5.0	0.0	7.3	1.4	0.1
Na <sub>2</sub> O	7.1	8.8	1.5	7.5	8.8	1.4	7.1	9.8	2.1
K <sub>2</sub> O	0.2	0.2	13.7	0.3	0.2	13.8	0.2	0.8	14.1
TOT	98.5	99.6	97.8	99.8	99.1	99.2	99.9	99.1	100.4

Mineral formula units based on 32 oxygens

Si	10.72	11.16	11.97	10.72	11.10	12.02	10.59	11.46	11.83
Ti	-	-	0.01	-	0.01	-	-	0.01	0.04
Al	5.26	4.79	4.03	5.25	4.84	4.04	5.43	4.57	4.09
Fe	0.03	0.02	0.02	0.02	0.01	0.02	0.01	0.07	0.01
Mn	-	-	0.01	-	-	-	-	-	0.02
Mg	0.02	0.07	0.06	0.02	0.01	0.01	0.03	0.08	0.06
Ca	1.34	0.85	-	1.30	0.96	0.01	1.40	0.27	0.02
Na	2.50	3.04	0.54	2.59	3.05	0.49	2.44	3.38	0.75
K	0.05	0.04	3.26	0.06	0.05	3.23	0.04	0.19	3.29
SUM	19.93	19.98	19.90	19.98	20.02	19.82	19.94	20.03	20.12

	Kilmelford			Garabal Hill			Ballachulish		
	KM5	KM5	KM6	GH10	GH17	GH3	GGF5	GGF6	GGF6
SiO <sub>2</sub>	56.4	67.2	64.0	56.6	67.0	63.8	54.1	67.4	62.3
TiO <sub>2</sub>	0.2	0.1	0.2	0.2	0.0	0.1	0.0	0.1	0.5
Al <sub>2</sub> O <sub>3</sub>	26.8	20.7	18.3	26.4	21.1	18.7	27.9	20.8	18.5
FeO	0.4	0.4	0.1	0.1	-	0.1	0.3	0.2	-
MnO	0.0	-	0.2	-	-	0.1	0.1	-	-
MgO	0.1	0.3	0.2	-	0.1	0.3	-	0.3	0.1
CaO	8.7	1.0	0.0	8.7	0.8	-	10.8	0.5	0.0
Na <sub>2</sub> O	5.9	10.7	0.9	6.2	10.4	1.4	5.1	11.1	0.4
K <sub>2</sub> O	0.3	0.6	14.7	0.3	0.4	15.5	0.2	-	16.1
TOT	98.9	100.9	98.6	98.4	99.9	99.9	98.5	100.4	97.9

Mineral formula units based on 32 oxygens

Si	10.24	11.71	11.95	10.31	11.73	11.84	9.92	11.75	11.81
Ti	0.03	0.01	0.03	0.03	0.01	0.01	0.01	0.01	0.08
Al	5.73	4.26	4.02	5.67	4.35	4.08	6.04	4.27	4.12
Fe	0.06	0.05	0.02	0.01	-	0.01	0.04	0.03	-
Mn	0.01	-	0.03	-	-	0.02	0.01	-	-
Mg	0.02	0.07	0.04	-	0.04	0.08	-	0.07	0.03
Ca	1.69	0.18	0.01	1.69	0.15	-	2.12	0.09	0.01
Na	2.09	3.63	0.34	2.18	3.54	0.49	1.81	3.76	0.14
K	0.07	0.12	3.50	0.07	0.09	3.67	0.04	-	3.88
SUM	19.94	20.03	19.93	19.96	19.91	20.19	19.99	19.99	20.07

TABLE 3:8 CONTINUED.

	Comrie Diorite			Ben Nevis			Etive		
	CM1	CM2	CM5	BN16	BN13	BN16	ET2	ET4	ET7
SiO <sub>2</sub>	55.6	63.7	63.3	59.9	61.2	63.8	54.9	67.9	63.9
TiO <sub>2</sub>	-	0.1	0.3	0.2	-	0.3	-	-	0.6
Al <sub>2</sub> O <sub>3</sub>	28.3	23.6	17.8	23.6	23.1	17.8	28.3	19.9	18.8
Fe <sub>2</sub> O <sub>3</sub>	0.4	0.2	0.4	0.2	0.3	0.2	0.4	-	0.1
MnO	0.0	0.1	0.1	0.0	0.1	-	-	0.1	0.1
MgO	0.4	0.3	0.0	0.3	-	-	0.4	0.2	0.0
CaO	9.8	4.4	-	5.9	4.8	-	10.4	0.1	0.0
Na <sub>2</sub> O	5.8	8.9	0.7	7.8	7.8	2.3	5.0	11.6	0.5
K <sub>2</sub> O	0.2	0.3	15.8	0.3	0.6	13.3	0.5	0.1	15.9
TOT	100.5	101.6	98.5	98.1	97.9	97.7	99.8	99.9	101.1

Mineral formula units based on 32 oxygens

Si	9.97	11.11	11.93	10.86	11.09	11.98	9.93	11.89	11.84
Ti	-	0.01	0.04	0.02	-	0.04	-	-	0.08
Al	5.98	4.85	3.96	5.05	4.93	3.94	6.04	4.11	4.10
Fe	0.05	0.03	0.06	0.03	0.05	0.03	0.05	-	0.01
Mn	0.01	0.01	0.02	0.01	0.01	-	-	0.01	0.02
Mg	0.11	0.08	0.01	0.08	-	-	0.10	0.05	0.01
Ca	1.89	0.82	-	1.15	0.94	-	2.01	0.02	0.01
Na	2.01	2.99	0.26	2.74	2.73	0.84	1.74	3.95	0.18
K	0.03	0.07	3.81	0.06	0.14	3.19	0.11	0.01	3.76
SUM	20.06	19.98	20.08	19.99	19.88	20.03	19.97	20.04	19.99

	Comrie granite			Helmsdale		Lochnagar		Dorback		
	CM7	CM5	CM5	35-87	35-87	BL48	LU20	LU20	TM21	TM21
SiO <sub>2</sub>	61.5	67.3	65.8	65.5	67.9	63.3	64.8	64.5	60.8	63.9
TiO <sub>2</sub>	-	0.1	0.1	0.1	-	0.1	0.0	-	0.1	0.2
Al <sub>2</sub> O <sub>3</sub>	24.7	19.7	19.0	20.8	19.7	22.7	21.8	17.9	23.7	17.8
Fe <sub>2</sub> O <sub>3</sub>	0.2	0.3	0.2	0.3	0.2	0.0	0.1	0.2	0.3	0.2
MnO	-	0.1	-	-	-	0.2	-	-	0.1	-
MgO	0.4	0.1	0.2	-	0.2	-	0.1	-	0.1	-
CaO	5.4	0.3	0.2	2.4	0.0	4.6	3.1	-	5.7	0.1
Na <sub>2</sub> O	8.5	11.5	4.4	9.5	11.0	8.4	9.1	1.3	7.7	0.6
K <sub>2</sub> O	0.4	0.2	10.1	0.4	0.3	0.3	0.3	15.5	0.3	16.3
TOT	101.1	99.5	100.1	98.9	99.2	99.7	99.1	99.4	98.5	99.1

Mineral formula units based on 32 oxygens

Si	10.84	11.86	11.91	11.64	11.95	11.23	11.48	11.99	10.95	11.97
Ti	-	0.02	0.02	0.01	-	0.01	0.01	-	0.01	0.03
Al	5.12	4.09	4.06	4.35	4.09	4.75	4.55	3.93	5.04	3.94
Fe	0.03	0.04	0.04	0.04	0.02	0.01	0.02	0.04	0.04	0.03
Mn	-	0.01	-	-	-	0.03	-	-	0.01	-
Mg	0.11	0.03	0.05	-	0.05	-	0.03	-	0.01	-
Ca	1.02	0.05	0.04	0.46	0.01	0.88	0.58	-	1.09	0.01
Na	2.90	3.92	1.54	3.27	3.75	2.91	3.12	0.47	2.68	0.23
K	0.09	0.04	2.33	0.09	0.06	0.07	0.03	3.68	0.06	3.90
SUM	20.10	20.06	19.98	19.85	19.91	19.87	19.82	20.11	19.89	20.09

TABLE 3:8 CONTINUED.

	Ben Rinnes			Bennachie			Moy	
	TM31	TM36	TM31	8A8	8A8	8A2	M6	M6
SiO	63.7	67.5	64.3	63.1	66.2	64.6	68.6	64.6
TiO <sup>2</sup>	-	0.1	-	0.0	-	-	-	-
Al <sup>2</sup> O	22.1	19.6	18.5	22.1	20.5	18.3	19.0	18.3
Fe <sup>2</sup> O <sup>3</sup>	0.2	0.2	0.1	0.2	0.1	-	0.2	0.1
MnO	-	-	-	-	0.0	0.1	-	-
MgO	-	0.2	0.0	0.1	0.1	0.1	0.3	-
CaO	3.4	0.2	0.1	3.9	1.2	-	1.9	0.2
Na <sup>2</sup> O	9.4	11.1	1.1	8.5	10.2	1.5	8.5	1.7
K <sup>2</sup> O	0.1	0.1	15.0	0.6	0.2	14.7	0.1	15.0
TOT	98.9	99.0	99.1	98.6	98.5	99.2	98.4	99.9

Mineral formula units based on 32 oxygens

Si	11.36	11.92	11.95	11.31	11.76	11.99	12.09	11.95
Ti	-	0.02	-	0.01	-	-	-	-
Al	4.64	4.08	4.05	4.67	4.29	3.99	3.94	3.99
Fe	0.03	0.03	0.02	0.03	0.01	-	0.02	0.01
Mn	-	-	-	-	0.01	0.01	-	-
Mg	-	0.06	0.01	0.02	0.02	0.02	0.07	-
Ca	0.65	0.03	0.02	0.75	0.23	-	0.36	0.03
Na	3.25	3.79	0.41	2.96	3.49	0.54	2.89	0.62
K	0.03	0.02	3.55	0.14	0.04	3.48	0.03	3.53
SUM	19.96	19.94	20.01	19.90	19.86	20.02	19.40	20.13

	Cromar			Cairngorm			Hill of Fare		
	LU33	LU33	LU33	TM24	CN3	CN3	LU17	LU8	LU10
SiO	65.1	68.4	64.5	63.0	67.7	63.7	62.7	66.4	63.6
TiO <sup>2</sup>	0.1	-	0.1	-	-	0.1	0.1	-	0.5
Al <sup>2</sup> O	21.4	20.1	18.1	21.5	19.5	18.0	22.7	20.4	18.4
Fe <sup>2</sup> O <sup>3</sup>	0.1	-	0.2	0.2	0.1	-	0.3	0.0	0.1
MnO	0.1	0.1	-	-	0.1	-	0.1	-	-
MgO	0.1	0.2	-	-	0.1	-	0.1	0.1	0.0
CaO	2.2	0.2	0.0	3.5	0.3	0.1	4.0	1.5	0.1
Na <sup>2</sup> O	9.6	10.9	0.9	9.2	10.9	0.8	8.3	9.9	1.2
K <sup>2</sup> O	0.5	0.1	16.0	0.3	0.1	15.8	0.4	0.2	15.2
TOT	99.1	99.9	100.0	97.7	98.6	98.6	98.6	98.5	99.1

Mineral formula units based on 32 oxygens

Si	11.55	11.92	11.97	11.38	11.97	11.96	11.22	11.78	11.87
Ti	0.01	-	0.02	-	-	0.02	0.01	-	0.07
Al	4.47	4.14	3.96	4.59	4.06	3.98	4.79	4.27	4.04
Fe	0.01	-	0.03	0.03	0.01	-	0.05	0.01	0.02
Mn	0.01	0.01	-	-	0.01	-	0.01	-	-
Mg	0.04	0.05	-	-	0.03	-	0.04	0.03	0.01
Ca	0.41	0.03	0.01	0.68	0.05	0.02	0.76	0.28	0.02
Na	3.31	3.69	0.32	3.23	3.72	0.31	2.89	3.39	0.42
K	0.10	0.03	3.79	0.06	0.03	3.77	0.08	0.04	3.61
SUM	19.91	19.87	20.09	19.97	19.87	20.07	19.86	19.80	20.06

TABLE 3:8 CONTINUED.

	Mt Battock		Glen Gairn		Aberdeen		Ardclach		
	LU4	LU4	GG9	TM53	33-71	33-71	AD4	AD3	AD4
SiO <sub>2</sub>	67.2	63.1	68.5	65.6	56.1	58.9	61.0	63.2	63.4
TiO <sub>2</sub>	-	0.2	0.1	-	-	0.0	-	-	0.2
Al <sub>2</sub> O <sub>3</sub>	19.7	18.0	20.2	18.7	24.9	23.4	23.7	22.7	18.3
FeO <sup>3</sup>	0.4	0.5	0.1	0.1	0.0	0.0	0.1	0.1	-
MnO	-	-	-	-	0.0	0.1	-	0.1	-
MgO	0.1	-	0.4	0.0	0.1	-	0.2	0.1	0.1
CaO	0.6	-	0.2	0.1	7.5	5.8	5.7	3.6	0.0
Na <sub>2</sub> O	10.7	0.6	11.2	0.7	6.3	7.6	8.1	9.1	0.4
K <sub>2</sub> O	0.1	15.5	0.2	14.8	0.2	0.2	0.1	0.2	15.8
TOT	98.7	97.9	100.9	100.1	95.1	96.1	98.8	99.0	98.2

Mineral formula units on the basis of 32 oxygens

Si	11.89	11.93	11.86	12.01	10.53	10.89	10.95	11.26	11.93
Ti	-	0.03	0.01	-	-	0.01	-	-	0.03
Al	4.10	4.02	4.13	4.04	5.49	5.10	5.01	4.77	4.06
Fe	0.06	0.08	0.02	0.02	0.01	0.01	0.01	0.01	-
Mn	-	-	-	-	0.01	0.02	-	0.01	-
Mg	0.03	-	0.09	0.01	0.01	-	0.04	0.04	0.02
Ca	0.11	-	0.04	0.02	1.50	1.15	1.09	0.68	0.01
Na	3.69	0.21	3.77	0.25	2.31	2.73	2.83	3.13	0.15
K	0.02	3.74	0.04	3.45	0.05	0.05	0.03	0.05	3.80
SUM	19.90	20.00	19.96	19.81	19.90	19.94	19.97	19.95	19.99

	Shap		Skiddaw			Eskdale		
	SH29	SH29	SH29	SD38	SD20	SD38	ED32	6153
SiO <sub>2</sub>	61.5	63.8	64.3	60.7	67.5	64.1	68.5	63.3
TiO <sub>2</sub>	0.0	-	0.1	0.0	0.0	0.2	-	-
Al <sub>2</sub> O <sub>3</sub>	25.0	21.4	18.7	22.2	19.6	19.7	20.0	17.8
FeO <sup>3</sup>	0.4	0.2	0.2	-	-	0.1	0.1	0.1
MnO	-	-	-	-	-	0.1	0.1	-
MgO	-	0.3	0.1	0.2	0.1	0.3	0.2	0.0
CaO	6.3	3.2	0.4	8.9	0.6	0.1	0.1	-
Na <sub>2</sub> O	7.2	8.7	1.3	7.4	10.8	2.0	11.3	0.4
K <sub>2</sub> O	0.5	0.5	14.6	0.1	0.1	13.8	0.0	16.5
TOT	100.9	98.0	99.5	99.4	98.8	100.3	100.3	98.1

Mineral formula units based on 32 oxygens

Si	10.84	11.46	11.89	10.93	11.93	11.74	11.92	11.98
Ti	0.01	-	0.01	0.01	0.01	0.03	-	-
Al	5.19	4.53	4.08	4.71	4.09	4.25	4.10	3.98
Fe	0.05	0.03	0.03	-	-	0.01	0.02	0.01
Mn	-	-	-	-	-	0.01	0.02	-
Mg	-	0.07	0.04	0.05	0.02	0.08	0.04	0.01
Ca	1.19	0.62	0.07	1.72	0.12	0.02	0.01	-
Na	2.46	3.02	0.45	2.59	3.71	0.72	3.83	0.14
K	0.12	0.12	3.44	0.02	0.03	3.24	0.01	3.97
SUM	19.86	19.84	20.01	20.02	19.89	20.08	19.95	20.09

TABLE 3:8 CONTINUED.

	Ennerdale		Threlkeld		Carrock Fell
	EN20	EN27	EN27	TK23	CF5
SiO	61.2	68.2	63.4	64.7	59.6
TiO <sup>2</sup>	0.1	0.1	0.2	0.1	0.0
Al <sup>3</sup>	23.0	19.6	18.2	20.7	24.0
FeO <sup>3</sup>	0.3	0.1	1.4	0.4	0.3
MnO	-	-	-	-	0.2
MgO	-	0.2	0.2	0.3	0.1
CaO	5.0	0.2	0.0	1.3	5.6
Na <sub>2</sub> O	7.7	10.9	0.4	9.9	7.6
K <sub>2</sub> O	0.9	0.0	16.4	0.5	0.4
TOT	98.3	99.2	100.1	97.8	98.1

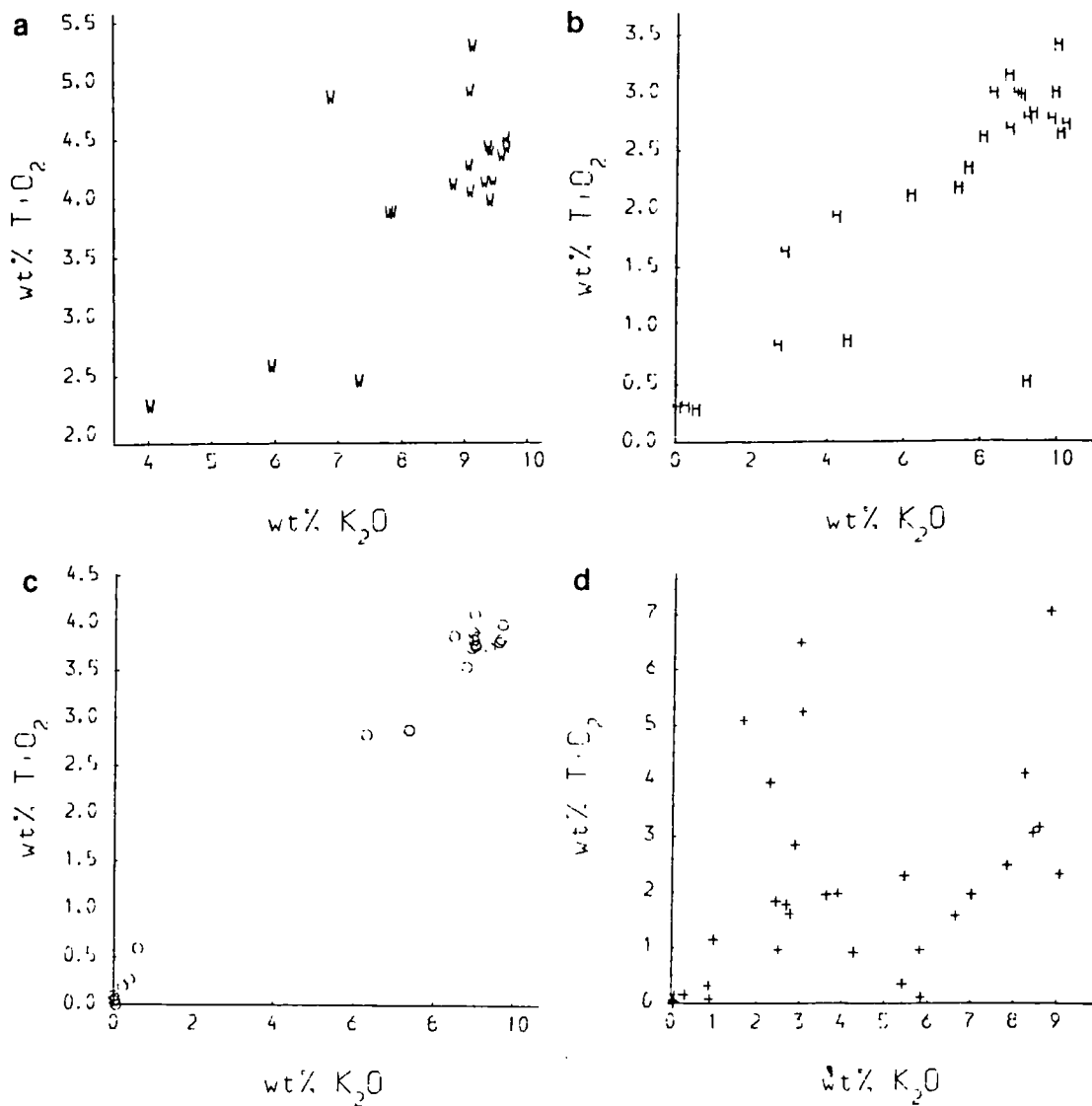
Mineral formula units based on 32 oxygens

Si	11.06	11.97	11.83	11.62	10.86
Ti	0.02	0.02	0.02	0.02	0.01
Al	4.91	4.05	4.01	4.37	5.13
Fe	0.05	0.01	0.21	0.06	0.05
Mn	-	-	-	-	0.03
Mg	-	0.05	0.05	0.08	0.02
Ca	0.97	0.03	0.01	0.25	1.09
Na	2.72	3.72	0.13	3.46	2.68
K	0.20	0.01	3.90	0.11	0.10
SUM	19.93	19.85	20.17	19.96	19.97

### 3:5:v. CHLORITES.

Chlorite is a frequent secondary mineral in the Caledonian granites commonly replacing biotite, and more rarely hornblende and pyroxene. The chemistry of chlorites and coexisting biotites from four Caledonian granites, Eskdale, Shap, Hill of Fare, and Ben Nevis, are compared in Figs. 3:8, 9 and 10, and it is apparent that with a decrease in K<sub>2</sub>O in the micas characteristic of chloritization there is a general decrease in TiO<sub>2</sub> (Fig. 3:8); with complete chloritization both K<sub>2</sub>O and TiO<sub>2</sub> are absent from the mineral. Potassium is highly mobile in aqueous solutions and may migrate out from the site of alteration, titanium on the other hand is not mobile in aqueous solutions and forms acicular crystals of rutile within the chlorite, as illustrated in Plate 3:8c. Together with

Fig. 3:8. Compositional variation during the change from biotite to chlorite, showing the variation of  $TiO_2$  with decreasing  $K_2O$  during chloritization of biotites (chlorites contain  $<1wt\% K_2O$ ) for biotite and chlorite analyses from a) Ben Nevis, b) Hill of Fare, c) Shap, d) Eskdale.



the decrease in  $K_2O$  content, a marked increase in the  $MgO$  and  $FeO$  content of the chlorites relative to that in the biotites is observed with the exception of chlorites from the Hill of Fare granite where  $MgO$  is depleted in the chlorites relative to the biotites, (Figs. 3:9 and 3:10). This behaviour is also observed in chlorites from the Cairngorm and Ben Rinnes granites, which all have low levels of  $MgO$  in the whole rock analysis. Representative analyses of chlorites from the Caledonian granites are shown in Table 3:9.

TABLE 3:9. REPRESENTATIVE MICROPROBE ANALYSES OF CHLORITES FROM CALEDONIAN INTRUSIONS. ANALYSES ARE QUOTED IN WT% OXIDES.

	Garabal Hill		Stron-	Kilmel-	Moor of Ballachulish			Comrie	Helmsdale	
	GH14	GH15	tian	ford	MR1	BN16	GGF6	CM6	CM6	36-102
			SRN6	KM8						
SiO <sub>2</sub>	30.0	26.2	26.2	31.0	35.7	32.7	26.7	29.0	36.1	27.9
TiO <sub>2</sub>	-	0.1	0.1	4.4	3.6	2.2	0.1	0.1	3.2	0.1
Al <sub>2</sub> O <sub>3</sub>	16.2	18.7	19.3	15.9	13.9	14.2	19.5	17.9	15.7	17.6
Fe <sub>2</sub> O <sub>3</sub>	16.4	23.6	21.4	20.6	17.4	19.7	23.3	18.9	13.6	20.9
MnO	0.2	0.2	0.6	0.1	0.3	0.1	0.4	0.5	0.5	1.0
MgO	23.7	17.0	18.1	13.6	14.1	15.3	17.5	20.6	15.9	17.7
CaO	0.1	-	0.0	0.3	0.2	0.2	0.1	0.0	0.3	0.1
Na <sub>2</sub> O	0.4	0.4	0.3	0.8	0.5	0.1	0.2	0.6	0.1	0.5
K <sub>2</sub> O	0.0	0.0	0.0	4.2	7.4	4.0	-	0.1	5.5	0.1
TOT	87.0	86.1	86.0	90.8	93.1	88.6	87.7	87.7	90.7	85.9

Mineral formula units based on 28 oxygens

Si	6.073	5.591	5.544	6.290	7.002	6.716	5.571	5.911	7.017	5.904
Ti	-	0.008	0.017	0.670	0.537	0.345	0.009	0.009	0.464	0.010
Al	3.868	4.710	4.807	3.811	3.221	3.443	4.798	4.305	3.594	4.394
Fe	2.773	4.214	3.782	3.493	2.860	3.396	4.073	3.218	2.210	3.696
Mn	0.031	0.040	0.111	0.019	0.042	0.023	0.064	0.088	0.077	0.174
Mg	7.139	5.403	5.704	4.106	4.137	4.704	5.446	6.265	4.604	5.582
Ca	0.028	-	0.007	0.054	0.040	0.042	0.027	0.002	0.056	0.018
Na	0.157	0.157	0.119	0.295	0.175	0.040	0.065	0.229	0.034	0.197
K	0.008	0.003	0.005	1.088	1.851	1.058	-	0.029	1.367	0.027
SUM	20.076	20.126	20.097	19.826	19.864	19.766	20.053	20.056	19.423	20.001

Fig. 3:9. Compositional variation during the change from biotite to chlorite, showing the variation of MgO with decreasing  $K_2O$  during chloritization of biotites (chlorites contain  $<1$  wt%  $K_2O$ ) for biotite and chlorite analyses from a) Ben Nevis, b) Hill of Fare, c) Shap, d) Eskdale.

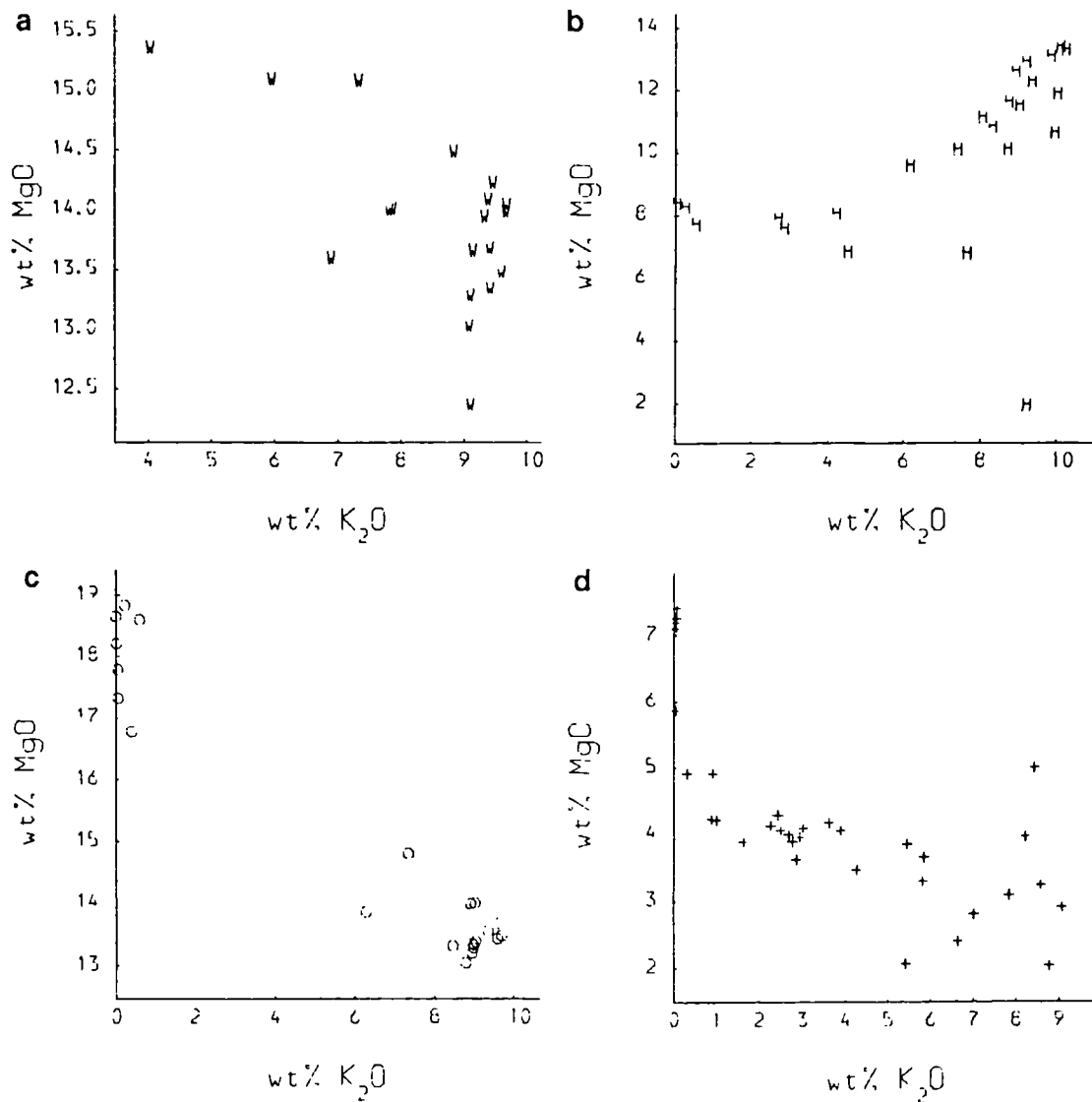


Fig. 3:10. Compositional variation during the change from biotite to chlorite, showing the variation of FeO with decreasing  $K_2O$  during chloritization of biotites (chlorites contain <1 wt%  $K_2O$ ) for biotite and chlorite analyses from a) Ben Nevis, b) Hill of Fare, c) Shap, d) Eskdale.

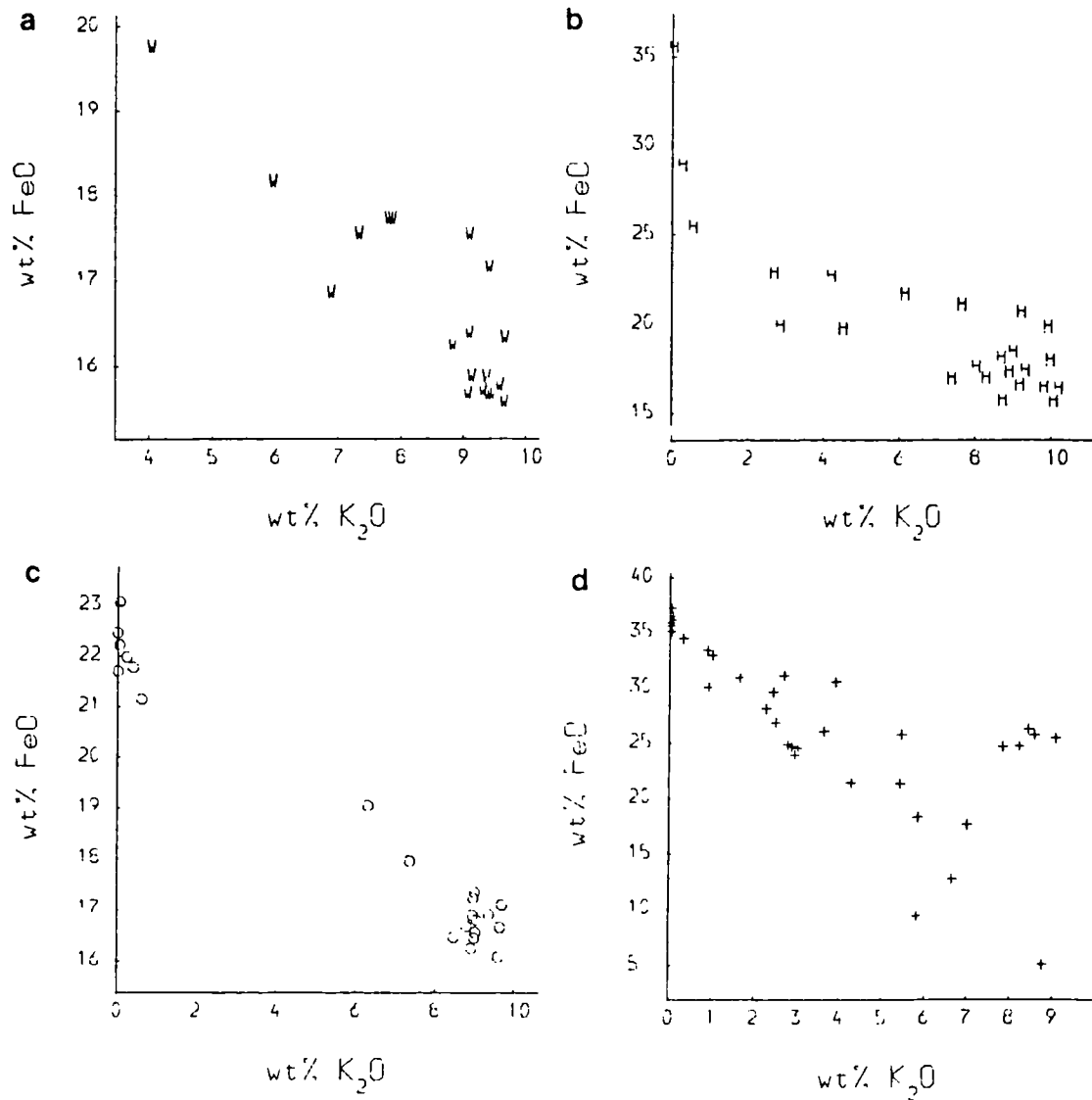


TABLE 3:9 CONTINUED.

	Etive		Loch- nagar	Moy M3	Mt. Battock LU4A	Hill of Fare LU10	Benn- achie BA2	Cove Bay 17-36	Ben Rinnes TM36
SiO	27.6	27.0	26.8	33.0	28.1	26.5	34.9	23.6	26.5
TiO <sup>2</sup>	-	2.6	-	2.1	0.3	0.3	1.7	1.2	0.1
Al <sup>3</sup>	19.4	17.7	18.9	15.2	19.2	21.8	13.8	19.4	20.9
Fe <sup>3</sup>	20.0	24.2	22.0	19.7	20.3	28.8	18.4	34.8	32.9
MnO	0.4	0.8	1.0	0.6	0.5	1.2	0.9	0.2	0.5
MgO	20.5	15.0	17.5	12.6	18.0	8.2	13.6	6.6	7.3
CaO	-	0.1	0.2	0.2	0.1	0.2	0.1	-	0.1
Na <sup>0</sup>	0.3	0.1	0.4	0.4	1.1	0.5	0.4	0.5	0.4
K <sup>0</sup>	0.1	0.1	0.1	4.4	0.1	0.3	5.8	0.2	0.0
TOT	88.3	87.5	86.8	88.0	87.6	87.6	89.5	86.5	88.7

Mineral formula units based on 28 oxygens.

Si	5.623	5.701	4.647	6.840	5.785	5.713	7.112	5.366	5.734
Ti	-	0.416	-	0.326	0.040	0.047	0.259	0.206	0.023
Al	4.653	4.398	4.696	3.718	4.654	5.523	3.317	5.210	5.322
Fe	3.412	4.263	3.871	3.412	3.507	5.181	3.147	6.624	5.957
Mn	0.009	0.147	0.185	0.109	0.086	0.213	0.159	0.041	0.083
Mg	6.227	4.716	5.477	3.885	5.520	2.630	4.134	2.230	2.365
Ca	-	0.020	0.047	0.036	0.029	0.035	0.015	-	0.012
Na	0.122	0.020	0.143	0.149	0.432	0.200	0.150	0.238	0.164
K	0.013	0.024	0.019	1.152	0.024	0.074	1.500	0.055	0.011
SUM	20.119	19.706	20.086	19.626	20.076	19.616	19.795	19.971	19.670

Cromar Cairn-  
gorm

	LU33	CN36	SH29	SD41	ED32
SiO	23.5	25.8	27.2	24.4	26.6
TiO <sup>2</sup>	-	0.1	-	0.1	0.3
Al <sup>3</sup>	20.3	20.3	18.3	19.0	22.0
Fe <sup>3</sup>	37.5	33.7	23.1	29.8	33.4
MnO	2.8	1.6	0.4	0.8	0.8
MgO	4.0	5.1	17.3	10.9	4.2
CaO	0.0	0.2	0.1	0.0	-
Na <sup>0</sup>	0.3	0.3	0.6	0.1	0.4
K <sup>0</sup>	-	0.4	0.1	0.1	0.9
TOT	88.5	87.5	87.0	85.0	88.8

mineral formula units based on 28 oxygens

Si	5.357	5.757	5.742	5.492	5.790
Ti	-	0.023	-	0.014	0.052
Al	5.437	5.328	4.534	5.037	5.657
Fe	7.146	6.274	4.067	5.608	6.085
Mn	0.530	0.296	0.070	0.149	0.151
Mg	1.368	1.708	5.442	3.649	1.376
Ca	0.010	0.045	0.014	0.002	-
Na	0.150	0.138	0.229	0.035	0.186
K	-	0.108	0.016	0.017	0.247
SUM	19.999	19.679	20.114	20.002	19.545

## 3:5:vi. MUSCOVITES.

The chemistry of muscovites, whether they are primary as in the Aberdeen, Ardclach and Cove Bay intrusions, or secondary as in most of the other granites, is similar. The iron and magnesium contents are variable in both groups, the only notable differences are the secondary muscovites in the Glen Gairn greisen which are relatively enriched in manganese. Representative microprobe analyses of primary muscovites are shown in Table 3:10, and secondary muscovites in Table 3:11.

---

TABLE 3:10. REPRESENTATIVE MICROPROBE DATA FOR PRIMARY MUSCOVITES IN CALEDONIAN GRANITES. ANALYSES QUOTED IN WT% OXIDES.

	Aberdeen 33-71A	Ardclach AD3	Cove Bay 17-36
SiO <sub>2</sub>	43.2	45.5	45.9
TiO <sub>2</sub>	1.1	2.0	1.0
Al <sub>2</sub> O <sub>3</sub>	33.1	29.9	33.6
Fe <sub>2</sub> O <sub>3</sub>	1.6	3.8	2.6
MnO	-	0.1	0.0
MgO	0.8	1.2	1.2
CaO	-	0.0	0.0
Na <sub>2</sub> O	0.7	0.5	0.7
K <sub>2</sub> O	9.8	10.8	11.2
TOT	90.2	93.9	96.2

Mineral formula units based on 22 oxygens

Si	6.099	6.281	6.138
Ti	0.113	0.206	0.103
Al	5.500	4.864	5.299
Fe	0.188	0.442	0.293
Mn	-	0.013	0.001
Mg	0.166	0.253	0.229
Ca	-	0.006	0.004
Na	0.183	0.126	0.171
K	1.761	1.902	1.915
SUM	14.010	14.094	14.153

---

TABLE 3:11 REPRESENTATIVE MICROPROBE ANALYSES OF SECONDARY MUSCOVITES IN CALEDONIAN GRANITES. ANALYSES QUOTED IN WT% OXIDES.

	Kilmel- ford KM10	Garabal Hill GH17	Cromar LU33	LU33	Ben Rinnes TM36	Cairn- gorm CN3	Glen GG7	Gairn GG9	Hill of Fare LU10
SiO	49.3	47.6	45.3	45.2	44.2	45.6	47.0	47.4	44.8
TiO <sup>2</sup>	-	0.0	-	0.3	0.9	0.3	0.1	-	0.6
Al <sup>3+</sup>	31.1	28.8	34.8	27.3	31.0	26.8	28.8	34.5	32.2
Fe <sup>3+</sup>	2.3	2.9	2.4	7.6	4.3	6.7	5.8	1.3	4.1
MnO	0.2	0.0	0.2	0.5	0.2	0.3	1.4	0.7	0.1
MgO	1.6	3.4	0.2	1.7	0.7	1.9	-	0.5	1.0
CaO	0.1	0.1	-	-	-	0.0	0.1	-	0.1
Na <sup>0</sup>	0.2	0.3	0.7	0.6	0.7	0.4	0.1	0.2	0.6
K <sup>2+</sup>	9.9	11.2	10.7	10.4	10.3	10.9	9.9	10.4	11.1
TOT	94.9	94.4	94.3	93.7	92.1	93.0	93.2	95.0	94.6

Mineral formula units based on 22 oxygens

Si	6.585	6.497	6.151	6.389	6.217	6.465	6.563	6.317	6.157
Ti	-	0.004	-	0.030	0.090	0.032	0.007	-	0.064
Al	4.899	4.626	5.570	4.542	5.136	4.483	4.744	5.428	5.208
Fe	0.252	0.335	0.270	0.903	0.507	0.798	0.672	0.144	0.473
Mn	0.017	0.003	0.020	0.061	0.023	0.041	0.167	0.079	0.006
Mg	0.327	0.689	0.036	0.362	0.136	0.393	-	0.093	0.201
Ca	0.011	0.016	-	-	-	0.006	0.016	-	0.010
Na	0.060	0.074	0.189	0.167	0.183	0.121	0.019	0.044	0.170
K	1.690	1.954	1.843	1.881	1.848	1.963	1.757	1.773	1.943
SUM	13.840	14.200	14.080	14.335	14.141	14.303	13.946	13.878	14.232

Eskdale                      Skiddaw Threlkeld

	ED40	ED40	SD31	TK23
SiO	46.8	47.0	45.8	46.8
TiO <sup>2</sup>	-	-	0.5	-
Al <sup>3+</sup>	30.9	30.9	34.9	27.7
Fe <sup>3+</sup>	4.9	1.2	1.6	4.8
MnO	0.1	0.1	0.1	0.0
MgO	1.6	1.2	1.1	1.5
CaO	-	0.1	0.1	0.1
Na <sup>0</sup>	0.6	0.7	0.9	0.0
K <sup>2+</sup>	10.5	9.6	9.6	9.5
TOT	95.4	90.7	94.5	90.3

Mineral formula units based on 22 oxygens

Si	6.356	6.534	6.140	6.647
Ti	-	-	0.048	-
Al	4.941	5.056	5.510	4.631
Fe	0.553	0.144	0.184	0.565
Mn	0.014	0.009	0.016	0.001
Mg	0.326	0.240	0.210	0.322
Ca	-	0.018	0.013	0.011
Na	0.153	0.178	0.224	0.008
K	1.817	1.694	1.648	1.712
SUM	14.159	13.873	13.992	13.897

## 3:5:vii. OXIDES.

Both ilmenite and magnetite are common accessory minerals in the British Caledonian granites. The Fe/Ti ratio in ilmenites is variable but the available data do not indicate any systematic variation. However ilmenites from the more evolved granites, Bennachie, Mt Battock and Skiddaw contain appreciable amounts of manganese (Fig. 3:11a and b), similar to the biotites in these evolved granites. Rutile is found as a secondary mineral within chlorites in most of the granites.

## 3:5:viii. GARNETS.

The Eskdale granite is the only garnet bearing granite studied. All garnets analysed are of similar composition and are almandine rich with an end-member ratio alm:gross:spess:pyrop of 86:2:7:5.

## 3:5:ix. ACCESSORY RARE EARTH BEARING MINERALS.

The most important rare earth bearing minerals observed in granites are allanite, monazite and xenotime. Due to problems with standards for the rare earths, uranium and thorium, only partial analyses of these minerals were possible and therefore only limited observations can be made on variations in the compositions of these minerals. The distribution of these minerals has some bearing on both the total rare earth contents and the rare earth patterns observed in the granitoids. Generally speaking allanite is common in the less evolved granitoids whereas monazite and xenotime are more common in the more highly evolved granites such as Cairngorm, Bennachie and Skiddaw.



### 3:6 SUMMARY AND CONCLUSIONS.

a) Texturally cumulate phases can be recognized in Caledonian intrusives, and the cumulus assemblage varies from pyroxenes and oxides in the least evolved diorites, through pyroxene, hornblende, sphene, biotite, oxides and plagioclase, to biotite, oxides and plagioclase in the most evolved plutons.

b) S-type granites can be recognized texturally by the presence of early euhedral quartz, together with primary muscovite.

c) A large variation in biotite compositions is observed, with manganese enrichment in the biotites of the more evolved granites; conversely biotites from S-type granites have low manganese contents possibly reflecting residual garnet in the source retaining manganese. This is also seen in the Eskdale granite where manganese is preferentially partitioned into garnets.

## CHAPTER 4. CRITERIA FOR THE CLASSIFICATION OF THE CALEDONIAN GRANITES.

The earliest attempt at a classification of the British Caledonian granites (Read 1961) was based on field relations and for that reason it is still of value today. Read divided the granites into several groups on the basis of their time relationship with the various tectonic and metamorphic events of the Caledonides.

The first group includes the pre-Caledonian granites or "older granites" which display regional foliation trends in their fabric, for example Carn Chuinneag and Inchbae within the Moines and Ben Vuirich in the Dalradian. This grouping has later been substantiated by isotopic dating (Long 1964, Pankhurst & Pidgeon 1976, Pidgeon & Johnson 1974).

The second group Read identified was the migmatites formed during the regional metamorphic event of the Scottish Caledonides (the Grampian orogeny). Large areas of regional migmatites are found north of the Great Glen Fault in the Moines of Ross and Sutherland, in the Moines south of the Great Glen Fault and in the Dalradian of the Grampian Region.

The third group in Reads classification was the Assynt alkali suite of Ben Loyal, Loch Borrolan and Loch Ailsh which was identified as being later than the migmatization event. However the time relationships of this group with the "newer granites" of the Caledonides was at that stage unclear.

The next group of granitoid rocks in Reads classification is the appinite suite which are small bodies of various rock types which are generally diorites, monzonites and more alkaline types such as kentallanite. The appinite suite is closely associated both in time and space with the major "newer granite" intrusions, although from field relations they are rather earlier than the granites.

The next and by far the largest group of intrusions in the Read classification are the "newer granites". These are regarded as having been forcefully intruded into the Caledonian orogen and are in some cases (for example the Moor of Rannoch and Lairg-Rogart intrusions) surrounded by contact migmatites and are therefore early in the post-deformational events; indeed many of these are considered to have been unroofed before the deposition of the Lower Devonian conglomerates. These granites are separated in the Read classification from the "last" granites by a period of volcanic activity in the Lower Devonian. The "last" granites were intruded "passively" by cauldron subsidence and have associated ring faults and frequently have associated down faulted blocks of lava. A summary of Reads classification is to be found in table 4:1.

Later workers have subsequently modified the Read classification; Dewey and Pankhurst (1970) noted that some unfoliated granites belonged on the basis of their isotopic dates to the "older" granites and that the "newer" and "last" granites are of a similar age and not necessarily separated by a substantial time interval. Although this modification to Read's scheme was based on the available isotopic age data, it should be noted that most of the age determinations available at that time were K-Ar results which do not necessarily record intrusion ages. More recent

isotopic age data appear to uphold this modification (Table 2:1).

---

TABLE 4:1 SUMMARY OF READS CLASSIFICATION OF THE CALEDONIAN GRANITES.

<u>1</u>	<u>2</u>	<u>3</u>	<u>4</u>	<u>5</u>	<u>6</u>
<u>older</u>	<u>miqmatites</u>	<u>alkaline</u>	<u>appinites</u>	<u>newer</u>	<u>last</u>
<u>granites</u>		<u>suite</u>		<u>granites</u>	<u>granites</u>
				<u>(forceful)</u>	<u>(passive)</u>
Carn-	Strath-	Loch Borrolan		Helmsdale	Ben Nevis
Chuinneag	Hallidale	Ben Loyal		Rogart	Lochnagar
Ben Vuirich	Loch Coire	Loch Ailsh		Grudie	Etive
				Migdale	Glen Coe
				Cluanie	
				Strontian	
				Kilmelford	
				Ballachulish	
				Foyers	
				Moy	
				Ardclach	
				Ben Rinnes	
				Stritchen	
				Peterhead	
				Cove Bay	
				Aberdeen	
				Blackburn	
				Bennachie	
				Hill of Fare	
				Mt Battock	
				Cromar	
				Glenlivet	
				Dorback	
				Glen Gairn	
				Cairngorm	
				Strath Ossian	
				Moor of Rannoch	
				Garabal Hill	
				Comrie	

---

More recent work of Pankhust and Sutherland (1982) divided this now enlarged group of newer or post-metamorphic granites into three subgroups. Group 1 comprises the earliest post-metamorphic granites which on the basis of isotopic dating fall within 10-25 Ma of the climax of regional metamorphism; this group includes the Stritchen, Aberchider, Longmanhill, Aberdeen and Findhorn (Strathdearn) granites. These group 1 granites all have high  $Sr^{87}/Sr^{86}$  initial ratios indicative of a large

crustal component in their source. On the basis of petrography and mineral chemistry the Ardclach and Cove Bay granites may also belong to this group. The group 2 granites are of Late Ordovician to Early Silurian age (c 440-410 Ma), i.e. post dating the metamorphism by c 50 Ma. The group includes many of Read's forceful granites along with some "passively" intruded granites. The intrusions of this group comprise a wide variety of rock types, ranging from diorite to adamellite, which are often associated with appinites and more mafic and ultra-mafic rock types such as those seen in the Garabal Hill complex. Group 3 granites are of Lower Devonian age and younger (i.e. <410 Ma) and include both forcefully and passively intruded granites, (see Table 4:2 for further details of this classification). However even this classification does not conform with published isotopic dates for these granites (Table 2:1), for instance many of the granites classified as belonging to group 2 have isotopic dates which would place them in group 3, for example the Garabal Hill, Foyers, Ballachulish, Grudie, Strath Ossian and Moor of Rannoch intrusions.

---

TABLE 4:2 RECLASSIFICATION OF READ'S NEWER AND LAST GRANITES ACCORDING TO PANKHURST AND SUTHERLAND (1982)

<u>Group 1</u>	<u>Group 2</u>	<u>Group 3</u>
Stritchen	Strantian	Etive
Aberdeen	Kilmelford	Cairngorm
	Helmsdale	Ben Nevis
	Cluanie	Glen Coe
	Lochnagar	
	Hill of Fare	
	Garabal Hill	
	Foyers	
	Rogart	
	Ballachulish	
	Grudie	
	Migdale	
	Strath Ossian	
	Moor of Rannoch	

---

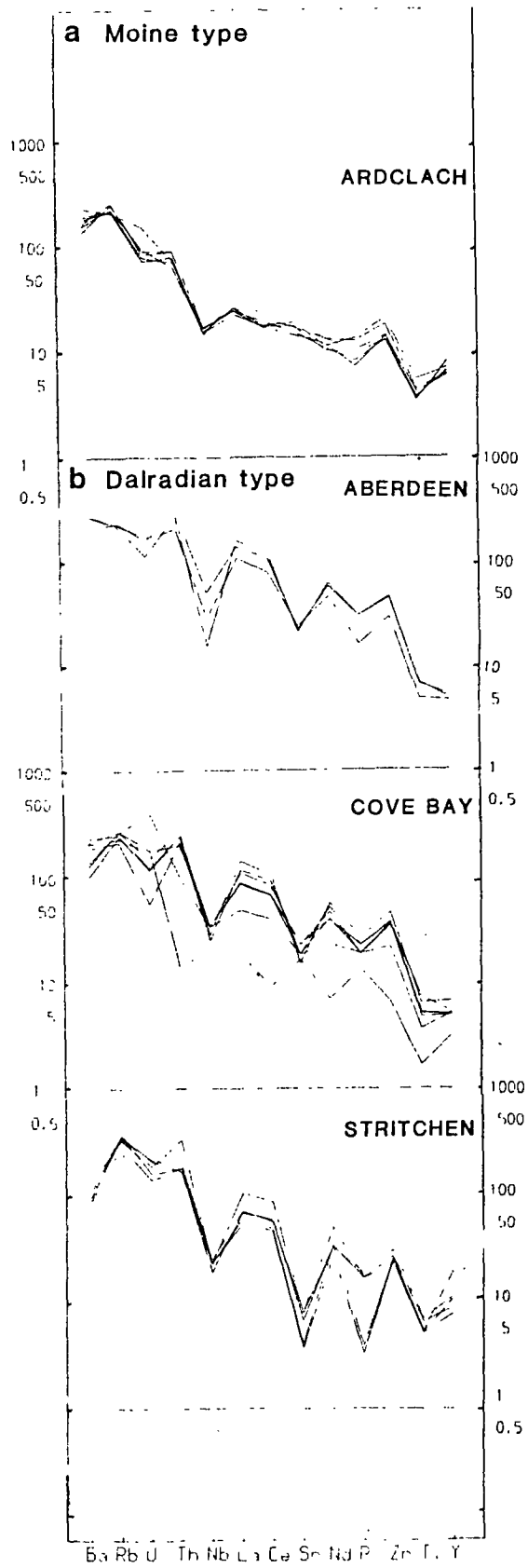
An alternative method of classification of the Caledonide granites could be one based on their geochemical characteristics and may of course be more relevant to the problem of their petrogenesis than a classification solely on the basis of relative timing of intrusion. A simple way of characterizing different types of intrusion on the basis of geochemistry is the use of mantle normalized plots for a comprehensive range of trace elements. However such methods must also take account of the petrography of the various intrusions as the proportion of cumulus phases (such as plagioclase and hornblende) can modify the observed whole rock trace element abundances. Consideration of their isotope geochemistry is also important where this indicates a large crustal component in the granite.

Pankhurst and Sutherland's group 1 granites may be further subdivided on the basis of whole rock geochemistry. Mantle normalized trace element patterns for these granites fall into two distinct groups, which are related to the host rocks of the intrusions. The S-type (crustal derived) granites which lie within the Moine (group 1a) have markedly different patterns from the S-type granites within the Dalradian (group 1b) (Fig 4:1).

The remainder of the granitoids which appear on the basis of their petrography, mineral chemistry and isotope geochemistry to be predominantly juvenile in origin, can be divided into two main groups; less evolved juvenile granitoids (group 3) and more evolved juvenile granitoids (group 2). However these two groupings may also be further subdivided. The more evolved group can be subdivided into three groups, the Cairngorm type (group 2a), the intermediate group (group 2b) and the

Fig. 4:1. Mantle normalized trace element patterns for the group 1 (a and b) granites (see over page).

Fig. 4:1



West Scotland group (group 2c) as detailed in Fig 4:2. The Cairngorm type granites are geochemically fairly evolved, having strong relative depletion of Ba, Sr, P and Ti and highly enriched in Rb, U, Th and Y as may be seen from their mantle normalized trace element plots. The intermediate group are less fractionated and are transitional between the less evolved juvenile granites and the Cairngorm type showing similar depletions and enrichments but less strongly. The west Scotland group of granites show similar relative depletions in P and Ti; however they are strongly enriched in Sr and Ba. This enrichment in Sr and Ba does not appear to be related to any difference in mineralogy between these and other evolved Caledonian granitoids, thus some form of source variation is implied.

The less evolved group 3 granitoids can also be divided into three sub-groups; the high phosphorous and strontium granitoids of west Scotland (group 3c), the high strontium and zirconium granitoids of west Scotland (group 3b), and the north east Scotland group (group 3a), as illustrated in Fig 4:3. The less evolved granitoids as a whole do not show the enrichments (Rb, U, Th, Y) and depletions (Ti, P, Ba, Sr) of the evolved granites, and generally have very different patterns. Many of these plutons also generally contain higher proportions of probable cumulus phases (plagioclase, pyroxene and hornblende) than the evolved group. The high P and Sr granitoids are exclusively granodiorite, tonalite and diorite in composition and show positive anomalies on mantle normalized trace element diagrams for P and Sr, and often also for Zr and Ba; they are perhaps the least evolved group of Caledonian granites and contain the largest proportions of cumulus minerals. The group 3b high Sr and Zr granites are similar to the group 3c rocks, but encompass only

Fig. 4:2. Mantle normalized trace element patterns for the group 2 granites (see over page).

Fig. 4:2. Mantle normalized trace element patterns for the more evolved juvenile granites (Group 2); Group 2a (Cairngorm type), Group 2b (Intermediate group), and Group 2c (West Scotland type).

Fig. 4:2.

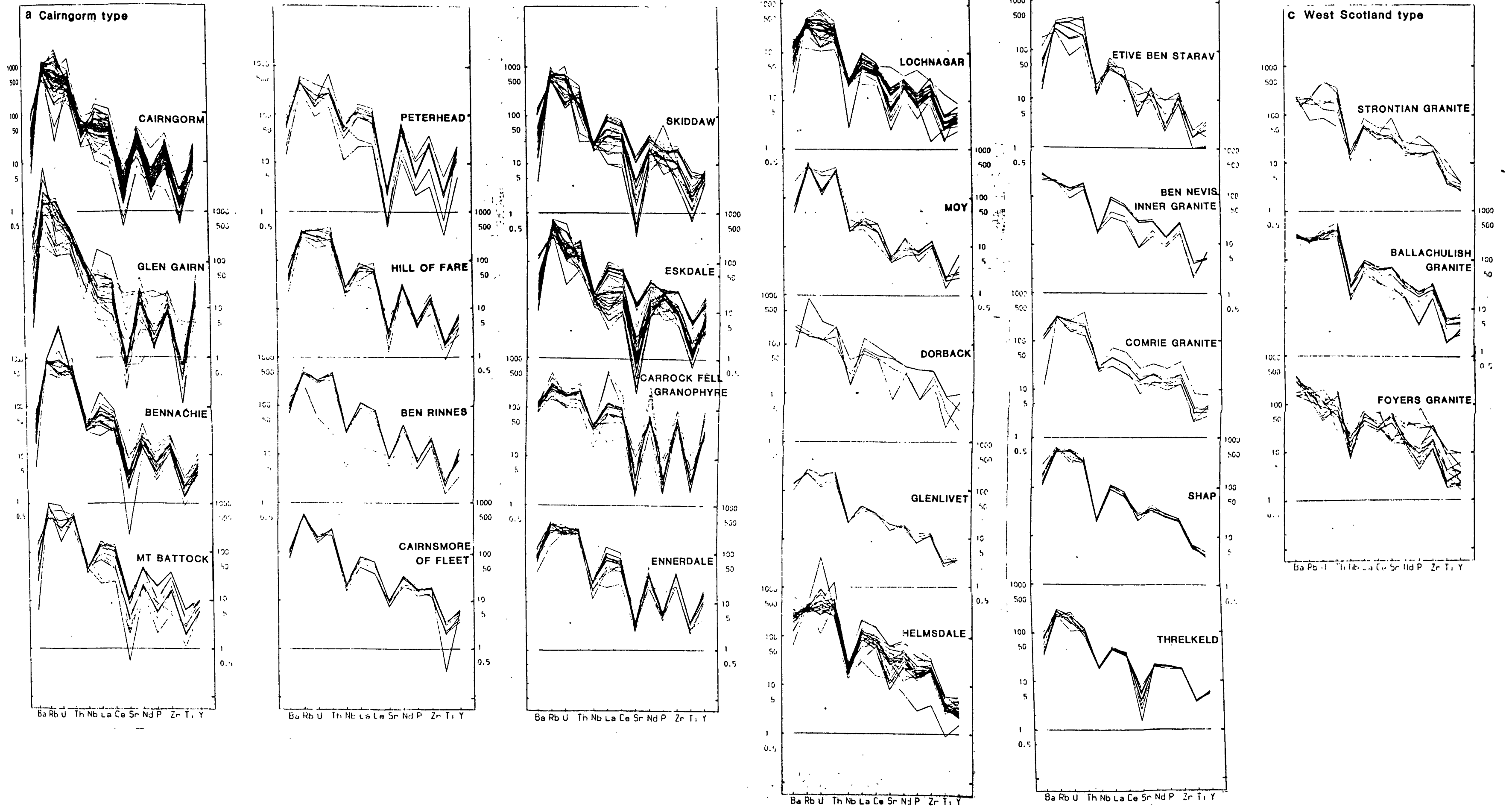
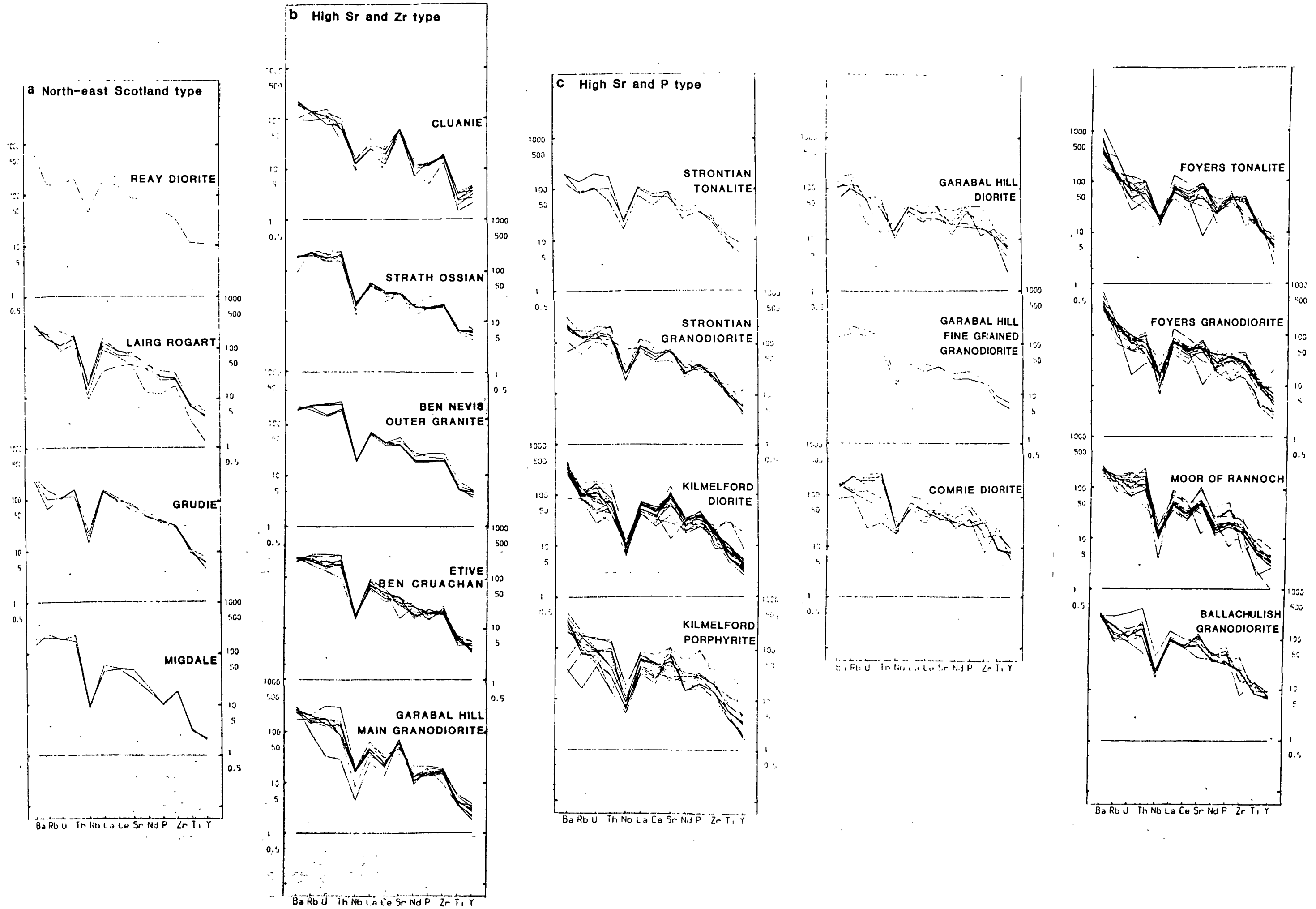


Fig. 4:3. Mantle normalized trace element patterns for the less evolved juvenile granitoids (Group 3); Group 3a (North-east Scotland type), Group 3b (high Sr and Zr type), and Group 3c (high Sr and P type).

Fig. 4:3



---

TABLE 4:3 GEOCHEMICAL CLASSIFICATION OF THE CALEDONIAN GRANITES.

GROUP 1. (S-TYPE GRANITES).

a	b
<u>Moine type</u>	<u>Dalradian Type</u>
Ardclach	Stritchen
	Aberdeen
	Cove Bay

GROUP 2. MORE EVOLVED JUVENILE GRANITES.

a	b	c
<u>Cairngorm Type</u>	<u>Intermediate group</u>	<u>West Scotland group</u>
Cairngorm	Glenlivet	Foyers granite
Peterhead	Moy	Strontian granite
Ben Rinnes	Dorback	Ballachulish
Mt Battock	Lochnagar	granite
Hill of Fare	Blackburn	
Bennachie	Comrie granite	
Cairnsmore of Fleet	Etive Ben Starav	
Glen Gairn	Ben Nevis inner granite	
Eskdale	Helmsdale	
Skiddaw	Shap	
Ennerdale	Threlkeld	
Carrock Fell granophyre		

GROUP 3. LESS EVOLVED JUVENILE GRANITES.

a	b	c
<u>north-east Scotland type</u>	<u>High Sr and Zr type</u>	<u>High Sr and P type</u>
Reay	Etive Ben Cruachan	Garabal Hill fine
Rogart	Ben Nevis outer	grained granodiorite
Migdale	granite	Garabal Hill diorite
Grudie	Garabal Hill main	Foyers granodiorite
	granodiorite	Foyers tonalite
	Cluanie	Ballachulish
	Strath Ossian	granodiorite
		Kilmelford porphyrite
		Kilmelford diorite
		Moor of Rannoch
		Comrie diorite
		Strontian tonalite
		Strontian granodiorite

---

Key to Figs. in Chapter 5.

Figs. 5:10, 5:11 and 5:12.

- - Shap granite.
- \* - Eskdale granodiorite.
- + - Eskdale granite.
- ⌘ - Eskdale greisen.
- ⊕ - Ennerdale granophyre.
- ⊗ - Skiddaw less geochemically evolved granite.
- △ - Skiddaw more geochemically evolved granite.
- ⊠ - Skiddaw greisen.
- - Carrock Fell granophyre.
- H - Carrock Fell hybrid granophyre and ferrogabbro.
- L - Carrock Fell leached granophyre.

Fig. 5:14.

- ⊗ - Skiddaw less geochemically evolved granite.
- △ - Skiddaw more geochemically evolved granite.
- ⊠ - Skiddaw greisen.

Fig. 5:15.

- \* - Eskdale granodiorite.
- + - Eskdale granite.
- ⌘ - Eskdale greisen.

Fig. 5:16.

- H - Carrock Fell hybrid granophyre and ferrogabbro.
- - Carrock Fell granophyre.
- L - Carrock Fell leached granophyre.
- - Shap granite.

Fig. 5:18.

- I - Kilmelford diorite.
- J - Kilmelford porphyritic granodiorite.

Fig. 5:22.

- ▽ - Glen Gairn granite.
- ▼ - Glen Gairn greisen.

## CHAPTER 5. MINERALIZATION, METALLOGENESIS AND LATE STAGE PROCESSES IN THE CALEDONIAN GRANITES.

### 5:1 INTRODUCTION.

The Caledonian province, unlike the later Hercynian province of Britain does not have widespread mineralization of economic importance. However the English Lake District contains an important orefield with numerous mineral veins of hydrothermal origin (Stanley & Vaughan 1982, Dagger 1977, Shepherd et al. 1976). This mineralization is thought to be associated with the buried granite batholith under the Lake District (Simpson et al. 1979, Brown et al. 1980, Moore 1982). In Scotland there is no widespread mineralization, although some granites contain localized porphyry-type mineralization, mostly in south west and central Scotland. The granites of eastern Scotland, although they are not mineralized, are metalliferous, with above background levels of tin, uranium and tungsten. In northern Scotland the Helmsdale granite has associated uranium mineralization. It must be noted however that none of the Scottish granites contains mineralization of economic importance.

The objectives of this chapter are to discuss the mineralized and metalliferous granites in the context of their major and trace element chemistry, with a view to observing the connections between mineralization and granite petrogenesis. Therefore it is also necessary to discuss the late stage processes of greisenization and sericitization where these are observed in the Caledonian granites and the geochemistry of the altered granites in relation to the mineralization process.

5:2. MINERALIZATION, METALLOGENESIS AND LATE STAGE PROCESSES IN THE CALEDONIAN GRANITES OF THE ENGLISH LAKE DISTRICT.

The Lake District contains an important orefield with numerous mineral veins of hydrothermal origin (Stanley & Vaughan 1982, Dagger 1977, Shepherd et al. 1976). Shepherd et al. (1976) postulated on the basis of isotopic and fluid inclusion evidence that the tungsten ores of the province were deposited soon after the consolidation of the granites from saline solutions of mixed magmatic and circulating ground water origin and Firman (1978b) suggested a similar origin for the other vein systems in the lower Palaeozoic rocks of the Lake District. Radiometric age dating indicates that the first episodes of hydrothermal activity in the district, which deposited tungsten-molybdenum minerals in and around granites and copper in volcanics and slates, took place 390 Ma ago (Shepherd et al. 1976). Lead-zinc mineralization occurred later at c 360 Ma, contemporaneous with the basal Carboniferous conglomerates (Firman 1978b), while K-Ar analyses of clays suggest that hydrothermal activity continued intermittently until Jurassic times (Ineson & Mitchell 1974).

Recently a link has been proposed between the orefield generally and the buried Lake District Batholith which has been suggested to have high heat production and hence to have been capable of maintaining hydrothermal convective cells in periods of increased tectonism and increased mantle heat flow (Simpson et al. 1979, Brown et al. 1980, Moore 1982). The extant geothermal field of Wairakei in New Zealand is considered to provide an appropriate model for the Lake District mineralization. However the complex distribution of veins in the Lake

District is thought to have been the product of several generations of single pass hydrothermal cells with varying metal sources. Moreover erosion of the Lake District is thought to have exposed structural levels in the fossil hydrothermal systems several kilometres below those visible in active geothermal fields.

The most important mineralization associated with the Lake District granites is the tungsten mineralization at Carrock Mine near to and within the Skiddaw granite (Shepherd et al. 1976). However most of the Lake District granites contain higher than background levels of tin, tungsten, molybdenum and copper, as can be seen from Figs. 5:1,2,3 and 4. Shap and Skiddaw contain higher than background levels of molybdenum (Fig. 5:3), Shap, Skiddaw and Threlkeld contain above background levels of copper (Fig. 5:4), all the Lake District granites with the exception of Threlkeld contain above background levels of tungsten (Fig. 5:2), and all the Lake District granites contain above background levels of tin (Fig. 5:1). For elements which are frequently associated with metalliferous and mineralized granites frequency distribution patterns for boron, uranium, thorium, lithium and beryllium are shown in Figs. 5:5, 6, 7, 8 and 9. Boron is present at above the background levels observed in the Caledonian granites generally in most of the Lake District granites with the exception of the Ennerdale and Carrock granophyres (Fig. 5:5). Above background levels of uranium are observed in the Shap and Skiddaw granites, and the distribution of uranium levels in the Eskdale granite is skewed towards high concentrations, although the bulk of the samples are at background levels (Fig. 5:6). None of the Lake District granites has noticeably high levels of thorium except Shap which is just above background (Fig. 5:7). Above background levels

Fig. 5:1. Frequency distribution of tin in Caledonian granites (see over page).

Fig. 5:1. Frequency distribution of tin in Caledonian granites; values less than 6 ppm Sn are considered to represent background values.

Fig. 5:1 Frequency distribution of tin in Caledonian granites.

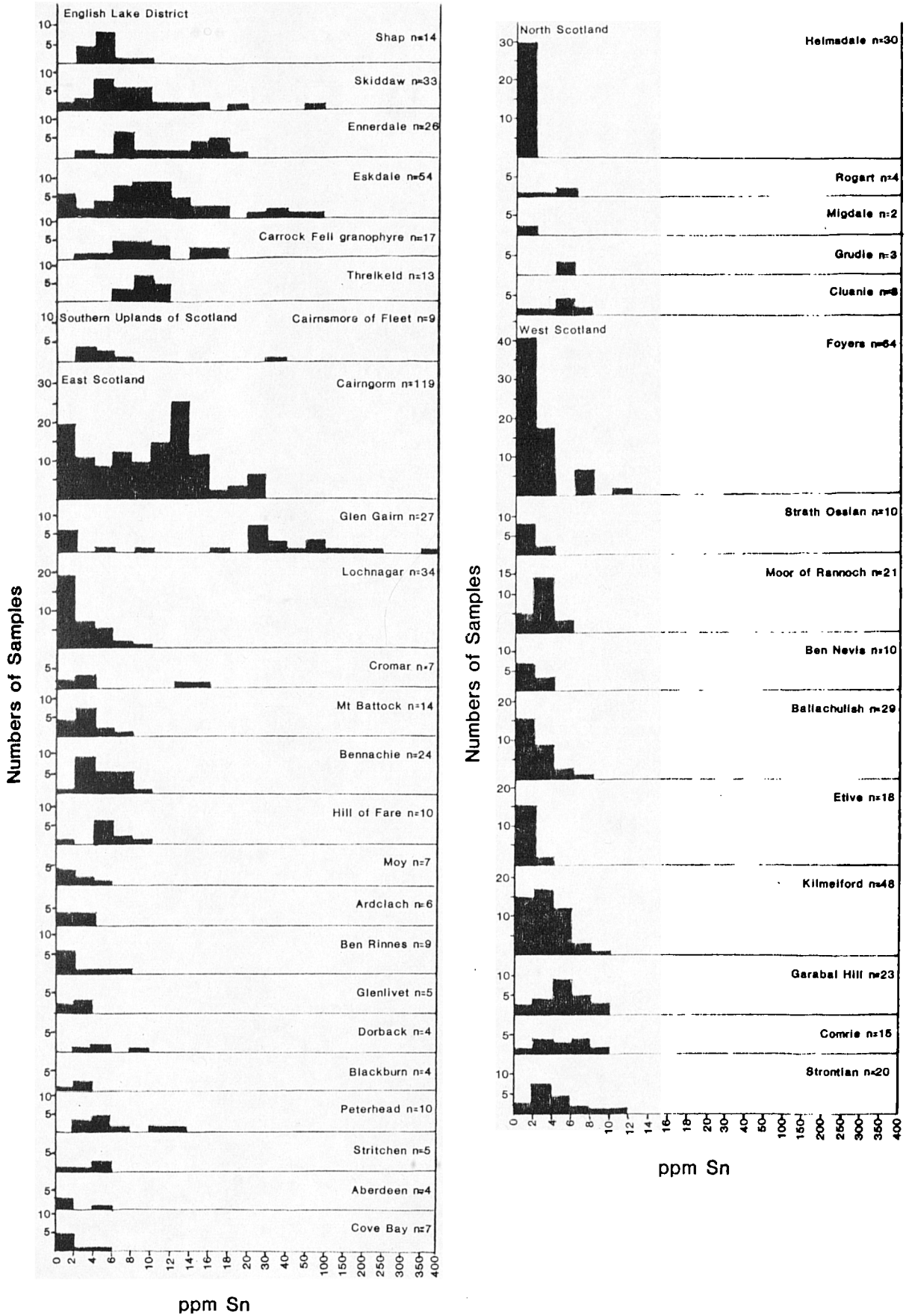


Fig. 5:2. Frequency distribution of tungsten in Caledonian granites (see over page).

Fig. 5:2. Frequency distribution of tungsten in Caledonian granites; values less than 4 ppm W are considered to represent background values.

Fig. 5:2 Frequency distribution of tungsten in Caledonian granites.

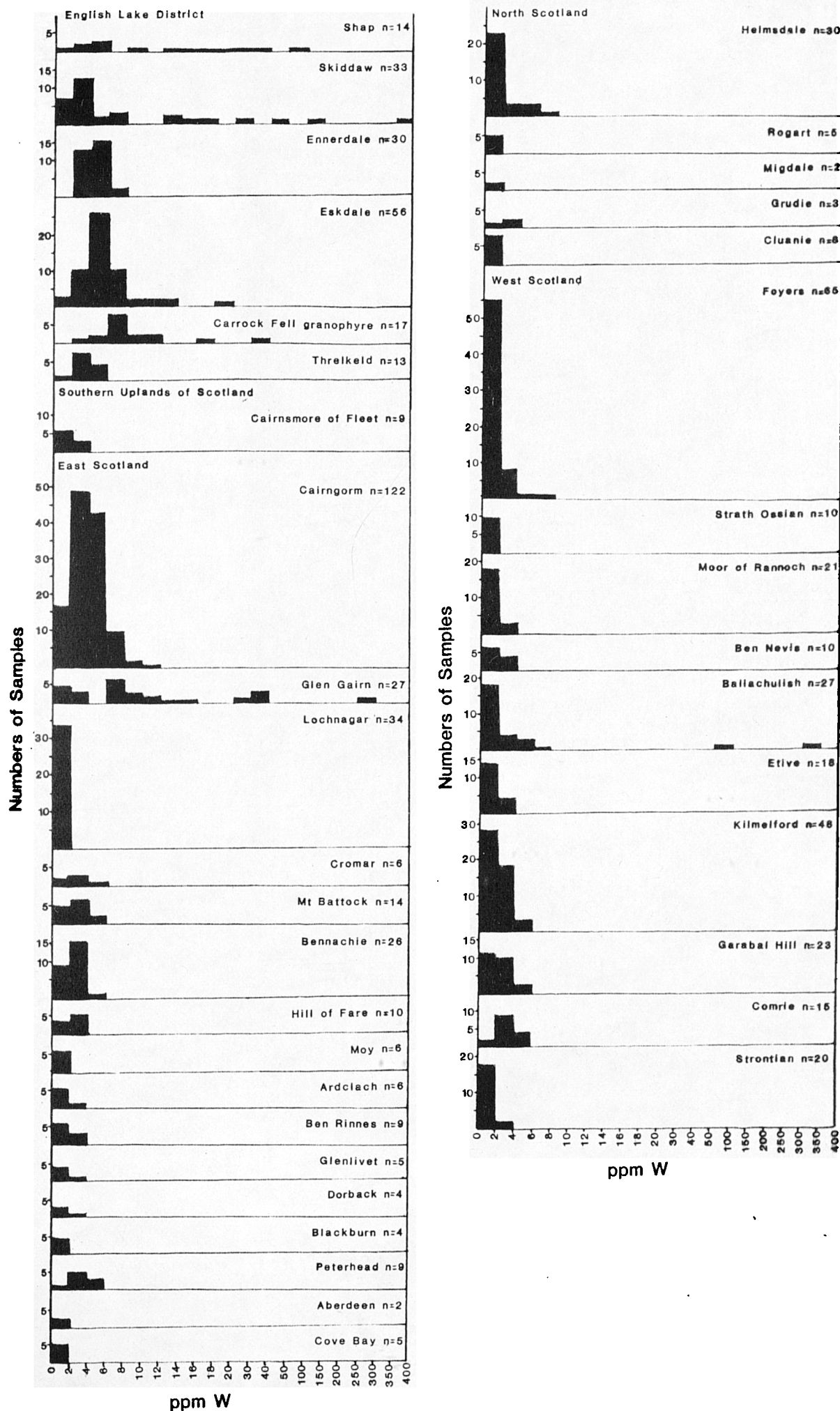


Fig. 5:3. Frequency distribution of molybdenum in Caledonian granites  
(see over page).

Fig. 5:3. Frequency distribution of molybdenum in Caledonian granites; values less than 2 ppm Mo are considered to represent background values.

Fig. 5:3 Frequency distribution of molybdenum in Caledonian granites.

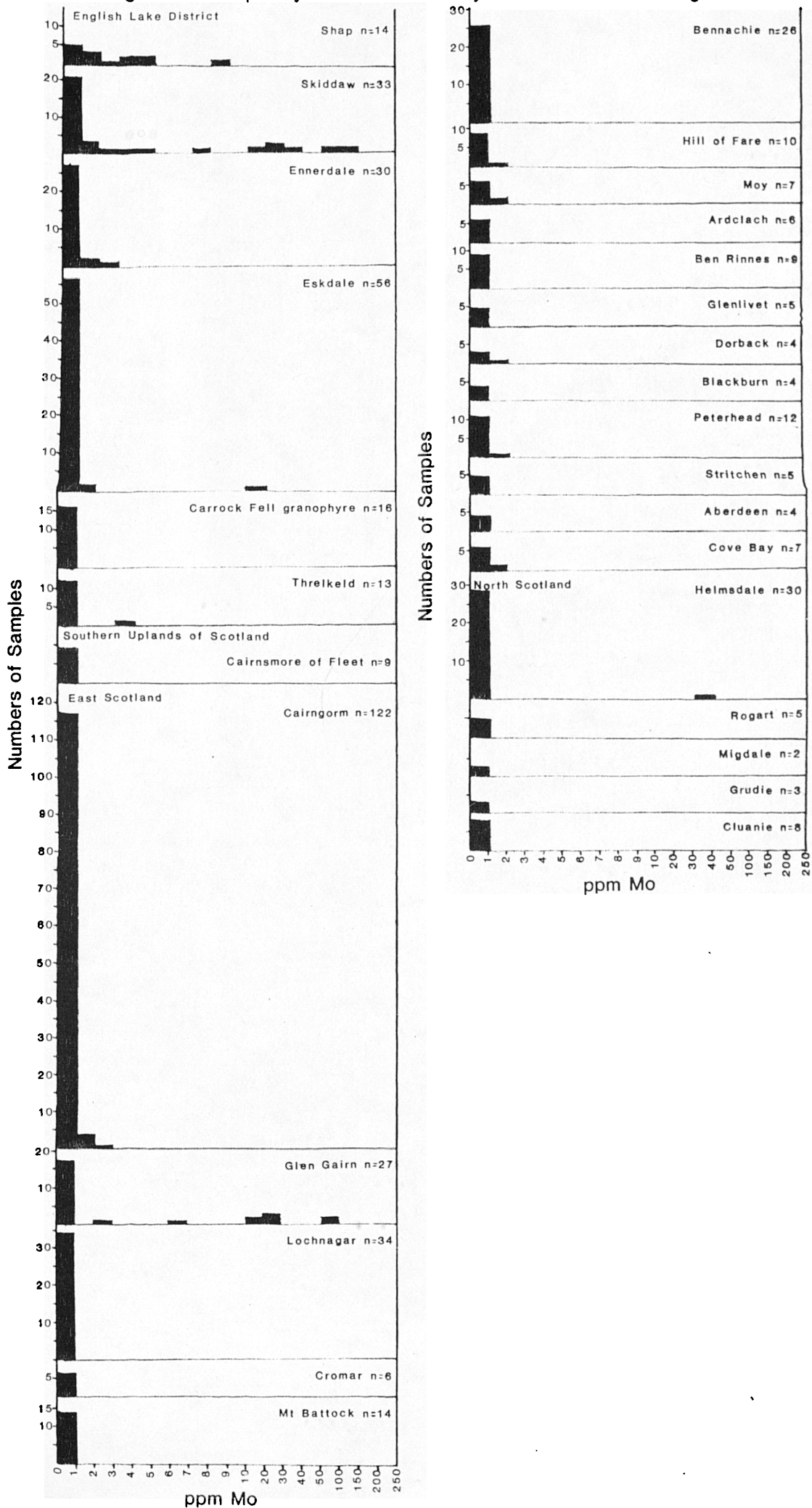


Fig. 5:3 Continued. Frequency distribution of molybdenum in Caledonian granites.

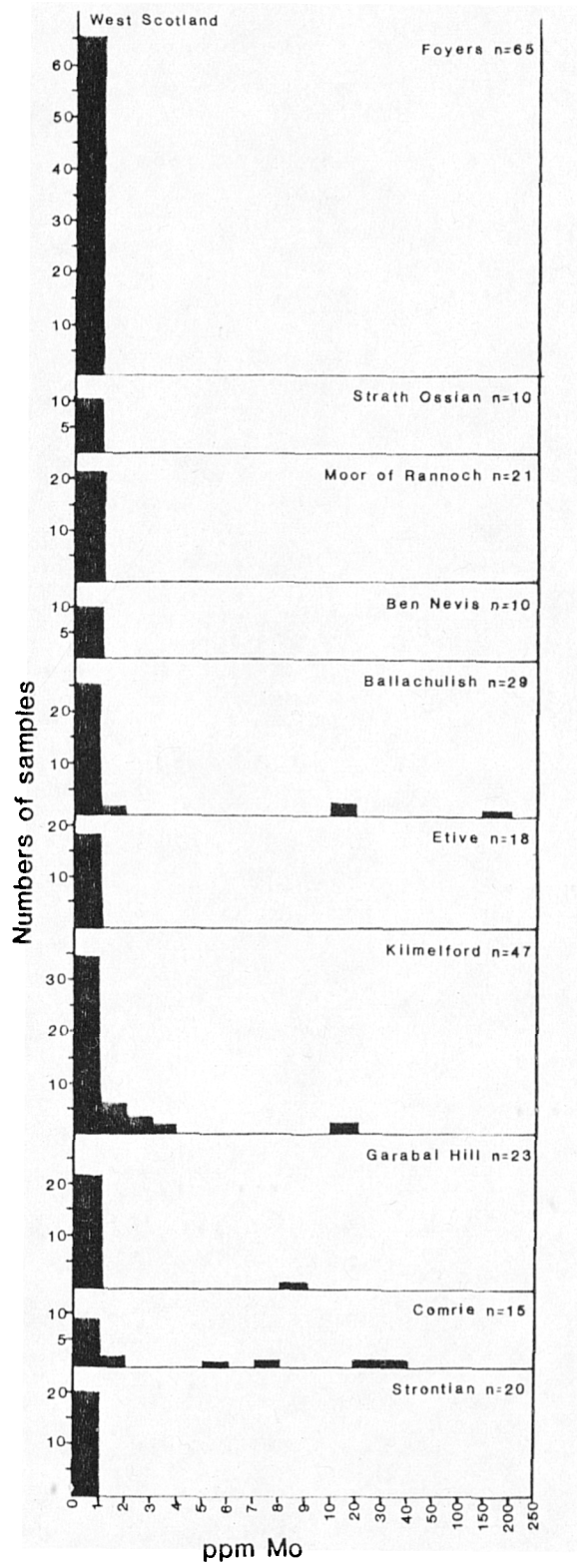


Fig. 5:4. Frequency distribution of copper in Caledonian granites (see over page).

Fig. 5:4. Frequency distribution of copper in Caledonian granites; values less than 15 ppm Cu are considered to represent background values.

Fig. 5:4 Frequency distribution of copper in Caledonian granites.

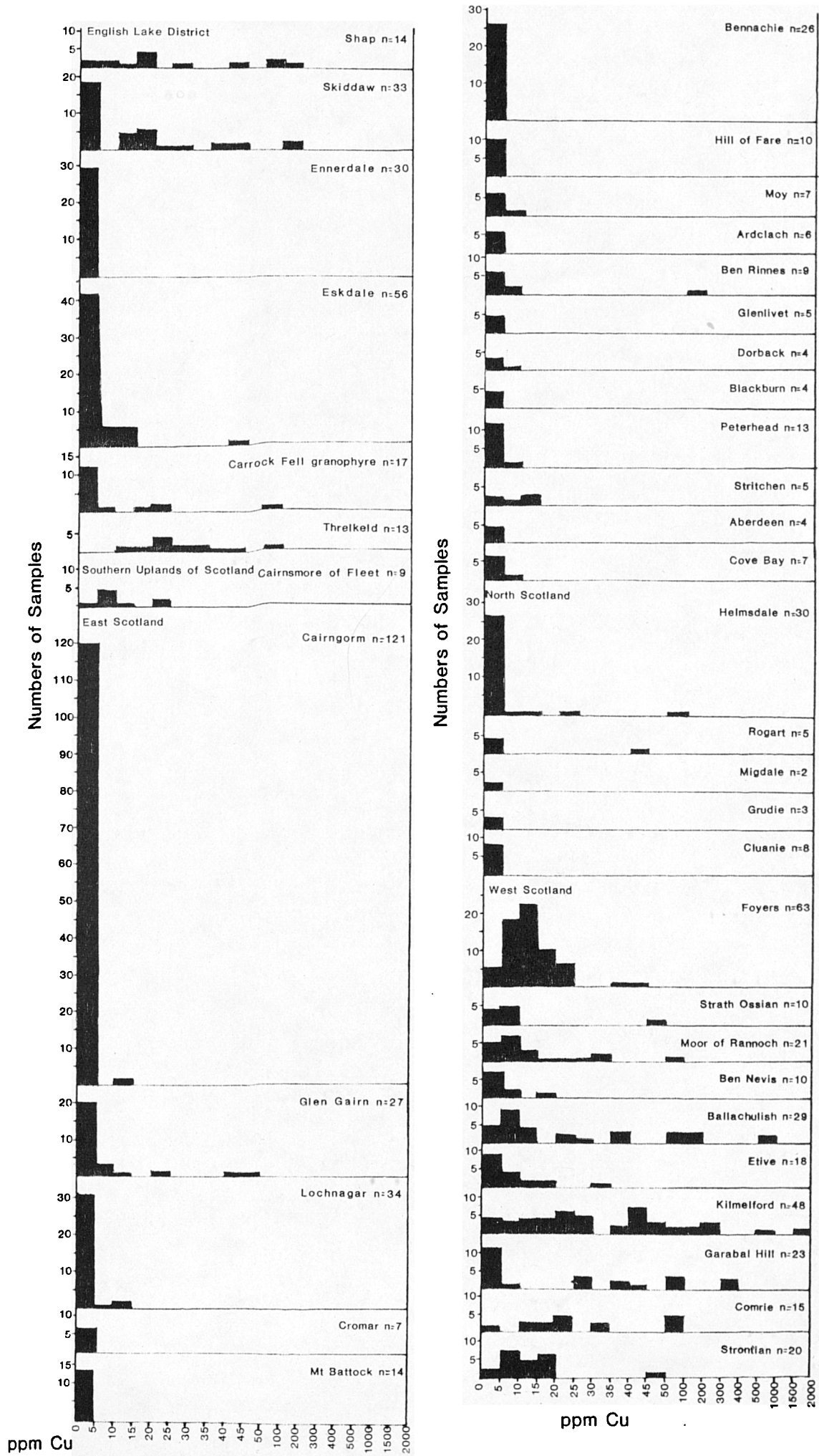


Fig. 5:5. Frequency distribution of boron in Caledonian granites (see over page).

Fig. 5:5. Frequency distribution of boron in Caledonian granites; values less than 10 ppm B are considered to represent background values.

Fig. 5:5 Frequency distribution of boron in Caledonian granites.

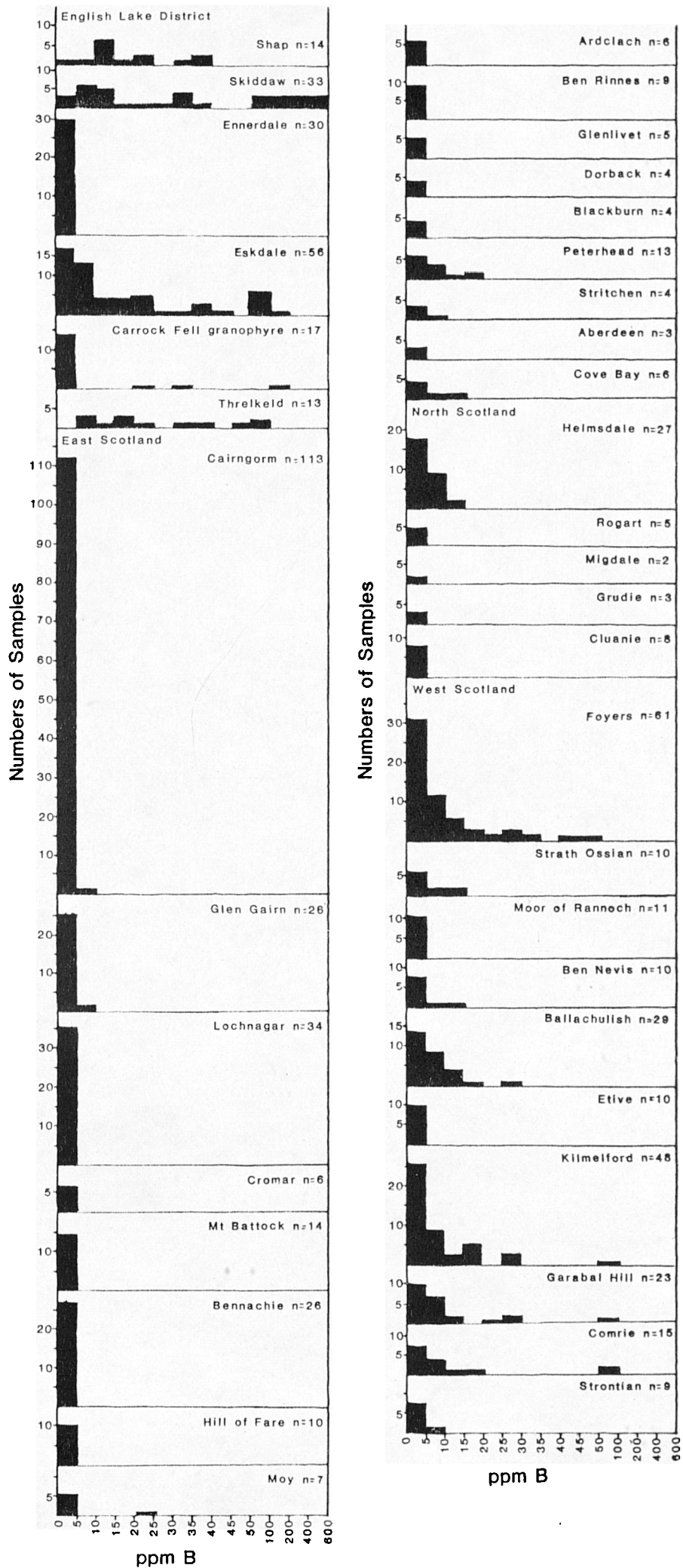


Fig. 5:6. Frequency distribution of uranium in Caledonian granites (see .  
over page).

Fig. 5:6. Frequency distribution of uranium in Caledonian granites; values less than 8 ppm U are considered to represent background values.

Fig. 5:6 Frequency distribution of uranium in Caledonian granites.

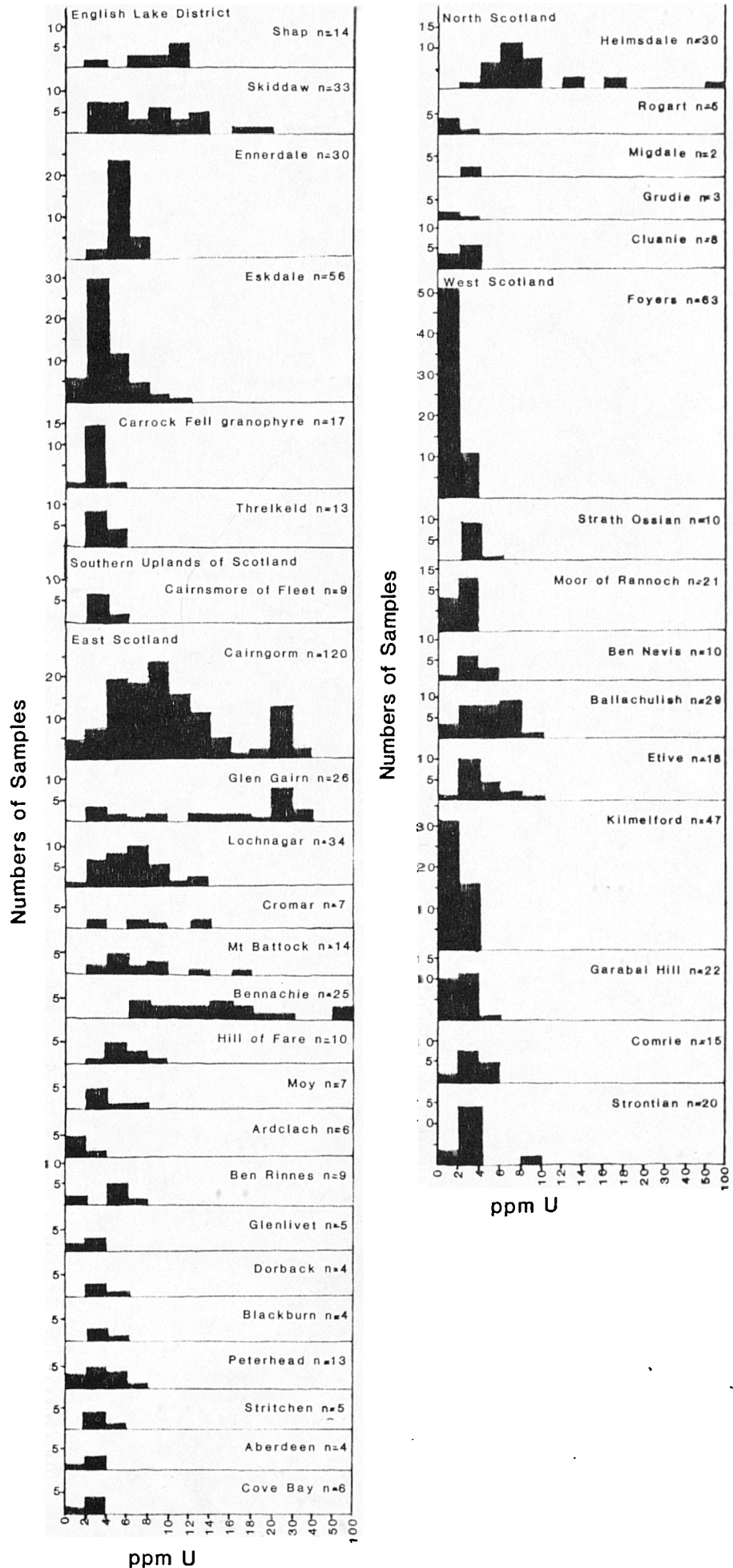
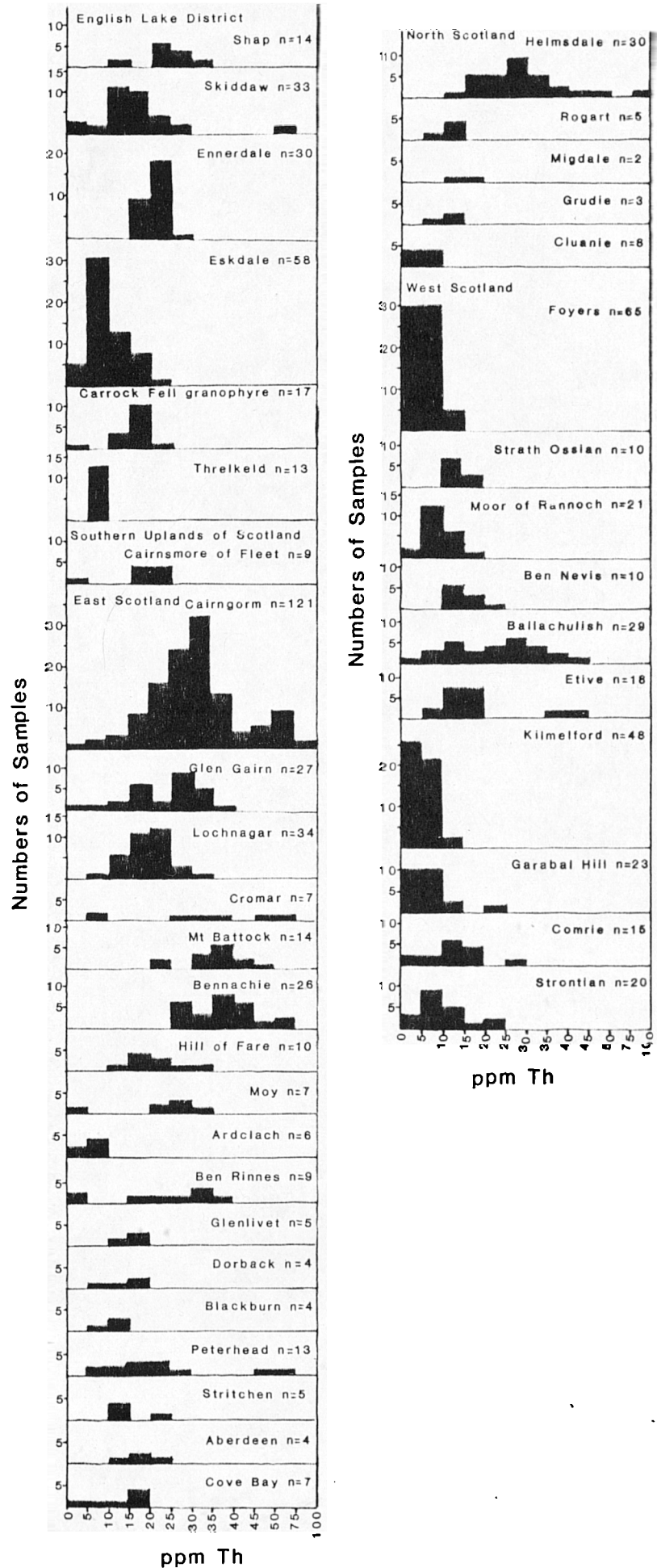


Fig. 5:7. Frequency distribution of thorium in Caledonian granites (see over page).

Fig. 5:7. Frequency distribution of thorium in Caledonian granites; values less than 25 ppm Th are considered to represent background values.

Fig. 5:7 Frequency distribution of thorium in Caledonian granites.



of lithium are observed in the Shap and Skiddaw granites, with some high values in the Eskdale granites (Fig. 5:8), high values of lithium are characteristic of the Cairngorm type granites and are commonly associated with granites with high levels of tin and tungsten (Tauson & Kozlov 1973). Similarly beryllium is at above background levels in Shap and Skiddaw and a few samples from Eskdale also show above background levels (Fig. 5:9). The Eskdale granite has also been subject to haematization, producing deposits within the granite which were of economic importance in the past; this event is probably of post-Carboniferous age (Firman 1978b).

The high levels of lithium, beryllium, uranium and thorium observed in the Skiddaw granite are typical of granites belonging to the Cairngorm group of more evolved juvenile granites according to the classification set up in Chapter 4, and although the enrichments in these elements in the Eskdale granite are not as great as those observed in the Skiddaw granite, this granite also belongs to the Cairngorm type group of granites. However the enrichments of lithium, beryllium, uranium and thorium observed in the Shap granite are unusual, particularly the high lithium and beryllium which is not observed in any of the other granites of the intermediate group of the more evolved granitoids to which the Shap granite otherwise has close geochemical affinities.

Many of the granites show visible effects of metasomatism, the extent and temperature of which varies partly in relation to the exposed structural level of the intrusions and to the geothermal field. Skiddaw, Shap and to some extent Eskdale show various high temperature effects of water-rock interaction (Greenwood et al. in press, Shepherd et al. 1976) with greisenization at Skiddaw and Eskdale and subsolidus

Fig. 5:8. Frequency distribution of lithium in Caledonian granites (see over page).

Fig. 5:8. Frequency distribution of lithium in Caledonian granites; values below 100 ppm Li are considered to represent background values.

Fig. 5:8 Frequency distribution of lithium in Caledonian granites.

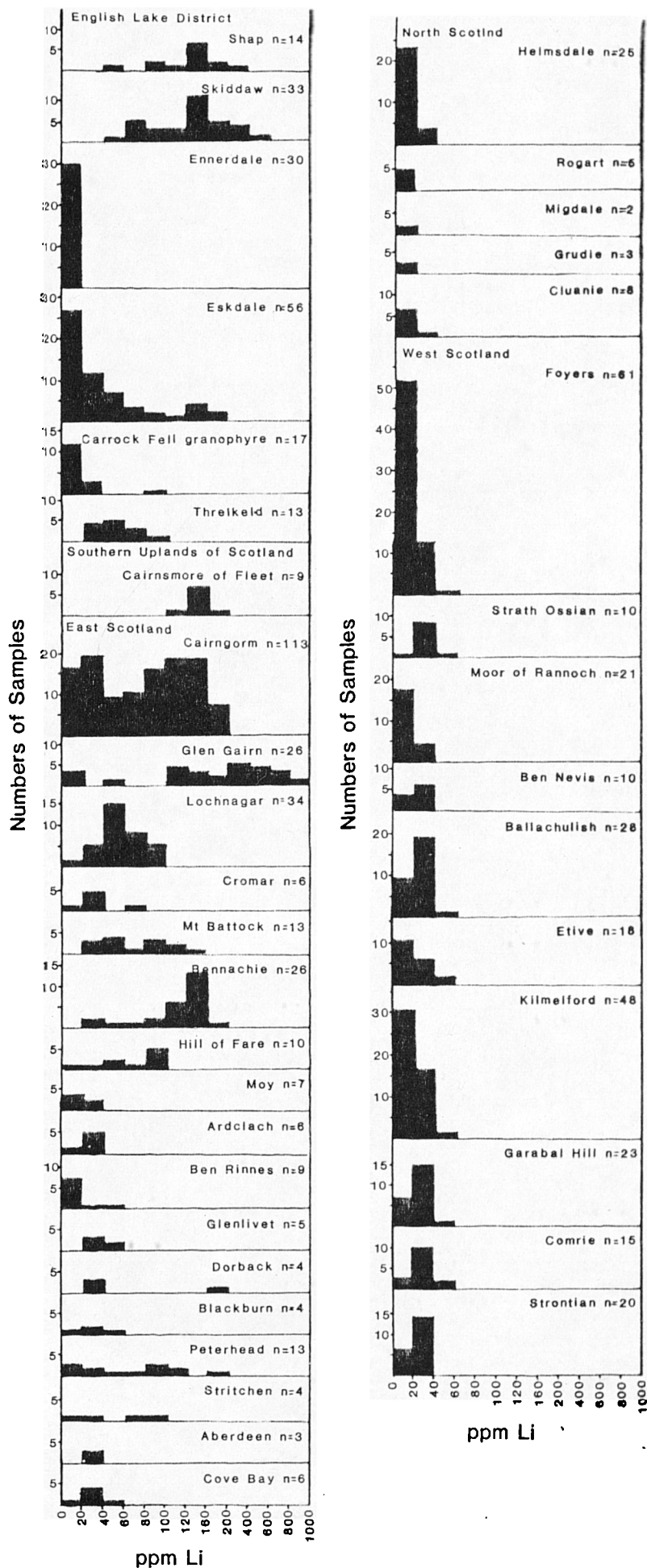
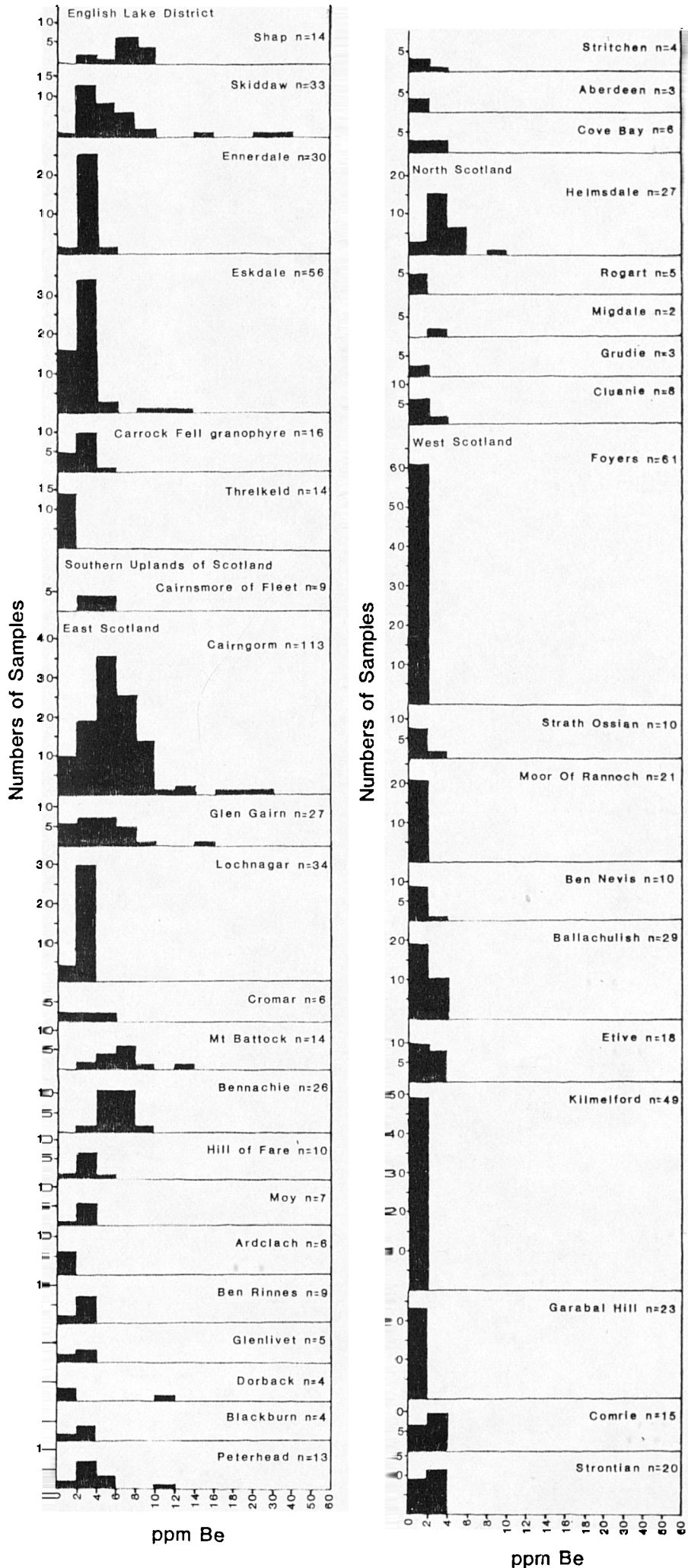


Fig. 5:9. Frequency distribution of beryllium in Caledonian granites (see over page).

Fig. 5:9. Frequency distribution of beryllium in Caledonian granites; values less than 6 ppm Be are considered to represent background values.

Fig. 5:9 Frequency distribution of beryllium in Caledonian granites.



K-feldspar growth at Shap, phenomena commonly attributed to high temperature acid leaching and postmagmatic potassic metasomatism respectively (Korzinski 1953, 1964; Beus 1963). The Threlkeld, Ennerdale and Eskdale intrusions have been variably affected by low temperature alteration with the development of sericite, chlorite and calcite, the Threlkeld intrusion having been pervasively altered.

There are large numbers of secondary minerals present in the main Lake District granites. In the Shap granite, chlorite, calcite, pyrite, anatase, fluorite, tourmaline, muscovite, rutile, baryte, haematite, chalcopryrite, bismuthinite, scheelite, molybdenite, sphalerite, and galena have been recorded (Davidson 1957, Grantham 1928). In the Skiddaw granite, chlorite, muscovite, tourmaline, calcite, dolomite, apatite, ankerite, rutile, baryte, scheelite, arsenopyrite, pyrite, pyrrhotite, sphalerite, molybdenite, chalcopryrite, bismuthinite, wolframite, native bismuth, and bismuth-sulpho-tellurides have been found (Shepherd et al. 1976, Hitchen 1934, Ewart 1962). In the Eskdale granite the hematite veins also contain manganese oxides, ankerite, dolomite, calcite, malachite, and chalcopryrite (Firman 1978b).

#### 5:2:i. EFFECTS OF METASOMATISM AND HYDROTHERMAL ALTERATION ON THE MAJOR AND TRACE ELEMENT COMPOSITION OF THE INTRUSIONS.

The extensive metasomatism which has affected the Lake District granites has resulted in the remobilization of certain major and trace elements. In general the elements most likely to have been redistributed in aqueous systems are those of low ionic potential (<3.0) e.g. Cs, Rb, K, Na, Li, Ba, Sr, Ca, and Mg, which behave as hydrated cations, or those

of high ionic potential ( $>12.0$ ) e.g. B, P, and S which behave as soluble complex oxyanions. The former group includes the important LIL elements which are commonly used as petrogenetic indicators. The elements of intermediate ionic potential which are generally held in refractory accessory minerals e.g. Y and the REE, Zr, Ti, Hf, Ta, Nb (all HFS elements), Th and U, are generally the most resistant to alteration although where there is a high activity of acid ligands (e.g.  $F^-$ ,  $Cl^-$ ) (usually during high temperature metasomatism) redistribution of elements such as Sn, W, Be, Ta, U and REE may occur (Eugster 1984). Uranium is subsequently readily remobilized from easily leachable sites as a result of the number of its complexes which are stable over a wide range of Eh, pH and temperature conditions (Langmuir 1978).

The effects of extensive hydrothermal activity on the geochemistry of the Lake District granites can be examined at the simplest level by plotting trace element or trace element-major element pairs which on the basis of their similar chemistry in silicate systems would normally show relatively simple igneous fractionation trends. For example Rb v. Sr, Rb v. Ba, K v. Rb, and U v. Th, which show simple igneous trends for some Caledonian in northern Scotland (Plant et al. 1980, Pankhurst 1979) but show a wide scatter of values for the Lake District province generally, (Figs. 5:10 and 11), and for the Eskdale intrusion in particular. On the other hand HFS elements and HFS element pairs such as  $TiO_2$  v. Y or V should retain igneous fractionation trends despite intense alteration. For example the variably altered Eskdale, Skiddaw and Shap granites fall on a simple igneous trend on a plot of  $TiO_2$  v. V, (Fig. 5:12a), hence evidence of alteration may become apparent by plotting LIL elements against HFS elements such as  $TiO_2$ .

Fig. 5:10. a) Rb vs. Sr variation diagram for the Lake District granitoids. b) Rb vs. Ba variation diagram for the Lake District granitoids. (key to symbols on fold out sheet).

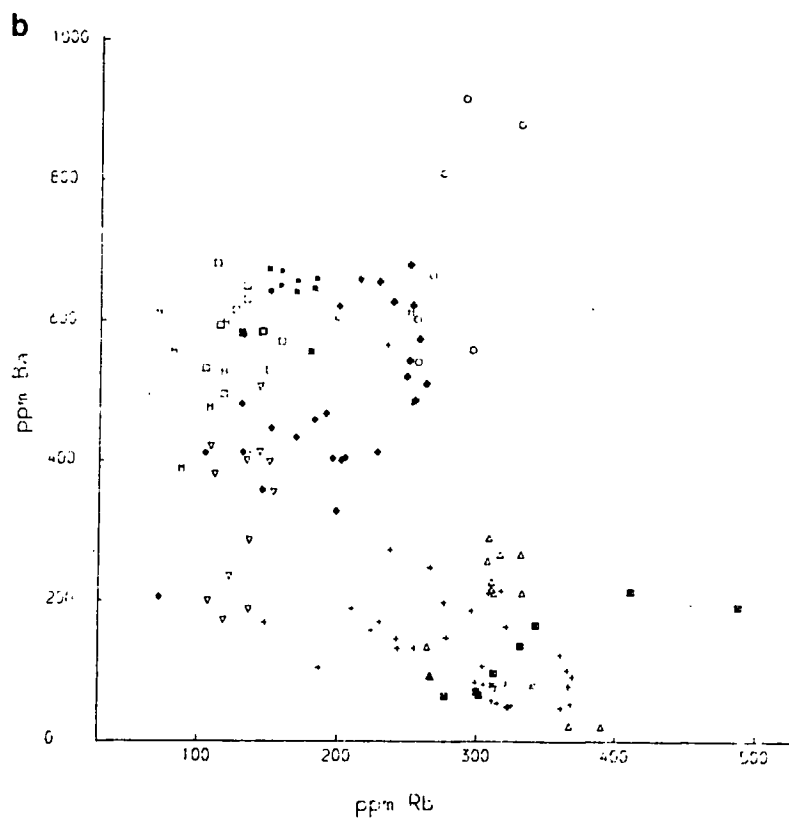
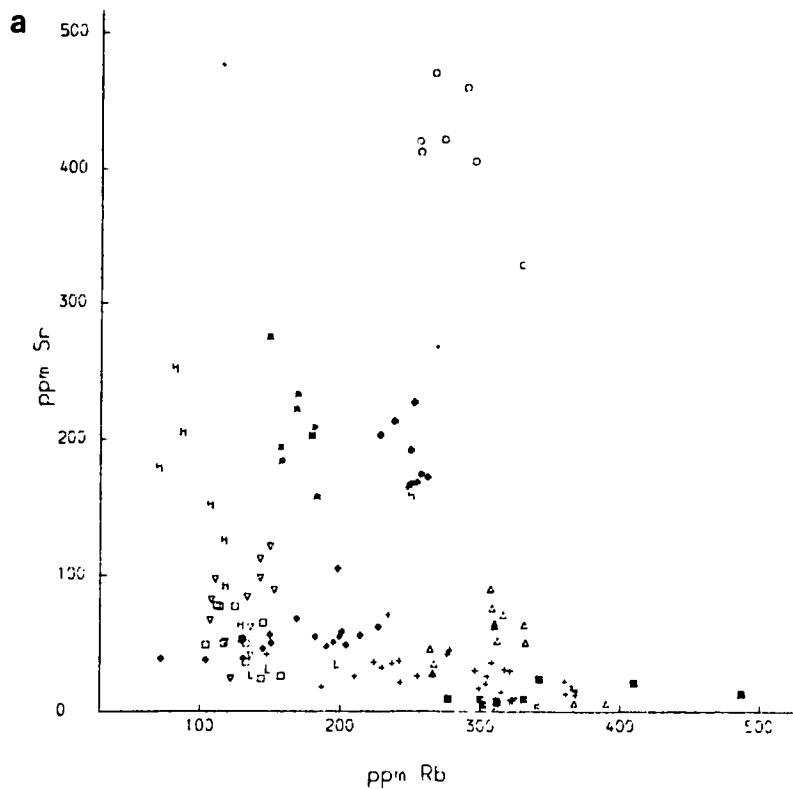


Fig. 5:11. a) Rb vs.  $K_2O$  variation diagram for the Lake District granitoids. b) U vs. Th variation diagram for the Lake District granitoids. (key to symbols on fold out sheet).

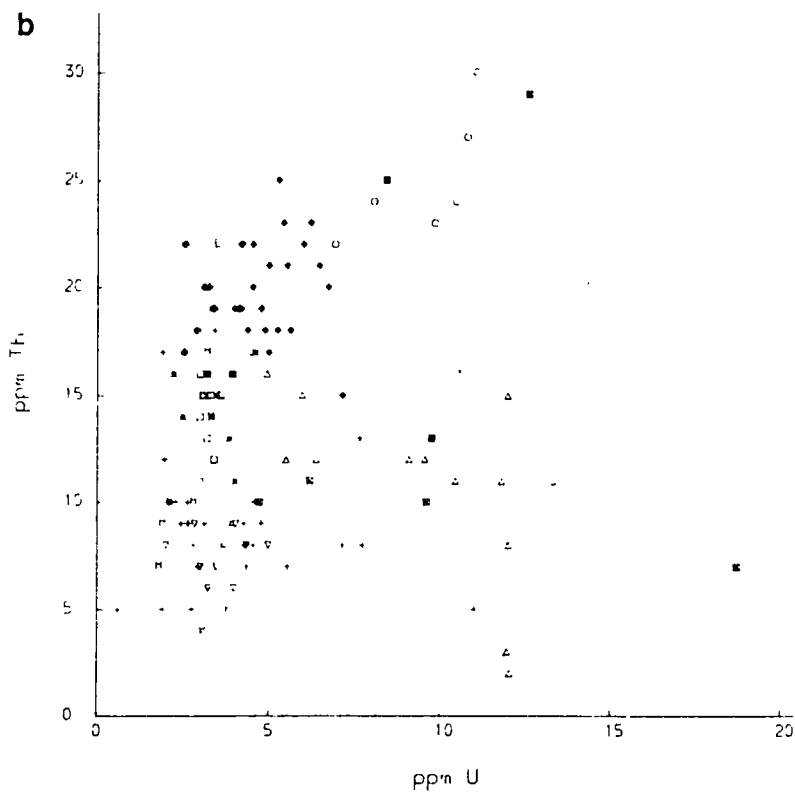
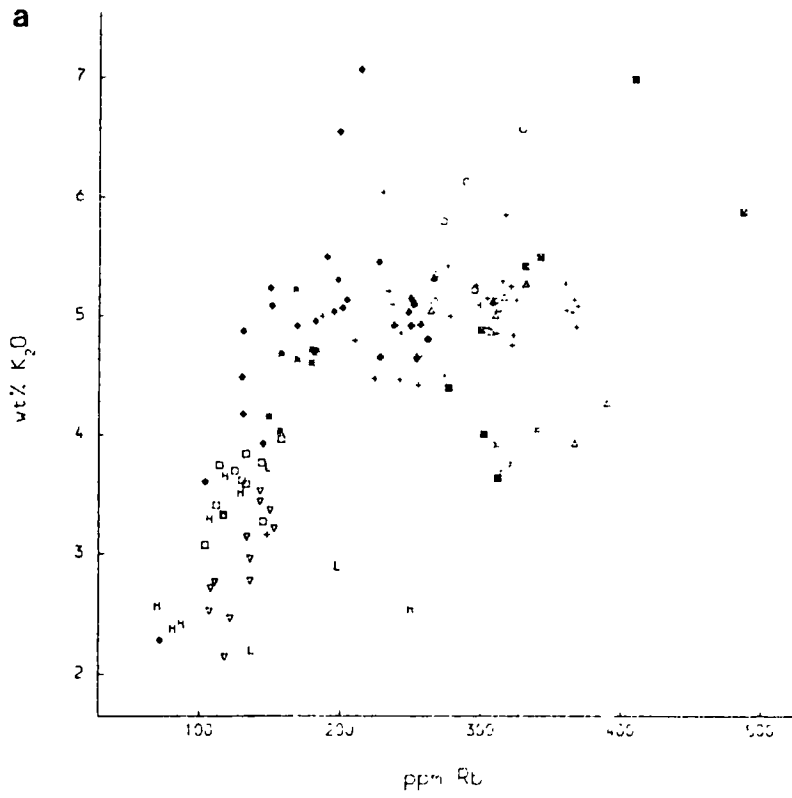
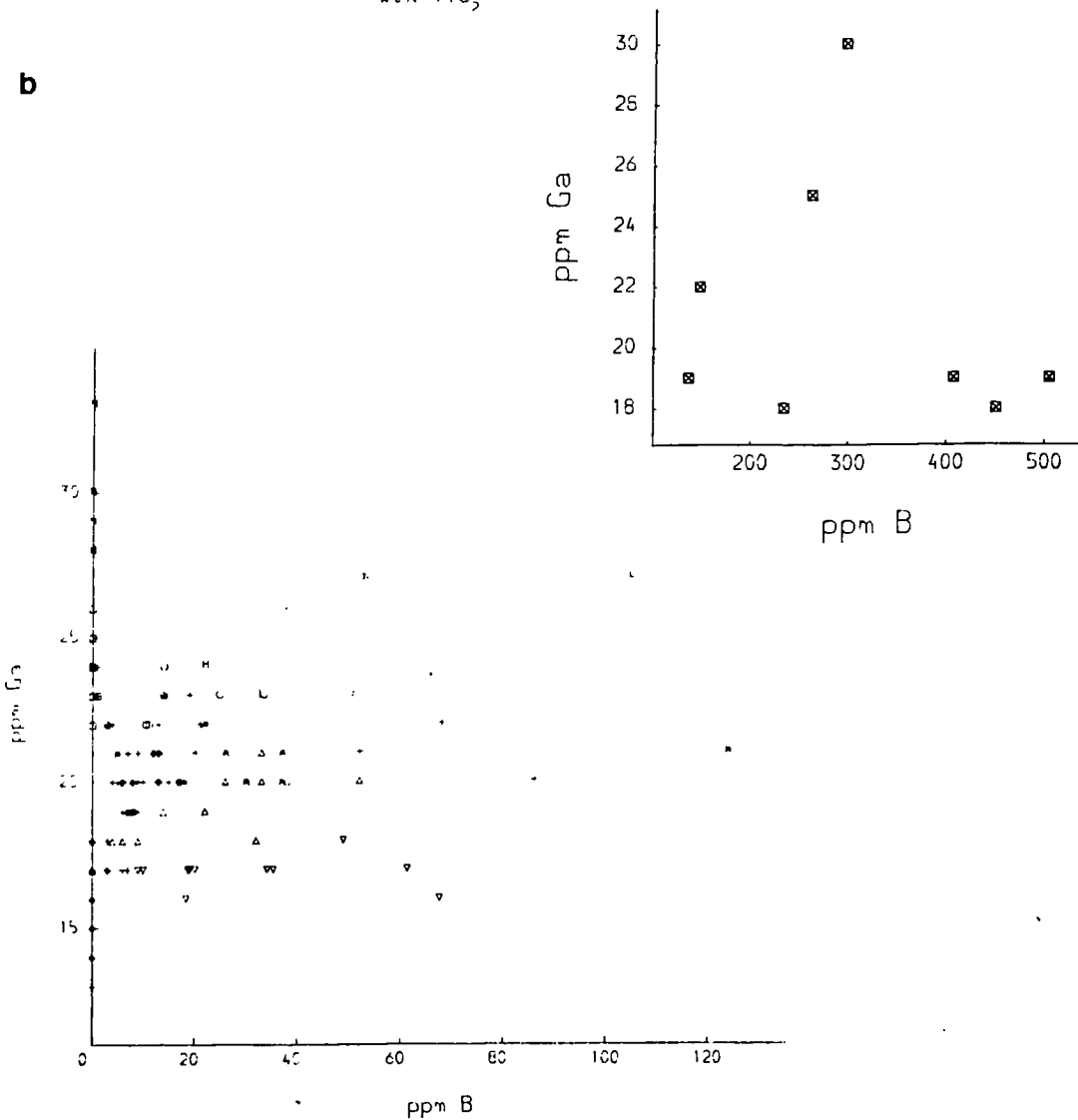
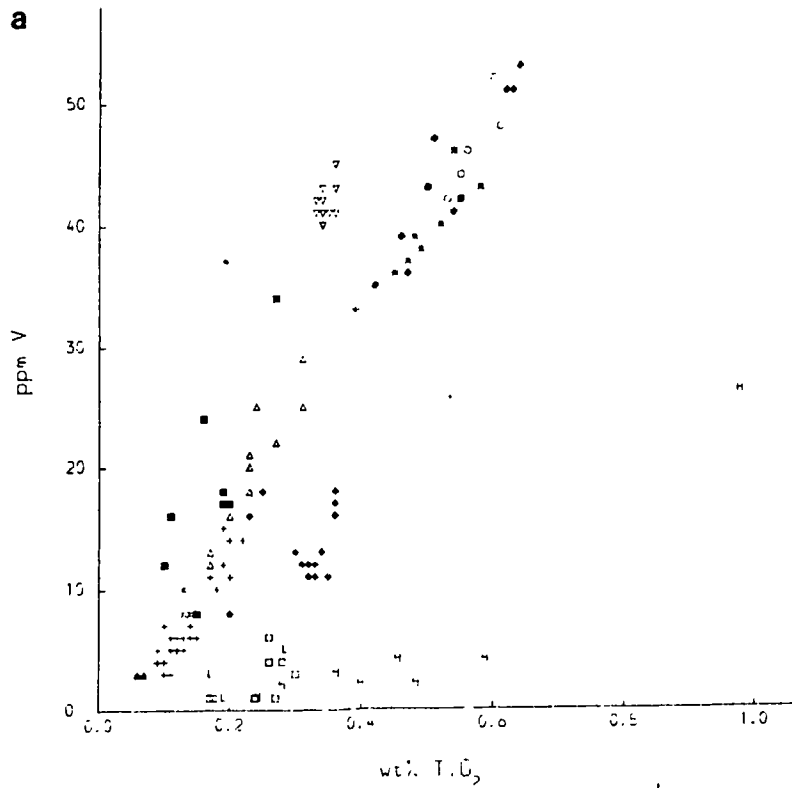


Fig. 5:12. a)  $TiO_2$  vs. V variation diagram for the Lake District granitoids. b) B vs. Ga variation diagram diagram for the Lake District granitoids with an inset for high B samples. (Key to symbols on fold out sheet).



Increased B/Ga and B/SiO<sub>2</sub> ratios have been shown to be an indicator of boron metasomatism as a result of high temperature granite-shale derived fluid interaction (Simpson et al. 1979, Lister 1979). Most of the Lake District granites have elevated levels of boron, (Fig. 5:12b), with the exception of the Ennerdale and Carrock Fell granophyres which on the basis of other isotopic, geochemical and mineralogical evidence are the least metasomatized; the secondary epidote noted in Chapter 3 for these intrusions is probably related to the regional greenschist metamorphic event. The Shap granite contains the lowest levels of boron of the metasomatized/mineralized granites of the Lake District and the significance of this is discussed further below. The absence of any correlation between boron and TiO<sub>2</sub> (unaffected by metasomatism) in the Skiddaw granite (Fig. 5:14f) implies that the high levels of boron in the Skiddaw granite is of secondary origin and not the result of volatile build up during crystallization.

On the basis of these criteria the geochemistry of the Skiddaw and Eskdale intrusions and the Shap granite appear to be the most affected by hydrothermal activity particularly in the early high temperature event consistent with the petrographical evidence of metalliferous mineralization discussed above. The Threlkeld intrusion also appears to have been affected by a lower temperature event. The Ennerdale and Carrock granophyres (away from mineral veins) appear to be largely unaffected by metasomatism although secondary epidote and chlorite after pyroxene in these intrusions may be related to regional greenschist facies metamorphism. Some of the geochemical changes affecting individual intrusions are discussed below.

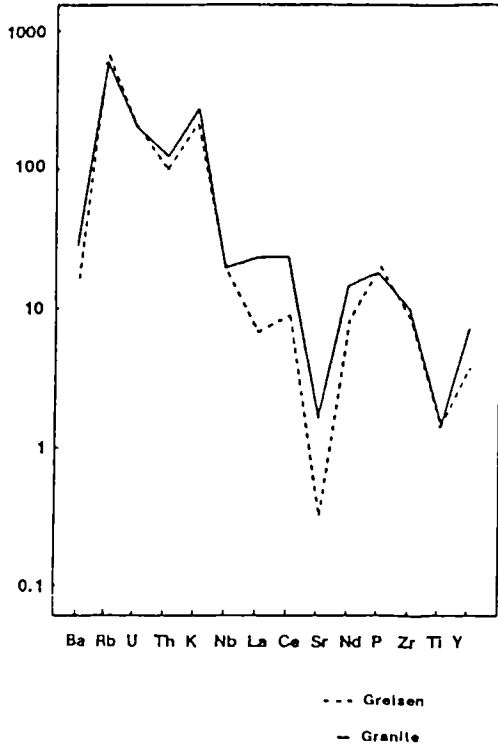
## 5:2:ii. THE EFFECTS OF GREISENIZATION.

In the case of the Skiddaw and Eskdale granites and the Carrock granophyre adjacent to mineral veins where high temperature acid leaching has occurred, a study of greisens provides additional information on geochemical changes associated with hydrothermal activity. The mantle normalized trace element patterns for the Skiddaw, Carrock and Eskdale greisens are compared with those for the respective less altered granites in Fig. 5:13. Considerable depletion of LREE and Sr is observed in the greisens relative to the granites. The effects of greisenization are also considered using plots of LIL elements against  $TiO_2$  which mineralogical studies indicate to be retained in secondary rutile in the greisens. Moreover  $TiO_2$  v. V plots (Figs. 5:14e and 5:15e), for the greisens indicate that they lie on the overall magmatic trend for the intrusions.

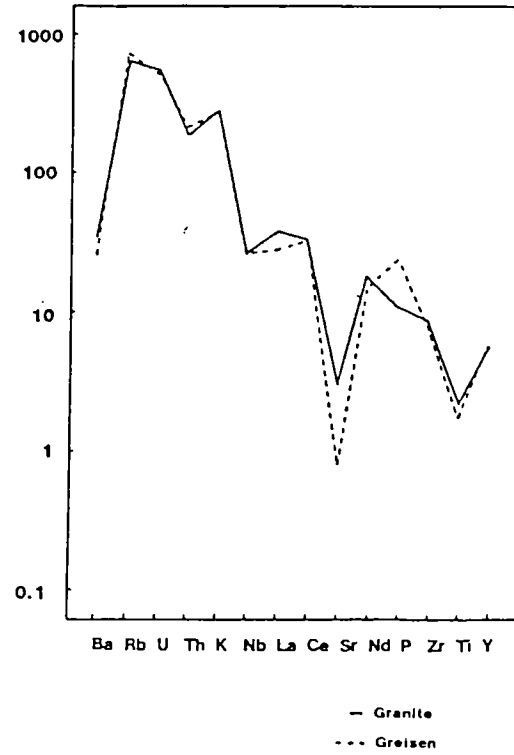
The chemistry of the Skiddaw and Eskdale greisens differ considerably. Rb in the Skiddaw greisen is significantly enriched above the "magmatic" trend (Fig. 5:14a), whereas in the Eskdale greisen there is no overall enrichment but considerable scatter when plotted against  $TiO_2$ , (Fig. 5:15a), suggesting large scale introduction and remobilization of Rb in the Skiddaw and Eskdale hydrothermal systems respectively at the present level of erosion. Li shows a similar distribution in the two greisenized intrusions (Figs. 5:14b and 5:15b), while Ba does not appear to have been mobile during greisenization of either the Eskdale or Skiddaw intrusions (Figs. 5:14c and 5:15c), probably reflecting the retention of Ba in secondary muscovite in the greisens. Sr on the other hand appears to be significantly depleted in the greisens of Eskdale and Skiddaw

Fig. 5:13. Comparison of mantle normalized trace element plots for average values of Lake District granites and average values for their respective greisens.

ESKDALE GREISEN vs. GRANITE



SKIDDAW GREISEN vs. GRANITE



CARROCK LEACHED GRANOPHYRE vs. GRANOPHYRE

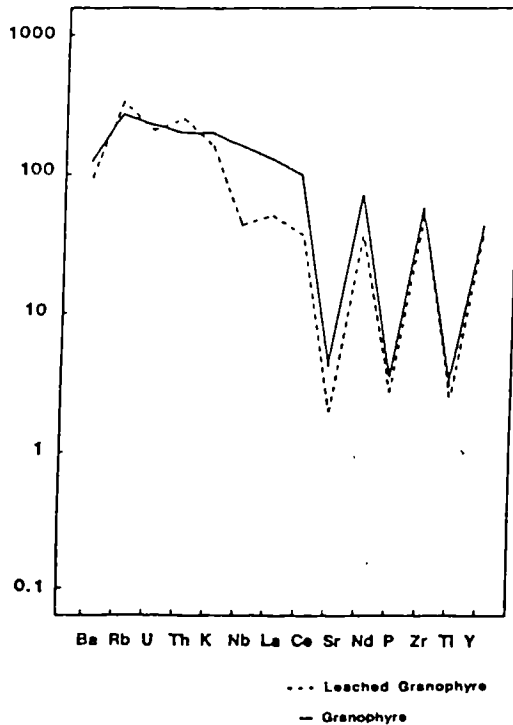


Fig. 5:14. Bi-element variation diagrams for the Skiddaw intrusion. a)  $TiO_2$  (immobile) vs. Rb (mobile), b)  $TiO_2$  (immobile) vs. Li (mobile), c)  $TiO_2$  (immobile) vs. Ba (mobile), d)  $TiO_2$  (immobile) vs. Sr (mobile), e)  $TiO_2$  (immobile) vs. V (immobile), f)  $TiO_2$  (immobile) vs. B (mobile); key to symbols on fold out sheet.

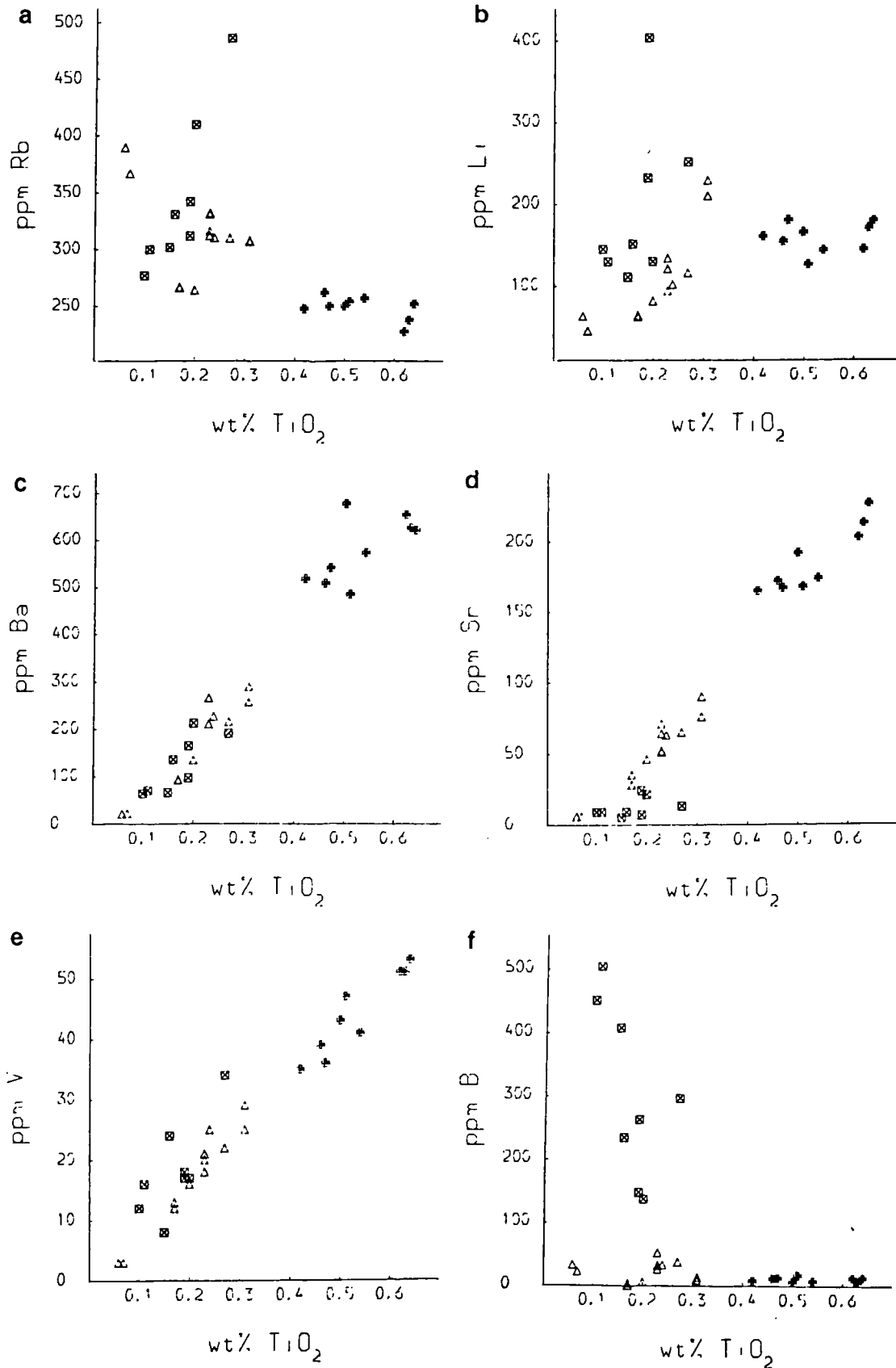
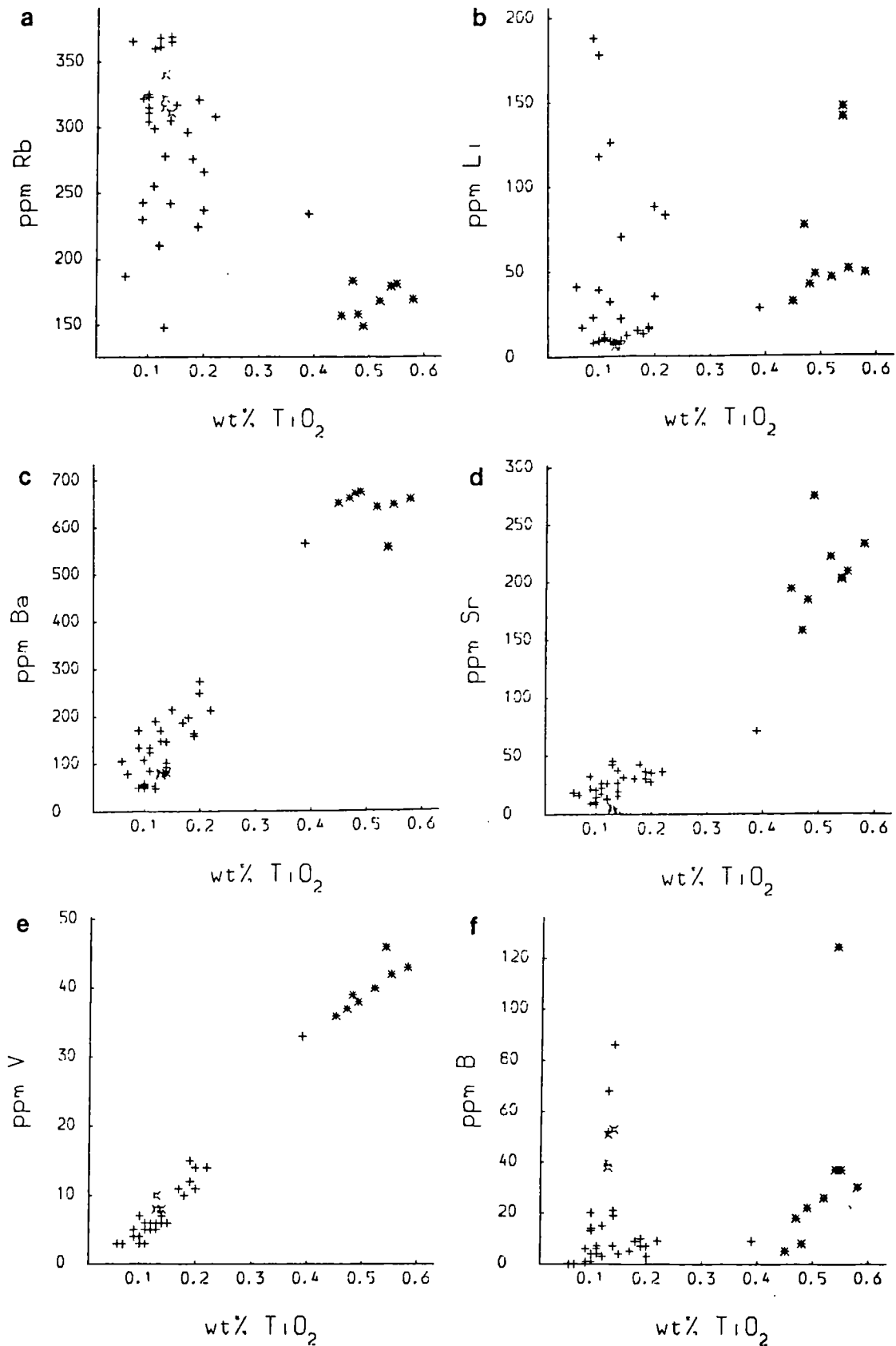


Fig. 5:15. Bi-element variation diagrams for the Eskdale intrusion. a)  $TiO_2$  (immobile) vs. Rb (mobile), b)  $TiO_2$  (immobile) vs. Li (mobile), c)  $TiO_2$  (immobile) vs. Ba (mobile), d)  $TiO_2$  (immobile) vs. Sr (mobile), e)  $TiO_2$  (immobile) vs. V (immobile), f)  $TiO_2$  (immobile) vs. B (mobile); key to symbols on fold out sheet.



(Figs. 5:14d and 5:15d), reflecting the breakdown of plagioclase and its replacement by muscovite which cannot accommodate Sr in its lattice. The Skiddaw and Eskdale granites show significant and extensive sericitization associated with low levels of Sr, probably reflecting some component of metasomatic alteration combined with magmatic fractionation.

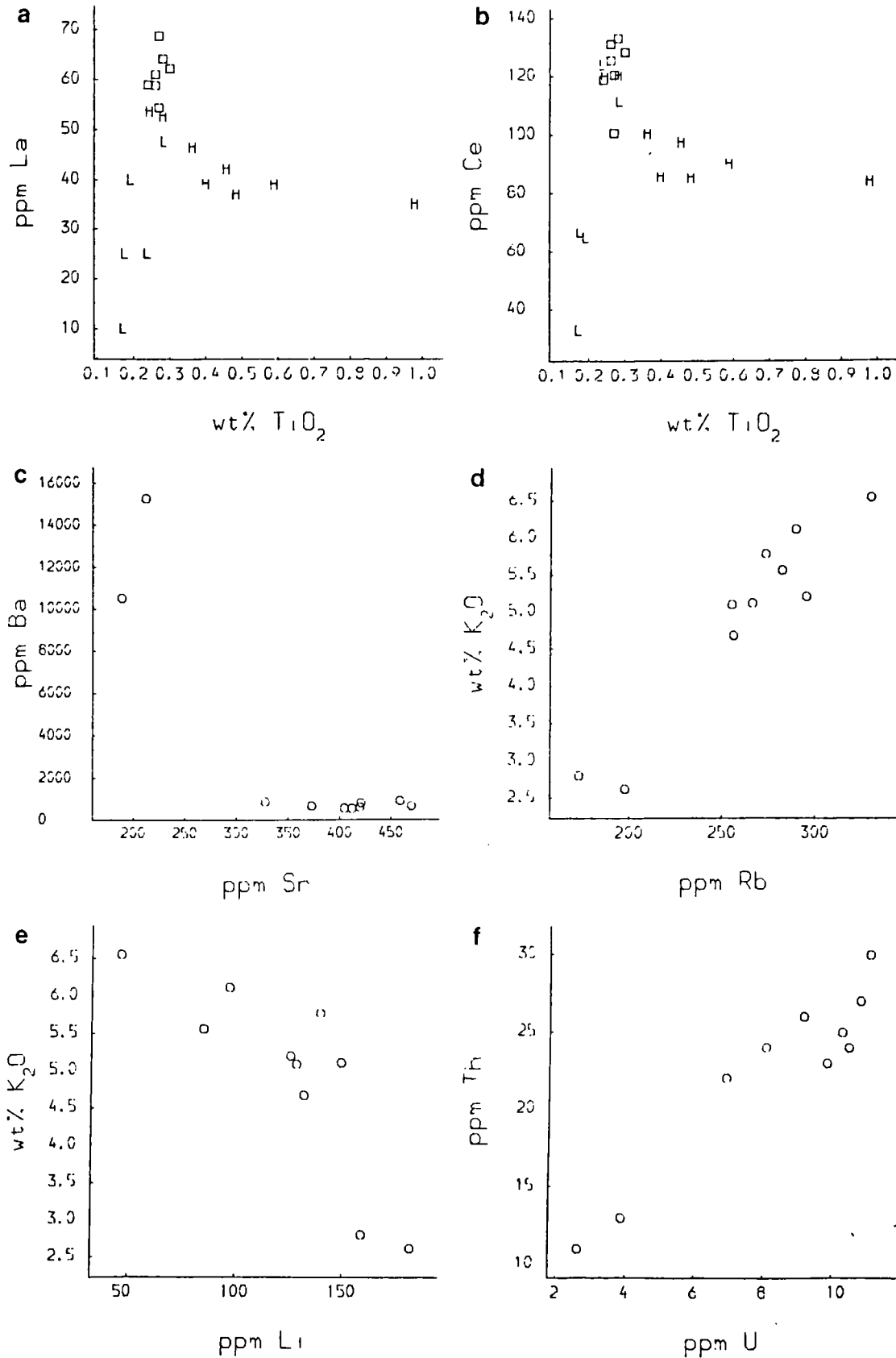
The Skiddaw greisens contain particularly high concentrations of boron, and boron also tends to be high in most Skiddaw granite samples. The high levels of boron are not the result of magmatic fractionation of a granite formed by melting of the Skiddaw slates which like all argillaceous sediments are enriched in boron. This is shown in the relationship of boron with HFS elements shown to be immobile during the process of hydrothermal alteration such as  $TiO_2$  where no correlation of boron with  $TiO_2$  (Fig. 5:14f) and no enrichment of boron in the most evolved samples with low  $TiO_2$  is observed. The use of  $TiO_2$  as an index of fractionation is not ideal; however Rb (the only element which behaves consistently incompatibly in all the Caledonian granites studied) is highly mobile under metasomatism and enriched as a result of the development of secondary muscovite particularly during the process of greisenization. Titanium however is immobile during these processes and in all intrusions shows a strong negative correlation with  $SiO_2$  during magmatic fractionation although variations in the fractionating mineral assemblage will result in variations in the gradient of the correlation. Moreover the muscovite which is probably in this case the main boron carrying phase and may contain high levels of boron (Stavrov & Khitrov 1962) appears in all cases to be secondary. The addition of boron is thus considered to be due to a high temperature metasomatism similar to that described for the Cornubian batholith (Simpson et al. 1979, Lister 1979). The source of the boron is believed to be fluids from the Skiddaw

slates. Phosphorous also appears to have been mobile to a limited extent in the Skiddaw greisen, with appreciably higher levels in the greisen relative to the granite reflecting the growth of secondary apatite.

The Eskdale greisens contain relatively little boron compared with those of the Skiddaw greisens; this is consistent with the generally lower levels of boron in the Eskdale granite which is emplaced largely into Borrowdale volcanics and which generally have much lower boron contents than the Skiddaw slates (Fig. 5:15f). It should be noted at this point that the high levels of boron observed in some samples of the Eskdale granodiorite are associated with contamination from xenoliths of the Skiddaw Slate which are numerous in the Waberthwaite quarries (Simpson 1934) the sampling locality for these granodiorites.

The Carrock Fell granophyre shows no evidence of the pervasive metasomatism, such as occurs in the Skiddaw and Eskdale intrusions, although alteration ranging from chloritization to microgreisenization occurs adjacent to mineral veins, for example adjacent to the west vein at Brandy Gill near Carrock Mine. Samples of the microgreisen and chloritized granophyre show many of the features of the Skiddaw greisen with elevated B, Rb, Li and depleted Sr contents. Moreover the LREE appear to have been strongly depleted (Figs. 5:16a and 5:16b), which is thought to reflect the breakdown of apatite in hydrothermal fluids in which the activity of fluorine was high; indeed fluorite is present in many samples of the adjacent mineralized Skiddaw granite.

Fig. 5:16. Bi-element variation diagrams for the Carrock granophyre and ferrogabbros (a and b); and the Shap granite (c, d, e and f). a)  $TiO_2$  (immobile) vs. La (mobile), b)  $TiO_2$  (immobile) vs. Ce (mobile), c) Sr (mobile) vs. Ba (mobile), d) Rb (mobile) vs.  $K_2O$  (mobile), f) U (mobile) vs. Th (mobile); key to symbols on fold out sheet.



## 5:2:iii. GEOCHEMISTRY OF METASOMATISM OTHER THAN GREISENIZATION.

The Shap granite is unique amongst the Caledonian granites studied in having high levels of Sr, Rb, Ba, U, Th, Li, and  $K_2O$  (Figs 5:16c, d, e and f), although on the basis of immobile HFS element trends (Fig. 5:12a), it is one of the least magmatically evolved plutons in the Lake District. The high values of Ba and Sr together with Rb, Li, U, Th and  $K_2O$  may be the result of a unique source for this granite which is not sampled by any other Caledonian granite. However the close proximity of the Shap granite in time and space to the Skiddaw granite in the Lake District, which is geochemically similar to the granites of eastern Scotland, and no discernable difference in the isotope geochemistry of the Shap granite from the remaining Caledonian granites renders a unique source for the Shap granite unlikely.

The Shap granite has visible effects of metasomatism. Samples of the Shap granite which contain very high levels of Ba are pervasively mineralized with the development of microveins and overgrowths of baryte. The high  $K_2O$  and Rb values are also thought to be secondary and related to the subsolidus growth of potassium feldspar which occurs in xenoliths and autoliths in the granite. These large potassium feldspar crystals also contain numerous anhedral inclusions of other minerals as illustrated in chapter 3. The high U and Th levels observed in the Shap granite have also probably been enhanced by metasomatism; this is supported by the presence of uranium in secondary hematite pseudomorphing sphene and grain boundary sites as seen in leucans. The relatively low levels of boron in the Shap granite suggest the origin of the metasomatic fluids was not the sediments surrounding the granite and a model whereby

the Shap granite was the site of volatile discharge from the larger Lake District batholith system at depth is suggested as a possible source of the enrichments in Li, Rb, U, Th, and  $K_2O$  observed in the Shap granite.

The Threlkeld microgranite appears to have been affected by a pervasive low temperature metasomatism as seen in the abundant sericitization of the feldspars within this intrusion and numerous calcite veins within the granite. Geochemically this has resulted in the loss of principally Ba, and Sr, which give vertical trend when plotted against  $TiO_2$ , similarly Cr, V and Ni appear to have become mobile producing similar trends although the REE and other HFS elements appear to have been unaffected (Figs. 5:17a, b, c, d, e and f).

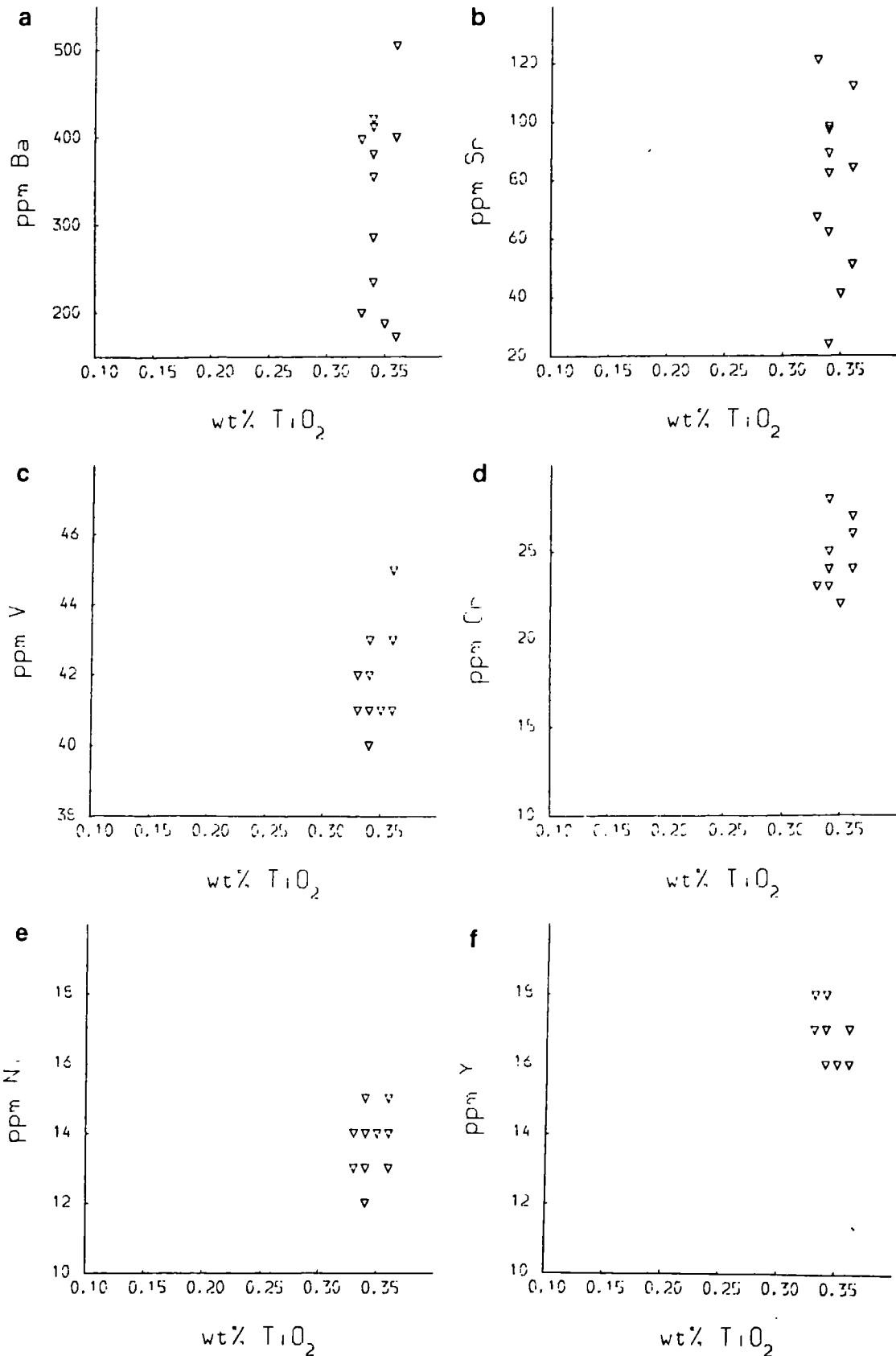
### 5:3. MINERALIZATION AND METASOMATISM IN THE CALEDONIAN GRANITES OF SCOTLAND.

The Caledonian igneous province of Scotland is not generally mineralized. However there are isolated plutons in west Scotland with associated porphyry copper mineralization. In east Scotland there are metalliferous tin-uranium granites and in north Scotland the Helmsdale granite has uranium mineralization.

#### 5:3:i. THE PORPHYRY COPPER MOLYBDENUM GRANITES.

The porphyry copper molybdenum granites were were recognized during the BGS regional geochemical survey (Plant et al. 1980) and earlier studies (Ellis 1977, Evans et al. 1977). These are the Kilmelford, Ballachulish and Comrie intrusions located in southwest and central Scotland (Fig. 1:2). The Kilmelford, Comrie and Ballachulish granitoid bodies are the

Fig. 5:17. Bi-element variation diagrams for the Threlkeld microgranite. a)  $TiO_2$  (immobile) vs. Ba (mobile), b)  $TiO_2$  (immobile) vs. Sr (mobile), c)  $TiO_2$  (immobile) vs. V (immobile), d)  $TiO_2$  (immobile) vs. Cr (immobile), e)  $TiO_2$  (immobile) vs. Ni (immobile), f)  $TiO_2$  (immobile) vs. Y (immobile); key to symbols on fold out sheet.



only intrusions covered in this study which have positively identifiable "porphyry type" low grade copper and molybdenum deposits, although high levels of copper are also associated with the Foyers, Strath Ossian, Moor of Rannoch, Ben Nevis, Etive, Garabal Hill and Strontian granites (Fig. 5:4), and high molybdenum levels are reported for one sample from the Garabal Hill complex (Fig. 5:3). These high levels of copper and molybdenum are exclusively associated with basic members of these intrusions and appear not to be associated with any porphyry type mineralization.

The granites with associated porphyry mineralization have elevated copper and molybdenum (Figs. 5:3 and 5:4). These intrusions also have high levels of boron (Fig. 5:5) which, as in the Lake District, appears to be secondary in origin, the high levels correlating with visible secondary alteration. However boron is also found at above background levels in the Foyers and Garabal Hill intrusions (Fig. 5:5), thus enhanced levels of this element is not in itself conclusive evidence for potential mineralization, but rather as evidence of fluid rock interaction which does not necessarily result in mineralization. Tin and tungsten are at background levels in these granites, (Figs. 5:1 and 5:2), as are the levels of lithium, uranium and beryllium, (Figs. 5:6, 5:8 and 5:9). However thorium is present in above background levels in the Ballachulish intrusion, (Fig. 5:7).

According to the geochemical classification of these granites set up in Chapter 4, the Kilmelford diorite and porphyrite and the Ballachulish granodiorite belong to the high strontium and phosphorous group of the less evolved juvenile granitoids, with the Ballachulish granite belonging

to the West Scotland group of the more evolved juvenile granites which are also characterized by high levels of strontium. The Comrie granite which is more molybdenum rich, with little associated copper, belongs to the intermediate group of the more evolved juvenile granitoids.

The elements which are likely to have become mobile during the process of porphyry copper mineralization are the same as those outlined in the discussion of mineralization of the Lake District granites although because of the strong links between copper mineralization and high levels of zinc (Olade & Fletcher 1976) the behaviour of this element is also discussed. In the Kilmelford diorite and porphyrite, which appear to have suffered the most pervasive mineralization of the intrusions with porphyry type mineralization, all the elements which are mobile in aqueous solutions appear to have been redistributed. Thus although vanadium correlates with  $TiO_2$  both elements being immobile, (Fig. 5:18a), rubidium, strontium, barium, lithium, uranium and thorium do not correlate with  $TiO_2$  and are highly scattered, thus indicating remobilization (Figs. 5:18c, d, e, f, g and h). Boron, as in the Lake District granites, does not correlate with  $TiO_2$  and therefore may be thought to have been introduced into the Kilmelford complex from the Dalradian metasediments which have high levels of boron (Fig. 5:18b). Zinc does not correlate closely with  $TiO_2$ , which would be expected if this element had not been involved in the mineralization process (Fig. 5:18i).

The Ballachulish intrusion does not appear to have been strongly affected by the mineralization. Both vanadium and strontium correlate closely with  $TiO_2$  displaying the original igneous trends with  $TiO_2$ , V and

Fig. 5:18. Bi-element variation diagrams for the Kilmelford complex. a)  $TiO_2$  (immobile) vs. V (immobile), b)  $TiO_2$  (immobile) vs. B (mobile), c)  $TiO_2$  (immobile) vs. Rb (mobile), d)  $TiO_2$  (immobile) vs. Li (mobile), e)  $TiO_2$  (immobile) vs. Sr (mobile), f)  $TiO_2$  (immobile) vs. Ba (mobile), continued on next page; key to symbols on fold out sheet.

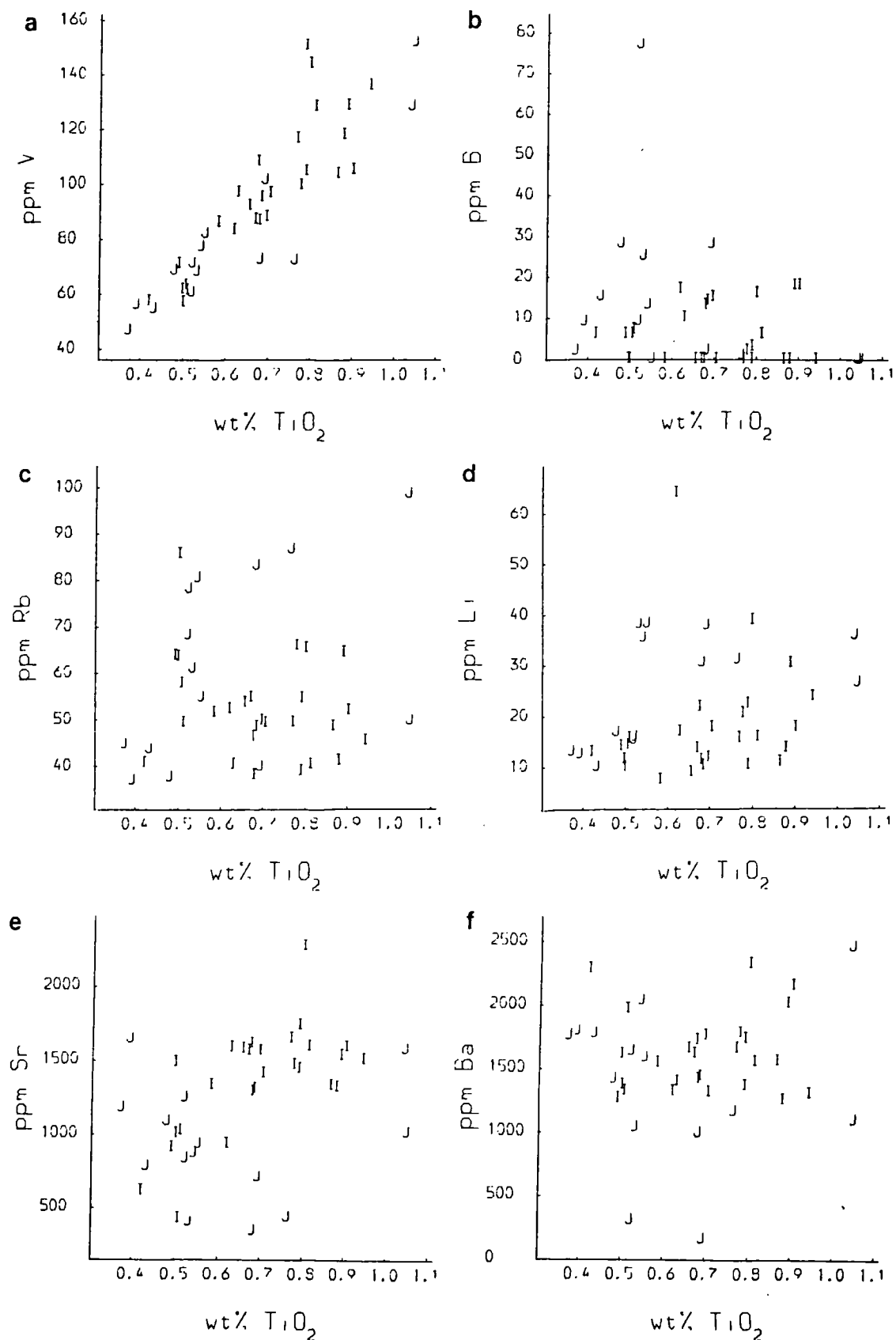
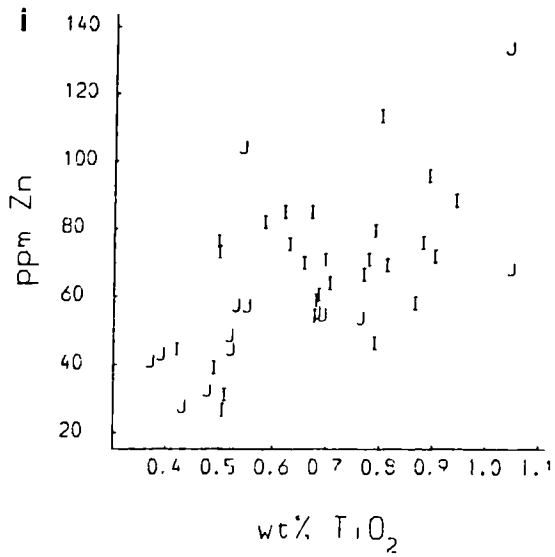
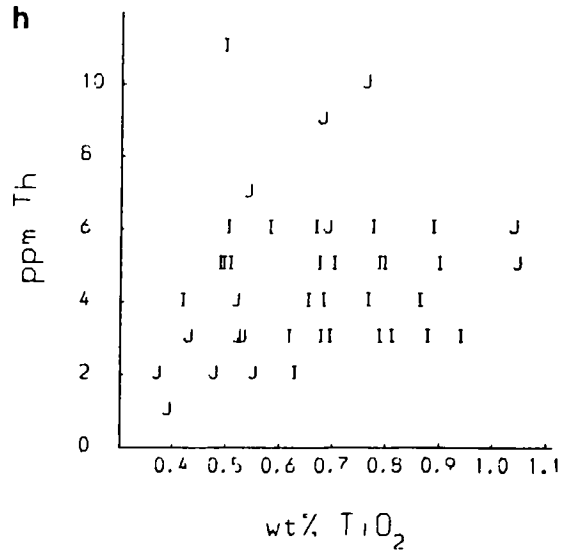
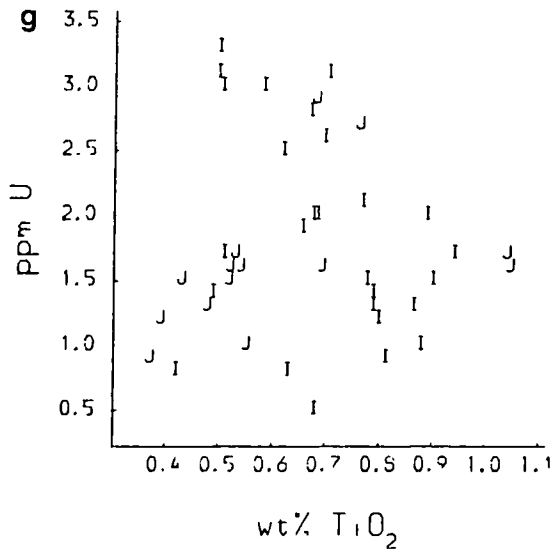


Fig. 5:18. Continued. Bi-element variation diagrams for the Kilmelford complex. g)  $TiO_2$  (immobile) vs. U (mobile), h)  $TiO_2$  (immobile) vs. Th (mobile), i)  $TiO_2$  (immobile) vs. Zn (mobile); key to symbols on fold out sheet.



Sr behaving compatibly in the granitoid magmatic system (Fig. 5:19a and e). Also uranium, thorium and rubidium correlate with  $TiO_2$  although not as closely - thus there may be some remobilization of these elements - but in general their behaviour is consistent with igneous processes giving enrichment of uranium, thorium and rubidium in the samples with low  $TiO_2$  (Figs. 5:19c, g and h). In this case zinc correlates with  $TiO_2$  indicating that its distribution is controlled by igneous processes rather than by mineralizing fluids. The compatible behaviour zinc (Fig 5:19i) indicates fractionation of hornblende or biotite which have crystal liquid distribution coefficients for Zn of 7 and 20 respectively (Henderson 1982). Boron does not correlate with  $TiO_2$  (Fig. 5:19b) and this would be consistent with its derivation from the Dalradian metasediments and its introduction into the Ballachulish intrusion during metasomatism. Both lithium and barium do not correlate with  $TiO_2$  and appear to have been redistributed during the mineralization process (Figs. 5:19d and f).

The geochemistry of the Comrie intrusion is similar to the Ballachulish intrusion. Vanadium, strontium, barium and zinc behave in a fashion consistent with their distribution being controlled by igneous fractionation processes (Figs. 5:20a, e, f and i). Also rubidium, uranium and thorium show igneous trends with enrichment of these elements in samples with low  $TiO_2$  (Figs. 5:20c, g and h). Boron, as in the Kilmelford and Ballachulish intrusions, does not correlate with  $TiO_2$  (Fig. 5:20b), which would be consistent with its introduction into the intrusion during mineralization. Lithium appears to have been substantially remobilized during the mineralization process as shown by the absence of any correlation with  $TiO_2$  (Fig. 5:20d).

Fig. 5:19. Bi-element variation diagrams for the Ballachulish complex. a)  $TiO_2$  (immobile) vs. V (immobile), b)  $TiO_2$  (immobile) vs. B (mobile), c)  $TiO_2$  (immobile) vs. Rb (mobile), d)  $TiO_2$  (immobile) vs. Li (mobile), e)  $TiO_2$  (immobile) vs. Sr (mobile) f)  $TiO_2$  (immobile) vs. Ba (mobile), continued on next page; key to symbols on fold out sheet.

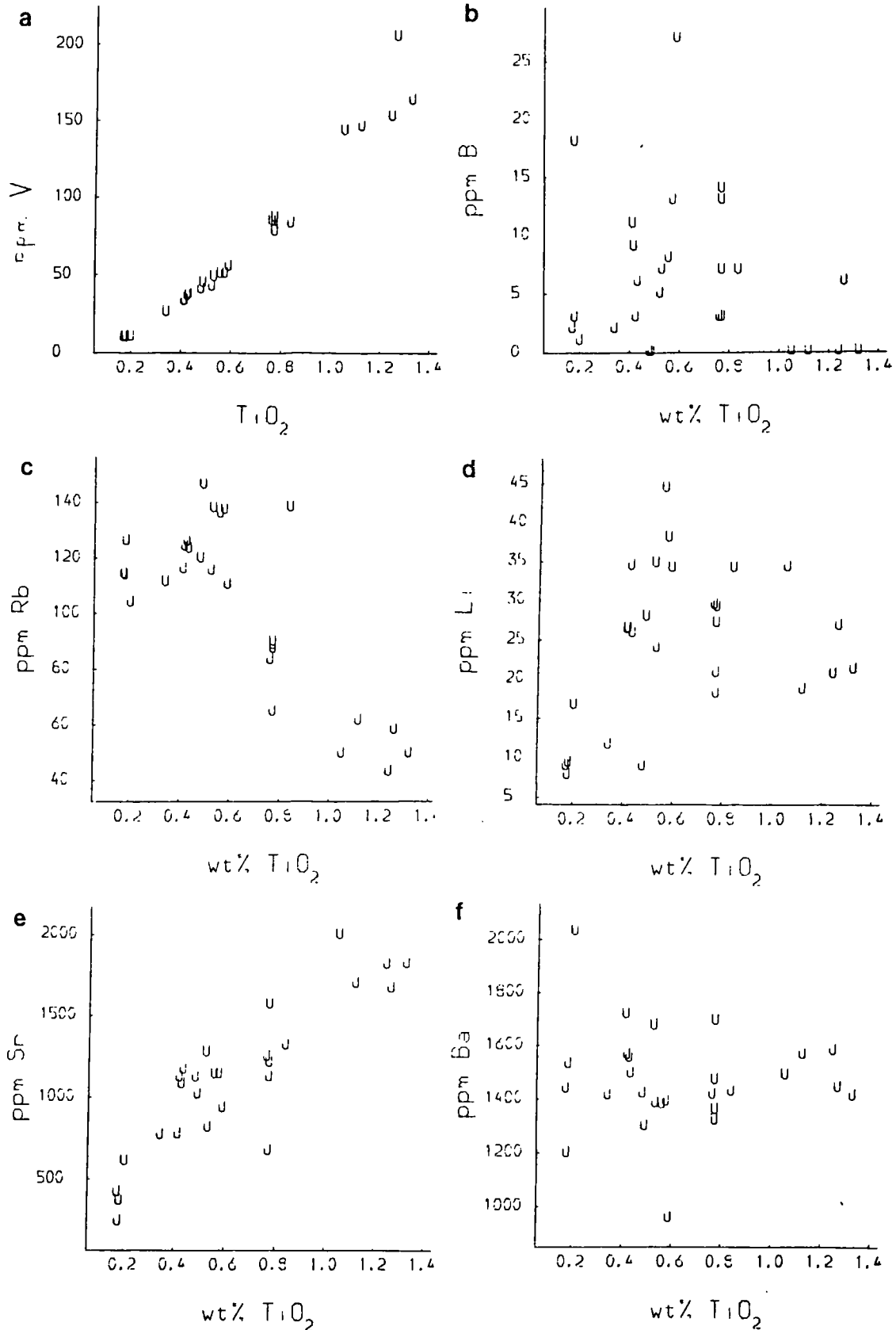


Fig. 5:19. Continued. Bi-element variation diagrams for the Ballachulish complex. g)  $TiO_2$  (immobile) vs. U (mobile), h)  $TiO_2$  (immobile) vs. Th (mobile), i)  $TiO_2$  (immobile) vs. Zn (mobile); key to symbols on fold out sheet.

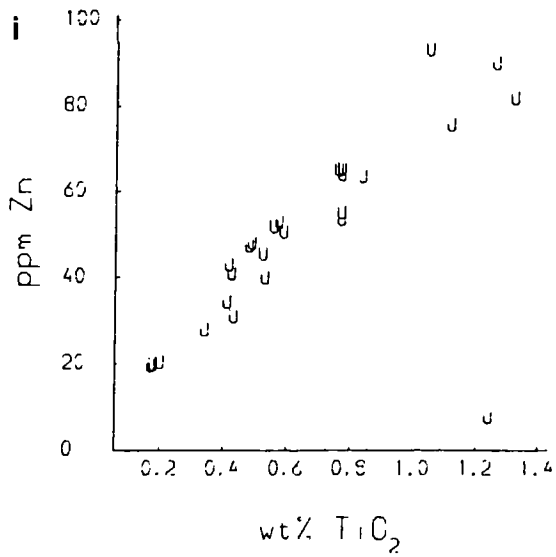
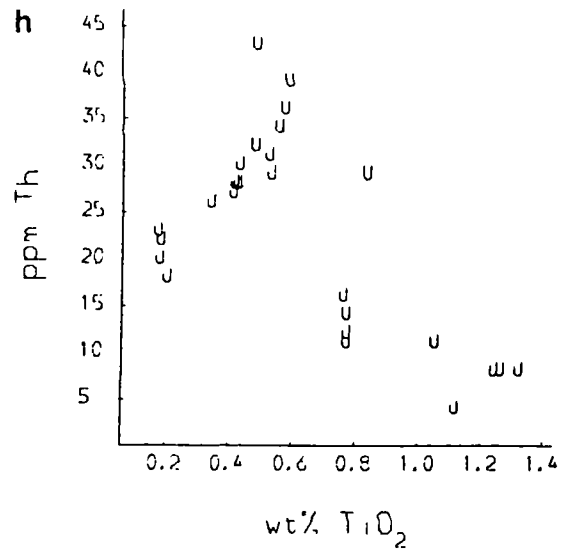
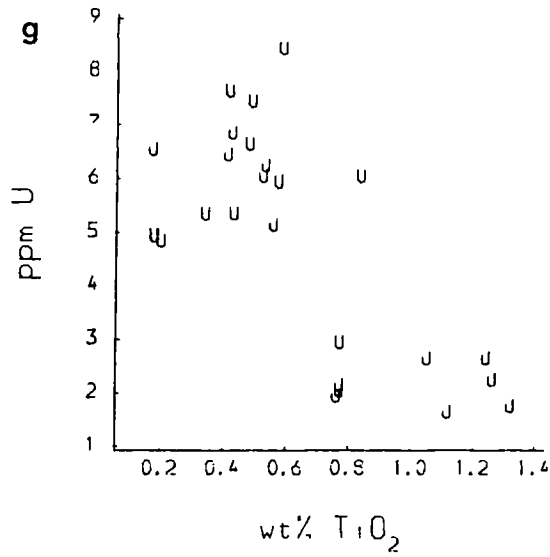


Fig. 5:20. Bi-element variation diagrams for the Comrie complex. a)  $TiO_2$  (immobile) vs. V (immobile), b)  $TiO_2$  (immobile) vs. B (mobile), c)  $TiO_2$  (immobile) vs. Rb (mobile), d)  $TiO_2$  (immobile) vs. Li (mobile), e)  $TiO_2$  (immobile) vs. Sr (mobile), f)  $TiO_2$  (immobile) vs. Ba (mobile), continued on next page; key to symbols on fold out sheet.

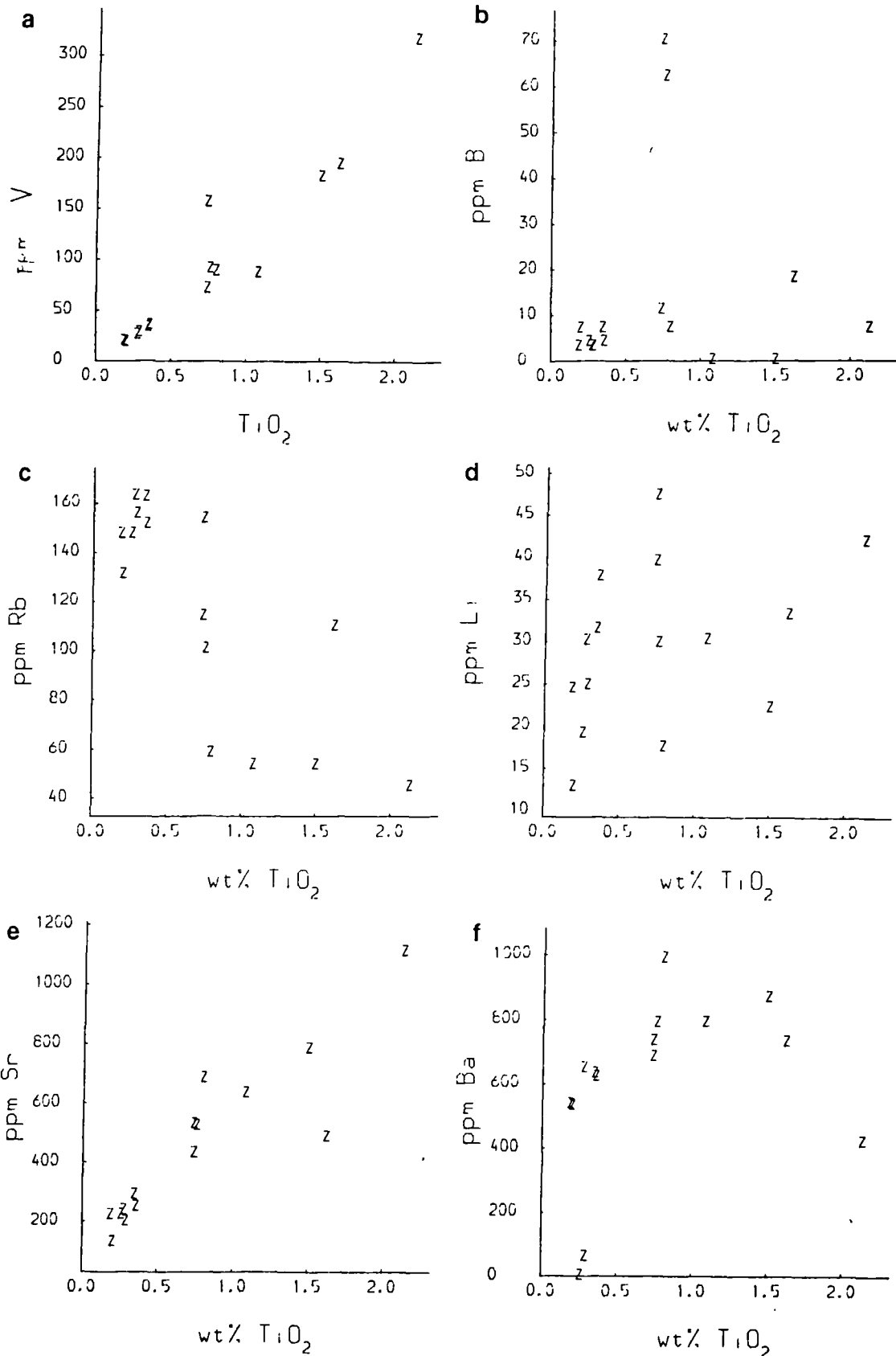
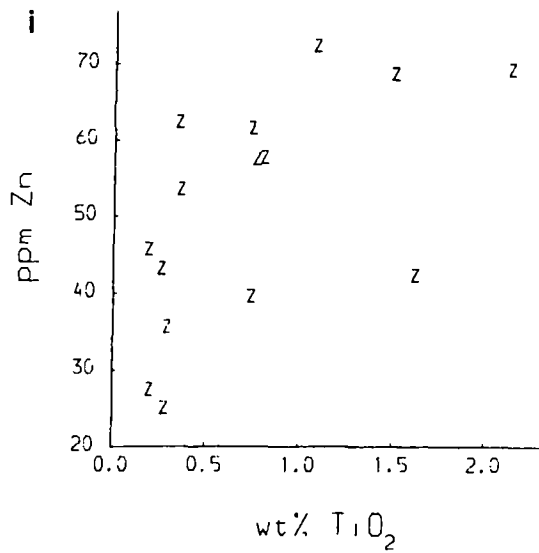
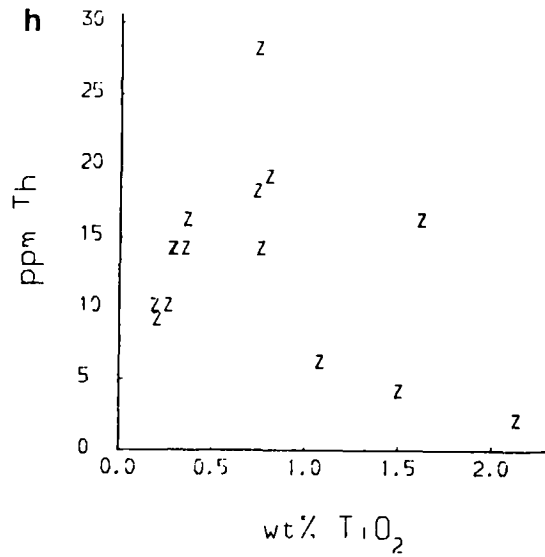
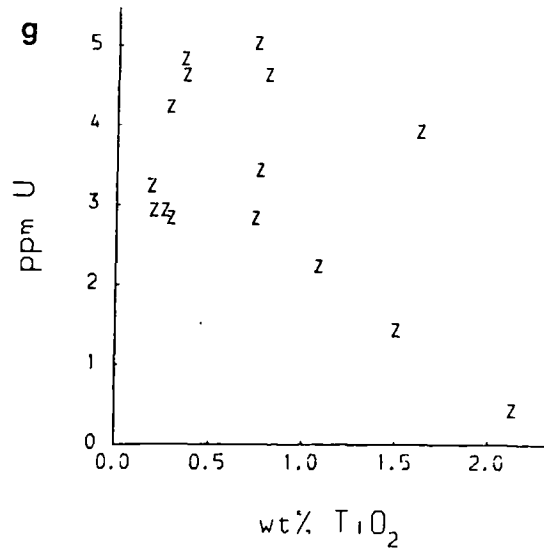


Fig. 5:20. Continued. Bi-element variation diagrams for the Comrie complex. g)  $TiO_2$  (immobile) vs. U (mobile), h)  $TiO_2$  (immobile) vs. Th (mobile), i)  $TiO_2$  (immobile) vs. Zn (mobile); key to symbols on fold out sheet.



## 5:3:ii. THE METALLIFEROUS TIN TUNGSTEN GRANITES OF EASTERN SCOTLAND.

Many of the Caledonian granites of the Grampian region of Scotland are characterized by high levels of tin, tungsten, uranium, thorium, lithium and beryllium (Simpson et al. 1979, Johnstone et al. 1979, Plant et al. 1980, Plant et al. 1983), although these granites are not mineralized. The intrusions with significant (above background) levels of tin and tungsten are the Cairngorm and Glen Gairn granites (Figs. 5:1 and 5:2), although slightly above background values for tin are observed in the Lochnagar, Cromar, Mt Battock, Bennachie, Hill of Fare and Peterhead granites (Fig. 5:1). Copper and molybdenum are present at below background levels in all these granites except at Glen Gairn where the greisen samples with high tin and tungsten also contain above background levels of molybdenum and copper (Figs. 5:3 and 5:4). Boron however is at background levels in all the metalliferous granites of this region (Fig. 5:5). Above background levels of uranium and thorium are found in the Cairngorm, Glen Gairn, Lochnagar, Cromar, Mt Battock and Bennachie granites (Fig. 5:6) and of thorium in the Hill of Fare, Moy, Ben Rinnes and Peterhead granites (Fig. 5:7). Similarly high levels of lithium are found in the Cairngorm, Glen Gairn, Lochnagar, Mt Battock, Bennachie, Hill of Fare and Peterhead granites (Fig. 5:8), and above background levels of beryllium are observed in the Cairngorm, Glen Gairn, Mt Battock and Bennachie granites (Fig. 5:9).

All the intrusions in the Grampian region which have above background levels of tin and tungsten belong to the Cairngorm type group of evolved juvenile granites with the exception of the Lochnagar granite which belongs to the intermediate group and is the only hornblende bearing

granite with high levels of tin. The overall geochemistry of this group of granites with high levels of tin is similar to that of the Cornubian batholith (Simpson & Plant 1984) (Fig. 5:21).

The absence of boron in most of the metalliferous tin-tungsten granites of the Grampian region is significant, because these intrusions are hosted by boron-rich Dalradian metasediments (Plate 5:1) (Plant et al. 1984) as are the granitoids with porphyry copper mineralization. Thus the absence of boron together with the generally fresh nature of the granites implies that there was no circulation of connate or meteoric water through these intrusions which could have resulted in mineralization. Presumably this is a consequence of the higher metamorphic grade of the host metasediments, because the high concentrations of uranium and thorium in these large intrusions implies no lack of a long term heat source; the only possible exception to this is the Peterhead granite where some hydrothermal alteration is observed and boron is present.

Growth of secondary muscovite is however observed in most Scottish granites and also local hematitization; moreover the samples with the highest levels of tin and tungsten are found in the zinwaldite greisen at Glen Gairn. This latter greisen shares many of the geochemical features of the Skiddaw greisen, such as high rubidium and lithium and low strontium, but in contrast to the Skiddaw greisen it has low boron: a feature characteristic of the parent granite (Table 5:1). As the host rocks to this intrusion contain high levels of boron there is an implication that the fluids involved in this greisenization process were magmatic rather than connate. If so it is possible that the secondary

Fig. 5:21. A comparison of mantle normalized trace element patterns for the Cairngorm and Dartmoor granites; patterns separated by one log scale, from Simpson and Plant (1984).

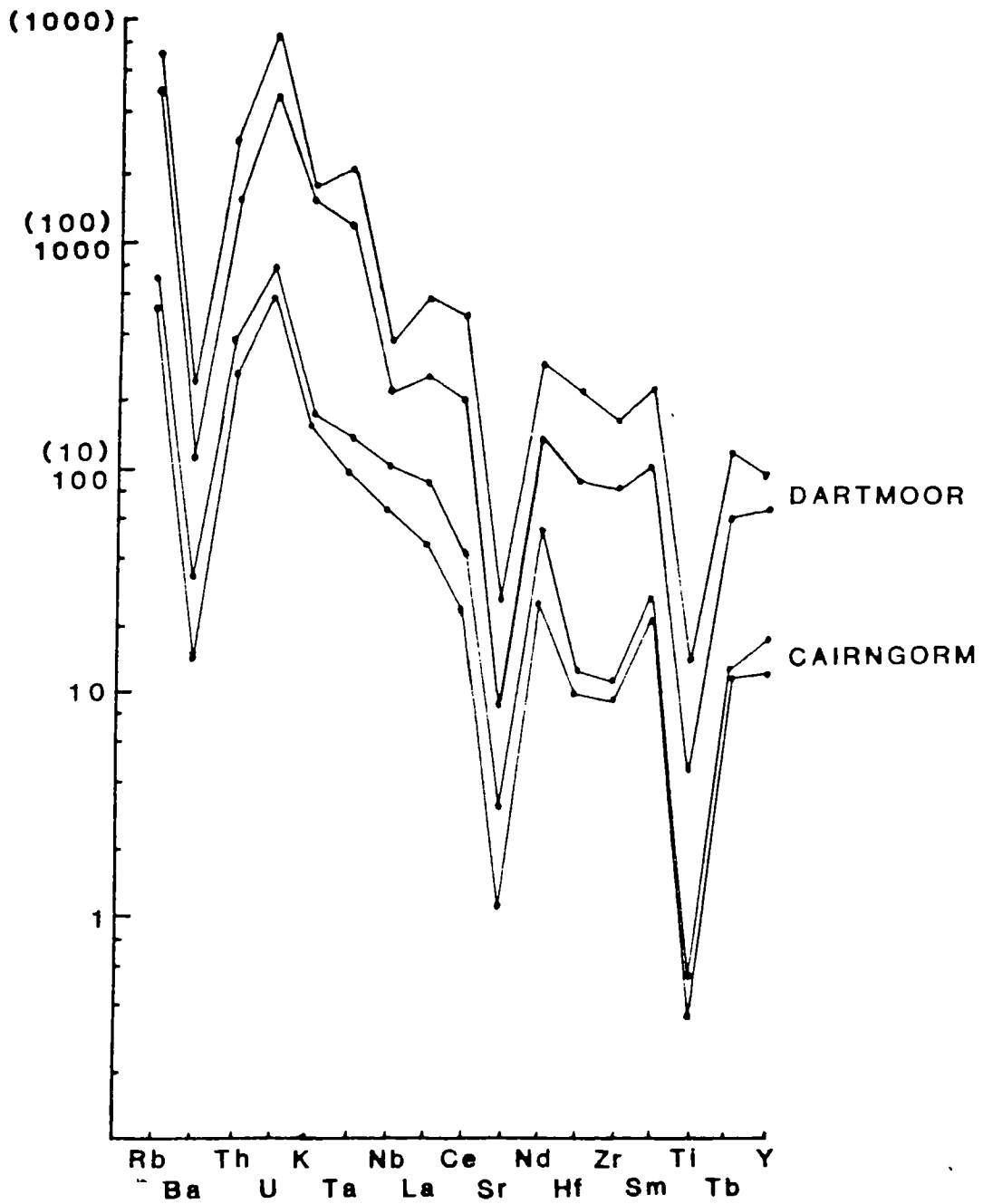
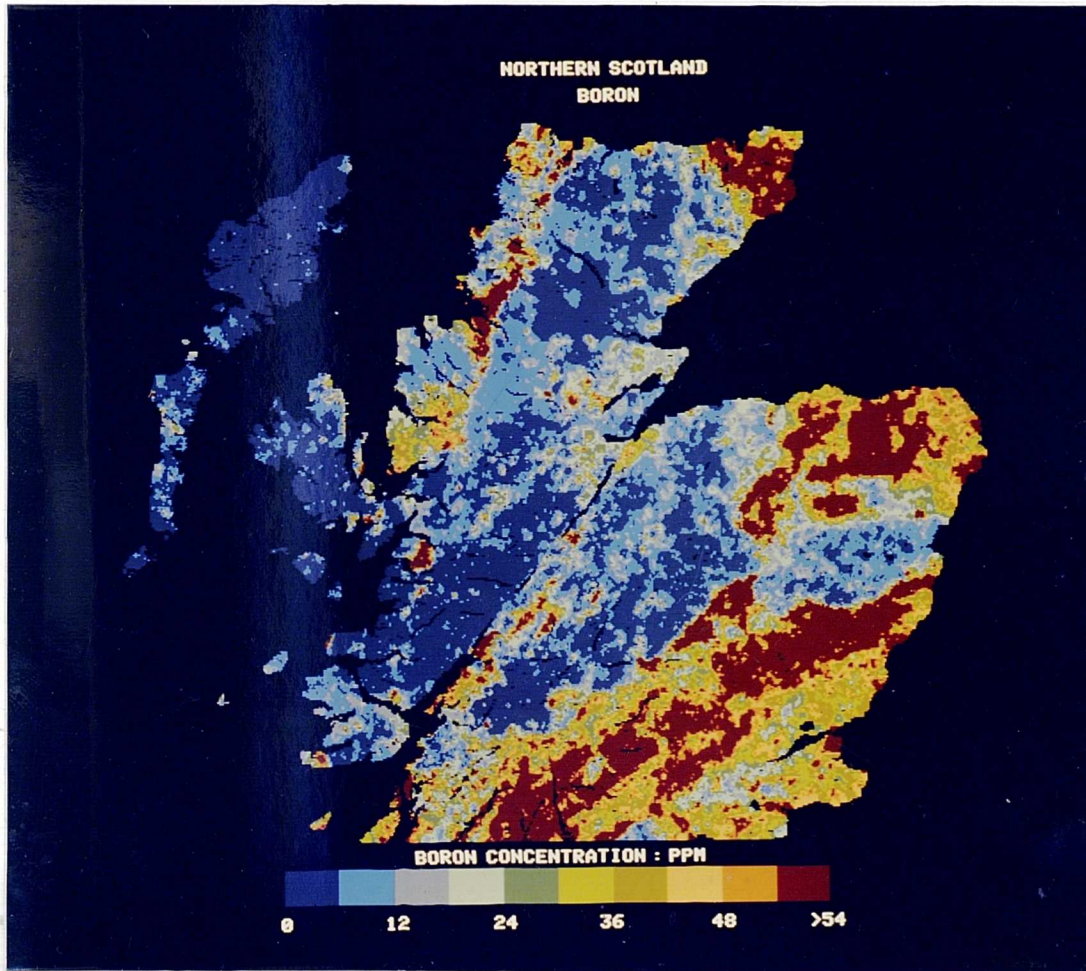


PLATE 5:1. (See over page).

PLATE 5:1.

Map of boron concentrations from stream sediments over Scotland  
(reproduced with the permission of Dr J. Plant British Geological  
Survey).



muscovite in many of the Cairngorm type granites may have resulted from the action of magmatic water. The greisen samples from the Glen Gairn granite are among the most geochemically evolved parts of the intrusion, having the lowest levels of  $TiO_2$  and vanadium (Fig. 5:22a); also levels of Sr in the Glen Gairn greisen are compatible with the igneous magmatic trend observed for the rest of the granite (Fig. 5:22b) with no obvious Sr depletion. The Glen Gairn greisen is strongly enriched in lithium, barium, rubidium, yttrium and niobium along with tin and tungsten (Figs. 5:22c, d, e, h and i). It is to be noted that yttrium and niobium behave incompatibly in the Cairngorm type granites - this will be discussed in more detail in Chapters 6 and 7. Uranium and thorium are also present at high levels in the greisen, although there is no enrichment over the unaltered granite (Figs. 5:22f and g). Apparently these greisens, which are small and quite localized, seem to be the result of a reaction between the more evolved parts of the Glen Gairn intrusion and a volatile component enriched in residual magmatic components.

---

TABLE 5:1 SELECTED TRACE ELEMENT ABUNDANCES FOR AVERAGE GLEN GAIRN AND SKIDDAW GREISENS.

	Rb	Li	Sr	Ba	U	Th	Nb	Y	V	La	Ce	Nd	Mo	Cu	Sn	W	Bi	Be	B
Glen Gairn greisen n=8	2106	567	17	701	13.9	20	43	81	2	7	14	7	32	19	144	14	59	2.2	<1
Skiddaw greisen n=8	345	195	13	125	9.2	15	16	17	18	14	42	14	20	47	18	79	83	3.3	306

---

There are a number of interesting implications arising from the marked compositional differences between the Glen Gairn and Skiddaw greisens. The high boron contents in the latter are a result of interaction between the granite and shale derived fluids during hydrothermal activity. However at Glen Gairn there is no boron enrichment, but many other trace

Fig. 5:22. Bi-element variation diagrams for the Glen Gairn intrusion. a)  $TiO_2$  (immobile) vs. V (immobile), b)  $TiO_2$  (immobile) vs. Sr (mobile), c)  $TiO_2$  (immobile) vs. Ba (mobile), d)  $TiO_2$  (immobile) vs. Rb (mobile), e)  $TiO_2$  (immobile) vs. Li (mobile), f)  $TiO_2$  (immobile) vs. U (mobile), continued on next page; key to symbols on fold out sheet.

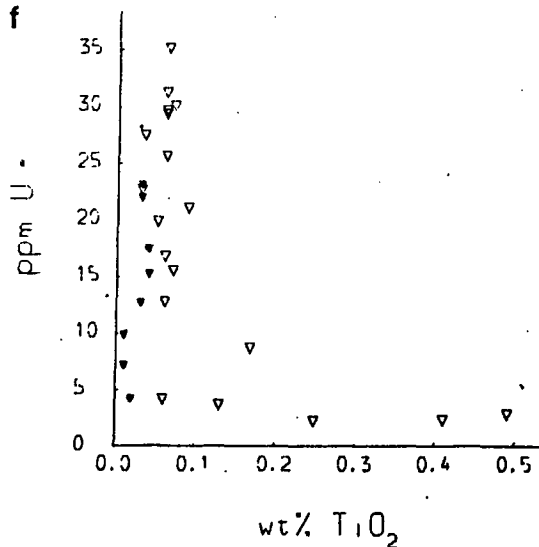
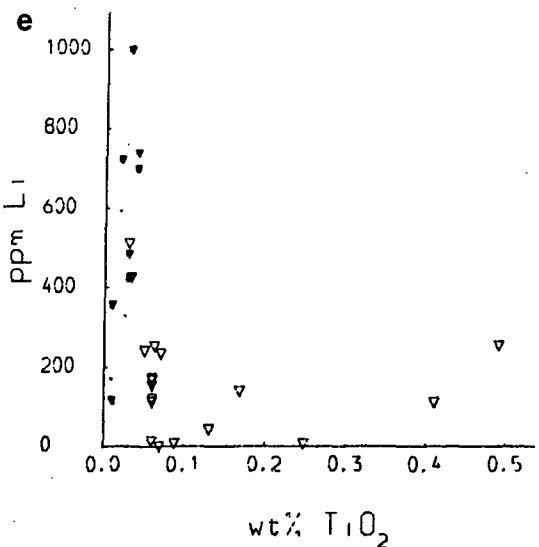
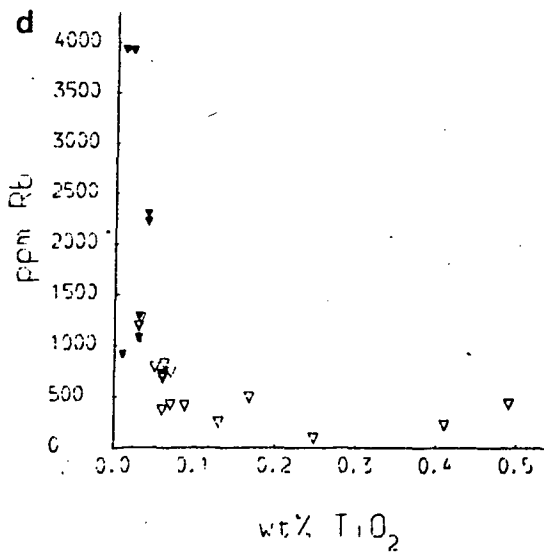
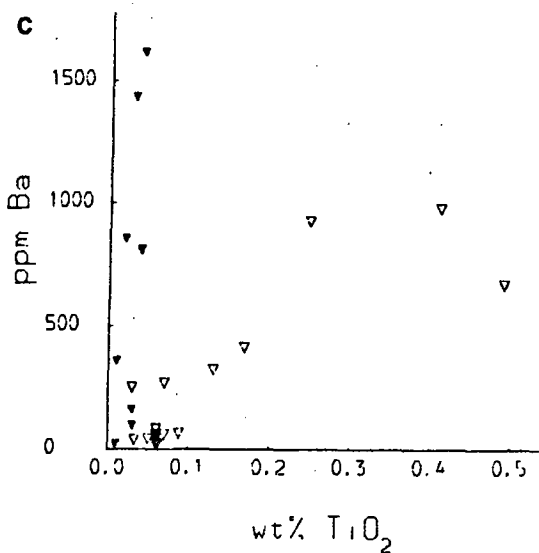
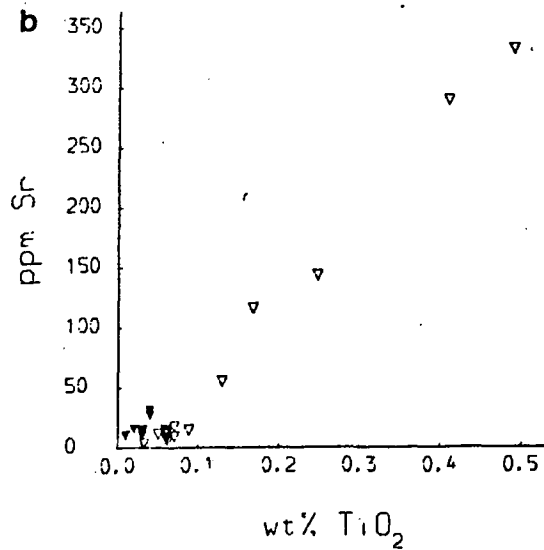
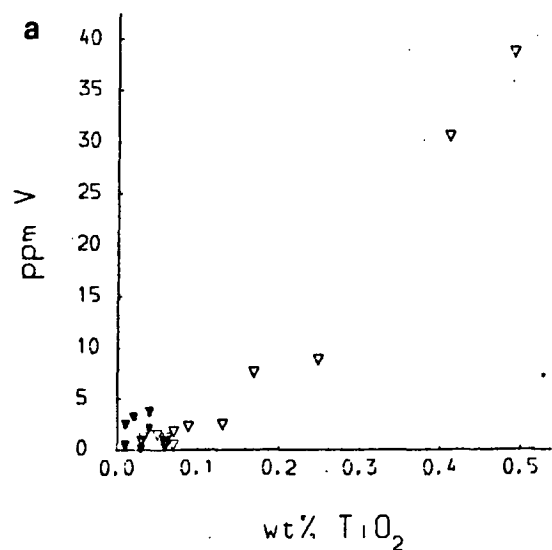
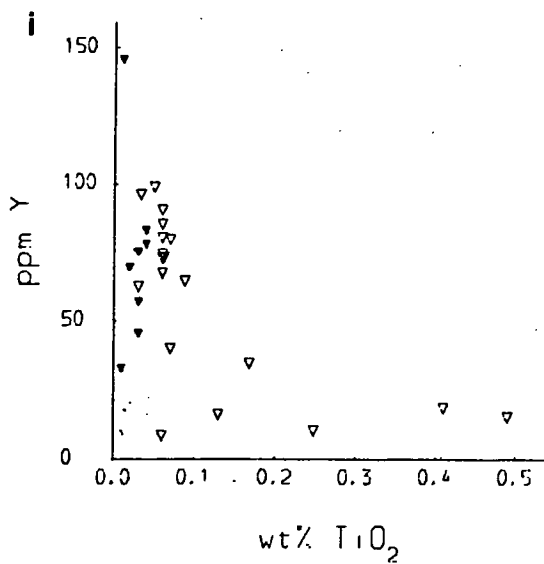
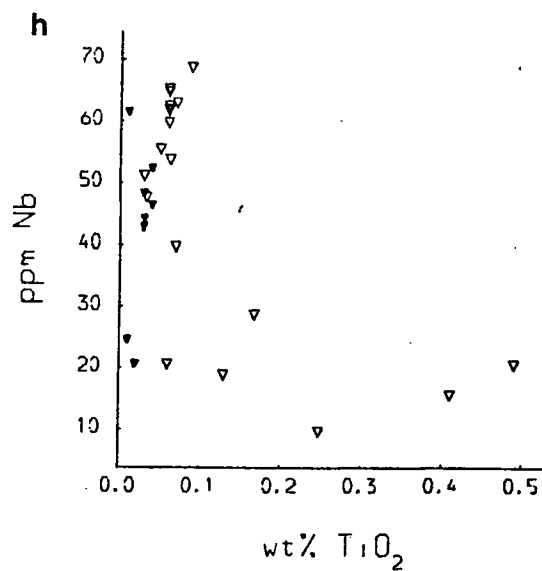
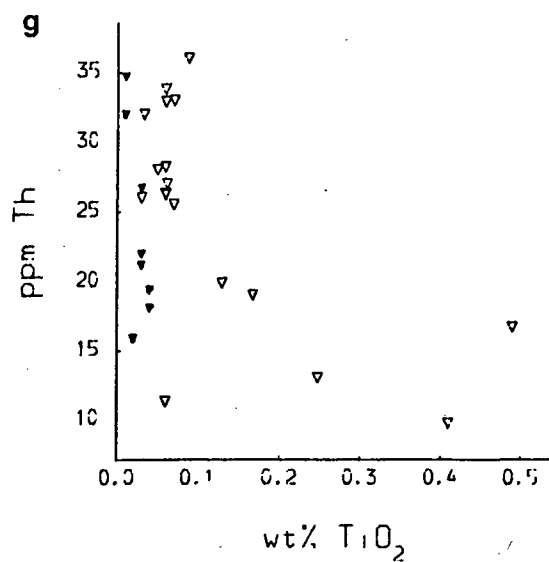


Fig. 5:22. Continued. Bi-element variation diagrams for the Glen Gairn intrusion. g)  $\text{TiO}_2$  (immobile) vs. Th (mobile), h)  $\text{TiO}_2$  (immobile) vs. Nb (mobile), i)  $\text{TiO}_2$  (immobile) vs. Y (mobile); key to symbols on fold out sheet.



elements are considerably enriched over their values in the Skiddaw greisen, tin and tungsten included. Hence it is probable that high levels of boron in any mineralized granite are likely to be the result of interaction between a juvenile granite and shale derived water.

#### 5:3:iii. FRACTURE INDUCED URANIUM MINERALIZATION AT HELMSDALE.

The Helmsdale granite is intruded into Moine granulites and cut by the Helmsdale Fault, part of the Great Glen Fault system. Uranium mineralization was recognized as a result of a BGS reconnaissance study between 1955 and 1971 (Bowie et al. 1966, Gallagher et al. 1971), and a more detailed study of the uranium mineralization was undertaken by Tweedie (1979), who concluded that U mineralization is generally associated with fracture systems within the Helmsdale granite. The mineralization is thought to have resulted from uranium enrichment during a low to medium temperature hydrothermal event (Tweedie 1979). Published stable isotope data for the Helmsdale intrusion is limited to one  $\delta^{18}$  value of +12.4 (Harmon et al. 1984) which is more compatible with a model involving the interaction of the granite with sediment derived connate water rather than meteoric water as suggested by Tweedie (1979). The origin of this water cannot be the "dry" Moine granulites and a more realistic model would be to derive the uranium from down-faulted Devonian sediments to the south of the exposed granite with migration upwards through the fractured granite.

The Helmsdale granite is enriched in uranium and thorium (Figs. 5:6 and 5:7), although unlike the Cairngorm type granites it is not enriched in lithium and beryllium (Figs. 5:8 and 5:9). Levels of boron are above

the Caledonian background level but are not greatly enriched, thus suggesting some interaction with sediment derived fluids (Fig. 5:5). A few samples of the Helmsdale granite have elevated levels of copper and molybdenum (Figs. 5:4 and 5:3), corresponding to observations of localized copper-molybdenum mineralization within the granite (Tweedie 1979). Both tin and tungsten are at essentially background levels throughout the granite (Figs. 5:1 and 5:2).

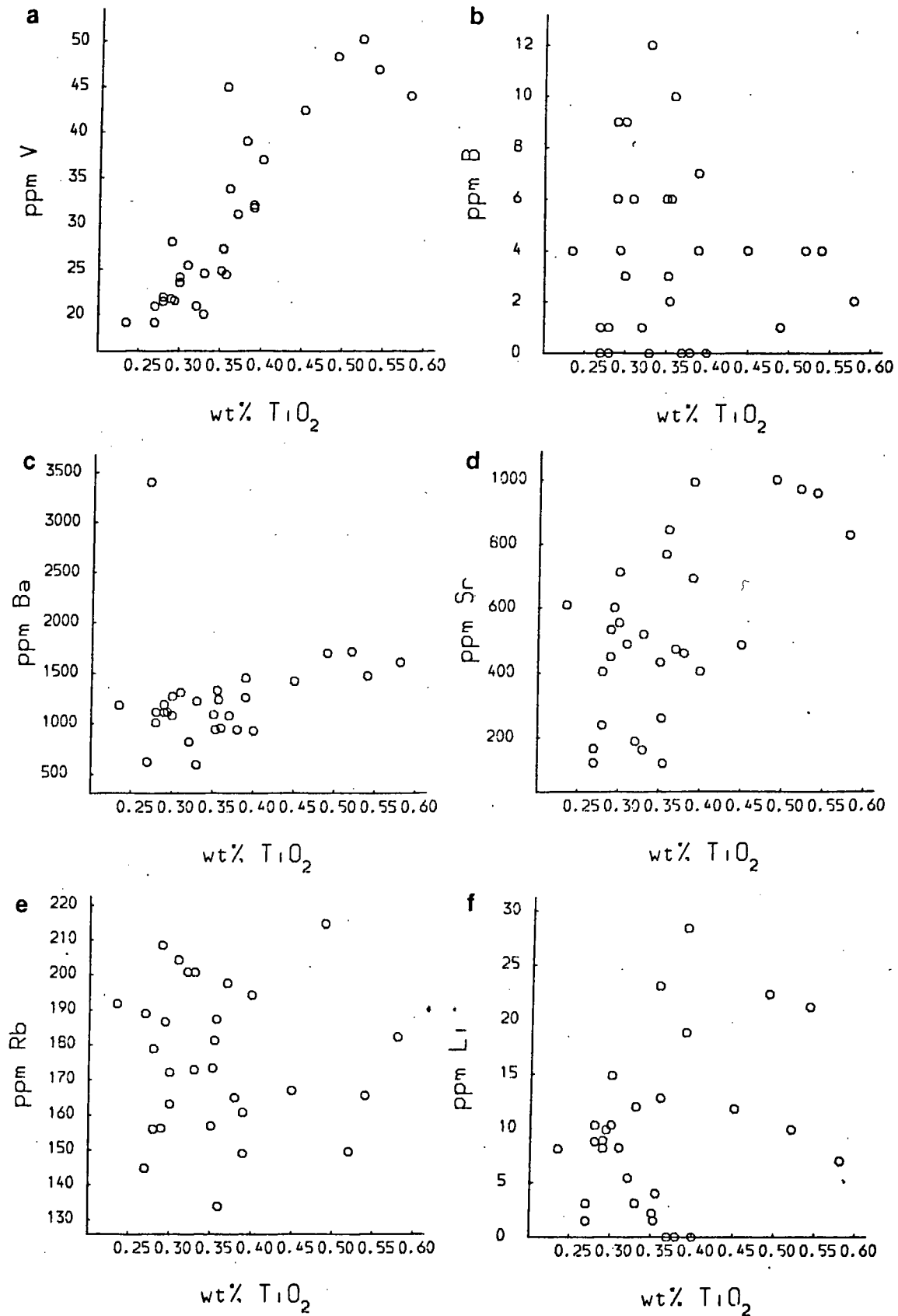
Element mobility in the Helmsdale mineralized granite can be assessed in the same way as for the Lake District granites. Vanadium correlates quite closely with  $TiO_2$  in the Helmsdale granite (Fig. 5:23a), with boron showing no relationship with  $TiO_2$  (Fig. 5:23b), thus indicating its secondary origin. Both barium and strontium show evidence of redistribution with increased scatter when plotted against  $TiO_2$ , high levels of barium in one sample is associated with the fluorite mineralization in the northeast part of the pluton (Figs. 5:23c and d). Additionally rubidium and lithium appear to have been remobilized and show increased scatter when plotted against  $TiO_2$  (Figs. 5:23e and f).

#### 5:4. SUMMARY AND CONCLUSIONS.

This geochemical approach to mineralization and metasomatism in the Caledonian granites has revealed a number of important factors.

a) During the water-rock interaction which results in mineralization and metasomatism a variety of trace elements become mobile: mainly rubidium, lithium, barium, strontium, uranium, thorium and boron.

Fig. 5:23. Bi-element variation diagrams for the Helmsdale intrusion. a)  $TiO_2$  (immobile) vs. V (immobile), b)  $TiO_2$  (immobile) vs. B (mobile), c)  $TiO_2$  (immobile) vs. Ba (mobile), d)  $TiO_2$  (immobile) vs. Sr (mobile), e)  $TiO_2$  (immobile) vs. Rb (mobile), f)  $TiO_2$  (immobile) vs. Li (mobile); key to symbols on fold out sheet.



b) The use of elements which remain immobile during this process helps to evaluate the extent to which the metasomatism has caused redistribution in the mobile elements especially where the metasomatism is localized. The use of immobile elements also defines igneous fractionation trends.

c) Boron enrichments in mineralized granites are shown to be unrelated to igneous fractionation processes and therefore boron must be introduced into the granites during the associated hydrothermal activity; the most likely source of this element is generally argillaceous host rocks of low metamorphic grade. Conversely boron enrichment is unlikely where the host rocks are of high metamorphic grade.

d) The unmineralized but metalliferous Caledonian tin-tungsten granites of eastern Scotland display enrichments in tin, tungsten, uranium, thorium, rubidium and lithium relative to their mineralized counterparts such as Skiddaw and the Cornubian batholith, but lack boron enrichments: The high grade nature of the host rocks to these intrusions indicates the lack of connate water necessary to cause mineralization, thus the high levels of tin, tungsten, uranium, thorium, rubidium, and lithium observed in tin granites are a primary magmatic feature.

e) The effects of metasomatism on the overall geochemical patterns of mineralized intrusions, as shown on mantle normalized trace element diagrams, is limited, and does not change the overall characteristics of the mantle normalized patterns, although some elements are depleted.

Key to Figs. in Chapter 6.

Figs. 6:1 and 6:24.

- \* - Skiddaw less geochemically evolved granite.
- △ - Skiddaw more geochemically evolved granite.
- ⊗ - Skiddaw greisen.

Figs. 6:2 and 6:25.

- \* - Eskdale granodiorite.
- + - Eskdale granite.
- ⌘ - Eskdale greisen.

Figs. 6:3 and 6:26.

- G - Carrock Fell gabbro.
- H - Carrock Fell hybrid granophyre and ferrogabbro.
- - Carrock Fell granophyre.
- L - Carrock Fell leached granophyre.

Fig. 6:4.

- - Shap granite.
- ▽ - Threlkeld microgranite.
- ◆ - Ennerdale granophyre.

Fig. 6:6.

- + - Grudie granite.
- 0 - Rogart complex.
- M - Migdale granite.

Fig. 6:7.

- S - Strontian complex.
- \* - Cluanie granodiorite.

Fig. 6:9.

- W - Ben Nevis outer granite.
- Ⓜ - Ben Nevis inner granite.
- E - Etive Ben Cruachan.
- ⓔ - Etive Ben Starav.

Fig. 6:10.

⌘ - Moor of Rannoch granodiorite.

□ - Strath Ossian granodiorite.

Fig. 6:12.

R - Ben Rinnes granite.

P - Peterhead granite.

\* - Moy granite.

Fig. 6:13.

A - Aberdeen granite.

T - Stritchen granite.

△ - Ardclach granite.

⊕ - Cove Bay granite.

Fig. 6:14.

D - Dorback granite.

B - Blackburn granite.

V - Glenlivet granite.

Fig. 6:15.

K - Mt. Battock granite.

Q - Cromar granite.

H - Hill of Fare granite.

## CHAPTER 6. THE GEOCHEMISTRY OF THE CALEDONIAN GRANITOIDS AND GEOCHEMICAL MODELLING OF SELECTED INTRUSIONS.

### 6:1. INTRODUCTION.

The objective of this chapter is to consider the geochemistry of the various Caledonian granites studied in the context of major and trace element models which might constrain their petrogenesis. For this purpose some 950 intrusive rock samples from 40 plutons covered in this study were analysed by wavelength dispersive X-ray fluorescence techniques (XRF), delayed neutron method (DNM) and direct reading optical spectrometry (DR). Small subsets of these samples were also analysed by instrumental neutron activation (INAA) and inductively coupled plasma spectrometry (ICP).

The elements determined were Si, Ti, Al, Fe, Mn, Mg, Ca, Na, K, P, Ba, Rb, Sr, Y, Nb, Zr, Ga, Zn, Ni, Th, La, Ce, Nd, Cr, V, Pb, Cu, Mo, Sn, W, (by XRF) U, (by DNM) Co, Li, Be, B, Ag, Cd, Bi, (by DR) La, Ce, Nd, Sm, Eu, Gd, Tb, Tm, Yb, Lu, U, Th, Ta, Hf, (by INAA) and La, Ce, Pr, Nd, Sm, Eu, Gd, Dy, Ho, Er, Yb, Lu (by ICP). Further details of the analytical techniques used are documented in Appendix B, and the data are listed in Appendices C, D, E and F.

### 6:2. MAJOR AND TRACE ELEMENT VARIATIONS.

The large number of plutons covered in this study and the large range of rock types has naturally given rise to equally large geochemical variations. To provide a convenient summary of these, average analyses

of the various plutons, or their main components, are given in Table 6:1. Variations in the major and selected trace element compositions of individual plutons, and groups of plutons where the data sets are small are shown in diagrams plotting selected elements against  $\text{SiO}_2$  in Figs. 6:1 to 6:22. Additionally the whole data set for Scotland and for the Lake District are shown separately for certain selected major and trace elements in order to show the geochemical relationships between individual plutons, in Chapter 7 (Figs. 7:1-7:14 and 7:14-7:38).

A summary of the important features of the  $\text{SiO}_2$  covariation diagrams for individual plutons is given below. In the interests of clarity this is dealt with in two main sections: the Lake District intrusives, and the Scottish granitoids.

TABLE 6:1. MEAN ANALYSES FOR THE BRITISH CALEDONIAN INTRUSIVES.

	1.	2.	3.	4.	5.	6.	7.	8.
	n=8	n=12	n=30	n=12	n=6	n=17	n=9	n=31
SiO <sub>2</sub>	69.8	72.3	74.0	75.4	65.9	51.5	67.9	76.3
TiO <sub>2</sub>	0.56	0.34	0.30	0.25	0.50	2.07	0.40	0.13
Al <sub>2</sub> O <sub>3</sub>	14.9	15.0	14.2	12.9	13.8	18.2	16.5	13.1
Fe <sub>2</sub> O <sub>3</sub>	2.3	3.0	1.7	3.0	7.9	10.6	4.1	1.7
MnO	0.05	0.08	0.07	0.09	0.27	0.25	0.11	0.03
MgO	1.2	1.1	0.6	0.2	0.3	4.7	0.9	0.2
CaO	1.8	1.2	0.9	0.9	2.6	8.3	2.2	0.5
Na <sub>2</sub> O	3.3	4.0	3.3	4.5	4.6	2.9	3.2	3.2
K <sub>2</sub> O	5.6	2.9	4.9	3.6	4.1	1.2	4.7	4.9
P <sub>2</sub> O <sub>5</sub>	0.24	0.18	0.13	0.03	0.12	0.14	0.20	0.17
Nb	13	11	16	26	20	8	14	12
Zr	169	137	95	424	412	121	199	79
Y	12	17	31	117	85	27	45	21
Sr	408	86	82	62	156	223	208	26
U	9.2	3.5	7.6	4.0	3.5	2.1	3.4	3.8
Rb	282	132	307	129	99	44	170	289
Th	25	7	15	14	11	3	15	9
Pb	41	14	45	27	19	12	30	16
Ga	23	17	20	24	29	23	21	21
Zn	26	39	82	82	162	83	42	20
Ni	14	14	5	3	2	27	5	2
Cr	32	24	14	4	3	82	18	6
V	46	42	26	2	3	349	41	8
La	52	23	26	93	42	18	40	12
Ce	95	47	58	128	95	35	85	31
Nd	36	20	22	91	53	20	37	15
Ba	801	329	284	591	524	230	633	143
Li	117	51	148	25	20	34	71	42
Be	7.4	1.2	5.6	2.4	2.3	1.1	2.4	2.5
B	16	29	95	2	<1	3	35	14
Co	6	8	5	2	2	38	9	2
Cu	31	28	8	2	10	32	12	1
Mo	2.4	0.5	5.0	<0.1	<0.1	<0.1	0.5	<0.1
Sn	44	9	6	9	5	1	4	12
W	8.5	2.7	4.5	8.0	5.0	2.0	4.1	4.5
Ag	0.1	<0.1	0.1	<0.1	<0.1	0.1	<0.1	<0.1
Cd	0.1	<0.1	0.2	<0.1	<0.1	<0.1	0.1	<0.1
Bi	1.4	0.1	24.3	0.1	<0.1	0.6	0.5	<0.1

n = No. of samples.

1. Shap
2. Threlkeld
3. Skiddaw
4. Carrock Fell granophyre
5. Carrock Fell hybrid suite
6. Carrock Fell gabbro
7. Eskdale granodiorite
8. Eskdale granite

TABLE 6:1 CONTINUED.

	1.	2.	3.	4.	5.	6.	7.	8.
	n=17	n=30	n=2	n=8	n=5	n=8	n=6	n=11
SiO <sub>2</sub>	74.3	70.7	74.3	63.2	68.7	69.7	69.6	62.5
TiO <sub>2</sub>	0.32	0.35	0.25	0.84	0.54	0.23	0.49	0.92
Al <sub>2</sub> O <sub>3</sub>	13.7	14.5	15.5	16.8	16.0	16.5	15.5	16.4
Fe <sub>2</sub> O <sub>3</sub>	1.8	1.6	1.1	4.9	3.1	1.8	2.7	5.0
MnO	0.03	0.03	0.02	0.08	0.04	0.05	0.05	0.08
MgO	0.4	0.6	0.3	3.3	1.8	0.4	1.4	3.3
CaO	0.6	0.9	0.9	4.0	2.2	2.1	2.5	4.4
Na <sub>2</sub> O	4.2	4.4	5.0	4.7	5.0	6.3	4.5	4.6
K <sub>2</sub> O	4.9	5.2	4.0	2.5	3.5	2.6	3.4	2.7
P <sub>2</sub> O <sub>5</sub>	0.05	0.19	0.11	0.38	0.24	0.10	0.18	0.32
Nb	15	13	5	11	9	8	9	18
Zr	279	171	139	228	181	132	141	182
Y	36	9	6	17	12	10	9	18
Sr	55	523	607	1096	916	947	706	1059
U	5.1	10.2	3.4	1.9	2.1	2.0	4.6	2.7
Rb	167	177	106	51	79	62	87	59
Th	20	29	14	10	10	5	14	9
Pb	9	65	33	18	22	33	20	19
Ga	17	19	21	22	21	24	20	21
Zn	13	37	36	71	54	55	42	62
Ni	2	10	2	53	25	3	29	76
Cr	5	21	9	130	61	5	29	106
V	13	29	19	97	54	22	45	91
La	38	50	26	73	48	14	30	43
Ce	84	106	65	126	89	25	50	77
Nd	32	35	19	48	34	10	18	31
Ba	439	1213	845	1278	1205	890	922	979
Li	6	10	8	12	12	12	22	23
Be	2.6	3.3	2.3	1.6	1.5	1.9	2.2	2.2
B	<1	4	<1	1	<1	<1	<1	<1
Co	3	5	4	16	9	2	6	22
Cu	0.2	5	0.4	1.4	10	0.4	7.1	15.2
Mo	0.4	1.1	<0.1	<0.1	<0.1	<0.1	0.1	0.2
Sn	8	1	2	5	4	5	3	3
W	4.7	1.6	0.4	2.6	0.6	0.1	1.7	1.1
Ag	<0.1	0.5	<0.1	<0.1	<0.1	<0.1	<0.1	0.1
Cd	<0.1	<0.1	<0.1	<0.1	<0.1	<0.1	<0.1	0.1
Bi	<0.1	0.1	<0.1	<0.1	<0.1	<0.1	0.5	0.1

n = No. of samples.

1. Ennerdale
2. Helmsdale
3. Migdale
4. Grudie
5. Rogart
6. Cluanie
7. Strontian granite
8. Strontian granodiorite

TABLE 6:1 CONTINUED.

	1. n=3	2. n=12	3. n=16	4. n=3	5. n=7	6. n=8	7. n=10	8. n=21
SiO <sub>2</sub>	62.0	58.5	68.5	70.8	69.4	75.5	69.1	65.9
TiO <sub>2</sub>	0.98	0.96	0.41	0.39	0.46	0.16	0.55	0.52
Al <sub>2</sub> O <sub>3</sub>	17.0	16.0	15.2	15.4	15.5	12.8	15.3	15.5
Fe <sub>2</sub> O <sub>3</sub>	5.0	5.9	2.5	2.2	2.7	0.9	3.1	3.8
MnO	0.08	0.09	0.04	0.05	0.04	0.03	0.05	0.07
MgO	3.2	3.9	1.1	0.7	1.4	0.2	1.5	2.6
CaO	4.6	4.9	1.5	1.2	1.9	0.6	2.2	3.3
Na <sub>2</sub> O	4.9	4.0	4.5	4.7	4.5	3.8	4.2	4.1
K <sub>2</sub> O	2.4	3.1	4.2	4.1	4.4	4.9	4.2	3.3
P <sub>2</sub> O <sub>5</sub>	0.38	0.39	0.15	0.13	0.17	0.05	0.18	0.20
Nb	13	15	16	11	12	10	11	7
Zr	199	186	201	233	165	80	170	112
Y	16	22	15	16	16	7	13	11
Sr	1241	1440	872	475	539	135	421	780
U	2.4	2.5	6.1	2.6	3.5	5.0	3.5	2.2
Rb	49	75	122	97	112	156	109	68
Th	8	13	29	13	16	21	14	9
Pb	19	24	27	19	21	26	23	19
Ga	22	20	16	18	17	15	18	18
Zn	61	63	37	31	34	18	46	52
Ni	57	42	9	6	22	4	15	55
Cr	74	93	18	7	40	7	26	120
V	91	116	33	19	41	9	52	67
La	47	50	42	47	31	25	37	25
Ce	84	96	74	84	53	43	61	44
Nd	34	43	27	32	20	13	22	18
Ba	877	1453	1464	1483	1091	338	1115	1029
Li	22	25	24	19	21	21	20	17
Be	1.9	1.8	1.9	1.3	1.6	2.0	1.7	1.1
B	2	5	7	<1	3	<1	2	<1
Co	21	20	6	3	6	3	10	14
Cu	12	39	123	1	6	2	12	15
Mo	<0.1	<0.1	11.3	<0.1	<0.1	<0.1	0.2	<0.1
Sn	4	3	1	2	1	<1	3	3
W	1.1	0.8	28.8	2.3	1.4	1.0	1.5	1.2
Ag	0.1	<0.1	0.2	<0.1	<0.1	<0.1	<0.1	<0.1
Cd	0.1	<0.1	<0.1	<0.1	<0.1	<0.1	<0.1	<0.1
Bi	0.7	0.2	<0.1	<0.1	<0.1	<0.1	0.6	<0.1

n = No. of samples.

1. Strontian granodiorite
2. Ballachulish granodiorite
3. Ballachulish granite
4. Ben Nevis inner granite
5. Ben Nevis outer granite
6. Etive Ben Starav
7. Etive Ben Cruachan
8. Moor of Rannoch

TABLE 6:1 CONTINUED.

	1. n=10	2. n=17	3. n=25	4. n=19	5. n=7	6. n=6	7. n=9	8. n=5
SiO <sub>2</sub>	65.8	68.2	69.9	56.3	73.8	73.4	76.8	73.1
TiO <sub>2</sub>	0.64	0.44	0.88	1.15	0.27	0.37	0.22	0.52
Al <sub>2</sub> O <sub>3</sub>	15.1	14.8	15.9	18.8	14.1	14.4	12.9	14.5
Fe <sub>2</sub> O <sub>3</sub>	4.1	2.4	4.9	6.0	1.8	2.3	1.4	2.9
MnO	0.07	0.05	0.09	0.10	0.03	0.05	0.03	0.05
MgO	2.7	0.9	2.6	2.6	0.5	0.6	0.3	0.6
CaO	3.4	1.6	3.3	4.1	0.8	1.5	0.8	0.9
Na <sub>2</sub> O	3.9	4.0	4.1	4.6	3.7	3.5	3.2	3.2
K <sub>2</sub> O	3.6	4.7	3.8	3.6	4.9	3.8	5.0	5.2
P <sub>2</sub> O <sub>5</sub>	0.18	0.15	0.32	0.44	0.12	0.09	0.07	0.12
Nb	12	10	10	11	14	9	18	14
Zr	161	149	216	278	108	119	166	208
Y	17	11	17	17	11	20	25	34
Sr	565	590	871	1137	88	266	131	95
U	3.3	1.8	1.4	1.3	3.4	1.7	3.3	2.6
Rb	106	84	72	73	214	107	222	167
Th	14	7	5	5	23	5	30	15
Pb	22	23	18	20	26	24	31	26
Ga	17	17	19	22	18	16	19	19
Zn	41	39	56	76	34	34	27	34
Ni	29	8	12	11	6	10	4	5
Cr	66	19	24	17	9	25	11	15
V	66	39	82	98	21	35	16	31
La	27	25	38	37	17	13	47	37
Ce	46	48	66	66	30	25	92	79
Nd	19	20	27	29	12	11	34	35
Ba	917	1408	1859	2220	537	855	478	571
Li	24	12	18	17	20	29	21	47
Be	1.7	1.2	1.3	1.3	2.9	1.6	2.5	1.8
B	4	4	12	7	3	<1	<1	2
Co	7	6	12	17	3	5	2	n.d.
Cu	5	8	15	14	2	<1	9	7
Mo	<0.1	<0.1	<0.1	<0.1	0.2	<0.1	<0.1	<0.1
Sn	1.2	1.6	2.6	2.0	1.8	2.1	2.0	3.7
W	1.6	1.2	1.3	0.5	0.9	1.1	1.8	n.d.
Ag	<0.1	<0.1	0.1	0.1	<0.1	<0.1	<0.1	0.1
Cd	<0.1	<0.1	<0.1	<0.1	<0.1	<0.1	0.1	<0.1
Bi	0.5	<0.1	0.5	0.7	<0.1	<0.1	<0.1	<0.1

n = No. of samples.

1. Strath Ossian
2. Foyers granite
3. Foyers granodiorite
4. Foyers tonalite
5. Moy
6. Ardclach
7. Ben Rinnes
8. Stritchen

TABLE 6:1 CONTINUED.

	1.	2.	3.	4.	5.	6.	7.	8.
	n=9	n=4	n=7	n=4	n=10	n=26	n=14	n=7
SiO <sub>2</sub>	77.1	68.3	71.5	73.5	76.5	76.1	74.2	74.6
TiO <sub>2</sub>	0.16	0.71	0.44	0.27	0.17	0.21	0.32	0.16
Al <sub>2</sub> O <sub>3</sub>	13.2	15.5	15.0	14.7	13.0	12.9	13.5	14.0
Fe <sub>2</sub> O <sub>3</sub>	1.6	4.7	2.8	1.8	1.0	1.2	1.7	1.1
MnO	0.02	0.04	0.04	0.04	0.04	0.06	0.05	0.03
MgO	0.2	1.2	0.7	0.5	0.2	0.3	0.5	0.3
CaO	0.4	2.5	1.9	1.4	0.6	0.7	0.7	0.8
Na <sub>2</sub> O	3.2	3.4	3.3	4.3	3.8	3.6	3.7	3.9
K <sub>2</sub> O	5.3	3.9	4.0	4.0	4.9	4.9	5.1	5.0
P <sub>2</sub> O <sub>5</sub>	0.06	0.27	0.18	0.11	0.05	0.07	0.09	0.05
Nb	28	29	18	14	15	23	30	25
Zr	191	324	245	140	119	111	181	114
Y	50	16	15	14	15	16	25	31
Sr	41	333	296	275	57	55	107	183
U	3.6	1.8	4.1	3.6	5.8	18.8	7.2	7.4
Rb	222	122	120	112	177	368	344	305
Th	20	18	13	12	21	36	35	31
Pb	24	21	20	21	31	41	32	35
Ga	21	23	21	19	18	18	19	19
Zn	44	49	48	31	20	26	31	28
Ni	2	4	3	2	4	2	2	3
Cr	6	5	6	5	8	5	5	9
V	9	32	21	19	8	11	18	11
La	59	65	44	25	33	33	52	25
Ce	124	125	87	52	78	62	103	62
Nd	51	51	36	20	26	19	32	21
Ba	334	1090	847	940	262	152	413	423
Li	67	26	27	30	65	124	69	35
Be	2.9	0.8	1.8	1.9	2.9	6.3	6.4	3.5
B	2	<1	5	<1	<1	<1	<1	<1
Co	3	17	10	2	2	3	3	2
Cu	0.6	2	1.5	<0.1	<0.1	<0.1	0.1	0.3
Mo	0.1	0.1	0.2	<0.1	0.1	<0.1	<0.1	0.1
Sn	6	1	2	2	5	2	3	5
W	3.6	n.d.	1.0	1.0	1.6	4.1	2.8	2.2
Ag	<0.1	<0.1	<0.1	<0.1	<0.1	<0.1	<0.1	<0.1
Cd	0.1	<0.1	<0.1	<0.1	<0.1	<0.1	<0.1	<0.1
Bi	<0.1	<0.1	0.1	0.3	<0.1	<0.1	<0.1	<0.1

n = No. of samples.

1. Peterhead
2. Aberdeen
3. Cove Bay
4. Blackburn
5. Hill of Fare
6. Bennachie
7. Mt. Battock
8. Cromar

TABLE 6:1 CONTINUED.

	1.	2.	3.	4.	5.	6.	7.	8.
	n=31	n=1	n=20	n=5	n=4	n=121	n=7	n=8
SiO <sub>2</sub>	73.7	57.2	76.1	73.5	70.4	76.0	58.7	70.6
TiO <sub>2</sub>	0.31	1.30	0.11	0.28	0.48	0.16	1.23	0.33
Al <sub>2</sub> O <sub>3</sub>	13.5	17.5	13.5	14.6	15.9	13.1	17.3	15.4
Fe <sub>2</sub> O <sub>3</sub>	1.7	6.9	1.0	1.7	2.8	1.2	6.5	2.2
MnO	0.04	0.10	0.07	0.04	0.06	0.04	0.11	0.05
MgO	0.7	3.5	0.2	0.8	1.3	0.2	4.1	1.0
CaO	1.2	6.0	0.5	1.3	2.4	0.5	5.4	1.2
Na <sub>2</sub> O	3.6	3.7	3.9	4.4	4.2	3.5	3.6	4.0
K <sub>2</sub> O	4.6	2.2	4.7	3.8	3.4	4.9	3.1	4.6
P <sub>2</sub> O <sub>5</sub>	0.10	0.39	0.04	0.10	0.18	0.05	0.33	0.13
Nb	15	13	45	14	16	30	13	17
Zr	138	207	92	96	185	118	175	149
Y	13	26	56	11	17	39	22	13
Sr	191	798	56	296	576	63	675	241
U	6.2	1.9	17.5	3.1	3.2	10.2	2.7	3.8
Rb	192	57	629	119	167	375	76	151
Th	19	8	25	14	12	33	11	15
Pb	32	14	45	29	24	33	18	25
Ga	18	22	23	19	20	21	19	16
Zn	32	70	41	30	42	31	61	41
Ni	5	27	4	9	14	4	62	10
Cr	12	77	4	23	28	4	141	21
V	24	137	5	27	45	8	159	33
La	32	33	19	23	45	31	31	22
Ce	57	67	40	45	80	70	61	42
Nd	21	32	18	18	30	27	30	19
Ba	514	685	225	608	952	234	749	610
Li	57	20	183	41	71	76	31	28
Be	2.7	1.8	5.3	2.2	3.9	5.8	1.6	2.5
B	<1	<1	<1	<1	1	<1	23	5
Co	4	29	2	6	9	2	24	4
Cu	1.9	13	2.6	0.2	2.6	0.3	38	30
Mo	<0.1	<0.1	3.9	<0.1	0.5	0.1	0.8	9.0
Sn	3	3	22	2	6	9	5	4
W	0.8	0.6	20.4	1.0	1.7	3.8	2.6	3.0
Ag	<0.1	0.1	<0.1	<0.1	<0.1	<0.1	0.1	<0.1
Cd	<0.1	0.2	<0.1	<0.1	<0.1	<0.1	<0.1	<0.1
Bi	<0.1	<0.1	2.5	<0.1	0.5	0.6	0.6	<0.1

n = No. of samples.

1. Lochnagar granite
2. Lochnagar diorite
3. Glen Gairn granite
4. Glenlivet
5. Dorback
6. Cairngorm
7. Comrie diorite
8. Comrie granite

TABLE 6:1 CONTINUED.

	1.	2.	3.	4.	5.	6.	7.	8.
	n=10	n=2	n=8	n=2	n=1	n=38	n=8	n=9
SiO <sub>2</sub>	69.7	61.9	51.4	54.4	43.6	59.3	64.7	73.3
TiO <sub>2</sub>	0.38	0.71	1.24	0.99	0.49	0.84	0.52	0.24
Al <sub>2</sub> O <sub>3</sub>	16.0	16.8	13.2	14.8	1.4	16.2	16.6	14.7
Fe <sub>2</sub> O <sub>3</sub>	2.3	5.3	9.8	8.4	13.6	5.5	3.6	1.5
MnO	0.04	0.10	0.17	0.14	0.23	0.08	0.05	0.05
MgO	1.1	3.3	10.0	7.9	34.4	3.3	2.1	0.5
CaO	1.9	4.6	5.1	6.9	11.4	4.7	2.9	1.1
Na <sub>2</sub> O	5.0	4.0	2.5	3.2	0.1	3.9	4.1	3.5
K <sub>2</sub> O	3.7	2.9	1.8	1.5	0.1	3.2	3.8	5.0
P <sub>2</sub> O <sub>5</sub>	0.14	0.21	0.27	0.33	0.01	0.31	0.26	0.17
Nb	9	10	9	8	<1	6	6	13
Zr	122	136	160	110	34	139	115	112
Y	8	17	21	17	17	14	8	14
Sr	893	510	494	665	23	1282	908	126
U	3.0	2.8	0.8	1.9	0.3	1.8	1.6	3.7
Rb	82	86	55	74	1	54	59	327
Th	9	7	3	4	<1	5	5	17
Pb	23	21	23	17	8	25	17	31
Ga	18	20	19	19	3	20	18	20
Zn	42	63	48	71	89	68	51	49
Ni	9	37	161	92	383	35	28	n.d.
Cr	21	120	540	374	1614	69	55	n.d.
V	35	115	224	194	213	109	66	18
La	22	21	19	24	1	29	24	31
Ce	32	41	37	46	7	57	43	60
Nd	13	21	21	23	9	28	20	23
Ba	1283	616	473	543	13	1485	1562	421
Li	23	31	29	25	5	19	23	144
Be	1.4	1.5	1.2	1.3	0.5	1.1	0.9	8.3
B	4	31	8	16	30	8	9	n.d.
Co	5	22	58	43	151	23	15	1
Cu	0.4	2	66	74	302	73.8	209.7	11
Mo	<0.1	<0.1	1.3	0.1	0.6	1.5	0.3	<0.1
Sn	5	6	5	6	3	3	4	7
W	1.1	2.0	2.1	2.0	2.0	1.6	1.9	1.8
Ag	<0.1	<0.1	<0.1	<0.1	1.6	0.2	0.1	<0.1
Cd	<0.1	<0.1	<0.1	<0.1	<0.1	<0.1	<0.1	<0.1
Bi	<0.1	<0.1	<0.1	<0.1	8	0.9	<0.1	0.2

n = No. of samples.

1. Garabal Hill main granodiorite
2. Garabal Hill fine grained granodiorite
3. Garabal Hill diorite
4. Garabal Hill gabbro
5. Garabal Hill hornblendite
6. Kilmelford diorite
7. Kilmelford porphyrite
8. Cairnsmore of Fleet

## 6:2:i. INTERNAL GEOCHEMICAL VARIATIONS OF THE LAKE DISTRICT INTRUSIVES.

Because the Lake District intrusions appear to have been affected by varying degrees of metasomatism, many of the inter-element variations described below may not be related to magmatic processes. The intrusions most affected are Shap, Skiddaw, Eskdale and Threlkeld. However variations in the less mobile elements Ti, Cr, V, Nb, Y, Zr, and possibly Ca, Mg, Th and Be, are more likely to reflect magmatic processes.

## 1) The Skiddaw granite (Fig. 6:1).

Silica values for the Skiddaw granite vary continuously from 70 to 78 wt% with higher values for the greisens. MgO, MnO, Fe<sub>2</sub>O<sub>3</sub>, TiO<sub>2</sub>, Al<sub>2</sub>O<sub>3</sub>, CaO and P<sub>2</sub>O<sub>5</sub> define negative correlations with SiO<sub>2</sub>. Na<sub>2</sub>O and K<sub>2</sub>O increase slightly with increasing silica, but with very low levels of Na<sub>2</sub>O in the greisens. Cr, V, Sr, Ba, Li, La, Ce, Th and Zr concentrations decrease with increasing SiO<sub>2</sub>; Be, U, Rb, Y and Nb concentrations appear to increase with increasing SiO<sub>2</sub>.

## 2) The Eskdale granite (Fig. 6:2).

SiO<sub>2</sub> values for the Eskdale intrusion show a compositional gap between the granodiorite and granite. MgO, MnO, Fe<sub>2</sub>O<sub>3</sub>, TiO<sub>2</sub>, Al<sub>2</sub>O<sub>3</sub>, CaO and P<sub>2</sub>O<sub>5</sub> define negative correlations with SiO<sub>2</sub>, whereas Na<sub>2</sub>O and K<sub>2</sub>O increase slightly with increasing SiO<sub>2</sub>. Cr, V, Sr, Ba, La, Ce, Y, Nb, Th, and Zr concentrations decrease with increasing SiO<sub>2</sub>; Rb concentrations increase with increasing SiO<sub>2</sub> whilst Li, Be and U do not form coherent trends.

Fig. 6:1. Major and trace element variation diagrams for the Skiddaw intrusion, key to symbols on fold out sheet.

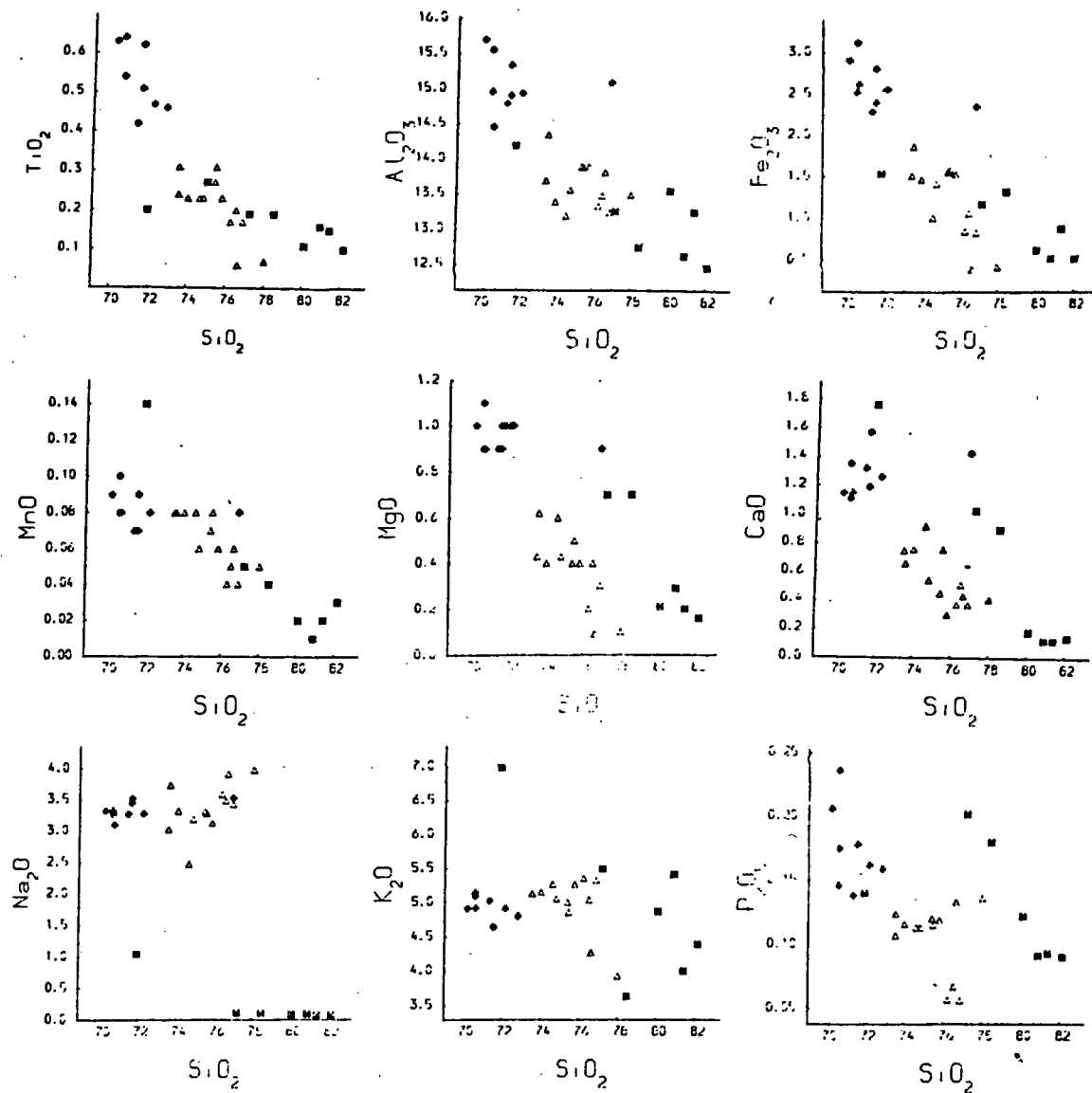


Fig. 6:1. Continued.

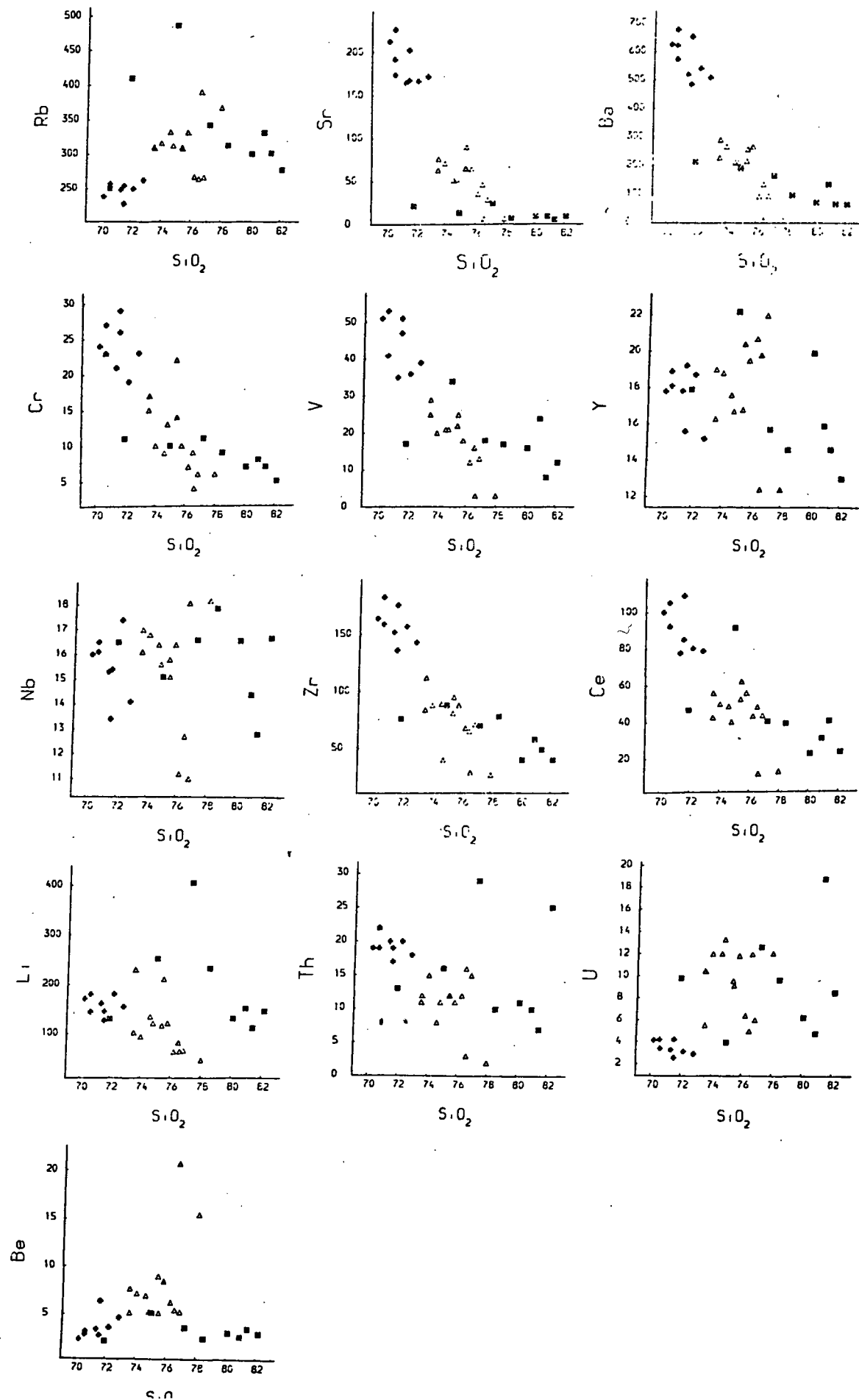


Fig. 6:2. Major and trace element variation diagrams for the Eskdale intrusion, key to symbols on fold out sheet.

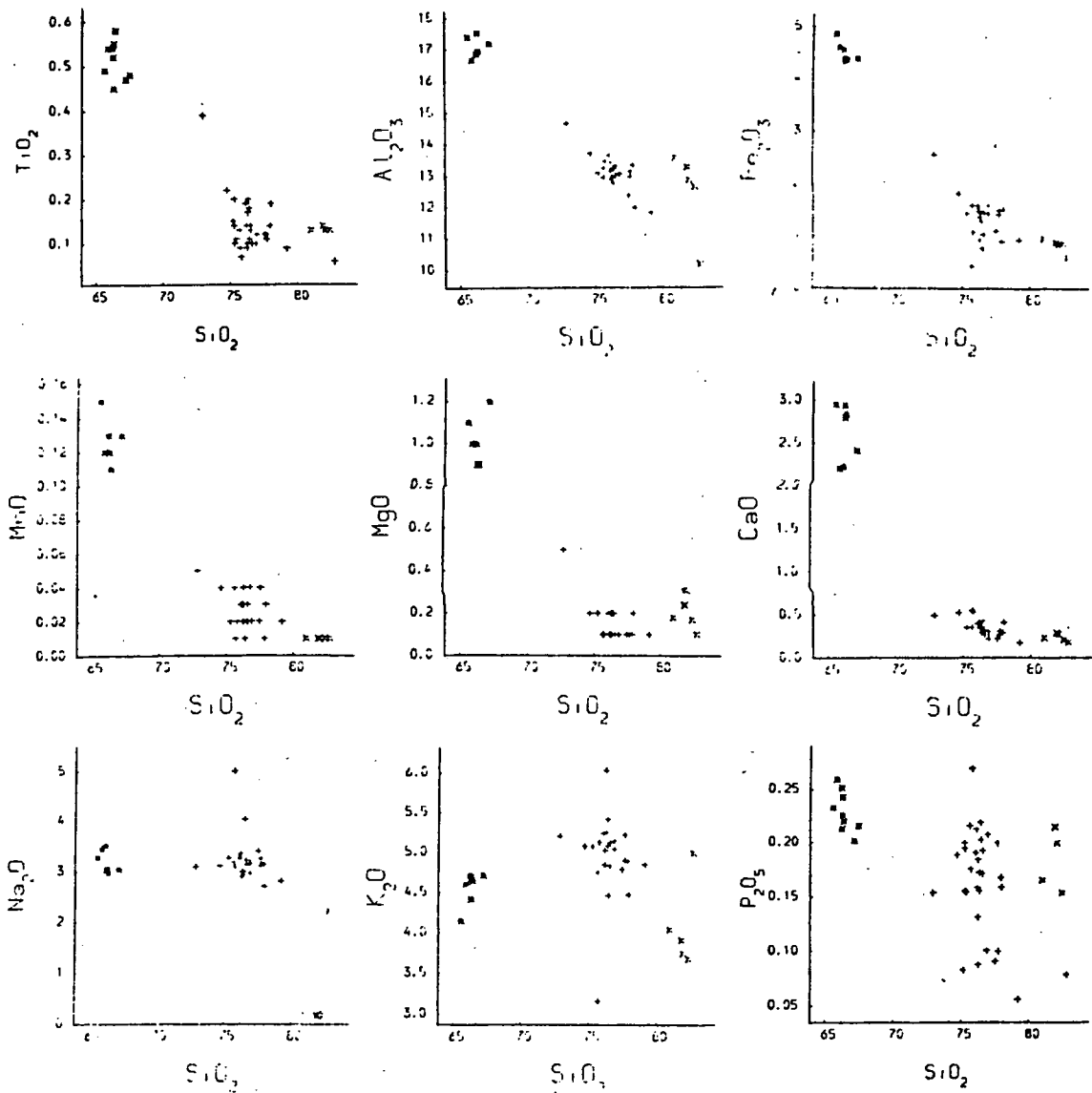
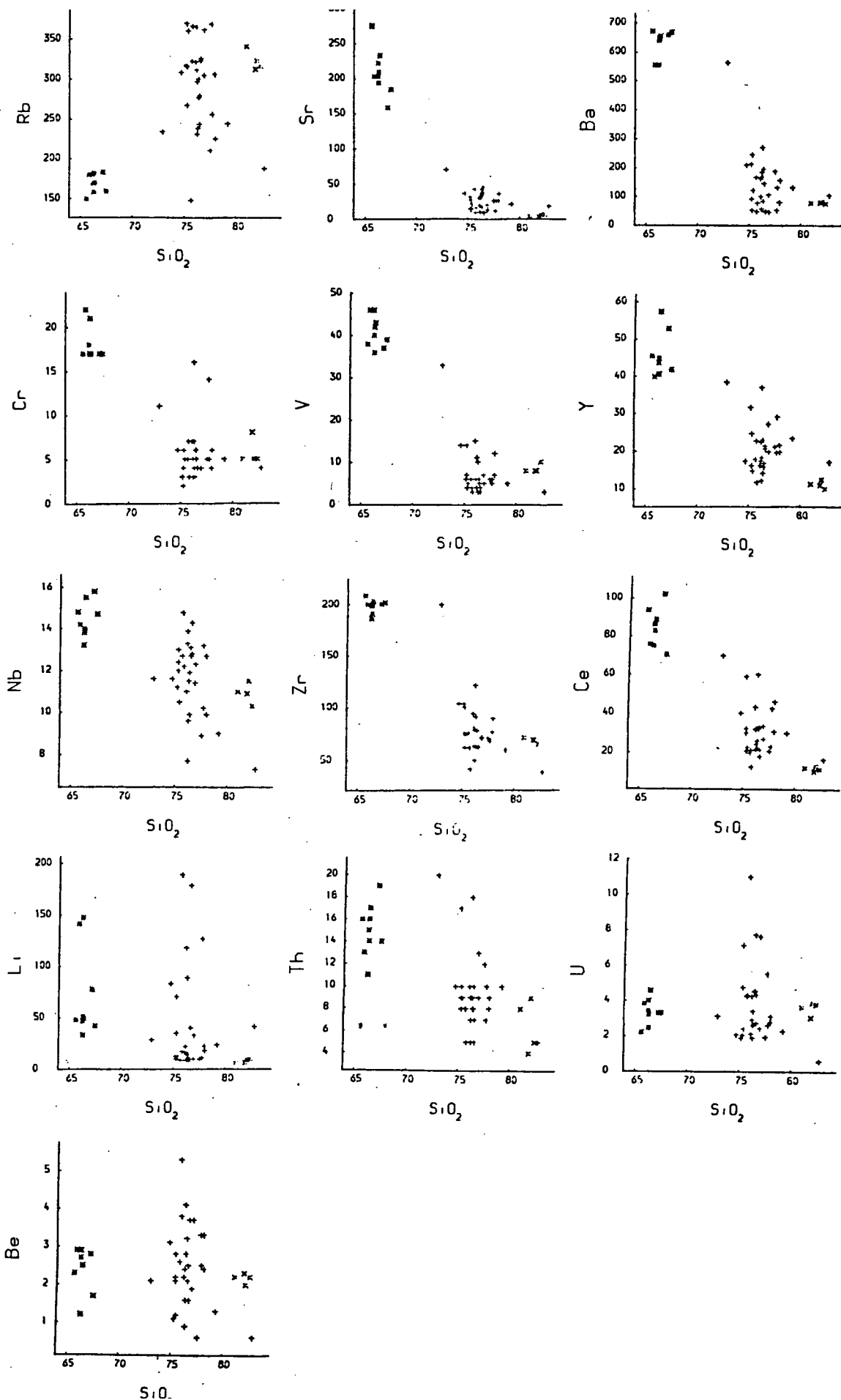


Fig. 6:2. Continued.



### 3) The Carrock Fell complex (Fig. 6:3).

The Carrock Fell gabbro has been shown to be unrelated to the Carrock Fell granophyre, hybrid suite and ferrogabbros; the former being a calc-alkali gabbro and the latter tholeiitic (Hunter 1980).

The Carrock Fell gabbros occupy a range of  $\text{SiO}_2$  from 45 to 55 wt% with decreasing  $\text{Fe}_2\text{O}_3$ , MnO,  $\text{TiO}_2$ , MgO,  $\text{Al}_2\text{O}_3$ , CaO and  $\text{P}_2\text{O}_5$  as  $\text{SiO}_2$  increases;  $\text{Na}_2\text{O}$  and  $\text{K}_2\text{O}$  increase with increasing  $\text{SiO}_2$ . Cr, V, Sr and Li concentrations decrease with increasing  $\text{SiO}_2$ ; whereas Y, Rb, U, Ba, Nd, La, Ce, Th, Nb, Zr, and Be concentrations increase with increasing  $\text{SiO}_2$ .

The tholeiitic Carrock hybrid suite and granophyre have  $\text{SiO}_2$  ranging from 60 to 73 wt%;  $\text{Fe}_2\text{O}_3$ , MnO,  $\text{TiO}_2$ ,  $\text{Al}_2\text{O}_3$ , CaO and  $\text{P}_2\text{O}_5$  define negative correlations with  $\text{SiO}_2$ ; MgO is at very low levels throughout this suite but shows a slight decrease as  $\text{SiO}_2$  increases.  $\text{Na}_2\text{O}$  decreases slightly with high  $\text{SiO}_2$  values but  $\text{K}_2\text{O}$  increases with increasing  $\text{SiO}_2$ . Cr and V like MgO are at low concentrations throughout the hybrid suite and granophyres. Sr and Li concentrations decrease with increasing  $\text{SiO}_2$ ; Rb, Ba, Ce, Y, Nb, Be, Th and U concentrations however increase in the hybrid suite and granophyre.

### 4) The Ennerdale granophyre (Fig. 6:4).

$\text{SiO}_2$  in the Ennerdale granophyre ranges from 72 to 78 wt%. MgO,  $\text{Fe}_2\text{O}_3$ , MnO,  $\text{TiO}_2$ ,  $\text{Al}_2\text{O}_3$ , CaO and  $\text{P}_2\text{O}_5$  correlate negatively with  $\text{SiO}_2$ , whereas  $\text{Na}_2\text{O}$  and  $\text{K}_2\text{O}$  increase with increasing  $\text{SiO}_2$ . Trace element variations within this intrusion are relatively small; Sr, V, Ba, Rb, Be, Y, and Ce all appear to decrease in abundance with increasing  $\text{SiO}_2$ . Li and Cr appear constant; Nb and Zr concentrations increase slightly although some samples are scattered; U and Th increase with increasing  $\text{SiO}_2$ .

Fig. 6:3. Major and trace element variation diagrams for the Carrock Fell complex, key to symbols on fold out sheet.

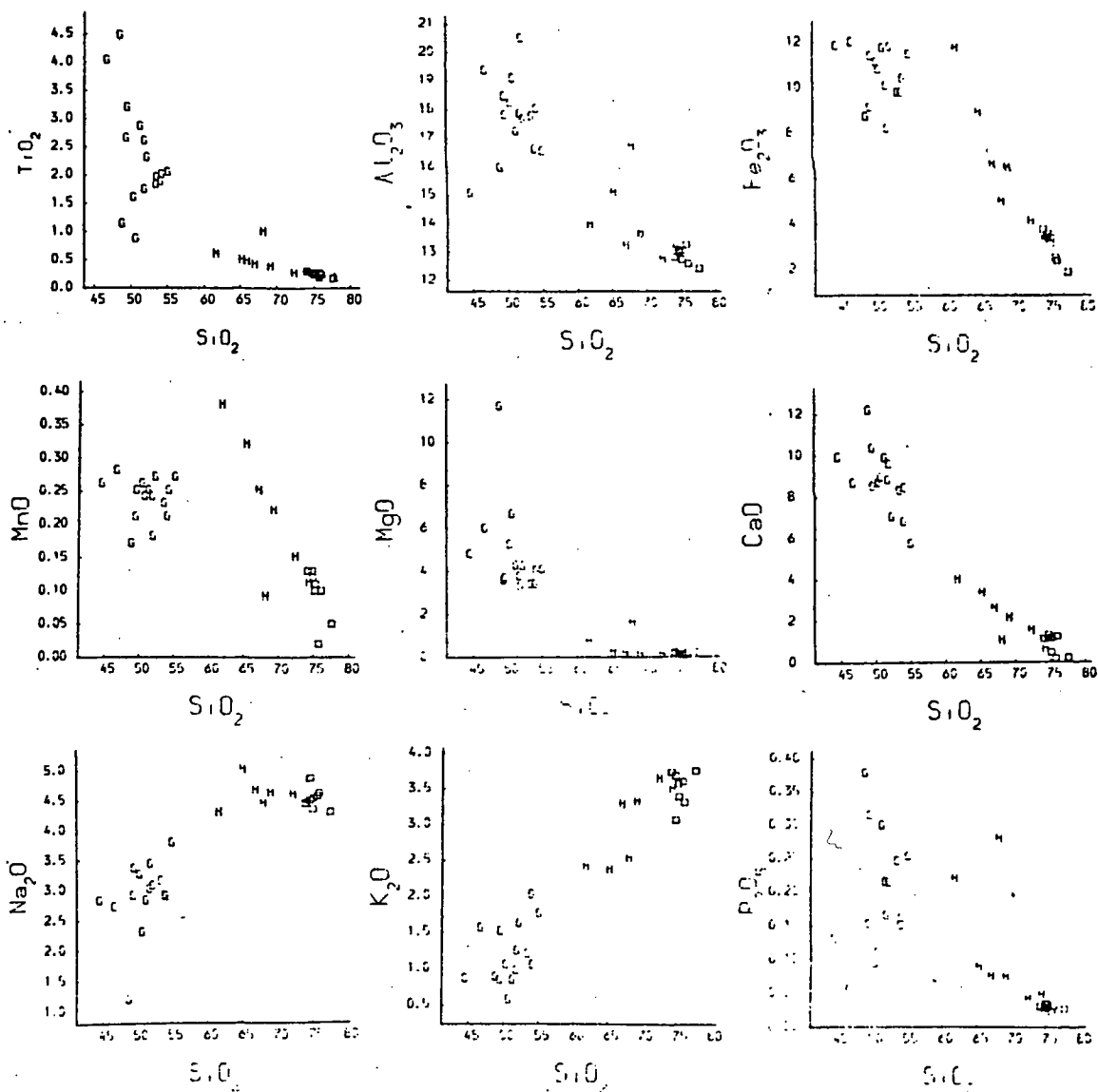


Fig. 6:3. Continued.

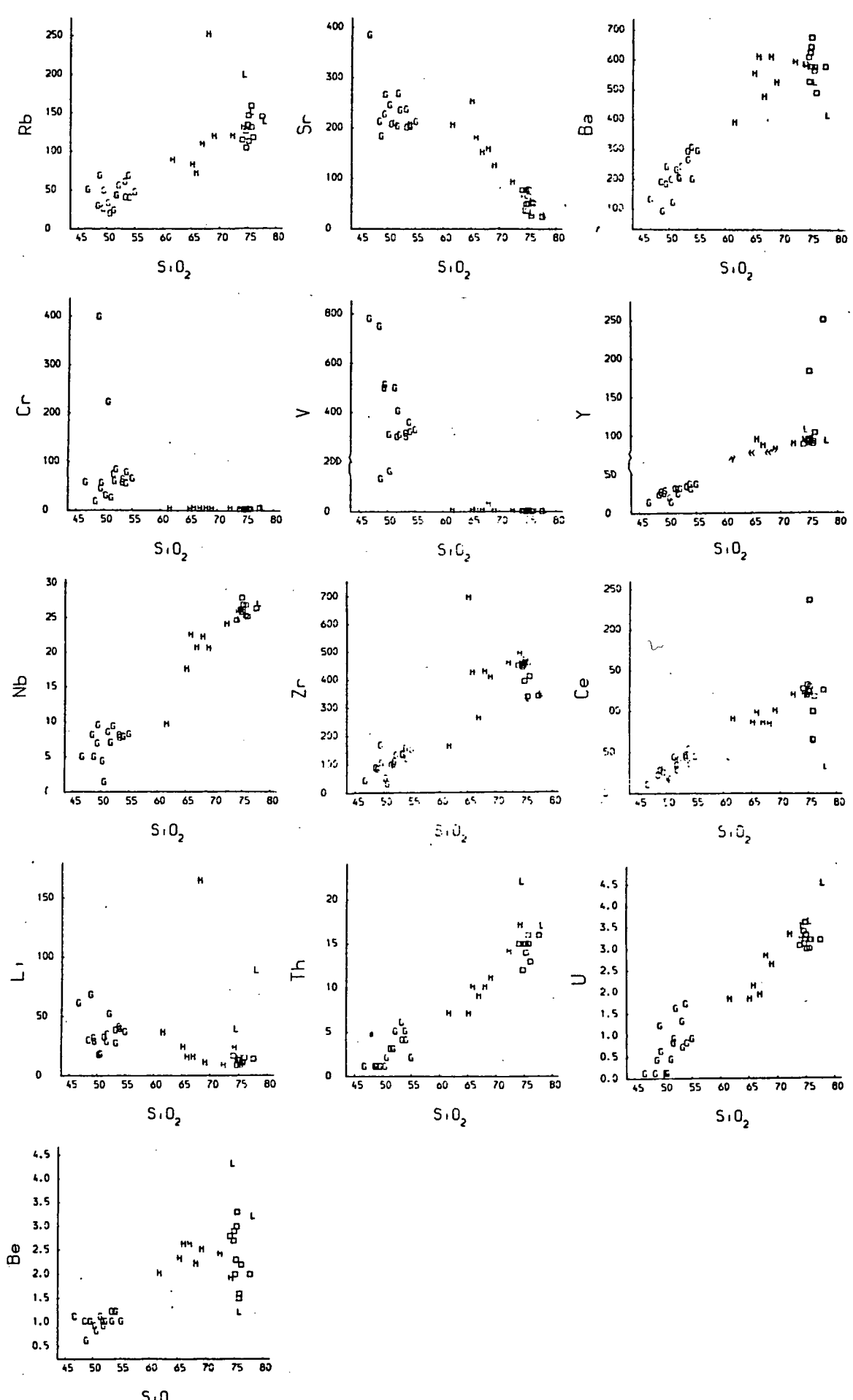


Fig. 6:4. Major and trace element variation diagrams for the Shap granite, the Ennerdale granophyre and the Treklled microgranite, key to symbols on fold out sheet.

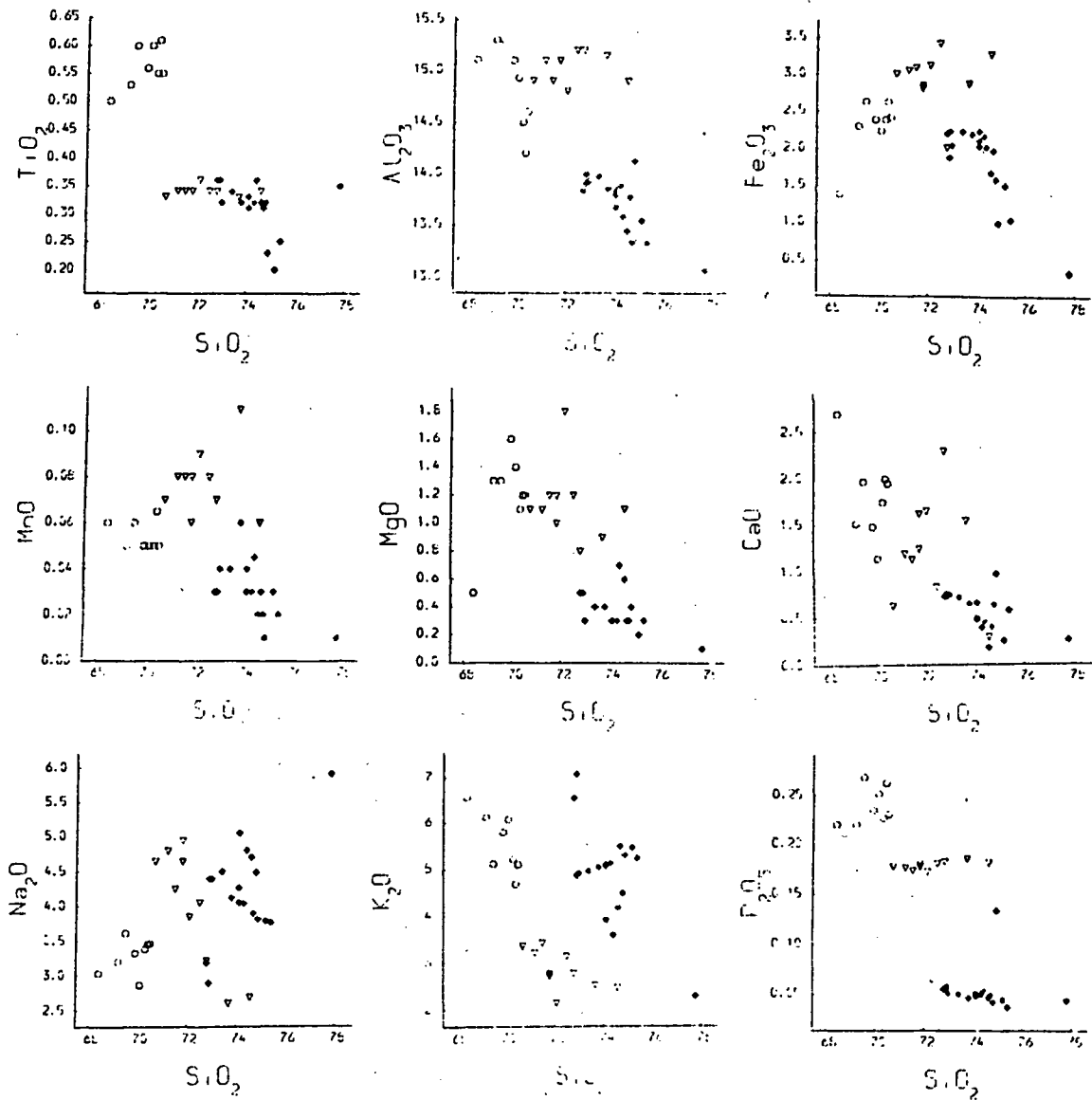
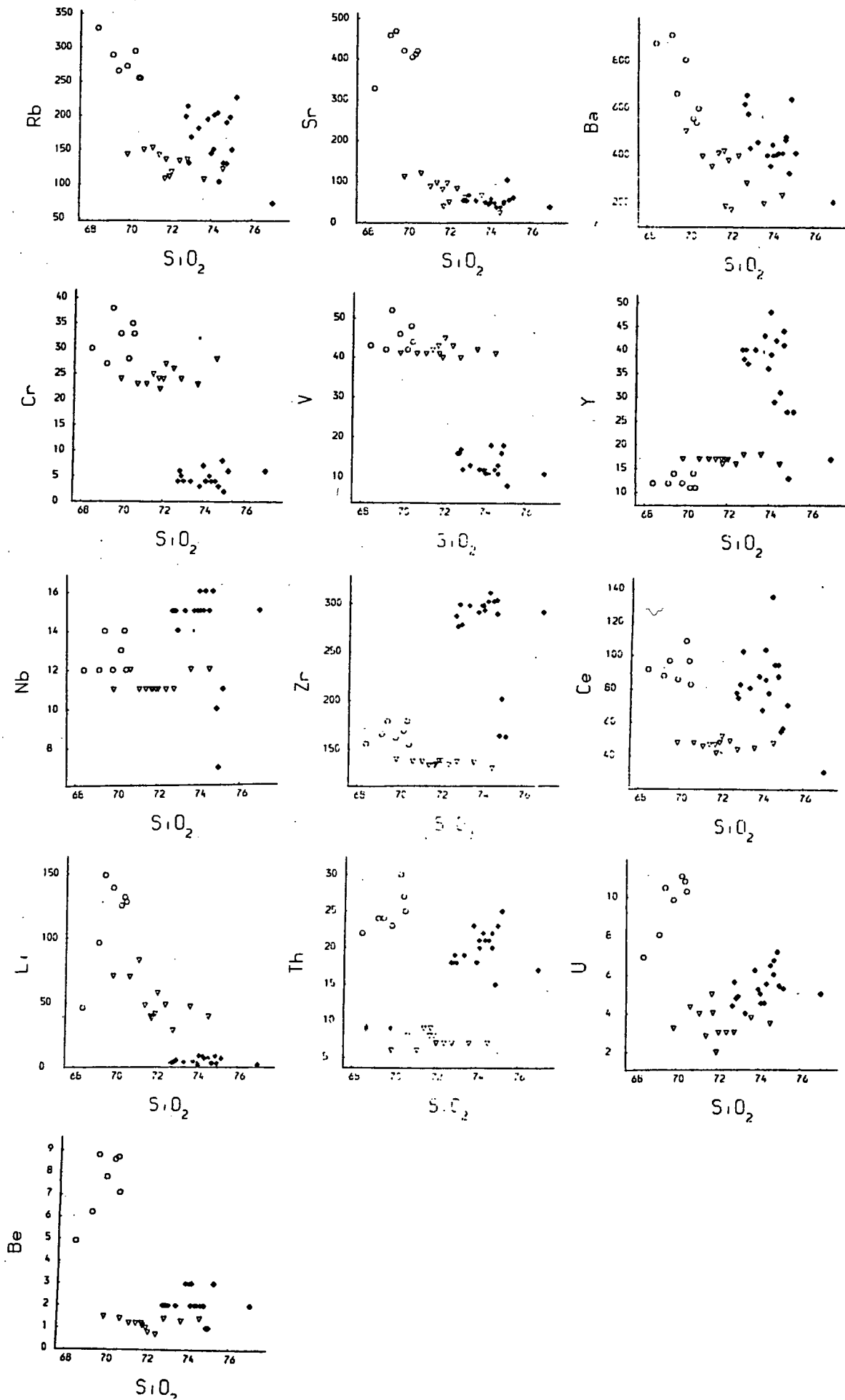


Fig. 6:4. Continued.



5) The Threlkeld microgranite (Fig. 6:4).

$\text{SiO}_2$  in the Threlkeld microgranite ranges from 70 to 75 wt%, MnO, MgO,  $\text{Na}_2\text{O}$  and  $\text{K}_2\text{O}$  decrease with increasing  $\text{SiO}_2$ ;  $\text{TiO}_2$ ,  $\text{P}_2\text{O}_5$ ,  $\text{Fe}_2\text{O}_3$  and  $\text{Al}_2\text{O}_3$  remain constant, whilst CaO increases with increasing  $\text{SiO}_2$ . Li, Rb, Sr, and Ba concentrations decrease slightly with increasing  $\text{SiO}_2$ ; Ce, Y, Th, Cr, V, Nb, Be and Zr concentrations remain constant and U shows considerable scatter when plotted against  $\text{SiO}_2$ .

6) The Shap granite (Fig 6:4).

The range of  $\text{SiO}_2$  observed in the Shap granite is small, from 68 to 71 wt% and is almost certainly the result of sampling;  $\text{K}_2\text{O}$ ,  $\text{Al}_2\text{O}_3$  and CaO correlate negatively with  $\text{SiO}_2$ ;  $\text{TiO}_2$ , MgO,  $\text{Fe}_2\text{O}_3$ ,  $\text{Na}_2\text{O}$  and  $\text{P}_2\text{O}_5$  increase with increasing  $\text{SiO}_2$  and MnO remains roughly constant. Rb and Ba concentrations decrease slightly with increasing  $\text{SiO}_2$ ; Zr, Cr, V, Ce, Y, and Nb show little or no variation; whilst Li, Sr, Th, Be and U concentrations increase with increasing  $\text{SiO}_2$ .

#### 6:2:ii INTERNAL GEOCHEMICAL VARIATIONS IN THE SCOTTISH CALEDONIAN INTRUSIVES.

Some plutons in this group have been shown to be affected by metasomatism, particularly Helmsdale, Ballachulish, Kilmelford, Comrie and possibly Foyers; thus some of the geochemical variations listed below may not be related to magmatic processes.

1) The Helmsdale granite (Fig. 6:5).

$\text{SiO}_2$  varies from 68 to 78 wt% in the Helmsdale granite;  $\text{TiO}_2$ , MgO,  $\text{Fe}_2\text{O}_3$ , MnO,  $\text{Al}_2\text{O}_3$ , CaO and  $\text{P}_2\text{O}_5$  define negative correlations with  $\text{SiO}_2$ .

Fig. 6:5. Major and trace element variation diagrams for the Helmsdale granite, key to symbols on fold out sheet.

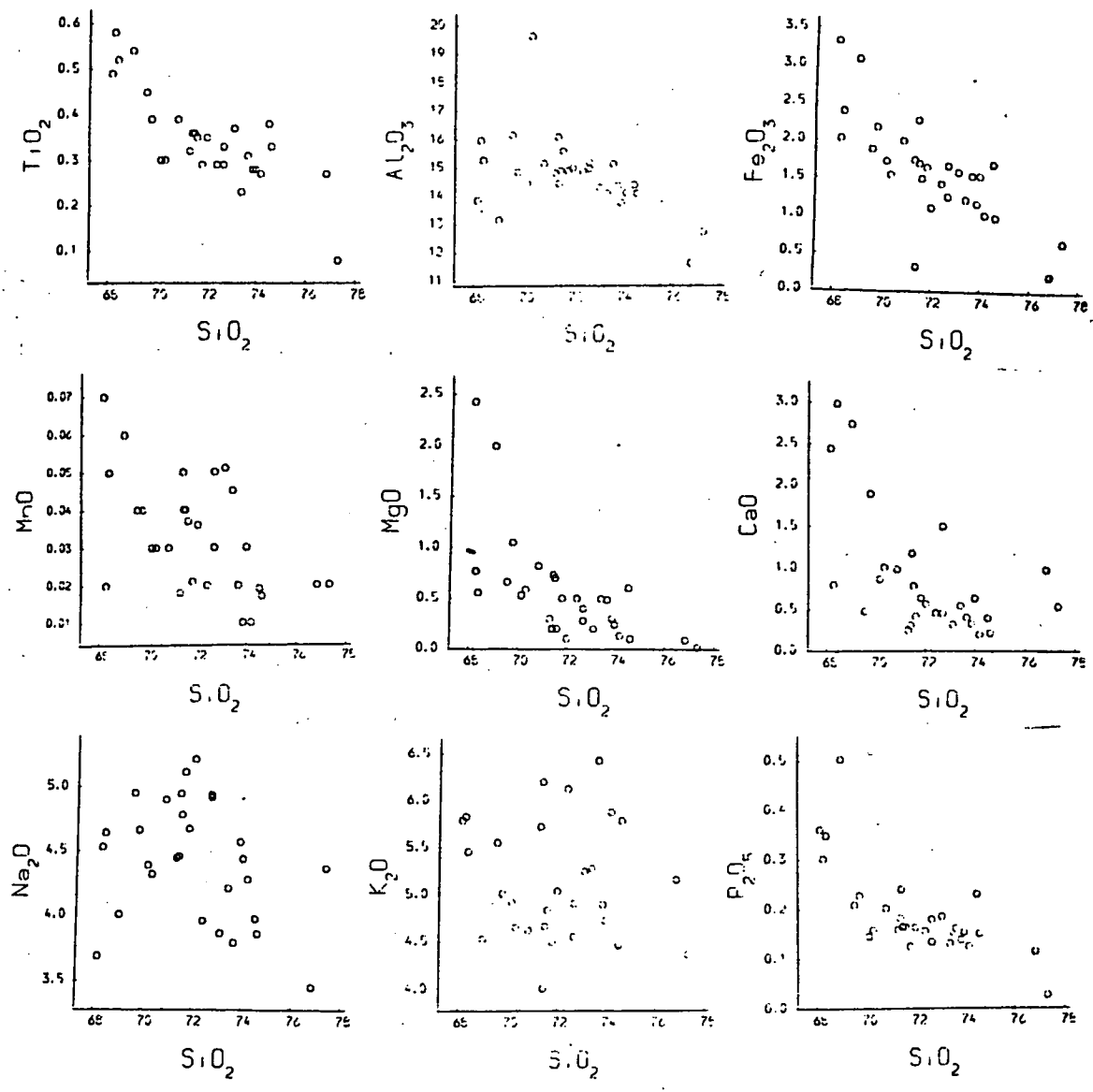
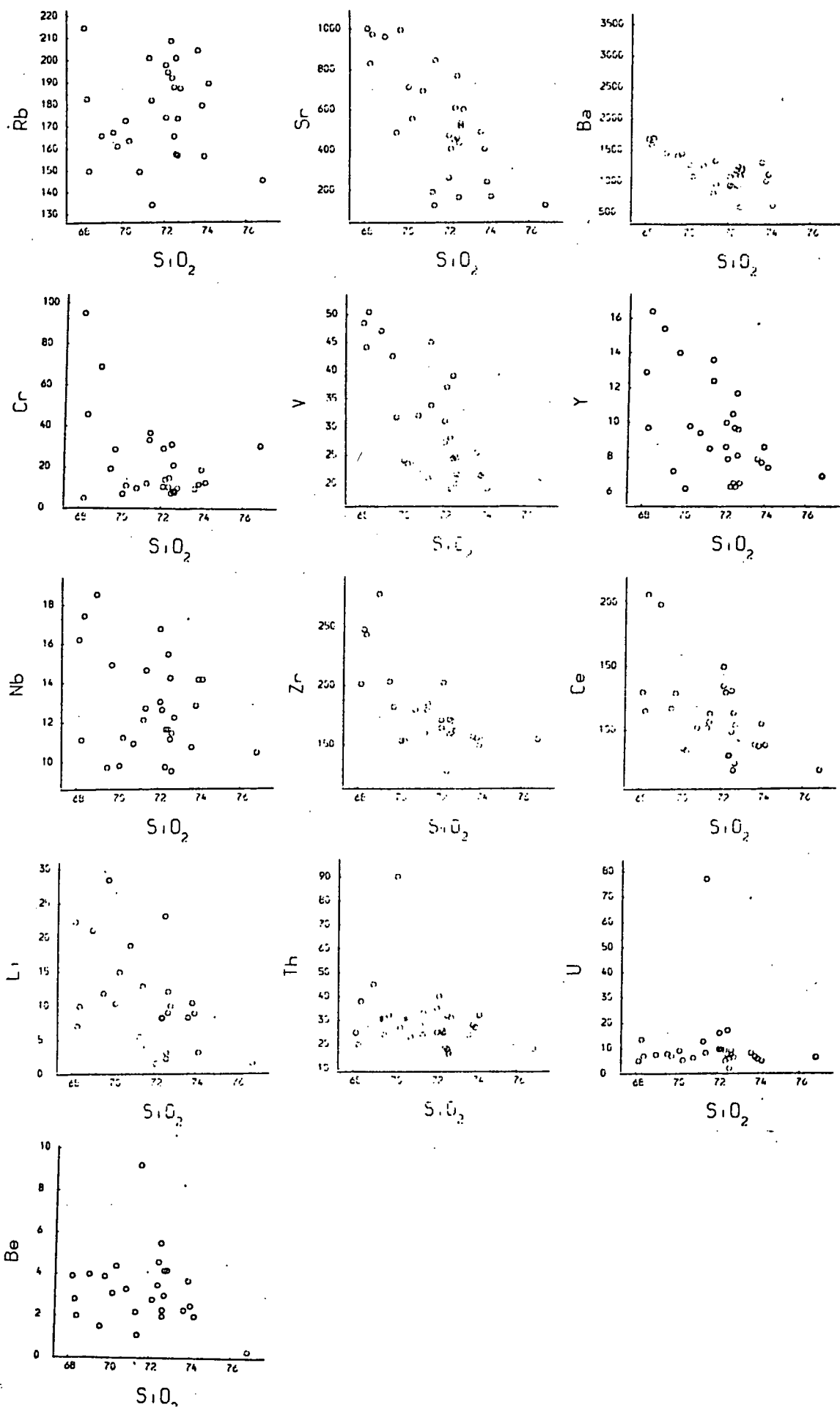


Fig. 6:5. Continued.



some showing considerable scatter;  $\text{Na}_2\text{O}$  and  $\text{K}_2\text{O}$  are severely scattered and do not define any noticeable trend. Sr, Ba, Ce, Y, Zr, Cr, V and Li define negative correlations with  $\text{SiO}_2$ , with varying dispersion; Rb concentrations increase with increasing  $\text{SiO}_2$  with considerable scatter; U, Th and Be do not show any apparent correlation with  $\text{SiO}_2$  as a result of mineralization.

2) The Migdale, Grudie and Rogart intrusions (Fig. 6:6).

The sample suites examined for the Migdale and Grudie granite are too small for any meaningful geochemical variation to be observed, as these granitoids are geochemically similar to the Rogart complex which has a range of  $\text{SiO}_2$  from 64 to 74 wt% the geochemical trends for this intrusion are outlined.  $\text{Fe}_2\text{O}_3$ , MnO, MgO,  $\text{TiO}_2$ ,  $\text{Al}_2\text{O}_3$ , CaO and  $\text{P}_2\text{O}_5$  correlate negatively with  $\text{SiO}_2$ ,  $\text{K}_2\text{O}$  increases with increasing  $\text{SiO}_2$  and  $\text{Na}_2\text{O}$  remains roughly constant; major element data from the Grudie and Migdale granites fall roughly on the same trends as the Rogart intrusion. Ba, Sr, Li, Y, Ce, Zr, Nb, Cr and V define negative correlations with  $\text{SiO}_2$ ; U, Th and Be concentrations remain roughly constant and Rb concentrations increase with increasing  $\text{SiO}_2$ . The gradients of the trends for Grudie and Migdale are different to the Rogart intrusion for trace elements.

3) The Cluanie granodiorite (Fig. 6:7).

The Cluanie granodiorite occupies a narrow range of  $\text{SiO}_2$  values from 68 to 73 wt%. All major elements decrease in abundance with increasing  $\text{SiO}_2$ . Sr, Ba, Cr, V, Nb, Zr, Ce, Y and Rb appear constant, whilst U and Th concentrations increase with increasing  $\text{SiO}_2$ .

Fig. 6:6. Major and trace element variation diagrams for the Migdale, Rogart and Grudie intrusions, key to symbols on fold out sheet.

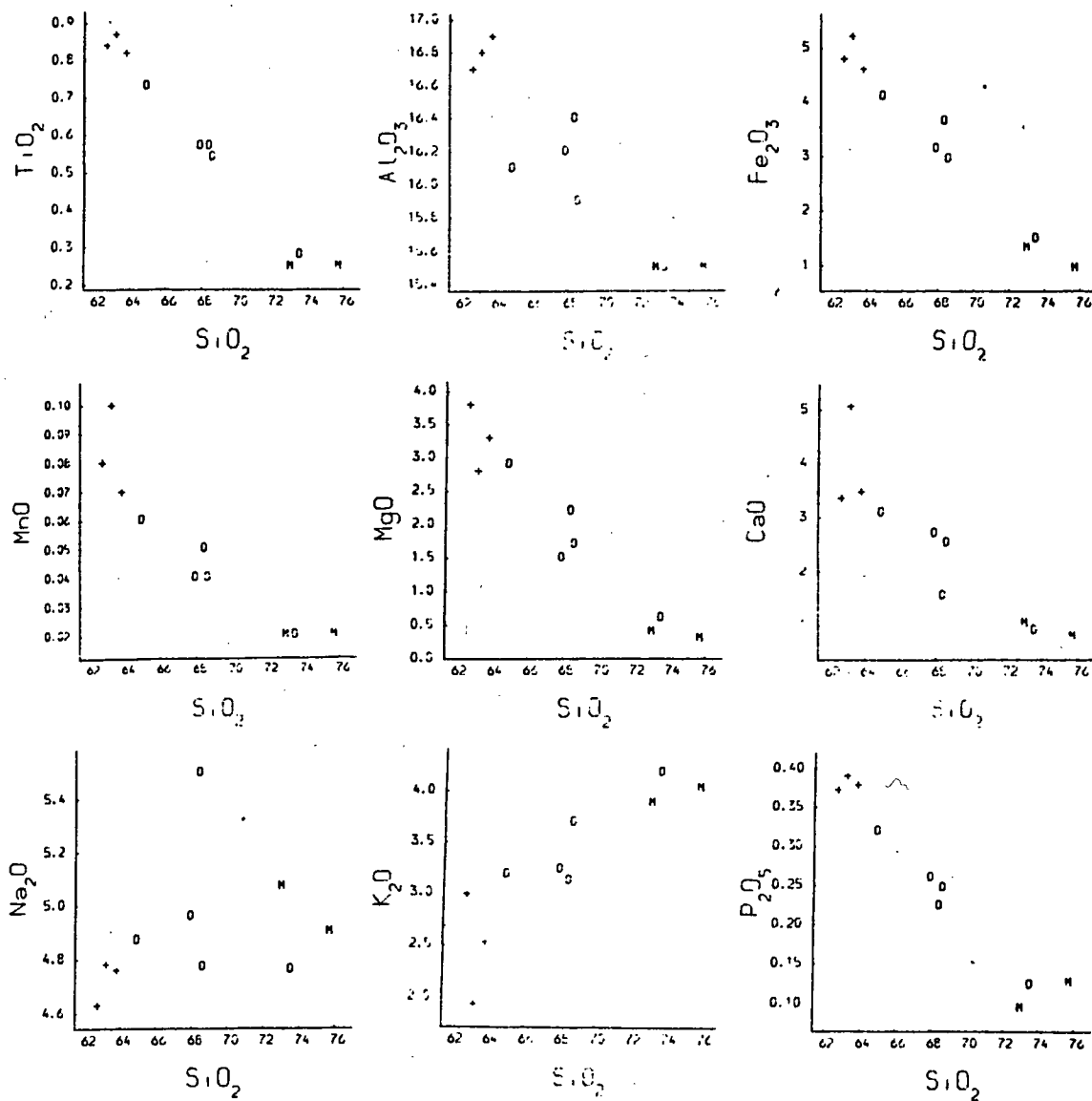


Fig. 6:6. Continued.

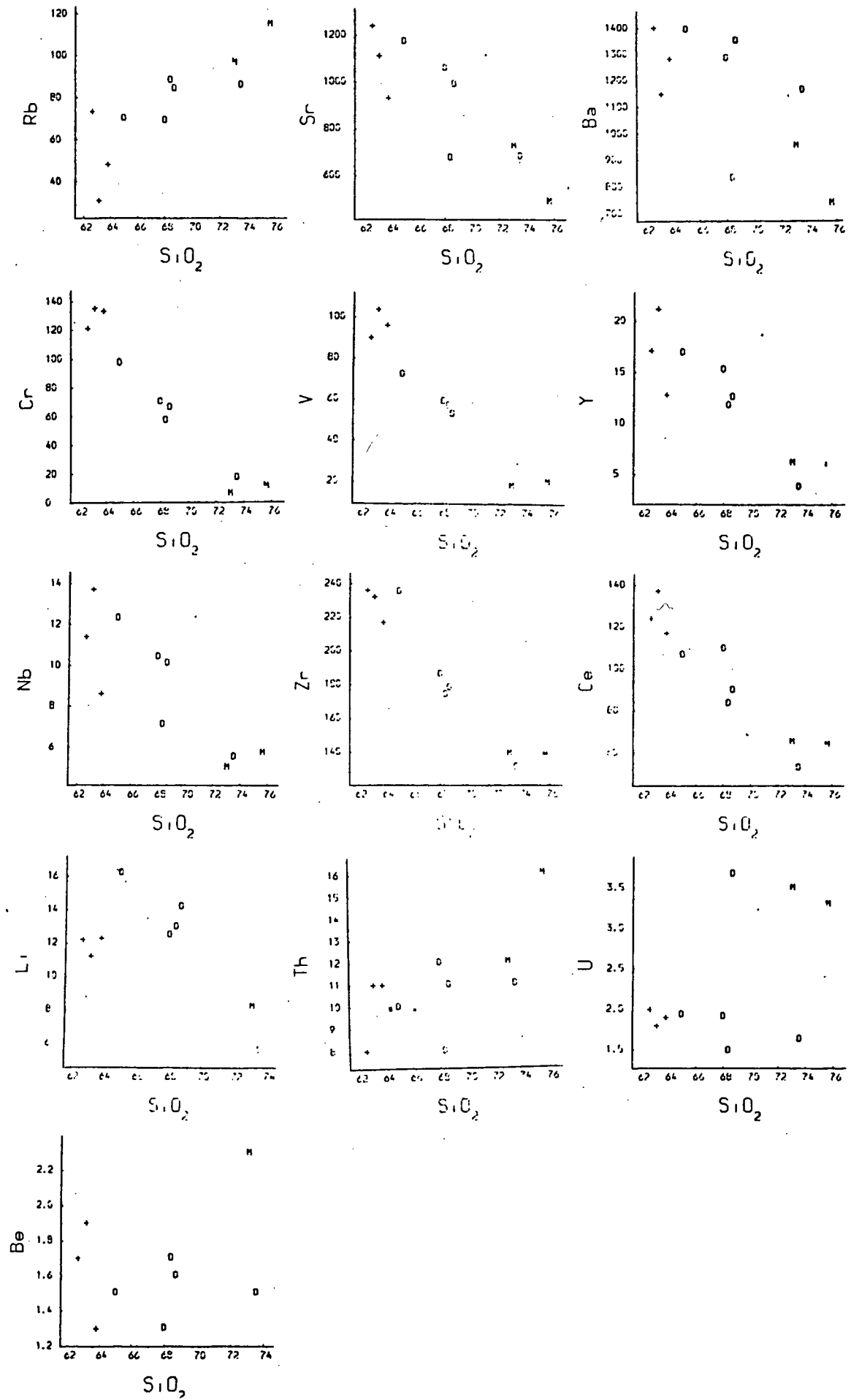


Fig. 6:7. Major and trace element variation diagrams for the Strontian complex and the Cluanie granodiorite, key to symbols on fold out sheet.

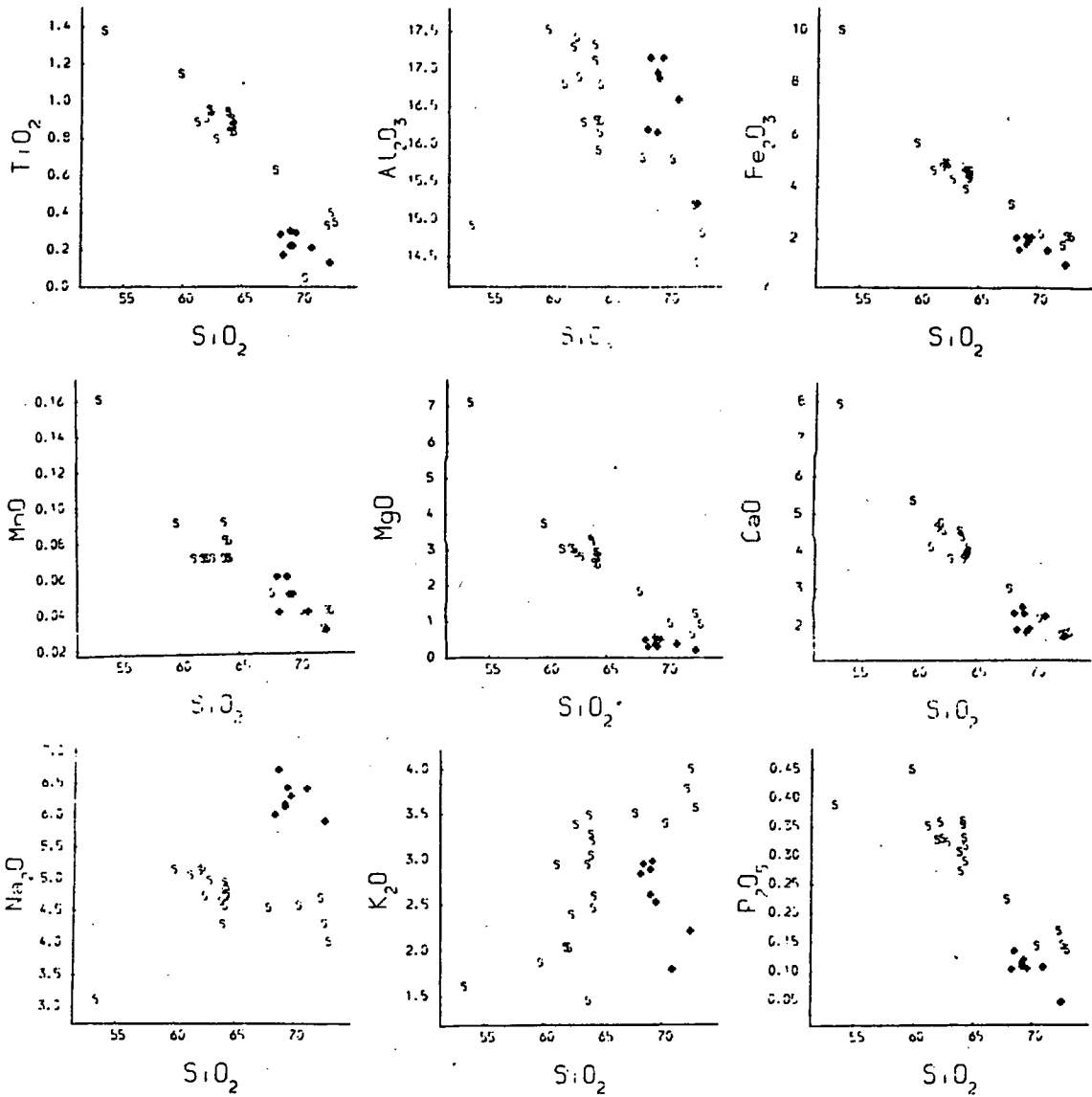
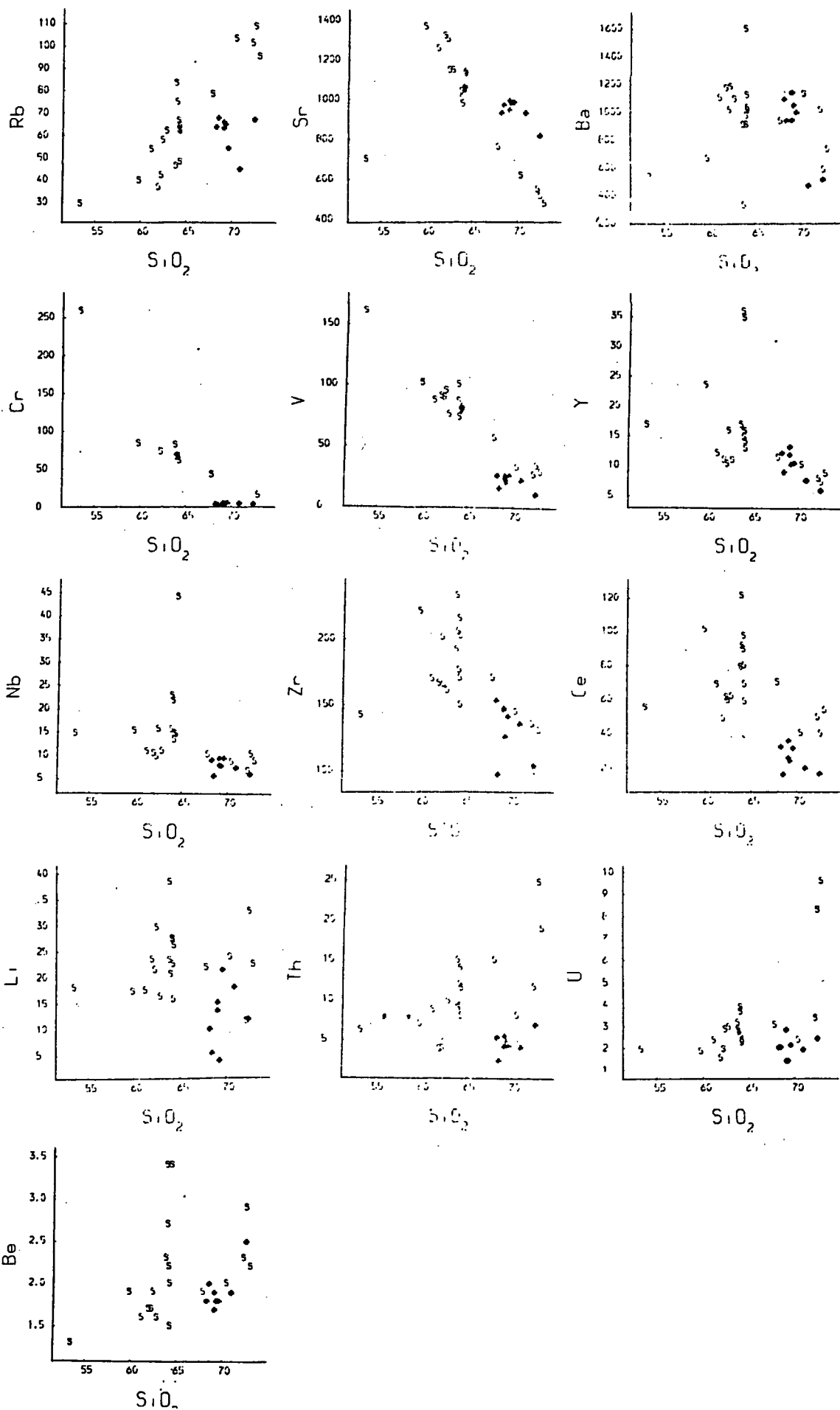


Fig. 6:7. Continued.



4) The Strontian complex (Fig. 6:7).

The compositional range of the Strontian complex is large, with  $\text{SiO}_2$  ranging from 53 to 72 wt%. Over this range  $\text{MgO}$ ,  $\text{TiO}_2$ ,  $\text{Fe}_2\text{O}_3$ ,  $\text{MnO}$  and  $\text{CaO}$  display good negative correlations with  $\text{SiO}_2$ ;  $\text{Al}_2\text{O}_3$ ,  $\text{Na}_2\text{O}$  and  $\text{P}_2\text{O}_5$  appear to increase at first (between 53 and 58%  $\text{SiO}_2$ ) and then decrease; this is poorly defined due to poor sample coverage.  $\text{K}_2\text{O}$  increases with increasing  $\text{SiO}_2$  but does not display a linear trend.  $\text{V}$ ,  $\text{Cr}$  and  $\text{Nb}$  concentrations decrease with increasing  $\text{SiO}_2$ ;  $\text{Sr}$ ,  $\text{Ba}$ ,  $\text{Zr}$ ,  $\text{Y}$  and  $\text{Ce}$  display trends similar to  $\text{Al}_2\text{O}_3$ ,  $\text{Na}_2\text{O}$  and  $\text{P}_2\text{O}_5$ , increasing in concentration at first then decreasing.  $\text{Be}$ ,  $\text{U}$ ,  $\text{Th}$  and  $\text{Rb}$  increase in concentration with increasing  $\text{SiO}_2$ , whilst  $\text{Li}$  concentrations remain roughly constant. It is noted that the more  $\text{SiO}_2$  rich samples from the Strontian granite (67-72%  $\text{SiO}_2$ ) define rather different trends from the basic suite for  $\text{K}_2\text{O}$ ,  $\text{Al}_2\text{O}_3$ ,  $\text{Be}$ ,  $\text{Zr}$ ,  $\text{U}$ ,  $\text{Th}$ ,  $\text{Ce}$ ,  $\text{Ba}$ ,  $\text{Nb}$ ,  $\text{Rb}$  and  $\text{Li}$ .

5) The Ballachulish complex (Fig. 6:8).

$\text{SiO}_2$  ranges from 53 to 75 wt% in the Ballachulish complex.  $\text{Fe}_2\text{O}_3$ ,  $\text{MnO}$ ,  $\text{MgO}$ ,  $\text{TiO}_2$ ,  $\text{CaO}$  and  $\text{P}_2\text{O}_5$  display tight negative correlations with  $\text{SiO}_2$ ,  $\text{Al}_2\text{O}_3$  increases in the low silica part of the trend and decreases with increasing  $\text{SiO}_2$  from 60 to 75%  $\text{SiO}_2$  with considerable scatter;  $\text{Na}_2\text{O}$  increases with  $\text{SiO}_2$  generally but with considerable scatter, whilst  $\text{K}_2\text{O}$  displays a good positive correlation with  $\text{SiO}_2$ . The major elements do not appear to give any distinction of trend between the granodiorite and the granite. However trace elements display different trends for the granodiorite and the granite, and indicate an overlap in silica contents between 63 and 66%  $\text{SiO}_2$  for the two parts of the intrusion.  $\text{Sr}$ ,  $\text{Cr}$ ,  $\text{V}$ ,  $\text{Ce}$  and  $\text{Y}$  concentrations decrease with increasing  $\text{SiO}_2$  for both parts of the intrusions although the gradients of the trends are not always

Fig. 6:8. Major and trace element variation diagrams for the Ballachulish complex, key to symbols on fold out sheet.

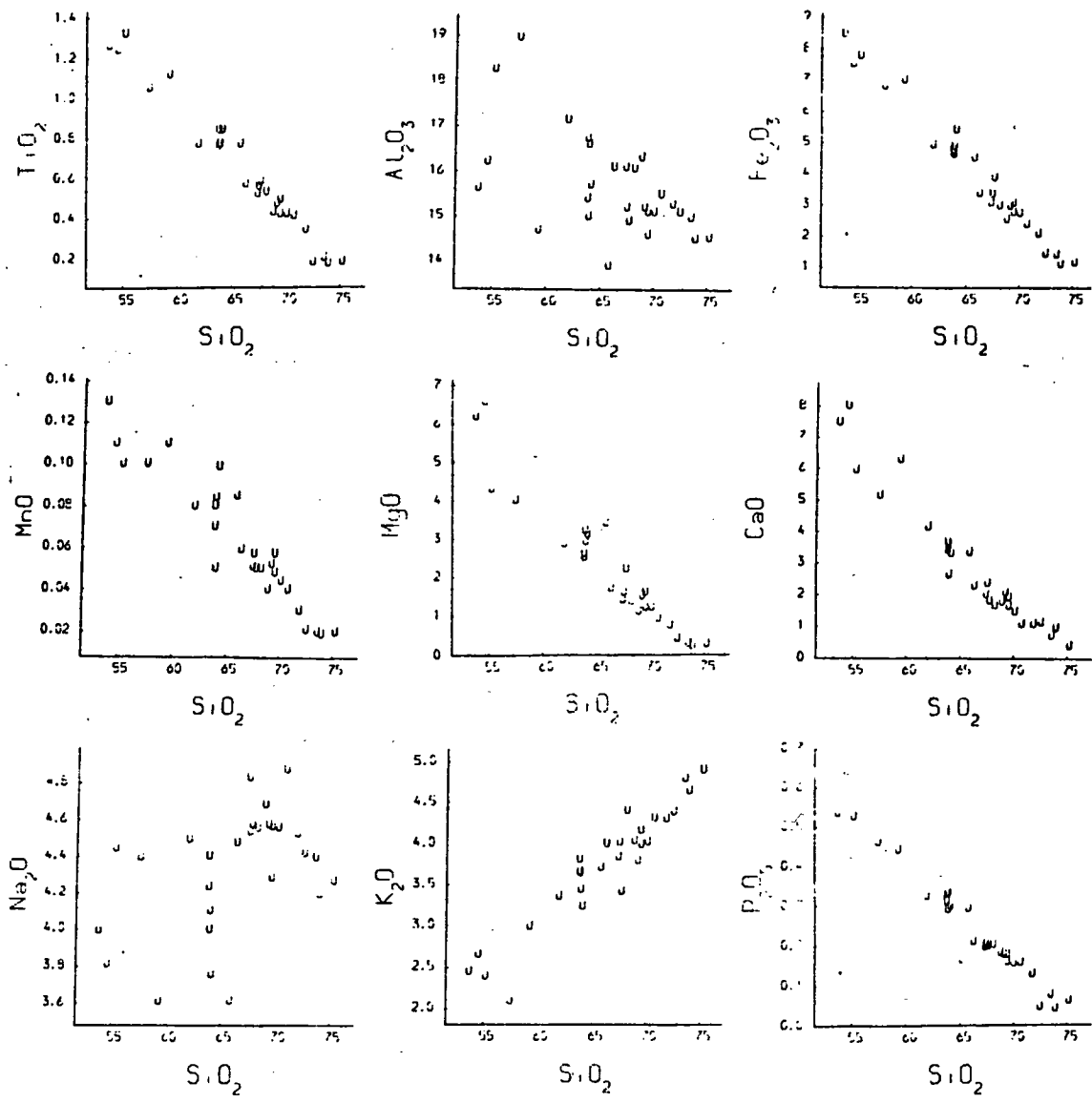
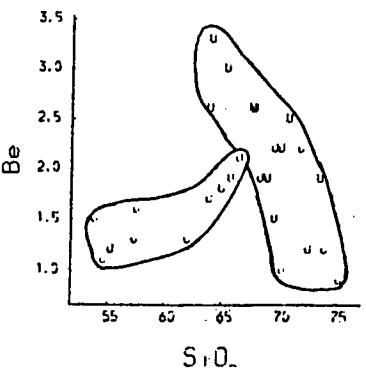
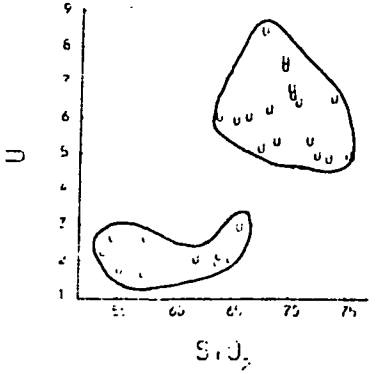
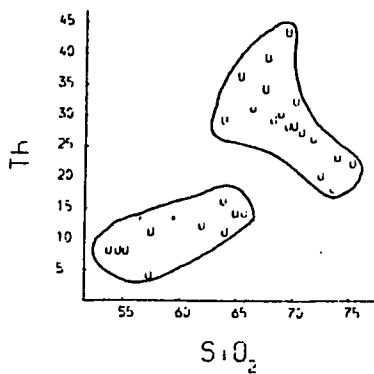
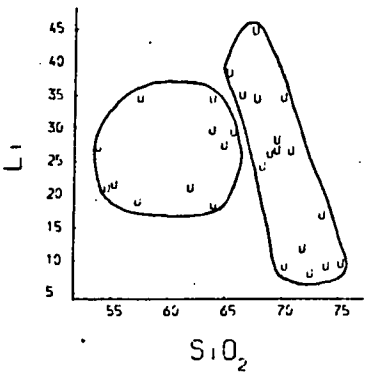
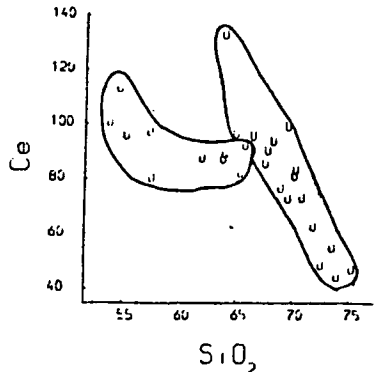
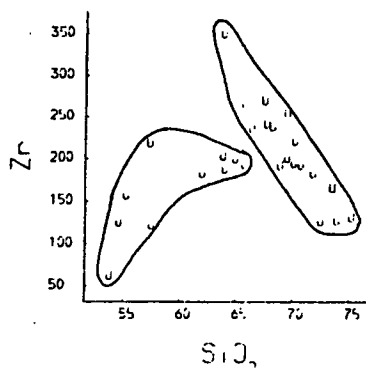
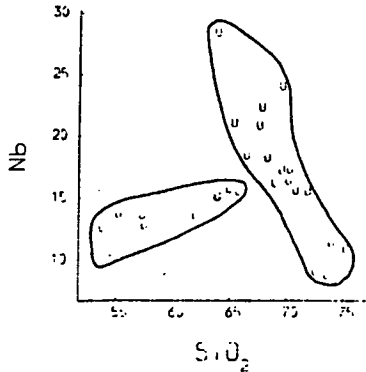
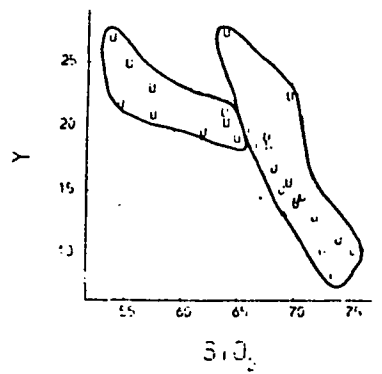
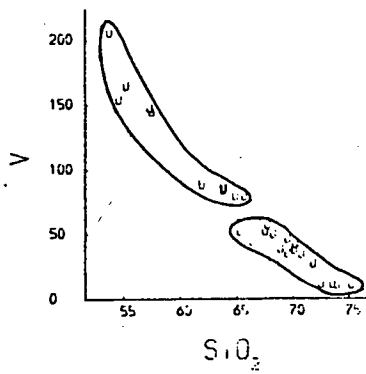
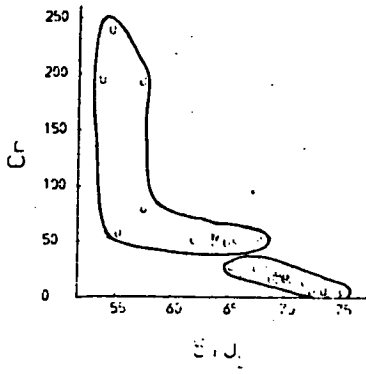
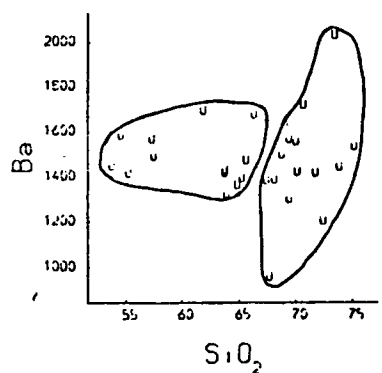
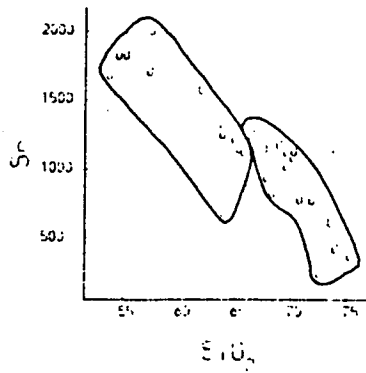
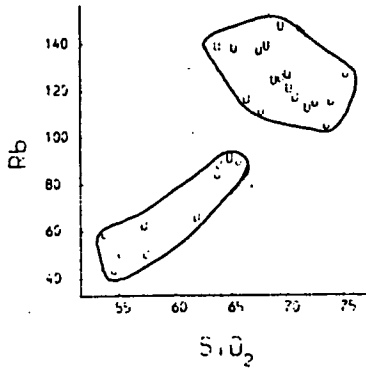


Fig. 6:8. Continued.



similar; this is particularly noticeable for Ce and Y. Nb, Th, Zr, Rb, U, Li and Be concentrations decrease with increasing  $\text{SiO}_2$  in the Ballachulish granite whilst in the Ballachulish granodiorite these elements increase in abundance with increasing  $\text{SiO}_2$ , with the exception of Li which remains constant in the granodiorite. Ba shows considerable scatter when plotted against  $\text{SiO}_2$  for both components of the Ballachulish complex.

6) The Ben Nevis complex (Fig. 6:9).

The range of  $\text{SiO}_2$  values observed in the Ben Nevis complex is from 64 to 73 wt%; MgO,  $\text{Fe}_2\text{O}_3$ , MnO,  $\text{TiO}_2$ , CaO and  $\text{P}_2\text{O}_5$  display good negative correlations with  $\text{SiO}_2$ ;  $\text{Al}_2\text{O}_3$  decreases rapidly at first and then less rapidly between 68 and 73%  $\text{SiO}_2$ ;  $\text{Na}_2\text{O}$  appears to fall at first then rises rapidly between 68 and 73%  $\text{SiO}_2$ ;  $\text{K}_2\text{O}$  defines a tight positive correlation with  $\text{SiO}_2$  over the whole compositional range. As in the Ballachulish complex the differences between the Ben Nevis inner and outer granites are negligible in terms of major elements; however there are some important differences in trace element variations between the two components of this intrusion. Cr, V, Zr, Li, Ce and Sr display negative correlations with  $\text{SiO}_2$ , although the trends vary between the two components of this intrusion, and this is particularly evident for Ce and Zr. Be, Rb, Nb, U and Th concentrations increase in the  $\text{SiO}_2$  64 to 70 wt% compositional range and fall with increasing  $\text{SiO}_2$  in the more evolved compositions. Y concentrations fall with increasing  $\text{SiO}_2$  between 64 and 70%  $\text{SiO}_2$ ; Ba concentrations remain roughly the same throughout the compositional range of the outer granite with somewhat higher values in the inner granite.

Fig. 6:9. Major and trace element variation diagrams for the Etive and Ben Nevis complexes, key to symbols on fold out sheet.

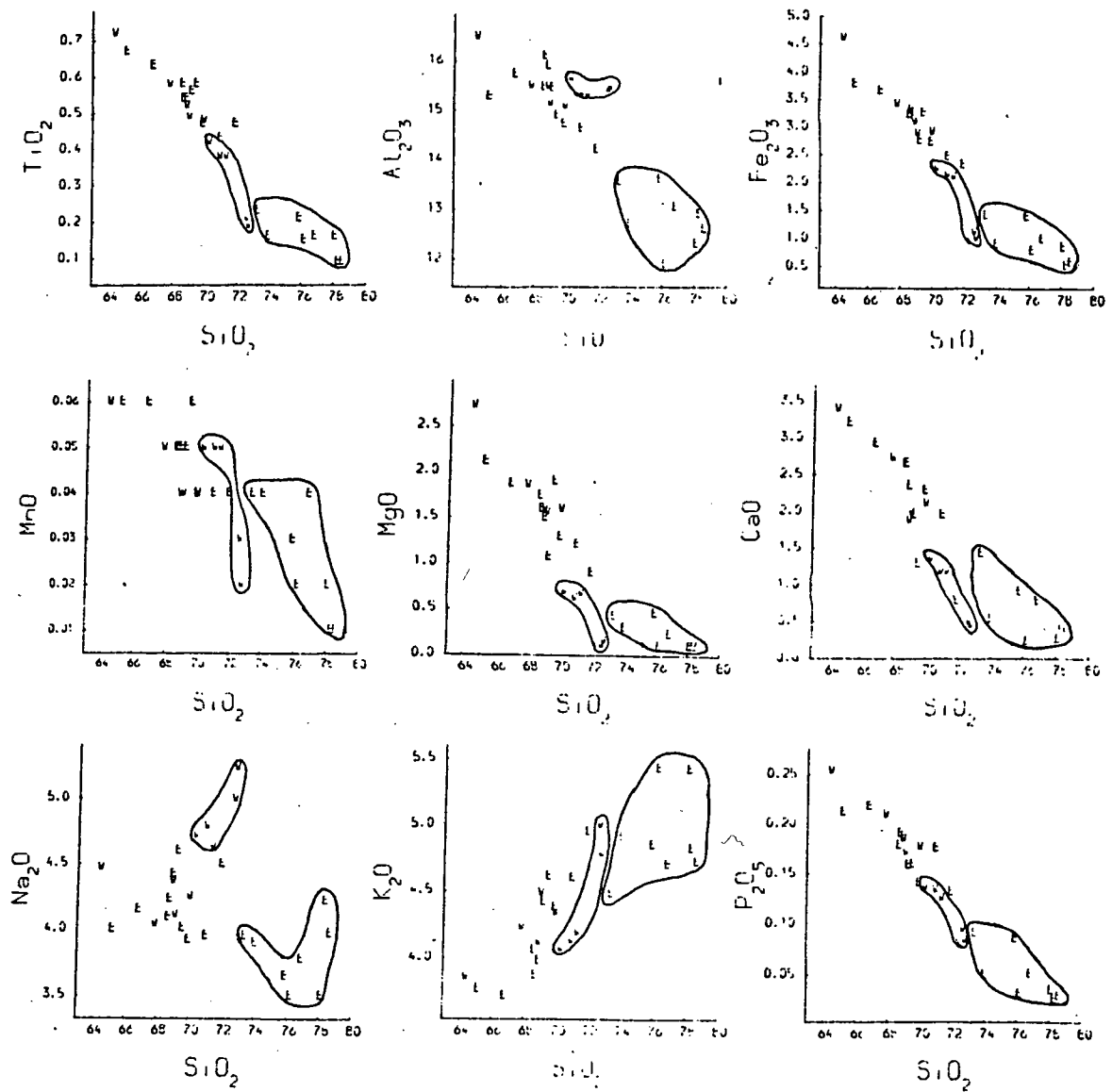
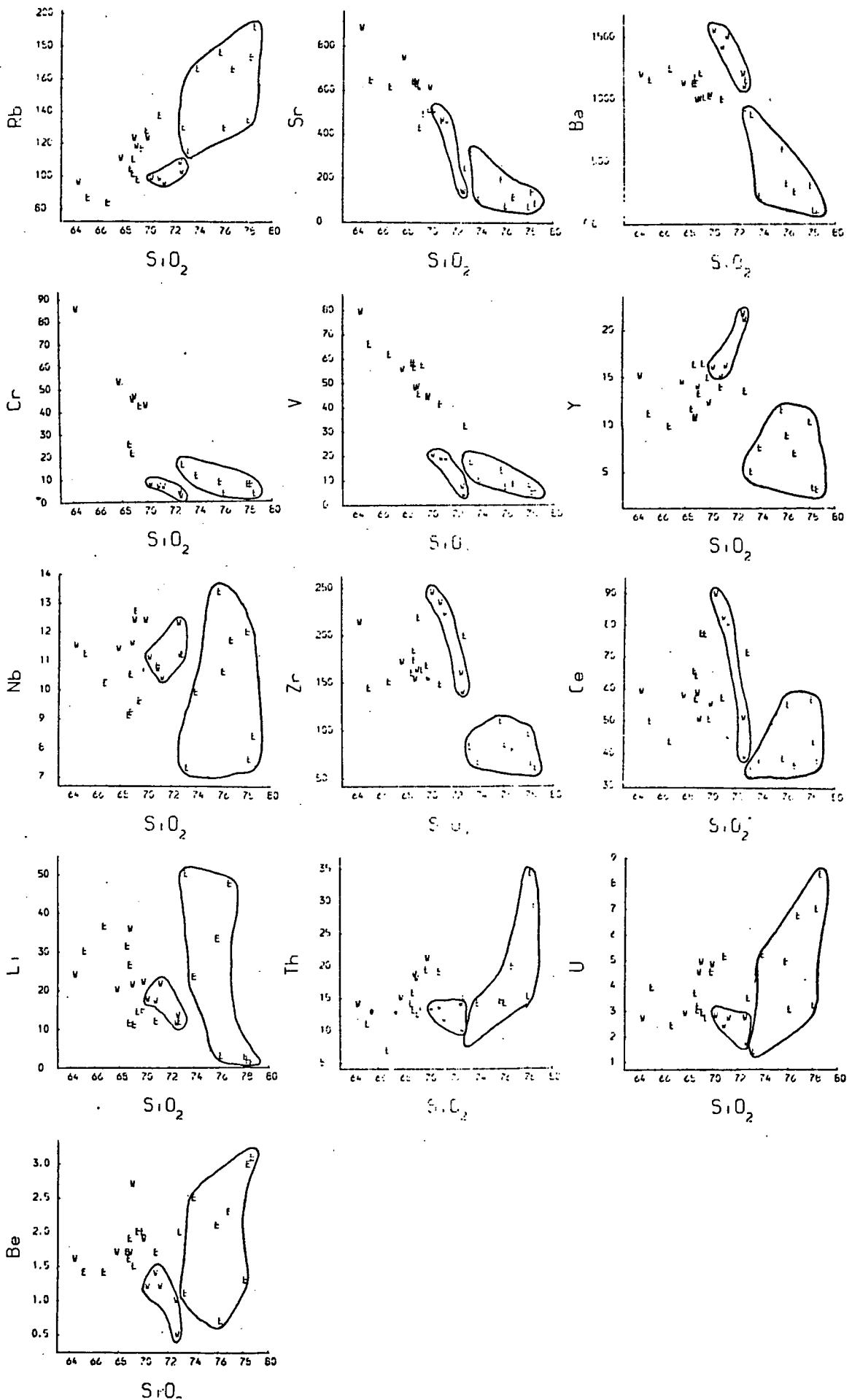


Fig. 6:9. Continued.



7) The Etive complex (Fig. 6:9).

$\text{SiO}_2$  concentrations range from 65 to 78% over the Etive complex.  $\text{Fe}_2\text{O}_3$ ,  $\text{MnO}$ ,  $\text{MgO}$ ,  $\text{TiO}_2$ ,  $\text{Al}_2\text{O}_3$ ,  $\text{CaO}$  and  $\text{P}_2\text{O}_5$  display good negative correlations with  $\text{SiO}_2$  for both the Starav and Cruachan units of the Etive complex, the gradients of the correlations differ slightly between the two intrusive components.  $\text{Na}_2\text{O}_3$  increases slightly with increasing  $\text{SiO}_2$  in the Cruachan unit, in the Starav unit  $\text{Na}_2\text{O}$  decreases between 72 and 76%  $\text{SiO}_2$  and increases in the more  $\text{SiO}_2$  rich samples.  $\text{K}_2\text{O}$  increases with increasing  $\text{SiO}_2$  in both the Cruachan and Starav units.  $\text{Cr}$ ,  $\text{V}$  and  $\text{Sr}$  concentrations decrease with increasing  $\text{SiO}_2$  over both the Cruachan and Starav units with differing gradients.  $\text{Li}$  and  $\text{Nb}$  concentrations decrease with increasing  $\text{SiO}_2$  in the Cruachan unit but show considerable scatter in the Starav unit.  $\text{Zr}$  concentrations increase in the low silica members of the Cruachan unit but decrease slightly in the silica rich samples, concentrations of  $\text{Zr}$  are lower in the Starav unit and decrease with increasing  $\text{SiO}_2$ .  $\text{Ce}$ ,  $\text{Y}$ ,  $\text{Be}$ ,  $\text{Th}$ ,  $\text{U}$  and  $\text{Rb}$  concentrations increase with increasing  $\text{SiO}_2$  in both the Cruachan and Starav units of the Etive complex, these elements show considerable scatter in the Starav unit. Concentrations of  $\text{Ba}$  decrease slightly with increasing  $\text{SiO}_2$  in the Cruachan unit and decrease more rapidly in the Starav unit.

8) The Moor of Rannoch granodiorite (Fig. 6:10).

$\text{SiO}_2$  ranges from about 55% in the hornblendic inclusions to 76% in the more evolved granitic samples.  $\text{MgO}$ ,  $\text{Fe}_2\text{O}_3$ ,  $\text{MnO}$ ,  $\text{TiO}_2$ ,  $\text{Al}_2\text{O}_3$  and  $\text{CaO}$  display good negative correlations with  $\text{SiO}_2$ .  $\text{Na}_2\text{O}$  also correlates negatively with  $\text{SiO}_2$  although the trend is less well defined.  $\text{K}_2\text{O}$  decreases over the range 55 to 60%  $\text{SiO}_2$ , then correlates positively with  $\text{SiO}_2$  in the more evolved samples.  $\text{Cr}$ ,  $\text{Y}$  and  $\text{V}$  define tight negative

Fig. 6:10. Major and trace element variation diagrams for the Moor of Rannoch and Strath Ossian granodiorites, key to symbols on fold out sheet.

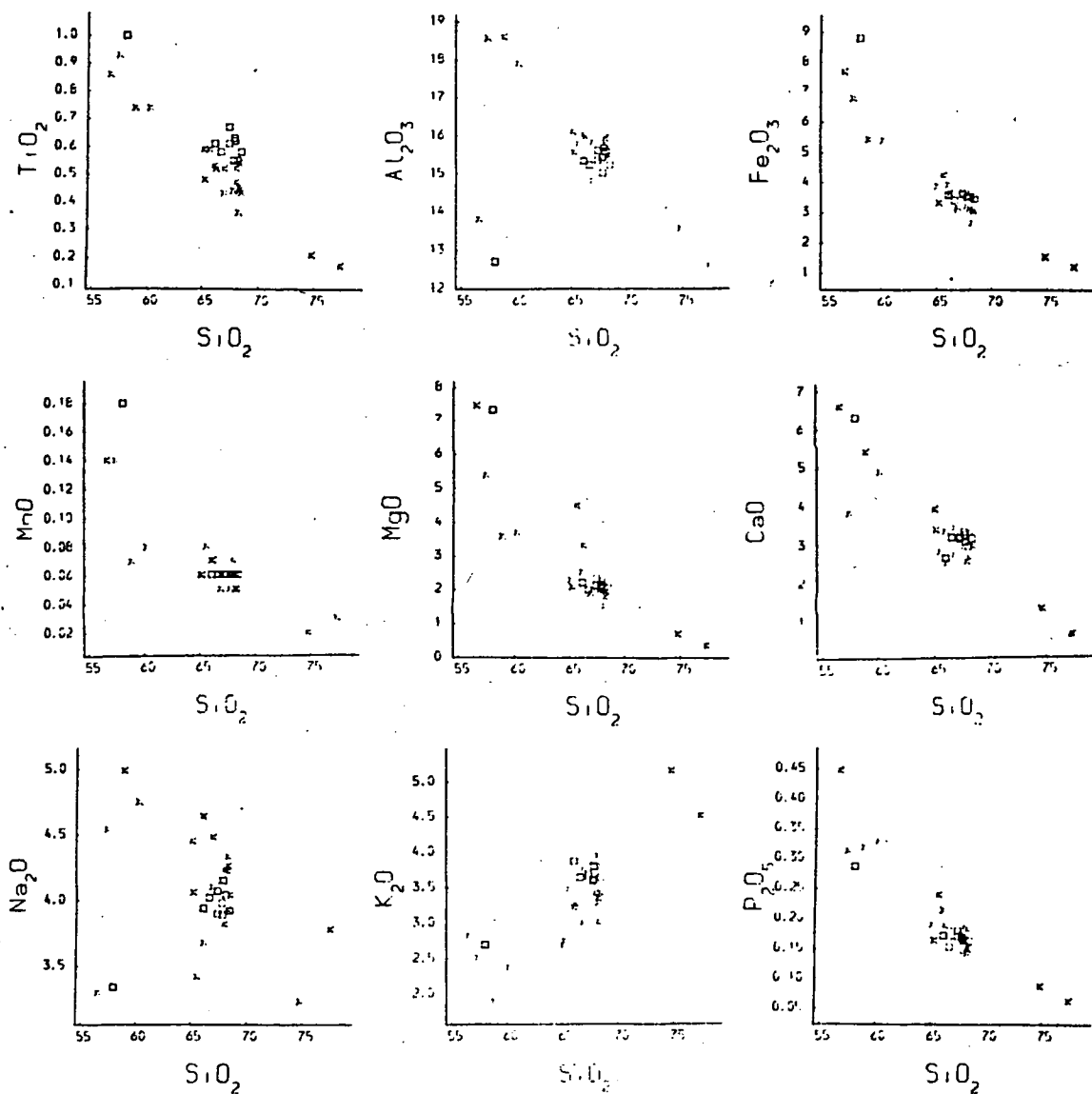
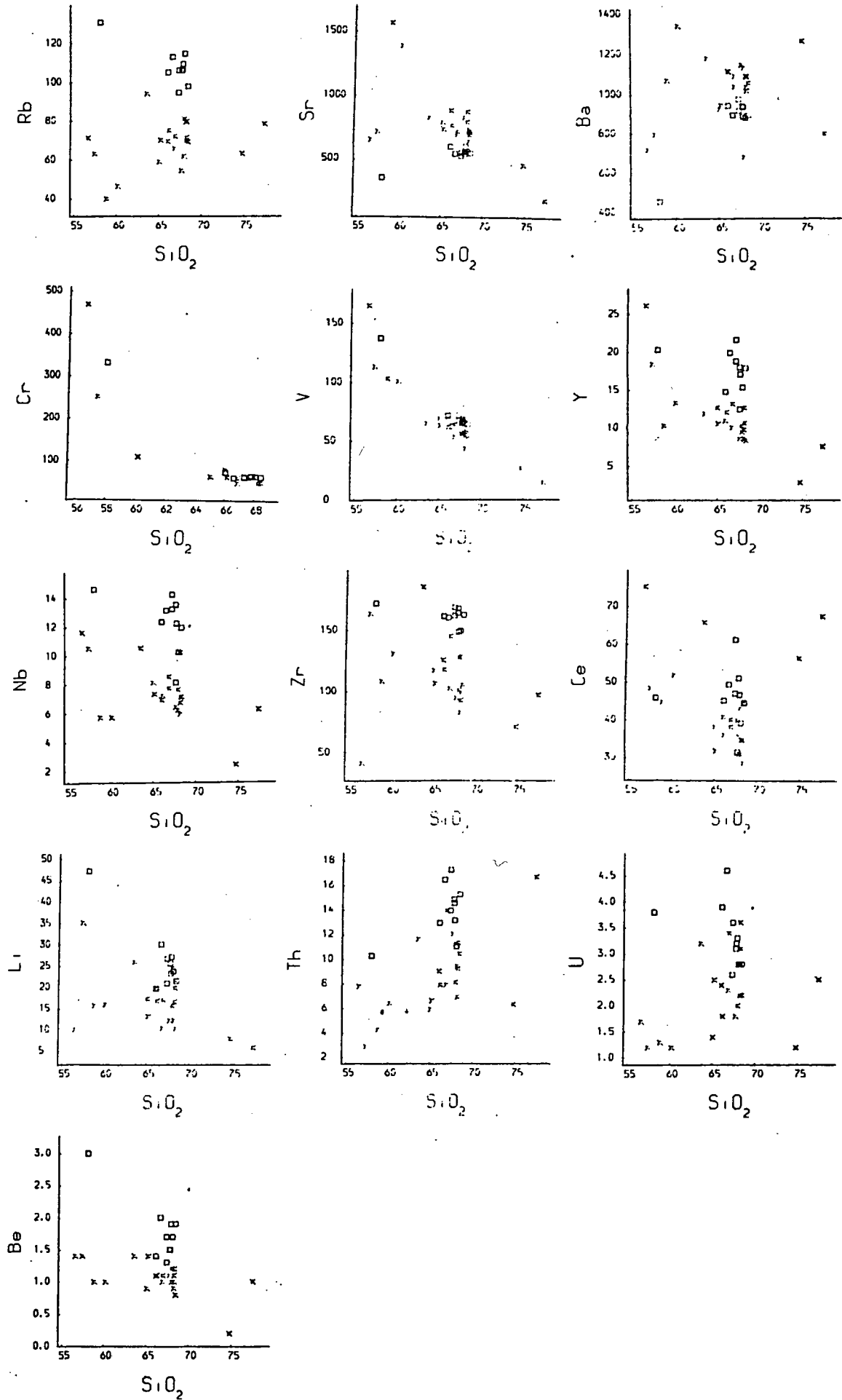


Fig. 6:10. Continued.



correlations with  $\text{SiO}_2$  for all samples whilst Sr, Li, Nb, Zr, Ba and Be display negative correlations with  $\text{SiO}_2$  except for the hornblendite samples which do not plot on the general trends defined by the diorite and granodiorite samples, the quality of the correlations for these elements is variable. Rb, Th and U concentrations generally increase with increasing  $\text{SiO}_2$  although there is considerable scatter. Ce concentrations increase in the range 55 to 70%  $\text{SiO}_2$  but decrease in the silica rich samples.

9) The Strath Ossian granodiorite (Fig. 6:10).

The silica contents of the granodiorite have a restricted range between 65 and 68 wt% (with a hornblendic inclusion at  $\text{SiO}_2$  58%). Major element variations in this intrusion are similar to those of the Moor of Rannoch intrusion: Variations in trace elements over the small compositional range are probably meaningless but comparison of trace element concentrations with the Moor of Rannoch intrusion may have some significance. Concentrations of Cr, Zr, Y, Ce and V are very similar to the Moor of Rannoch intrusion; concentrations of Sr and Ba are similar in the granodiorite but are significantly lower in the Strath Ossian hornblendic inclusion than similar material from the Moor of Rannoch intrusion. Concentration of U, Th, Rb, Li, Nb and Be are slightly higher in the granodiorite than similar materials from the Moor of Rannoch intrusion, but these elements are higher in the hornblendic inclusions than corresponding hornblendic inclusions from the Moor of Rannoch.

10) The Foyers complex (Fig. 6:11).

$\text{SiO}_2$  ranges from 53 to 78 wt% over the Foyers complex;  $\text{TiO}_2$ ,  $\text{MgO}$ ,  $\text{Fe}_2\text{O}_3$ ,  $\text{MnO}$ ,  $\text{Al}_2\text{O}_3$ ,  $\text{CaO}$ ,  $\text{Na}_2\text{O}$  and  $\text{P}_2\text{O}_5$  define negative correlations with

Fig. 6:11. Major and trace element variation diagrams for the Foyers complex, key to symbols on fold out sheet.

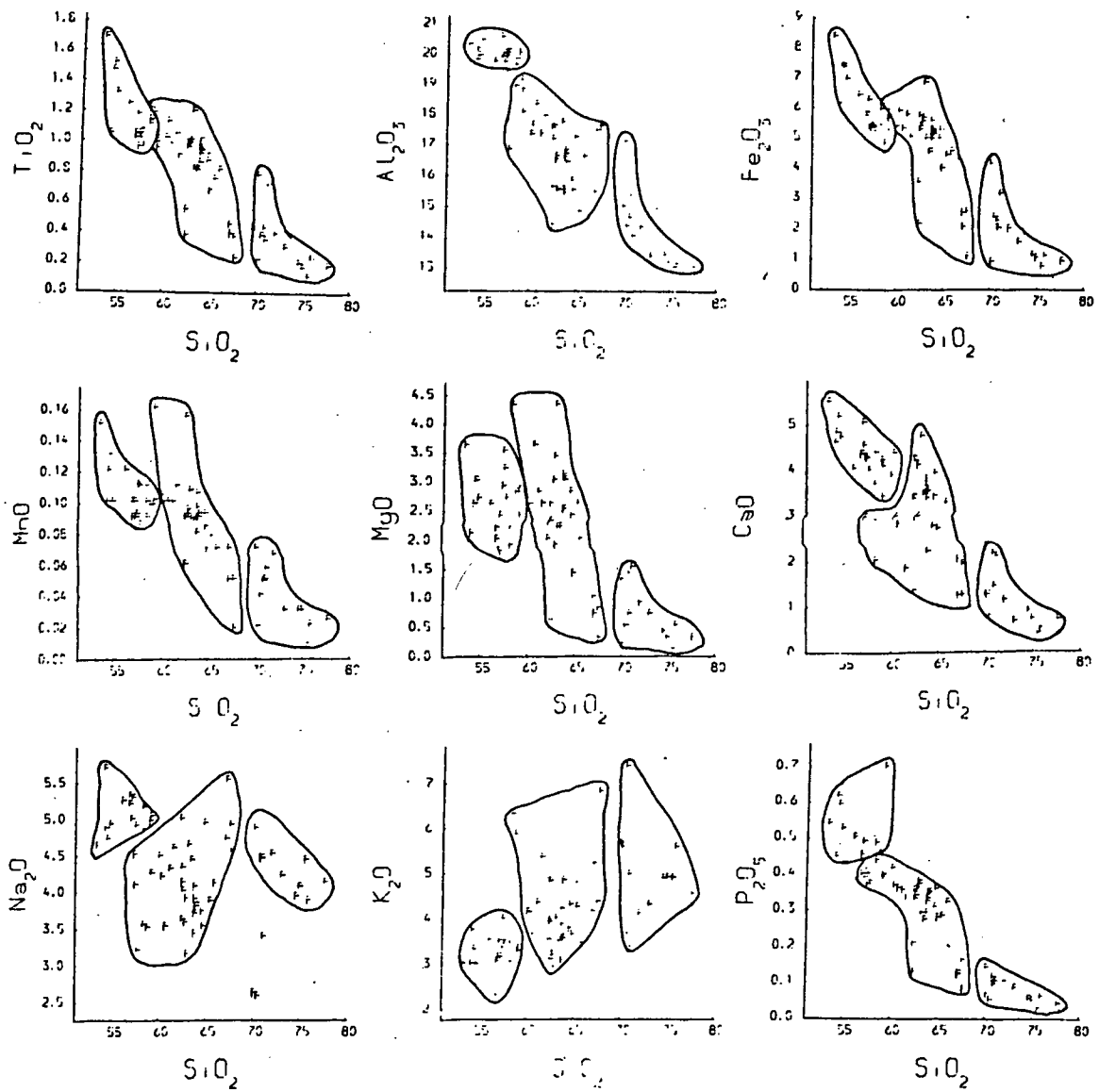
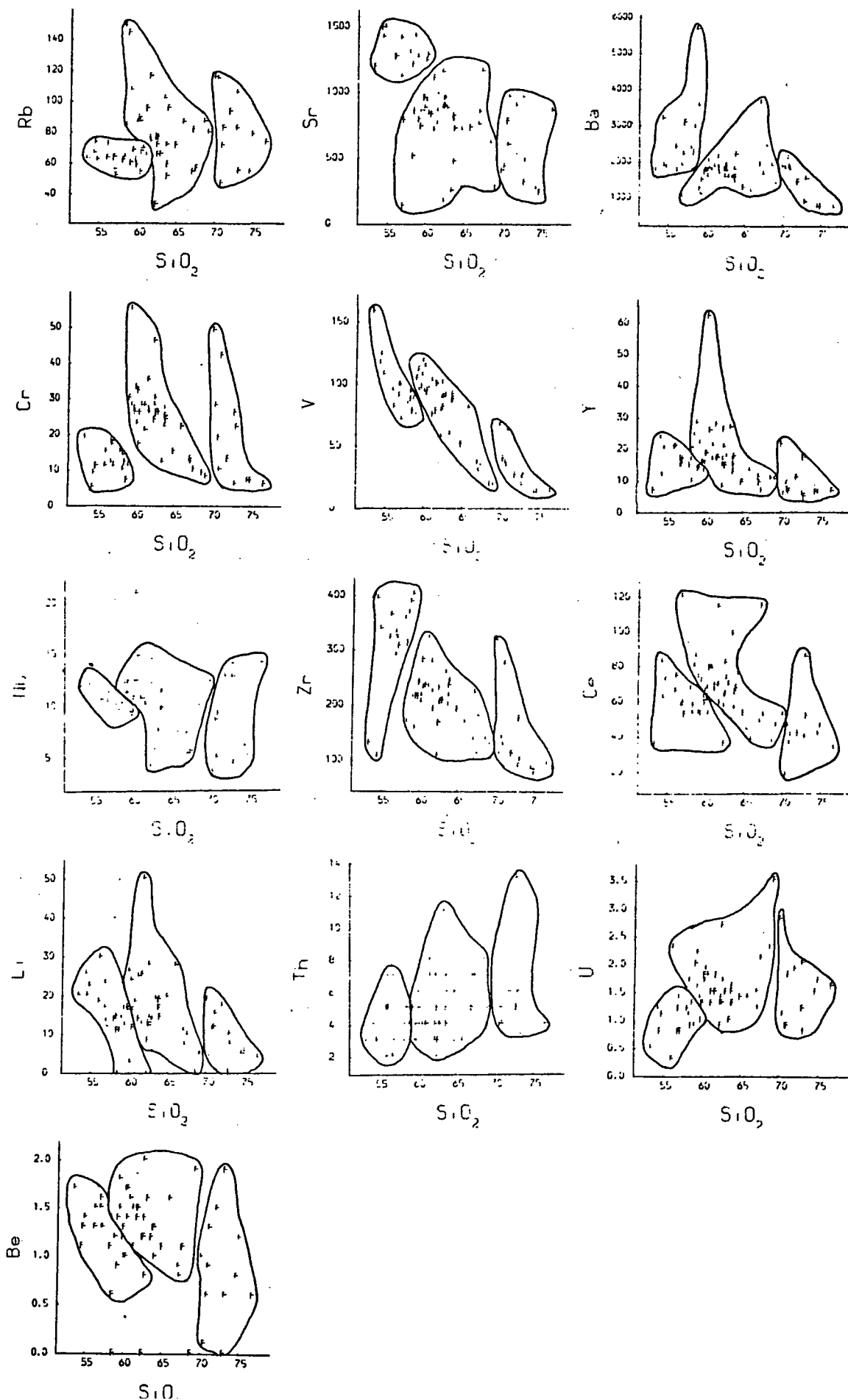


Fig. 6:11. Continued.



$\text{SiO}_2$  although there appear to be three sections to these trends defining separate correlations for the tonalite, granodiorite and granite, this is particularly noticeable for  $\text{MnO}$  and  $\text{P}_2\text{O}_5$ .  $\text{K}_2\text{O}$  increases with increasing  $\text{SiO}_2$  with considerable scatter. Cr and V define three separate negative correlations with  $\text{SiO}_2$ . All the remaining trace elements for the Foyers intrusion display separate but poor correlations with  $\text{SiO}_2$  for each unit of the Foyers intrusion.

11) The Moy granite (Fig. 6:12).

The silica variation in the Moy granite is small (74 to 76%).  $\text{MgO}$ ,  $\text{Fe}_2\text{O}_3$ ,  $\text{TiO}_2$ ,  $\text{Al}_2\text{O}_3$ ,  $\text{CaO}$ ,  $\text{P}_2\text{O}_5$  and  $\text{Na}_2\text{O}$  appear to decrease with increasing  $\text{SiO}_2$ , whereas  $\text{MnO}$  and  $\text{K}_2\text{O}$  appear to increase with increasing  $\text{SiO}_2$ . Trace element variations over such a small compositional range may not be significant; Zr, Be, Cr, V, Nb, Sr, Ba, Y, Ce and Th concentrations appear to decrease with increasing  $\text{SiO}_2$ , whilst U, Li and Rb concentrations appear to increase with increasing  $\text{SiO}_2$ .

12) The Peterhead granite (Fig. 6:12).

$\text{SiO}_2$  ranges from 75 to 78 wt% in the Peterhead granite.  $\text{MnO}$ ,  $\text{TiO}_2$  and  $\text{K}_2\text{O}$  appear to decrease with increasing  $\text{SiO}_2$ ;  $\text{Na}_2\text{O}$ ,  $\text{Al}_2\text{O}_3$  and  $\text{Fe}_2\text{O}_3$  appear to remain constant;  $\text{MnO}$ ,  $\text{CaO}$  and  $\text{P}_2\text{O}_5$  appear to increase with increasing  $\text{SiO}_2$ . As in the Moy granite trace element variations may not be meaningful for this restricted compositional range; Zr, Cr, V and Ce concentrations appear to decrease with increasing  $\text{SiO}_2$ ; Y, U, Sr, Ba, Nb, Be, Rb and Li concentrations appear to increase with increasing  $\text{SiO}_2$ .

Fig. 6:12. Major and trace element variation diagrams for the Ben Rinnes granite, the Peterhead granite and the Moy granite, key to symbols on fold out sheet.

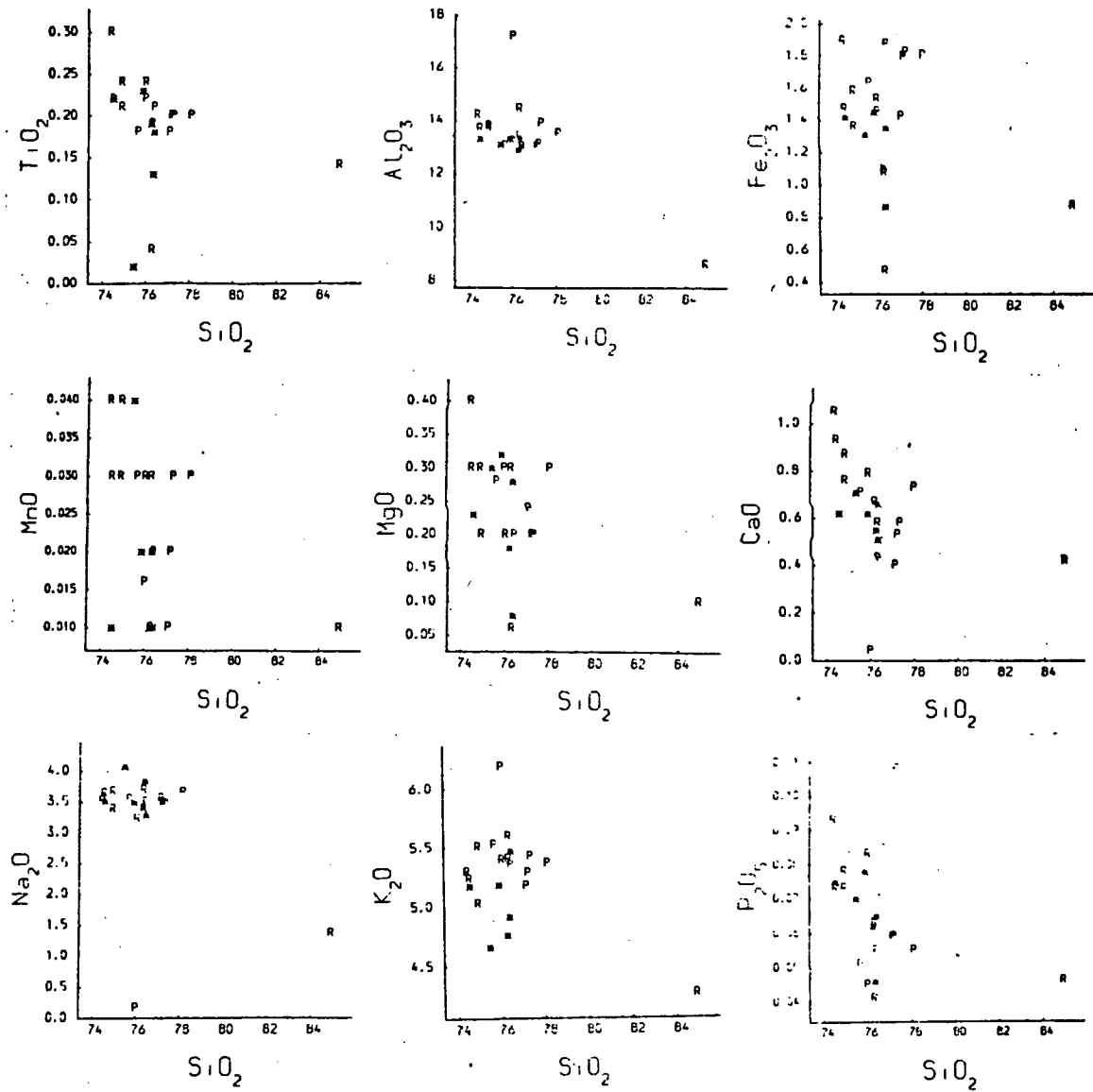
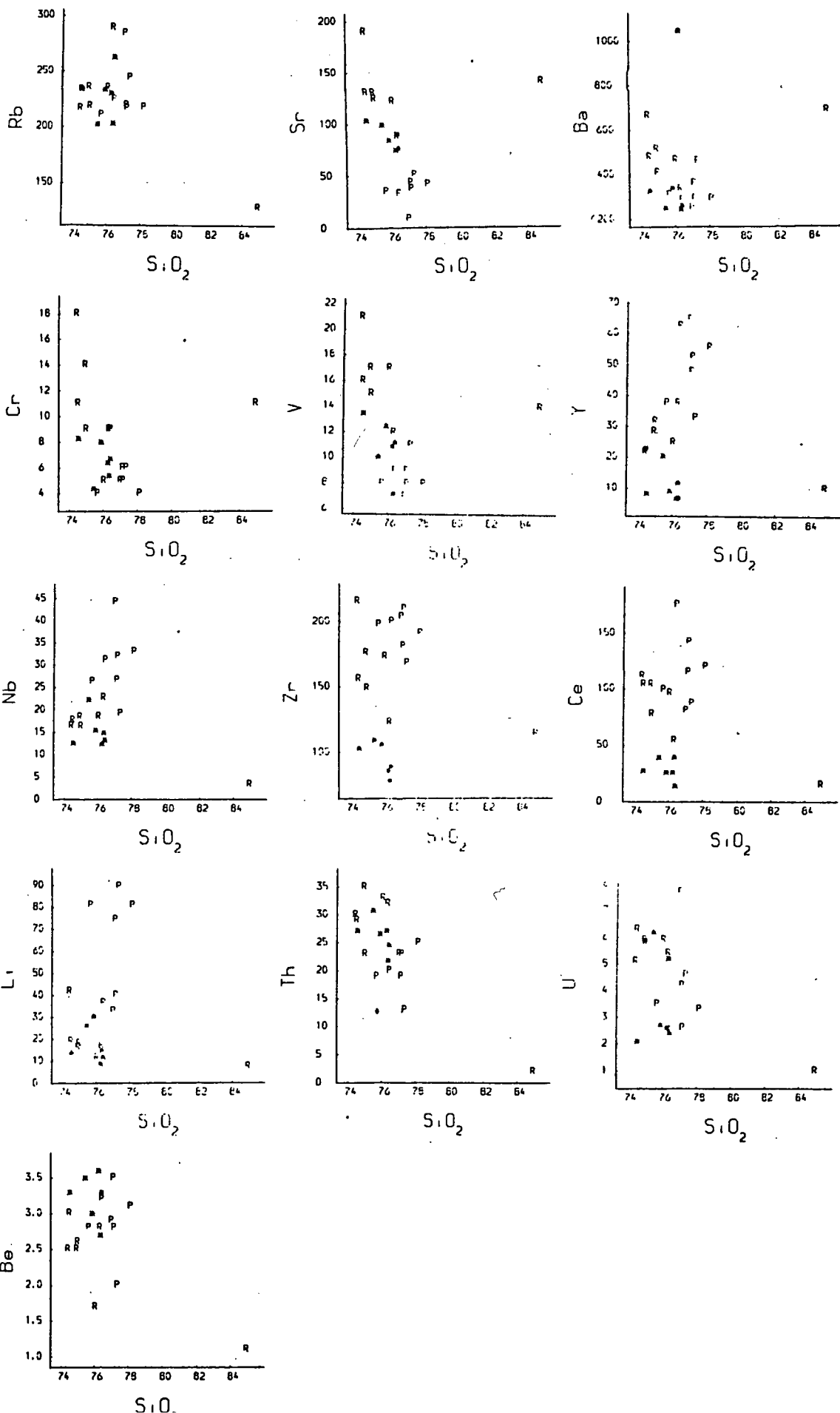


Fig. 6:12. Continued.



13) The Ben Rinnes granite (Fig. 6:12).

SiO<sub>2</sub> variation in the main granite is small, from 74 to 76% but a sample from near the contact has SiO<sub>2</sub> 85% and has obviously suffered contamination with the host metasediments. MgO, MnO, Fe<sub>2</sub>O<sub>3</sub>, TiO<sub>2</sub>, Al<sub>2</sub>O<sub>3</sub>, CaO, P<sub>2</sub>O<sub>5</sub> and Na<sub>2</sub>O correlate negatively with SiO<sub>2</sub>; K<sub>2</sub>O increases with increasing SiO<sub>2</sub> in the normal granite but the contaminated sample has lower K<sub>2</sub>O levels. Li, Zr, Cr, V, Sr, Ba and Ce concentrations decrease with increasing SiO<sub>2</sub> in the main granite; Ba, Sr, Cr and V concentrations increase in the contaminated granite. Y, Th, Be, Rb and Nb concentrations increase with increasing SiO<sub>2</sub> in the main granite, and are lower in the contaminated granite. U concentrations remain constant in the main granite and are severely depleted in the contaminated granite.

14) The Ardclach granite (Fig. 6:13).

The range of SiO<sub>2</sub> observed in the Ardclach granite is small, from 72 to 75 wt%. Over this range of compositions Fe<sub>2</sub>O<sub>3</sub>, MnO, TiO<sub>2</sub>, MgO, Al<sub>2</sub>O<sub>3</sub>, CaO, K<sub>2</sub>O and P<sub>2</sub>O<sub>5</sub> display negative correlations with SiO<sub>2</sub>, whereas Na<sub>2</sub>O increases with increasing SiO<sub>2</sub>. Trace element variations over this small range of SiO<sub>2</sub> may be misleading, however all the selected trace elements correlate negatively with SiO<sub>2</sub> except Li and Be. Levels of Cr and V are relatively high for granites of this composition, possibly reflecting a metasedimentary source.

15) The Strichen granite (Fig. 6:13).

The range of SiO<sub>2</sub> observed in the Strichen granite is small from 72 to 74%. Over this small range of compositions Fe<sub>2</sub>O<sub>3</sub>, MnO, TiO<sub>2</sub>, MgO, Al<sub>2</sub>O<sub>3</sub>, CaO and P<sub>2</sub>O<sub>5</sub> display negative correlations with SiO<sub>2</sub> whereas Na<sub>2</sub>O and K<sub>2</sub>O increase with increasing SiO<sub>2</sub>. Trace element variations are similar to

Fig. 6:13. Major and trace element variation diagrams for the Ardclach granite, the Aberdeen granite, the Cove Bay granite and the Stritchen granite, key to symbols on fold out sheet.

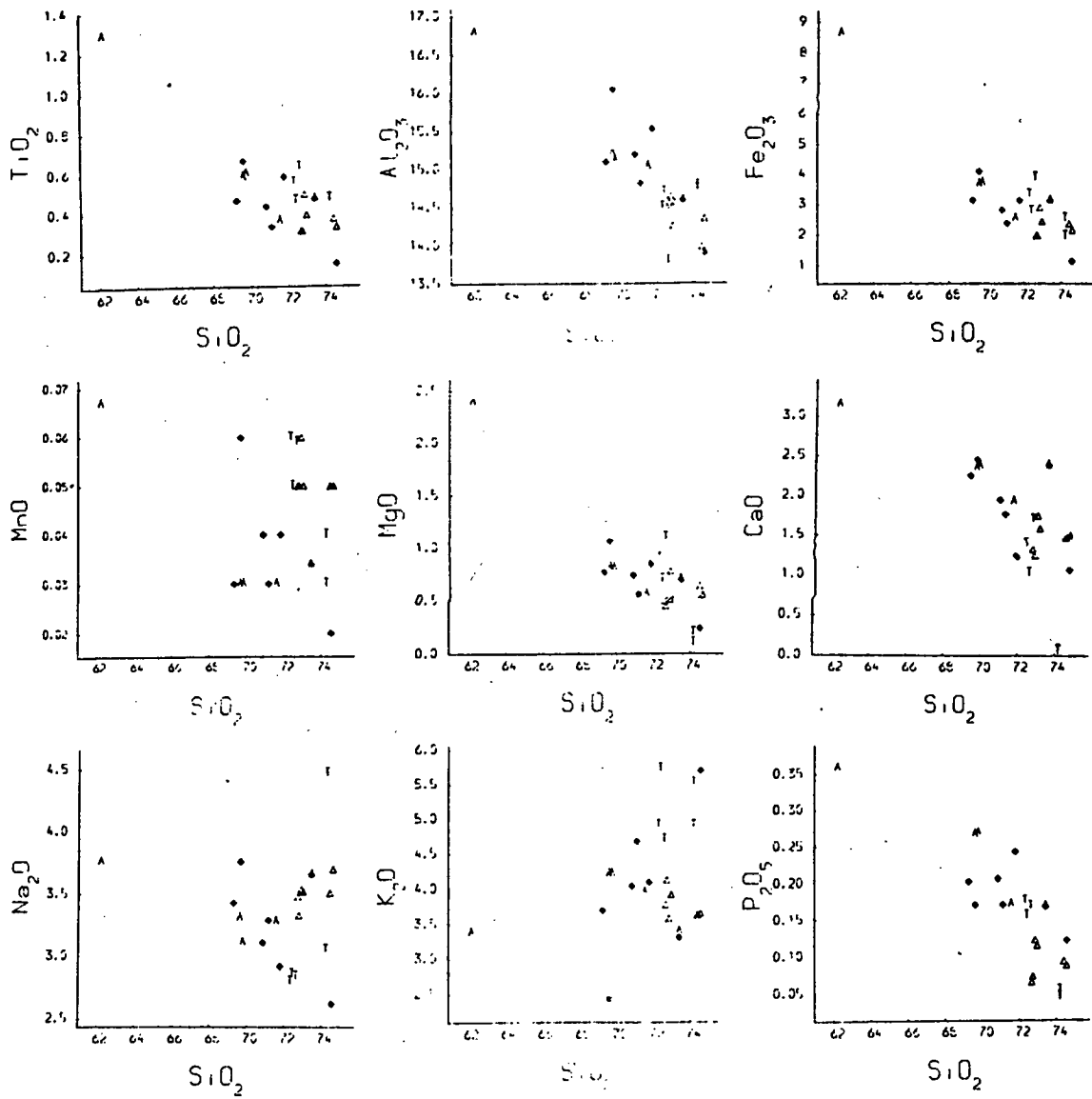
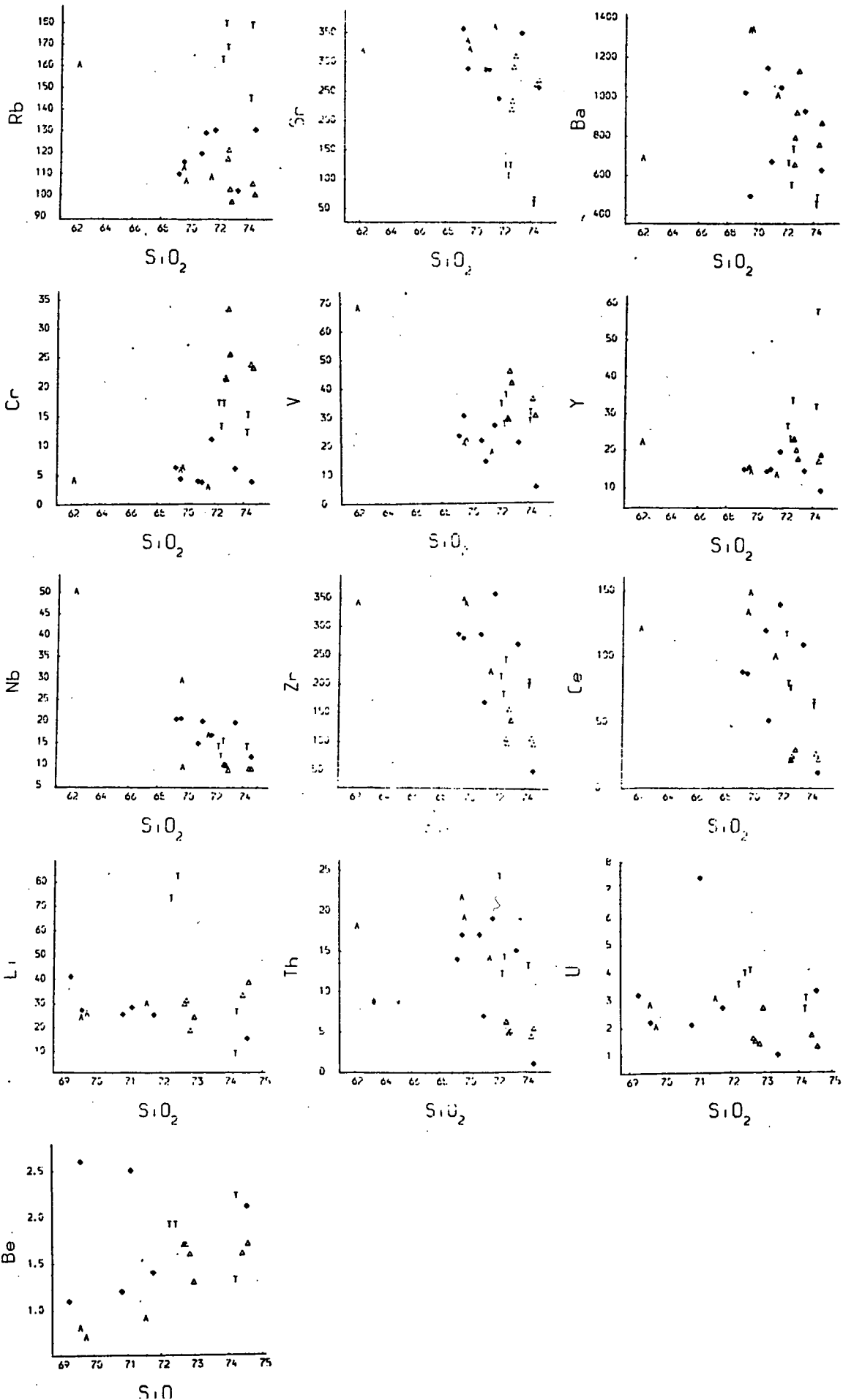


Fig. 6:13. Continued.



the Ardclach granite with the exception of Y which increases rapidly with increasing  $\text{SiO}_2$ . Rb and Li are generally more abundant and Sr concentrations are generally lower than in the other "S" type granites.

16) The Aberdeen granite (Fig. 6:13).

The Aberdeen granite has  $\text{SiO}_2$  ranging from 62 to 72 wt%.  $\text{Fe}_2\text{O}_3$ , MnO, MgO,  $\text{TiO}_2$ ,  $\text{Al}_2\text{O}_3$ , CaO and  $\text{P}_2\text{O}_5$  define negative correlations with  $\text{SiO}_2$ .  $\text{Na}_2\text{O}$  decreases from  $\text{SiO}_2$  62 to 70% and increases in the  $\text{SiO}_2$ -rich compositions, whereas  $\text{K}_2\text{O}$  increases over the range  $\text{SiO}_2$  62 to 68% and decreases in the  $\text{SiO}_2$  rich compositions. Y, Nb, V and Rb concentrations decrease with increasing  $\text{SiO}_2$ , Cr and Zr concentrations remain constant from 62 to 70%  $\text{SiO}_2$  and decrease in the more  $\text{SiO}_2$  rich compositions. Ce, Ba and Th concentrations increase from  $\text{SiO}_2$  62 to 70% and decrease in the more evolved samples. Sr concentrations remain constant from 62 to 70%  $\text{SiO}_2$  and increase slightly in the more silica rich samples. The data set for Li, U and Be is not complete for this suite.

17) The Cove Bay granite (Fig. 6:13).

$\text{SiO}_2$  varies from 69 to 74 wt% in the Cove Bay granite. The major element trends, with the exception of  $\text{Na}_2\text{O}$  and  $\text{K}_2\text{O}$ , which show considerable scatter, are similar to the Aberdeen granite. Silica covariation diagrams for Cr, V, Nb, Th, Zr, Ce, Y, Sr, Ba and Rb are also similar to those of the Aberdeen granite.

18) The Blackburn granite (Fig. 6:14).

The observed variation of  $\text{SiO}_2$  is from 72 to 76% in the Blackburn granite. Over this compositional range  $\text{TiO}_2$ ,  $\text{Fe}_2\text{O}_3$ , MnO, MgO,  $\text{Al}_2\text{O}_3$ , CaO,  $\text{P}_2\text{O}_5$  and  $\text{Na}_2\text{O}$  display negative correlations with  $\text{SiO}_2$ , whereas  $\text{K}_2\text{O}$

Fig. 6:14. Major and trace element variation diagrams for the Dorback granite, the Glenlivet granite and the Blackburn granite, key to symbols on fold out sheet.

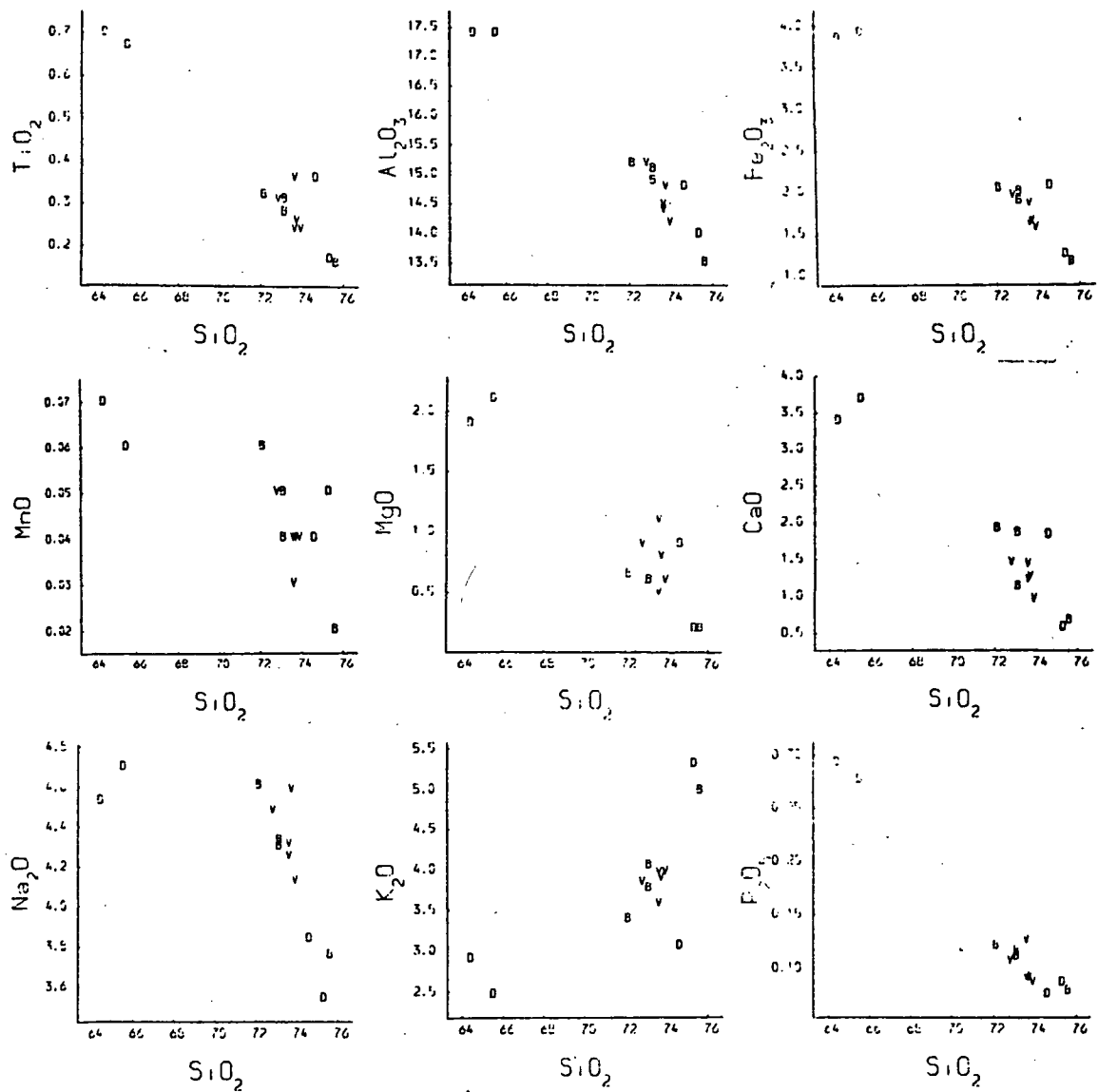
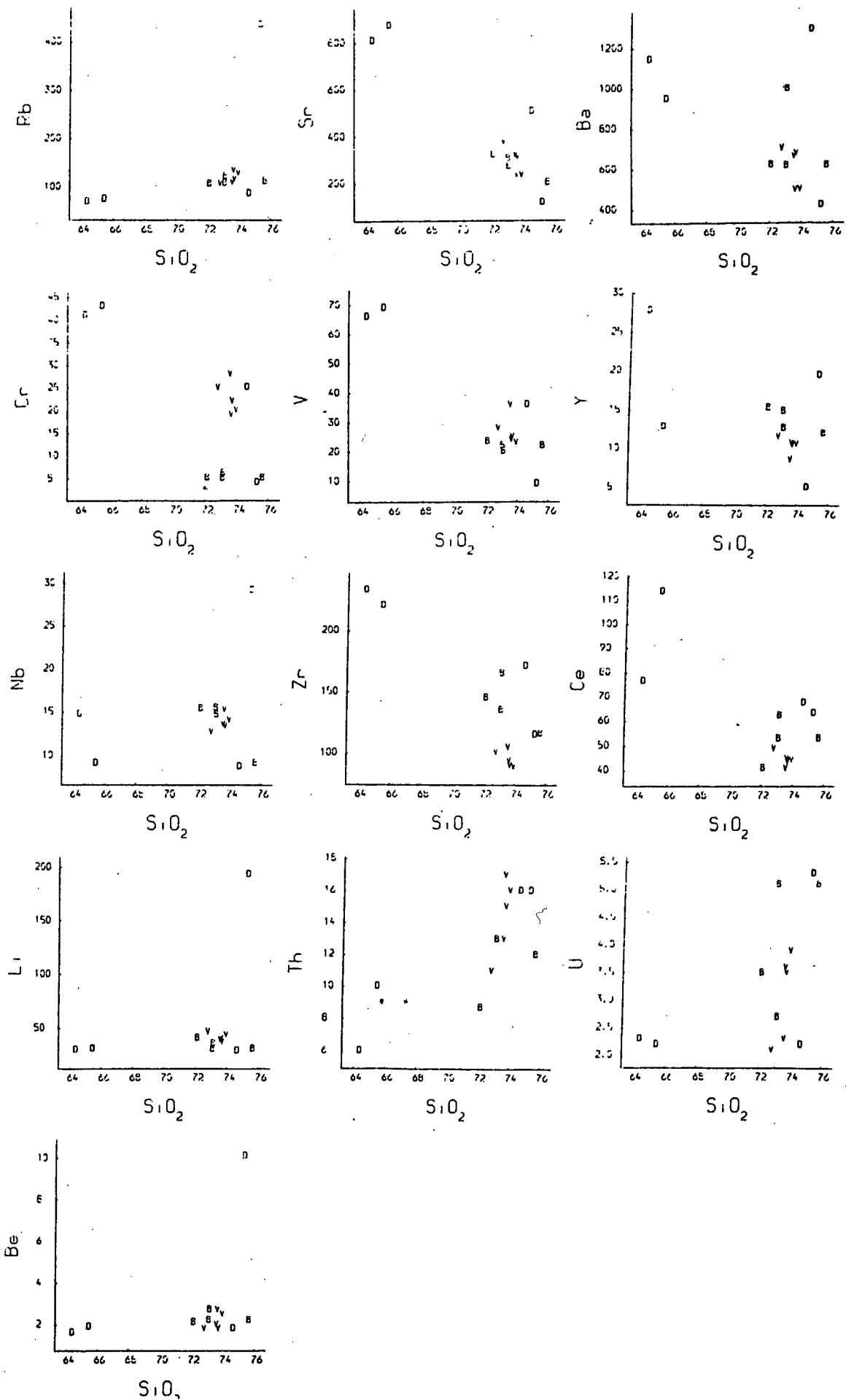


Fig. 6:14. Continued.



increases with increasing  $\text{SiO}_2$ . Trace element variations over this small compositional range do not always produce defineable trends; Zr, Sr, Li, Y and Nb concentrations appear to decrease with increasing  $\text{SiO}_2$ ; Cr, V and Be concentrations remain roughly constant; Rb, U and Th concentrations appear to increase with increasing  $\text{SiO}_2$ .

19) The Glenlivet granite (Fig. 6:14).

The observed variation of  $\text{SiO}_2$  is vary small (72 to 74%), major element variations are similar to the Blackburn granite. Ce, Y, Sr, Ba, Zr, Li, Cr and V concentrations appear to decrease with increasing  $\text{SiO}_2$ , whereas Nb, Rb, Be, U and Th concentrations appear to increase with increasing  $\text{SiO}_2$ .

20) The Dorback granite (Fig. 6:14).

The four samples collected from this intrusion form two distinct groups one at 64-66%  $\text{SiO}_2$  and the other at 74-76%  $\text{SiO}_2$  and although many major and trace elements define coherent trends with  $\text{SiO}_2$  (CaO, MgO,  $\text{Na}_2\text{O}$ ,  $\text{TiO}_2$ ,  $\text{Al}_2\text{O}_3$ ,  $\text{Fe}_2\text{O}_3$ , MnO,  $\text{P}_2\text{O}_5$ , Th, Sr, Zr, Cr and V) others are so scattered as to cast doubt on any genetic relationship between the two groups (Nb, Rb, Li, Be, Ba, U, Y, Ce and  $\text{K}_2\text{O}$ ).

21) The Hill of Fare granite (Fig. 6:15).

$\text{SiO}_2$  values range from 76 to 78% in the Hill of Fare granite.  $\text{TiO}_2$ ,  $\text{Fe}_2\text{O}_3$ , MnO, MgO,  $\text{Al}_2\text{O}_3$ , CaO,  $\text{P}_2\text{O}_5$  and  $\text{Na}_2\text{O}$  decrease slightly with increasing  $\text{SiO}_2$ , whereas  $\text{K}_2\text{O}$  increases slightly with increasing  $\text{SiO}_2$ . Zr, Be, V, Th, Sr, Ba, Nb, Y, Rb and Li display poor negative correlations with  $\text{SiO}_2$ ; Ce, U and Cr concentrations appear to increase with increasing  $\text{SiO}_2$ .

Fig. 6:15. Major and trace element variation diagrams for the Cromar granite, the Mt Battock granite and the Hill of Fare granite, key to symbols on fold out sheet.

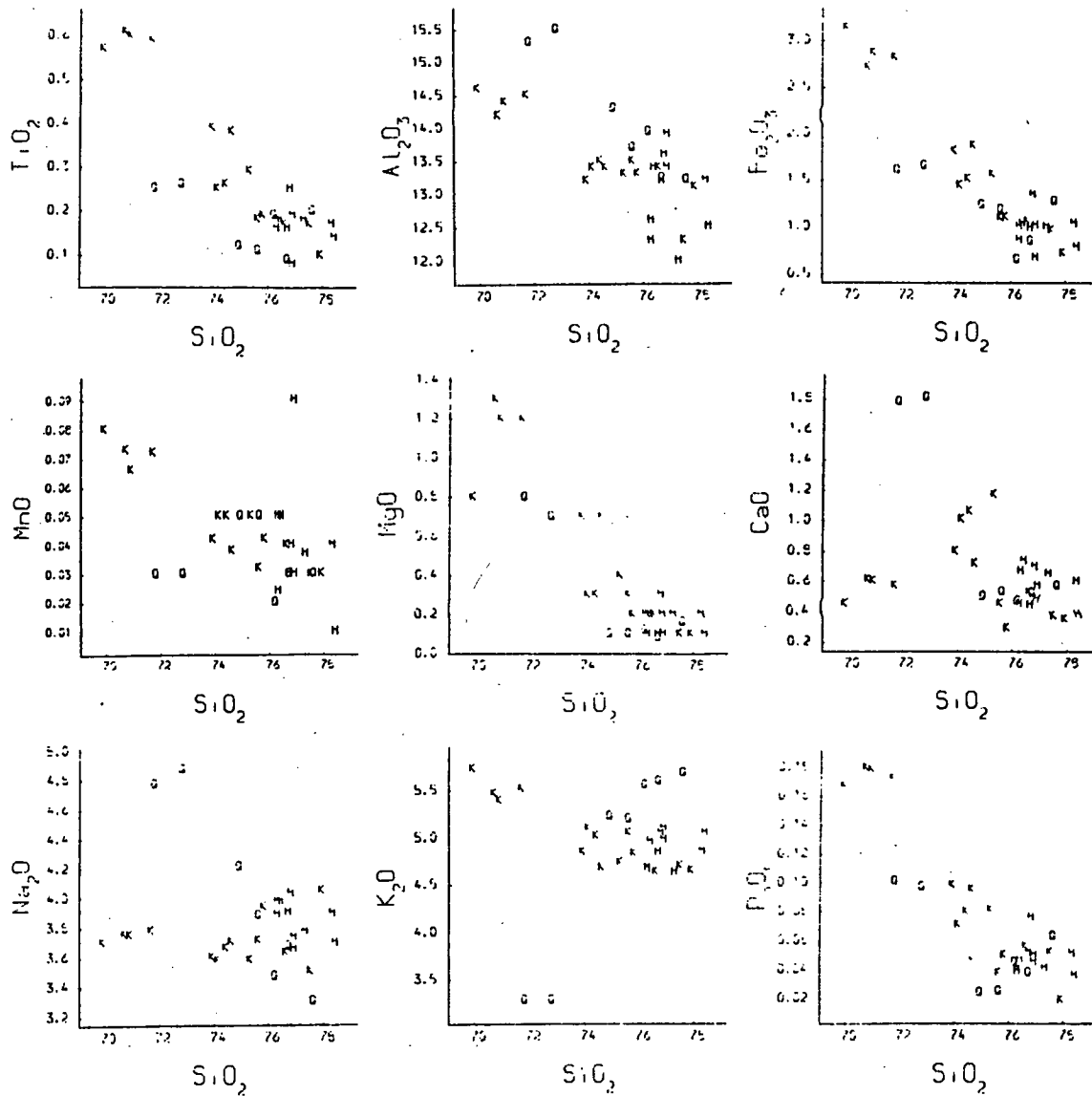
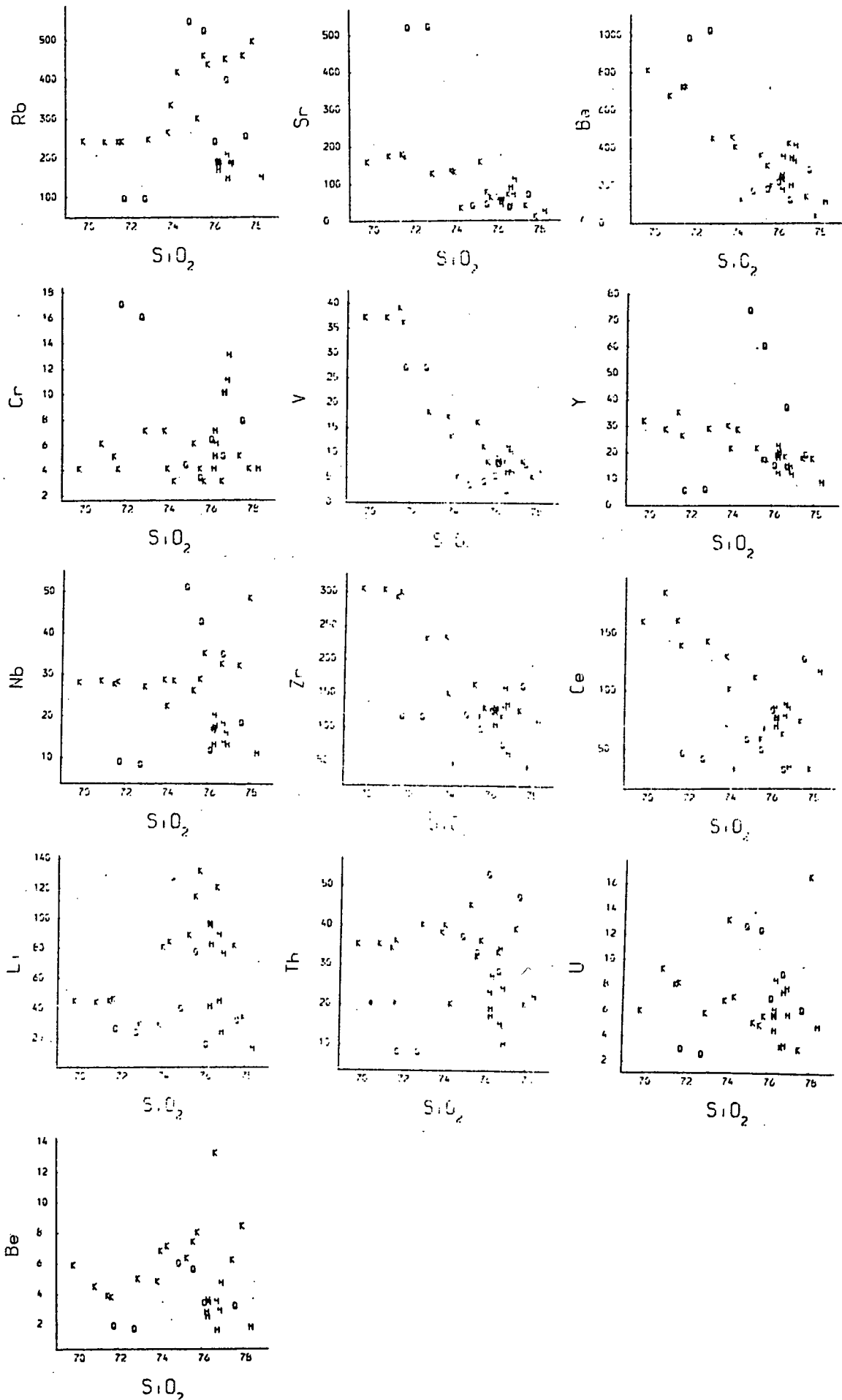


Fig. 6:15. Continued.



22) The Mt. Battock granite (Fig. 6:15).

$\text{SiO}_2$  ranges from 70 to 78% in the Mt. Battock granite.  $\text{TiO}_2$ ,  $\text{Fe}_2\text{O}_3$ ,  $\text{MnO}$ ,  $\text{K}_2\text{O}$ ,  $\text{Al}_2\text{O}_3$  and  $\text{P}_2\text{O}_5$  decrease with increasing  $\text{SiO}_2$ , but  $\text{Na}_2\text{O}$  remains roughly constant.  $\text{CaO}$  increases over the range  $\text{SiO}_2$  70 to 76% and decreases in the silica rich samples. V, Zr, Ba, Sr, Y and Ce concentrations decrease with increasing  $\text{SiO}_2$ , whereas U and Th concentrations remain roughly constant over the range  $\text{SiO}_2$  70 to 76% and decrease slightly in the more silica rich samples. Cr remains roughly constant, but Li and Be concentrations increase over the range  $\text{SiO}_2$  70 to 76% and decrease in the more silica rich samples. Rb and Nb concentrations remain roughly constant in the range  $\text{SiO}_2$  70 to 74% and increase rapidly in the more silica rich samples.

23) The Cromar granite (Fig. 6:15).

$\text{SiO}_2$  ranges from 71 to 78% in the Cromar granite.  $\text{MgO}$ ,  $\text{CaO}$ ,  $\text{TiO}_2$ ,  $\text{Al}_2\text{O}_3$ ,  $\text{Fe}_2\text{O}_3$  and  $\text{Na}_2\text{O}$  all decrease with increasing  $\text{SiO}_2$ , whereas MnO increases over the range  $\text{SiO}_2$  71 to 75% and decreases in the high silica samples.  $\text{P}_2\text{O}_5$  decreases over the range  $\text{SiO}_2$  71 to 75% and decreases in the high silica samples, and  $\text{K}_2\text{O}$  increases with increasing  $\text{SiO}_2$ . Although the major elements give coherent trends for this intrusion, the trace element variations show two separate groups, one with  $\text{SiO}_2$  at 72 to 73% and the other from 74 to 78%  $\text{SiO}_2$ . The low  $\text{SiO}_2$  samples are characterized by high Sr, Ba, Cr and V and low Rb, Ce, Y, U, Th, Be and Nb. The high silica samples are characterized by high Nb, Be, U, Th, Y, Ce and Rb, and low Cr and V. U, Th, Nb, Be, Y, Li and Rb display negative correlations with  $\text{SiO}_2$ . In the high silica samples, Cr, V and Ce concentrations increase with increasing  $\text{SiO}_2$ , but in these samples, concentrations of Zr, Ba and Sr remain roughly constant.

24) The Bennachie granite (Fig. 6:16).

The range of  $\text{SiO}_2$  observed in the Bennachie granite is effectively from 73 to 78%.  $\text{MgO}$ ,  $\text{Fe}_2\text{O}_3$ ,  $\text{TiO}_2$ ,  $\text{Al}_2\text{O}_3$ ,  $\text{CaO}$  and  $\text{P}_2\text{O}_5$  display negative correlations with  $\text{SiO}_2$ .  $\text{K}_2\text{O}$  remains roughly constant,  $\text{MnO}$  also remains roughly constant but shows considerable scatter;  $\text{Na}_2\text{O}$  increases with increasing  $\text{SiO}_2$  between  $\text{SiO}_2$  73 and 76% and decreases in the more silica rich samples. Th, V, Zr, Sr, Ba and Ce concentrations decrease with increasing  $\text{SiO}_2$ ; Cr, Nb and Y concentrations decrease with increasing  $\text{SiO}_2$  for the range  $\text{SiO}_2$  73 to 76% and increase in the more silica rich samples; Rb and Be concentrations increase with increasing  $\text{SiO}_2$  whilst U and Li do not define recognisable trends.

25) The Lochnagar complex (Fig. 6:17).

With the associated diorite the Lochnagar complex has a range of  $\text{SiO}_2$  from 57 to 77%, although there is a large gap in the data between the diorite sample and the granites between 57 and 70%  $\text{SiO}_2$ .  $\text{TiO}_2$ ,  $\text{MgO}$ ,  $\text{Fe}_2\text{O}_3$ ,  $\text{MnO}$ ,  $\text{Al}_2\text{O}_3$ ,  $\text{CaO}$  and  $\text{P}_2\text{O}_5$  define tight negative correlations with  $\text{SiO}_2$ .  $\text{Na}_2\text{O}$  decreases with increasing  $\text{SiO}_2$  in the granite but is lower in the diorite,  $\text{K}_2\text{O}$  increases with increasing  $\text{SiO}_2$  in the granite but is lower in the diorite,  $\text{K}_2\text{O}$  increases with increasing  $\text{SiO}_2$ . Cr, V, Zr and Sr define good negative correlations with  $\text{SiO}_2$ , Nb concentrations increase from the diorite to the granite and decrease with increasing  $\text{SiO}_2$  between 70 and 75%  $\text{SiO}_2$ . Nb concentrations then increase with increasing  $\text{SiO}_2$  in the more silica rich samples. Y concentrations decrease with increasing  $\text{SiO}_2$  from 57 to 75%  $\text{SiO}_2$  and increase in the more silica rich samples. Ce and Ba concentrations increase from the granite and then decrease with increasing  $\text{SiO}_2$  from 70 to 77%  $\text{SiO}_2$ . Rb, Be, U, Th and Li concentrations increase with increasing  $\text{SiO}_2$ .

Fig. 6:16. Major and trace element variation diagrams for the Bennachie granite, key to symbols on fold out sheet.

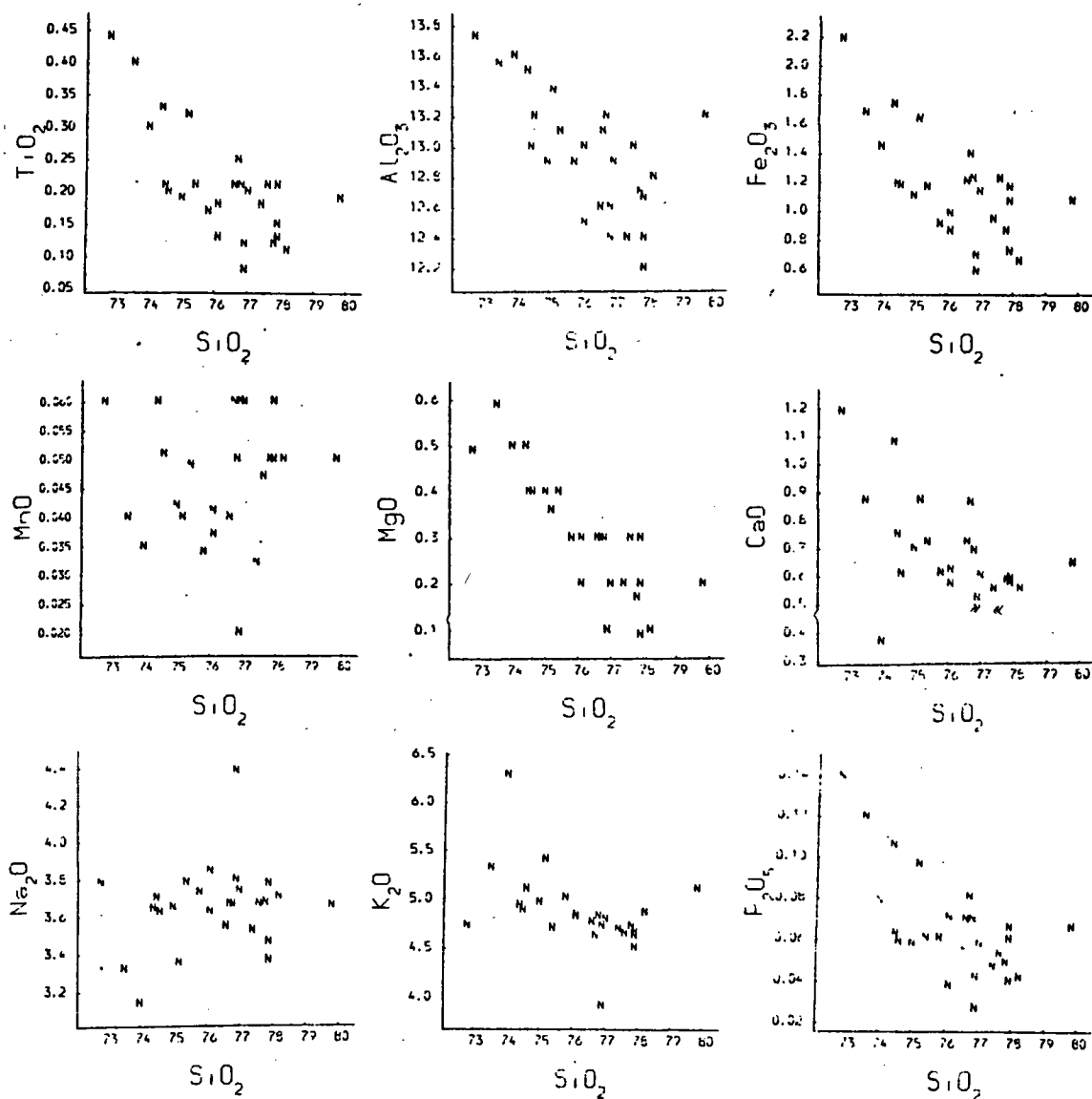


Fig. 6:16. Continued.

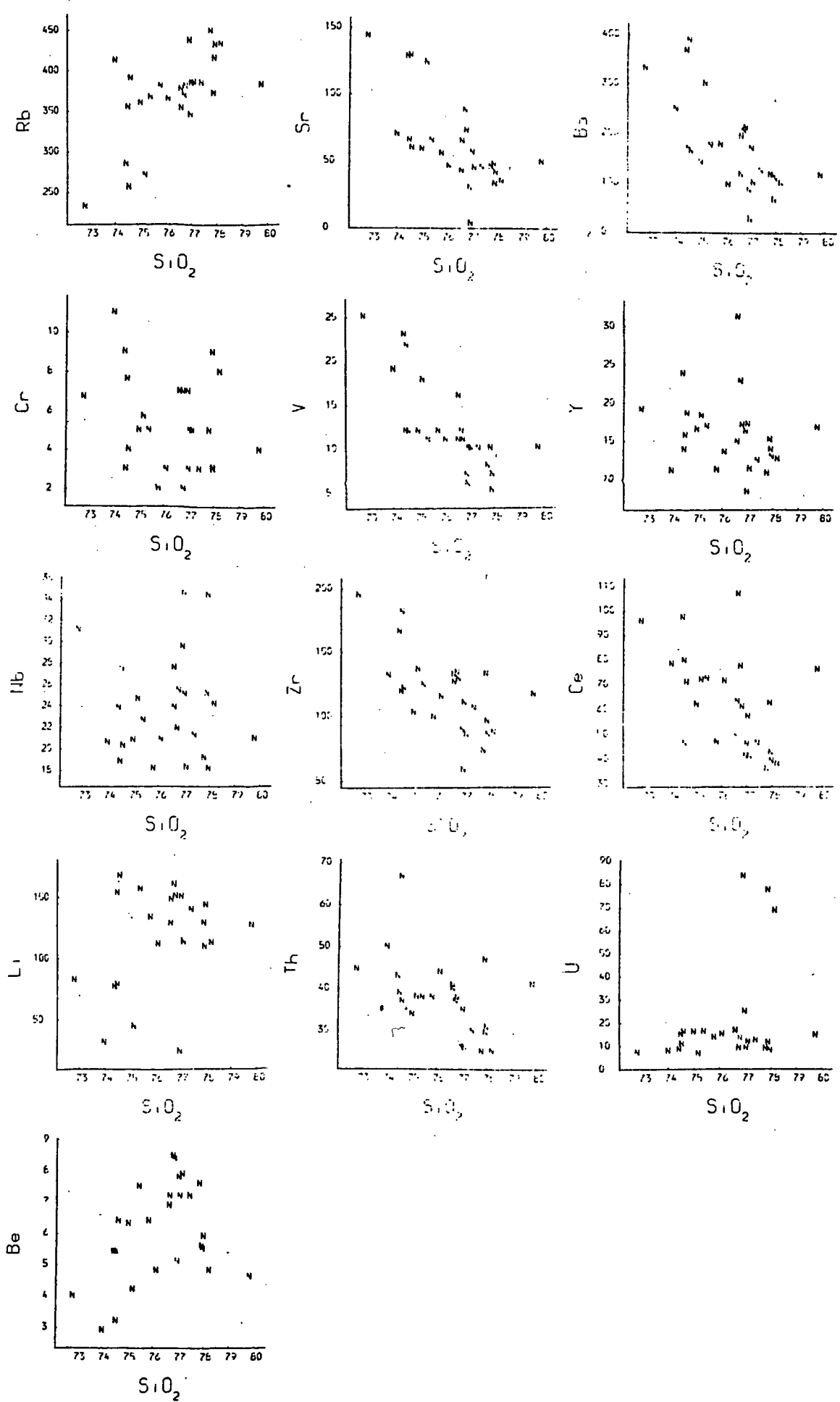


Fig. 6:17. Major and trace element variation diagrams for the Lochnagar complex, key to symbols on fold out sheet.

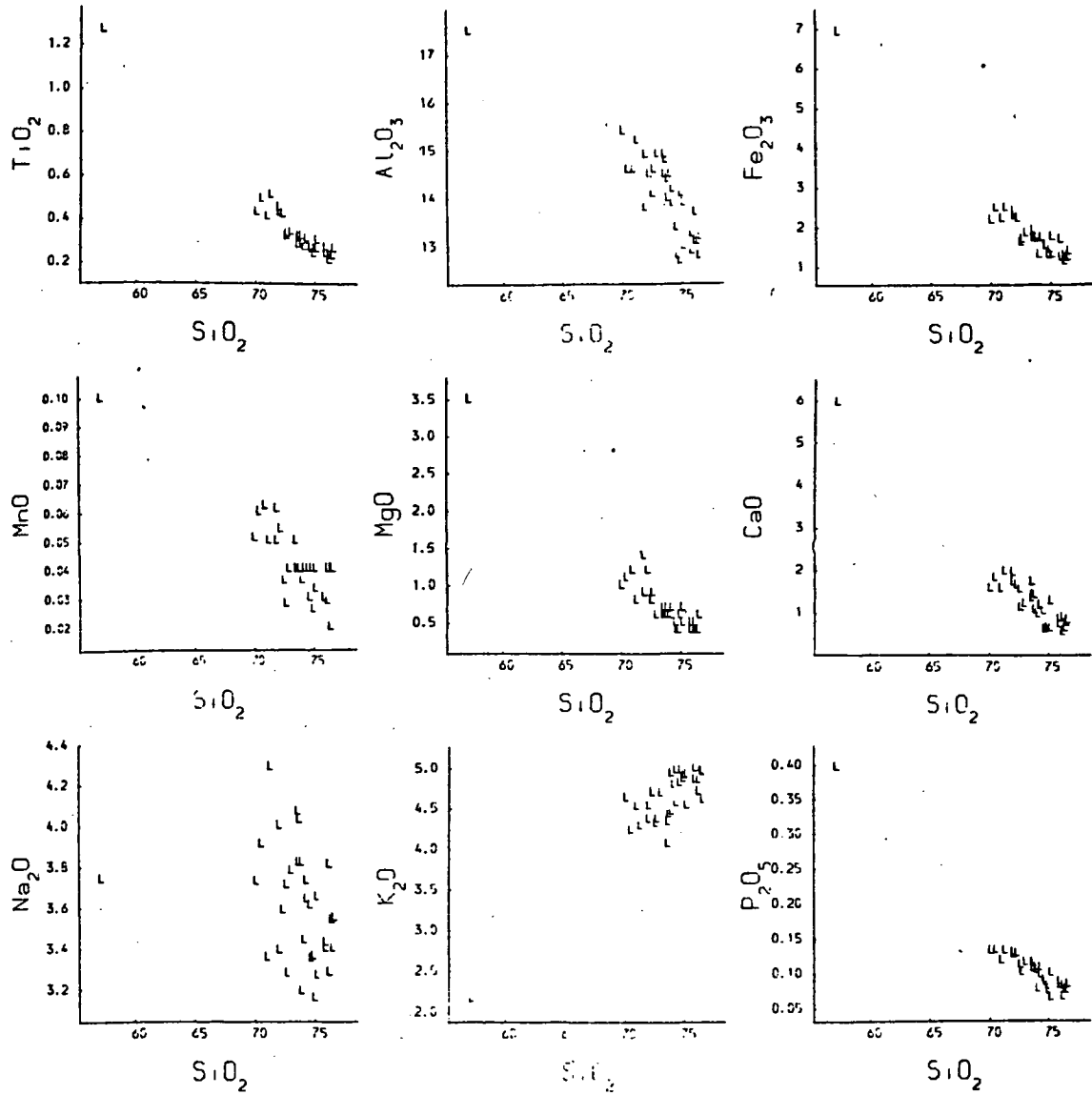
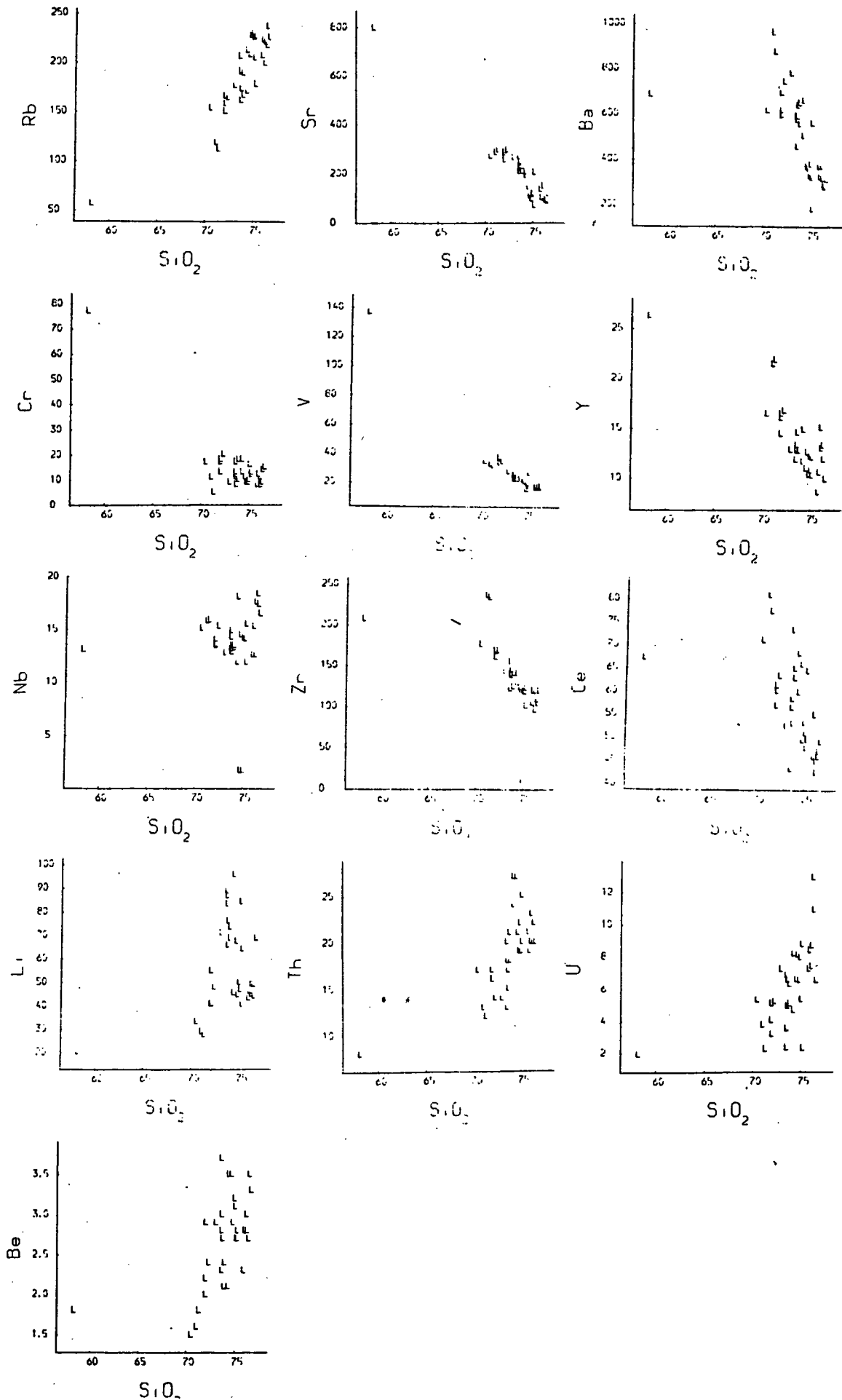


Fig. 6:17. Continued.



26) The Glen Gairn granite (Fig. 6:18).

$\text{SiO}_2$  in the granite ranges from 70 to 78%. Greisen samples have  $\text{SiO}_2$  values both higher and lower than the granite.  $\text{Fe}_2\text{O}_3$ ,  $\text{TiO}_2$ ,  $\text{MgO}$ ,  $\text{Al}_2\text{O}_3$ ,  $\text{CaO}$ ,  $\text{Na}_2\text{O}$  and  $\text{K}_2\text{O}$  appear to decrease with increasing  $\text{SiO}_2$ , but  $\text{MnO}$  remains roughly constant. Ce, Be, Zr, Cr, V, Ba and Sr concentrations decrease with increasing  $\text{SiO}_2$ , but Li, Rb, Nb, Y, U and Th concentrations generally increase with increasing  $\text{SiO}_2$ .

27) The Cairngorm granite (Fig. 6:19).

$\text{SiO}_2$  ranges from 68 to 82% in the Cairngorm granite.  $\text{Fe}_2\text{O}_3$ ,  $\text{MgO}$ ,  $\text{TiO}_2$ ,  $\text{Al}_2\text{O}_3$ ,  $\text{CaO}$  and  $\text{P}_2\text{O}_5$  define negative correlations with  $\text{SiO}_2$ , but  $\text{Na}_2\text{O}$  remains constant.  $\text{MnO}$  decreases with increasing  $\text{SiO}_2$  although there is considerable scatter.  $\text{K}_2\text{O}$  decreases with increasing  $\text{SiO}_2$ , up to 80%  $\text{SiO}_2$ , and decreases in the silica rich samples. Cr, V, Zr, Sr and Ba concentrations decrease with increasing  $\text{SiO}_2$  although some elements show considerable scatter. U, Th, Be, Li, Rb, Nb and Y concentrations generally increase with increasing  $\text{SiO}_2$ , whereas Th shows considerable scatter; U, Be, Li, Rb, Nb and Y concentrations decrease very slightly or remain constant from 70 to 74%  $\text{SiO}_2$  before increasing rapidly from 74 to 78%  $\text{SiO}_2$ .

28) The Comrie complex (Fig. 6:20).

$\text{SiO}_2$  values range from 50 to 74% in the Comrie complex.  $\text{Fe}_2\text{O}_3$ ,  $\text{MnO}$ ,  $\text{TiO}_2$ ,  $\text{MgO}$ ,  $\text{Al}_2\text{O}_3$ ,  $\text{CaO}$  and  $\text{P}_2\text{O}_5$  display negative correlations with  $\text{SiO}_2$ , but  $\text{Na}_2\text{O}$  appears to define three separate correlations with  $\text{SiO}_2$ , two with negative gradients with  $\text{SiO}_2$  from 50 to 70% and one with a positive gradient with  $\text{SiO}_2 > 70\%$ .  $\text{K}_2\text{O}$  increases with increasing  $\text{SiO}_2$ . All the trace elements appear to define three separate trends for the Comrie

Fig. 6:18. Major and trace element variation diagrams for the Glen Gairn granite, key to symbols on fold out sheet.

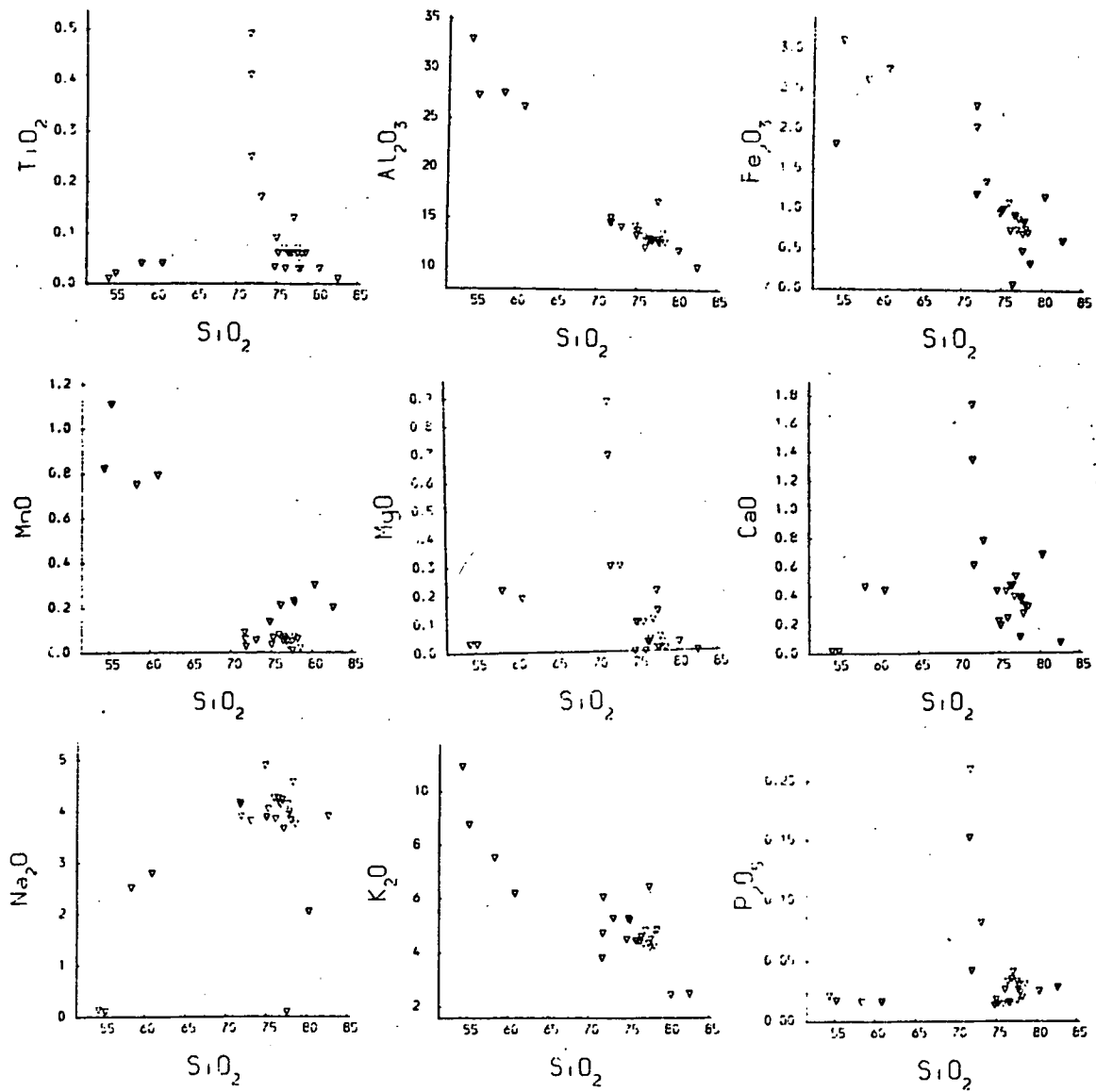


Fig. 6:18. Continued.

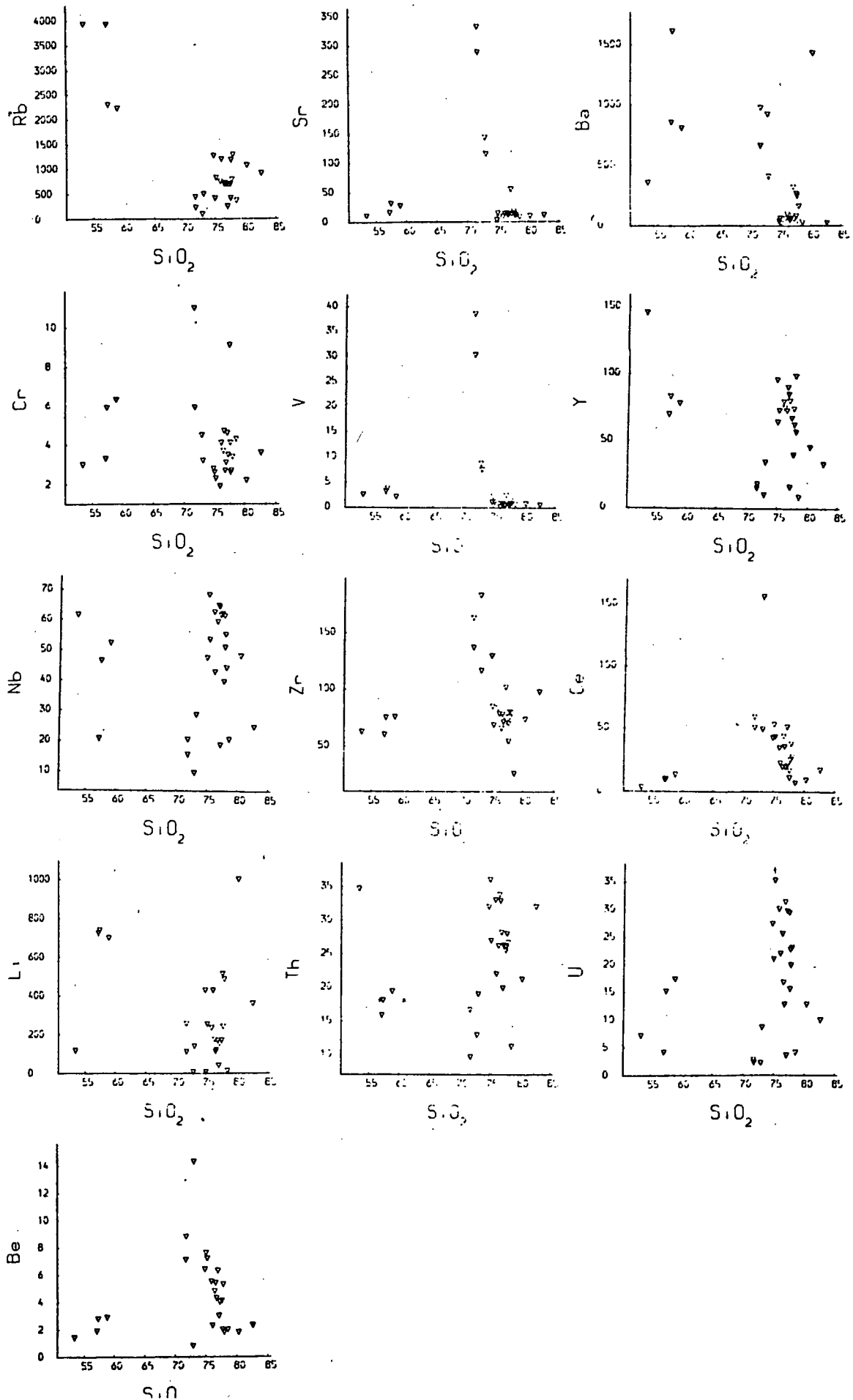


Fig. 6:19. Major and trace element variation diagrams for the Cairngorm granite, key to symbols on fold out sheet.

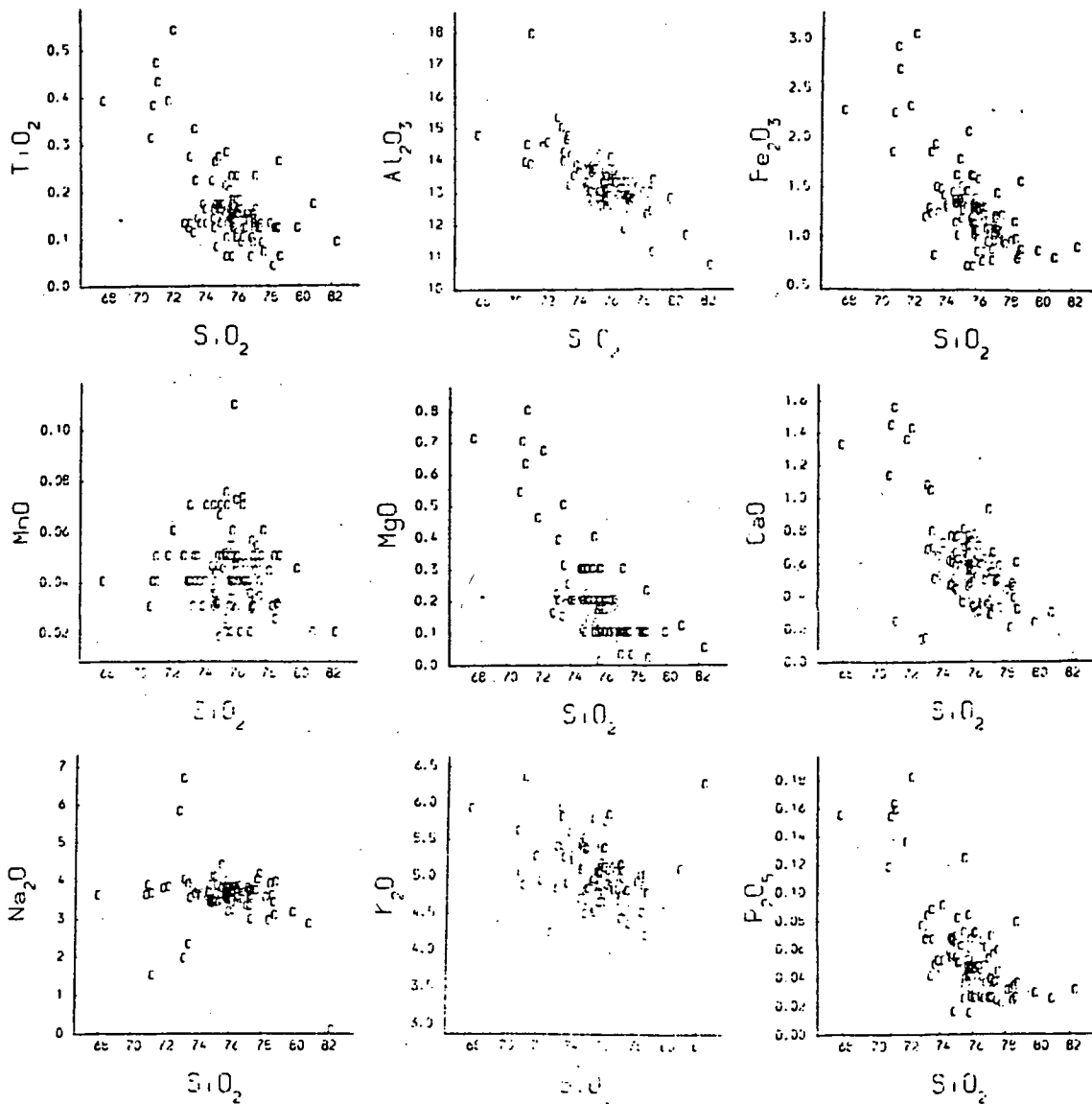


Fig. 6:19. Continued.

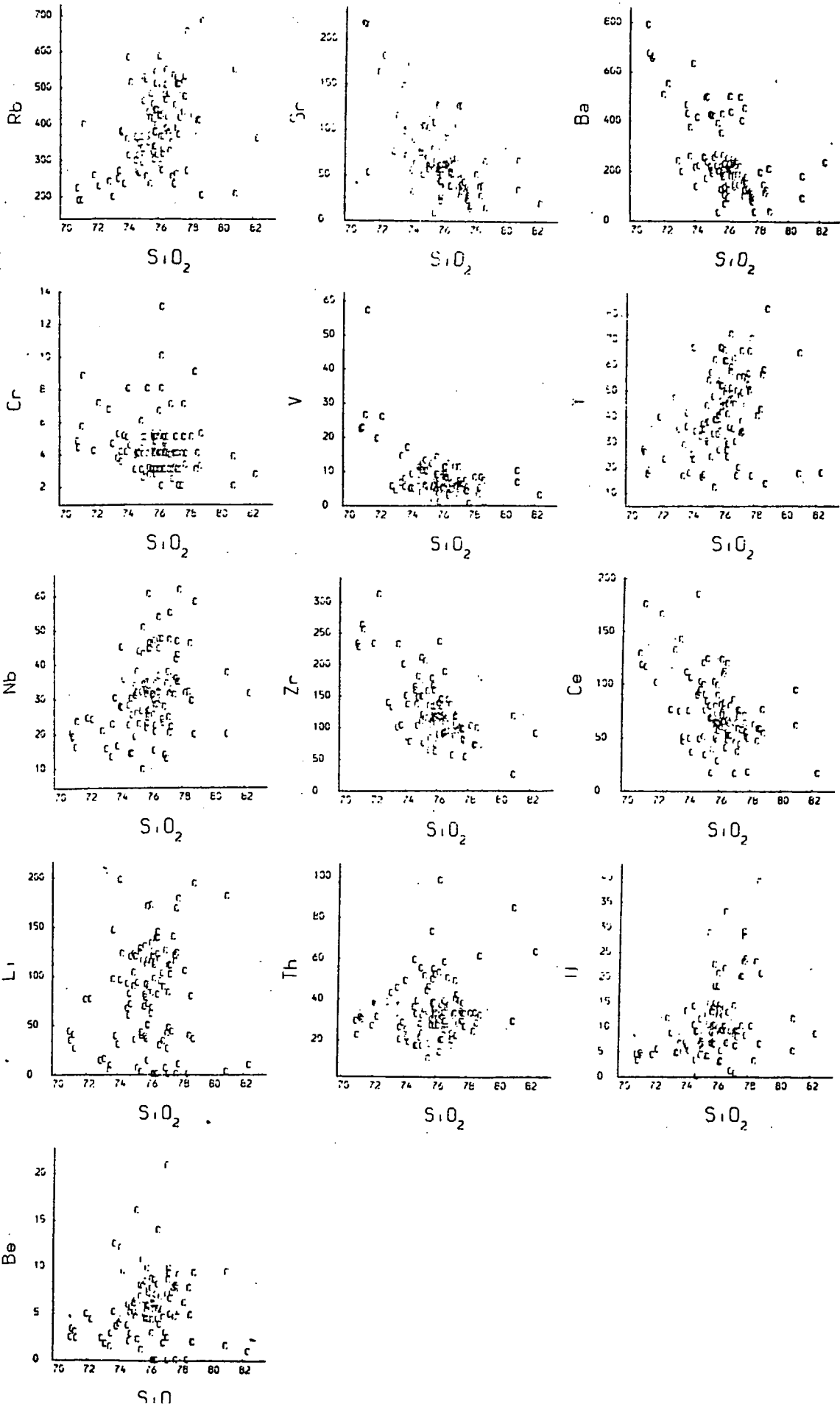


Fig. 6:20. Major and trace element variation diagrams for the Comrie complex, key to symbols on fold out sheet.

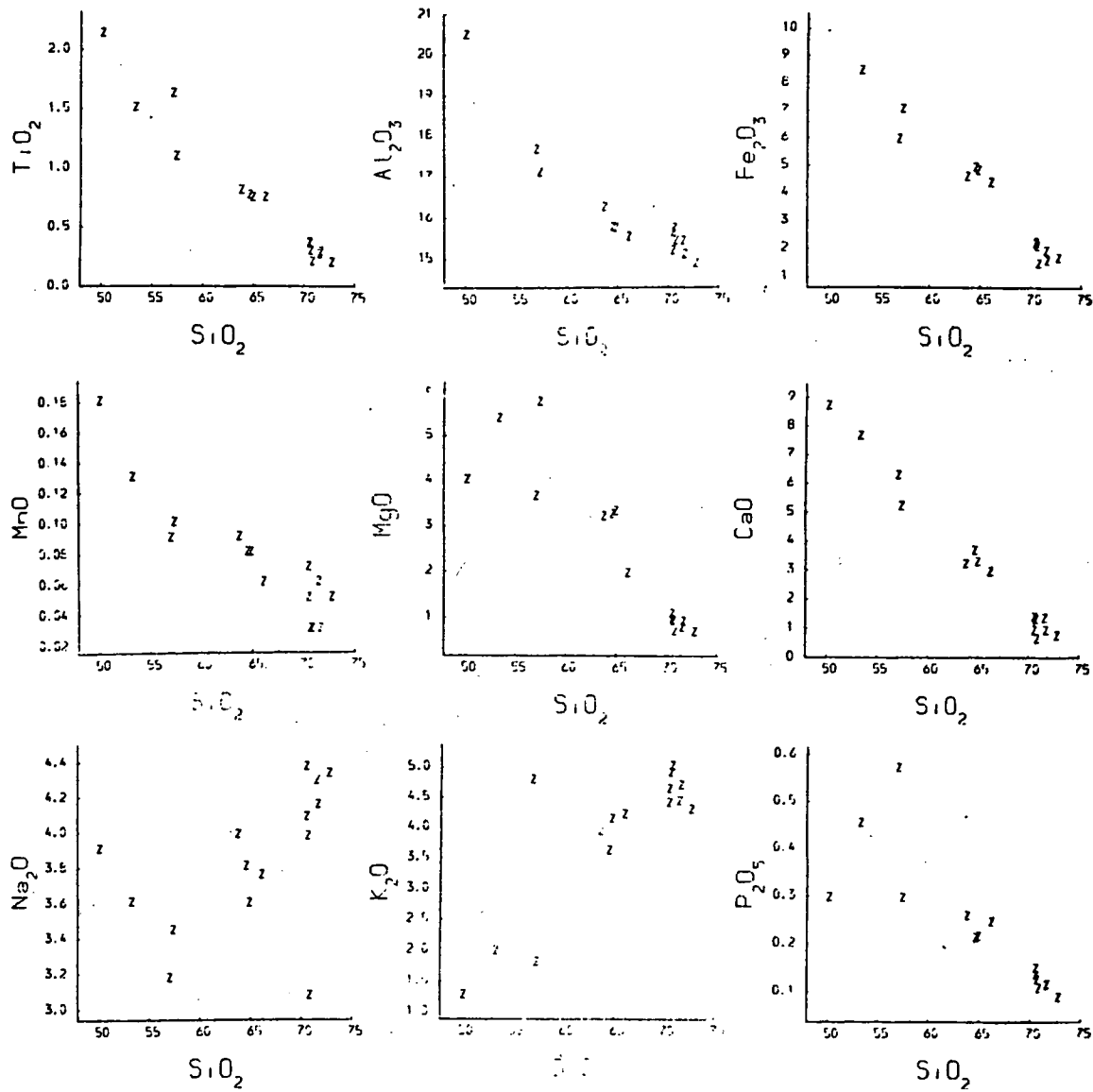
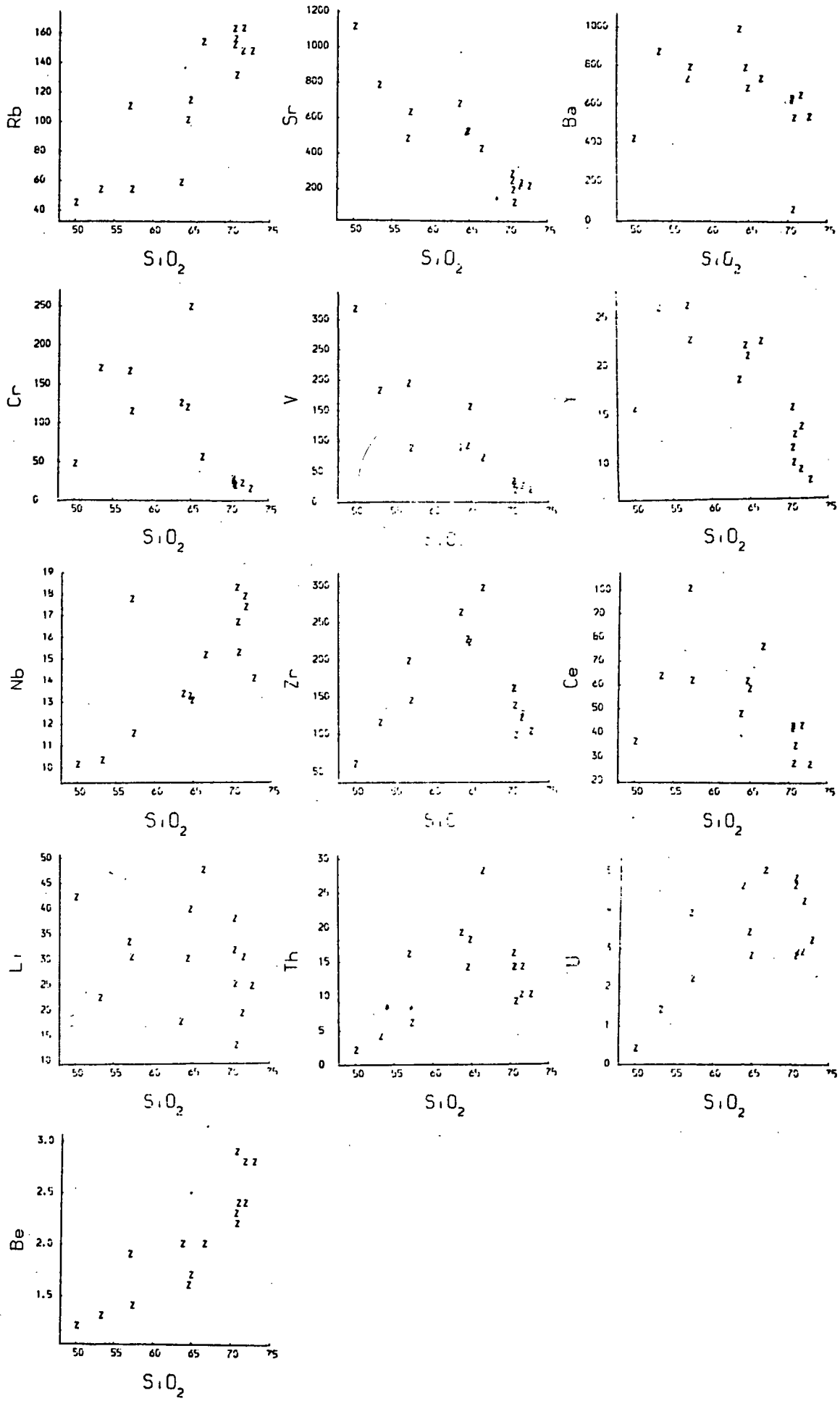


Fig. 6:20. Continued.



complex. Sr and V concentrations correlate negatively with  $\text{SiO}_2$  in all three trends. Ba and Cr concentrations increase with increasing  $\text{SiO}_2$  from 50 to 57%  $\text{SiO}_2$  and correlate negatively with  $\text{SiO}_2$  with two separate trends from 62 to 73%  $\text{SiO}_2$ . Zr, Y and Ce concentrations increase with increasing  $\text{SiO}_2$  for the two trends between 50 and 67%  $\text{SiO}_2$  and decrease with increasing  $\text{SiO}_2$  in the Comrie granite. Nb and Th concentrations increase with increasing  $\text{SiO}_2$  in the two trends from 50 to 67%  $\text{SiO}_2$  and decrease with increasing  $\text{SiO}_2$  in the Comrie granite. Li concentrations decrease with increasing  $\text{SiO}_2$  from 50 to 57% and correlate positively with  $\text{SiO}_2$  in the more silica rich samples. Be, Rb and U define three separate positive correlations with  $\text{SiO}_2$ .

29) The Garabal Hill complex (Fig. 6:21).

$\text{SiO}_2$  values range from 43 to 72% in the Garabal Hill complex, MgO,  $\text{Fe}_2\text{O}_3$ , MnO,  $\text{TiO}_2$  and CaO define negative correlations with  $\text{SiO}_2$ ,  $\text{P}_2\text{O}_5$  decreases generally with  $\text{SiO}_2$  although some samples with low silica define a rather different trend where  $\text{P}_2\text{O}_5$  increases with increasing  $\text{SiO}_2$ .  $\text{Al}_2\text{O}_3$  increases with increasing  $\text{SiO}_2$  between 43 and 57%  $\text{SiO}_2$  and then decreases between  $\text{SiO}_2$  60 and 73%.  $\text{Na}_2\text{O}$  and  $\text{K}_2\text{O}$  increase with increasing  $\text{SiO}_2$ . Sr, Ba, U, Th, Nb, Be and Rb concentrations increase with increasing  $\text{SiO}_2$ , Li, Zr and Ce concentrations increase with increasing  $\text{SiO}_2$  from 43 to 57%  $\text{SiO}_2$  and decrease in the more silica rich samples. Y, Cr and V concentrations decrease with increasing  $\text{SiO}_2$ .

30) The Kilmelford complex (Fig. 6:22).

$\text{SiO}_2$  varies from 50 to 70% in the Kilmelford complex. MgO,  $\text{Fe}_2\text{O}_3$ , MnO,  $\text{TiO}_2$  and CaO define negative correlations with  $\text{SiO}_2$  whereas  $\text{Na}_2\text{O}$ ,  $\text{K}_2\text{O}$  and  $\text{Al}_2\text{O}_3$  increase with increasing  $\text{SiO}_2$  although with considerable scatter.

Fig. 6:21. Major and trace element variation diagrams for the Garabal Hill complex, key to symbols on fold out sheet.

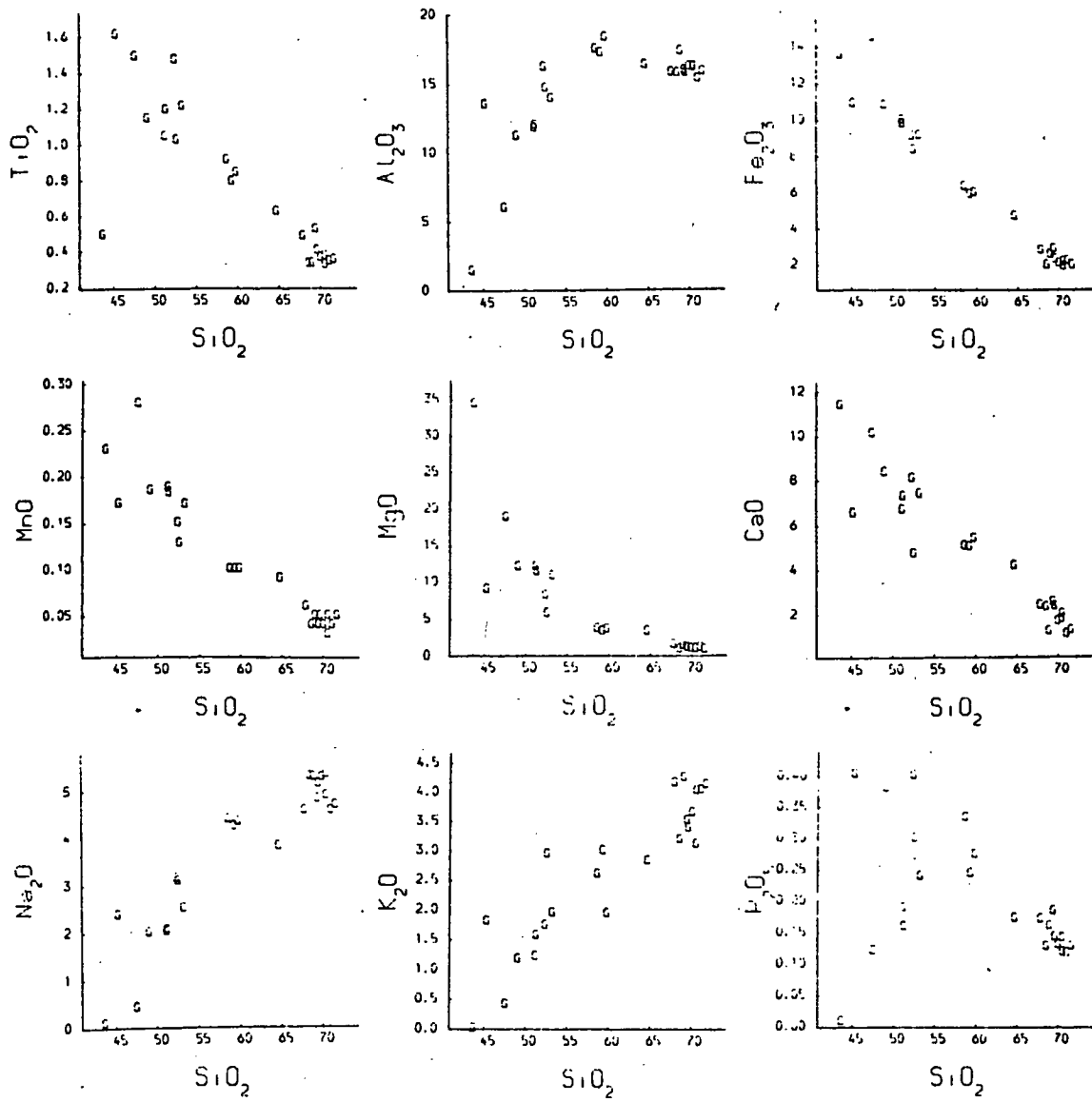


Fig. 6:21. Continued.

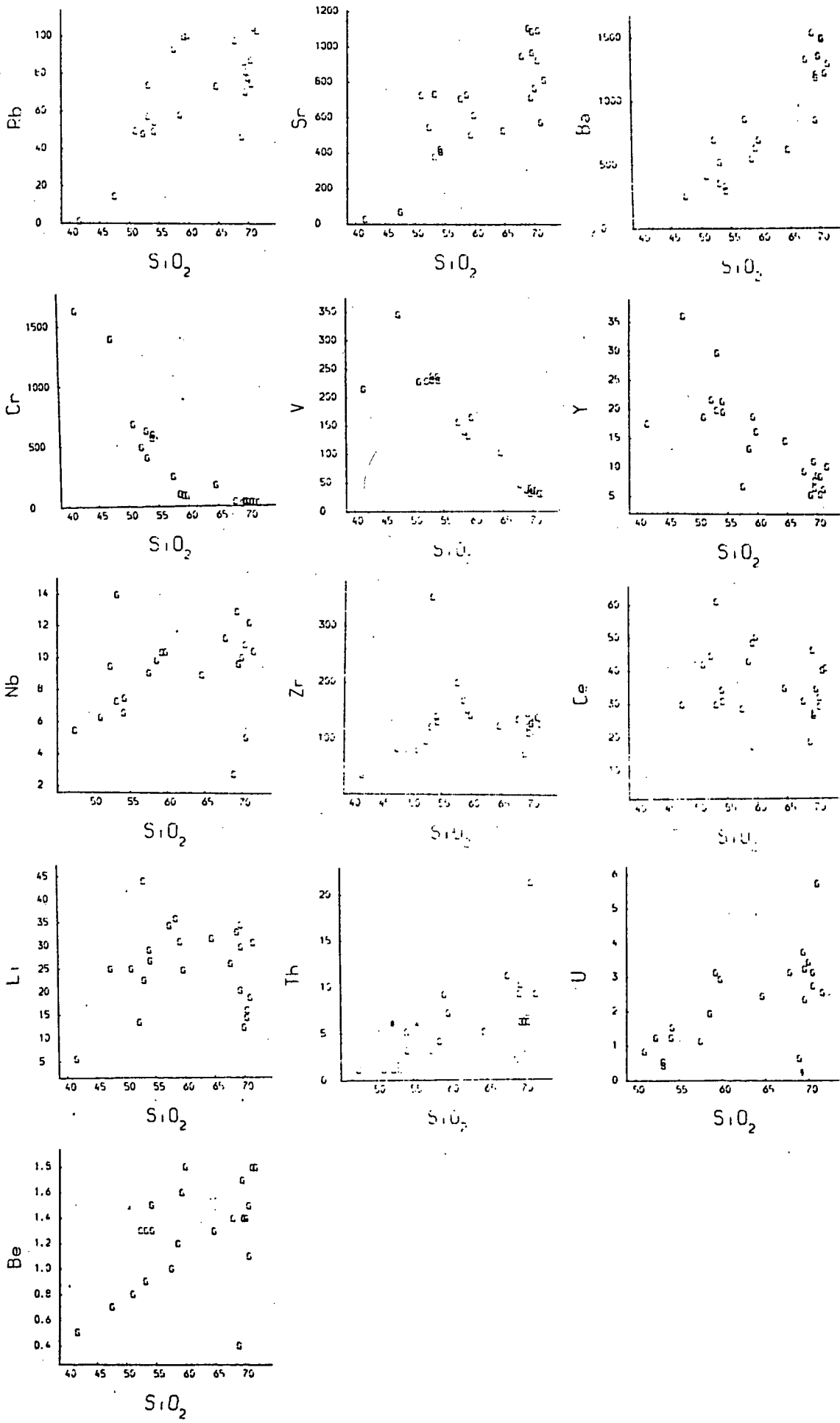


Fig. 6:22. Major and trace element variation diagrams for the Kilmelford complex, key to symbols on fold out sheet.

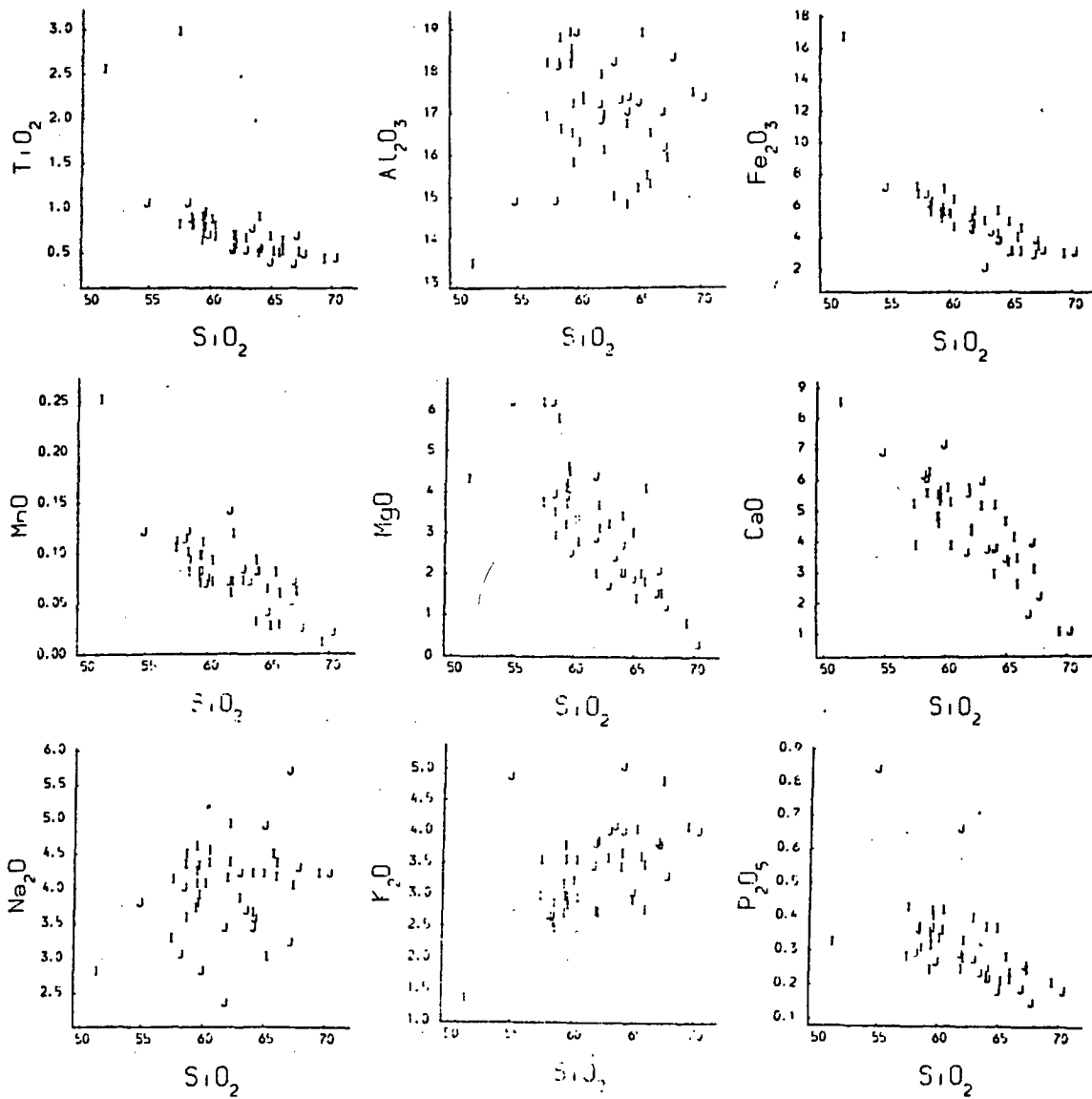
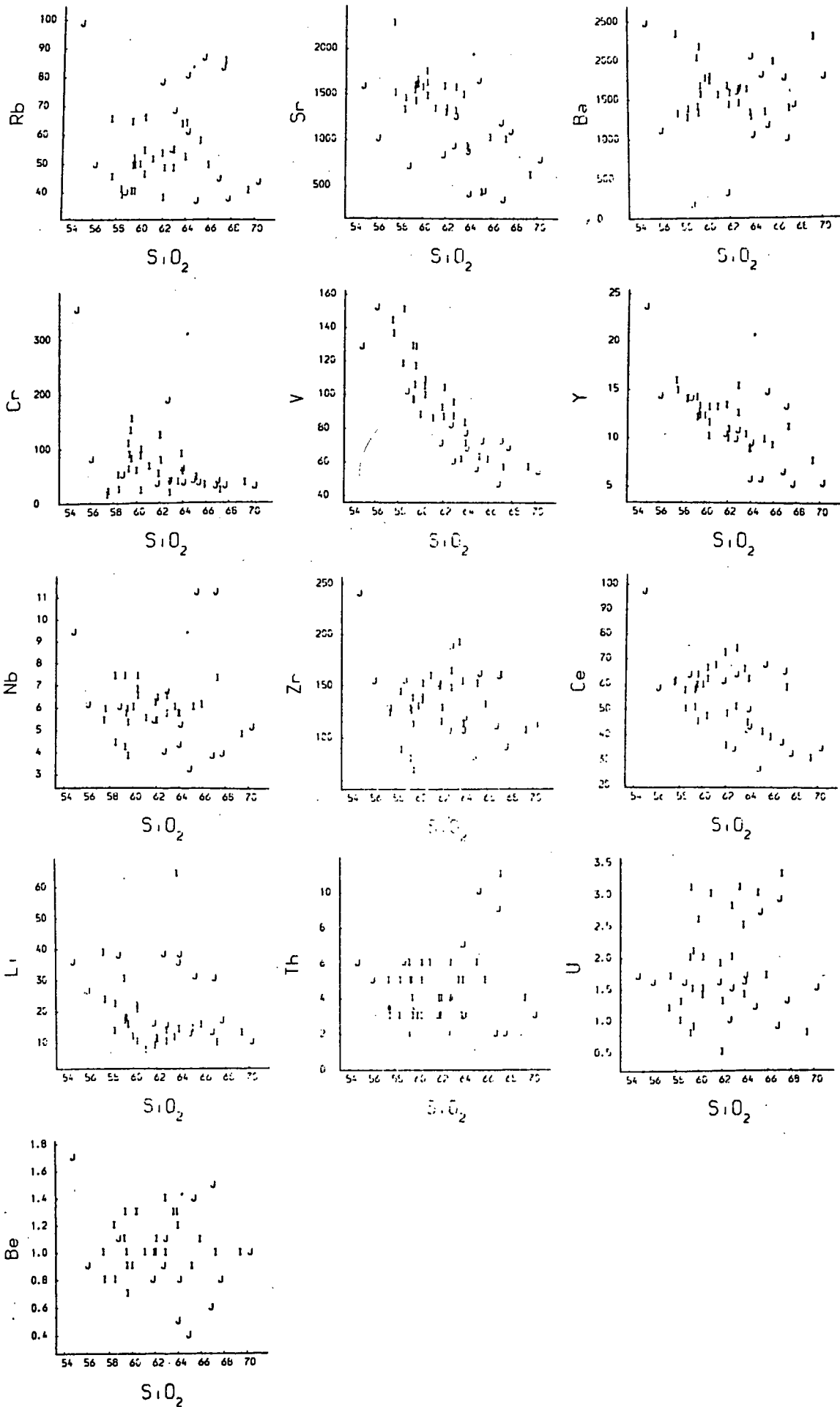


Fig. 6:22. Continued.



Trace elements plotted against  $\text{SiO}_2$  generally show considerable scatter although the general trends can be defined; Ce, Y, Cr, V, Sr, Li, Zr and Nb concentrations decrease generally with increasing  $\text{SiO}_2$ ; U, Th, Be, Ba and Rb concentrations increase generally with increasing  $\text{SiO}_2$ .

31) The Cairnsmore of Fleet granite (Fig. 6:23).

The observed  $\text{SiO}_2$  range is between 71 and 76% in the Cairnsmore of Fleet granite.  $\text{TiO}_2$ , MgO,  $\text{Fe}_2\text{O}_3$  and CaO define negative correlations with  $\text{SiO}_2$ .  $\text{Na}_2\text{O}$ ,  $\text{P}_2\text{O}_5$  and MnO remain roughly constant between 71 and 74%  $\text{SiO}_2$ , then increasing in the silica rich samples.  $\text{Al}_2\text{O}_3$  does not obviously correlate with  $\text{SiO}_2$ ,  $\text{K}_2\text{O}$  increases over the range  $\text{SiO}_2$  71 to 74%, with lower  $\text{K}_2\text{O}$  in the most silica rich sample. Sr, Ba, Th, Ce, Y, Zr and V concentrations decrease with increasing  $\text{SiO}_2$ ; Li, Rb, Nb and U concentrations increase with increasing  $\text{SiO}_2$ , Be concentrations are generally constant with one sample having extremely high levels of Be.

### 6:3. GEOCHEMICAL MODELLING.

Detailed numerical modelling of the geochemistry of granites has highlighted certain problems which render the study of acid magmas in the plutonic environment more problematic than their extrusive equivalents. Crystallization within acid (viscous) melts is unlikely to produce any clear division between true cumulates and liquids. Thus granitoid rocks are probably best described as crystal "mushes" comprising various proportions of "cumulus" minerals surrounded by the crystalline products of the interstitial melt (McCarthy & Groves 1979). The proportions of "cumulus" and "intercumulus" minerals are difficult to determine by modal analysis because subsolidus reactions may ultimately determine final

Fig. 6:23. Major and trace element variation diagrams for the Cairnsmore of Fleet granite, key to symbols on fold out sheet.

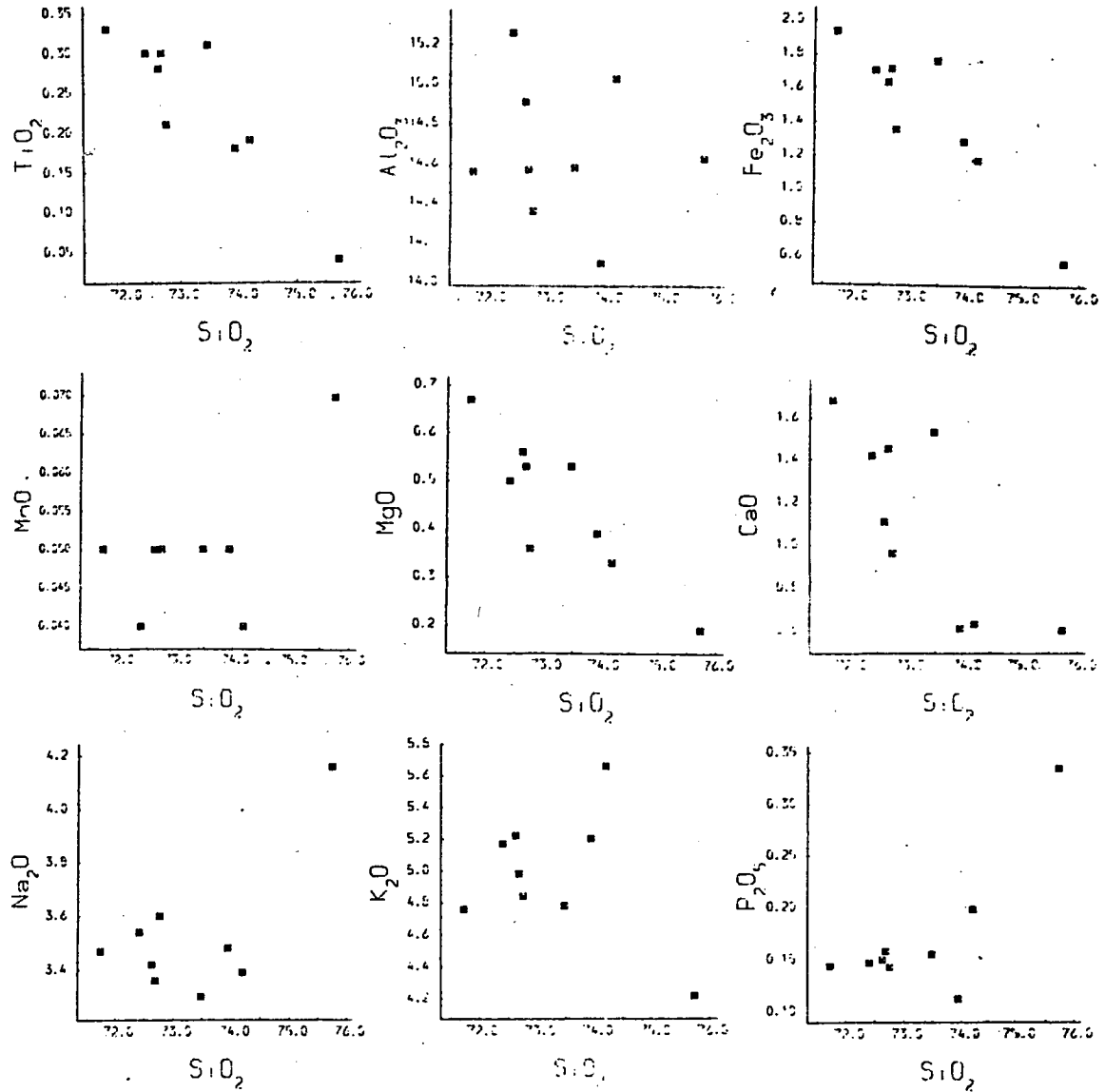
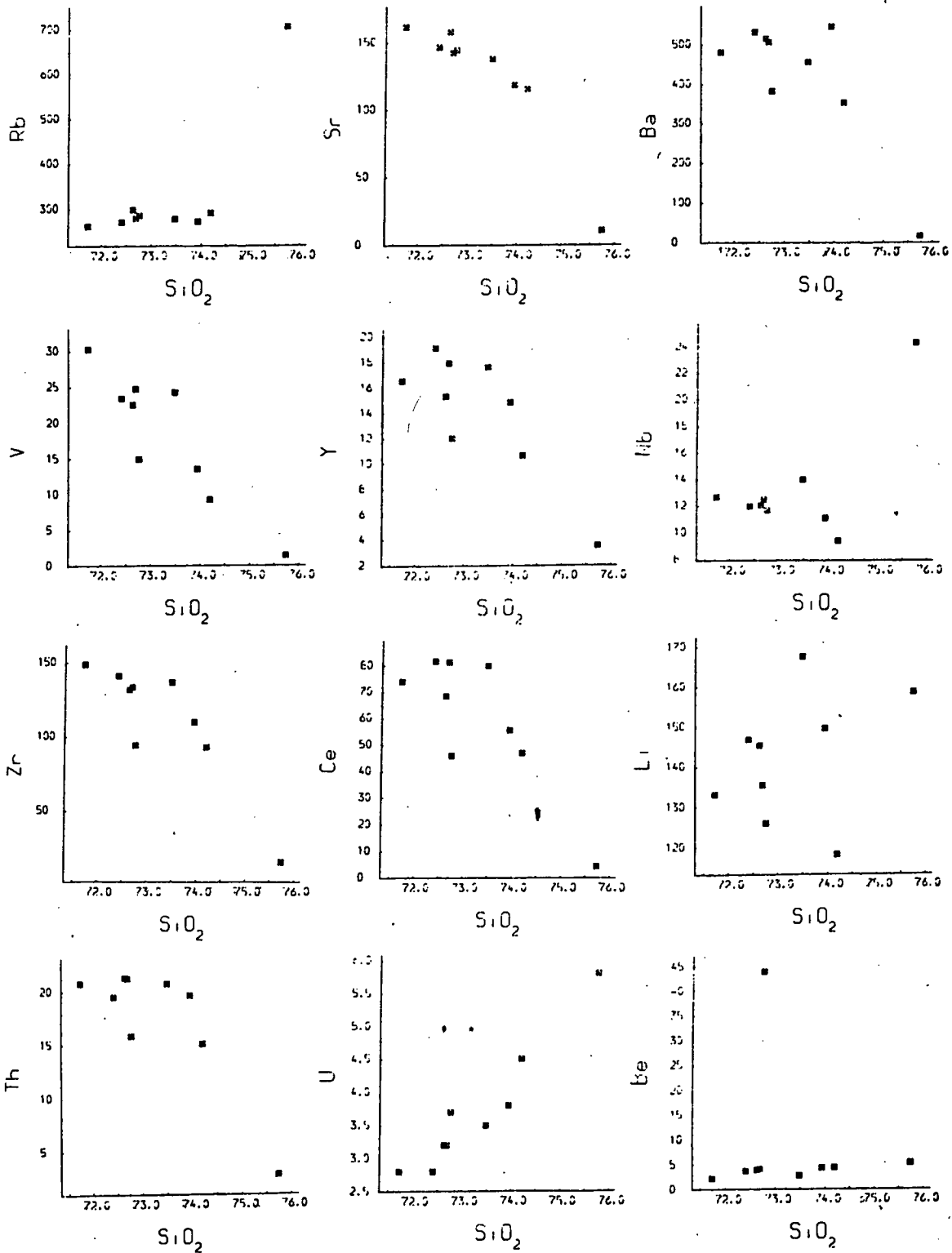


Fig. 6:23. Continued.



textures. However textural evidence as described in Chapter 3 indicates which minerals may be regarded as "cumulus".

The type of crystallization which takes place in the plutonic environment is disputed, and may lie somewhere between the extremes of equilibrium crystallization (where the whole of each solid phase remains in equilibrium with the melt) and perfect or Rayleigh fractional crystallization (where only the surface of the crystal remains in equilibrium with the melt). As diffusion rates are temperature dependant, generally increasing with increasing temperature, and granitic melts are generally low temperature, slow diffusion will tend to favour Rayleigh fractional crystallisation. However as diffusion is also dependent on ionic charge and ionic radius (Magaritz & Hofmann 1978), each element may behave slightly differently in the spectrum between Rayleigh and equilibrium crystallisation.

Any model is only as good as the trace element distribution coefficients used. Mineral-melt distribution coefficients are dependent on temperature and melt composition (e.g. Watson 1976), and ideally should be continuously varied. Additionally high concentrations of halogen-rich residual magmatic fluids may add further complications during the final stages of crystallization (Hanson 1978).

Many trace element concentrations are controlled by minor and accessory phases such as zircon, apatite, sphene, allanite and more rarely monazite and xenotime (Dodge & Mays 1972, Condie 1978, McCarthy & Kable 1978). These minor phases are difficult to incorporate into petrogenetic models because of their low abundance and poorly determined distribution

coefficients. The net result of this is that there is no trace element which behaves perfectly incompatibly (i.e. has a bulk distribution coefficient = 0) over the whole range of compositions observed in the Caledonian granites (this is probably true of most granites), thus rendering the trace element characteristics of the magma source or variations in melt proportion at source less accessible than in simpler systems such as mid-ocean ridge basalt.

For intrusions where subsolidus mineralization resulting from water rock interaction is observed, both major and trace element modelling may be misleading. Therefore care must be taken to assess the extent of mobilization of each element before attempting any form of petrogenetic modelling. Trace element mobility in the mineralization plutons is discussed in Chapter 5.

#### 6:3:1 MAJOR ELEMENT MODELLING.

Major element trends for many of the Caledonian granites can be modelled using a petrological mixing model based on Bryan et al. (1969) using the equation;

$$\text{"parent magma"} = \text{liquidus crystals} + \text{residual liquid}$$

However this equation is based on the assumption that the compositions represent liquids and this is probably not so in the majority of cases discussed here. Another interpretation of this equation would be

composition A = composition B + "cumulus mineral assemblage"

where composition A is less geochemically evolved than composition B.

In this case neither composition is necessarily a liquid, and an indication of the proportion of various "cumulus" minerals may be ascertained in this way. The results of this method of modelling are summarized in Table 6:2, this is however only a summary of the results of major element modelling based on a very large number of small compositional steps calculated by least squared method where the sum of the residuals is less than 0.1. Only plutons with a large compositional range are treated in this fashion; those intrusions with small compositional ranges or small sample suites will not give meaningful results. The mineral compositions used are based on energy dispersive microprobe analyses from the respective plutons, with the exception of plagioclase where the model required more calcic plagioclase compositions than were recorded from microprobe analyses, although the range of samples covered by microprobe analysis is incomplete and does not cover the range of whole rock compositions adequately for each intrusion. In order to minimise errors in the major element modelling, mean compositions along the observed trends were taken at 2 or 2.5% SiO<sub>2</sub> intervals, these values were used for modelling and where compositional gaps were encountered trends, were extrapolated.

TABLE 6:2. MEAN CUMULUS MINERAL ASSEMBLAGES CALCULATED USING MAJOR ELEMENT MODELLING. WHERE THE CUMULUS ASSEMBLAGE VARIES SIGNIFICANTLY TWO ASSEMBLAGES ARE RECORDED WITH THE SiO<sub>2</sub> RANGE FOR EACH ASSEMBLAGE.

	gt	cpx	hbl	bt	mt	il	plag	kspar	qtz	ap	sphn	SiO <sub>2</sub> range
Carrock Fell	15				18		65			1		
Skiddaw				27			46	16	11			
Eskdale	9			15			56	20				
Rogart			23	19	1		56			1		
Cluanie			7		1		68	18	5	1		
Strontian			31	16	1		46		4	1	1	52.5-62.5
			5	3			39	26	27			62.5-75.0
Ballaculish			16	22	2		59			1		
Ben Nevis			21	16	1		50	10		2		65.0-70.0
				16	1		52	5	25	1		70.0-75.0
Etive			43	20			31			5	1	65.0-67.5
			1	11	2		46	19	20	1		67.5-80.0
Moor of Rannoch			16	18	1		65					57.5-65.0
			2	6	1		39	26	26			65.0-75.0
Foyers			1	26	4		67			1	1	52.5-75.0
							31	31	38			75.0-80.0
Aberdeen				17			37	19	26	1		
Bennachie				28			44	15	12	1		
Mt. Battock				13			34	29	24			
Cromar				1	1		31	34	33			
Lochnagar			6	18	2		63	2	6	1	2	
Glen Gairn				6			35	35	23	1		
Cairngorm				5			32	33	29	1		
Comrie	2	25	17	1			52			1	2	50.0-70.0
				13	2		35	32	12	3	3	70.0-75.0
Garabal Hill	41	21	12				26					45.0-55.0
		31	18	1			49			.5	.5	55.5-67.5
			13	1			52	16	16	2		67.5-75.0
Kilmelford	65			24	9					2		50.0-57.5
	18		14	4			63			1		57.5-70.0

The results shown in Table 6:2 fit the general variation observed from petrographic studies. An exception is the Foyers complex where more hornblende involvement would be expected on the basis of petrography. However the observed trace element variations (Fig. 6:11) indicate at least three overlapping geochemical trends in the Foyers complex and it would therefore appear that a mean major element trend for this intrusion has no meaning. With this exception, the major element modelling therefore provides in most cases a geologically reasonable background for trace element modelling.

### 6:3:2. TRACE ELEMENT MODELLING.

The behaviour of trace elements in the Caledonian granites is generally more complex than the observed behaviour of major elements. Many of the trends expressed in Harker type diagrams are complex with the behaviour of elements such as Zr, Ce, Y, Nb, Li, Ba, Sr and Be implying large changes in the bulk distribution coefficient as different phases begin or cease to be a part of fractionating assemblages. Of the trace elements discussed Zr, Ce, Nb, Th, U and Be are probably controlled by minor phases and are therefore difficult to incorporate into the quantitative trace element models as the amounts of these phases are generally difficult to quantify and they have poorly defined distribution coefficients. The behaviour of Li is also difficult to assess in that there are few mineral/melt distribution coefficients published for this element, and all of these are less than 1 (Nagasawa & Schnetzler 1971, Henderson 1982). Thus although this element should behave incompatibly, this is not always so, and Li appears to behave compatibly in some more mafic intrusions such as Kilmelford (Fig. 6:22) and the Moor of Rannoch granodiorite (Fig. 6:10), and in some geochemically evolved plutons such as Bennachie (Fig. 6:16) and Hill of Fare (Fig. 6:15). In the less geochemically evolved plutons Li is probably substituting for Mg in pyroxenes and amphiboles, but in the more evolved plutons Li may be affected by late stage volatile expulsion; for instance the high levels of Li in the Glen Gairn greisens may result from this process. Variation in bulk distribution coefficients for Ba, Sr and Y are generally related to variations in the proportions of potassium feldspar, plagioclase and hornblende in the fractionating assemblage respectively, and therefore can be modelled quantitatively.

It is not practical, in the space available, to model in detail the trace element variations for all the Caledonian granitoids, therefore an attempt will be made to model quantitatively a representative selection of the studied plutons and the rest of the plutons are discussed in more general terms. The LIL elements Ba, Rb and Sr are most commonly used in trace element modelling of granitoids (Tindle & Pearce 1981, McCarthy 1978, McCarthy & Hasty 1976, McCarthy & Robb 1978, McCarthy & Fripp 1980, Robb 1983, Arth 1976) - these elements characterise the involvement of feldspars and biotite in fractional crystallization. This type of model may be extended to include Y as the behaviour of this element is dominantly controlled by hornblende or pyroxene during fractional crystallization, although distribution coefficients for Y are also substantially greater than 1 in garnet, apatite and zircon assuming distribution coefficients derived for Ho or Er are accepted as comparable to the behaviour of Y (Henderson 1982, Arth 1976). The role of garnet in fractional crystallization for most of the suites studied is negligible, the exception being the Eskdale complex, and the affects of apatite or zircon on Y concentrations will be small in comparison with that of hornblende since in percentage terms these minerals have a minor affect on the bulk distribution coefficient for Y.

It is unfortunate that the LIL elements most commonly used in magmatic modelling are very mobile in the aqueous environment, therefore problems may occur in attempting to model granites which have suffered metasomatism e.g. Skiddaw and Eskdale in particular. However it is demonstrated in Chapter 5 that although some samples indicate that the LIL elements have been mobile particularly in the greisens, the overall trends for these elements as plotted against immobile HFS elements such as Ti are probably of magmatic origin.

The detailed magmatic models included in the following sections of this chapter are based on the Rayleigh fractional crystallization equation.

$$C_l(i)/C_o(i) = F^{(D_i-1)}$$

Where  $C_o(i)$  = the concentration of element  $i$  in the original melt.

$C_l(i)$  = the concentration of element  $i$  in the residual melt.

$F$  = the weight fraction of melt remaining.

$D_i$  = the bulk distribution coefficient for element  $i$ .

( $D_i = \sum K_i^a \cdot X_a$  where  $K_i^a$  = distribution coefficient for element  $i$  in phase  $a$ ;  $X_a$  = weight fraction of phase  $a$ ).

The Rayleigh fractional crystallization model is used since this appears to be a better approximation of the trace element behaviour observed in the Caledonian granitoids than equilibrium crystallization. In general the fractional crystallization model used follows that described by McCarthy & Hasty (1976) where a cumulus trend is calculated defining cumulate compositions in equilibrium with the liquids produced by in-situ fractional crystallization, as shown by Tindle & Pearce (1981) for the Loch Doon pluton. The only exception to this is the model for the Carrock Fell granophyre where petrography indicates this to be of near liquid composition (Chapter 3). Also the bulk distribution coefficients used in these models were calculated on the basis that the most evolved composition represents the stage where crystallization is almost complete (i.e.  $F = 0.1$ ); this provides a minimum bulk distribution coefficient for the trend where  $D_i > 1$  and a maximum bulk distribution coefficient where  $D_i < 1$ . Distribution coefficients used in trace element modelling are shown in Table 6:3. Mineral/matrix distribution coefficients with a

value of less than 1 do not significantly affect the bulk distribution coefficient and have been assumed to approximate to zero.

method continued on page 127a.

---

TABLE 6:3. MINERAL/MELT DISTRIBUTION COEFFICIENTS USED IN MAGMATIC MODELS.

	Plag	Kfeld	Biot	Hbl	Cpx	Gt
Sr	4.4(1)	3.87(1)				
Ba		6.12(1)	6.4(3)			
Rb			3.3(3)			
Ho(&Y)				12(1)	2.25(2)	43(4)

(1) Arth 1976

(2) Nagasawa & Schnetzler 1971

(3) Gill 1978

(4) Henderson 1982

---

#### 6:3:2:i THE LAKE DISTRICT.

##### 1) The Skiddaw granite.

LIL element variations for the Skiddaw granite can be modelled, despite the extensive metasomatism affecting this intrusion, because the LIL elements appear to correlate with  $TiO_2$  (immobile during metasomatism) (c.f. Fig. 5:14) implying only limited redistribution of LIL elements during metasomatism; there is however a large degree of uncertainty in modelling metasomatized intrusions using LIL elements. There appear to be two fractional crystallization assemblages in the Skiddaw granite (Fig. 6:24) the early assemblage calculated on the basis of the method set out above of a maximum of 26% biotite with a minimum of 30% plagioclase and the second assemblage of a maximum of 27% biotite with a minimum of 43% plagioclase and 8% potassium feldspar. The low totals for both assemblages imply that the calculated bulk distribution coefficients with  $D_i > 1$  are too low and for elements with  $D_i < 1$  are too high, suggesting

The Raleigh fractional crystallization equation is used here to provide constraints on the crystallizing mineral assemblages. For each trend considered (which may represent a section of a trend i.e. in Fig. 6:31 for Lochnagar the trend l3 to l4) the most evolved sample is assumed to represent the point where crystallization is nearly complete (i.e.  $F=0.1$ ). Thus  $C_1$  and  $C_0$  are fixed points and  $D_i$  for Sr, Ba, Rb and Y are calculated assuming  $F$  is equal to 0.1 using the equation in the form

$$\frac{\log C_1 - \log C_0}{\log F} = D_i - 1$$

The mineral proportions quoted are then derived using the bulk distribution coefficients calculated on the basis of the above equation assuming  $F$  is equal to 0.1 and the following equations with mineral/melt distribution coefficients from Table 6:3. The minerals used in these calculations were chosen on the basis of petrographic observations using only minerals which are observed to be present.

For example.

$$D_{Rb} = (X_{biot} \times 3.3) + (X_{hbl} \times 0.0) + (X_{plag} \times 0.0) + (X_{kfeld} \times 0.0)$$

$$D_{Rb} = X_{biot} \times 3.3$$

$$X_{biot} = \frac{D_{Rb}}{3.3} \quad \text{where } D_{Rb} - 1 = \frac{\log C_1 - \log C_0}{\log F}$$

similarly

$$D_{Ba} = (X_{kfeld} \times 6.12) + (X_{biot} \times 6.4) + (X_{hbl} \times 0.0) + (X_{plag} \times 0.0)$$

$$D_{Ba} = (X_{kfeld} \times 6.12) + (X_{biot} \times 6.4)$$

and

$$D_{Sr} = (X_{plag} \times 4.4) + (X_{kfeld} \times 3.87) + (X_{hbl} \times 0.0) + (X_{biot} \times 0.0)$$

$$D_{Sr} = (X_{plag} \times 4.4) + (X_{kfeld} \times 3.87)$$

and

$$D_Y = (X_{hbl} \times 12) + (X_{plag} \times 0.0) + (X_{kfeld} \times 0.0) + (X_{biot} \times 0.0)$$

$$D_Y = X_{hbl} \times 12 \quad (\text{if garnet and clinopyroxene are not part of the observed mineral assemblage}).$$

Ideally  $X_{biot} + X_{hbl} + X_{plag} + X_{kfeld} = 1.0$

However it is clear in all cases that

$$X_{biot} + X_{plag} + X_{kfeld} + X_{hbl} \neq 1.0$$

For example in the case of Lochnagar

for trend 1 (L1 to L2)

$$X_{biot} = 0.27, X_{plag} = 0.31, X_{kfeld} = 0.0, X_{hbl} = 0.09 \quad \Sigma = 0.67$$

for trend 2 (L3 to L4)

$$X_{biot} = 0.27, X_{plag} = 0.27, X_{kfeld} = 0.0, X_{hbl} = 0.1 \quad \Sigma = 0.64$$

for trend 3 (L5 to L6)

$$X_{biot} = 0.29, X_{plag} = 0.32, X_{kfeld} = 0.0, X_{hbl} = 0.06 \quad \Sigma = 0.67$$

The low totals for the derived assemblages cannot just be a function of rounding error in the equations used and implies that either the initial assumption that  $F$  is equal to 0.1 is not correct, or that minerals which have mineral/melt distribution coefficients for all elements used is equal to 0 (such as quartz) are involved in fractional crystallization.

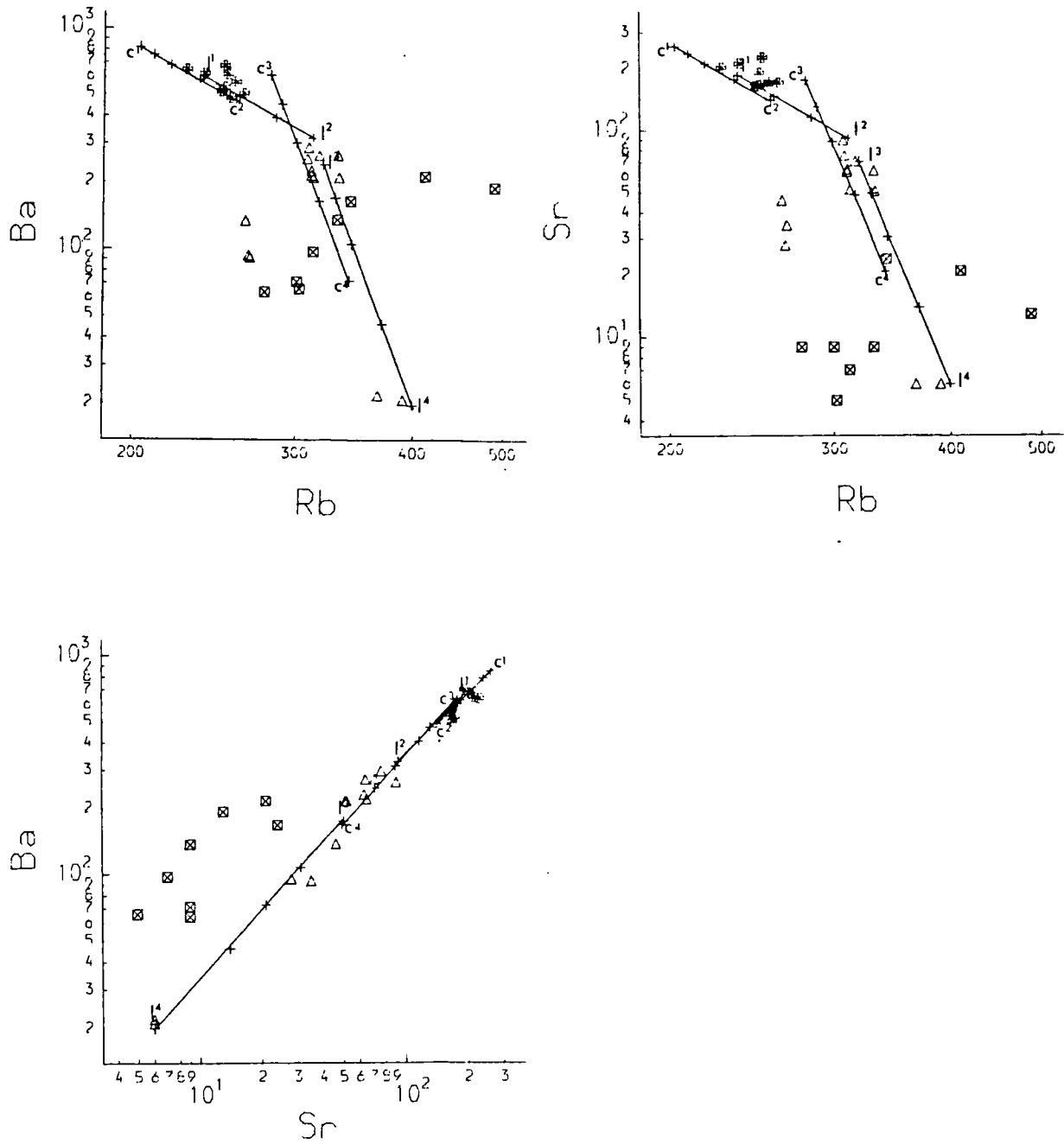
If  $F$  does not equal 0.1 and is indeed greater than 0.1 then for elements with  $D_i$  greater than 1.0 the calculated  $D_i$  on the basis that  $F$  is equal to 0.1 represents a minimum value for  $D_i$ , implying that the derived proportions of minerals will represent minimum percentages in the crystallization assemblage.

If  $F$  does not equal 0.1, and is indeed greater than 0.1 then for elements with  $D_i$  greater than 1.0 the calculated  $D_i$  on the basis that  $F$  is equal to 0.1 represents a maximum value for  $D_i$ , implying that the derived proportions of minerals will represent maximum percentages in the crystallization assemblage.

Another result of the use of a low value for  $F$  is that the biotite factor calculated is a maximum value. This has implications for the calculated potassium feldspar component from the Ba equation which is often calculated to have a small negative value. If  $F$  is greater than 0.1 the biotite factor is smaller, because  $D_{i_{Rb}}$  is always less than 1, which will allow for a small positive potassium feldspar component from the Ba equation.

Therefore the mineral proportions quoted represent maximum or minimum percentages and not necessarily precise percentages of the fractionating assemblage. Although they place constraints on the mineral assemblages involved in fractional crystallization, they are not intended as accurate assessments of the proportions of minerals removed during fractionation. Despite these limitations the modelling does allow estimation of the phases involved in granite genesis, and of the relative importance of different phases during the formation of the different granite bodies. The modelling carried out here is also dependent on the mineral/melt distribution coefficients used, obviously for a complex diorite-granodiorite-granite intrusion such as Lochnagar several sets of mineral/melt distribution coefficients should be used.

Fig. 6:24. Modelled LIL element variation diagrams for the Skiddaw intrusion,  $l^1$ - $l^4$  represent modelled liquid compositions,  $c^1$ - $c^4$  represent modelled cumulate compositions, key to symbols on fold out sheet.

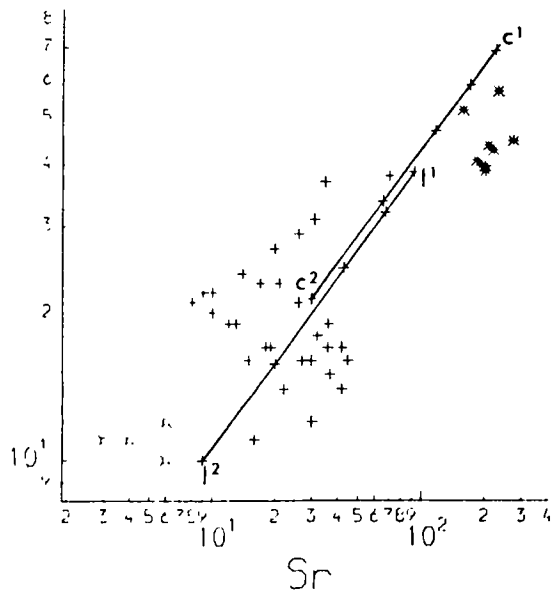
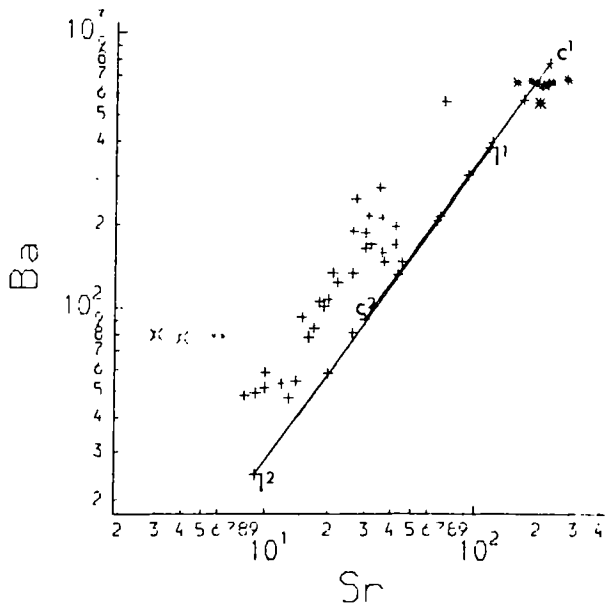
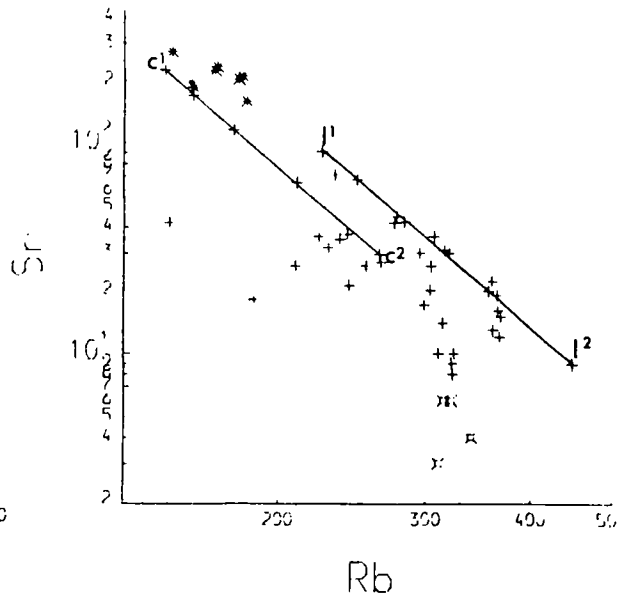
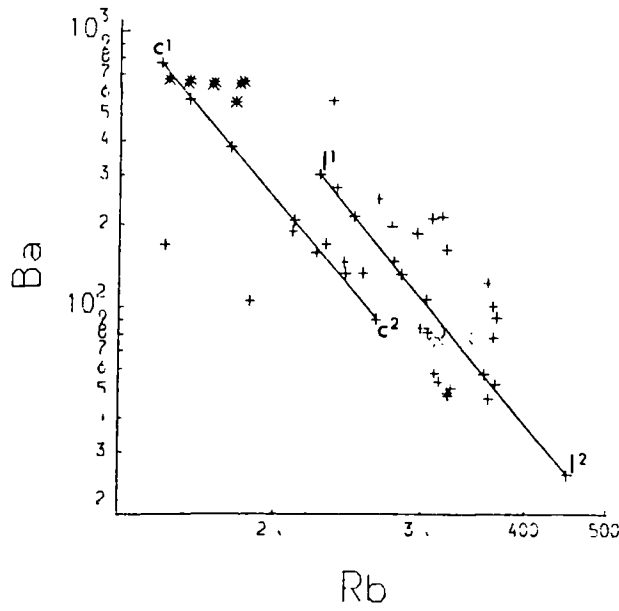


that either fractional crystallization processes did not proceed to completion, or minerals such as quartz which have bulk distribution coefficients of 0 for all elements discussed are involved in fractional crystallization. From the previous section and Fig. 6:1, it is apparent that Cr, V, Li, Ce, Th and Zr are being removed from the melt during fractional crystallization. Cr and V have very large distribution coefficients for biotite of 19 (Henderson 1982) and 50 (Gill 1978) respectively, thus the behaviour of these elements can be explained by the biotite in the modelled fractionating assemblage. Ce, Th and Zr are almost certainly controlled by minor phases, in this case monazite (Ce, Th) and zircon.

## 2) The Eskdale intrusion.

LIL element variations for the Eskdale granite can also be modelled despite the extensive metasomatism affecting this intrusion for the same reasons as for the Skiddaw intrusion, there does not appear to be any significant change in the fractionating assemblage over the range in compositions (Fig. 6:25) with an assemblage calculated on the basis of the method set out above of a maximum of 20% biotite, with a minimum of 4% garnet, 15% potassium feldspar, 35% plagioclase. The low total for this assemblage implies that the calculated bulk distribution coefficients for elements with  $D_i > 1$  are too low and for elements with  $D_i < 1$  are too high, implying that either fractional crystallization processes did not proceed to completion, or minerals such as quartz which have bulk distribution coefficients of 0 for all elements discussed are involved in fractional crystallization. From the previous section and Fig. 6:2, it is apparent that Cr, V, Nb, Zr, Ce and Th are being removed from the melt during fractional crystallization. Cr and V are removed in

Fig. 6:25. Modelled LIL element variation diagrams for the Eskdale intrusion,  $l^1$  and  $l^2$  represent modelled liquid compositions,  $c^1$  and  $c^2$  represent modelled cumulate compositions, key to symbols on fold out sheet.

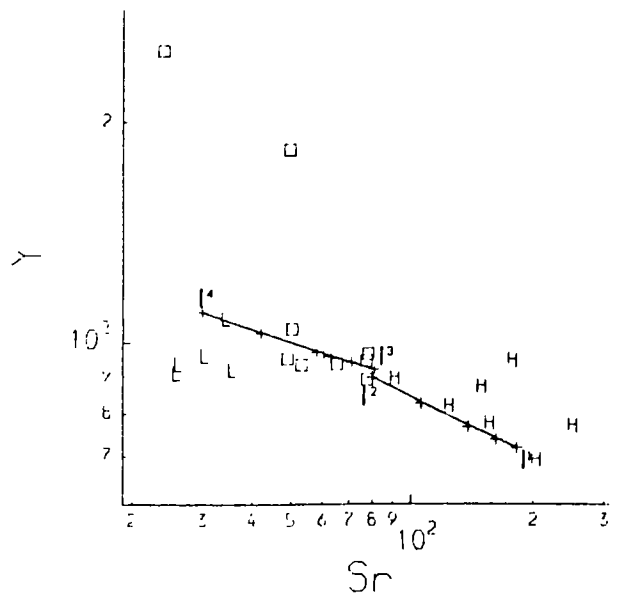
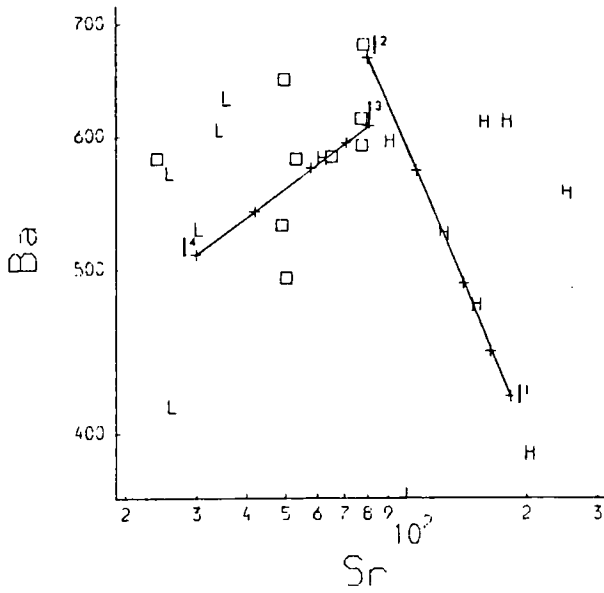
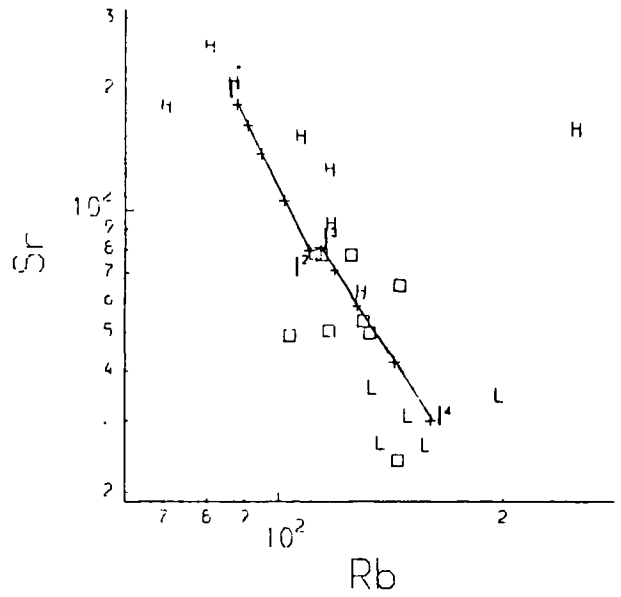
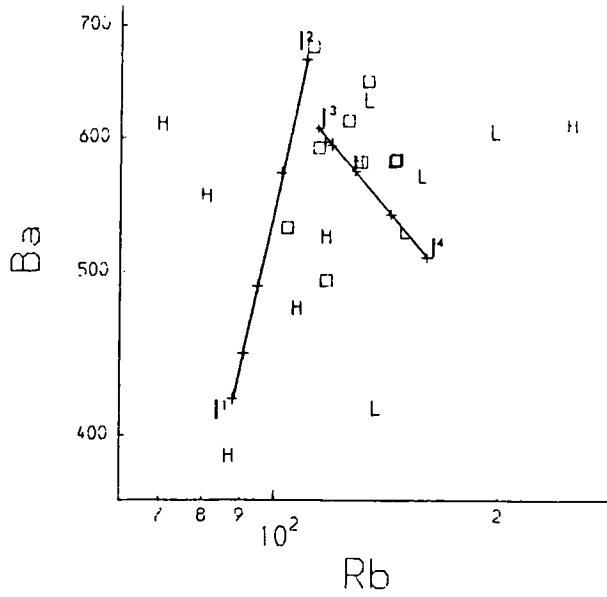


biotite; Nb, Zr, Ce and Th are probably controlled by minor phases, in this case monazite (Ce, Th), sphene (Nb) and zircon.

### 3) The Carrock Fell complex.

The Carrock Fell gabbro is not modelled in this thesis, however the Carrock Fell granophyre and hybrid suite are of interest. LIL element variations for this complex can be modelled, and trends for this intrusion indicate a significant change in the fractionating mineral assemblage (Fig. 6:26) with two mineral assemblages calculated on the basis of the previously defined method of firstly a maximum of 27% biotite, and 40% clinopyroxene with a minimum of 32% plagioclase; followed by a maximum of 25% biotite, and 41% clinopyroxene with a minimum of 28% plagioclase, and 6% potassium feldspar. However there are problems with this model in that biotite is not observed in this complex. If therefore we then recalculate this model on the basis that  $D_{Rb} = 0$ , which would be more correct, we have an assemblage of firstly 63% plagioclase, 23% clinopyroxene; and secondly 21% clinopyroxene, 12% potassium feldspar, 67% plagioclase. If magnetite which has  $D = 0$  for all elements discussed here is considered to form a substantial component of the first crystallization assemblage then this is very similar to the assemblage derived by major element modelling. For this intrusion only the modelled liquid trends are included as the low levels of Cr and V, together with textural observations from Chapter 3, imply that the cumulates that would be in equilibrium with the observed liquid compositions must have been effectively separated during fractional crystallization. From the previous section and Fig. 6:3 the only other elements which behave compatibly in this complex are Li and Zr, in the granophyre with  $SiO_2 > 73\%$ ; Li as noted earlier is probably being removed

Fig. 6:26. Modelled LIL element variation diagrams for the Carrock Fell granophyre and ferrogabbros, 1<sup>1</sup>-1<sup>4</sup> represent modelled liquid compositions, key to symbols on fold out sheet.



in pyroxenes, and zircon becomes part of the liquidus mineral assemblage in the high silica granophyres.

4) The Ennerdale granophyre.

Since the observed compositional range for the Ennerdale granophyre is very small no quantitative modelling has been attempted. In general however the low levels of Cr and V (Fig. 6:4) indicate that pyroxene, which is present in small amounts, has been removed from the magma. Both Ce and Y also appear to be behaving compatibly although there is no obvious explanation for this.

5) The Threlkeld microgranite.

No quantitative modelling has been attempted for this intrusion, and levels of LIL elements are suspect due to the intense low temperature alteration suffered by this intrusion. There are no significant variations in the trace elements observed (Fig. 6:4). However this intrusion is characterized by high levels of Cr and V, indicating that the magma was not highly evolved geochemically.

6) The Shap granite.

No quantitative modelling is attempted for this intrusion because of the small sample suite and the geoghemical effects of metasomatism. The high levels of Ba and Sr (Fig. 6:4) are thought to be primary and along with the high levels of Cr and V indicate the low degree of fractional crystallization in the genesis of this intrusion.

## 6:3:2:ii. THE SCOTTISH CALEDONIAN GRANITOIDS.

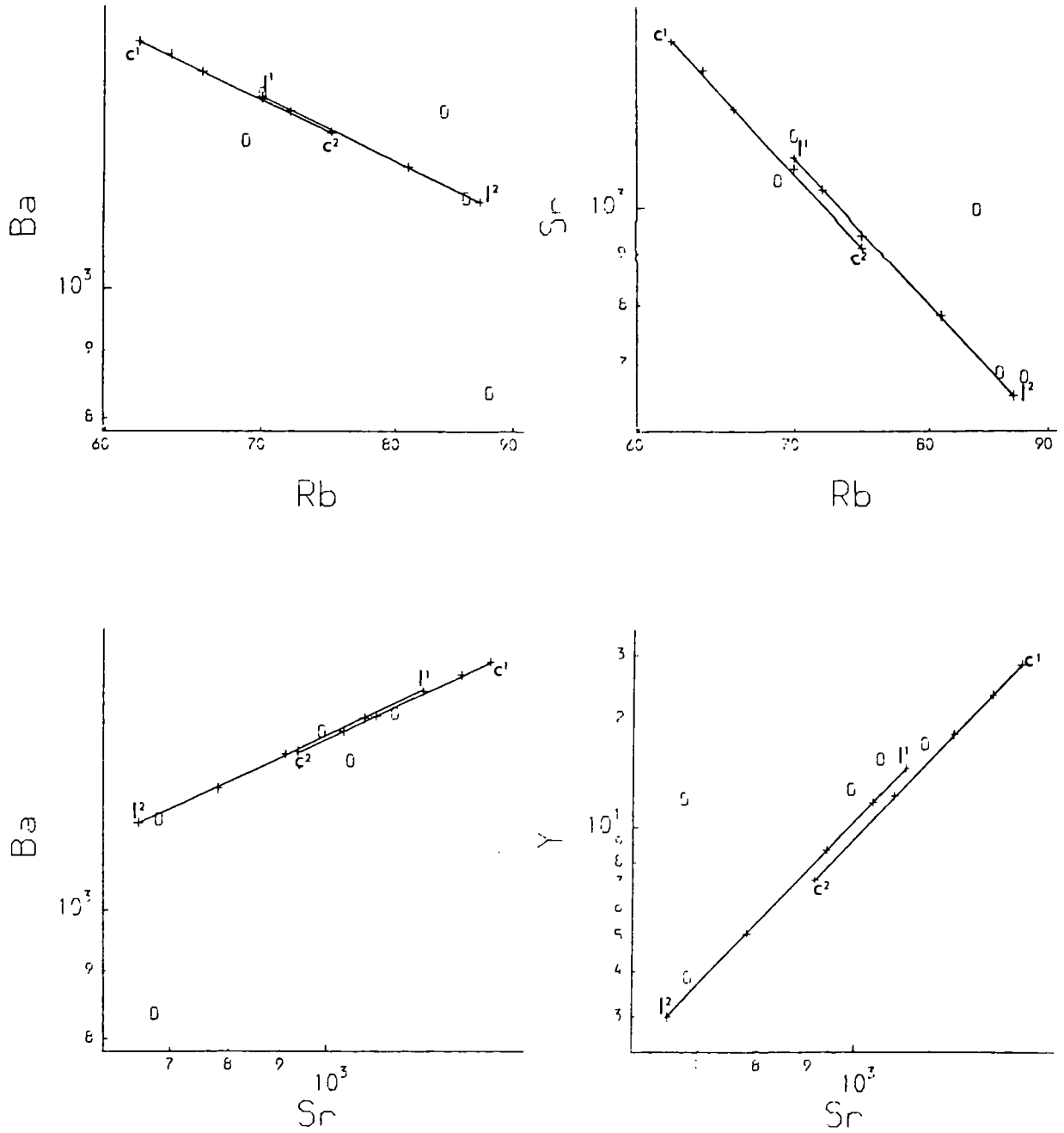
## 1) The Helmsdale granite.

No quantitative modelling is attempted for this intrusion due to the considerable scatter in the data for this intrusion (Fig. 6:5) as a result of mineralization. In general however the compatible behaviour of Sr and Ba indicate plagioclase and potassium feldspar as part of the fractionating assemblage. The compatible behaviour of Y indicates hornblende fractionation and the compatible behaviour of Cr and V could be the result of hornblende or biotite in the crystallizing assemblage. Also Nb, Zr and Ce behave compatibly indicating sphene or ilmenite (Nb), zircon (Zr) and probably allanite (Ce) in the crystallizing assemblage; allanite is thought to be the main cause of light rare earth depletion with increasing  $\text{SiO}_2$ , based on the presence of hornblende as these two minerals are generally found together; monazite is generally restricted to biotite granites.

## 2) The Rogart intrusion.

LIL element and Y variations for the Rogart intrusions can be modelled with some uncertainty due to the small number of samples. Again there does not appear to be any significant change in the fractionating assemblage over the range of compositions (Fig. 6:27) with an assemblage calculated on the basis of the previously defined method of a maximum of 27% biotite, with a minimum of 15% hornblende, and 29% plagioclase. The low total for this assemblage implies that the bulk distribution coefficients calculated on this basis are too low for elements with bulk distribution coefficient  $>1$  and too high for elements with  $D_i < 1$ , implying that either fractional crystallization processes did not proceed to

Fig. 6:27. Modelled LIL element variation diagrams for the Rogart intrusion,  $l^1$  and  $l^2$  represent modelled liquid compositions,  $c^1$  and  $c^2$  represent modelled cumulate compositions, key to symbols on fold out sheet.



completion or that minerals such as quartz which has a bulk distribution coefficient of 0 for all elements discussed are involved in fractional crystallization. It is apparent from Fig. 6:6 that Cr, V, Nb, Zr, Ce and Li are being removed from the melt during fractional crystallization. Distribution coefficients for V and Cr in hornblende and biotite are  $>1$ ; for V 32 and 50 (Gill 1978) respectively and for Cr in biotite 19 (Henderson 1982) with no published data for hornblende; thus the behaviour of these elements can be explained by the calculated assemblage. The behaviour of Li may also be related to hornblende fractionation. Nb, Zr and Ce are probably being controlled by minor phases, in this case sphene or ilmenite (Nb), allanite (Ce) and zircon.

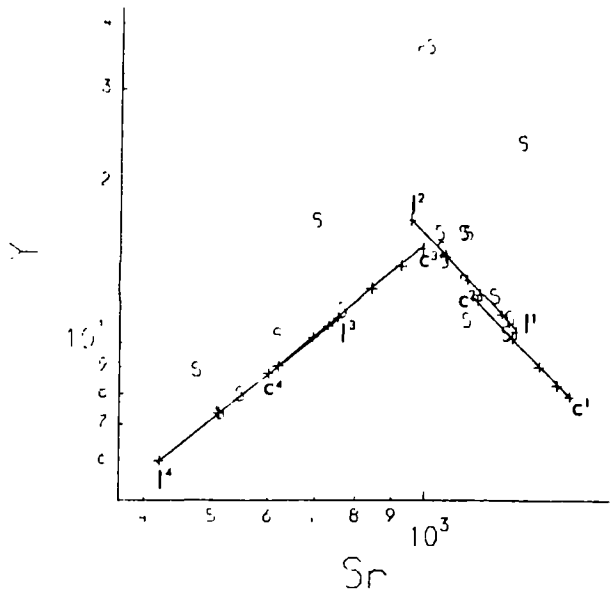
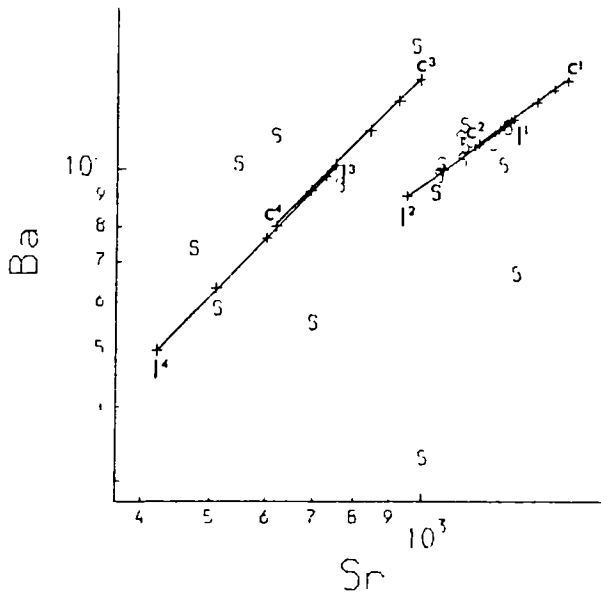
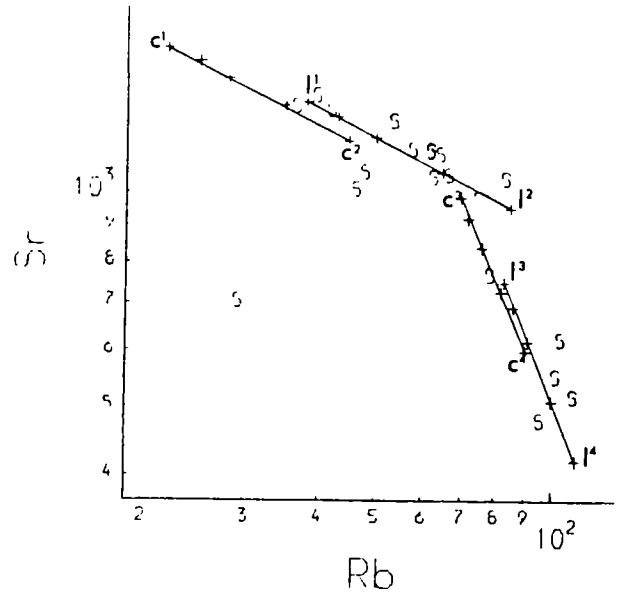
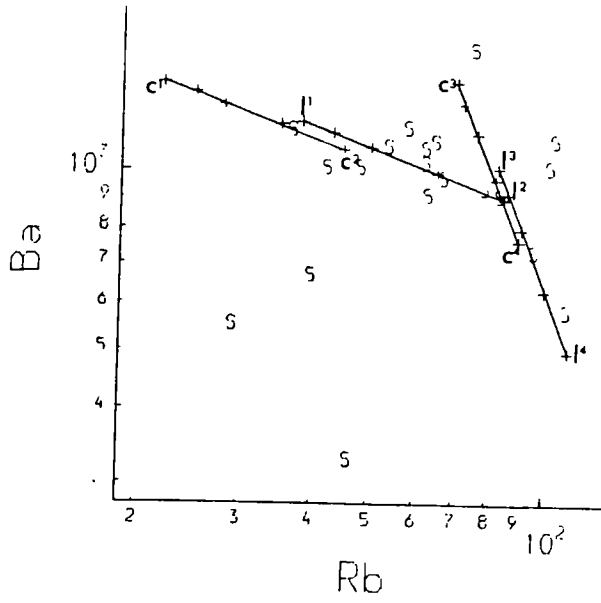
### 3) The Cluanie granodiorite.

No quantitative modelling is attempted for this intrusion due to the small sample suite and small compositional range. In general however the compatible behaviour of Sr, Ba and Y (Fig. 6:7) indicate plagioclase, potassium feldspar and hornblende are probably fractionating phases. The low levels of Cr and V reflect the low content of mafic minerals in this intrusion. The compatible behaviour of Zr indicates zircon fractionation.

### 4) The Strontian complex.

It is clear from Fig. 6:7 that there are at least two trends described by trace elements in the Strontian complex. The low silica trend covers the granodiorite and tonalite and the high silica trend represents the granite; this therefore has to be reflected in the trace element modelling of this intrusion. Quantitative modelling of Rb, Sr, Ba and Y (Fig. 6:28) for this intrusion based on the previously described method

Fig. 6:28. Modelled LIL element variation diagrams for the Strontian complex,  $l^1-l^4$  represent modelled liquid compositions,  $c^1-c^4$  represent modelled cumulate compositions, key to symbols on fold out sheet.



defines both trends; with an assemblage of a maximum of 22% biotite and 6% hornblende, with a minimum of 26% plagioclase for the granodiorite and tonalite, and a maximum of 25% biotite with a minimum of 9% hornblende, and 30% plagioclase for the granite. The low total for both assemblages implies that the calculated bulk distribution coefficients for elements with  $D_i > 1$  are too low and for elements with  $D_i < 1$  are too high, implying that either fractional crystallization processes did not proceed to completion or that minerals such as quartz which have bulk distribution coefficients of 0 for all elements discussed are involved in fractional crystallization. The low silica sample (c.f. Fig. 6:7 ( $\text{SiO}_2$  53%)) is contaminated with a Tertiary dyke cutting the sample, and is therefore excluded from this model. Cr, V, Nb, Zr and Ce appear to behave compatibly, Cr and V being controlled by biotite and hornblende as described before. Similarly Nb is probably controlled by ilmenite or sphene, Zr by zircon and Ce by allanite in the crystallizing assemblage. The difference in the trends for the Strontian granite and the Strontian tonalite and granodiorite is such that insitu processes cannot explain the variation and different pulses of magma must be involved.

##### 5) The Ballachulish complex.

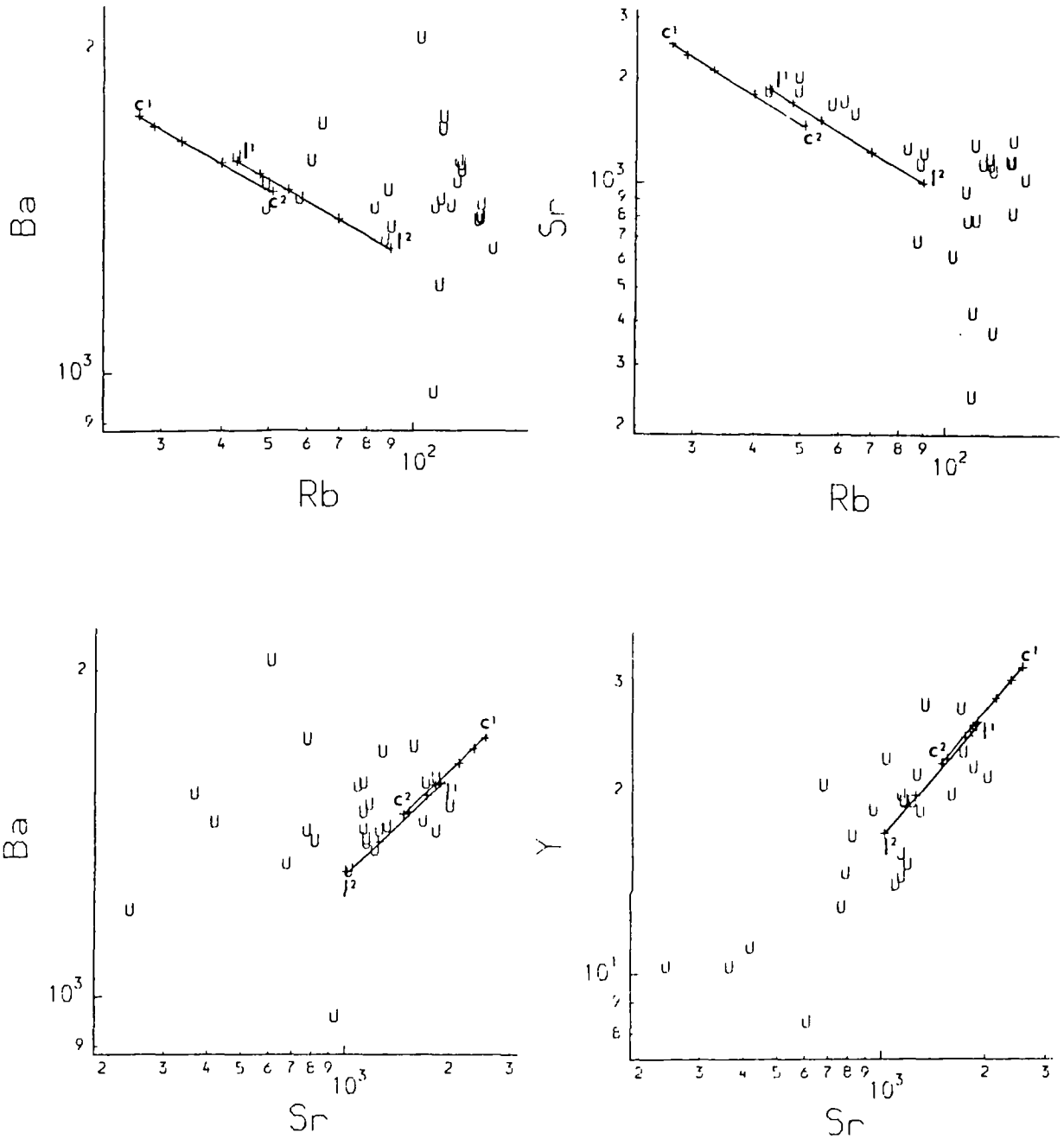
It is clear from Fig. 6:8 that there are two trends described by the trace element data from the Ballachulish complex; the low silica trend represents the granodiorite, with the high silica trend representing the granite. Whereas both trends may be modelled quantitatively, the apparently compatible behaviour of Rb in the high silica trend for the granite would require very substantial amounts of biotite in the fractional crystallization assemblage for the granite. However there is no evidence for this in the petrography of the Ballachulish granite, and

since the granitic portion of the Ballachulish complex has undergone considerable metasomatism related to porphyry copper mineralization (Evans 1977, Evans et al. 1979, Fortey 1980, Haslam & Kimbell 1981). It is possible therefore that Rb has undergone considerable remobilization although this was not observed in Fig. 5:19 where the LIL elements were plotted against  $TiO_2$  and therefore it is not possible to use LIL element modelling for the Ballachulish granite; the Ballachulish granodiorite however does not appear to be as severely affected by this process and therefore can be modelled using quantitative techniques (Fig. 6:29). The resultant fractional crystallization assemblage on the basis of the previously described method is a minimum of 10% hornblende and 30% plagioclase with a maximum of 20% biotite. The low total for this assemblage implies that the calculated bulk distribution coefficients for elements with  $D_i > 1$  are too low and too high for elements with  $D_i < 1$ , implying that either fractional crystallization processes did not proceed to completion or minerals such as quartz which have bulk distribution coefficients of 0 for all elements discussed are involved in fractional crystallization. In this case the latter explanation is unlikely. Of the other trace elements discussed, Cr, V and Ce behave compatibly (Fig. 6:8), Cr and V are controlled by biotite and hornblende and Ce by allanite in the crystallizing assemblage. The trend described by Zr in the granodiorite suite indicates that zircon becomes part of the fractional crystallization assemblage at about 60%  $SiO_2$ .

#### 6) The Ben Nevis complex.

It is clear from Fig. 6:9 that the trace element trends for the Ben Nevis complex define two separate trends on the Harker type diagrams; a low silica trend for the samples from the outer granite and a slightly

Fig. 6:29. Modelled LIL element variation diagrams for the Ballachulish granodiorite,  $l^1$  and  $l^2$  represent modelled liquid compositions,  $c^1$  and  $c^2$  represent modelled cumulate compositions, key to symbols on fold out sheet.

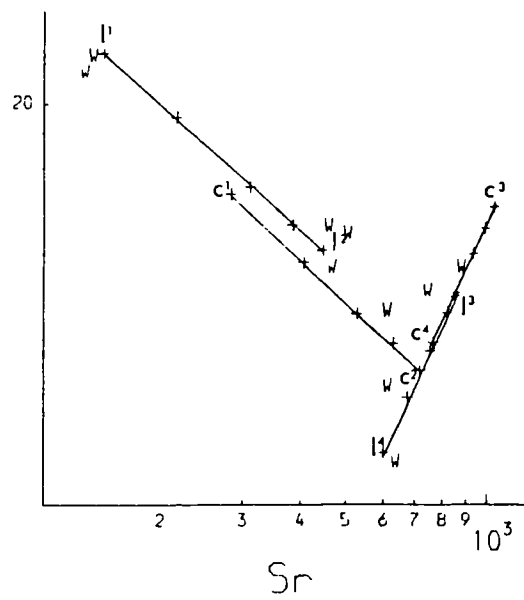
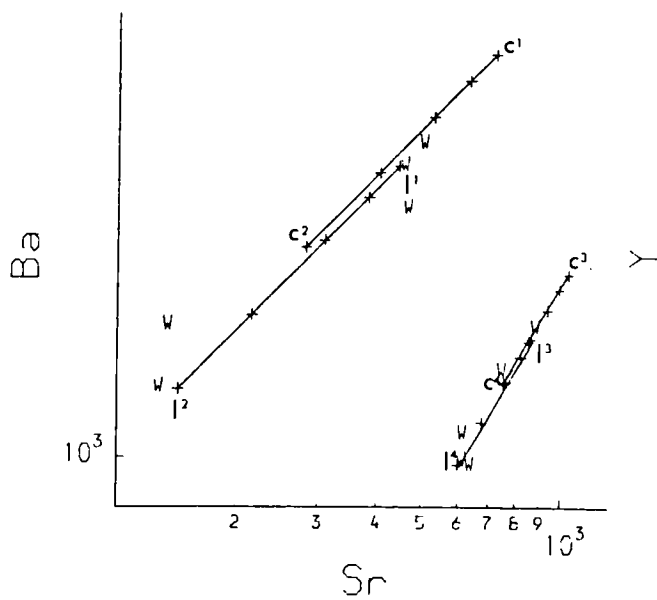
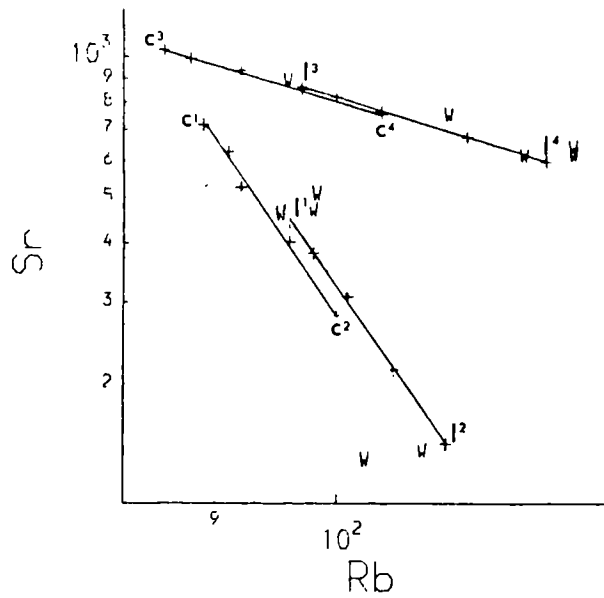
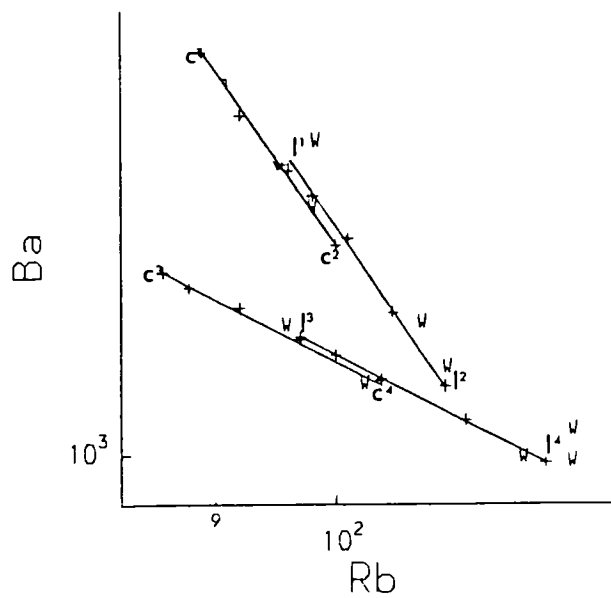


higher silica trend for the inner porphyritic granite. Both these trends may be quantitatively modelled (Fig. 6:30). The modelled crystallization assemblage for the Ben Nevis outer granite on the basis of the previously described method represents a minimum of 27% plagioclase and 10% hornblende and a maximum of 27% biotite in the assemblage; for the inner granite a minimum of 28% plagioclase and a maximum of 28% biotite and 6% hornblende in the assemblage. As before it is clear that the calculated bulk distribution coefficients are too low for elements with  $D_i > 1$  and too high for elements with  $D_i < 1$ , implying that either fractional crystallization did not proceed to completion or minerals such as quartz, which have bulk distribution coefficients of 0 for all elements discussed, are involved in fractional crystallization. The marked difference in the trends expressed both in Fig. 6:9 and Fig. 6:30 for the two components of this intrusion imply that these cannot be related by in situ fractional crystallization and must therefore represent two magma pulses. In the outer granite it is clear from Fig. 6:9 that Ce, V, Zr and Cr are behaving compatibly, Cr and V concentrations are controlled by biotite and hornblende in the assemblage, and Ce and Zr respectively indicate allanite and zircon in the assemblage. This is also the case in the Ben Nevis inner granite.

#### 7) The Etive complex.

Although the sample suite shown in Fig. 6:9 for the Etive complex is not as small as that shown for the Ben Nevis complex the samples particularly for the inner Starav granite show considerable scatter. In view of this it is inappropriate to attempt to model this intrusion quantitatively. In general however the LIL elements indicate plagioclase and potassium feldspar are fractionating phases in the Starav intrusion.

Fig. 6:30. Modelled LIL element variation diagrams for the Ben Nevis complex,  $l^1-l^4$  represent modelled liquid compositions,  $c^1-c^4$  represent modelled cumulate compositions, key to symbols on fold out sheet.



Potassium feldspar does not appear to be part of the fractionating assemblage in the outer Cruachan intrusion. The behaviour of Y is ambiguous and more data would be required to constrain the hornblende involvement in fractional crystallization for both intrusions.

8) The Moor of Rannoch granodiorite.

The large range in  $\text{SiO}_2$  observed in the Moor of Rannoch intrusion implies extensive fractional crystallization (Fig. 6:10). However the inter-element relationships of the trace elements do not provide suitable trends for fractional crystallization modelling. The two samples with  $\text{SiO}_2 = 55\%$  are from hornblendic xenoliths and may represent fragments of an earlier cumulus assemblage beneath this intrusion, although the wide range of levels of Li, Th, Ce and Zr cast doubt on this.

9) The Strath Ossian granodiorite.

The suite of samples from the granodiorite have a very limited compositional range (Fig. 6:10) and are therefore not suitable for quantitative trace element modelling. The hornblendic inclusion with  $\text{SiO}_2 = 57\%$  may represent an early cumulus assemblage although the high levels of Li and Be may be difficult to account for.

10) The Foyers complex.

Trace element data from the Foyers complex form three separate and complex trends on Harker type diagrams (Fig. 6:11). The range of silica values within each trend is relatively small and no quantitative modelling is attempted for this intrusion. However there does not appear to be any possible fractional crystallization relationship between the tonalite, granodiorite and granitic members of this complex contrary to

the opinion expressed by Pankhurst (1979). LIL elements show considerable scatter for all members of this complex, implying some remobilization of these elements. Trends for HFS elements such as Cr and V are tighter, indicating internal variations within each unit.

11) The Moy granite.

The sample suite for the Moy granite is small and is therefore not suitable for quantitative modelling. In general however the compatible behaviour of Sr and Ba (Fig. 6:12) indicates both plagioclase and potassium feldspar fractionation. The compatible behaviour of Cr and V implies either hornblende or biotite fractionation, and although Y appears to behave compatibly there is no observed hornblende in the samples analysed which suggests that biotite is the main mafic phase in the fractional crystallization assemblage.

12) The Peterhead granite.

The Peterhead granite is geochemically similar to the Cairngorm granite and is characterized by low levels of Sr, Ba, V and Cr (Fig. 6:12). Fractional crystallization trends are poorly defined for Sr and Ba; however the incompatible behaviour of Y and Nb indicates no hornblende and sphene or ilmenite as part of the fractional crystallization assemblage. The sample suite is too small to give meaningful fractional crystallization models.

13) The Ben Rinnes granite.

The small sample suite and restricted range in compositions (Fig. 6:12) preclude quantitative modelling. In general terms the compatible behaviour of Sr and Ba indicate plagioclase and potassium feldspar as a

major part of the fractional crystallization assemblage. The compatible behaviour of Cr and V together with the incompatible behaviour of Y indicate biotite rather than hornblende as the main mafic mineral in the fractional crystallization assemblage. The incompatible behaviour of Nb indicates sphene or ilmenite are not part of the crystallization assemblage. Ce and Zr appear to be behaving compatibly, suggesting monazite (Ce) and zircon fractionation.

14) The Mt. Battock granite.

Although there is a wide range of composition (Fig. 6:15) quantitative modelling has not been attempted for this pluton. However in general terms the compatible behaviour of Sr and Ba indicate plagioclase and potassium feldspar in the fractional crystallization assemblage. Cr, V and Y also behave compatibly although there is no hornblende present in this intrusion and biotite is considered to be the main mafic phase present. Thus the compatible behaviour of Y cannot be related to insitu hornblende fractionation but may be related to minor phases in the assemblage. Increased levels of Nb in the high silica samples imply that sphene or ilmenite are not part of the fractionating assemblage. Zr and Ce both behave compatibly suggesting zircon and monazite as part of the crystallizing assemblage.

15) The Bennachie granite.

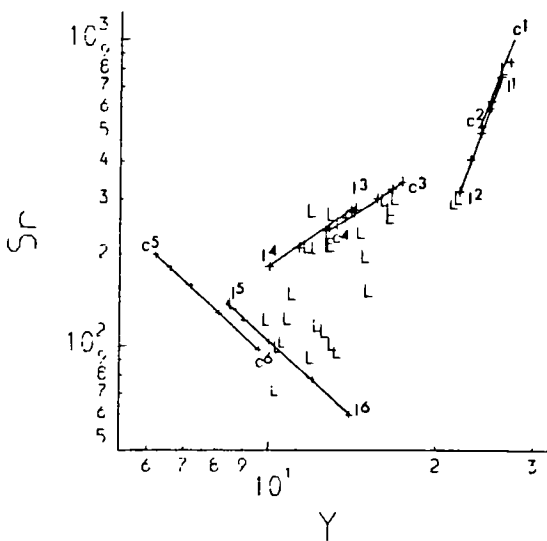
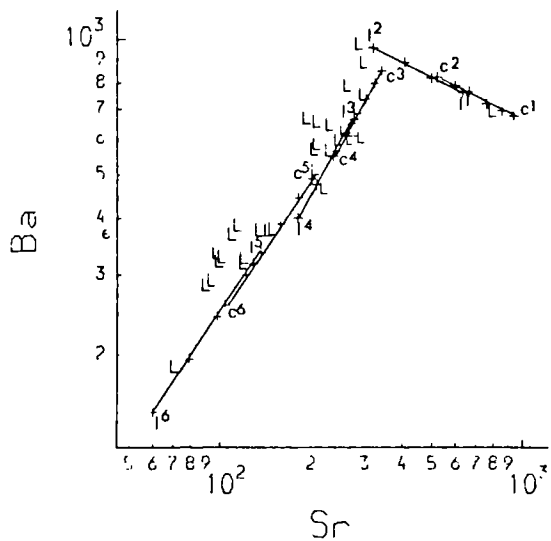
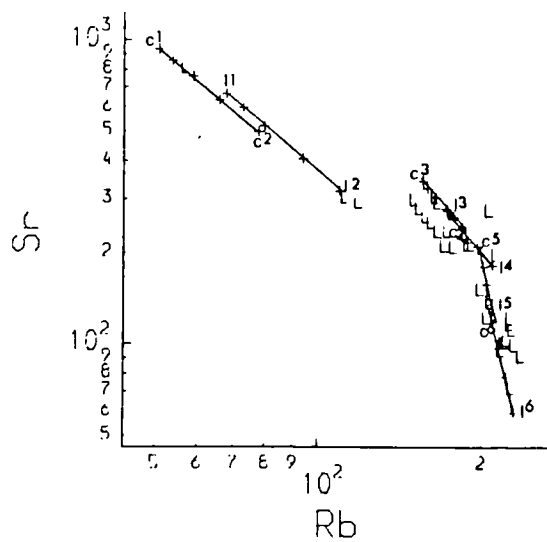
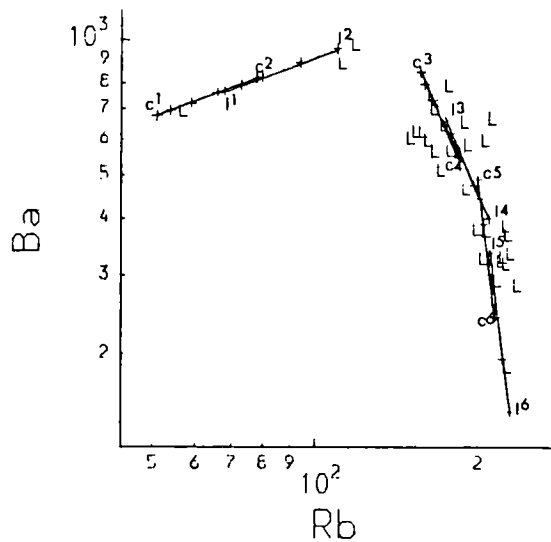
Although there is some variation in composition in this intrusion (Fig. 6:16) no quantitative modelling is attempted here. However in general terms the compatible behaviour of Sr and Ba indicate plagioclase and potassium feldspar in the crystallizing assemblage. The compatible behaviour of Cr and V with the ambiguous behaviour of Y and the absence

of hornblende in this intrusion indicates biotite as the main mafic mineral in the insitu crystallization assemblage. The behaviour of Y may be related to minor phases in the insitu fractional crystallization assemblage. The observed increase in Nb with increasing  $\text{SiO}_2$  indicates that sphene and ilmenite do not form part of the crystallization assemblage. The compatible behaviour of Zr, Ce and Th indicate zircon (Zr) and monazite (Ce, Th) are involved in fractional crystallization.

#### 16) The Lochnagar complex.

Data from the Lochnagar complex covers a wide range of compositions (Fig. 6:17). Although there is limited data for the diorite, work by Rennie (1984) indicates that there is a continuum of compositions from 60 to 70%  $\text{SiO}_2$ . Quantitative modelling of the trace element compositions for this intrusion indicates three distinct geochemical trends (Fig. 6:31). The modelled crystallization assemblages on the basis of the previously described method are: for trend 1 (diorite) a minimum of 31% plagioclase and 9% hornblende with a maximum of 27% biotite; for trend 2 a minimum of 27% plagioclase and 10% hornblende with a maximum of 27% biotite; and for trend 3 a minimum of 32% plagioclase with a maximum of 6% hornblende and 29% biotite. It is clear from the low totals for assemblages in these models that the calculated distribution coefficients for elements with  $D_i > 1$  are too low and too high for elements with  $D_i < 1$ , this would allow for some potassium feldspar in all three trends with substantial amounts of potassium feldspar in trends 2 and 3; this may also imply that either fractional crystallization processes did not proceed to completion or minerals such as quartz which have bulk distribution coefficients of 0 for all elements discussed here are involved in fractional crystallization. The absence of any overlap

Fig. 6:31. Modelled LIL element variation diagrams for the Lochnagar complex, 1<sup>1</sup>-1<sup>6</sup> represent modelled liquid compositions, c<sup>1</sup>-c<sup>6</sup> represent modelled cumulate compositions, key to symbols on fold out sheet.



between trends 1, 2 and 3 would indicate the possibility of an insitu fractional crystallization relationship between at least trends 2 and 3, however the small compositional gap between the diorite of trend 1 and trends 2 and 3 suggests that the diorite may represent a separate pulse of magma. The behaviour of Cr and V (Fig. 6:17) are controlled by biotite and hornblende in the fractional crystallization assemblage. Nb appears to decrease in trend 1 and 2 but increase in trend 3 indicating that in trend 3 sphene and ilmenite do not form part of the crystallizing assemblage. Zr and Ce behave compatibly in trends 2 and 3 indicating zircon and allanite or monazite fractionation.

#### 17) The Glen Gairn granite.

The Glen Gairn intrusion appears to be a multiple intrusion, in that the rapid changes in concentration of Sr and V (Fig. 6:18) between 70 and 75%  $\text{SiO}_2$  are probably too large to be the result of fractional crystallization. However the samples with >75%  $\text{SiO}_2$  appear to be from one single intrusive phase with little variation in  $\text{SiO}_2$ . The samples with between 50 and 60%  $\text{SiO}_2$  are small scale greisen pockets within the high silica granite which have very little free quartz, being composed almost entirely of zinwaldite and muscovite, as described in Chapters 3 and 5 (there are also greisen samples with much more free quartz). Generally it appears that Y and Nb behave incompatibly in this intrusion indicating no hornblende and ilmenite or sphene in the crystallizing assemblage. The very low levels of Sr and Ba in the granite with >75%  $\text{SiO}_2$  require that large amounts of plagioclase and potassium feldspar have been removed by fractional crystallization and it would appear that this granite represents the volatile enriched top of a pluton.

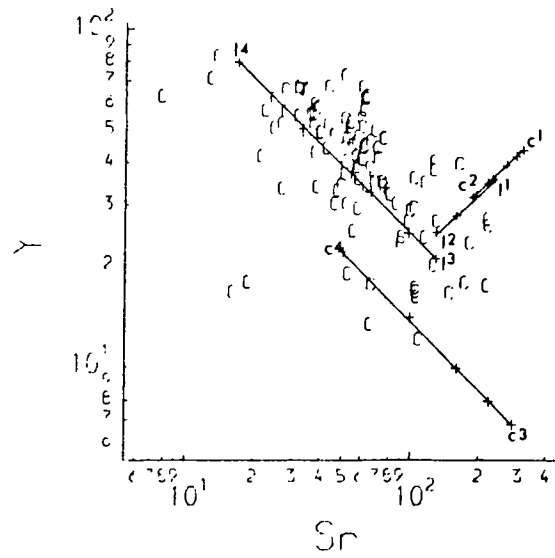
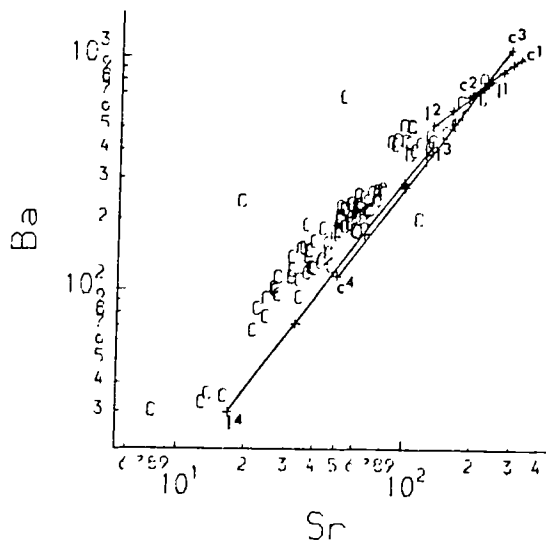
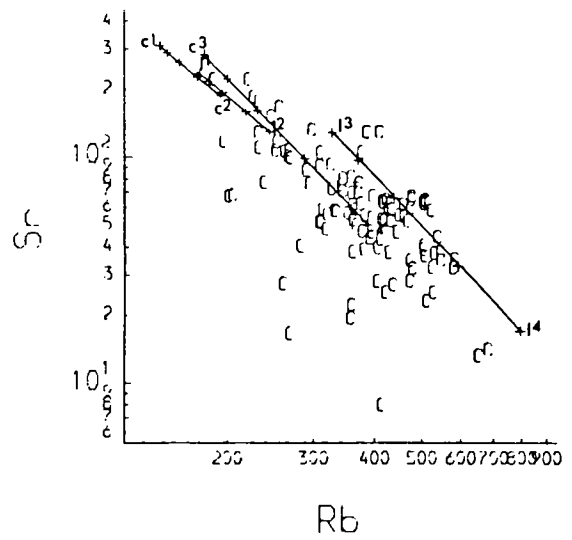
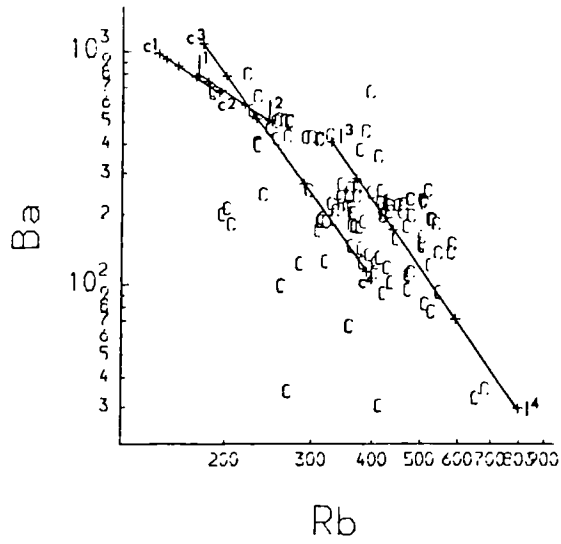
#### 18) The Cairngorm granite.

The Cairngorm granite is one of the largest plutons in the British Caledonides and one of the best sampled intrusions in this study. Although the range in major element compositions of this intrusion is relatively small, the range in trace element composition is quite large (Fig. 6:19). Quantitative modelling of this intrusion reveals two trends which are only observed in the behaviour of Y; the trends for Rb, Sr and Ba do not show any significant change in fractional crystallization assemblage (Fig. 6:32). The modelled fractional crystallization assemblages on the basis of the previously defined method are a minimum of 8% potassium feldspar, 22% plagioclase and 9% hornblende or 0.04% apatite with a maximum of 25% biotite for trend 1; and a minimum of 19% plagioclase and 29% potassium feldspar with a maximum of 17% biotite. It is apparent from the low totals for these assemblages that the calculated bulk distribution coefficients for elements with  $D_i > 1$  are too low and too high for elements with  $D_i < 1$ , implying that either fractional crystallization processes did not proceed to completion or minerals such as quartz which have bulk distribution coefficients of 0 for all elements discussed are involved in fractional crystallization. The behaviour of Cr and V is controlled by biotite in the fractionating assemblage. The incompatible behaviour of Nb indicates that ilmenite or sphene are not represented in the fractionating assemblage. Zr and Ce behave compatibly indicating zircon and monazite as part of the fractionating assemblage.

#### 19) The Garabal Hill complex.

A much larger suite of samples would be required in order to quantitatively model the trace element behaviour in the Garabal Hill

Fig. 6:32. Modelled LIL element variation diagrams for the Cairngorm granite,  $l^1$ - $l^4$  represent modelled liquid compositions,  $c^1$ - $c^4$  represent modelled cumulate compositions, key to symbols on fold out sheet.



complex than is presented here (Fig. 6:21). In general however the hornblendite sample cannot be related to the rest of the plutonics in a simple liquid cumulate relationship but may represent an earlier cumulus phase related to parental liquids for the more silica rich trends. This is seen in relatively low levels of Y and V for the hornblendite where Y and V are behaving compatibly in the main trend. Also on the basis of the behaviour of Sr, Ba, Nb, Zr, Li, Th, U and Be there appears to be more than one intrusive phase to this intrusion which cannot be related by insitu fractional crystallization but may be related by fractional crystallization in a magma chamber at depth. However the data set for this intrusion is insufficient to make further comments.

#### 20) The Kilmelford complex.

The data from this complex shows considerable scatter (Fig. 6:22), probably related to the associated porphyry copper mineralization. It is apparent that the diorite and porphyrite have a similar crystallization history. Quantitative modelling for this intrusion is not attempted due to the apparent remobilization of trace elements in this complex. The apparently compatible behaviour of Sr indicates some plagioclase in the fractional crystallization assemblage; the behaviour of Ba is ambiguous. The compatible behaviour of Cr, V, Y and Nb imply pyroxene, hornblende and ilmenite or sphene in the fractional crystallization assemblage. Ce also appears to behave compatibly indicating a minor phase in the fractional crystallization assemblage.

## 6:4 THE RARE EARTH ELEMENTS.

It is clear from trace element modelling that in most cases both light and heavy rare earth elements behave compatibly. The only exceptions to this are the biotite granites where the heavy rare earth elements behave incompatibly. The notable exception to this is the Carrock Fell granophyre where both heavy and light rare earths behave incompatibly. The rare earth pattern for this intrusion is fairly flat (Fig. 6:33) and since both light and heavy rare earths are behaving incompatibly the parental liquids to this intrusion would also be expected to have a flat pattern fairly similar to the Sarmiento complex in Chile (Saunders et al. 1979). The negative Eu anomaly for the granophyre indicates plagioclase fractionation, which would be expected from the trace element model for this intrusion. The flat REE pattern of the Carrock Fell granophyre would be the typical result of a fractionation sequence for an assemblage of plagioclase, pyroxenes and oxides, all of which do not significantly alter the  $La_N/Lu_N$  ratio of the rare earth pattern.

Fairly flat rare earth patterns are also characteristic of several other Lake District intrusions; the rare earth pattern for the Threlkeld intrusion is slightly light rare earth enriched (Fig. 6:33), the negative Eu anomaly indicating that plagioclase has been a fractionating phase as would be expected from the relatively low levels of Sr and the presence of plagioclase phenocrysts. Similarly the rare earth patterns for the Ennerdale granophyre are also slightly light rare earth enriched, with negative Eu anomalies (Fig. 6:33) indicating plagioclase fractionation. The heavy rare earths for this intrusion however show a slightly dish pattern. This might result from apatite or hornblende



fractionation; apatite fractionation would be consistent with the low levels of phosphorous in this intrusion (Fig. 4:2). The rare earth patterns for the Eskdale intrusion are also slightly light rare earth enriched (Fig. 6:33) in the granodiorite and becomes more light rare earth enriched in the granite, probably the result of garnet in the fractionating assemblage. Both the light and heavy rare earths behave compatibly in this intrusion, the depletion of the light rare earths probably being the result of monazite in the fractionating assemblage. The total observed variation in the rare earth patterns for the Eskdale intrusion corresponds to a fractional crystallization assemblage of 45wt% plagioclase, 30wt% potassium feldspar, 5.5wt% garnet, 0.15wt% monazite, 0.5wt% apatite and 0.9wt% sphene (Fig. 6:34b) and, although sphene is not observed in the Eskdale granite Nb, which could be controlled by sphene in the fractional crystallization assemblage, appears to behave compatibly (Fig. 6:2).

The Shap and Skiddaw granites of the Lake District however are characterized by much more fractionated rare earth patterns. The Shap granite has a steep rare earth pattern with no noticeable negative Eu anomaly (Fig. 6:33). This could be caused by combined hornblende and plagioclase fractionation or residual garnet in the source; however combined hornblende and plagioclase fractionation would produce a pronounced concave pattern in the heavy rare earths (Fig. 6:34a) since the distribution coefficients for Gd, Tb, Dy, Ho and Er in hornblende are much greater than those for Tm, Yb and Lu (Henderson 1982). Similarly residual garnet in the source cannot fully explain the observed patterns unless the parental magmas are at least andesitic if not basaltic in composition, since the distribution coefficients for Lu are lower than

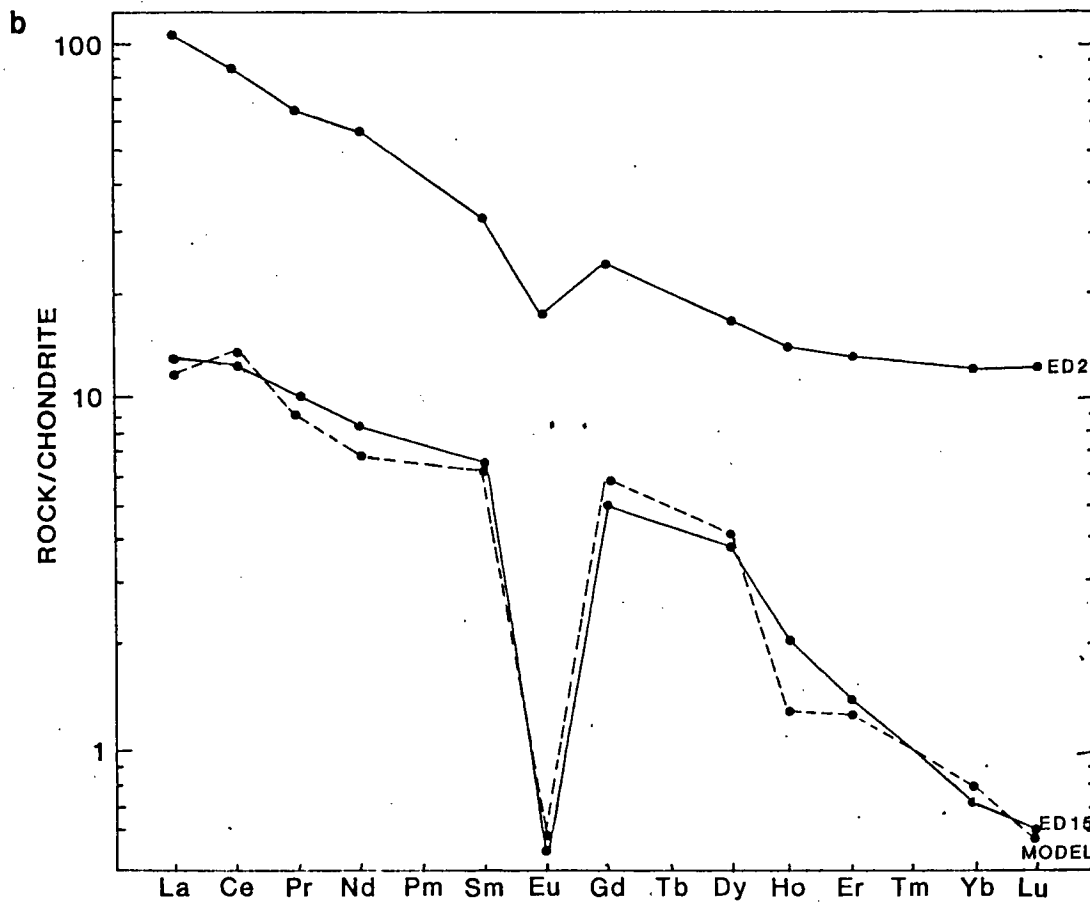
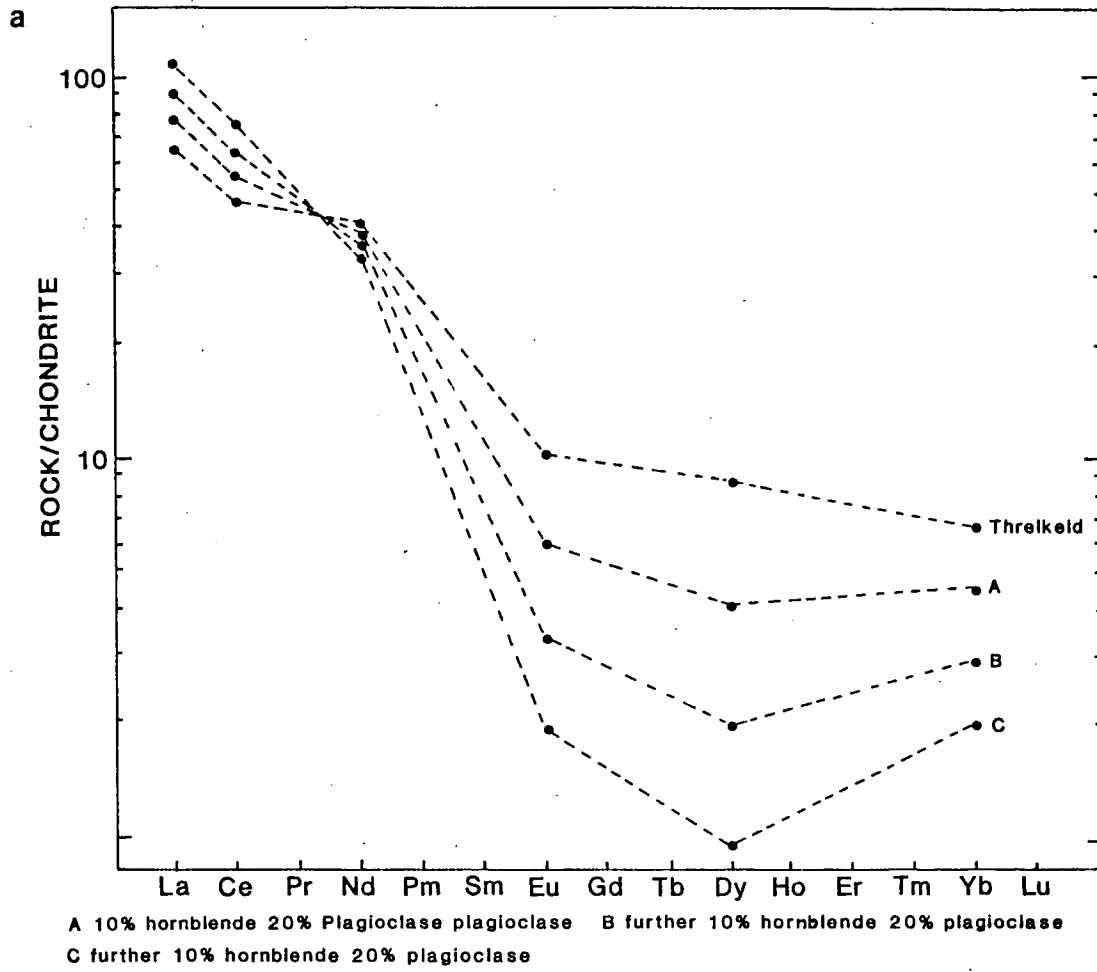
Fig. 6:34. REE modelling (see over page).

Fig. 6:34.

a) REE modelling of the effects of fractional crystallization of a plagioclase and hornblende assemblage on the slightly light REE enriched rare earth pattern of the Threlkeld microgranite.

b) REE modelling from the Eskdale granodiorite to the Eskdale granite using a fractional crystallization assemblage of 45 wt% plagioclase, 30 wt% potassium feldspar, 5.5 wt% garnet, 0.15 wt% monazite, 0.5 wt% apatite and 0.9 wt% sphene.

Fig. 6:34



those for Er and Yb for garnet in rhyolitic rocks (Table 6:5). The skiddaw granite is also characterized by a steep rare earth pattern with a small negative Eu anomaly for the least evolved samples (Fig. 6:33). In the more silica rich samples however the patterns are less fractionated with a larger negative Eu anomaly. The decrease in light rare earth elements is thought to be the result of monazite fractionation, with no garnet or hornblende to control the heavy rare earth elements, which then increase with fractional crystallization.

TABLE 6:4.a) AVERAGE MINERAL-MELT DISTRIBUTION COEFFICIENTS OF THE RARE EARTH ELEMENTS IN BASALTIC AND ANDESITIC ROCKS, FROM HENDERSON 1982.

	Olivine	Ortho- pyroxene	Clino- pyroxene	Amphibole	Plagioclase	Phlogopite	Garnet
La	--	--	0.08	0.27	0.14	--	0.05
Ce	0.009	0.02	0.34	0.34	0.14	0.03	0.05
Nd	0.009	0.05	0.6	0.19	0.08	0.03	--
Sm	0.009	0.05	0.9	0.91	0.08	0.03	0.6
Eu	0.008	0.05	0.9	1.0	0.32	0.03	0.9
Gd	0.012	--	0.9	1.1	0.10	--	3.7
Tb	--	0.05	1.0	1.4	--	--	5.6
Dy	0.012	0.20	1.1	0.64	0.09	0.03	--
Ho	--	--	--	--	--	--	19
Er	0.013	0.31	1.0	0.48	0.08	--	--
Tm	--	--	1.1	--	--	0.03	--
Yb	--	0.34	1.0	0.97	0.07	--	30
Lu	--	0.11	0.8	0.89	0.08	0.04	35

TABLE 6:4.b) AVERAGE MINERAL-MELT DISTRIBUTION COEFFICIENTS OF RARE EARTH ELEMENTS IN DACITIC AND RHYOLITIC ROCKS, FROM HENDERSON 1982.

	opx	cpx	amph	plag	ksp	gt	mt	al	ap	sp	zir
La	0.65	0.6	0.9	0.32	--	0.39	0.5	820	--	--	--
Ce	0.5	0.9	1.2	0.24	0.04	0.62	0.6	635	31	53	4.2
Nd	0.6	2.1	3.2	0.19	0.03	0.63	0.9	460	50	88	3.6
Sm	0.7	2.7	5.4	0.13	0.02	2.2	0.9	205	54	102	4.3
Eu	0.5	1.9	3.6	2.0	1.13	0.7	0.6	80	27	101	3.4
Gd	1.1	3.1	--	0.16	--	7.7	0.8	130	22	102	--
Tb	1.2	3.0	3.0	0.15	--	12	0.8	71	--	--	--
Dy	0.7	3.3	9.0	0.13	0.006	29	--	--	42	81	48
Ho	--	--	--	--	--	28	--	--	--	--	--
Er	0.61	--	8.0	0.05	0.006	43	--	--	31	59	140
Tm	1.4	--	5.0	0.1	--	--	0.8	--	--	--	--
Yb	1.0	2.1	6.2	0.08	0.012	43	0.4	8.9	21	37	280
Lu	1.1	2.3	4.5	0.06	--	38	0.4	7.7	17	27	345

Light rare earth enriched rare earth patterns are also characteristic of the Scottish granitoids. The granitoids of the high Sr groups 3b and c (Chapter 4) generally have rare earth patterns similar to the Shap granite with fractionated  $La_N/Lu_N$  ratios, although the heavy rare earths are generally less depleted than for the Shap granite, often with a slightly dish-shaped heavy rare earth pattern which may be the result of hornblende fractionation. Rare earth patterns for the Ben Nevis outer granite, Garabal Hill main granodiorite, Kilmelford diorite and the Ballachulish granodiorite all show no Eu anomaly but have slight depletion of Dy-Yb relative to Lu indicating some hornblende fractionation (Figs. 6:35 & 6:36). Rare earth patterns for the Moor of Rannoch granodiorite, Etive Ben Cruachan, Foyers granodiorite and Strontian granodiorite (Figs. 6:35, 6:36 & 6:37 (data from Pankhurst 1979)) are also characterized by the absence of a Eu anomaly and have a marked depletion of Dy-Er relative to Yb and Lu indicating hornblende fractionation. The absence of a positive Eu anomaly for all these suites indicates that the high levels of Sr observed cannot be the result of feldspar accumulation and must therefore be a source characteristic. Rare earth patterns for the Strontian and Foyers tonalites however are characterized by small positive Eu anomalies (Fig. 6:37 (data from Pankhurst 1979)) but are otherwise similar to the patterns for the respective granodiorites; this could indicate a cumulus feldspar component. The rare earth pattern for the Cluanie granodiorite has the least light rare earth enrichment observed in the high Sr granitoids (Fig. 6:36). The rare earth patterns from the group 2c West Scotland group of granites (that is the Strontian and Foyers granites (data from Pankhurst 1979)) which although they are petrographically granites are still characterized by high levels of Sr, are similar to the rest of the

Fig. 6:35. Chondrite normalized REE patterns for the Etive, Ben Nevis and Ballachulish intrusions, patterns for individual intrusions are separated by one log scale.

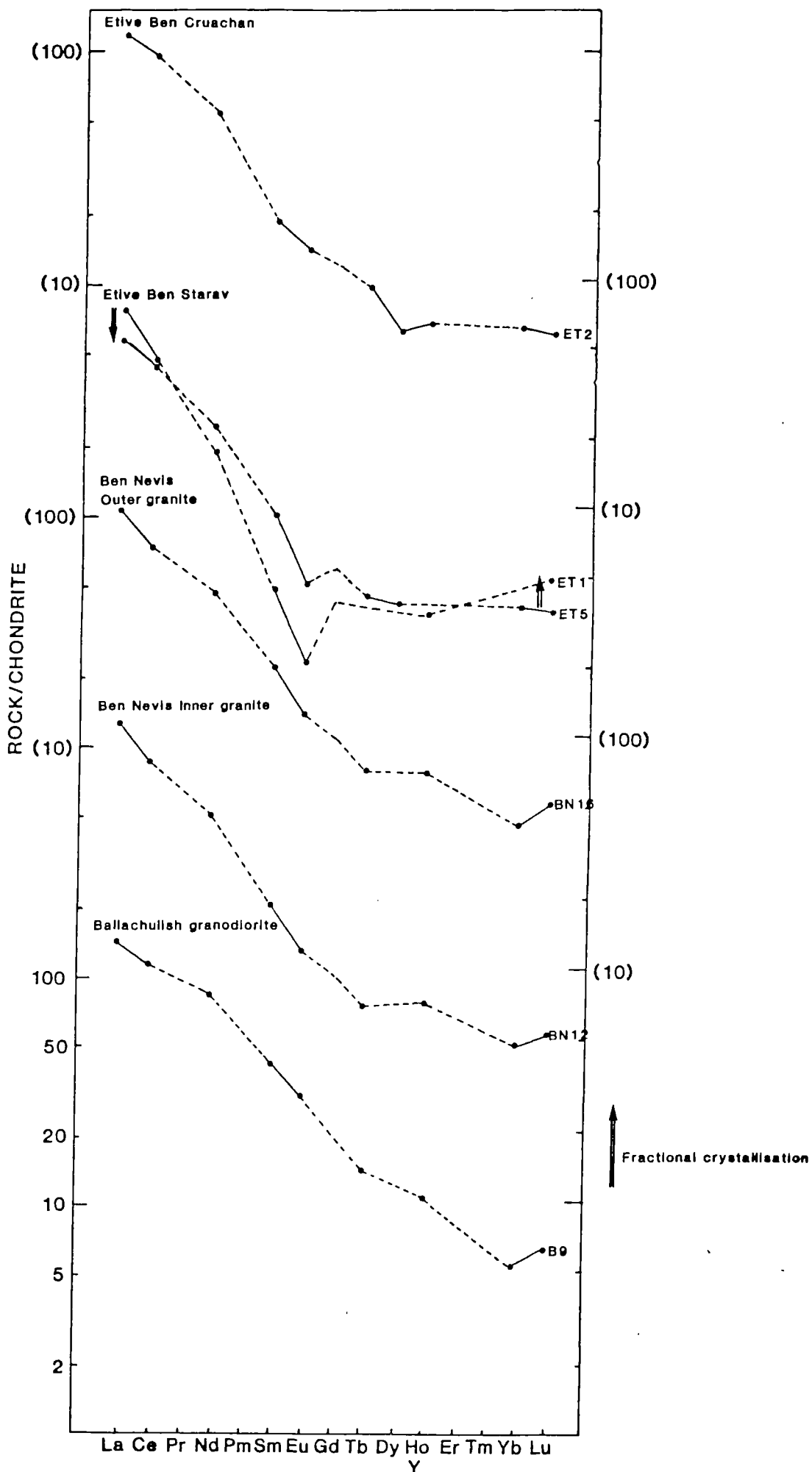


Fig. 6:36. Chondrite normalized REE patterns for the Cluanie, Moor of Rannoch, Kilmelford, Garabal Hill and Comrie intrusions, patterns for individual intrusions are separated by one log scale.

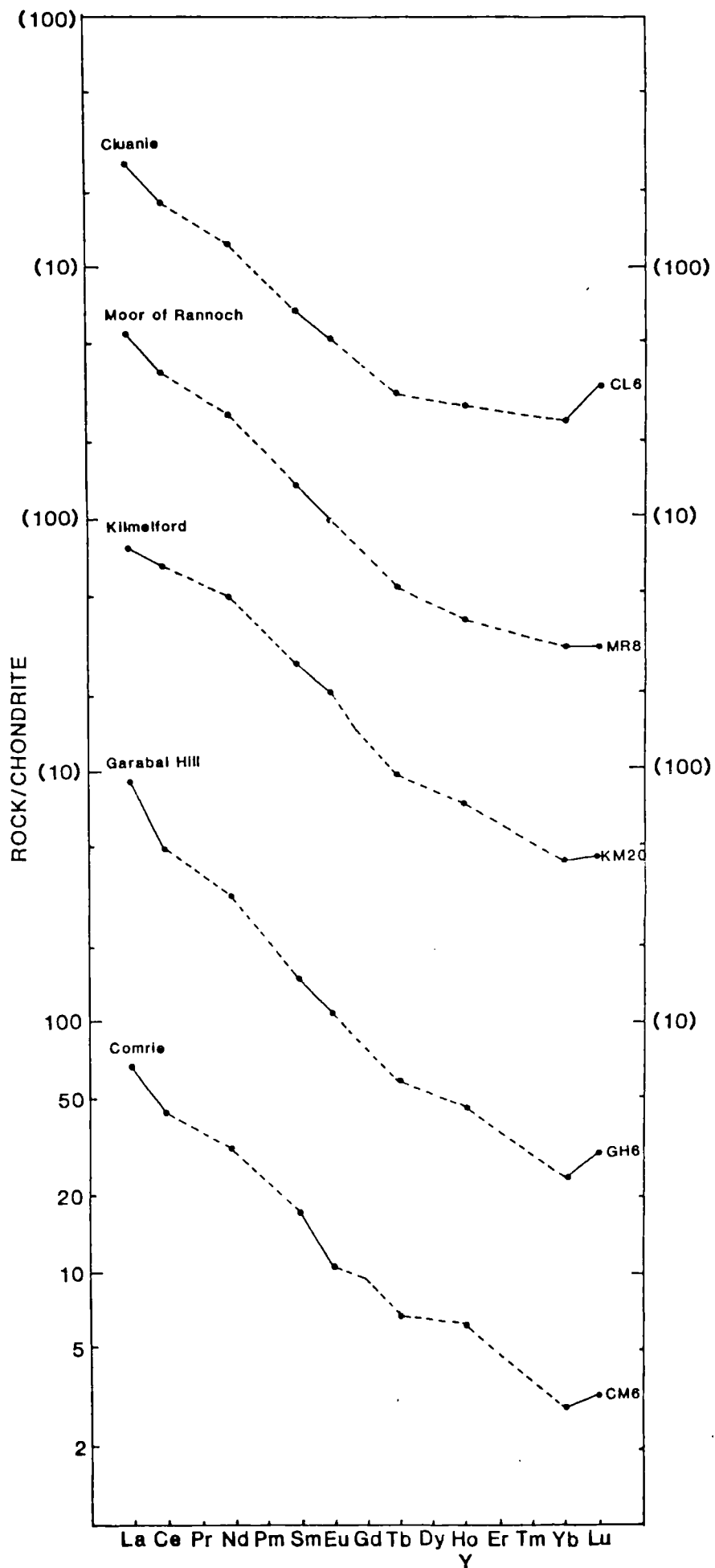
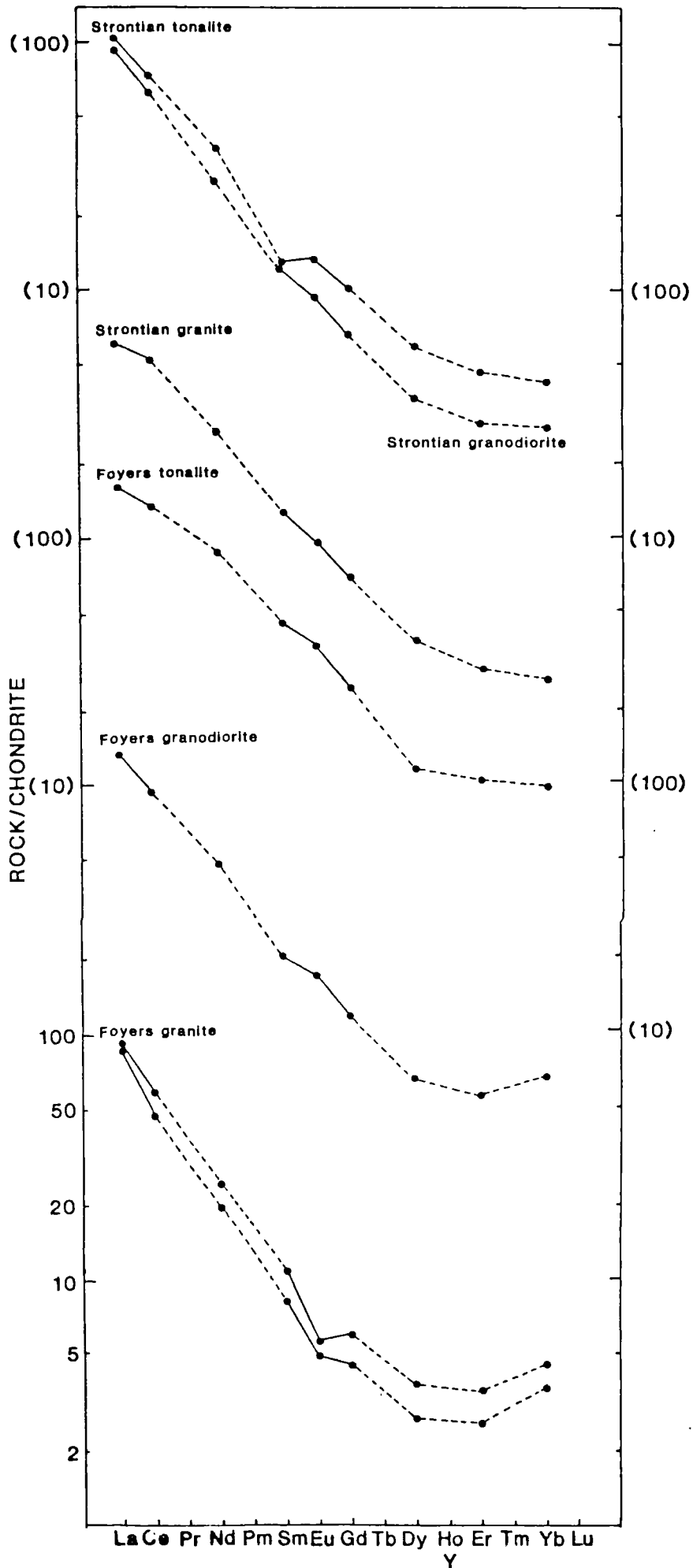


Fig. 6:37. Chondrite normalized REE patterns for the Strontian and Foyers intrusions (data from Pankhurst 1979), patterns for individual intrusions are separated by one log scale.

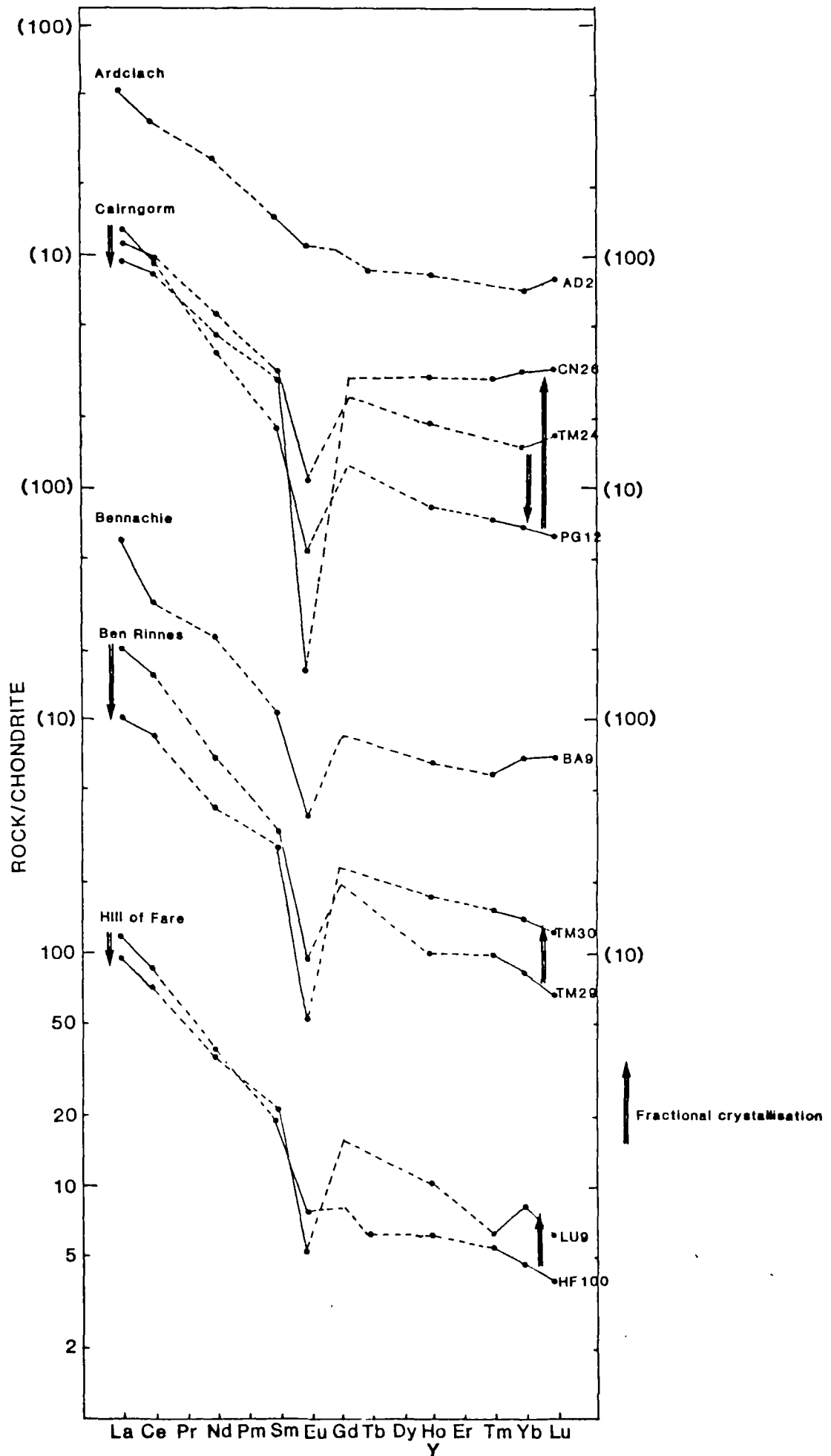


high Sr granitoids apart from showing small negative Eu anomalies (Fig. 6:37) indicating some plagioclase fractionation.

Granites of the intermediate group (group 2b from Chapter 4) have variable rare earth patterns. The Ben Nevis inner granite and the Comrie granite are characterized by fractionated  $La_N/Lu_N$  ratios and no Eu anomalies (Fig. 6:35 & 6:36), and are similar to the Shap granite. The rare earth patterns for Etive Ben Starav however have variable negative Eu anomalies (Fig. 6:35) indicating variable amounts of plagioclase fractionation. They have fractionated  $La_N/Lu_N$  ratios similar to the majority of the Scottish Caledonian granitoids, although the levels of heavy rare earth elements increases slightly with fractional crystallization, a feature similar to that seen in the Skiddaw granite.

The granites of the Cairngorm type (group 2a from Chapter 4) have variable rare earth patterns, and the variation appears to be the result of fractional crystallisation. The samples with the smallest negative Eu anomalies generally have higher levels of light rare earths and lower levels of heavy rare earths. With increased fractional crystallization the levels of light rare earths decrease and heavy rare earths increase, and is accompanied by an increase in the magnitude of the negative Eu anomaly. The best example of this is the Cairngorm granite itself (Fig. 6:38) the modelled fractional crystallization assemblage required is 35wt% plagioclase, 40wt% potassium feldspar, 9wt% biotite, 0.1wt% allanite or monazite and 0.5wt% apatite (Fig. 6:39). The levels of light rare earths in these granites are variable with the rare earth pattern for Ben Rinnes showing the highest levels of light rare earths (Fig. 6:38) and the Bennachie granite having the lowest levels of light

Fig. 6:38. Chondrite normalized REE patterns for the Ardclach, Cairngorm, Bennachie, Ben Rinnes and Hill of Fare granites, patterns for individual intrusions separated by one log scale.



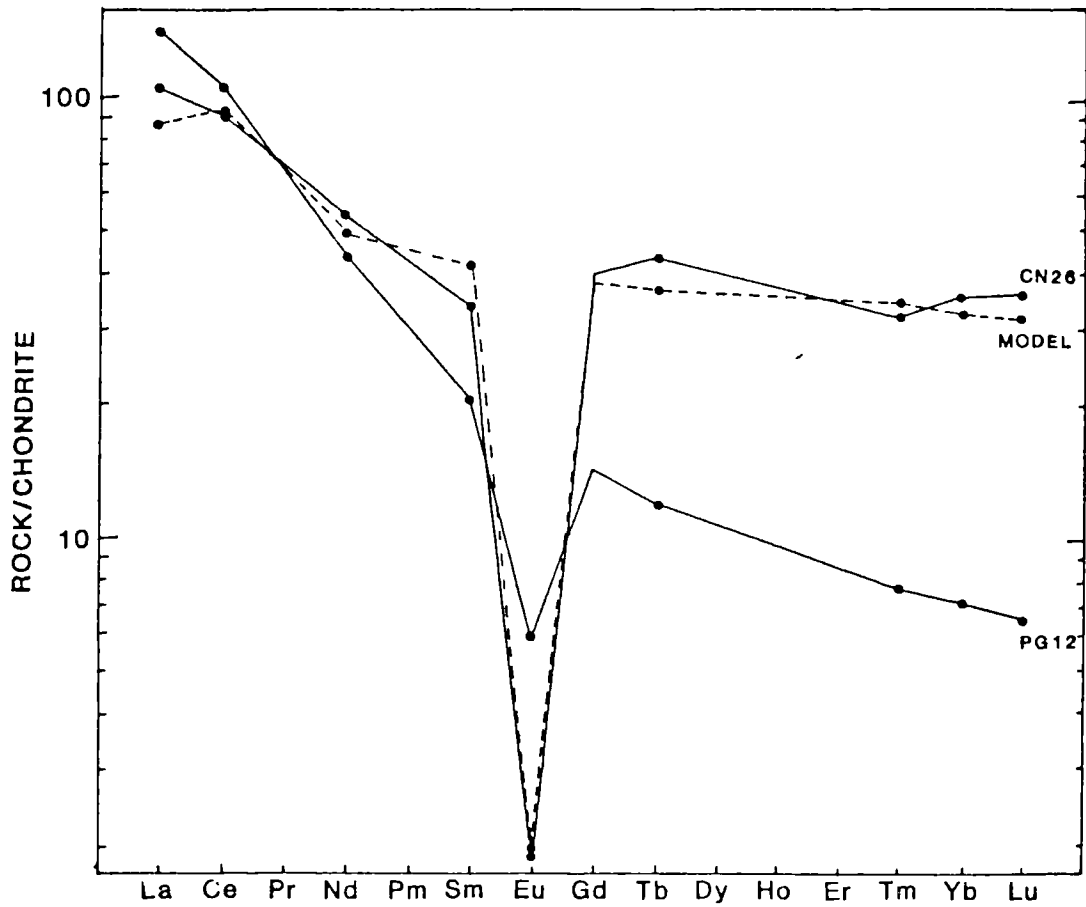


Fig. 6:39. REE modelling for the Cairngorm granite using a fractional crystallization assemblage of 35 wt% plagioclase, 40 wt% potassium feldspar, 9 wt% biotite, 0.1 wt% allanite or monazite and 0.5 wt% apatite.

rare earths. Because the levels of heavy rare earths appear to increase with fractional crystallization in these granites, the parental liquids for these granites probably had very fractionated  $La_N/Lu_N$  ratios, similar perhaps to the Ballachulish granodiorite.

The rare earth pattern for the Ardclach granite, which appears to be an "S" type granite belonging to group 1a from Chapter 4, is mildly light rare earth enriched with only a small negative Eu anomaly (Fig. 6:38). Levels of Sr are low in this intrusion (Table 6:1) but the size of the negative Eu anomaly precludes much plagioclase fractionation which would imply derivation of this granite from a low Sr source within the crust compatible with its derivation from the Moine metasediments.

#### 6:5. THE ROLE OF THE CONTINENTAL CRUST IN THE GENERATION OF THE CALEDONIAN GRANITES.

There are several factors to take into consideration when discussing the role of crustal components in the generation of the Caledonian granites. Consideration must be taken of both the isotopic and trace element characteristics of the crustal units which may be involved in granite genesis and whether the prevailing tectonic conditions of the crust would allow significant amounts of crustal melting. In the Caledonides of Britain the exposed crustal members have been extensively studied by isotope, major and trace element geochemistry. It is therefore possible by a combination of these techniques to constrain the role of the continental crust in magma genesis. Although no new isotopic data for the Caledonian granitoids is presented here there is adequate reconnaissance isotopic data in the literature (Tables 2:1, 2:2, 2:3 & 2:4), to indicate the scale of involvement of crustal units in the genesis of these granitoids.

## 6:5:i. THE LAKE DISTRICT GRANITES.

The role of the Continental crust in the genesis of the Caledonian Lake District intrusions is more difficult to define than for the intrusions north of the Iapetus suture, since the nature of the basement under the Lake District is unclear. However the low initial  $^{87}\text{Sr}/^{86}\text{Sr}$  ratios (Table 2:4) require no large amounts of old upper crustal material which would impart high initial  $^{87}\text{Sr}/^{86}\text{Sr}$  ratios to be involved in the generation of these granitoids. This is also apparent in the lack of inherited zircons from published Pb isotopic data (Pidgeon & Aftalion 1978) (Table 2:2).

The role of the Skiddaw slates in the generation of these granites however is more difficult to assess on isotopic criteria in the absence of published data for this crustal unit. However geochemical data from the Skiddaw slates (Table 6:6) indicate that bulk assimilation or bulk partial melting would give rise to relatively silica poor intrusions; small scale partial melting however may give rise to melts with some of the geochemical characteristics of the Lake District granites with the exception of those with generally low levels of boron. Under melting conditions boron would be expected to be concentrated in the melt along with other volatile and incompatible elements and it is clear that the Lake District granites cannot be derived from this source although local contamination through stoping may occur, (as is noted in the Eskdale granodiorite). It is also unlikely that the required thermal conditions for large scale partial melting of the Skiddaw slates were achieved during the Caledonide orogeny since the exposed section of the Skiddaw slates is only at lower greenschist (prehnite to pumpellyite) grade

(Oliver in press). It is therefore considered that crustal melting was not an important factor in the genesis of the Lake District granites.

#### 6:5:ii. THE SCOTTISH GRANITOIDS.

The possible crustal sources for the Scottish Caledonian granites are better defined but are more complex; these comprise Lewisian granulite basement, Lewisian amphibolite basement, Moine metasediments and Dalradian metasediments. All of these components can be defined both isotopically and geochemically (Table 6:6 and Fig. 2:1); a further component may be gained through subducted crustal material similar to the sediments of the Southern uplands accretionary prism.

It is clear from the isotopic data that melts generated from Moine and Dalradian metasediments would have initial  $^{87}\text{Sr}/^{86}\text{Sr}$  ratios  $>0.71$  and this would rule out these components as significant contributors to the Caledonian granites studied with the exception of the group 1a and b granites which have compositions compatible <sup>with</sup> melting of these upper crustal sources. Isotopic dating of the group 1 granites indicates that these intrusions were emplaced relatively early in the Caledonide orogeny and were intruded not long after the peak of metamorphism; thus a crustal origin for these granites is consistent with geological evidence.

The low initial  $^{87}\text{Sr}/^{86}\text{Sr}$  ratios recorded for the remainder of the Scottish Caledonian granitoids show however that the Dalradian and Moine metasediments cannot be significantly involved in the genesis of these granitoids. This factor however does not preclude the involvement of Lewisian basement in the genesis of the Caledonian granites. For the

granites with published Nd isotopic data the involvement of Lewisian basement can be constrained by combined use of Sr and Nd isotopes and from this (Fig. 2:1) the involvement of Lewisian basement in the genesis of these granitoids is negligible.

The available trace element data for the exposed crustal units in the Caledonides appear to preclude the genesis of the majority of these granites through crustal melting. The concentrations of Sr in particular are quite low in the majority of the crustal units and it is inconceivable that granitoids with about 1000 ppm Sr, such as the Strath Ossian granodiorite, can be obtained through partial melting of any of the crustal units, although this intrusion has an inherited zircon component (Table 2:2). Granitoids with lower levels of Sr such as the Cluanie granodiorite and some members of the Foyers complex which have levels of Sr around 700 ppm may however be derived through partial melting of the lower crust, this is comparable with the inherited zircon component observed by Pidgeon and Aftalion (1979) (Table 2:2). The presence of an inherited zircon component in the high Sr granitoids (Table 2:2) does not appear to be related to crustal melting of any of the observed crustal units although there is no apparent mechanism other than substantial crustal contamination which could account for the presence of the inherited zircon component.

TABLE 6:5. AVERAGE MAJOR AND TRACE ELEMENT DATA FOR CRUSTAL UNITS IN THE CALEDONIDES OF BRITAIN.

	(1)	(2)	(3)	(4)	(5)	(6)	(7)	(8)	(9)	(10)
SiO <sub>2</sub>	53.4	63.6	75.0	61.4	60.3	77.3	64.7	78.7	63.1	69.2
TiO <sub>2</sub>	1.3	0.5	0.6	1.0	1.1	0.6	1.0	0.5	0.8	1.0
Al <sub>2</sub> O <sub>3</sub>	24.1	15.8	11.9	17.7	18.8	11.1	16.1	10.8	20.1	12.8
Fe <sub>2</sub> O <sub>3</sub>	9.7	4.5	3.1	7.0	7.5	3.1	5.8	2.3	6.0	6.7
MnO	0.18	0.06	0.06	0.09	0.10	0.07	0.10	0.06	0.08	0.09
MgO	1.9	2.6	0.8	2.4	2.4	0.9	1.8	0.7	2.3	3.6
CaO	0.9	4.9	1.3	2.6	1.8	1.6	2.3	1.7	1.2	2.4
Na <sub>2</sub> O	1.2	4.7	2.7	3.0	2.5	2.4	2.7	2.6	2.2	2.3
K <sub>2</sub> O	3.6	0.9	3.9	3.54	4.7	2.4	4.6	2.5	4.1	2.1
P <sub>2</sub> O <sub>5</sub>	0.11	0.17	0.15	0.28	0.23	0.10	0.23	0.08	0.14	0.20
Rb	211	9	117	146	173	66	184	94	207	71
Sr	136	631	348	403	296	290	287	250	165	274
Ba	890	728	879	932	1035	628	991	594	818	463
La	45	20	-	-	-	-	-	-	-	39
Ce	98	44	-	-	-	-	-	-	-	82
Nd	34	-	-	-	-	-	-	-	-	39
Y	25	5	17	41	40	21	51	29	55	30
Nb	18	5	8	18	20	13	23	14	19	16
Zr	219	191	257	316	260	273	500	374	343	287
Ni	48	44	6	24	30	15	20	9	24	60
Cr	130	52	106	191	74	30	55	24	-	147
V	102	-	-	-	-	-	-	-	-	-
U	2.2	-	-	-	-	-	-	-	-	-
Th	17	-	-	-	-	-	-	-	-	10
Li	34	-	-	-	-	-	-	-	-	-
Pb	61	12	19	23	34	24	27	15	-	-
Zn	88	-	32	112	116	48	83	28	118	92
Cu	104	-	13	50	20	12	6	3	22	-
B	36	-	-	-	-	-	-	-	-	-

- (1) Skiddaw Slates (Jeans 1973) and data from this study.  
(2) Average Lewisian acid hornblende biotite gneiss Assynt (Sheraton et al. 1973).  
(3) Average Morar psammite (Moine) (Winchester et al. 1981).  
(4) Average Morar pelite (Moine) (Winchester et al. 1981).  
(5) Average Glenfinnan pelite (Moine) (Winchester et al. 1981).  
(6) Average Glenfinnan psammite (Moine) (Winchester et al. 1981).  
(7) Average Loch Eil pelite (Moine) (Winchester et al. 1981).  
(8) Average Loch Eil psammite (Moine) (Winchester et al. 1981).  
(9) Average Dalradian Levan Schists (Lambert et al. 1982).  
(10) Average Suothern Uplands greywacke (Tindle 1982).

## 6:6. SUMMARY.

The Caledonian granitoids are compositionally varied, and it appears that the extent of fractional crystallization and the mineral phases involved in fractional crystallization are major factors in the large compositional variation observed within the individual Caledonian granitoids. Most of the granitoids covered in this study do not appear to have been derived through the partial melting of upper crustal material with the exception of the group 1 granites (Stritchen, Aberdeen, Cove Bay and Ardclach). The contribution of lower crustal material to the genesis of the Caledonian granitoids also does not appear to be great.

Many of the composite intrusions are not simply generated by insitu fractional crystallization of one batch of magma, and therefore have more complex histories. The Foyers intrusion on the basis of trace element data appears to comprise three separate pulses of magma, probably generated from a similar source since the rare earth patterns for all three components are similar. The Strontian intrusion also comprises two separate pulses of magma, but the tonalite and granodiorite appear to be related by in-situ fractional crystallisation; however the granite cannot be related to the other units in this fashion and therefore appears to be a separate body. The Strontian rare earth patterns are similar for both the granite and the granodiorite and tonalite, thus indicating a similar source. The Ballachulish intrusion also appears to have been generated by two separate pulses of magma since the granite cannot be related to the granodiorite through in-situ fractional crystallization although the relationship of the source of the granite to that of the granodiorite is

unclear but it is likely that a similar source region may be involved, by analogy with the Foyers and Strontian intrusions. This is also the case for the Ben Nevis intrusion where the inner granite and the outer granite cannot be related by in-situ fractional crystallization but the rare earth patterns for the two parts of the intrusion are so similar that the source must be similar; the only difference in the trace element trends for the two parts of the intrusion resulting from different fractional crystallization assemblages, different degrees of partial melting or differing degrees of crustal contamination. The Etive complex is also similar in that the Cruachan and Starav units may not be related by in-situ fractional crystallisation; the Starav unit shows evidence of a much larger degree of fractional crystallization of feldspars than the Cruachan unit and is transitional between the high Sr granites and those of Cairngorm type. For the Lochnagar granite, however, the three in-situ fractional crystallization trends are almost consistent with a single batch of magma; however the annular nature of the intrusion (Oldershaw 1974) and the small but marked difference between the trend for the diorite (trend 1) and the trends for the granite (trends 2 and 3) indicate that the diorite may be an earlier phase of intrusion perhaps related to the granite by fractional crystallization at depth. The Lochnagar intrusion is particularly important as its composition falls between the hornblende biotite granodiorites and the biotite granites of the Cairngorm type, with trends 1 and 2 involving hornblende in the fractional crystallization assemblage and trend 3 showing an increase in Y with fractional crystallization, implying minimal involvement of hornblende similar to the granites of the Cairngorm type.

The rare earth patterns for the Caledonian granitoids are mostly very fractionated, with the exception the Ardclach granite and the early intrusions in the Lake District which only have slightly light rare earth enriched patterns. The composition of the Ardclach granite is consistent with partial melting of Moine metasediments and its rare earth pattern probably reflects the rare earth chemistry of the source. The change from fairly flat rare earth patterns to strongly light rare earth enriched patterns in the Lake District intrusions cannot be explained by a change in the fractional crystallization assemblage and must therefore be attributed to a change in the source. This is discussed in more detail in Chapter 7.

Key to Figs. in Chapter 7.

Figs. 7:1 to 7:9.

- H - Carrock Fell hybrid granophyre and ferrogabbro.
- - Carrock Fell granophyre.
- L - Carrock Fell leached granophyre.
- ◇ - Ennerdale granophyre.
- \* - Eskdale granodiorite.
- + - Eskdale granite.
- ⌘ - Eskdale greisen.
- ✱ - Skiddaw less geochemically evolved granite.
- △ - Skiddaw more geochemically evolved granite.
- ⊠ - Skiddaw greisen.
- - Shap granite.
- ▽ - Threlkeld microgranite.

Figs. 7:10 and 7:11a.

- G - Carrock Fell gabbro.
- H - Carrock Fell hybrid granophyre and ferrogabbro.
- - Carrock Fell granophyre.
- L - Carrock Fell leached granophyre.
- ◇ - Ennerdale granophyre.
- \* - Eskdale granodiorite.
- + - Eskdale granite.
- ⊠ - Eskdale greisen.
- ✱ - Skiddaw less geochemically evolved granite.
- △ - Skiddaw more geochemically evolved granite.
- ⊠ - Skiddaw greisen.
- - Shap granite.
- ▽ - Threlkeld microgranite.

Figs. 7:11b, 7:14 to 7:38.

- A - Aberdeen granite.
- B - Blackburn granite.
- C - Cairngorm granite.
- D - Dorback granite.
- E - Etive complex.
- F - Foyers complex.
- G - Garabal Hill complex.
- H - Hill of Fare granite.
- I - Kilmelford diorite.
- J - Kilmelford porphyritic granodiorite.
- K - Mt. Battock granite.
- L - Lochnagar granite.
- M - Migdale granite.
- N - Bennachie granite.
- O - Rogart complex.
- P - Peterhead granite.
- Q - Cromar granite.
- R - Ben Rinnes granite.
- S - Strontian complex.
- T - Stritchen granite.
- U - Ballachulish complex.
- V - Glenlivet granite.
- W - Ben Nevis complex.
- Y - Reay diorite.
- Z - Comrie complex.
- △ - Ardclach granite.
- ◇ - Cove Bay granite.
- \* - Moy granite.
- ▽ - Glen Gairn granite.
- ⊛ - Cluanie granodiorite.
- - Strath Ossian granodiorite.
- ⌘ - Moor of Rannoch granodiorite.
- + - Grudie granite.
- ⊠ - Cairnsmore of Fleet granite.

## CHAPTER 7. PETROGENESIS AND REGIONAL VARIATIONS.

## 7:1 INTRODUCTION.

Previous regional geochemical studies of granitoids in the Caledonides (Hall 1969 & 1972) show a regional variation in the major element chemistry parallel to the regional tectonic trend. These studies were based on major elements and CIPW norms and the variation was related to crystallization under different pressure regimes, although no petrogenetic conclusions were drawn. More recent regional geochemical studies of subduction related lavas and granitoids using major and trace elements have identified geochemical variations related to height above the subduction zone or distance from the trench (Dickinson 1975, Saunders et al. 1980). These geochemical variations appear to be restricted to LIL elements and have been interpreted in terms of subduction zone processes or mantle heterogeneity. Similar geochemical variations in primitive Devonian volcanics from Scotland and in Ordovician age volcanics of the "southern" plate have also been interpreted as a result of subduction zone processes (Thirlwall 1982, Fitton & Hughes 1970).

The observed variations in the Caledonian granite suite are discussed in this chapter in terms of fractional crystallization and mantle heterogeneity. In view of the fact that the Lake District forms part of the "southern" plate, which had a separate tectonic history from the "northern" plate for most of the Caledonide orogeny, the Lake District granites are initially discussed separately. However certain aspects of the geochemistry of the late granites of the Lake District (Shap and Skiddaw) are similar to the granitoids of the northern plate which

implies some overall geochemical similarity in granitoid genesis in the two parts of the Caledonide fold belt and therefore an overall discussion is included.

## 7:2. PETROGENETIC VARIATION IN THE LAKE DISTRICT GRANITIDS.

The most obvious petrogenetic variation in the Lake District intrusions is in their rare earth distributions (Fig. 6:32). Those in earlier calc-alkali granites (Threlkeld, Ennerdale and Eskdale) are flat to slightly light rare earth enriched whereas the later granites (Shap and Skiddaw) have very fractionated  $La_N/Lu_N$  ratios. The Ordovician Borrowdale volcanics also have only slightly light rare earth enriched patterns (Thirlwall & Fitton 1983) and appear therefore to be similar to the earlier granites in this respect.

It has been demonstrated in chapter 6 that this change from flat to steep rare earth patterns is not a result of differences in fractional crystallization assemblages and must therefore be a function of the source composition or melting conditions. The derivation of granites with very steep rare earth patterns (as initial basaltic or more likely andesitic liquids) from a source with residual garnet appears to be the most likely explanation of the fractionated  $La_N/Lu_N$  ratios. It is difficult to envisage much fractional crystallization in the genesis of the Shap granite which shows no negative Eu anomaly in the rare earth pattern (Fig. 6:31) and no evidence of hornblende fractionation in the heavy rare earth pattern where fractional crystallization of a combined hornblende + plagioclase assemblage might not generate a negative Eu anomaly but would leave a hornblende "signature" in the heavy rare earth

pattern. The Skiddaw granite has obviously undergone some degree of fractional crystallization as shown by the small negative Eu anomalies in the rare earth patterns (Fig. 6:31) and the depleted levels of Sr seen in mantle normalized trace element patterns (Fig. 4:2). Sr and Ba also appear to be depleted in the mantle normalized trace element pattern for Shap (Fig. 4:2), which does not appear to have undergone significant fractional crystallization, therefore this depletion may be inherited from the source. If this is the case then the parental magmas to the Skiddaw granite may also have low Sr and Ba relative to the other LIL elements.

The Eskdale granite, Threlkeld microgranite, Ennerdale and Carrock granophyres all appear, from both mantle normalized trace element plots (Fig. 4:2) and rare earth patterns (Fig. 6:31), to have undergone considerable fractional crystallization. Although there are differences in the fractional crystallization assemblages, particularly noticeable in the effects on Zr, Nb, Cr, V, Y and the rare earth elements (Figs. 7:1, 7:2, 7:3, 7:4, 7:5 and 7:6), there does appear to be a fundamental compositional difference between these intrusions and the Shap and Skiddaw granites particularly for Sr, Ba and Rb (Figs. 7:7, 7:8 and 7:9) even allowing for the possibility that the Shap granite may have suffered Rb enrichment through metasomatism (cf. Chapter 5). Additionally, it is possible that their Rb/Sr ratios vary primarily as a result of source variation (Fig 7:10) with the later granites being more enriched in Rb relative to Sr.

The geochemical data suggest some source variation in the Caledonian granites of the Lake District which is expressed temporally rather than

Fig. 7:1. Harker type  $\text{SiO}_2$  vs. Zr variation diagram for the Lake District Caledonian granitoids; key to symbols on fold out sheet.

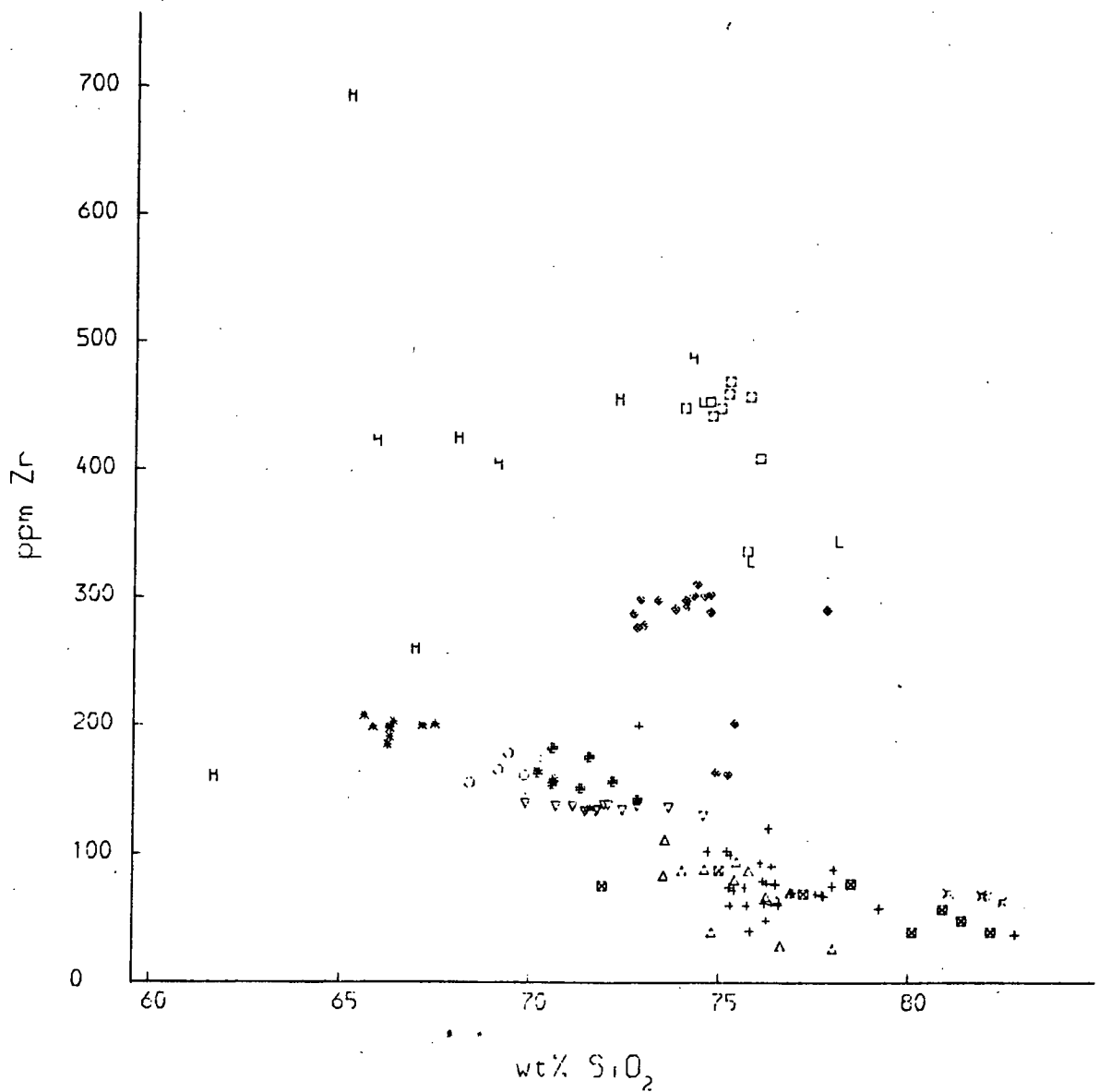


Fig. 7:2. Harker type  $\text{SiO}_2$  vs. Nb variation diagram for the Lake District Caledonian granitoids; key to symbols on fold out sheet.

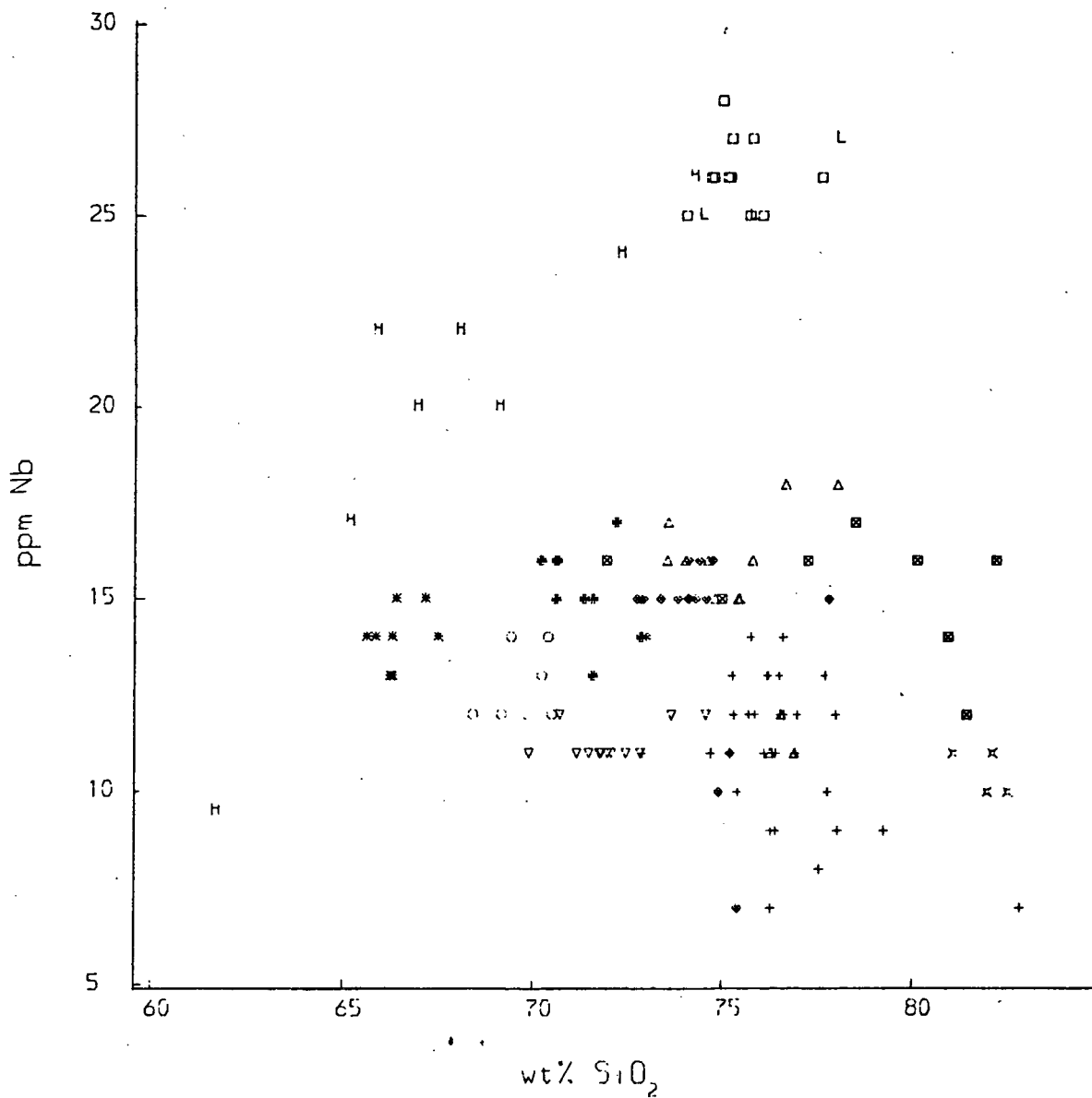


Fig. 7:3. Harker type  $\text{SiO}_2$  vs. Cr variation diagram for the Lake District Caledonian granitoids; key to symbols on fold out sheet.

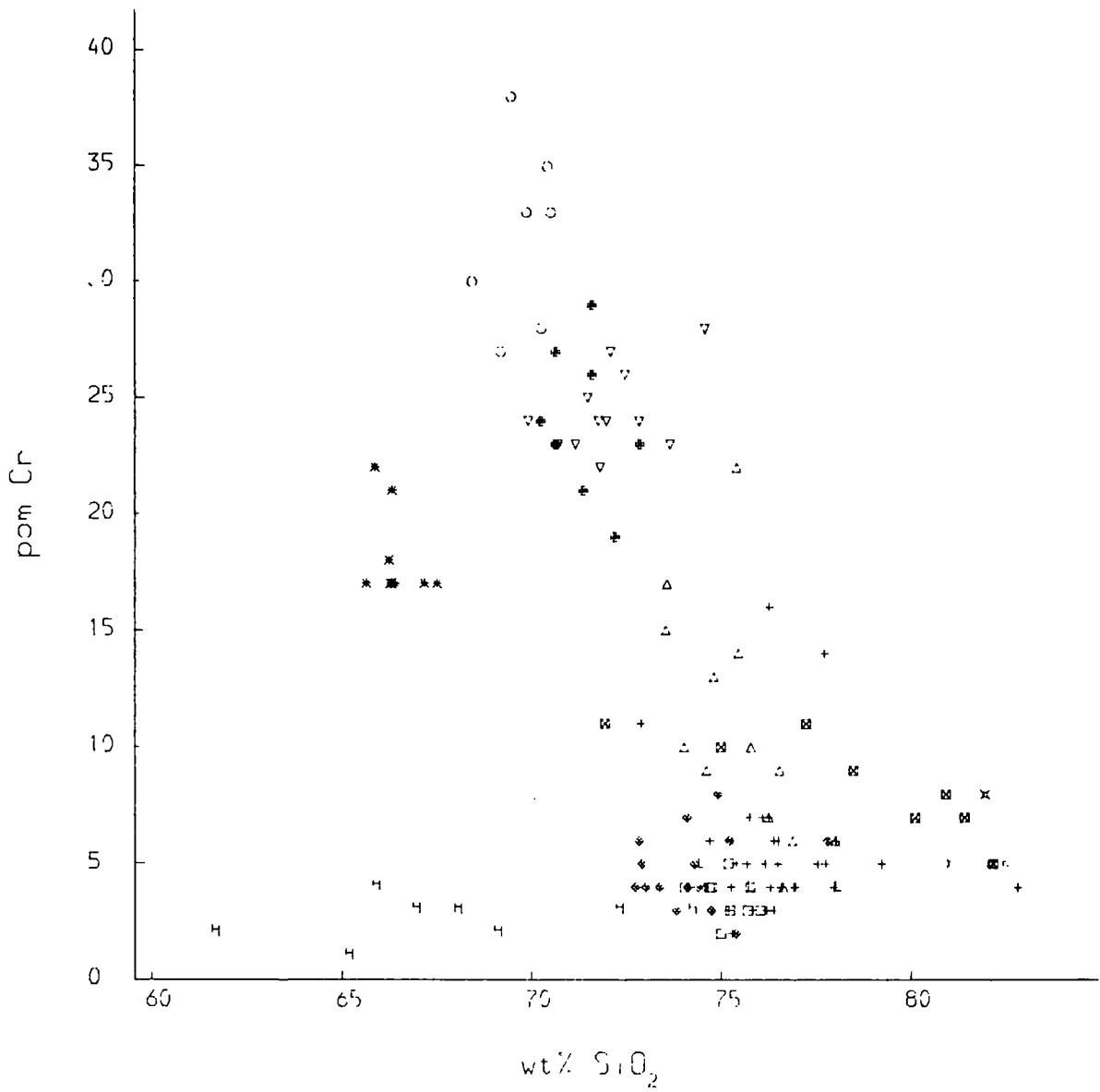


Fig. 7:4. Harker type  $\text{SiO}_2$  vs. V variation diagram for the Lake District Caledonian granitoids; key to symbols on fold out sheet.

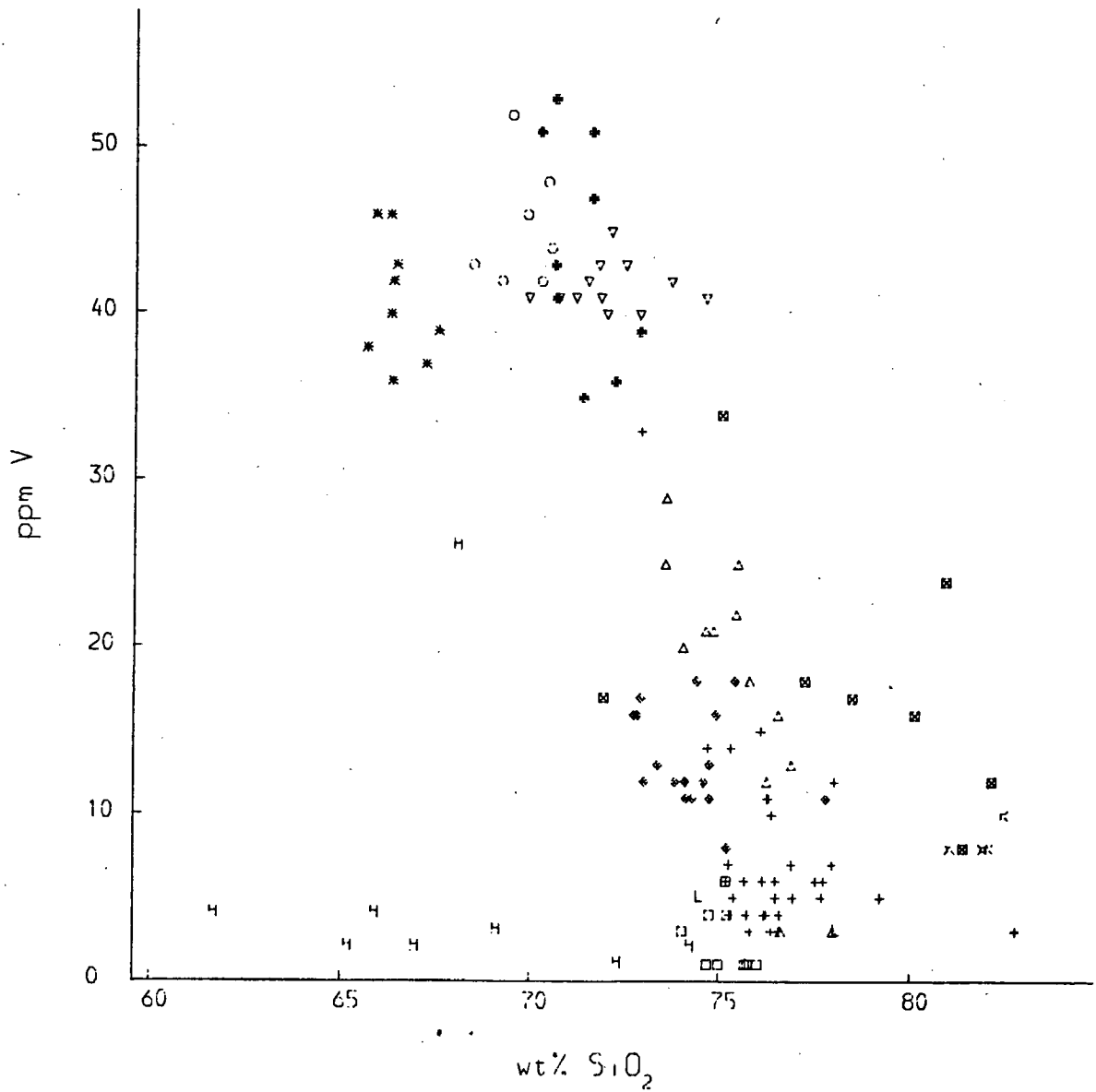


Fig. 7:5. Harker type  $\text{SiO}_2$  vs. Y variation diagram for the Lake District Caledonian granitoids; key to symbols on fold out sheet.

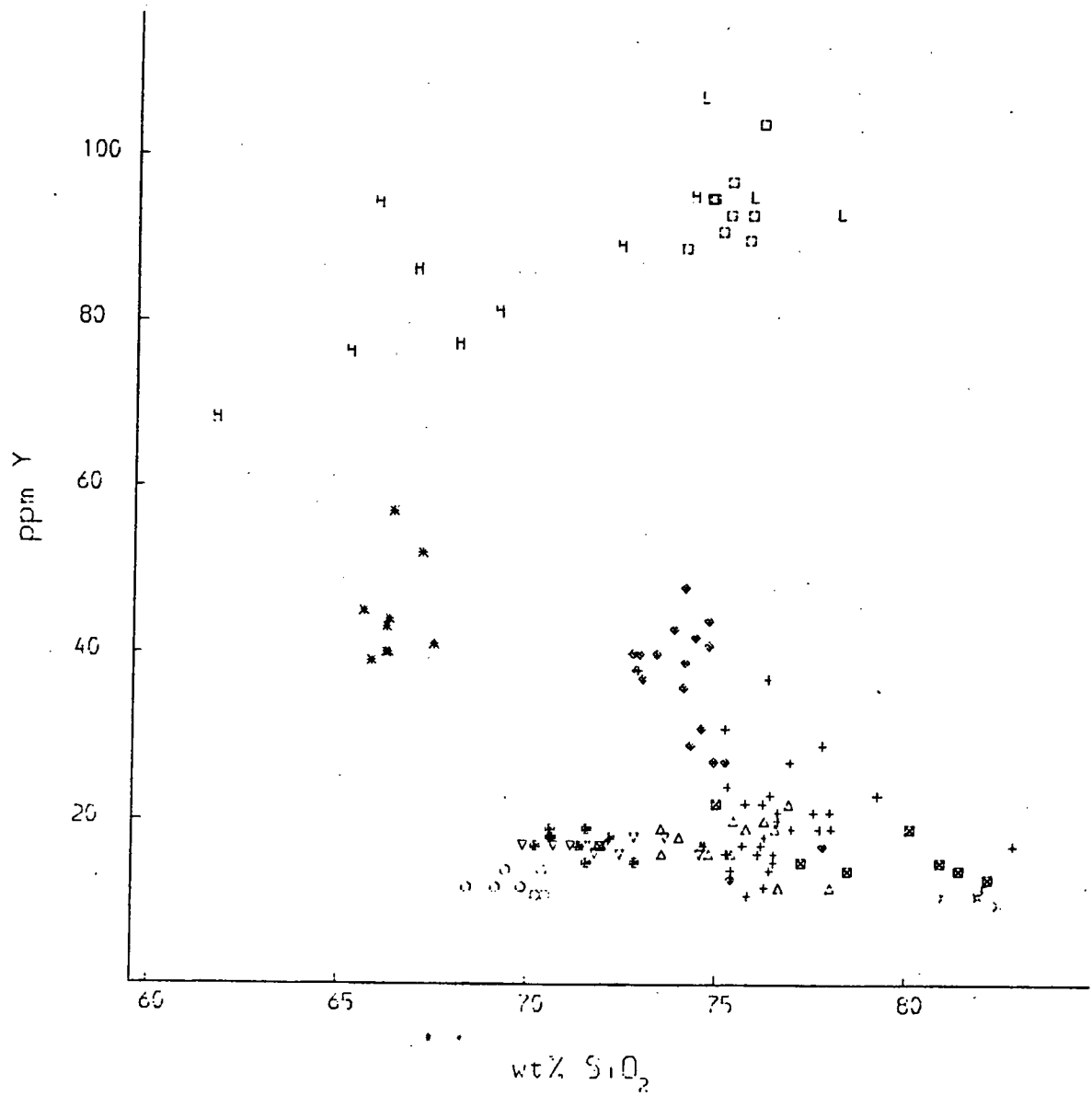


Fig. 7:6. Harker type  $\text{SiO}_2$  vs. Ce variation diagram for the Lake District Caledonian granitoids; key to symbols on fold out sheet.

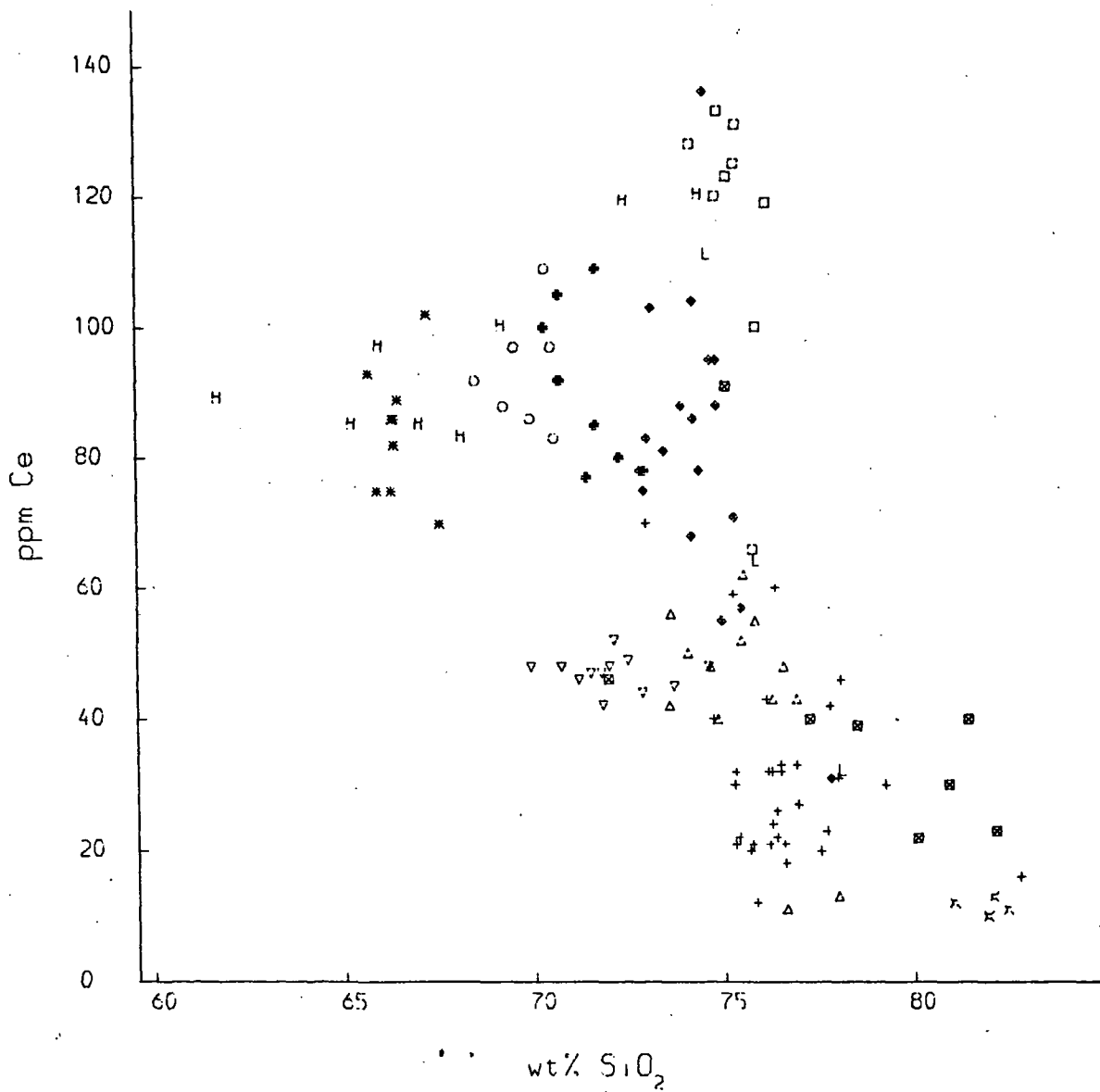


Fig. 7:7. Harker type  $\text{SiO}_2$  vs. Sr variation diagram for the Lake District Caledonian granitoids; key to symbols on fold out sheet.

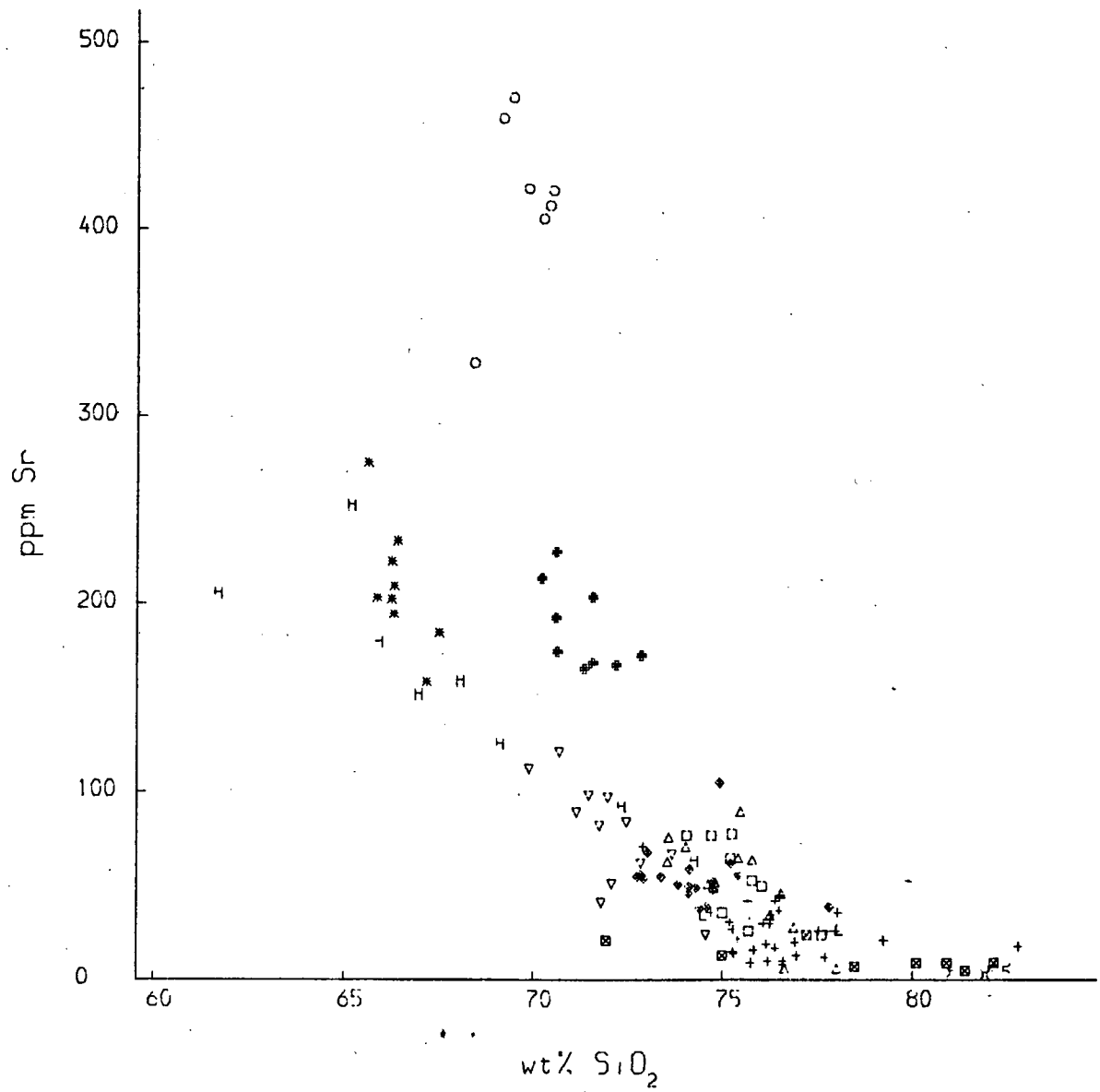


Fig. 7:8. Harker type  $\text{SiO}_2$  vs. Ba variation diagram for the Lake District Caledonian granitoids; key to symbols on fold out sheet.

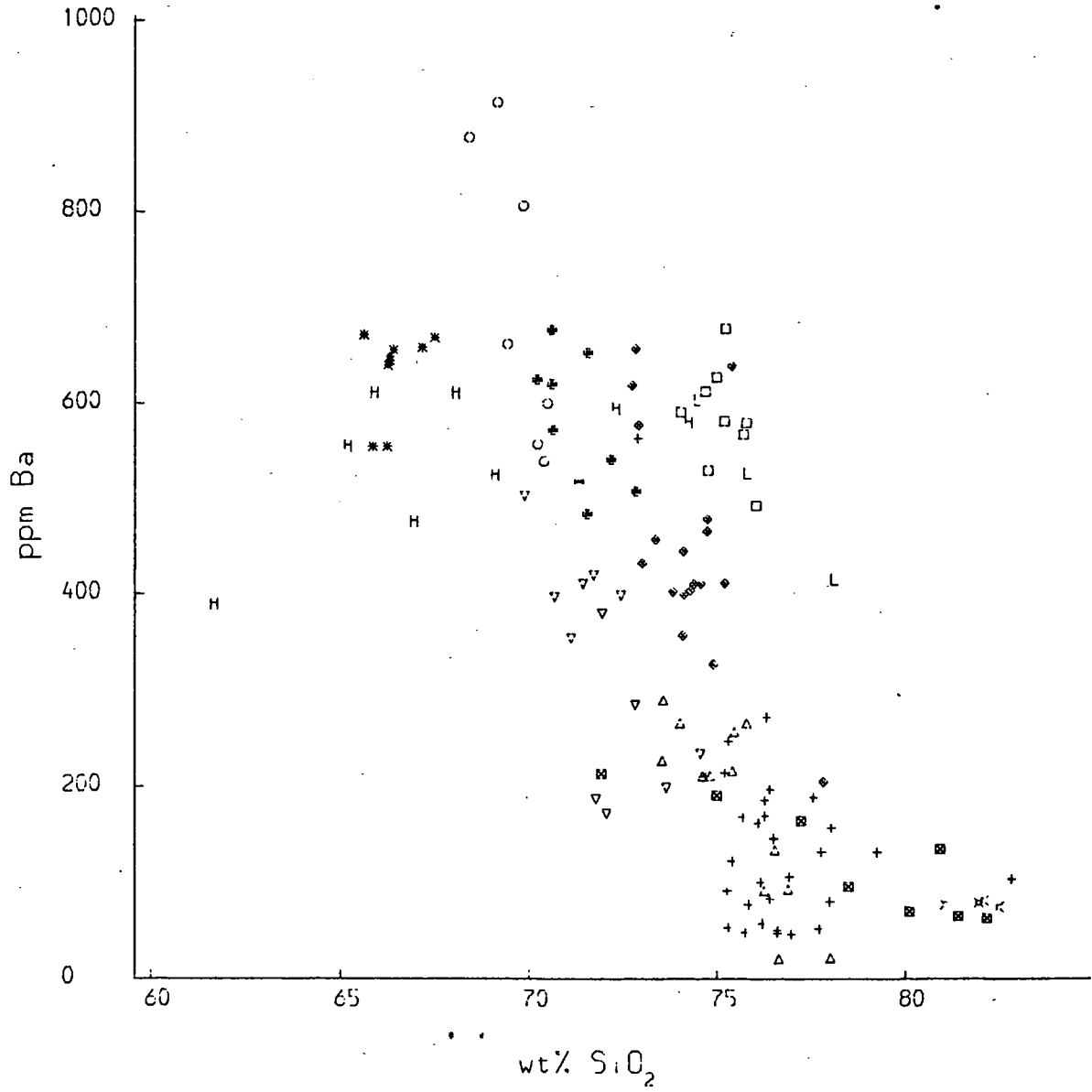


Fig. 7:9. Harker type  $\text{SiO}_2$  vs. Rb variation diagram for the Lake District Caledonian granitoids; key to symbols on fold out sheet.

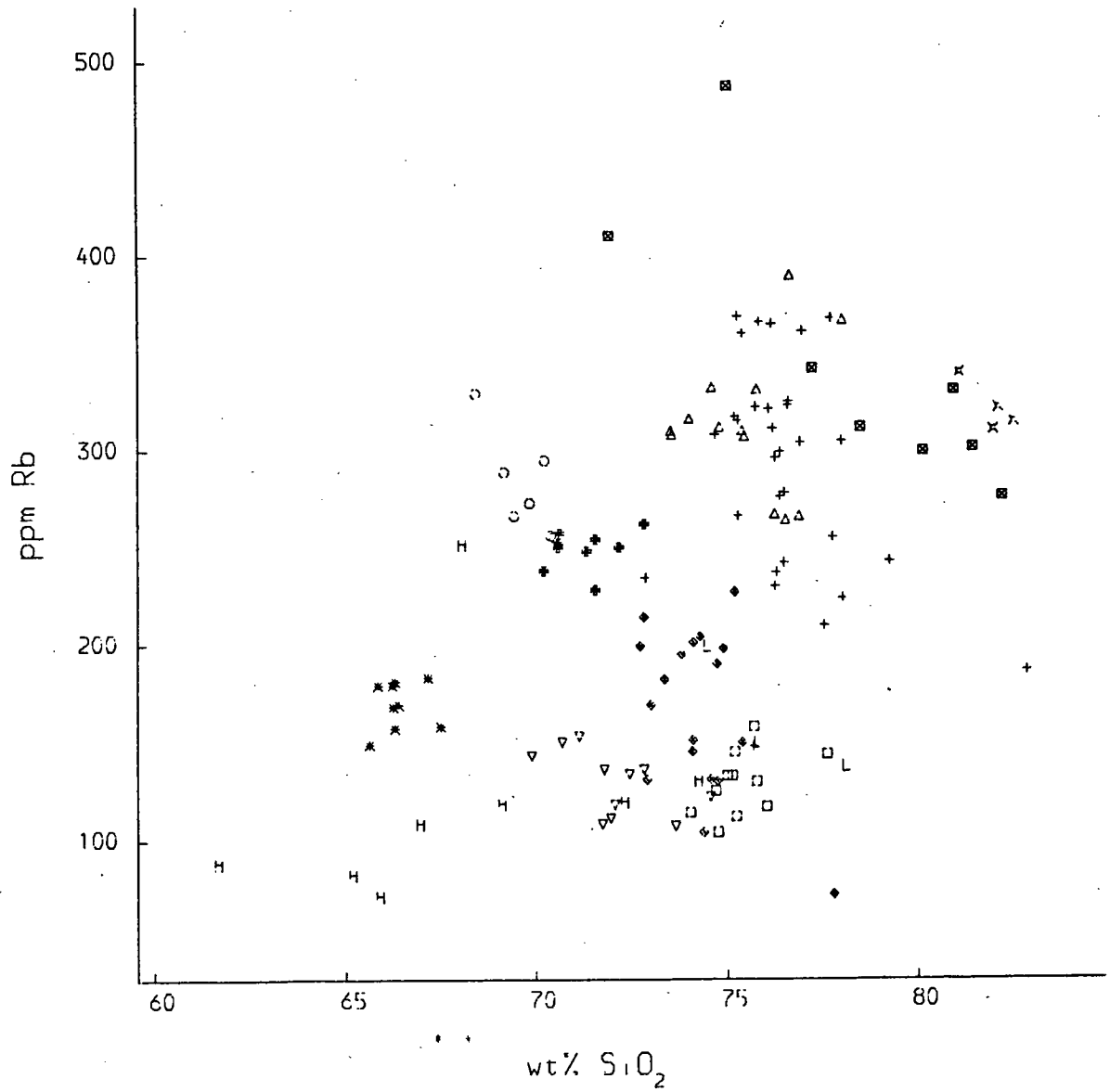
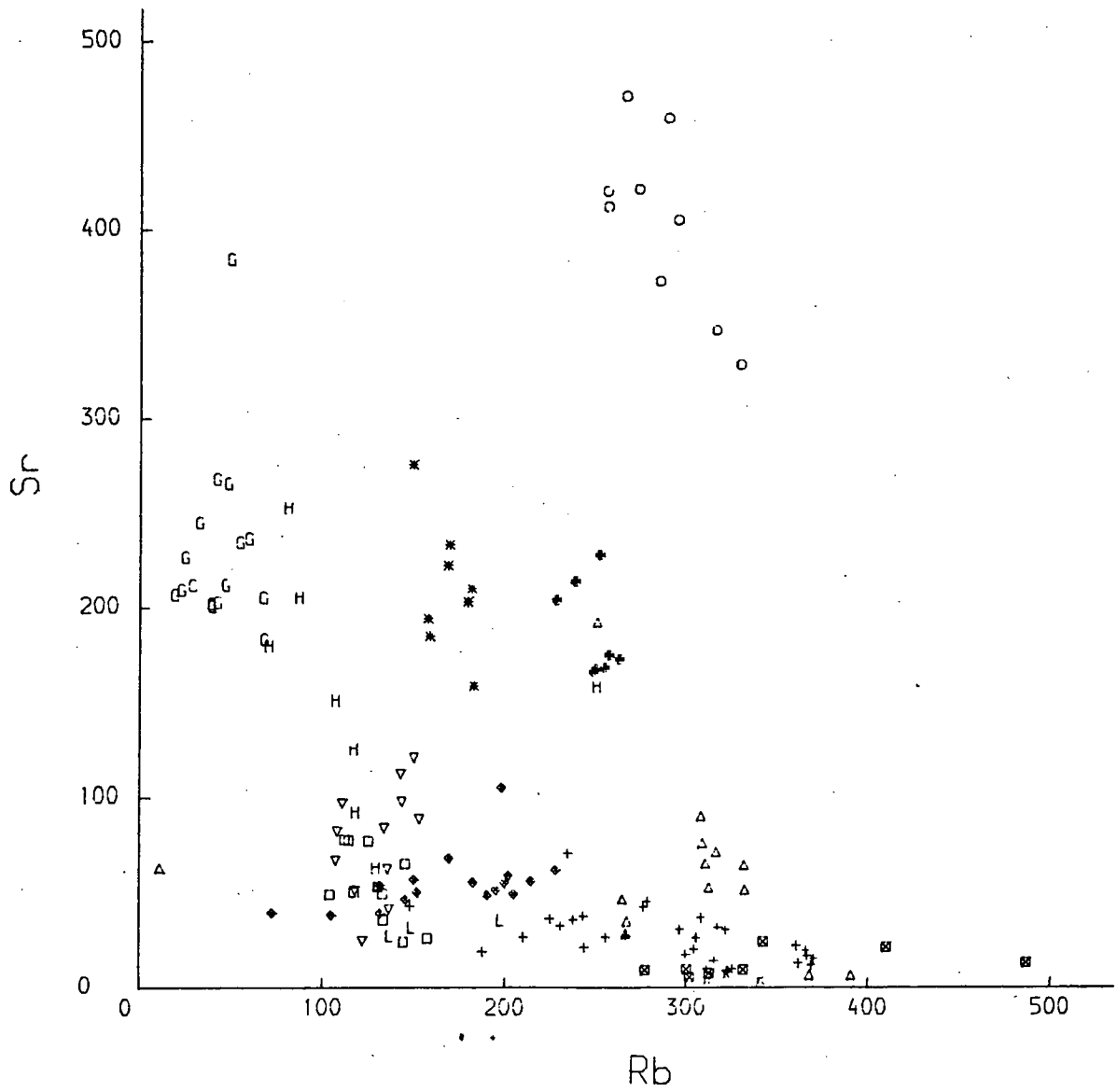


Fig. 7:10. Rb vs. Sr variation diagram for the Lake District Caledonian granitoids; key to symbols on fold out sheet.



spatially. The earlier intrusions, in particular the Carrock granophyre and hybrid suite, are related to the early tholeiitic magmatism and are characterized by flat REE patterns. The Ennerdale granophyre, Threlkeld microgranite and Eskdale granite are calc-alkaline (Fig 7:11) and are characterized by only mild light rare earth enrichment; similarly the Borrowdale volcanics are characterized by mild light rare earth enrichment (Fitton et al. 1982), and are similar to that of the early tholeiitic Carrock granophyre and hybrid suite. The two late calc-alkali granites of the Lake District Shap and Skiddaw have rather different chemistry to the earlier calc-alkali intrusions with rare earth patterns indicative of a basic source with residual garnet, unlike the earlier granitoids which cannot have residual garnet in the source. The implications of this temporal source variation are discussed in chapter 8.

### 7:3 PETROGENETIC VARIATIONS IN THE SCOTTISH CALEDONIAN GRANITOIDS.

It is evident from Table 6:1 that the composition of the Scottish granitoids is extremely variable. Some distinct regional variations are nevertheless apparent. For instance, granitoids with high levels of Sr are generally located in the central and western regions of Scotland, whereas granites with low Sr values predominate in eastern Scotland. This can be graphically demonstrated by choosing a range of  $\text{SiO}_2$ , in this case 68 to 73 wt%, and plotting a statistical map of Sr concentrations over the region (Fig. 7:12). A similar but inverse relationship is seen with Rb concentrations (Fig. 7:13). It is tempting to conclude that this spatial distribution is closely connected to some regional difference in the source across Scotland, as was inferred by Thirlwall

Fig. 7:11. a) AFM diagram for the Lake District Caledonain granitoids, b) AFM diagram for the Scottish Caledonian granitoids; key to symbols on fold out sheet.

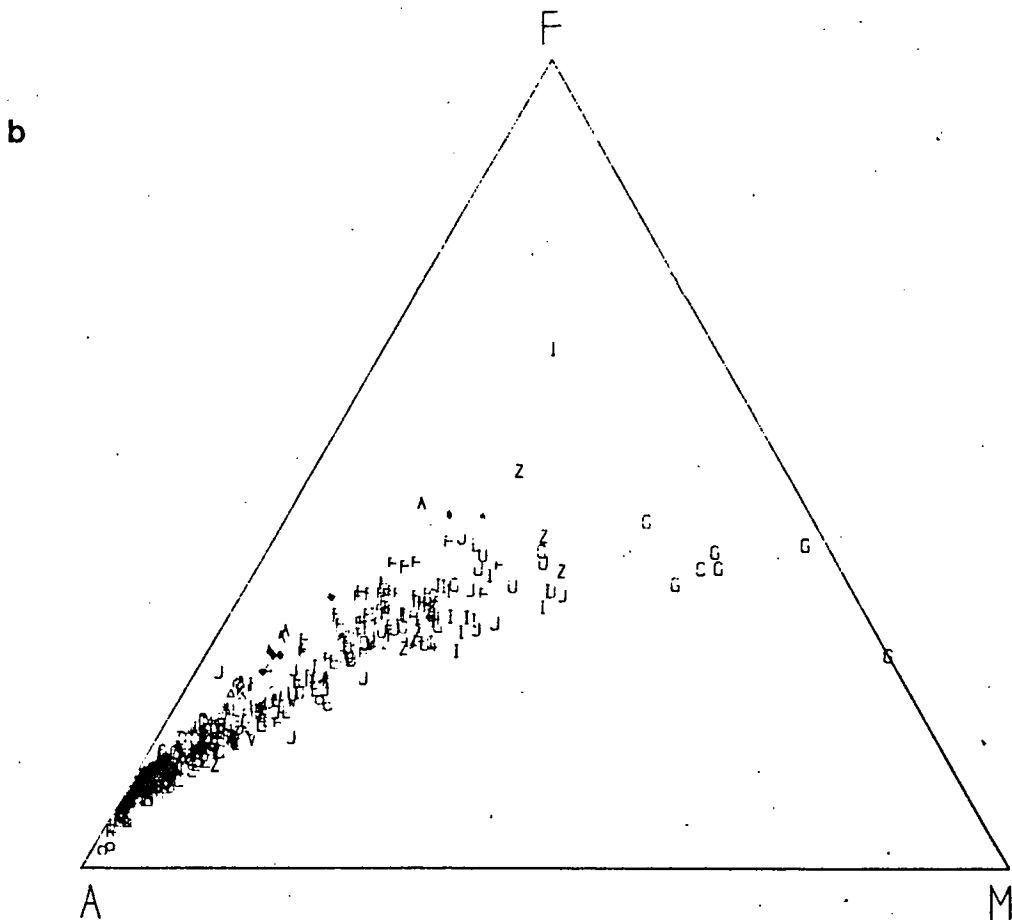
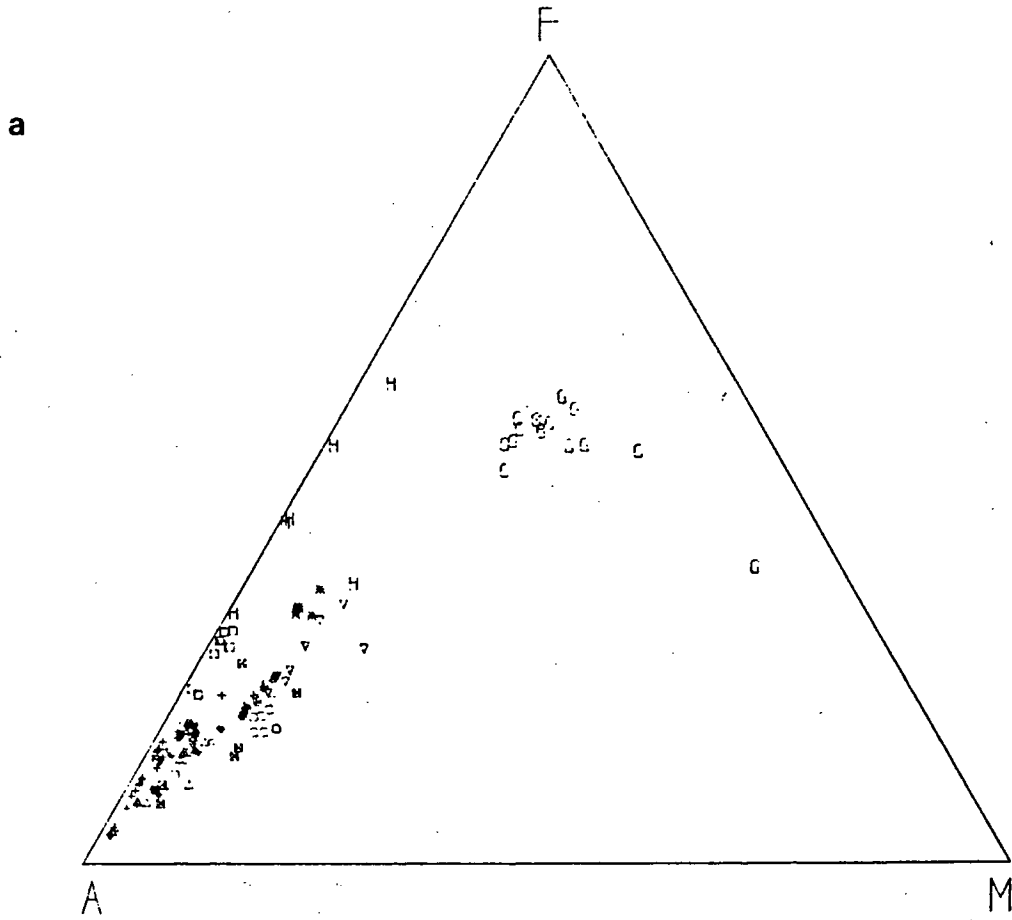


Fig. 7:12. Contoured map for Sr in Scottish granite samples with SiO<sub>2</sub>  
68-73 wt% (see over page).

Fig. 7:12. Contoured map for Sr in Scottish granite samples with  $\text{SiO}_2$   
68-73 wt%.

Fig. 7:12

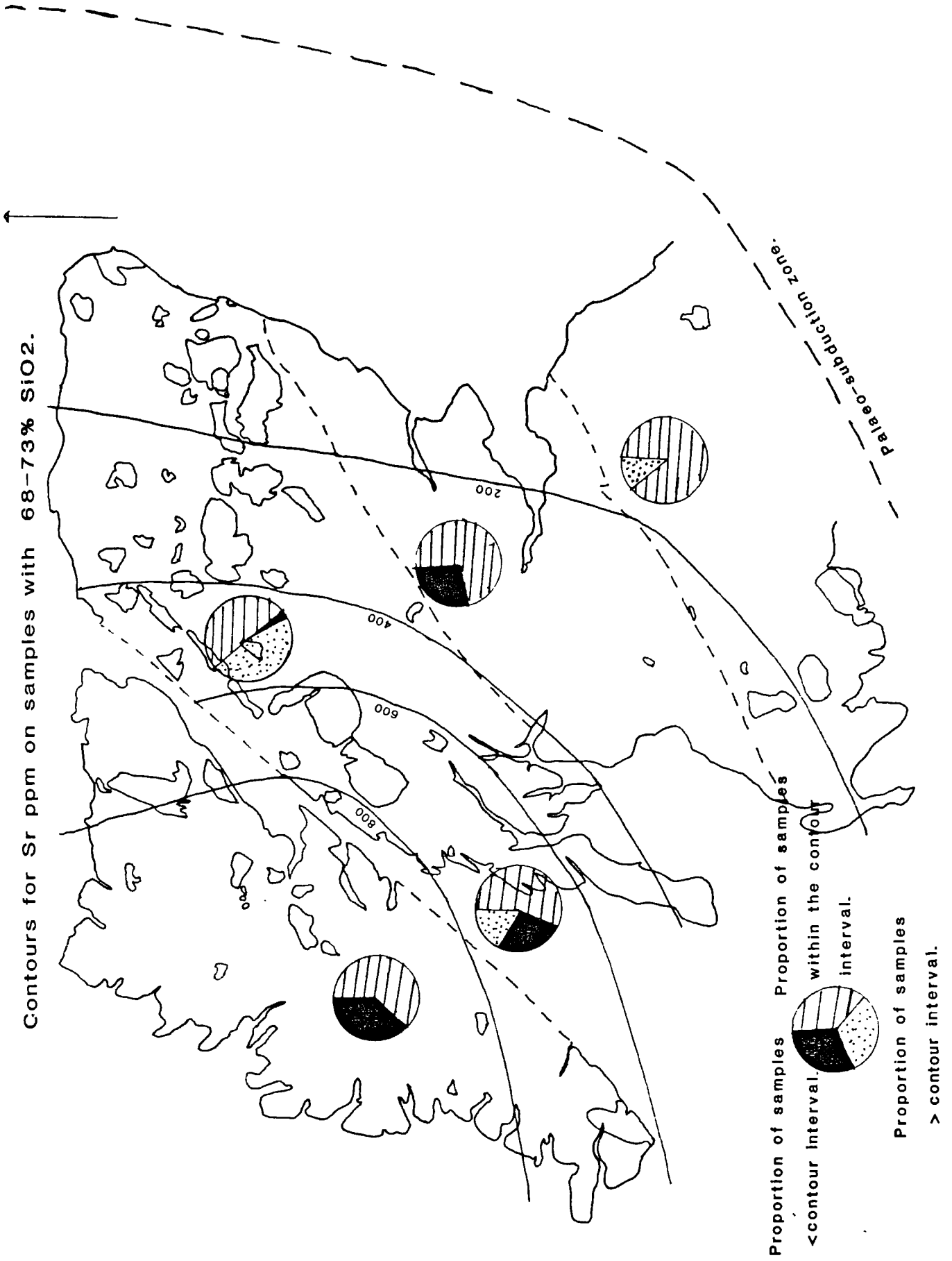
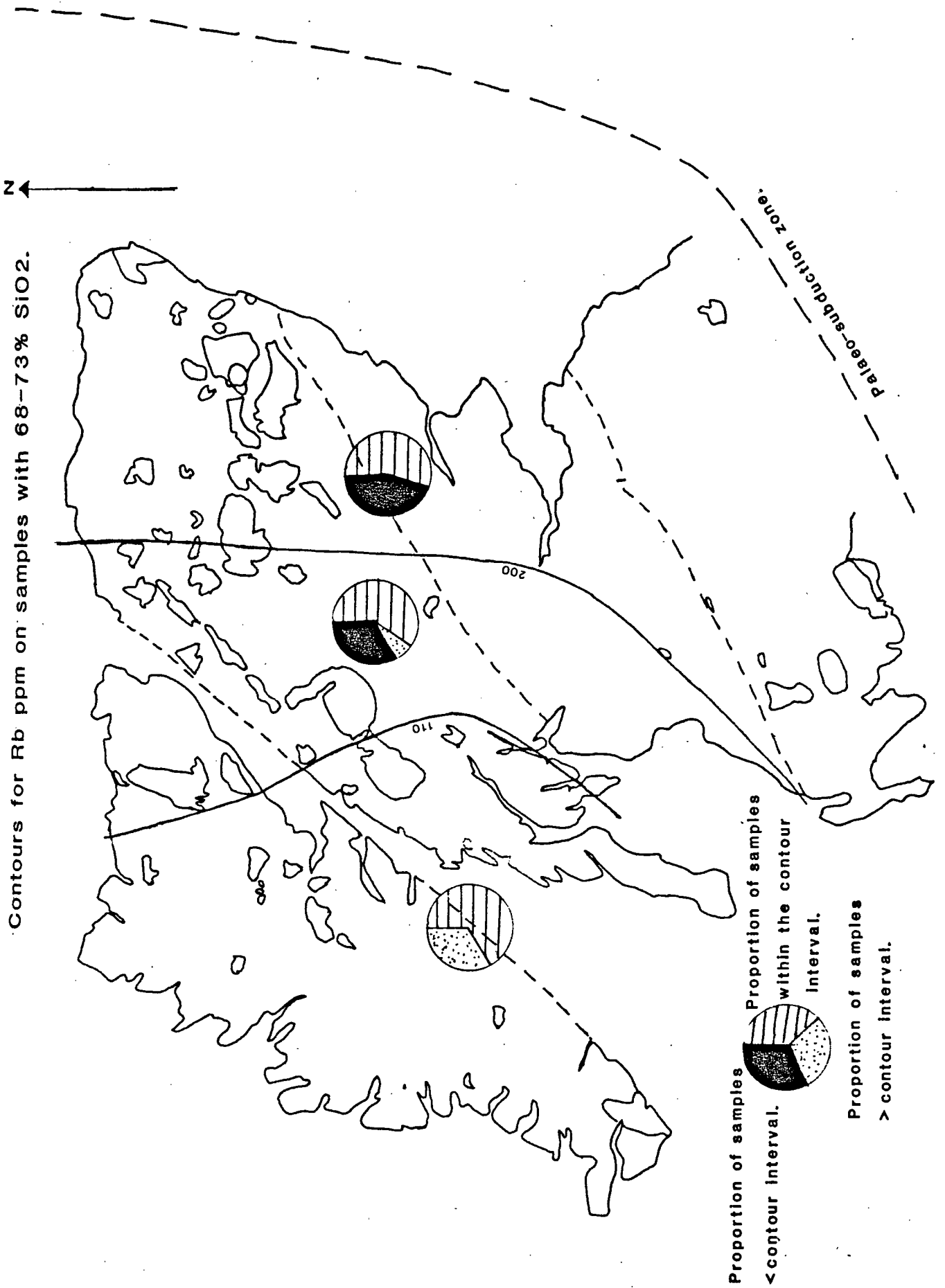


Fig. 7:13. Contoured map for Sr in Scottish granite samples with SiO<sub>2</sub>  
68-73 wt% (see over page).

Fig. 7:13. Contoured map for Rb in Scottish granite samples with SiO<sub>2</sub>  
68-73 wt%.

Fig. 7:13

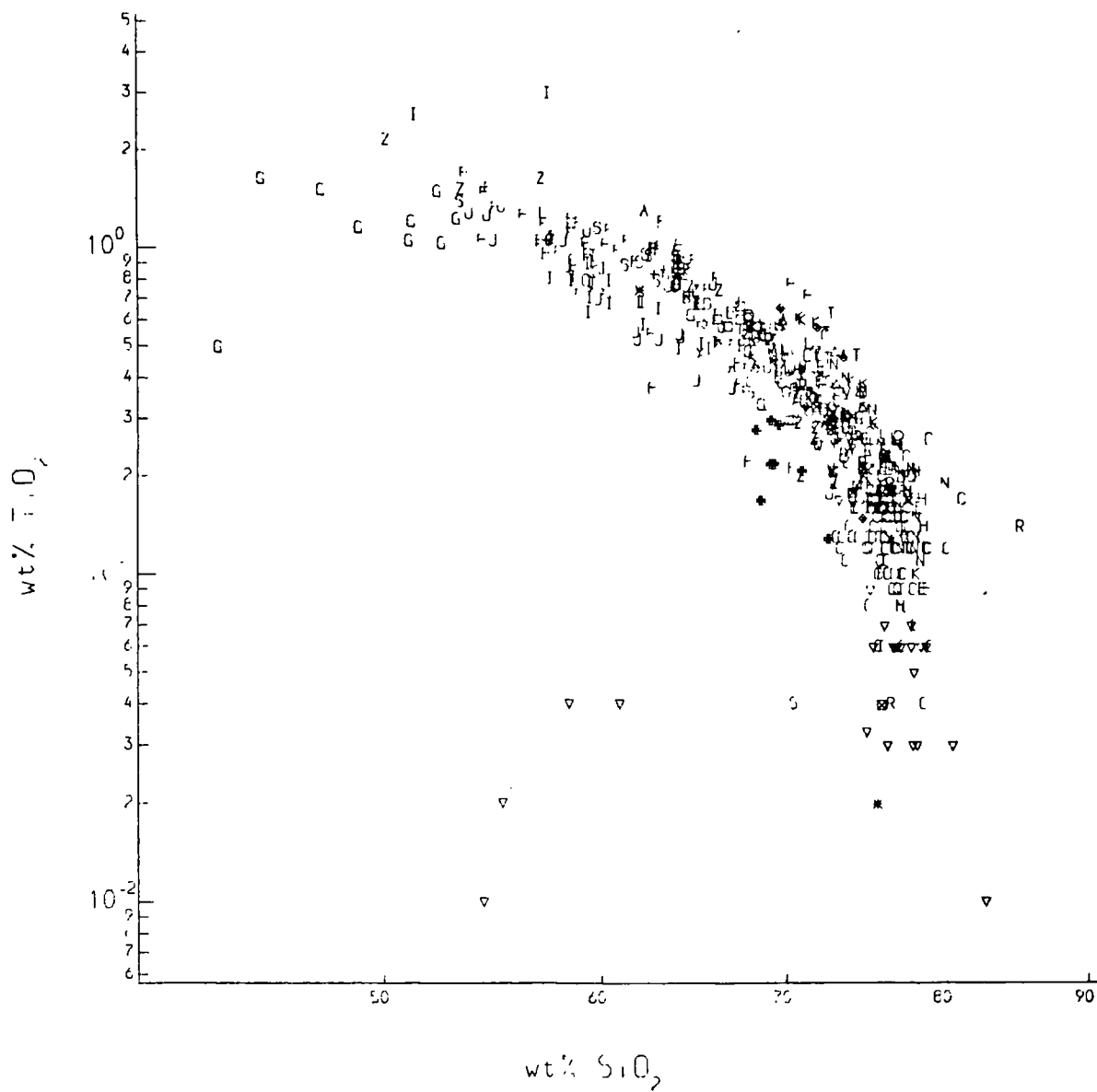


(1982) from geochemical studies of primitive samples of Devonian lavas. However the high levels of  $\text{SiO}_2$  used here in order to generate an even cover of samples across Scotland renders such a conclusion invalid since different fractional crystallization assemblages have a marked effect on the rate of increase of  $\text{SiO}_2$  with fractional crystallisation. The amount of feldspar involved in fractional crystallization is the most significant factor since a feldspar dominated fractional crystallization assemblage will not result in the rapid rate of  $\text{SiO}_2$  increase that is observed from a more mafic dominated assemblage. Since insitu fractional crystallization appears to be the sole cause of the internal geochemical variation within the individual intrusions and the fractional crystallization assemblages vary from pluton to pluton it is probable that much of the regional variation may be the result of differing degrees of both in-situ fractional crystallization and fractional crystallization processes prior to emplacement involving different fractional crystallization assemblages.

To pursue this hypothesis further it is necessary to study the major and trace element variations in the Scottish Caledonian granites; the simplest way of doing this is through Harker type diagrams since the behaviour of silica is relatively simple to predict. For the major elements (Figs. 7:14, 15, 16, 17, 18, 19, 20, 21 & 22) the bulk of the samples plot on smooth trends which would be explicable in terms of differing degrees of fractional crystallization and differing fractional crystallization assemblages.

For  $\text{TiO}_2$  (Fig. 7:14) the bulk of the samples indicate a decrease in  $\text{TiO}_2$  with increasing  $\text{SiO}_2$ . The rate of change of  $\text{TiO}_2$  concentrations is

Fig. 7:14. Harker type  $\text{SiO}_2$  vs.  $\text{TiO}_2$  variation diagram for the Scottish Caledonian granitoids; key to symbols on fold out sheet.



variable and consistent with changes in both the proportion and composition of the mafic minerals in the fractional crystallization assemblage. The data for certain plutons do not plot on the main trend, for instance samples from the Cluanie granodiorite have lower levels of  $TiO_2$  than intrusions with similar  $SiO_2$  contents and samples from the Kilmelford complex appear to follow a different trend to the other intrusions with relatively low  $SiO_2$ .

The trend described by  $Al_2O_3$  (Fig. 7:15) is more complex, the least  $SiO_2$  rich samples from the Garabal Hill complex, Kilmelford and the Ballachulish granodiorite show a rapid increase in  $Al_2O_3$  with increasing  $SiO_2$  which is compatible with the removal of a pyroxene or hornblende rich cumulate assemblage. The rest of the samples form a trend with decreasing  $Al_2O_3$  with increasing  $SiO_2$  compatible with a cumulus assemblage containing feldspars. The samples from the Foyers tonalite are significantly richer in  $Al_2O_3$  than the other samples on this second trend, which may be compatible with some entrained cumulus plagioclase. This second trend appears to form two sections, the significance of which is not clear. Samples from the Cluanie granodiorite are enriched in  $Al_2O_3$  relative to the main trend.

The trend for  $Fe_2O_3$  (Fig. 7:16) is similar in all respects to that for  $TiO_2$ . Samples from the Cluanie granodiorite are significantly lower in  $Fe_2O_3$  relative to the main trend. Samples from the Aberdeen, Cove Bay, Strichen and Ardclach granites have significantly higher  $Fe_2O_3$  relative to the main trend.

Fig. 7:15. Harker type  $\text{SiO}_2$  vs.  $\text{Al}_2\text{O}_3$  variation diagram for the Scottish Caledonian granitoids; key to symbols on fold out sheet.

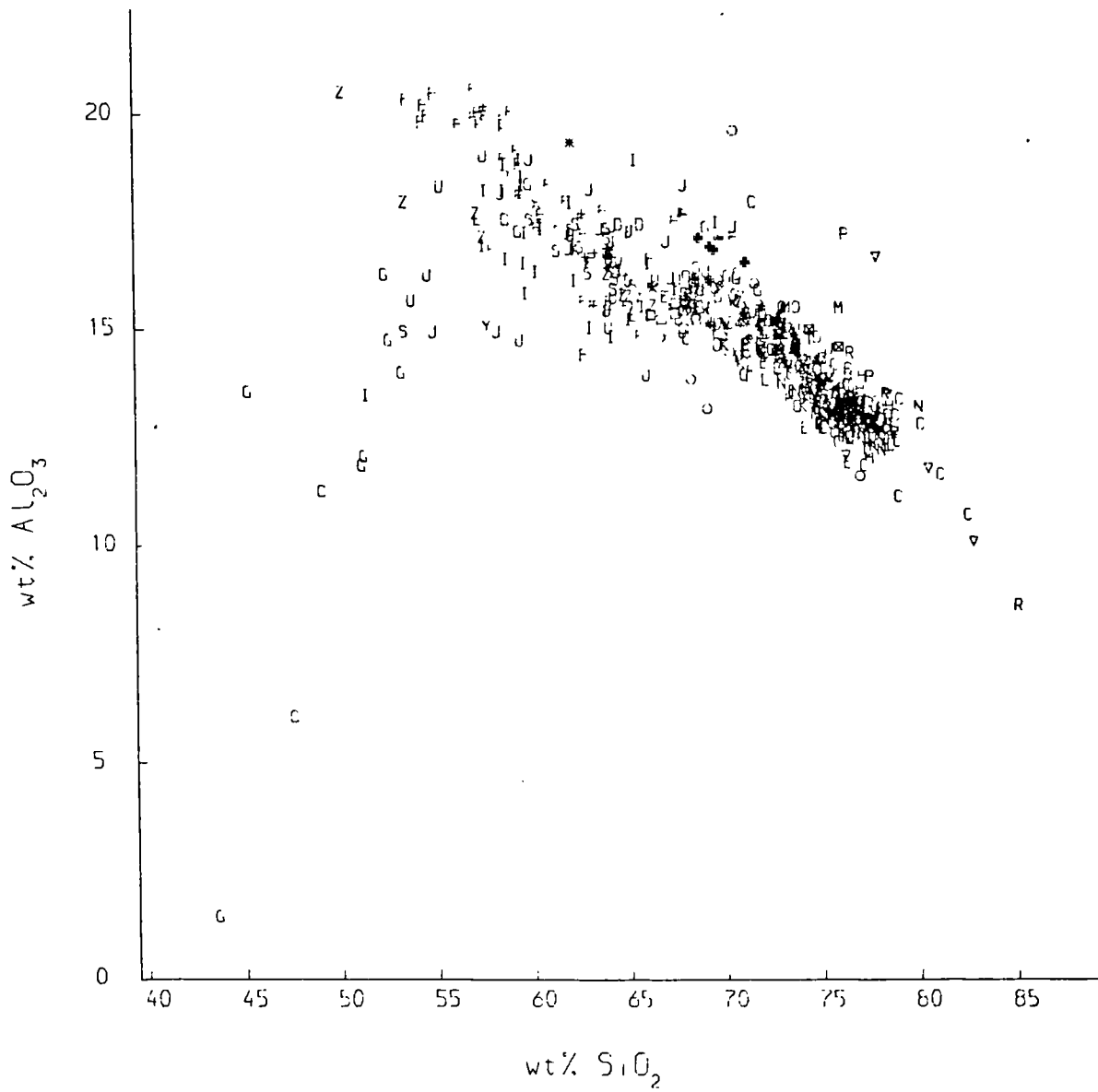
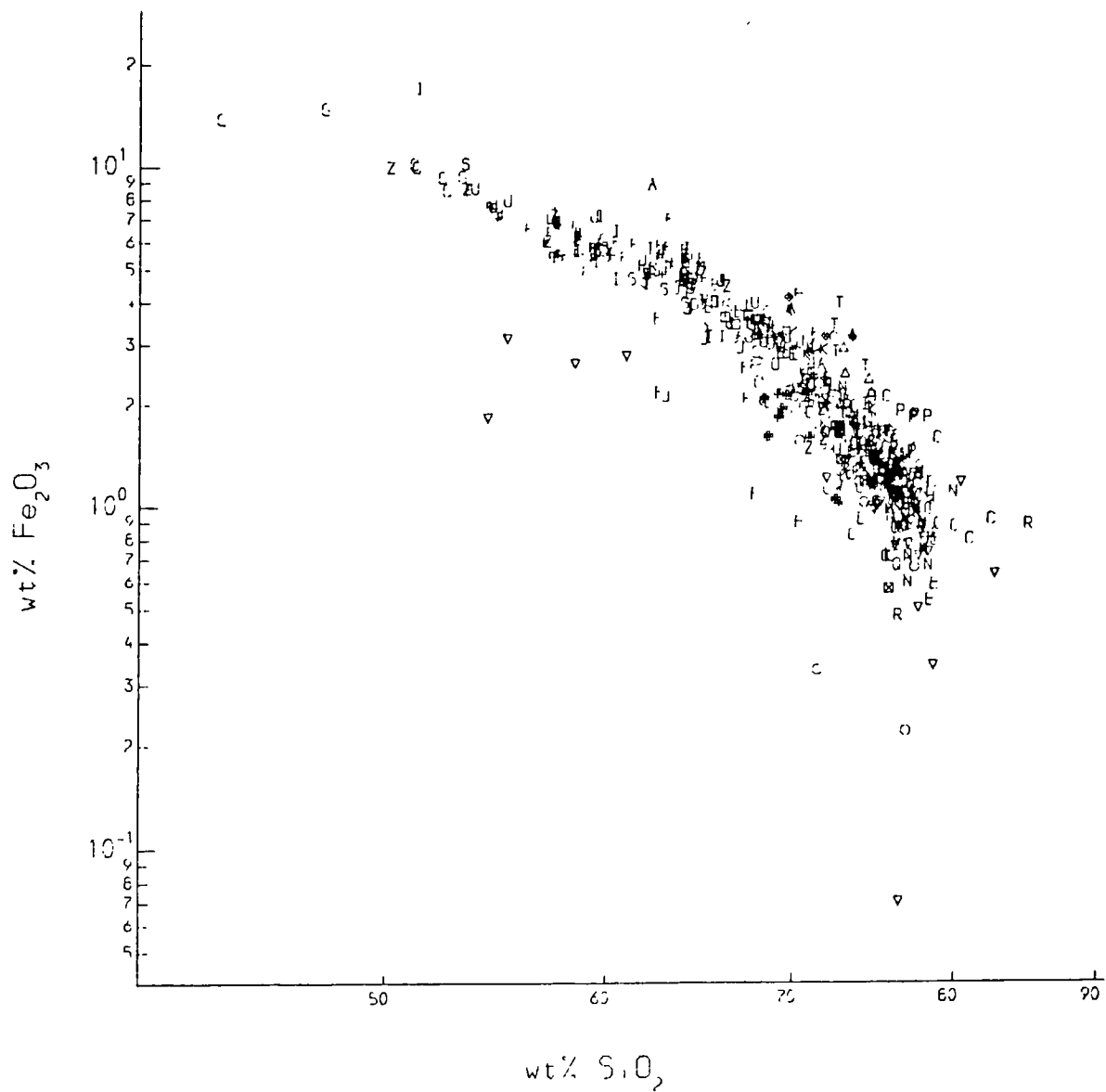


Fig. 7:16. Harker type  $\text{SiO}_2$  vs.  $\text{Fe}_2\text{O}_3$  variation diagram for the Scottish Caledonian granitoids; key to symbols on fold out sheet.



The behaviour of MnO (Fig. 7:17) is more difficult to understand. For samples with  $\text{SiO}_2 < 70\%$  this element behaves in the same way as MgO,  $\text{TiO}_2$  and  $\text{Fe}_2\text{O}_3$  indicating that it is removed from the melts in mafic minerals. However MnO appears to be enriched in the silica rich samples and reaches quite high levels in the Glen Gairn greisens and one sample of the Bennachie granite; it is also noted that MnO concentrations in the biotites within these evolved granites are high. Since igneous hornblendes are generally richer in MnO than igneous biotites (c.f. Appendix C), it may be that in these granites the lack of hornblende in the fractionating assemblages results in the increase in MnO.

The trend for MgO (Fig. 7:18) is similar in all respects to that for  $\text{TiO}_2$ . Samples from the Cluanie granodiorite are significantly lower in MgO relative to the main trend, also samples from the Foyers tonalite are depleted in MgO relative to the main trend.

The trend for CaO (Fig. 7:19) is similar in all respects to that for  $\text{TiO}_2$ . Samples from the Foyers tonalite are significantly lower in CaO relative to the main trend. Also the samples from the Helmsdale granite are significantly lower in CaO relative to the main trend.

$\text{Na}_2\text{O}$  does not form a tightly defined trend with  $\text{SiO}_2$  (Fig. 7:20). However a pattern is discernable. The samples with low silica show increasing  $\text{Na}_2\text{O}$  with  $\text{SiO}_2$ , compatible with the removal of pyroxene or hornblende rich cumulates. The samples with  $>55\text{wt}\% \text{SiO}_2$  show a decrease in  $\text{Na}_2\text{O}$  with fractional crystallization indicating the involvement of feldspars during fractional crystallisation, although within this there are trends at variance with the main trend, for example the Comrie

Fig. 7:17. Harker type  $\text{SiO}_2$  vs.  $\text{MnO}$  variation diagram for the Scottish Caledonian granitoids; key to symbols on fold out sheet.

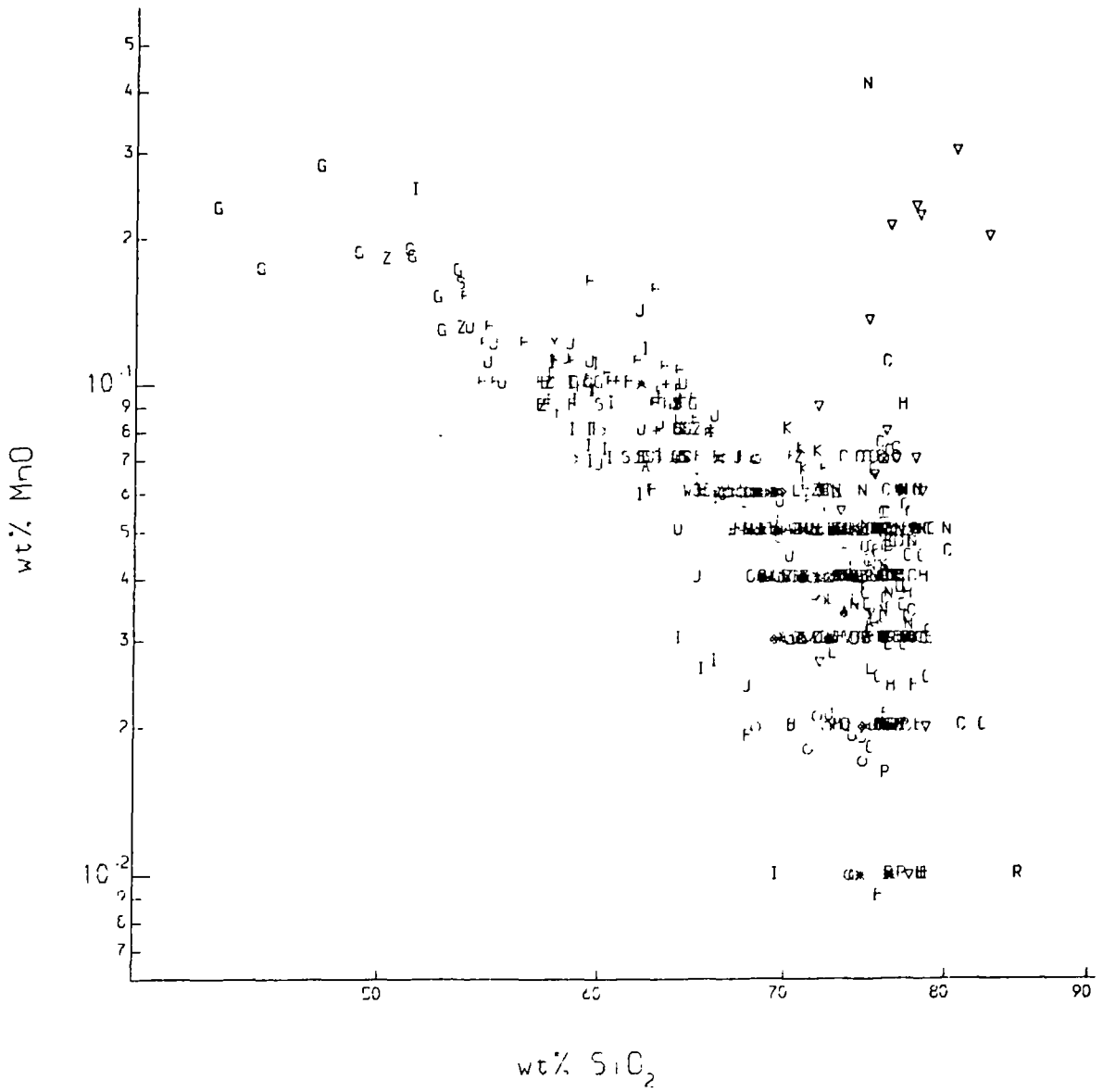


Fig. 7:18. Harker type  $\text{SiO}_2$  vs.  $\text{MgO}$  variation diagram for the Scottish Caledonian granitoids; key to symbols on fold out sheet.

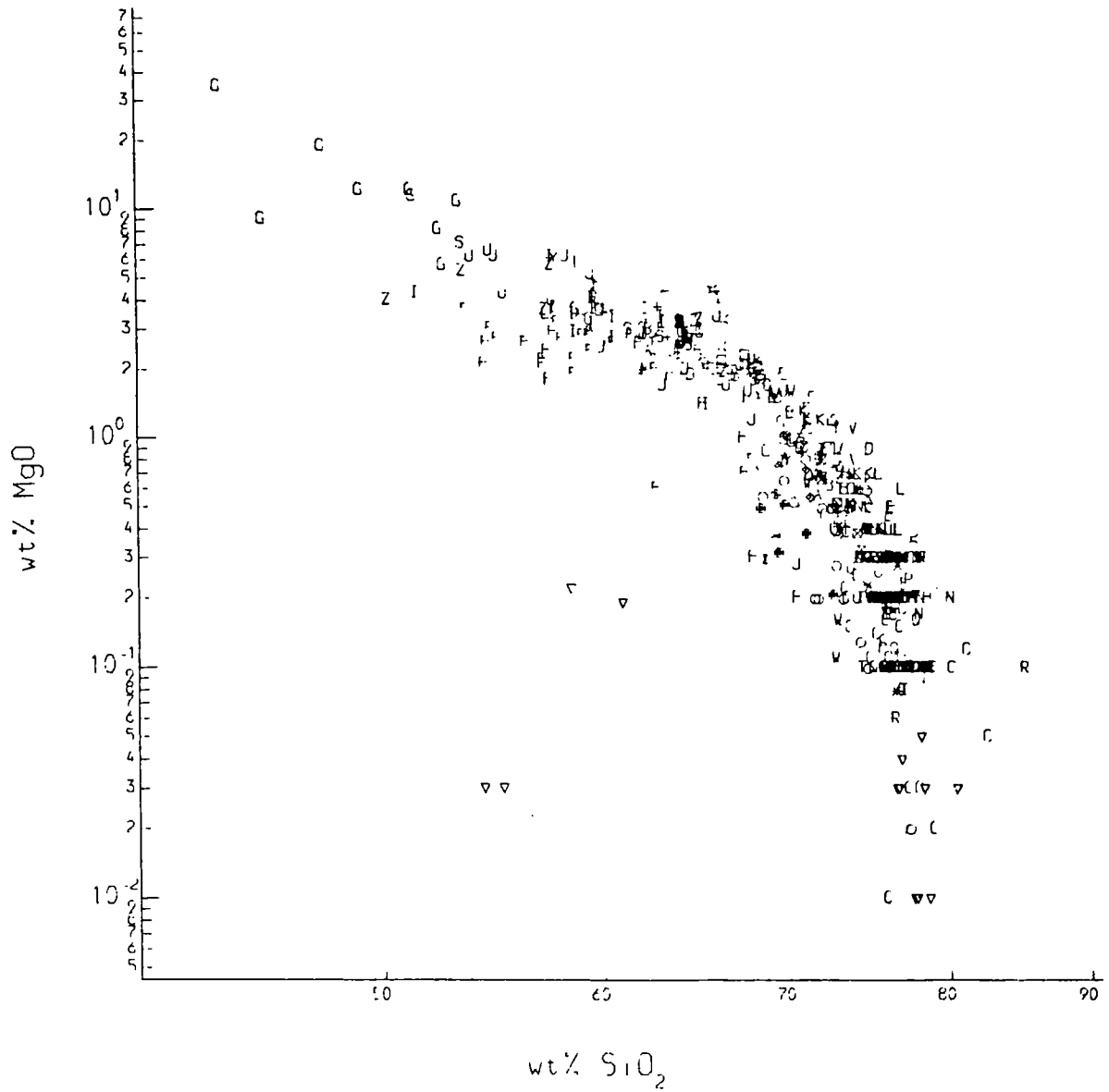


Fig. 7:19. Harker type  $\text{SiO}_2$  vs.  $\text{CaO}$  variation diagram for the Scottish Caledonian granitoids; key to symbols on fold out sheet.

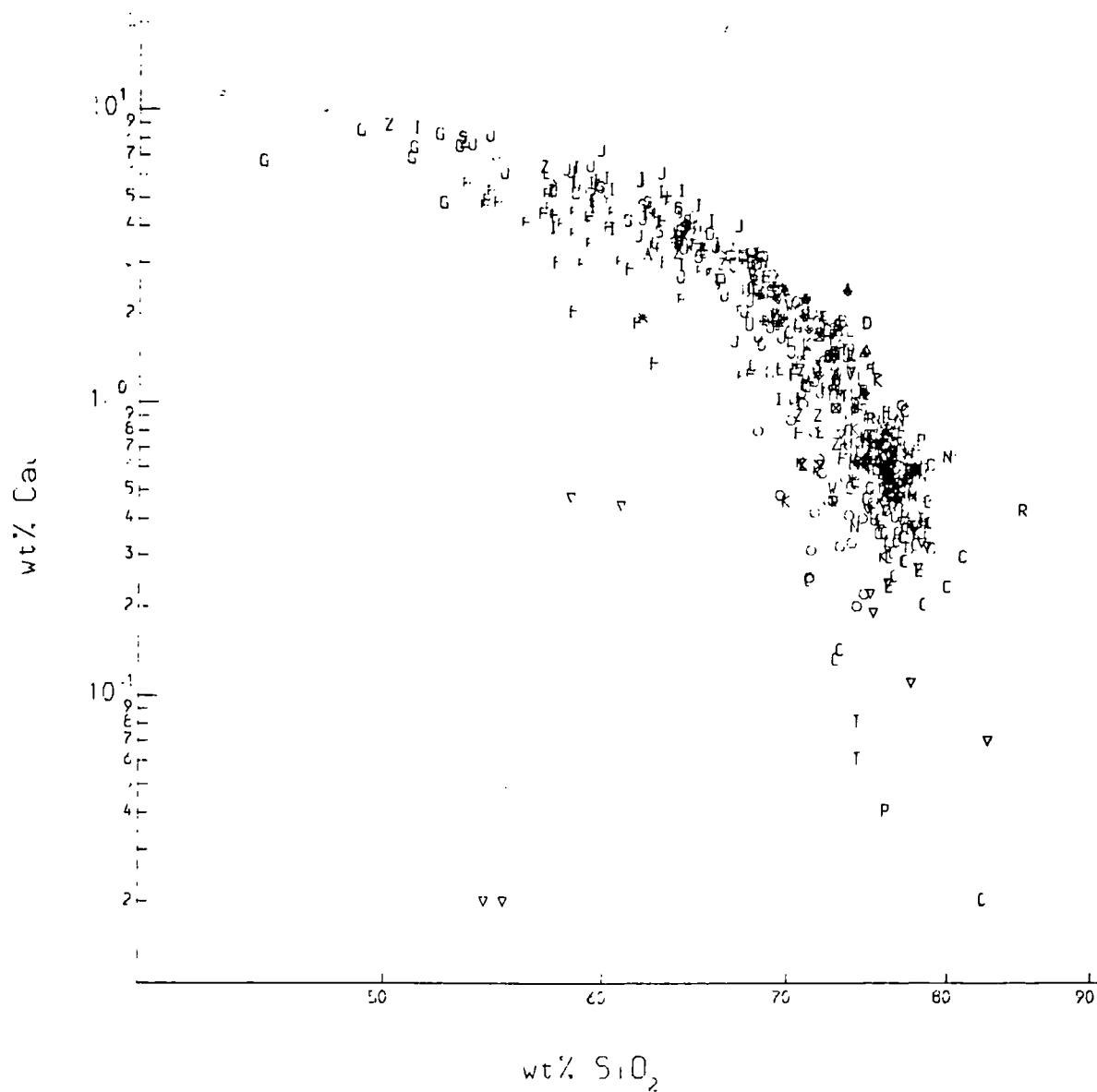
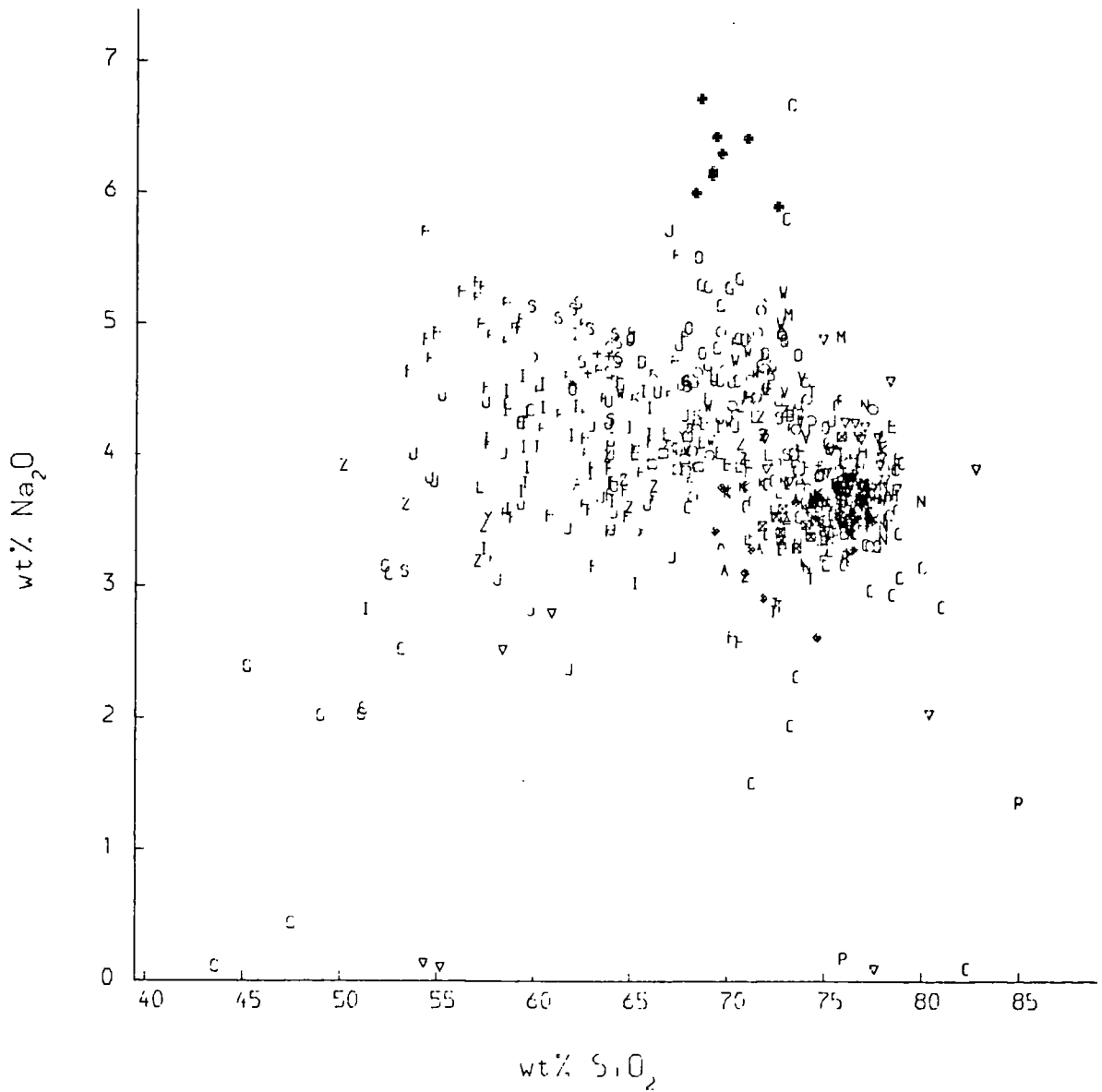


Fig. 7:20. Harker type  $\text{SiO}_2$  vs.  $\text{Na}_2\text{O}$  variation diagram for the Scottish Caledonian granitoids; key to symbols on fold out sheet.



diorite. The samples from the Cluanie granodiorite are significantly enriched in  $\text{Na}_2\text{O}$  relative to the main trend.

The general pattern for  $\text{K}_2\text{O}$  is a positive correlation with  $\text{SiO}_2$  (Fig. 7:21) implying that potassium feldspar is not a significant fractionating phase with the exception of the granite samples with  $\text{SiO}_2 > 75\%$  where some decrease in  $\text{K}_2\text{O}$  is observed. There does not appear to be a spatial variation in  $\text{K}_2\text{O}$  relative  $\text{SiO}_2$ . Again the samples from the Cluanie granodiorite have significantly lower  $\text{K}_2\text{O}$  relative to the main trend.

The behaviour of  $\text{P}_2\text{O}_5$  is determined by apatite fractionation. The samples with low  $\text{SiO}_2 < 55\%$  show an increase in  $\text{P}_2\text{O}_5$  with  $\text{SiO}_2$  (Fig. 7:22) implying that the cumulate assemblage does not include apatite. All the samples with  $> 55\%$   $\text{SiO}_2$  show a decrease in  $\text{P}_2\text{O}_5$  with increasing silica implying that apatite is part of the fractional crystallization assemblage for the more evolved samples.

The major element variations across Scotland can mostly be explained by fractional crystallization processes. The only intrusion with unusual major element chemistry is the Cluanie granodiorite which plots apart from the main trend for the majority of the major elements. The cause of this very different composition in the Cluanie granodiorite is presumably a different source from that of the majority of the Caledonian granites. Also some of the "S" type granites are distinguishable from the main trend for  $\text{Fe}_2\text{O}_3$  where  $\text{Fe}_2\text{O}_3$  is enriched in the "S" type granites, presumably the result of derivation from pelitic sediments.

Fig. 7:21. Harker type  $\text{SiO}_2$  vs.  $\text{K}_2\text{O}$  variation diagram for the Scottish Caledonian granitoids; key to symbols on fold out sheet.

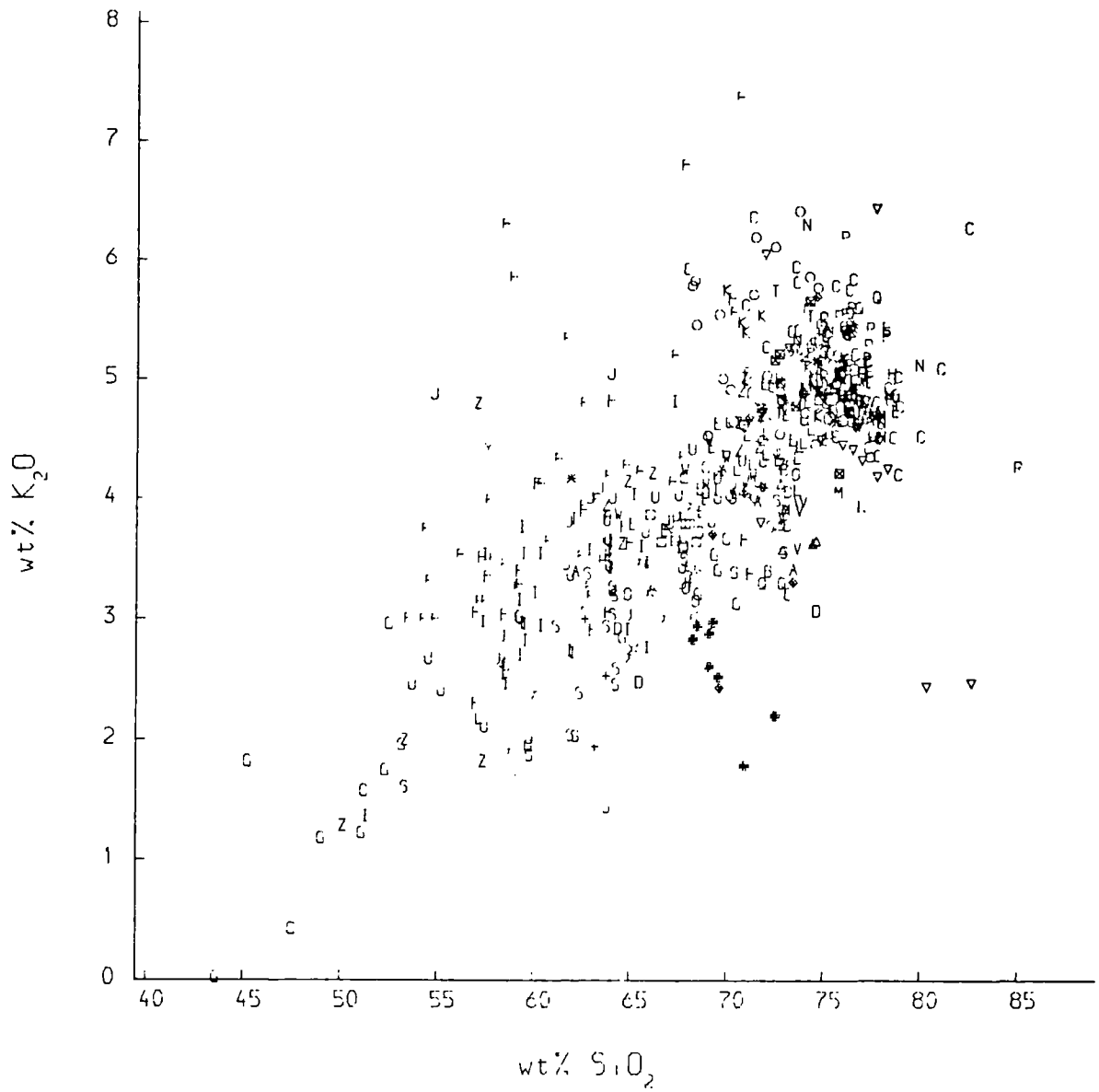
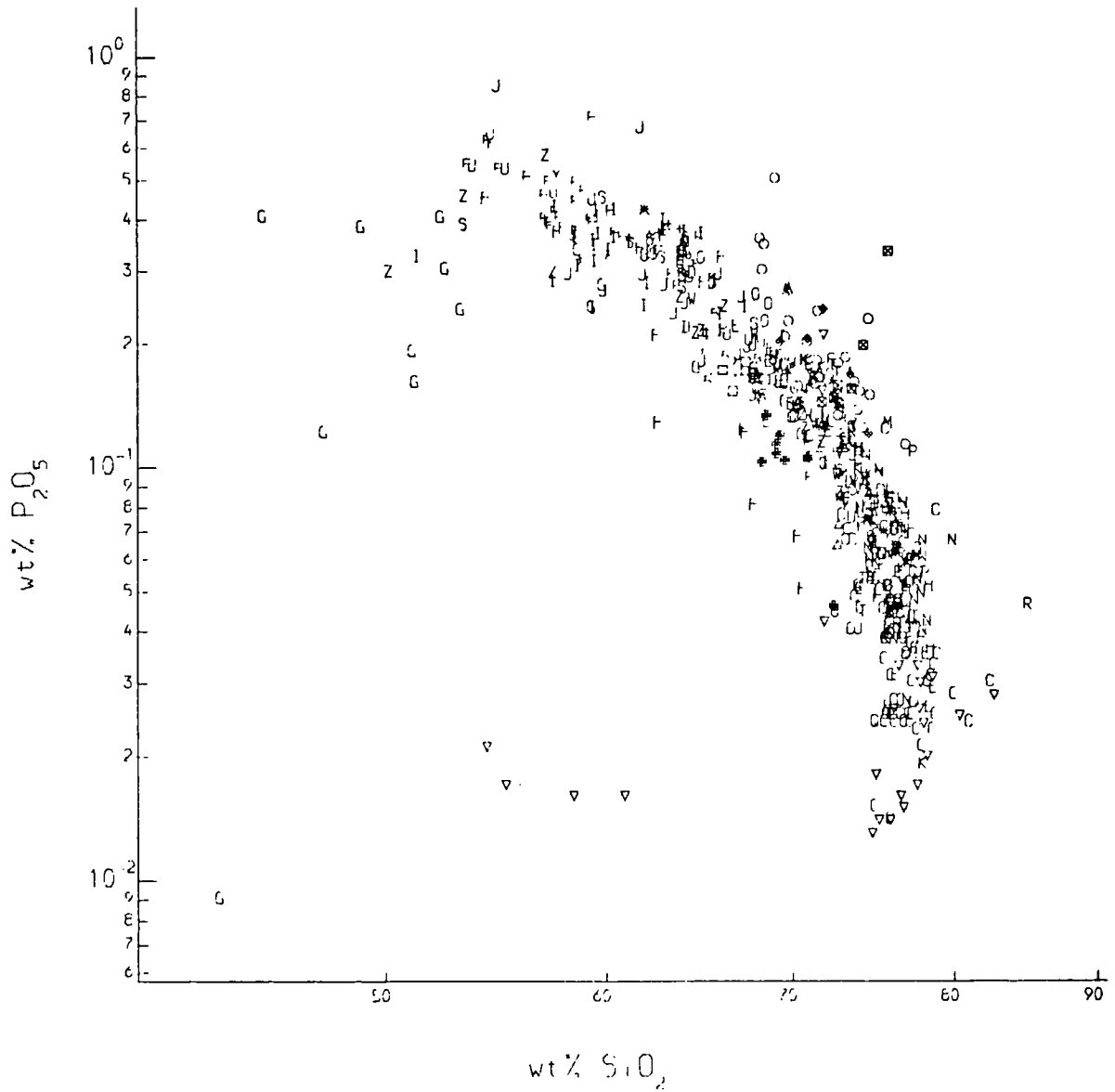


Fig. 7:22. Harker type  $\text{SiO}_2$  vs.  $\text{P}_2\text{O}_5$  variation diagram for the Scottish Caledonian granitoids; key to symbols on fold out sheet.



Variations in the levels of trace elements with  $\text{SiO}_2$  are less easy to define in terms of fractional crystallization since most of the trace element abundances are controlled by minor phases both during melting at the source and during fractional crystallization. The trace elements which are controlled primarily by main rock forming minerals are Rb, Ba, Sr, V, Cr and Y.

Rb behaves as an incompatible element throughout the compositional range (Fig. 7:23), the rate of increase in Rb changes over the compositional range with a more rapid increase with  $\text{SiO}_2$  where  $\text{SiO}_2 > 70\%$ . This is almost certainly due to the effects of different fractional crystallization assemblages on the rate of increase of  $\text{SiO}_2$  (as mentioned earlier a feldspathic assemblage will produce a slow rate of increase in  $\text{SiO}_2$  whereas Rb will continue to increase rapidly). This effect may be compounded by variation in the proportion of biotite in the fractional crystallization assemblage. The samples from the Glen Gairn granite with the highest levels of Rb represent the ultimate in residual liquids from fractional crystallisation. Although there is some variation in Rb which is probably the result of source variation seen in the spread of values for Rb at any given  $\text{SiO}_2$  value, there is no sensible regional variation in this and intrusions which are geographically close such as the Moor of Rannoch and Strath Ossian show distinct differences in Rb concentrations at a given level of  $\text{SiO}_2$ .

The behaviour of Ba is more complex (Fig. 7:24), the samples with  $\text{SiO}_2 < 55\%$  define a positive correlation for Ba with  $\text{SiO}_2$  indicating that Ba is an incompatible element consistent with the loss of a pyroxene or hornblende rich cumulate assemblage. From  $\text{SiO}_2$  55 to 70%, Ba behaves

Fig. 7:23. Harker type  $\text{SiO}_2$  vs. Rb variation diagram for the Scottish Caledonian granitoids; key to symbols on fold out sheet.

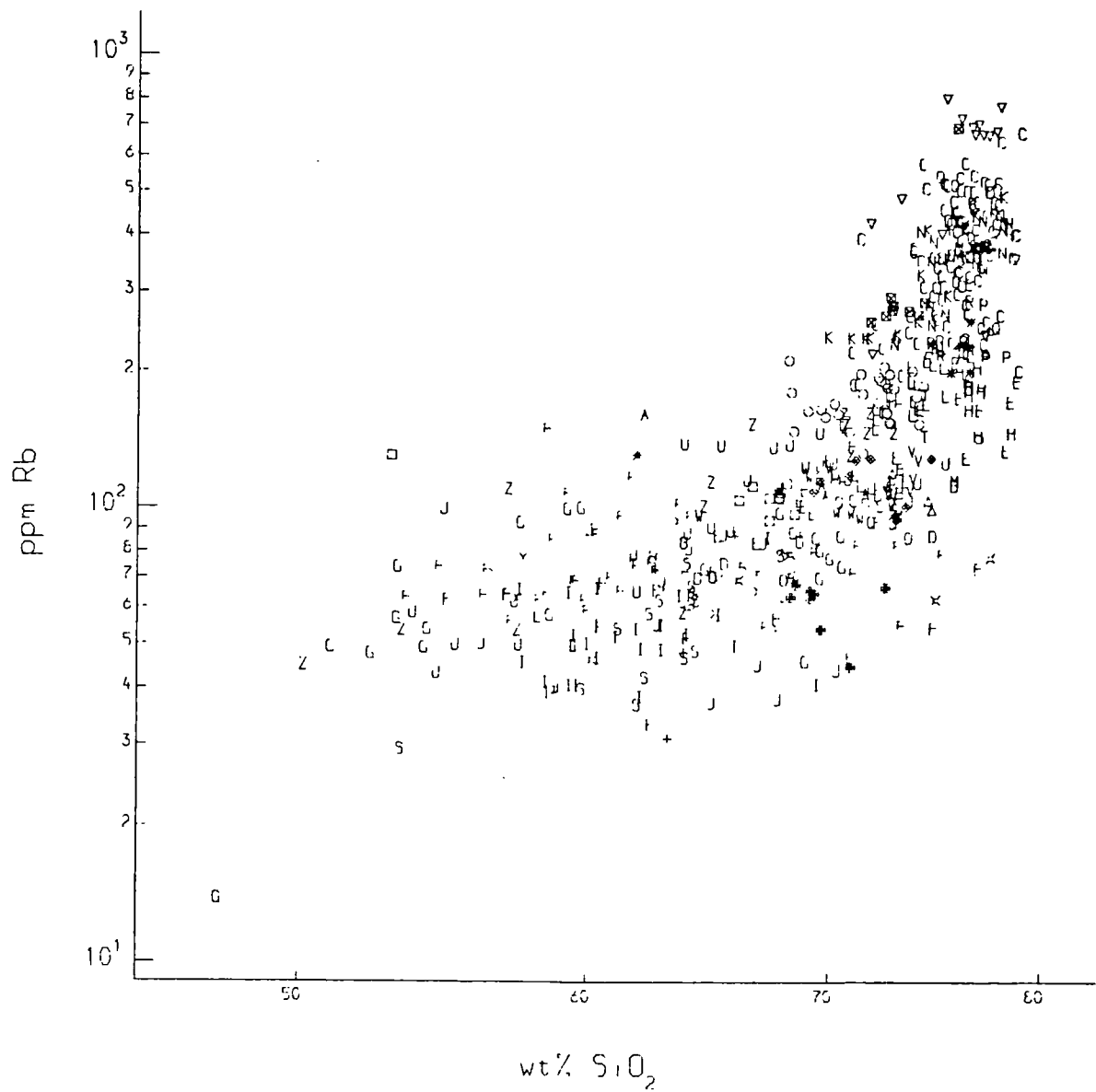
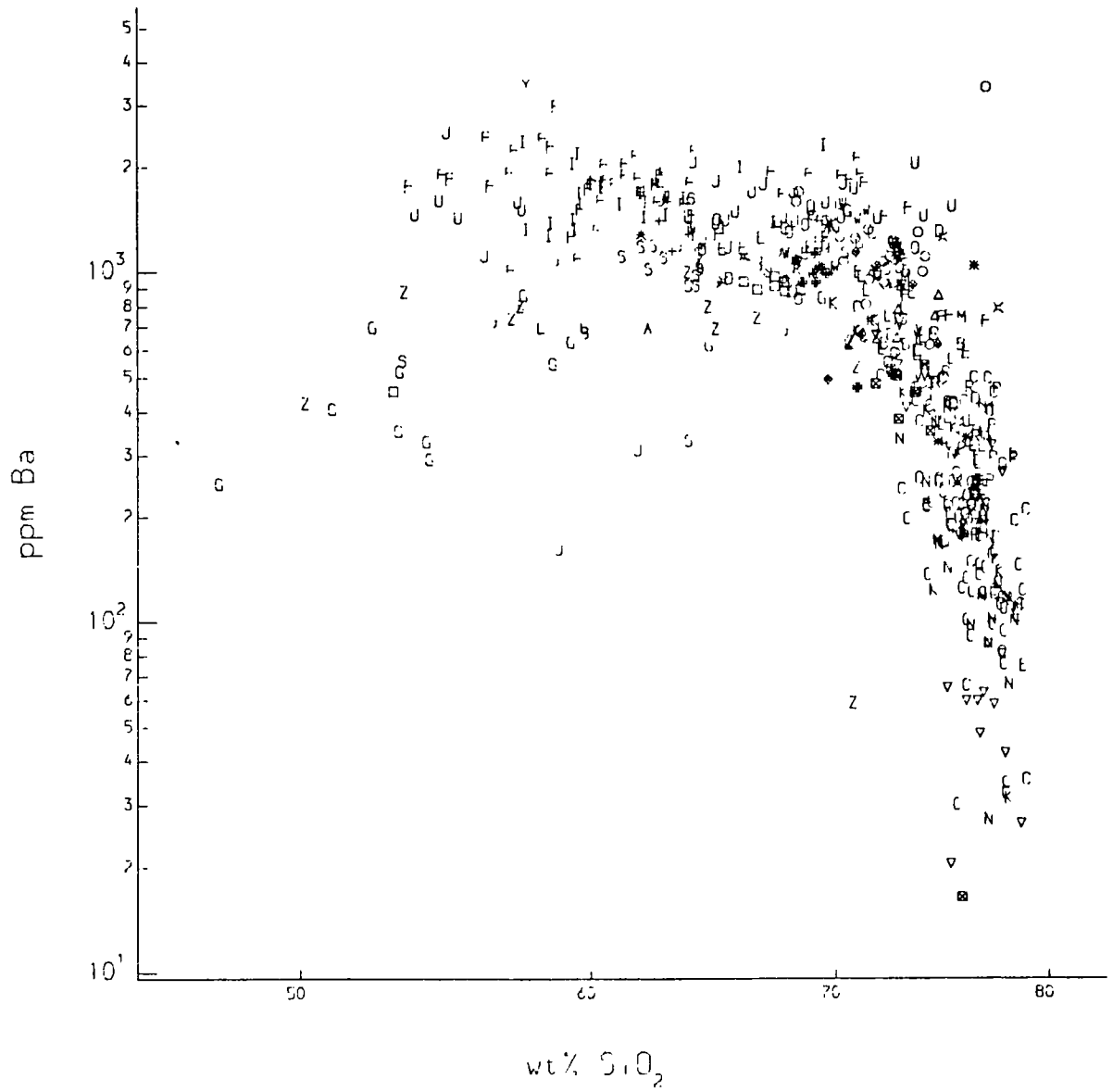


Fig. 7:24. Harker type  $\text{SiO}_2$  vs. Ba variation diagram for the Scottish Caledonian granitoids; key to symbols on fold out sheet.



slightly compatibly indicating perhaps some biotite is involved in fractional crystallisation. For the samples with  $>70\%$   $\text{SiO}_2$  the levels of Ba decrease rapidly, indicating both increased potassium feldspar involvement in fractional crystallization and the effects of a feldspathic crystallization assemblage on the rate of  $\text{SiO}_2$  increase. The behaviour of Sr is similar to that of Ba (Fig. 7:25) but reflects plagioclase in the crystallization assemblage.

The behaviour of V reflects the involvement of mafic minerals during fractional crystallization and as would be expected V behaves compatibly throughout the range in observed compositions (Fig. 7:26). The effects of the feldspathic fractional crystallization assemblage are also noticeable here with a steepening of the trend for the samples with  $\text{SiO}_2 >70\%$  even though the mafic content of the fractional crystallization assemblage is much less than for the less geochemically evolved plutons. The behaviour of Cr is less straightforward than V (Fig. 7:27), although the bulk of the samples define a single trend, samples from the Foyers complex show a marked depletion in Cr relative to samples with the same levels of  $\text{SiO}_2$  from other intrusions; there are insufficient published distribution coefficient data to comment further on this phenomena.

The behaviour of Y is dominantly controlled by hornblende during melting and crystallization processes and the observed trend (Fig. 7:28) reflects hornblende in the fractional crystallization assemblage. For samples with  $\text{SiO}_2 <70\%$ , Y behaves predominantly as a compatible element. This would tend to imply that the early cumulates separated from the samples with  $<55\%$   $\text{SiO}_2$  were hornblende rich rather than pyroxene rich. For the samples with  $\text{SiO}_2 >70\%$  however, Y behaves as an incompatible

Fig. 7:25. Harker type  $\text{SiO}_2$  vs. Sr variation diagram for the Scottish Caledonian granitoids; key to symbols on fold out sheet.

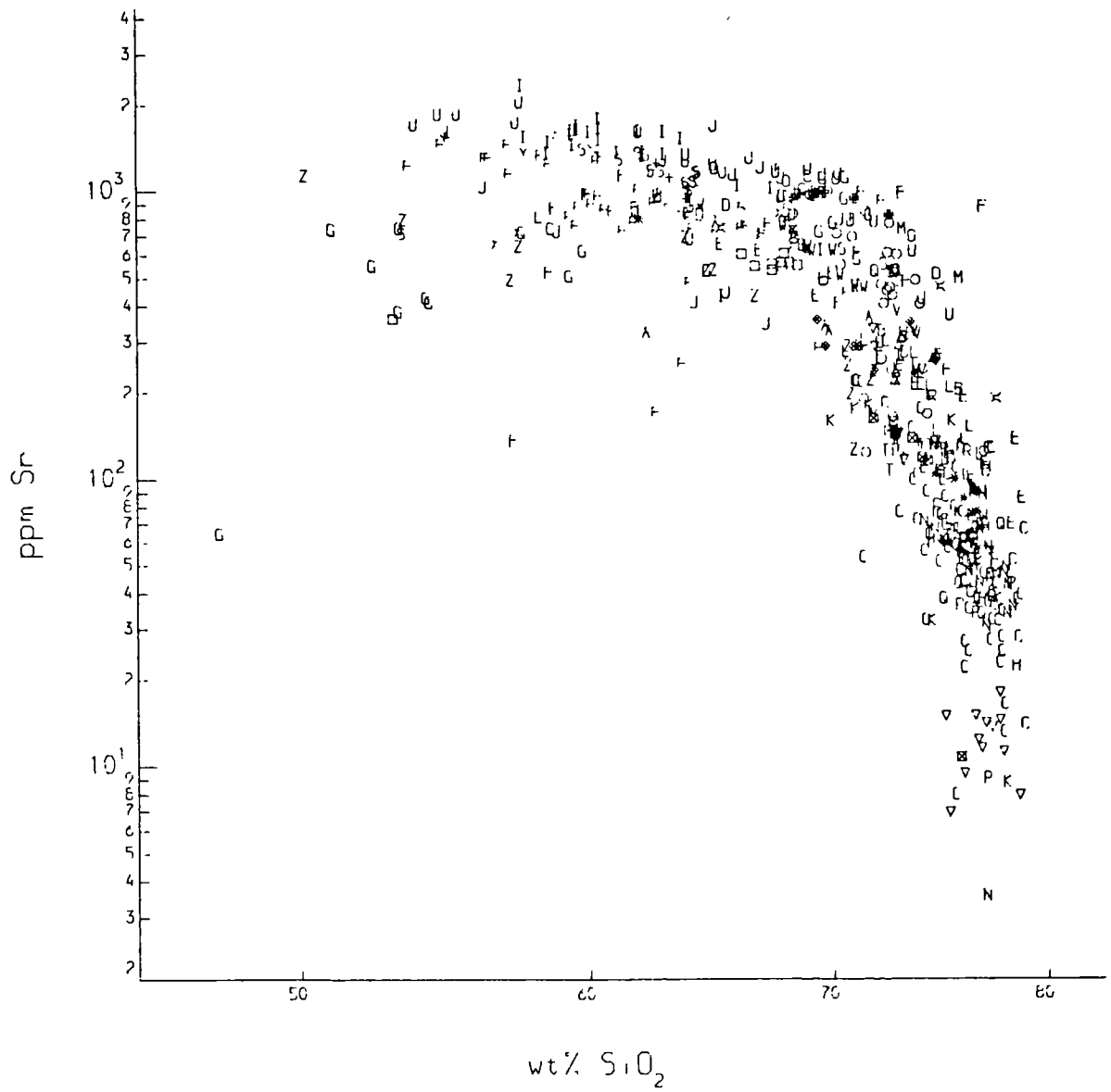


Fig. 7:26. Harker type  $\text{SiO}_2$  vs. V variation diagram for the Scottish Caledonian granitoids; key to symbols on fold out sheet.

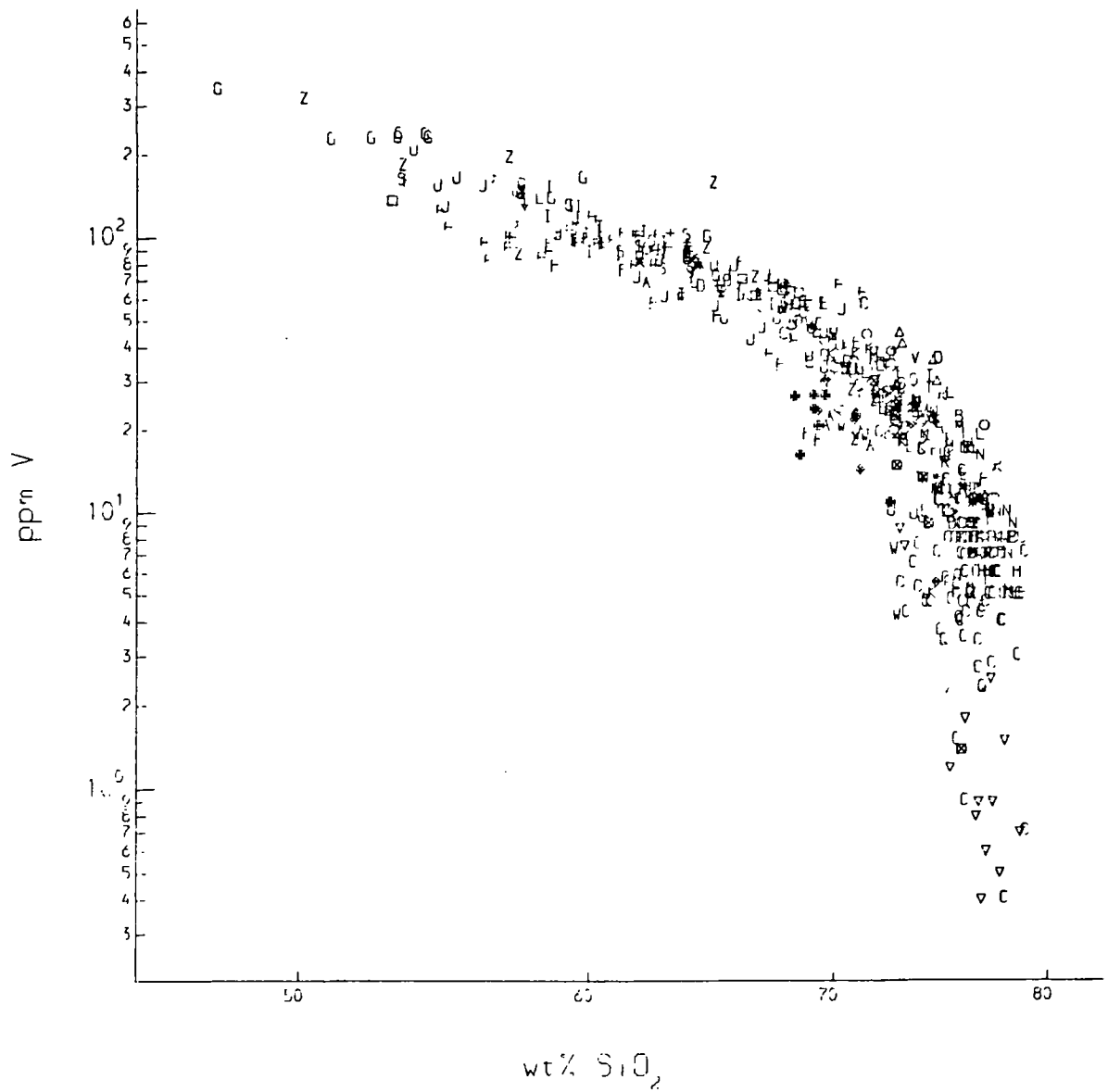


Fig. 7:27. Harker type  $\text{SiO}_2$  vs. Cr variation diagram for the Scottish Caledonian granitoids; key to symbols on fold out sheet.

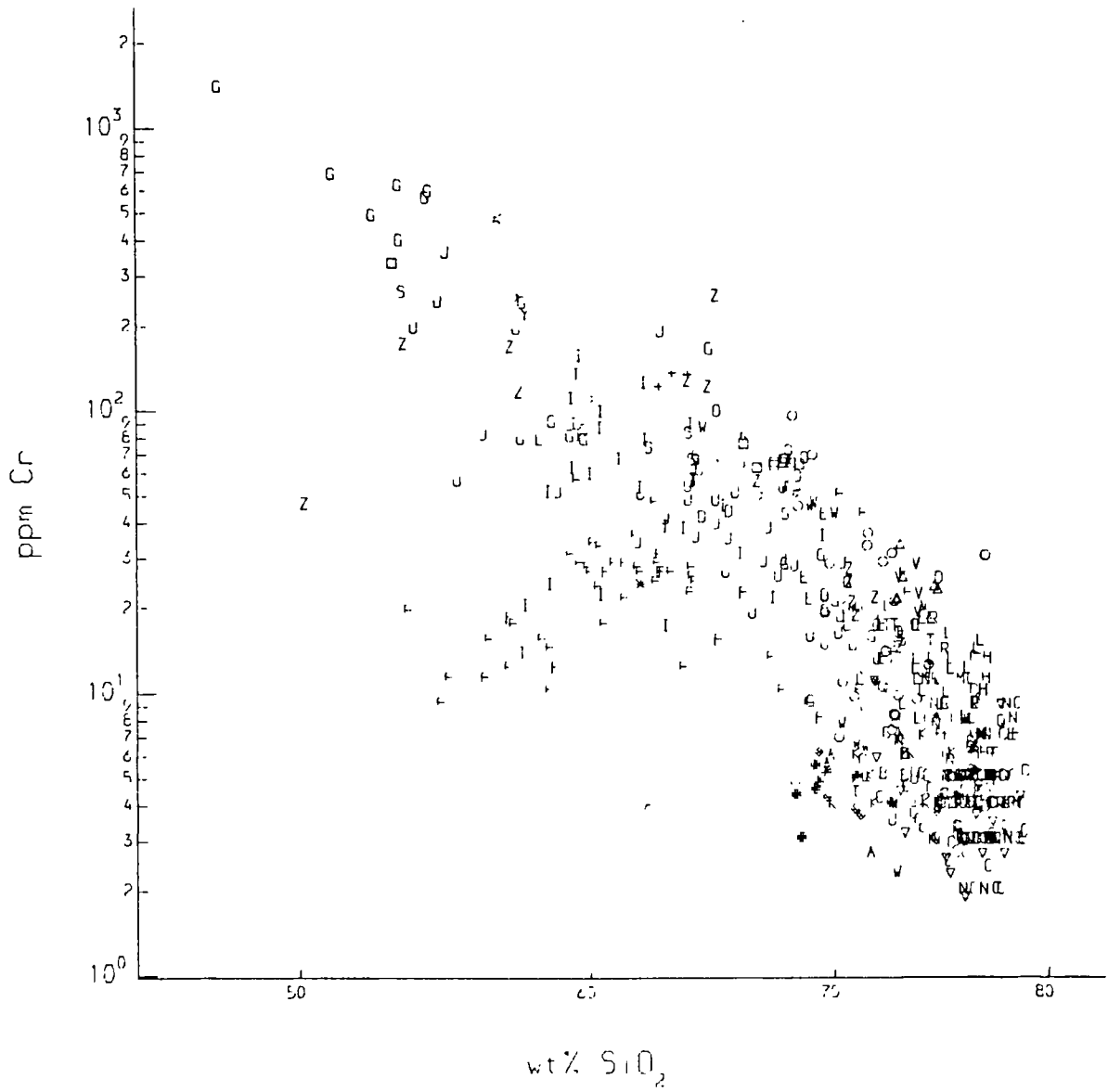
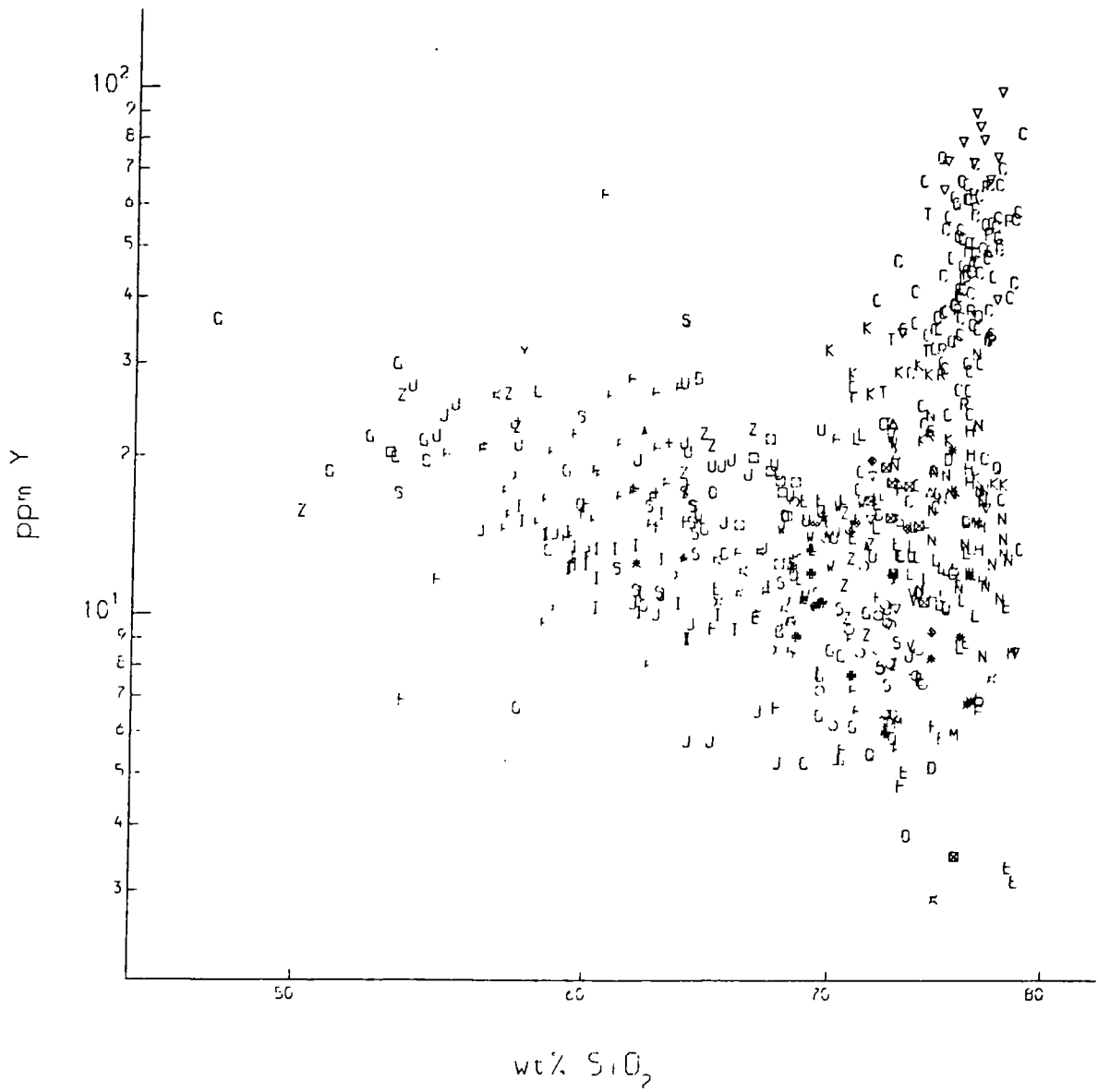


Fig. 7:28. Harker type  $\text{SiO}_2$  vs. Y variation diagram for the Scottish Caledonian granitoids; key to symbols on fold out sheet.



element, reflecting the negligible role of hornblende in the fractional crystallization assemblages for these granites. Again the effects of a feldspathic fractional crystallization assemblage on the rate of increase of  $\text{SiO}_2$  is very marked.

The rare earth patterns for the Scottish Caledonian granites do not show the large variation seen in the Lake District intrusions. The majority of the Scottish granitoids have steep rare earth patterns roughly similar to those of Shap and Skiddaw in the Lake District (Figs. 6:36 & 6:37). The exceptions to this generalization are the Ardclach and Cluanie intrusions which have much flatter rare earth patterns and may reflect derivation from a different source. The Ardclach granite may be derived by crustal melting and the Cluanie granodiorite may also be derived from a distinct source and is geochemically distinct also in terms of major elements. Superimposed on these generally steep REE patterns are the effects of fractional crystallization with some intrusions, in particular the Moor of Rannoch and Foyers intrusions (Figs. 6:35 & 6:37), showing the characteristic hornblende signature in the heavy rare earth pattern.

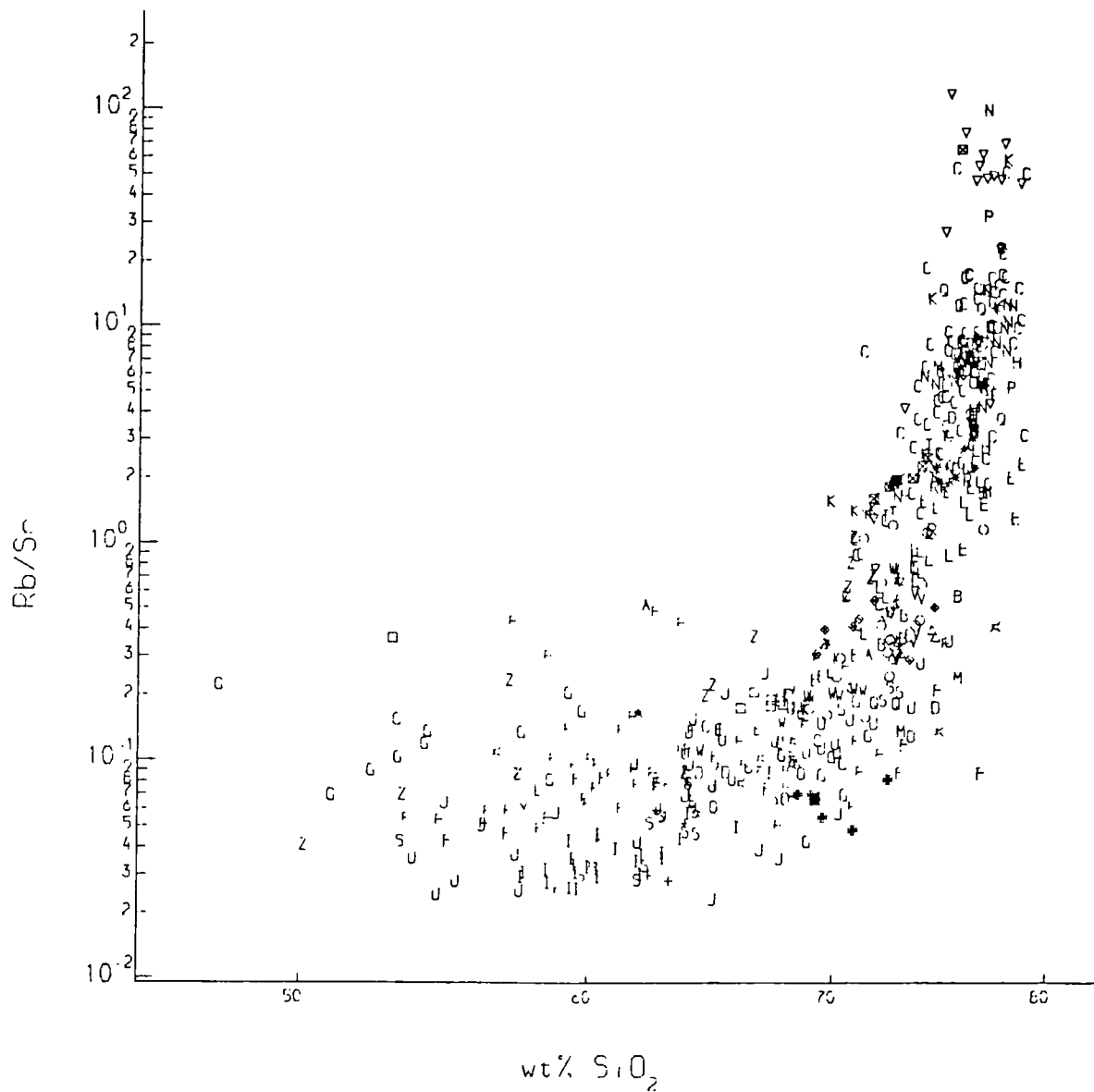
It therefore appears that the trace elements that are dominantly controlled by major phases in fractional crystallization are showing the same features as the major elements and that the major cause of compositional variation within the Caledonian granite suite is in some way connected to fractional crystallization processes. At this stage before looking into the behaviour of the trace elements controlled by minor phases it is worth observing that, as a result of the degree of fractional crystallization and the increasing role of feldspars in

fractional crystallization with increased magmatic evolution, the Rb/Sr ratios vary dramatically (Fig. 7:29). A dramatic increase in the Rb/Sr ratio is seen in the granites with  $>65\% \text{SiO}_2$ , this is the result of two components, firstly the increasing involvement of feldspars during fractional crystallization and secondly the effects of a feldspathic crystallization assemblage on the rate of increase in  $\text{SiO}_2$ .

Many of the remaining trace element abundances appear to be controlled by minor phases such as zircon, sphene, apatite, allanite, monazite, etc., although the behaviour of these trace elements is not clearly defined. The element Zr for instance will clearly be controlled by the presence of zircon. However Nb although generally thought of as behaving in a similar way to Ti cannot be substituting for Ti in all Ti bearing minerals because of the different behaviour of the two elements when plotted against  $\text{SiO}_2$  (Figs. 7:14 & 7:30). The element which has closest similarity to the behaviour of Nb in this case is Y, the abundance of which is dominantly controlled by hornblende. Although there are no experimentally determined distribution coefficients for Nb in hornblende, it may not be hornblende that is the controlling mineral phase for Nb but more probably sphene which is a major Ti bearing phase and tends to be found only in hornblende bearing assemblages. The light rare earth elements are dominantly controlled by phases such as allanite and monazite, also U and Th will be controlled to a certain extent by these phases.

It is perhaps necessary at this stage to discuss the role of these accessory phases in the process of fractional crystallisation. The traditional approach to these accessory phases regards their growth in

Fig. 7:29. Variation diagram for  $\text{SiO}_2$  vs. Rb/Sr ratio for the Scottish Caledonian granitoids; key to symbols on fold out sheet.

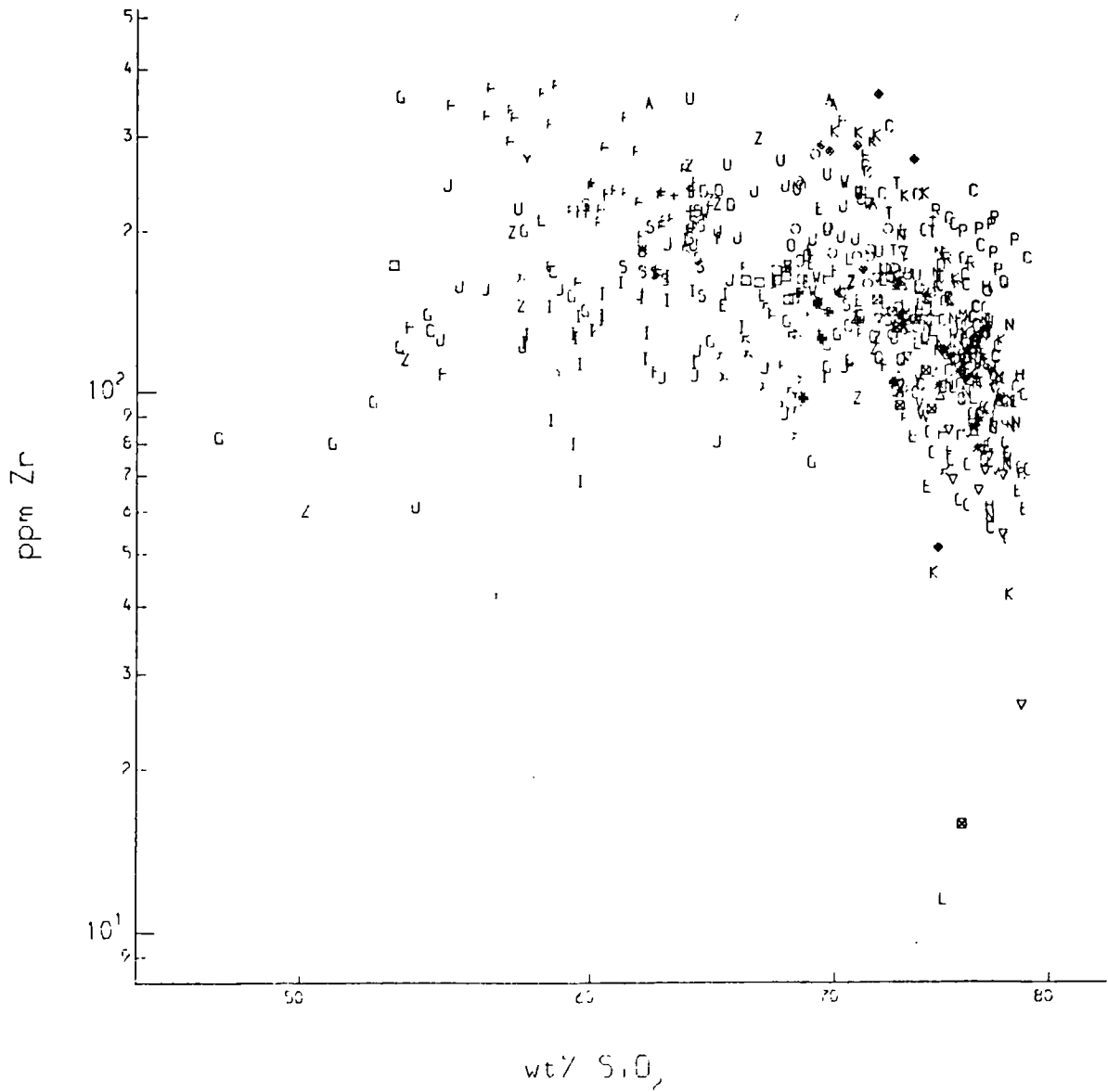




granitoids as late, (with the possible exception of zircon), and having crystallized from residual fluids and achieving their euhedral nature through the force of crystallization (Hatch, Wells & Wells 1972). This origin for the accessory phases does not explain the observed behaviour of (for instance)  $P_2O_5$  which clearly demonstrates that with increased fractional crystallization  $P_2O_5$  concentrations are decreasing, a clear indication of the involvement of apatite in fractional crystallisation. Also accessory minerals are frequently found enclosed within an early crystallizing phase, for example sphene within hornblende (Plate 3:2a) and apatite and zircon within biotite (Plate 3:2b). Moreover the frequent compositional zoning within larger accessory minerals seen through fission tracks of uranium (Barritt 1983) all tend to imply that the accessory minerals crystallize early and are involved in crystal fractionation.

It is therefore demonstrable that the change in behaviour of Nb (Fig. 7:30) is related to the absence of sphene as part of the fractional crystallization assemblage for the more evolved granites with  $SiO_2 > 70\%$ . The behaviour of Zr however, reflecting zircon crystallisation, is more complex and may reflect not only crystal fractionation but some element of source variation and/or the effects of assimilation of metasediments (Fig. 7:31). A general trend is observed in that samples with  $< 55\% SiO_2$  describe a positive correlation of Zr with  $SiO_2$  implying no zircon fractionation. For samples with between 55 and 70%  $SiO_2$  the levels of Zr remain roughly constant, although some individual plutons display a negative correlation of Zr with  $SiO_2$ , (e.g. Moor of Rannoch). However there is a large variation in Zr concentrations for a given  $SiO_2$  concentration implying some other process such as source variation or

Fig. 7:31. Harker type  $\text{SiO}_2$  vs. Zr variation diagram for the Scottish Caledonian granitoids; key to symbols on fold out sheet.



assimilation is involved. For the samples with  $>70\%$   $\text{SiO}_2$  Zr defines a negative correlation with  $\text{SiO}_2$  implying zircon as part of the fractional crystallization assemblage although the large range of Zr concentration at a given  $\text{SiO}_2$  content remains. The range of Zr concentrations for a given  $\text{SiO}_2$  value does not form a regional variation. However the presence of "S" type granites with relatively high Zr levels implies that this variation may be due to the effects of crustal assimilation as indicated by the presence of inherited zircons in crustally derived granites and those which may have assimilated crustal material. On the other hand this may represent a variation in the crystallization sequence relative to the point where zircon becomes a fractionating phase.

The behaviour of Ce is generally similar to that of Zr (Fig. 7:32), although the minerals involved are different in this case; allanite in the samples with  $\text{SiO}_2$  generally  $<70\%$   $\text{SiO}_2$  which have coexisting hornblende and sphene, and monazite in the samples with  $\text{SiO}_2$  generally  $>70\%$  with coexisting biotite. The arguments for assimilation and source variation as opposed to fractional crystallization being the cause of the spread of values for Ce at a given  $\text{SiO}_2$  value are the same as for Zr. The behaviour of Th and U is generally similar (Figs. 7:33 & 7:34) and both elements show a general increase in concentration with increasing  $\text{SiO}_2$  although Th in particular often behaves compatibly in insitu fractional crystallisation. This behaviour is consistent with varying degrees of fractional crystallisation prior to emplacement. The U/Th ratio of the Scottish Caledonian granitoids is generally constant over the compositional range (Fig. 7:35) at between 0.2 and 0.4; the few samples with low U/Th ratios have probably suffered surface leaching of U. However in the high silica samples the U/Th ratio increases.

Fig. 7:32. Harker type  $\text{SiO}_2$  vs. Ce variation diagram for the Scottish Caledonian granitoids; key to symbols on fold out sheet.

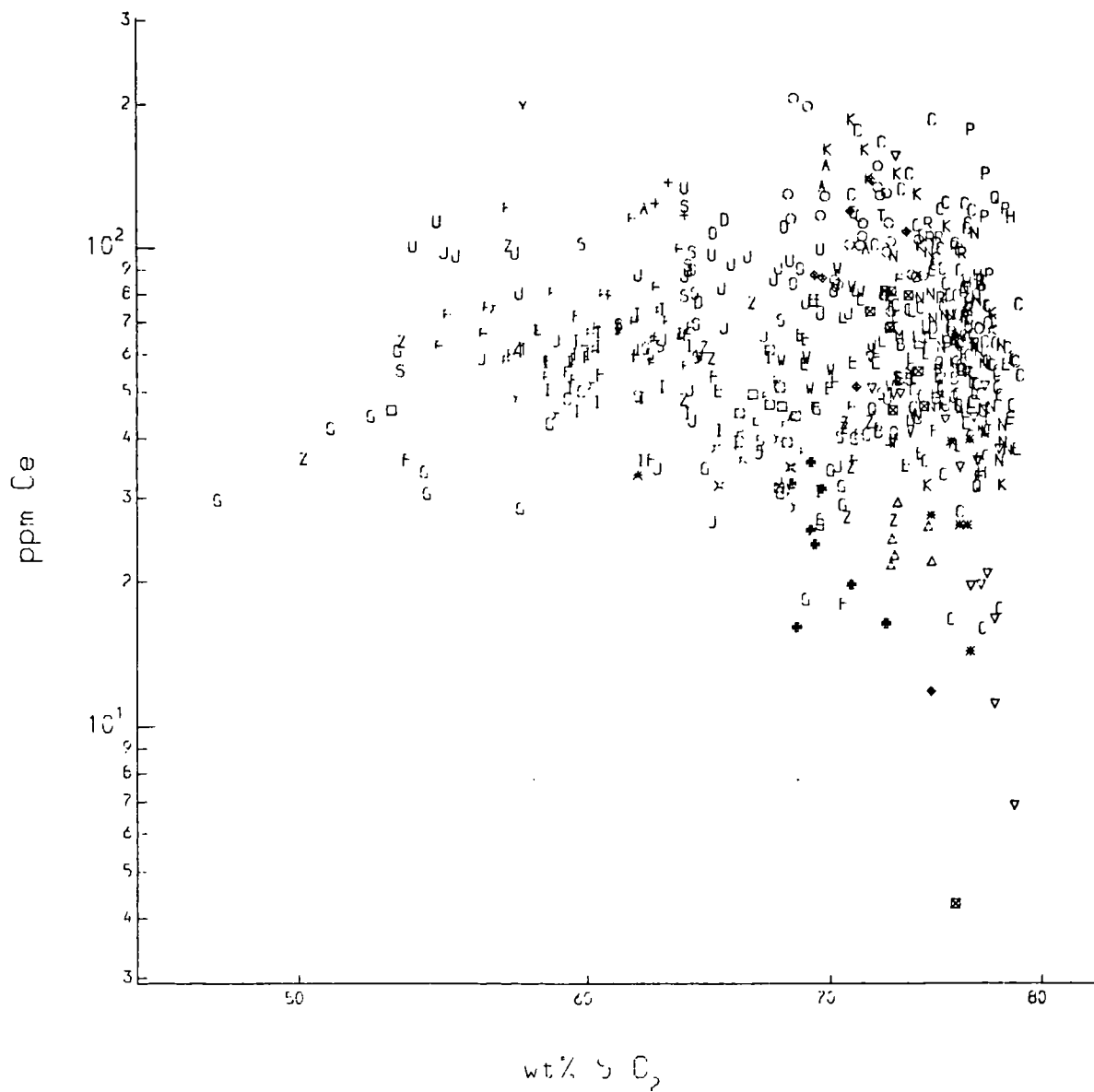


Fig. 7:33. Harker type  $\text{SiO}_2$  vs. Th variation diagram for the Scottish Caledonian granitoids; key to symbols on fold out sheet.

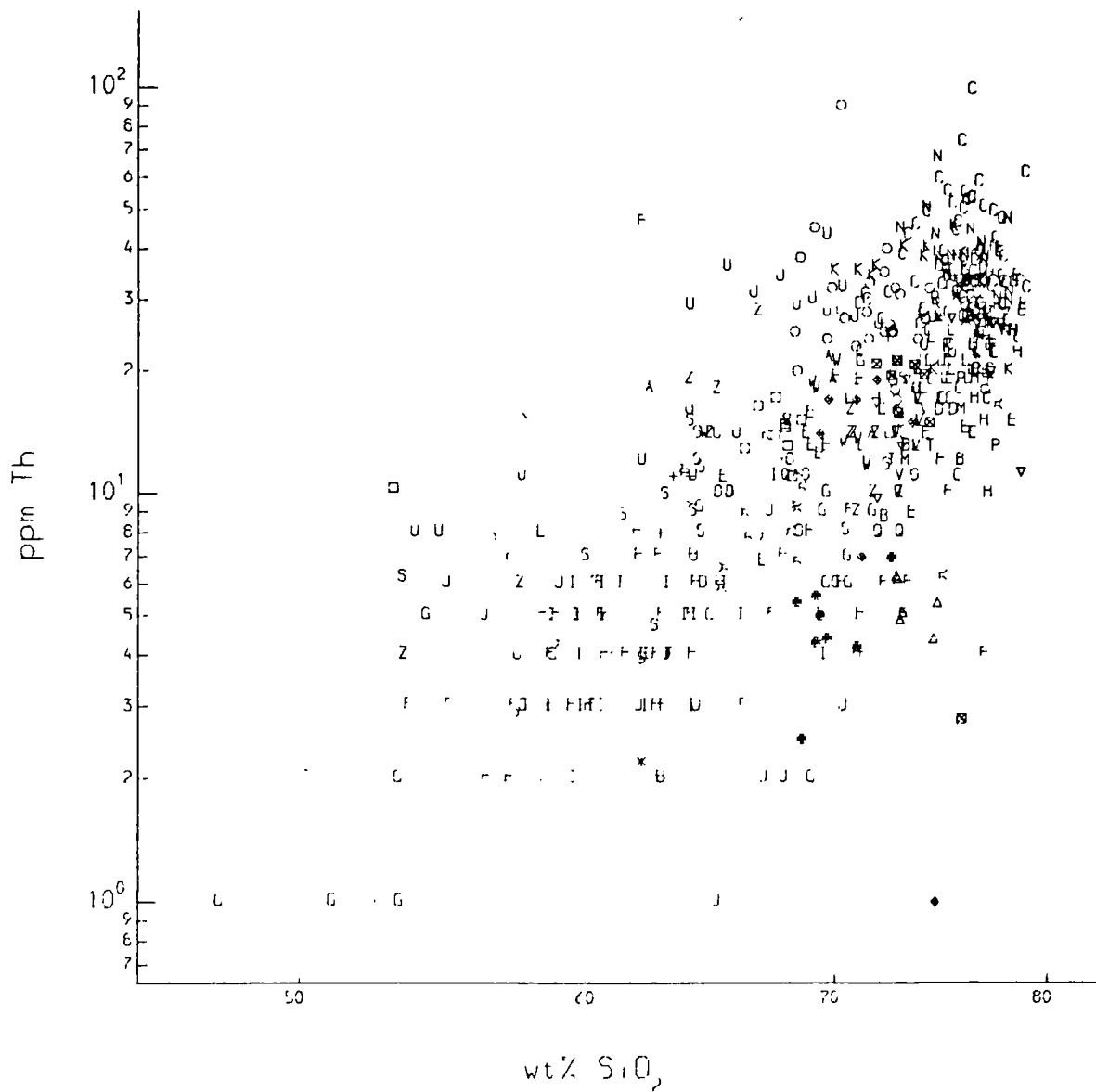


Fig. 7:34. Harker type  $\text{SiO}_2$  vs. U variation diagram for the Scottish Caledonian granitoids; key to symbols on fold out sheet.

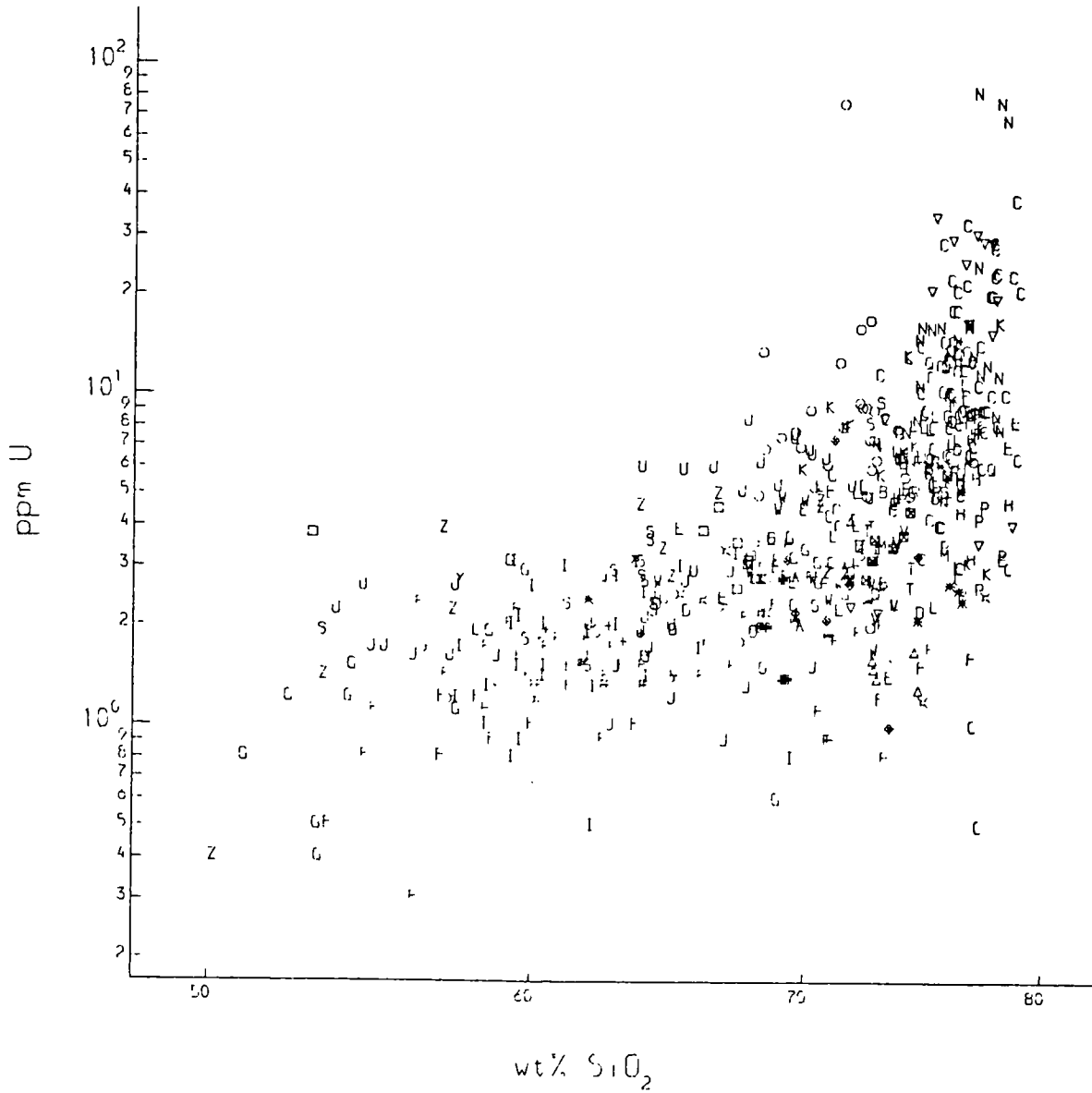
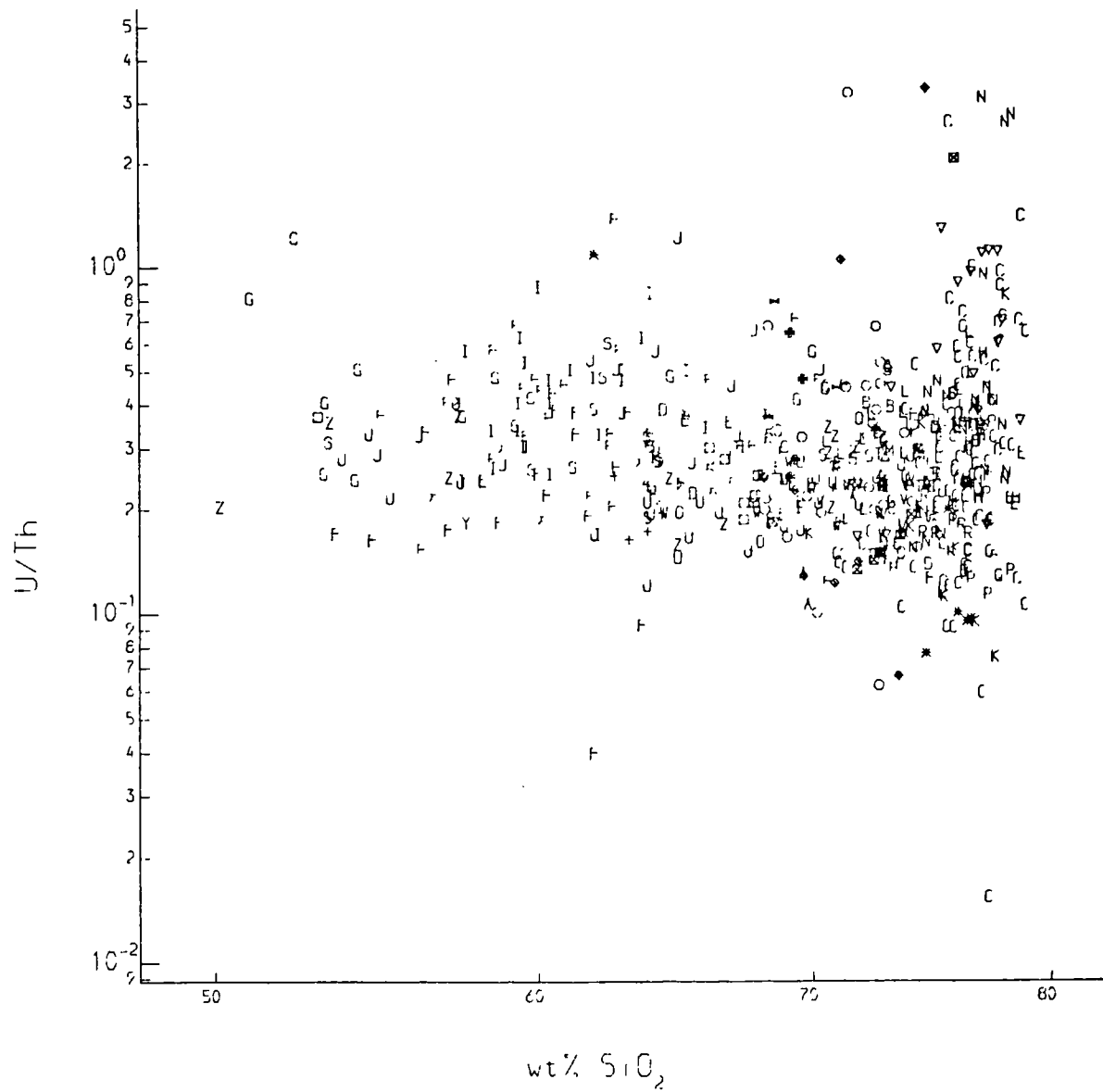


Fig. 7:35. Variation diagram for  $\text{SiO}_2$  vs. U/Th ratio for the Scottish Caledonian granitoids; key to symbols on fold out sheet.



reflecting perhaps the effects of fractional crystallization of allanite or monazite which remove Th in preference to U.

It appears that much of the geochemical variation in the Caledonian granitoid suite appears to be the result of differing degrees of fractional crystallization (both insitu and prior to emplacement). The possibility of source variation is not ruled out but assessing such variation is likely to be difficult. The type of source variation which might be expected within this granitoid suite may be an increased within-plate component away from the site of subduction as proposed by Brown et al. (1984), where the within plate component is expressed in terms of increased levels of Nb, Y, and Ta relative to the Rb/Zr ratio. However all of these trace elements are strongly affected by fractional crystallization (Figs. 7:28, 7:30 and 7:36). Thus although there may be differences in the mantle source between the Lake District granites and the Scottish granitoids, much of the variation within the Scottish granitoid suite on diagrams of the type used by Brown et al. (1984) are related to differences in insitu fractional crystallization assemblages as shown in Figs. 7:37 and 7:38. The differences in insitu fractional crystallization assemblages are however related to major element composition and presumably reflect the size of magma body in that large bodies of magma may undergo considerable fractional crystallization before emplacement at a high level in the crust. It is noticeable that the granites which show enrichment of Nb and Y during insitu fractional crystallization and are highly geochemically evolved (Cairngorm, Lochnagar, Bennachie, Mt Battock, Cromar, Glen Gairn and Hill of Fare), are associated with a large regional gravity low and geophysical modelling suggests that the granites extend to at least 10 Km depth

Fig. 7:36. Variation diagram for  $\text{SiO}_2$  vs.  $\text{Rb/Zr}$  ratio for the Scottish Caledonian granitoids; key to symbols on fold out sheet.

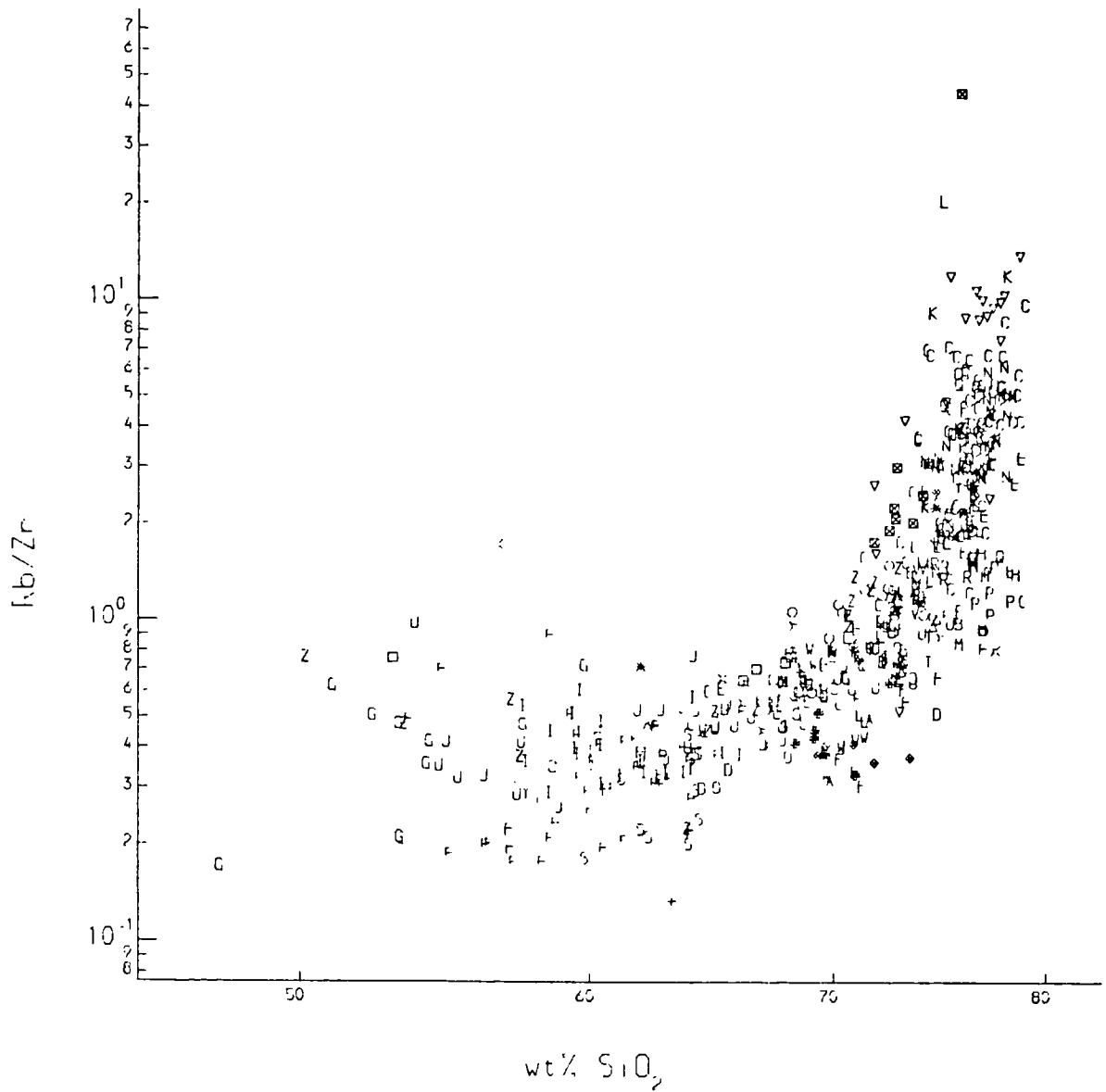


Fig. 7:37. Variation diagram for Nb vs. Rb/Zr ratio for the Scottish Caledonian granitoids with the effects of fractional crystallization variation shown diagrammatically; key to symbols on fold out sheet.

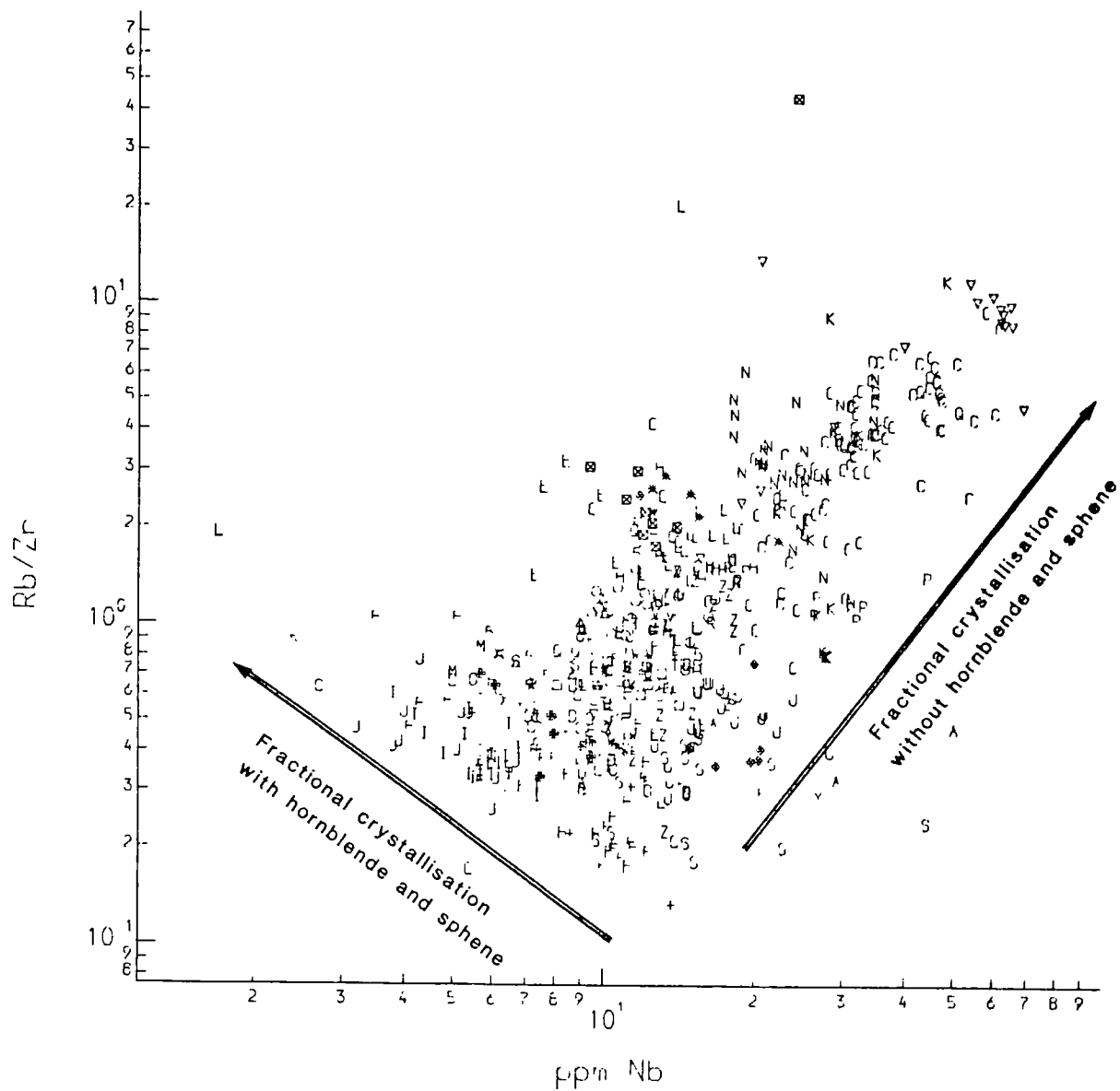
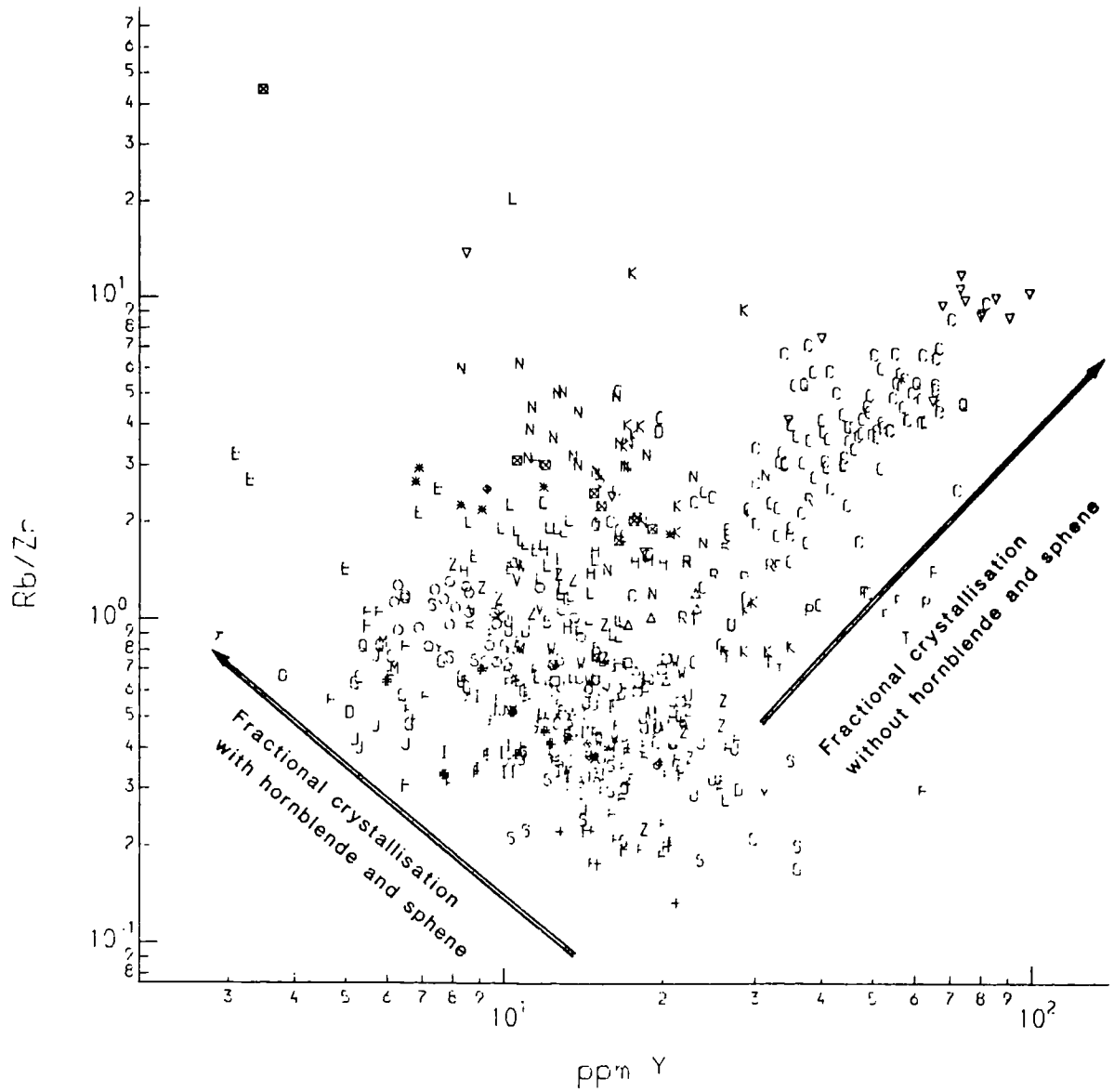


Fig. 7:38. Variation diagram for Y vs. Rb/Zr ratio for the Scottish Caledonian granitoids with the effects of fractional crystallization variation shown diagrammatically; key to symbols on fold out sheet.



(Rollin 1984) and therefore represent voluminous magmas which were capable of considerable degrees of fractional crystallisation. The geochemically less evolved granitoids do not have a large negative gravity expression (Brown & Locke 1979) and may also be of smaller volume thus inhibiting the amount of fractional crystallization which can take place both insitu and prior to emplacement.

It would therefore appear that since most of the geochemical variation observed in the Scottish Caledonian granitoids is probably the result of variations in degree of fractional crystallization, both insitu and prior to emplacement, and variations in the insitu fractional crystallization assemblage, the critical factor in the origin of these variations is the size of the magma body. However this cannot be the only factor since large batholiths are characteristic of the Andean margin and these batholiths are generally geochemically unevolved tonalites and granodiorites (Bartholomew 1984, McCourt 1981) and generally have a chemistry similar to the hornblende granodiorites and tonalites in western Scotland, there is also a close similarity with the geochemistry of granitoids of the Kohistan arc in the Himalayas (Pettersen 1984). The hydration state of the magmas would therefore be another contributing factor to the extent of fractional crystallization possible in a subduction related magma. Hydrous granitic magmas will solidify and crystallize rapidly with the reducing  $p(\text{H}_2\text{O})$  during ascent through the crust (Harris et al. 1970). It is hypothesized therefore that the voluminous "Cairngorm batholith" was a dry magma since it has obviously undergone considerable amounts of fractional crystallization and risen to a high structural level. Dry magmas are often associated with the products of crustal melting (Wyllie et al. 1976). However it does not

seem possible that the large "Cairngorm batholith" can be the result of crustal melting (c.f. Chapter 6) and therefore may have been derived from a dry andesitic melt from quartz eclogite in the subducted oceanic slab (Stern & Wyllie 1973) and undergone considerable amounts of fractional crystallization both insitu and before emplacement. The geochemical evolution of the smaller intrusions is inhibited by their size and possibly their water content.

One last comment on regional variations within the Scottish granitoid suite (which appears to be an unresolved paradox) is related to the spatial distribution of mineralized and metalliferous granitoids. If the palaeo-plate boundary shown on Figs. 7:12 and 7:13, adapted from Phillips et al. (1976), is correct, the spatial pattern of mineralized and metalliferous intrusions in the Scottish Caledonides is the inverse of that observed by Sillitoe (1972) in western America, with the porphyry copper intrusions being further from the site of subduction than the tin enriched granites of the "Cairngorm batholith". Whilst the enrichment of tin in the "Cairngorm batholith" may be the result of fractional crystallization processes (Fig. 7:39) seen in the correlation of Sn with Y and Nb, with rising levels of both elements where sphene and hornblende are not part of the fractional crystallization assemblages, the petrogenetic factors related to the development of porphyry copper intrusions are in this case less clear.

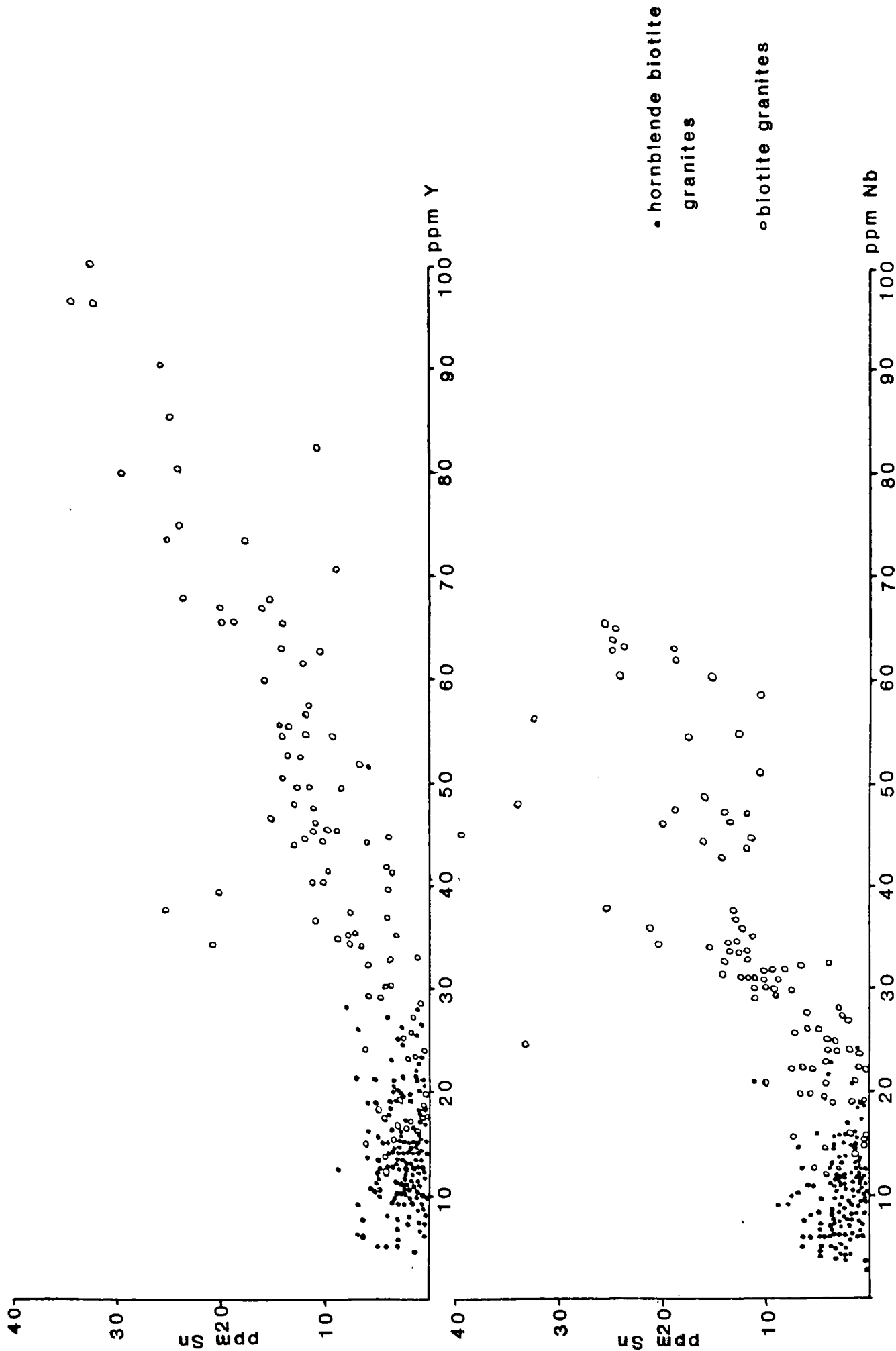
#### 7:4. ISOTOPIC EVIDENCE OF SOURCE VARIATION.

Although no new isotopic data is presented here it is appropriate to discuss the published isotopic data in relation to the granitoids covered

Fig. 7:39. Variation diagrams for Y vs. Sn and Nb vs. Sn for the Caledonian granitoids (see over page).

Fig. 7:39. Variation diagrams for Y vs. Sn and Nb vs. Sn for the Caledonian granitoids.

Fig. 7:39



in this study. The Caledonian granitoids have been studied using a variety of isotope techniques (Halliday et al. 1979, Halliday 1984, Hamilton et al. 1980, Harmon & Halliday 1980, Harmon et al. 1984, Clayburn et al. 1983, Pidgeon & Aftalion 1978, Blaxland et al. 1979). Combined Nd-Sm and Rb-Sr data for a variety of plutons presented by Harmon et al. (1980) and Halliday (1984) are shown on a [Sr vs. [Nd diagram (Fig. 2:1). Data from the Aberdeen and Stritchen granites plot to the right of the mantle array indicating an unequivocal upper crustal component in their genesis. Data from the Foyers granodiorite and tonalite, Strontian granite, Garabal Hill granodiorite, Cairnsmore of Fleet granite, Eskdale and Shap granites also plot to the right of the mantle array, although the enrichment in radiogenic Sr is somewhat less than observed in the crustally derived Aberdeen and Stritchen granites. This may be the result of crustal contamination as is also indicated by the presence of inherited zircons in the Foyers granodiorite (Pidgeon & Aftalion 1978) and in the Strontian granite (Halliday et al. 1979). The extent of crustal contamination does not however appear to have any significant effect on the trace element geochemistry of these intrusions, since these intrusions do not appear to be geochemically different from those which in isotopic terms are less contaminated such as Ben Nevis, Foyers granite, Strontian tonalite and granodiorite.

Detailed isotopic investigations of the Etive complex (Clayburn et al. 1983) suggest progressive contamination with lower crust during fractional crystallization at the base of the crust with time from the Quarry and Cruachan intrusions to the Starav intrusion, with only minor contamination from upper crustal metasediments. Pb isotope work on feldspars from the Caledonian granites also indicate a lower crustal

contribution to granites north of the Highland Boundary Fault which is absent from the granite to the south (Blaxland et al. 1979).

It would appear that many if not all of the granitic intrusions north of the Highland Boundary Fault have suffered some contamination with lower crustal material, however the extent of contamination is not reflected in the trace element geochemistry of these intrusions. The granites south of the Highland Boundary Fault appear to be contaminated with upper crustal material, again this is not reflected in the trace element behaviour. The available isotopic data for the majority of the intrusions is insufficient to make further comments on the provenance of individual intrusions and more detailed work such as is presented by Clayburn et al. (1983) is obviously required. Trace element abundance patterns in the granitoids however do not appear to reflect crustal contamination but rather the extent of and mineral assemblages involved in fractional crystallization processes, although crustal contamination and fractional crystallization processes may be closely linked.

#### 7:5. SOURCE VARIATION BETWEEN THE INTRUSIONS OF THE NORTHERN AND SOUTHERN PLATES.

Since the bulk of the granite magmatism in both plates involved in the Caledonide orogeny in Britain is restricted to the later stages of the evolution of the Caledonide orogeny, i.e. Silurian-Early Devonian in age, the distance separating the two plates at this time is likely to be relatively small (Scotese et al. 1979). In the Lake District (southern plate) there appears to be a temporally expressed source variation as seen in the changes in rare earth patterns of the intrusions with time.

In the suite of Caledonian granites from the northern plate (Scotland) there is also a temporal source variation but this is linked with the major crustal thickening event in the Ordovician which does not affect the southern plate, in that the early granites have a substantial component of old crustal material in their source, derived by crustal melting. The geochemical variations observed in the remaining granitoids of the northern plate are probably related to differing degrees of fractional crystallization as discussed in section 7:3 and the only source variation which can be inferred is a possible difference in  $H_2O$  contents of the magmas and the volume of magma emplaced into the crust at any one time.

The temporal source variation in the granites of the southern plate appears to be related to a change in subcrustal source mineralogy. Whilst all the granitoids have some element of light rare earth enrichment, which together with the enriched LIL elements are derived from the subducted oceanic lithosphere, the later granites of the southern plate (Shap and Skiddaw) together with the mantle derived granites of the northern plate have strongly depleted heavy rare earths, this is also a characteristic of the lavas of the Lorne Plateau (Thirlwall 1982). This depletion in heavy rare earths probably reflects residual garnet in the source and appears to be a common feature of the late Caledonian granitoids from both plates implying a similarity in source mineralogy for all the late granites.

## 7:6. DISCUSSION AND CONCLUSIONS.

On the basis of the geochemical evidence from over 950 samples taken from 40 Caledonian granites there appears to be little direct evidence of source variation except for the few granites with a distinct crustal component (the early "S" type granites) in the northern plate, and the early granitoids of the southern plate (Carrock granophyre, Ennerdale, Eskdale and Threlkeld) which appear to have been derived from a subcrustal source with a different mineralogy from that of the later granites. Whilst there may be source variations within the late granitoid suites of both plates this phenomena is not observed as a result of the effects of differing degrees of fractional crystallization of differing mineral assemblages both insitu and prior to emplacement. Therefore whilst the observations of Thirlwall (1981, 1982, 1983) on the chemical variation of primitive Devonian calc-alkaline lavas which may be contemporary with the late granite suite, and the implied source variation cannot be questioned by this study, however the evidence presented by Brown et al. (1984) for source variations in the Caledonide granite suite appears to be too simplistic and does not take into account the effects of fractional crystallization on trace element abundances. The dominant feature of the geochemistry of the Caledonian granitoid suite is the marked effects of variations in fractional crystallisation, the extent to which this process can effect the observed compositions is dependent on the water content and size of the magma body and these features are probably related to some difference in the magma source.

## CHAPTER 8. SUMMARY OF CONCLUSIONS.

The origin of the British Caledonian granites has been widely discussed in the literature, particularly on the basis of isotopic evidence. However this has resulted in several different interpretations of the same data set. Critical issues concern the extent of the crustal contribution in the petrogenesis of the granitoids and the relationship between the Caledonian granitoids and subduction. This is especially relevant in the case of the late granites which appear to have been intruded after active subduction ceased, although the date of the cessation of subduction is not precisely defined.

The role of crustal melting in the genesis of the Caledonian granites is limited by various considerations. The isotopic evidence indicates that the only unequivocal "S" type intrusions are those such as Stritchen and Aberdeen which were emplaced closely following the peak of metamorphism in the Grampians, which is perfectly reasonable in geological terms. Petrographic studies also show that these intrusions, together with the Cove Bay and Ardclach granites (for which there are no published isotopic data), have a different crystallization sequence from the majority of Caledonian granitoids, in particular in having primary early muscovite and quartz as an early crystallizing phase. Additionally the compositions of biotites from these intrusions are substantially different from the compositions of biotites from the remaining intrusions with respect to the Fe:Mg:Mn ratio.

The magnitude of the crustal contribution to the remaining intrusions is difficult to assess but appears from isotopic data to be relatively

small. Trace element geochemistry is a rather less suitable method for determining the relative contributions of crustal and subcrustal components to any parental granitic magma because of the dominating effects of fractional crystallization on trace element variations. The mechanism for assimilation of older crustal material may be limited in its effect in intrusions which do not appear to have an extensive fractional crystallization history within the crust, implying relatively rapid solidification. However the intrusions which have suffered the least fractional crystallization, such as the Cluanie granodiorite, the Strath Ossian granodiorite and the Foyers granite, appear on the basis of inherited zircons, to have some contribution from older crustal material. The more fractionated intrusions, such as the Hill of Fare granite and the Lochnagar complex have the potential for large scale crustal contamination through combined assimilation-fractional crystallization processes but show no evidence for this from inherited zircons, although the inherited zircon component may have settled out during crystal fractionation. It would therefore appear that the origin for the majority of the Caledonian granitoids lies in subcrustal processes with very little contribution from older crustal sources.

Apart from uncertainties over the nature and composition of the source of the Caledonian granites, their composition may also have been modified considerably by later fractional crystallization and by subsolidus water-rock interaction in associated hydrothermal systems. Clearly the chemical effects of these latter processes must be assessed before any conclusions can be drawn concerning the ultimate source of the Caledonian granites.

Unlike basic magmas, which produce cumulates with easily recognised petrographic features, fractional crystallization of granite magmas does not necessarily produce obvious differences between "cumulate" and "liquid" rock types. However differences in the amount of and the mineral assemblage involved in fractional crystallization appear to be the main causes of the large variation in trace element geochemistry of the Caledonian granitoids. The amount of fractional crystallization and to a certain extent the fractionating mineral assemblage in any one pluton may be related both to the hydration state of the magma and the size of the magma body. Thus small bodies of magma or wet magmas may not undergo appreciable fractional crystallization before becoming completely solid, and generally have a hornblende-dominated crystallization assemblage. This results in relatively primitive compositions with high levels of Sr, Ba, Cr, V, Ni and no negative anomalies on mantle normalized trace element diagrams or chondrite normalized REE patterns, for example the Moor of Rannoch granodiorite and the Kilmelford diorite. Large magma bodies undersaturated with respect to  $H_2O$  may undergo considerable fractional crystallization before complete solidification, resulting in very evolved compositions with low levels of Sr, Ba, Cr, V, Ni, but high levels of Li, Rb, U, Th, W and Sn. This manifests itself as negative anomalies on mantle normalized trace element plots and chondrite normalized REE patterns for Ba, Sr, Ti, P and Eu, as for example, in the Cairngorm granite. Although the processes of fractional crystallization are important, the main underlying factor controlling the geochemical variations appears to be the water content of the magma which is related to variation in the fluid phase at source.

After crystallization is complete any granite intrusion will act as a heat source within the crust until thermal equilibrium is attained. This may take many tens of millions of years, but during this cooling process the intrusion may act as a driving force for circulating ground or connate water. The type of host rocks to the intrusions are the main factor governing the magnitude of this process. High grade metamorphic terrains such as the Moines of Scotland do not have sufficient free water for circulating connate water systems to become established, which may explain the general absence of mineralized/metasomatized intrusions in the north of Scotland. The few granites which are mineralized, for example the Helmsdale granite, are cut by fault systems allowing ground water access to the intrusion. Low grade metamorphic terrains, such as are found in the Lake District, have sufficient free water for large scale regional circulating connate water systems to develop.

The passage of hydrothermal fluids through granitic rocks result in the dispersion of the more mobile elements such as Li, Rb, Sr, U and B. In the case of the Lake District intrusions several geochemical features of metasomatism are observed; firstly the B distribution clearly indicates that the source of this element is in the sediments outside the intrusions and is not present in significant quantities in the initial magmas; secondly, Sr is lost during the process of greisenization (Skiddaw and Eskdale) but not during high temperature potash metasomatism (Shap); thirdly, Li, Rb and U levels are generally enhanced by the metasomatic processes. The role of magmatic water (residual fluid after crystallization is complete) in the Lake District granites is overshadowed by the large scale regional connate water circulation. However in the Glen Gairn intrusion (Scotland) there are localised

greisens which appear to be the result of the action of magmatic water because no enrichment of B is observed in these greisens, although like the Lake District, the host rocks are B rich. The resulting greisens are geochemically similar to the greisens in the Lake District intrusions with enriched levels of Li, Rb, U, Sn, W and Mo, but they lack the high B characteristic of the Lake District greisens.

The geochemical study of processes such as fractional crystallization and water-rock interaction have considerable bearing on the broader petrogenetic aspects of this study. Since the majority of the intrusions appear to be subcrustal in origin, evidence such as the probable hydration state of the magma and the geochemical characteristics of the more primitive magmas relate to mantle or subduction zone processes. The chondrite normalized rare earth patterns provide some mineralogical information on the source. In the Lake District there appears on this basis to be a time integrated variation in the residual mineralogy of the subcrustal source, with early granitoids showing no evidence for residual garnet and the later granites, together with the more primitive Scottish intrusions, showing clear depletion of the heavy rare earth elements, indicating residual garnet in the source. The presence or absence of residual garnet may not be related to mineralogically different sources within the mantle but rather different degrees of partial melting.

A common feature of all the intrusions studied is the enhanced levels of LIL elements and the negative Nb anomaly on mantle normalized trace element patterns, although the latter is diminished by large degrees of fractional crystallization. This feature is common to all subduction related magmas and is caused by the mobility of the LIL elements in the

fluid phase and the retention of Nb by residual minerals in the downgoing slab of the subduction zone. The evidence from fractional crystallization on the water content of the Caledonian magmas appears also to be related to time. The later granites appear to be undersaturated in  $H_2O$  and whilst they display subduction zone characteristics such as negative Nb anomalies in the less geochemically evolved parts of the intrusions, these granites were probably derived from melting under a drier fluid phase in the mantle. This change in the fluid phase at source is probably the result of the cessation of subduction and may represent the transition from subduction related magmatism to continental magmatism although no contribution from a Nb enriched within plate source is necessary to explain their geochemistry.

## ACKNOWLEDGEMENTS.

I acknowledge the receipt of a N.E.R.C. grant and I thank Prof. J. Tarney and Dr Jane Plant for initiating this project. I am especially grateful to Dr Jane Plant and Peter Simpson for the use of the B.G.S. collection of British Caledonian granite samples, and I thank Dr A.M. Evans (Univ. of Leicester) and Prof. G.C. Brown (Open University) for the use of samples from their personal collections. I express my thanks to Nick Marsh and Rob Wilson for assistance with analytical techniques; Dr Ian Luff, Nick Marsh, Rob Wilson and Paul Tarney for the use of computer programmes; Sue Button and Jane Hurdley for assistance with drawing diagrams; and the departmental secretaries over the years for taking telephone messages. I am grateful to Dr Mike Norry, Dr Jane Plant, Dr Ian Luff, Dr Andy Saunders, Dr Dave Bartholomew, Dr Mike Petterson, John Pillar, Neil Hodgeson and Tony Rex for all those meaningful discussions on geochemistry; and the occupants of the Joe Coral Room over the years for putting up with my bad language and whose company I have enjoyed. Last but not least I express my thanks to Julian who has helped me to remain approximately sane against high odds and for whose personal support I am deeply grateful whatever happens in the future.